



**ISPRA**

Istituto Superiore per la Protezione e la Ricerca Ambientale

**SERVIZIO GEOLOGICO D'ITALIA**

Organo Cartografico dello Stato (legge n°68 del 2. 2. 1960)

# MEMORIE

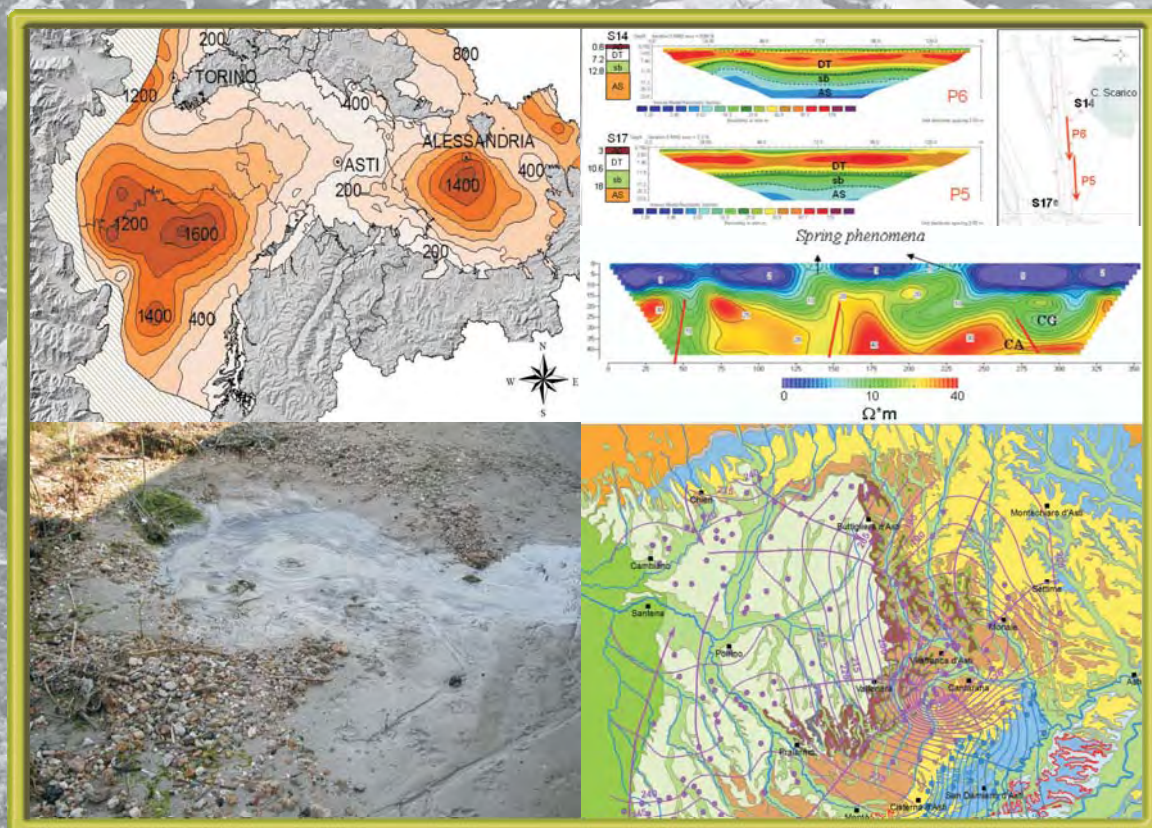
## DESCRITTIVE DELLA

# CARTA GEOLOGICA D'ITALIA

VOLUME XC

**Proceedings of the Second National Workshop  
Multidisciplinary approach for porous aquifer  
characterization**

*Atti del Secondo Workshop Nazionale  
L'approccio multidisciplinare allo studio degli  
acquiferi porosi*



*In copertina* : immagini relative al volume

*Realizzazione iconografica:* Maria Luisa VATOVEC



**ISPRA**

Istituto Superiore per la Protezione e la Ricerca Ambientale

**SERVIZIO GEOLOGICO D'ITALIA**

Organo Cartografico dello Stato (legge n° 68 del 2. 2. 1960)

# MEMORIE

## DESCRITTIVE DELLA

# CARTA GEOLOGICA D'ITALIA

VOLUME XC

---

### **Proceedings of the Second National Workshop Multidisciplinary approach for porous aquifer characterization**

*Atti del Secondo Workshop Nazionale  
L'approccio multidisciplinare allo studio degli acquiferi porosi*

*a cura di*

AMOROSI A., BERSEZIO R., BONOMI T., BONZI L., BUTTERI M., CALCAGNILE L.,  
CANEPÀ P., CANTONE M., CARLSON F., CAVALLI E., CILUMBRIELLO A., CLEMENTE P.,  
DELL'ARCIPRETE D., DEL ROSSO F., D'ONOFRIO S., DE LUCA D.A., DOVERI M.,  
FELLETTI F., FIORASO G., FIORUCCI A., FORNO M.G., FUMAGALLI L., GALLICCHIO S.,  
GATTAI P., GHIELMI M., GIANNECCHINI R., GIANOTTI F., GIUDICI M., GOVERNA M.,  
GRANATI C., GRIPPA A., GUADAGNINI A., GUADAGNINI L., IRACE A., LONGINELLI A.,  
LUPIS D., MAIORANO P., MARGIOTTA S., MARTELLI G., MARTINELLI G., MATEU-  
VICENS G., MAZZONE F., MELE M., MENZIANI M., MOSCA P., NATALICCHIO M.,  
NEGRI S., OSSELLA L., PAVESI M., PETRICIG M., PIANA F., PISANI V., POLINO R.,  
PUGNAGHI S., QUARTA G., RIVA M., ROSSI C.A., RUSI S., RUSNIGHI Y., SABATO L.,  
SCIUTO P.F., SELMO E., SPILOTRO G., TATANGELO F., TRENKWALDER S., TROPEANO M.,  
VASSENA C., VIGNA B., VINCENZI S., VIOLANTI D.

*Editors*

Riccardo BERSEZIO, Marco AMANTI

*Direttore responsabile:* Leonello SERVA

---

**REDAZIONE a cura del Servizio Cartografico, coordinamento base dati e tavoli europei**

*Capo Settore:* Domenico TACCHIA

*Coordinamento Editoriale, Allestimento Digitale:* Maria Luisa VATOVEC

---

*Stampa:* Tipografia CSR - Via di Pietralata n.157, Roma - 2010



### **Organizing Committee of the Workshop - *Comitato Organizzativo del Workshop***

RICCARDO BERSEZIO	Dipartimento di Scienze della Terra, Università di Milano
MARCO AMANTI	ISPRA, ROMA
ALESSANDRO AMOROSI	Dipartimento di Scienze Geologiche, Università di Bologna
MAURO GIUDICI	Dipartimento di Scienze della Terra, Università di Milano
GRAZIA MARTELLI	Dipartimento di Georisorse e Territorio, Università di Udine
RENZO VALLONI	Dipartimento di Scienze della Terra, Università di Parma

### **Scientific Committee of the Workshop - *Comitato Scientifico del Workshop***

MARCO AMANTI	ISPRA, Roma
ALESSANDRO AMOROSI	Dipartimento di Scienze Geologiche, Università di Bologna
GIOVANNI BERETTA	Dipartimento di Scienze della Terra, Università di Milano
RICCARDO BERSEZIO	Dipartimento di Scienze della Terra, Università di Milano
MAURO GIUDICI	Dipartimento di Scienze della Terra, Università di Milano
ALBERTO GUADAGNINI	Dip. di Ingegneria Idraulica, Ambientale, Infrastrutture Viarie, Rilevamento, Politecnico di Milano
ANTONIO LONGINELLI	Dipartimento di Scienze della Terra, Università di Parma
STEFANO MARGIOTTA	Dipartimento di Scienza dei Materiali, Università del Salento
GRAZIA MARTELLI	Dipartimento di Georisorse e Territorio, Università di Udine
SERGIO RUSI	Dipartimento di Geotecnologie per l'Ambiente e il Territorio, Università di Chieti
RENATO SANTANGELO	Dipartimento Ingegneria dei Materiali e dell'Ambiente, Università di Modena e Reggio Emilia
PAOLO SEVERI	Servizio Geologico, Sismico e dei Suoli, Regione Emilia - Romagna
RENZO VALLONI	Dipartimento di Scienze della Terra, Università di Parma
BARTOLOMEO VIGNA	Dip. di Ingegneria del Territorio, dell'Ambiente e delle Geotecnologie, Politecnico di Torino
ANDREA VITTURI	Settore Protezione Civile e Difesa del Suolo, Provincia di Venezia
ANNALISA ZAJA	Dipartimento di Geoscienze, Università di Padova

### **Reviewers Committee - *Comitato Revisori degli articoli***

LUCA ALBERTI	Dip. di Ingegneria Idraulica, Ambientale, Infrastrutture Viarie e Rilevamento, Politecnico di Milano
ALESSANDRO AMOROSI	Dipartimento di Scienze Geologiche, Università di Bologna
GIOVANNI BERETTA	Dipartimento di Scienze della Terra, Università di Milano
RICCARDO BERSEZIO	Dipartimento di Scienze della Terra, Università di Milano
MARCO BIANCHI	Department of Geological Sciences, University of Alabama
ALFREDO BINI	Dipartimento di Scienze della Terra, Università di Milano
TULLIA BONOMI	Dip. di Scienze dell'Ambiente e del Territorio Università degli Studi di Milano Bicocca
LUISA DE CAPITANI	Dipartimento di Scienze della Terra, Università di Milano
GIANFRANCO CIANCETTI	Dipartimento di Scienze della Terra, Università di Pavia
FABRIZIO FELLETTI	Dipartimento di Scienze della Terra, Università di Milano
LAURA FOGLIA	University of California, Davis
VINCENZO FRANCANI	Dip. di Ingegneria Idraulica, Ambientale, Infrastrutture Viarie e Rilevamento, Politecnico di Milano
MAURO GIUDICI	Dipartimento di Scienze della Terra, Università di Milano
ALBERTO GUADAGNINI	Dip. di Ingegneria Idraulica, Ambientale, Infrastrutture Viarie e Rilevamento, Politecnico di Milano
LAURA GUADAGNINI	Dipartimento di Scienze della Terra, Università di Parma
PETER HUGGENBERGER	Department of Geosciences, Applied and Environmental Geology, University of Basel
VINCENZO LAPENNA	IMAA – CNR, Potenza
ALFREDO LOZEJ	Dipartimento di Scienze della Terra, Università di Milano
ANTONIO LONGINELLI	Dipartimento di Scienze della Terra, Università di Parma
STEFANO MARGIOTTA	Dipartimento di Scienza dei Materiali, Università del Salento
GRAZIA MARTELLI	Dipartimento di Georisorse e Territorio, Università di Udine
GIOVANNI MARTINELLI	ARPA Emilia-Romagna
MARCO MASETTI	Dipartimento di Scienze della Terra, Università di Milano
SALVATORE MILLI	Dipartimento di Scienze della Terra, Università di Roma “La Sapienza”
SERGIO NEGRI	Dipartimento di Scienza dei Materiali, Università del Salento
PHILIPPE RENARD	Centre d'Hydrogéologie et de Géothermie, Institut de Géologie et d'Hydrogéologie, Université de Neuchâtel
EMANUELE ROMANO	CNR-IRSA, Roma
SERGIO RUSI	Dipartimento di Geotecnologie per l'Ambiente e il Territorio, Università di Chieti
PAOLO SEVERI	Servizio Geologico, Sismico e dei Suoli, Regione Emilia - Romagna
RENZO VALLONI	Dipartimento di Scienze della Terra, Università di Parma
CHIARA VASSENÀ	Dipartimento di Scienze della Terra, Università di Milano
BARTOLOMEO VIGNA	Dip. di Ingegneria del Territorio, dell'Ambiente e delle Geotecnologie, Politecnico di Torino
IRENE ZEMBO	Dipartimento di Scienze della Terra, Università di Milano
GIOVANNI MARIA ZUPPI	Dipartimento di Scienze Ambientali, Università di Venezia

## PREFACE

---

Groundwater is one of the main sources of drinking water in Italy and all over Europe; statistics from EuroGeoSurvey and European Environmental Agency show that about 60% of the drinking water in the European Union comes from it.

Because of that the knowledge of groundwater conditions, in terms of quality and quantity, is becoming day after day of vital importance for the Society needs such as:

- searching for and using good drinking water without colliding with the flora and fauna (environment) requirements and without threatening future water reserves;
- understanding the underground flow paths to be able to describe their variations in space and time;
- identifying and understanding the most important relationships between human intervention and related effects on groundwater aquifers;
- investigating the extent of human interventions in the hydrogeological cycle to establish appropriate planning and management measures.

Those are just some of the questions to which Geologists and Hydrogeologists are asked to answer; ISPRA is publishing this volume to contribute to the discussion. It comes 3 years after the proceedings of the first National Workshop held in Parma on June 2004, (*Developments in Aquifer Sedimentology and Groundwater Flow Studies in Italy*, R. VALLONI edr., Mem. Descr. Carta Geol. d'It., LXXVI (2007), pp. 316), and contains many papers produced by a large number of specialists who met in Rimini on September 2009 to take part in the Second National Workshop called "*Multidisciplinary approach for porous aquifer characterization*".

My sincere congratulations to all of them

## PREFAZIONE

---

*Le acque sotterranee sono una delle principali fonti di acqua potabile in Italia e in tutta Europa; statistiche realizzate da EuroGeoSurvey (Associazione dei Servizi Geologici dei paesi dell'Unione Europea) e Agenzia Europea per l'Ambiente mostrano che circa il 60% dell'acqua potabile nell'Unione Europea proviene da esse.*

*A causa di ciò, la conoscenza delle condizioni delle acque sotterranee, in termini di qualità e quantità, sta diventando giorno dopo giorno di sempre maggiore importanza per i bisogni della Società, tra i quali possiamo elencare:*

- *ricerca ed uso di acqua potabile di buona qualità senza scontrarsi con le necessità di flora e fauna (ambiente) e senza mettere in pericolo le riserve idriche future;*
- *conoscenza dei percorsi dei flussi sotterranei di acqua potabile, per essere in grado di descrivere le loro variazioni nello spazio e nel tempo;*
- *individuazione e comprensione delle relazioni che intercorrono tra le azioni dell'uomo e le variazioni delle falde acquifere sotterranee;*
- *verifica della portata degli interventi dell'uomo nel ciclo idrogeologico, per poter arrivare ad una adeguata pianificazione e gestione delle risorse disponibili.*

*Queste sono solo alcune delle domande a cui i geologi e gli idrogeologi sono invitati a rispondere; per contribuire alla discussione su queste fondamentali tematiche, ISPRA ha promosso la realizzazione e la pubblicazione di questo volume.*

*Esso rappresenta, a tre anni di distanza, la naturale continuazione degli atti del Primo Workshop Nazionale tenutosi a Parma nel giugno 2004, (*Developments in Aquifer Sedimentology and Groundwater Flow Studies in Italy*, R. VALLONI edr., Mem. Descr. Carta Geol. d'It., LXXVI (2007), pp. 316), e contiene i risultati di lavori e ricerche di altissima qualità scientifica realizzati da un gran numero di specialisti che si sono incontrati a Rimini, nel settembre 2009, per partecipare al Secondo Workshop Nazionale denominato "*Multidisciplinary approach for porous aquifer characterization*".*

*A tutti loro vanno le mie sincere congratulazioni*

Leonello SERVA

Direttore del Servizio Geologico d'Italia - ISPRA

Both surface and groundwaters are under increasing pressure from the continuous growth in demand for sufficient quantities of good quality water for all purposes. Hence the development of research aiming to provide the basic knowledge for management and protection tools of freshwater is a strategic matter all over the world and in Italy. At the beginning of the millennium, the European Parliament adopted a Directive that established a framework for Community action in the field of water policy. The purpose was the protection of inland surface waters, transitional waters, coastal waters and groundwater, promoting sustainable use based on a long-term protection of available water resources and ensuring the progressive reduction and prevention of pollution of groundwater. These challenging goals stimulated fast developments in the field of characterization and modelling of porous aquifers, with emphasis on surface-groundwater exchange, salt-freshwater interference, flow and contaminant transport paths, local vs. regional hydrogeological balances. These developments were possible thanks to a multidisciplinary approach, from geological and geophysical modelling of hydrostratigraphy and hydrogeochemical characterization, to mathematical modelling and simulation of flow and transport processes. During the last decades, innovative results in these fields have been achieved thanks to a renewed attention to the good knowledge of the geological architecture and evolution of aquifer stratigraphy, that is widely recognized as the starting point for any hydrogeological application.

A contribution to summarize the state of the art of these researches in Italy came from a first National Workshop held in Parma (June 2004), whose results are documented by the Proceedings Volume edited by Renzo VALLONI (Developments in Aquifer Sedimentology and Groundwater Flow Studies in Italy, *Mem. Descr. Carta Geol. d'It.*, **76** (2007), pp. 316). Following this line, the **Second National Workshop “Multidisciplinary approach for porous aquifer characterization”** was held in Rimini in September 2009, in the frame of the VII FIST Forum “Geotitalia 2009” (Workshop W1 Program and Abstracts of the 36 presentations can be found in *Epitome*, **3** (2009), p. 3 – 12). The Workshop aimed to contribute to update the state of the art, evaluate the research perspectives and stimulate scientific cooperation between different groups and expertises, stimulating a broad discussion about the multidisciplinary approach to characterization and modelling of porous aquifers, solution of flow and transport problems, quantification of the exchanges between atmospheric, surface and subsurface water reservoirs, and elaboration of sustainable scenarios for management of the water resource.

The good success of the Workshop stimulated printing of these Proceedings, that represent the ideal prosecution of the previous volume. Nineteen papers have been accepted for publication, all of them stressing the need for a multidisciplinary approach based on the robust geological knowledge of hydrostratigraphy.

Among the **review papers**, LONGINELLI & SELMO provide a summary of isotope geochemistry with respect to the water cycle with emphasis on Italy, GUADAGNINI *et alii*, discuss experiments and models on carbonates dissolution and heavy metals competition in porous media and GIUDICI reviews modelling water flow and solute transport in alluvial sediments.

Under the **methodology**, DELL’ARCIPRETE *et alii*, describe different techniques for simulation of heterogeneity in a meandering river aquifer analogue, MELE *et alii*, introduce an integrated geological-geophysical methodology for multiscale characterization of alluvial aquifers architecture, BONZI *et alii*, illustrate the Web 2.0 technology for the presentation of analytical data and results of the speciation calculation in groundwaters of the plain area of Emilia-Romagna region and VINCENZI *et alii*, demonstrate general analytical solutions of the linearized Richards equation that describes space and time evolution of the soil water content in an unsaturated medium.

A wide number of **regional case studies** has been collected. Under this group of papers, some deal with the **western Po plain hydrostratigraphy**: IRACE *et alii*, describe a new hydrostratigraphic framework of the Late Messinian-Quaternary basins of Southern Piedmont and VIGNA *et alii*, analyse the relations between stratigraphy, groundwater flow and hydrogeochemistry in some areas of the Tertiary Piedmont Basin. Still in Piedmont, FORNO *et alii* suggest the hydrogeological implications of the architecture of Pliocene-Pleistocene torrential and debris flow sediments of the Lanzo Massif region.

The **Central and Eastern Po plain hydrostratigraphy** are dealt with by AMOROSI & PAVESI, that illustrate aquifer stratigraphy from the Middle-Late Pleistocene succession of the Mantova area, BERSEZIO *et alii*, that describe the relations between aquifer building processes and Apennine tectonics in the southern most plain of Lombardy, BONOMI *et alii*, that provide the assessment of groundwater availability in the Milan province aquifers, MARTELLI & GRANATI that formulate a comprehensive hydrogeological view of the Friuli alluvial plain thanks to a multi-annual quantitative survey, and PISANI *et alii*, that show a case study of application of groundwater flow modelling to support a remediation project within a chemical facility.

Moving to **Central and Southern Italy**, BUTTERI *et alii*, describe the hydrogeological and hydrogeochemical frame of aquifers in the Arno coastal plain near Pisa, RUSI & TATANGELO provide the conceptual model of Sangro and Vomano plains for management of alluvial aquifers, CILUMBRIELLO *et alii*, illustrate sedimentology, stratigraphic architecture and hydrostratigraphy of the Metaponto coastal-plain and MARGIOTTA *et alii*, document the hydrogeological implications of the stratigraphic revision of the Brindisi-Taranto Plain.

Looking forward the next meeting on these relevant topics, we would like to thank all those who contributed to the success of the 2009 Workshop and to the edition of this Volume and specifically Maria Luisa VATOVEC who took care of the edition of this Volume.

## INTRODUZIONE

La disponibilità di acque superficiali e sotterranee di buona qualità subisce una pressione crescente dovuta al continuo aumento della domanda di grandi quantità d'acqua per uso civile, irriguo, industriale. Anche per questo, lo sviluppo della ricerca rivolta alle conoscenze di base per la gestione e protezione delle acque dolci è una necessità strategica nel mondo come in Italia. All'inizio del millennio il Parlamento Europeo adottò una direttiva che fornì il quadro di riferimento per le azioni comunitarie nel campo della politica dell'acqua. Lo scopo era la protezione delle acque superficiali continentali, dei corpi idrici transizionali e costieri e delle acque sotterranee, attraverso la promozione dell'utilizzo sostenibile fondata sulla protezione a lungo termine delle risorse idriche disponibili e sulla progressiva prevenzione e riduzione dell'inquinamento della falde acquifere. Questi obiettivi ambiziosi stimolarono sviluppi veloci nei campi della caratterizzazione e modellazione degli acquiferi porosi, con particolare riguardo agli scambi tra acque superficiali e sotterranee, all'interferenza tra acque dolci e saline, ai percorsi di flusso e di trasporto dei contaminanti, al calcolo dei bilanci idrologici locali e regionali. Questi sviluppi sono stati resi possibili dall'approccio multidisciplinare, che ha visto l'integrazione della modellistica geologica e geofisica dell'idrostratigrafia con l'idrogeochimica, la modellistica fisico-matematica e la simulazione dei processi di flusso e trasporto. Negli ultimi decenni in questi campi sono stati raggiunti risultati innovativi, anche grazie ad una rinnovata attenzione al miglioramento delle conoscenze relative all'architettura ed evoluzione stratigrafica degli acquiferi, che è ampiamente riconosciuta come il punto di partenza per ogni applicazione idrogeologica.

Un contributo a riassumere lo stato dell'arte delle ricerche in Italia in questi campi venne dal Primo Workshop Nazionale tenuto a Parma nel giugno 2004, i cui risultati sono raccolti nel Volume degli Atti edito da Renzo VALLONI (*Developments in Aquifer Sedimentology and Groundwater Flow Studies in Italy*, Mem. Descr. Carta Geol. d'It., **76**, 2007, pp. 316). Seguendo questa linea, si è organizzato e tenuto il **Secondo Workshop Nazionale "Multidisciplinary approach for porous aquifer characterization"** (Rimini, Settembre 2009) nell'ambito del VII Forum FIST "GeoItalia 2009" (Workshop W1, Programma e Riassunti delle 36 presentazioni in *Epitome*, **3**, 2009, p. 3 – 12). Il Workshop era rivolto a contribuire ad una nuova messa a punto dello stato dell'arte della ricerca a 5 anni di distanza dal precedente, valutando le nuove prospettive scientifiche e stimolando la collaborazione tra gruppi dotati di esperienze diverse e complementari. Il Workshop si proponeva inoltre di proseguire l'ampia discussione sull'approccio multidisciplinare alla caratterizzazione e modellazione degli acquiferi porosi, alla soluzione dei problemi di flusso e di trasporto, alla quantificazione degli scambi tra acque atmosferiche, superficiali e sotterranee ed all'elaborazione di scenari di gestione sostenibile della risorsa idrica.

Il buon successo del Workshop ha stimolato l'edizione di questo nuovo Volume di Atti, che costituisce l'ideale prosecuzione del precedente. Al termine della procedura di revisione, eseguita da un ampio Comitato di Revisori, sono stati accettati per la pubblicazione 19 contributi, che sottolineano in vario modo la necessità di un approccio pluridisciplinare basato su una robusta conoscenza geologica dell'idrostratigrafia.

Tra i **lavori con carattere di review**, LONGINELLI & SELMO forniscono una messa a punto delle metodologie della geochimica isotopica applicata al ciclo delle acque, con particolare attenzione al caso dell'Italia, GUADAGNINI et alii discutono la modellazione ed interpretazione dei processi di dissoluzione e di assorbimento competitivo di metalli pesanti nei mezzi porosi mentre GIUDICI rivede i metodi per la modellazione dei processi di flusso e trasporto dei soluti negli acquiferi alluvionali a diverse scale.

Tra i **lavori dedicati ad aspetti metodologici**, DELL'ARCIPRETE et alii presentano e confrontano tecniche differenti per la simulazione dell'eterogeneità di un analogo di acquifero fluviale meandriforme, MELE et alii descrivono una metodologia geologico-geofisica integrata per la caratterizzazione dell'architettura dei sistemi acquiferi fluviali a diverse scale, BONZI et alii illustrano la tecnologia Web 2.0 per la presentazione dei dati analitici e dei risultati del calcolo di speciazione nelle acque sotterranee della zona di pianura della Regione Emilia-Romagna e VINCENZI et alii dimostrano le soluzioni analitiche generali dell'equazione di Richards che descrive l'evoluzione spazio-temporale del contenuto in acqua del suolo e della zona insatura.

Un ampio numero di **studi relativi a casi a carattere regionale** descrive l'idrostratigrafia di diverse aree in Italia.

Tra questi un primo gruppo si riferisce alla **pianura padana occidentale**, come nel caso di IRACE et alii, che presentano un nuovo schema idrostratigrafico dei bacini Messiniano – Quaternari del Piemonte meridionale, e VIGNA et alii, che analizzano le relazioni tra stratigrafia, flusso idrico sotterraneo ed idrogeochimica in alcune aree del Bacino Terziario Ligure-Piemontese o FORNO et alii, che individuano le implicazioni idrogeologiche dell'architettura dei depositi torrentizi e di debris-flow della regione del Massiccio Ultrabassico di Lanzo.

L'idrostratigrafia della **pianura padana centro-orientale** è trattata da diversi autori, tra cui AMOROSI & PAVESI, che illustrano la stratigrafia degli acquiferi della successione del Pleistocene medio – superiore nel mantovano, BERSEZIO et alii, che descrivono le relazioni tra genesi degli acquiferi e tettonica appenninica nella Lombardia meridionale, BONOMI et alii, che stimano la disponibilità idrica negli acquiferi della provincia di Milano, MARTELLI & GRANATI, che formulano un quadro idrogeologico della pianura alluvionale friulana per mezzo di uno studio quantitativo pluriennale, e PISANI et alii, che presentano un caso di applicazione di modellistica idrogeologica al progetto di bonifica di un sito contaminato.

Diversi autori trattano **aree del centro e Sud Italia**, come BUTTERI et alii, che descrivono il contesto idrogeologico ed idrogeochimico della piana costiera dell'Arno vicino a Pisa, RUSI & TATANGELO, che forniscono il modello concettuale delle piane del Sangro e Vomano per la gestione degli acquiferi alluvionali, CILUMBRIELLO et alii, che illustrano la sedimentologia e l'architettura idrostratigrafica della piana costiera di Metaponto e MARGIOTTA et alii, che documentano le implicazioni idrogeologiche della revisione stratigrafica della piana di Brindisi – Taranto.

Nell'attesa del prossimo incontro-Workshop su queste tematiche di grande rilievo, ci è gradito ringraziare tutti coloro che hanno partecipato al Workshop 2009, gli autori degli articoli che compongono questi Atti, i componenti del Comitato Scientifico e del Comitato dei Revisori e la Responsabile del Coordinamento Editoriale, Maria Luisa VATOVEC, che hanno contribuito così efficacemente al buon successo dell'iniziativa e di questo volume.

Riccardo Bersezio, Marco Amanti



## Aquifer stratigraphy from the middle-late Pleistocene succession of the Po Basin

### *Stratigrafia di sistemi acquiferi nella successione medio - e tardo pleistocenica del Bacino Padano*

AMOROSI A. (\*), PAVESI M. (\*\*)

**ABSTRACT** - Detailed stratigraphic correlations based upon a large borehole data base, coupled with a multi-proxy investigation of cores and its framing into a sequence-stratigraphic context, enable for the first time the reconstruction of a high-resolution, unitary scheme of (hydro)stratigraphic architecture for a large portion of the Po Basin (Emilia-Romagna and SE Lombardy) over the last million years, including specific facies connotation of the aquifer systems. Two stratigraphic unconformities of tectonic origin, identified on a seismic basis and dated to about 450 and 870 ka, respectively, represent the lower bounding surfaces of two stratigraphic units (Lower Po Synthem and Upper Po Synthem) that can be tracked and mapped throughout the basin.

A striking cyclic architecture is identified within the the Upper Po Synthem. Each cycle, which is about 50-90 m thick and represents an interval of approximately 100 kyr (4<sup>th</sup>-order sequence), includes basal, silt-clay overbank deposits with thin and lenticular fluvial-channel sands, showing upward transition to increasingly amalgamated and more laterally extensive fluvial-channel sand bodies. Four aquifer systems (I to IV) in the upper portions of cycles, corresponding to alluvial-fan and fluvial channel-belt deposits, can be correlated from the basin margins to the Adriatic Sea. Shallow aquifer systems I and II display an impressive lateral continuity and are affected by local tectonic deformation only in the Ferrara area and close to the basin margins, whereas syn-depositional tectonics appears to have exerted a marked influence on facies and reservoir distribution of the relatively deeper aquifer systems (III and IV).

On the basis of the overall stratigraphic architecture and diagnostic pollen signature, the laterally extensive mud-prone intervals acting as permeability barriers between the aquifer

systems are interpreted to represent the landward equivalents of the transgressive nearshore deposits recognized at more distal locations. This allows subdivision of the fluvial succession into vertically stacked, transgressive-regressive sequences. The transgressive surfaces and their landward equivalents are readily identifiable stratigraphic markers that may be used to frame aquifer geometry within a sequence-stratigraphic context of fluvial architecture. The application of a hierarchy to subsurface stratigraphy in the Po Basin may thus represent the first step toward the interpretation and prediction of alluvial reservoir geometry and connectivity on a basin scale.

**KEY WORDS:** Aquifer stratigraphy, Alluvial deposits, Po Plain, Quaternary, Sequence stratigraphy

**RIASSUNTO** - Lo studio di dettaglio di un vasto database stratigrafico, integrato dall'analisi multidisciplinare di carote e dall'inquadramento di esse su base stratigrafico-sequenziale, consente per la prima volta la ricostruzione di un quadro (idro)stratigrafico unitario per i depositi medio- e tardopleistocenici di una vasta porzione del Bacino Padano (pianura emiliano-romagnola e mantovana). Due superfici di discontinuità, identificate su base sismica e datate rispettivamente a 450 e 870 ka, costituiscono i limiti di altrettante unità stratigrafiche (Sintema Padano Inferiore e Sintema Padano Superiore), riconoscibili e mappabili a scala bacinale.

Il Sintema Padano Superiore presenta una caratteristica architettura ciclica. I cicli deposizionali riconoscibili al suo interno hanno uno spessore di 50-90 m e rappresentano intervalli temporali di circa 100.000 anni (sequenze di quarto ordine). Ogni ciclo è dominato inferiormente da depositi sil-

(\*) Dipartimento di Scienze della Terra e Geologico-Ambientali, Università di Bologna, Via Zamboni 67, 40127 Bologna, Italy. E-mail: [alessandro.amorosi@unibo.it](mailto:alessandro.amorosi@unibo.it)

(\*\*) Via Trifoglio 128, 46040 Ceresara, Mantova, Italy. E-mail: [geolmart@gmail.com](mailto:geolmart@gmail.com)

toso-argillosi di piana inondabile, con isolate lenti sabbiose di canale fluviale; questi passano verso l'alto a corpi sedimentari grossolani a geometria tabulare, caratterizzati da un elevato grado di amalgamazione. In tutto sono riconoscibili quattro sistemi acquiferi (I-IV), che possono essere correlati dai margini del bacino al Mare Adriatico. Dal punto di vista sedimentologico i sistemi acquiferi sono impostati all'interno di depositi di conoide alluvionale e di channel belt fluviale. Gli acquiferi più superficiali (I e II) mostrano una rilevante continuità stratigrafica e sono deformati unicamente ai margini del bacino e in corrispondenza di alti strutturali quali, ad esempio, le pieghe ferraresi. E' evidente, al contrario, un forte controllo da parte della tettonica sindeposizionale sulle facies e sulla geometria dei sistemi acquiferi relativamente più profondi (III e IV).

Sulla base dell'architettura deposizionale e dei caratteri paleoclimatici (pollini) riscontrati in carota, i depositi prevalentemente fini, lateralmente continui, che formano le maggiori barriere di permeabilità tra sistemi acquiferi sono interpretati come gli equivalenti laterali dei depositi trasgressivi di ambiente costiero riconosciuti nel sottosuolo dell'attuale piana costiera, ponendo così le basi per la suddivisione della successione fluviale in sequenze trasgressivo-regressive. Le superfici di trasgressione ed il loro prolungamento verso terra costituiscono i principali marker stratigrafici alla scala dell'intero bacino, consentendo l'inquadramento degli acquiferi in un contesto stratigrafico-sequenziale. Questo studio dimostra come l'individuazione di una gerarchia di superfici all'interno del Bacino Padano costituisca un elemento imprescindibile per una ricostruzione realistica della geometria degli acquiferi a scala bacinale.

**PAROLE CHIAVE:** Acquiferi, Depositi alluvionali, Pianura Padana, Quaternario, Stratigrafia sequenziale

## 1. – INTRODUCTION

The Po Plain, a rapidly subsiding foreland basin bounded by the Alps to the North and the Apennines to the South, is one of the largest alluvial plains in Europe and makes up an appealing target for water research. For this reason, after the early studies mostly focused on basin formation and evolution (PIERI & GROPPi, 1981; PIERI, 1983; DONDI & D'ANDREA, 1986; DALLA *et alii*, 1992; ORI, 1993; MUTTONI *et alii*, 2003), extensive subsurface investigations have been performed in the Po Basin with the aims of defining a general framework of aquifer distribution within the middle-late Pleistocene alluvial succession, and of evaluating the volume and characteristics of the groundwater resource (REGIONE EMILIA-ROMAGNA & ENI-AGIP, 1998; REGIONE LOMBARDIA & ENI-DIVISIONE AGIP, 2002; BERSEZIO *et alii*, 2004). Through multiple-scale input data (from seismic mapping to well-log interpretation), these studies enabled the reconstruction of large-scale stratigraphic architecture, leading to internal subdivision of the Pliocene-Quaternary basin fill into six depositional sequences South of Po River (REGIONE EMILIA-ROMAGNA & ENI-AGIP, 1998), and four deposi-

tional sequences North of Po River (REGIONE LOMBARDIA & ENI-DIVISIONE AGIP, 2002). Each sequence, corresponding from a hydrostratigraphic viewpoint to an aquifer group, is bounded at its base by a tectonic unconformity, which is interpreted to have formed during a phase of significant basin reorganization.

A key issue featured in early stratigraphic studies was the concept of cyclic architecture on a variety of scales (AMOROSI & FARINA, 1995; REGIONE EMILIA-ROMAGNA & ENI-AGIP, 1998; REGIONE LOMBARDIA & ENI-DIVISIONE AGIP, 2002; AMOROSI *et alii*, 2008). Due to poor availability of continuous core data, however, facies received relatively little attention in these studies. As a consequence, most stratigraphic reconstructions did not incorporate information on the sedimentology of the aquifers, nor carried out a consistent analysis of the genetic relationships between alluvial and coastal depositional systems.

The widespread drilling campaign carried out by the Emilia-Romagna and Lombardy Geological Surveys in the Po Plain during the past 15 years has made it possible to focus recent stratigraphic work more specifically on facies characterization and multi-proxy investigation of continuous cores, up to 200 m long. After the pioneer work of AMOROSI *et alii* (1999a) on the 173 m-long Core S17 in the Romagna coastal plain, several studies have depicted stratigraphic and sedimentological characteristics of long cores in Emilia-Romagna (AMOROSI *et alii*, 2001, 2004, 2007) and Lombardy (MUTTONI *et alii*, 2003; SCARDIA *et alii*, 2006; AMOROSI *et alii*, 2008). A complete data set is offered by the Emilia-Romagna and Lombardy sheets of the 1:50,000 Geological Map. For a sequence-stratigraphic review, the reader is referred to AMOROSI & COLALONGO (2005) and AMOROSI (2008).

The aim of this paper is to provide for the first time a unitary scheme of aquifer architecture for the middle-late Pleistocene record of the Po Basin on a regional scale (fig. 1). Specific objectives are: i) the geometric characterization and facies connotation of the major aquifer bodies on the basis of a wide dataset, encompassing Emilia-Romagna and southern Lombardy, and ii) the construction of a framework of aquifer distribution into a sedimentological and sequence-stratigraphic context.

## 2. – REGIONAL STRATIGRAPHY

The recent mapping projects carried out by the geological surveys of Regione Emilia-Romagna and Lombardy have provided a wealth of infor-

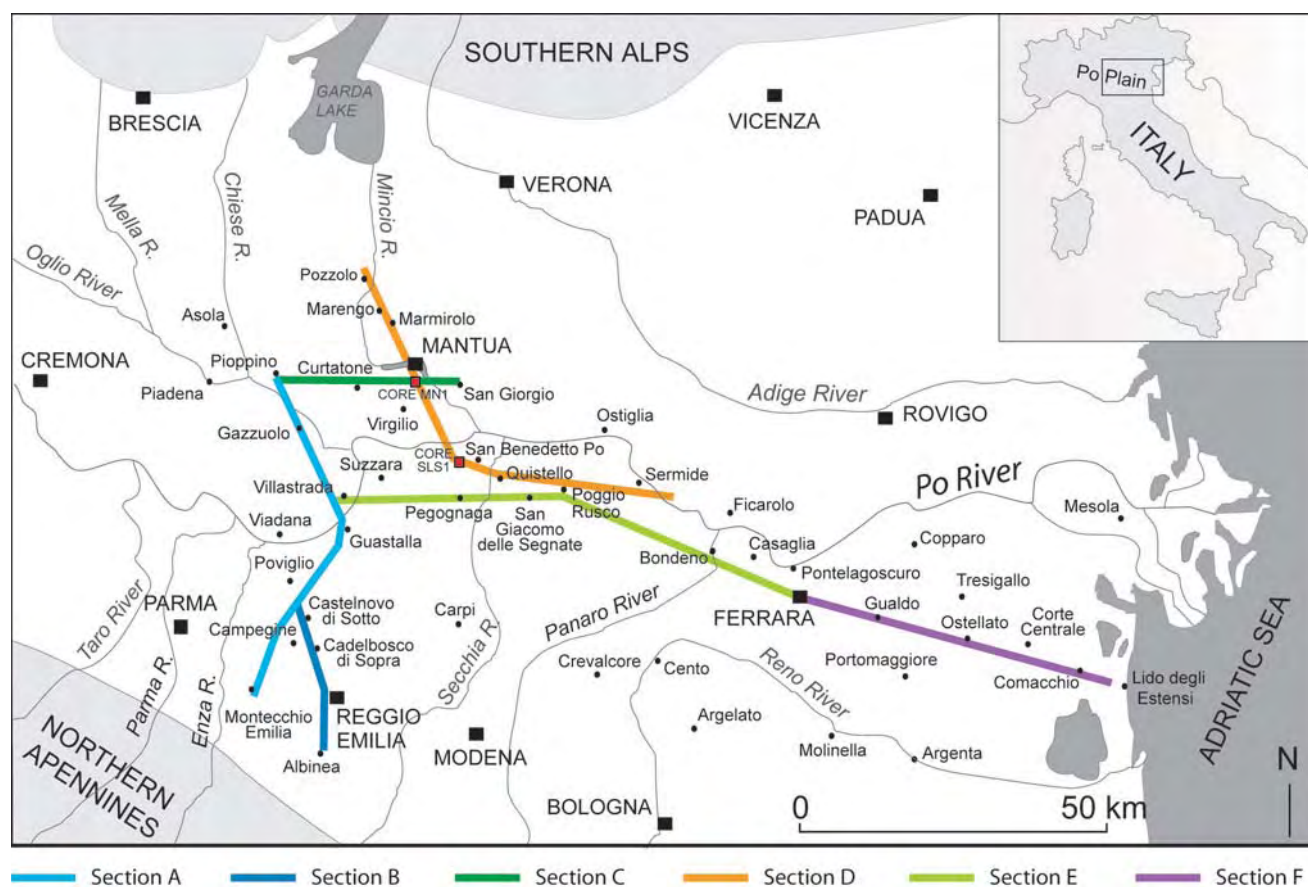


Fig. 1 - Study area, with indication of the section traces of figures 4-9.  
 - Area di studio con indicazione delle tracce di sezione relative alle figure 4-9.

mation, which has considerably improved previous knowledge on the Quaternary subsurface stratigraphy of the Po Basin. However, pragmatic use of the 1:50,000 geological maps beyond regional boundaries may be a difficult task, owing to i) mixed use of different types of stratigraphic units (depositional sequences, alloformations, unconformity-bounded stratigraphic units, hydrostratigraphic and lithostratigraphic units), ii) changes through time in age attribution of the bounding unconformities, and iii) use of locally inconsistent stratigraphic criteria across Po River (see below).

South of Po River, in Emilia-Romagna, the third-order depositional sequences (*sensu* MITCHUM *et alii*, 1977) recognized on a seismic basis have been mapped as unconformity-bounded stratigraphic units (UBSU) by REGIONE EMILIA-ROMAGNA & ENI-AGIP (1998) and by MOLINARI *et al.* (2007), but are labelled as alloformations (see “AES” or “AEI”) on the geological maps. The youngest USBU, which coincides in outcrop with the well-known Cycle Qc of RICCI LUCCHI *et alii* (1982), is termed the “Emilia-Romagna Supersynthem” (fig. 2). A stratigraphic unconformity of tec-

tonic origin allows subdivision of the Emilia-Romagna Supersynthem into two lower-rank units, namely “Lower Emilia-Romagna Synthem” and “Upper Emilia-Romagna Synthem”. This latter, in turn, is subdivided into a number of subsynthem (AES1 to AES8 in MOLINARI *et alii*, 2007 and in the Emilia-Romagna geological maps). From a hydrostratigraphic viewpoint, the Upper Emilia-Romagna Synthem coincides with Aquifer Group A, the Lower Emilia-Romagna Synthem with Aquifer Group B, while the underlying deposits, corresponding in outcrop to Cycle Qm of RICCI LUCCHI *et alii* (1982), to Aquifer Group C (fig. 2). Aquifer group A is subdivided into four aquifer systems (A1 to A4) according to REGIONE EMILIA-ROMAGNA & ENI-AGIP (1998), but five aquifer systems (A0 to A4) according to MOLINARI *et alii* (2007). Although event stratigraphy is advocated as the conceptual basis for all of these stratigraphic subdivisions, no one-to-one correlation is readily available between aquifer systems A0 to A4 and subsynthem AES1 to AES8 (fig. 2).

Unlike REGIONE EMILIA-ROMAGNA & ENI-AGIP (1998), REGIONE LOMBARDIA & ENI-DIVI-



Ricci Lucchi et al., 1982	Regione Emilia-Romagna & ENI-AGIP, 1998				Molinari et al., 2007			Regione Lombardia & ENI-Divisione AGIP, 2002		Amorosi et al., 2008 Amorosi & Colalongo, 2005		this paper		
STRATIGRAPHIC UNIT	STRATIGR. UNIT		AGE (Ma)	HYDROSTRATIGRAPHIC UNIT		AQUIFER SYSTEM	UBSU	AGE (Ma)	HYDRO-STRATIGRAPHIC UNIT (AGE Ma)	AGE (Ma) (Muttoni et al., 2003)	STRATIGRAPHIC UNIT (including transgressive - regressive -T/R- cycles)	OXYGEN ISOTOPE STAGE	AQUIFER SYSTEM	
CYCLE Qc	EMILIA-ROMAGNA SUPERSYNTHEM		~0.12	A	A1	A0	AES <sub>8</sub>	~0.12	A		PO SUPERSYNTHEM	T	OIS 1	
					A1	AES <sub>7</sub>	R						I	
					A2	AES <sub>3/6</sub>	T					OIS 5e		
					A3	AES <sub>2/5</sub>	R						II	
					A4	AES <sub>1/4</sub>	T					OIS 7		
	LOWER EMILIA-ROMAGNA SYNTHEM		~0.35-0.45	B	B1			~0.45	B	0.45		R		III
					B2							T	OIS 9	
					B3							R		IV
					B4							T	OIS 11	
CYCLE Qm			~0.65	C	C1			~0.80	C	0.65	0.87			
					C2									
					C3									
									D					

Fig. 2 - Generalized stratigraphic framework for the Quaternary deposits of the Po Basin.  
- *Quadro stratigrafico sintetico dei depositi quaternari del Bacino Padano.*

SIONE AGIP (2002) did not carry out a stratigraphic subdivision of the coeval deposits North of Po River into unconformity-bounded stratigraphic units, but just performed a hydrostratigraphic subdivision into aquifer groups (fig. 2). Although the aquifer groups identified in Lombardy are supposed to represent the lateral equivalents of those identified by Regione EMILIA-ROMAGNA & ENI-AGIP (1998), careful examination of the hydrostratigraphic sections South and North of Po River reveals obvious inconsistencies between these two studies. Specifically, while REGIONE EMILIA-ROMAGNA & ENI-AGIP (1998) used the tops of laterally extensive aquifers as bounding surfaces for their aquifer groups, REGIONE LOMBARDIA & ENI-DIVISIONE AGIP (2002) used their bases, thus making stratigraphic correlations across Po River very difficult (see figs. 2 and 3).

Age attributions also are ambiguous. Assignment of the uppermost two unconformities to 0.45 and 0.65 Ma, respectively (REGIONE EMILIA-ROMAGNA & ENI-AGIP, 1998; REGIONE LOMBARDIA & ENI-DIVISIONE AGIP, 2002 – see fig. 2), has been recently questioned by MUTTONI *et alii* (2003) who, on the basis of magnetostratigraphic data, documented that the latter (their “R-surface”) should be placed close to the Matuyama-Brunhes reversal, at 0.87 Ma. This latter interpretation is fully consistent with the age around 0.80 Ma estimated in outcrop by AMOROSI *et alii* (1998) for the Qm/Qc boundary (top of Imola Sands).

Recent identification, within the Upper Emilia-Romagna Synthem, of a depositional architecture controlled by a Milankovitch-scale (100 kyr) cyclicity (see pollen characterization in AMOROSI *et alii*,



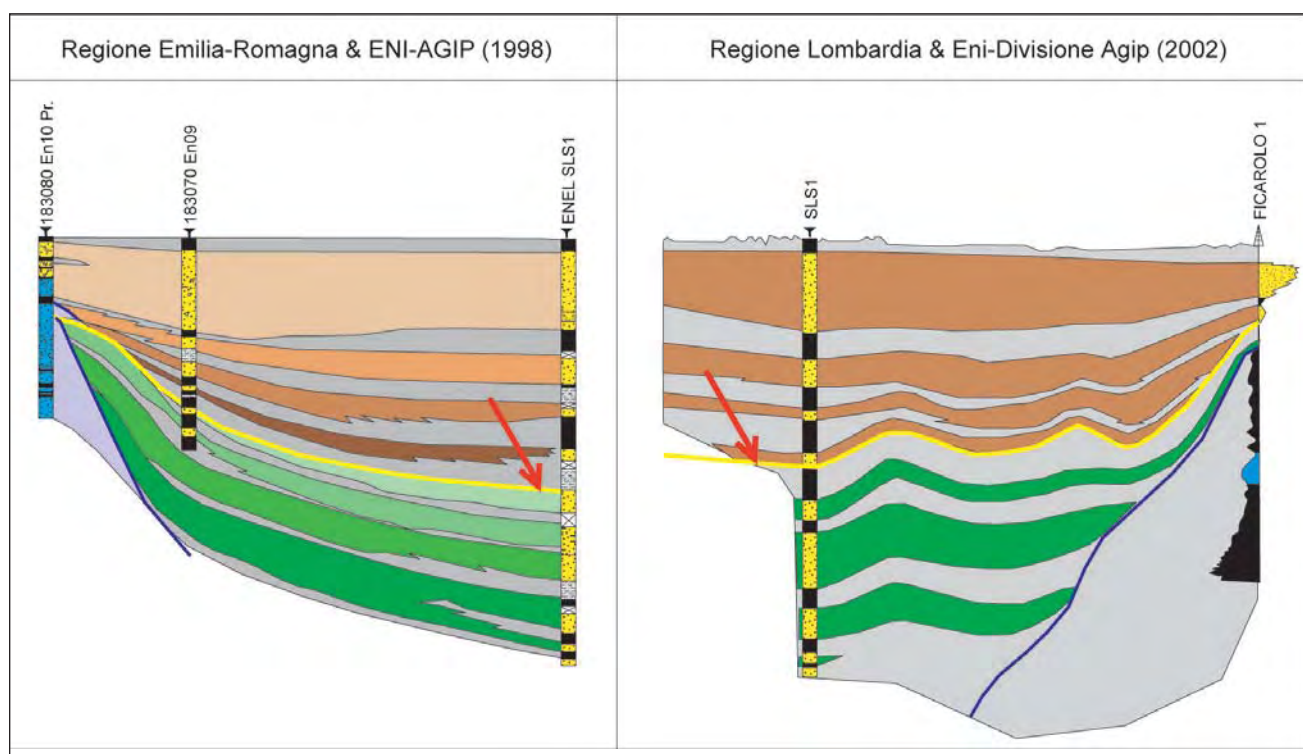


Fig. 3 - Inconsistent positioning, evidenced by arrow, of the lower boundary of Upper Po Synthem (yellow line) according to REGIONE EMILIA-ROMAGNA & ENI-AGIP (1998) and REGIONE LOMBARDIA & ENI-DIVISIONE AGIP (2002). Core SLS1 (see fig. 1), common to both sections, for reference.

- Posizionamento incoerente, evidenziato dalla freccia, del limite basale del Sintema Padano Superiore (linea gialla) da parte di REGIONE EMILIA-ROMAGNA & ENI-AGIP (1998) e REGIONE LOMBARDIA & ENI-DIVISIONE AGIP (2002). Il sondaggio SLS1 (v. fig. 1), comune ad entrambe le sezioni, funge da riferimento.

1999a, 2001, 2004, 2008) has allowed interpretation of the 4<sup>th</sup>-order depositional cycles (subsynthems) as transgressive-regressive (T-R) sequences, leading to the construction of a reliable chrono-stratigraphic framework. By placing age constraints on the key stratal surfaces, a linkage has been made between sedimentary cyclicity and climatic events, allowing correlation of the five basal transgressive surfaces (maximum regression surfaces of CATUNEANU *et alii*, 2009) on top of the aquifer systems with the onset of oxygen isotope stages 1, 5e, 7, 9 and 11 (AMOROSI & COLALONGO, 2005; AMOROSI, 2008) (fig. 2).

In order to avoid characterization of the Quaternary record of the Po Basin through stratigraphic units of local significance only, the “Emilia-Romagna Supersynthem” of REGIONE EMILIA-ROMAGNA & ENI-AGIP (1998) and Aquifer Groups A and B of REGIONE LOMBARDIA & ENI-DIVISIONE AGIP (2002) have been recently grouped into a new stratigraphic unit, provisionally referred to as “Po Supersynthem” (AMOROSI *et alii*, 2008; PAVESI, 2009), and subdivided into two lower-rank units (“Lower Po Synthem” and “Upper Po Synthem” - figure 2). This recent nomenclature is taken as a reference for this study.

### 3. – T-R SEQUENCES, AQUIFER SYSTEMS AND ALLUVIAL FACIES

As widely documented for selected portions of the Po Basin (AMOROSI & FARINA, 1995; REGIONE EMILIA-ROMAGNA & ENI-AGIP, 1998; REGIONE LOMBARDIA & ENI-DIVISIONE AGIP, 2002; AMOROSI & COLALONGO, 2005; AMOROSI *et alii*, 2008), stratigraphic architecture of the Upper Po Synthem reveals distinctive cyclic changes in lithofacies and channel stacking patterns of fluvial deposits, which allow their subdivision into five T-R sequences (fig. 2). Each sequence includes basal, silt-clay overbank deposits, with thin and lenticular fluvial-channel sands, showing upward transition to increasingly amalgamated and more laterally extensive fluvial-channel sand bodies. In hydrostratigraphic terms, the sheet-like fluvial bodies in the regressive portion of T-R sequences represent the major aquifer systems, termed here I to IV (fig. 2), while the overbank fines form the most important permeability barriers. The uppermost T-R sequence, of post-Last Glacial Maximum age (18 kyr-Present), is incomplete, and lacks almost entirely its upper, regressive portion. Despite this relatively simple picture of facies architecture, several heterogeneities are identified at both the lithofa-

cies and facies association scale (see WEBER, 1986; DREYER *et alii*, 1990) on the basis of core data (AMOROSI *et alii*, 2008). Sedimentological characteristics of the two major alluvial facies associations (*i.e.*, aquifer systems *versus* permeability barriers) are summarized below.

Fluvial-channel bodies represent complex systems of laterally migrating, braided- and low-sinuosity rivers, consisting of moderately well-sorted, medium to coarse sands. These are progressively replaced by gravels toward the basin margin (alluvial fan deposits). Individual fluvial-channel units, generally 3-20 m thick, are characterized by an erosional lower boundary and a fining-upward internal trend, and are commonly amalgamated into thicker (> 50 m) sedimentary bodies. Unidirectional, high-angle cross bedding and sub-horizontal bedding are commonly observed. Silt and clay intercalations are largely subordinate. Wood fragments represent common accessory material, while fossils are virtually absent. Organic-rich layers locally capping the FU successions are interpreted to have formed following channel abandonment.

The overbank facies association consists of a monotonous succession of massive, locally pedogenized, floodplain silts and clays, with subordinate sand intercalations and faint horizontal lamination.

Clays with fine disseminated plant debris, freshwater gastropods, and peat horizons are present at distinct stratigraphic levels, and interpreted to have formed in freshwater swamps. Sand-silt alternations, showing either sharp or gradational transitions, are inferred to represent natural levee deposits. Major sedimentary structures include horizontal lamination and subordinate, small-scale cross lamination. Sediment bodies with sharp lower boundary and internal fining-upward trends, but lesser thickness and grain size than their fluvial counterparts, are interpreted to represent crevasse-channel deposits, while coarsening-upward successions with transition to underlying mud are argued to represent crevasse splays. Laterally extensive organic-rich clays, interpreted as paludal deposits, are locally abundant.

#### 4. – AQUIFER STRATIGRAPHY OF THE UPPER PO SYNTHEM

The following section explores the stratigraphic zonation of the Upper Po Synthem based on mappable aquifer systems and clay-dominated permeability barriers, with the aid of six geological cross-sections (figs. 4 to 9). For each section, the

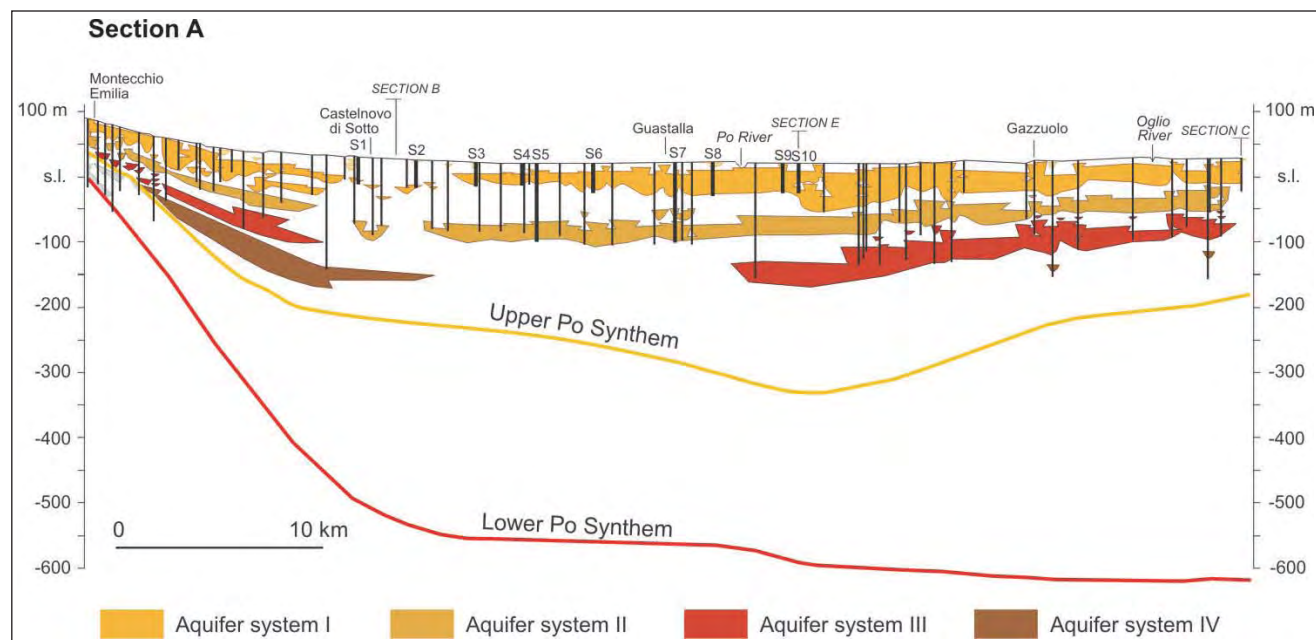


Fig. 4 - Stratigraphy of Po Supersystem, transversal to the Apenninic chain, across alluvial fan and alluvial plain deposits (see fig. 1, for location). Selected stratigraphic data only are shown. Fluvial-channel gravel and sand deposits (aquifer systems) are highlighted with colours. The grey color indicates indifferenciated coarse-grained bodies of the Lower Po Synthem. Small light yellow bodies below ground surface are Holocene coarse-grained deposits. The two major unconformities (red and yellow lines) are drawn based upon seismic and well-log data from REGIONE EMILIA-ROMAGNA & ENI-AGIP (1998) and REGIONE LOMBARDIA & ENI-DIVISIONE AGIP (2002).

- *Stratigrafia del Supersistema Padano attraverso depositi di conoide e pianura alluvionale (v. ubicazione in fig. 1). In sezione sono riportati i dati stratigrafici maggiormente attendibili. In colore sono indicati unicamente corpi sedimentari sabbioso-ghiaiosi (sistemi acquiferi). In grigio sono indicati corpi sedimentari grossolani indifferenziati appartenenti al Sintema Padano Inferiore. I corpi lenticolari di limitata estensione al di sotto del piano campagna corrispondono a corpi sedimentari grossolani di età olocenica. Le due superfici di discontinuità principali sono ricostruite sulla base della calibrazione con dati di sismica e di pozzo operata da REGIONE EMILIA-ROMAGNA & ENI-AGIP (1998) e da REGIONE LOMBARDIA & ENI-DIVISIONE AGIP (2002).*

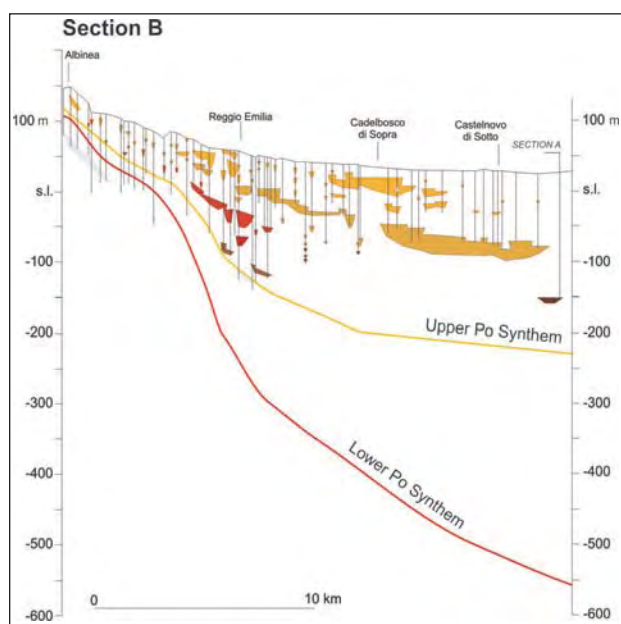


Fig. 5 - Stratigraphy of Po Supersynthem, transversal to the Apenninic chain, between alluvial fan depositional systems (see figure 1, for location).

- *Stratigrafia del Supersistema Padano in area di interconoide (v. ubicazione in figura 1).*

lower boundaries of Po Supersynthem (red line) and Upper Po Synthem (yellow line) were derived from REGIONE EMILIA-ROMAGNA & ENI-AGIP (1998) and REGIONE LOMBARDIA & ENI-DIVISIONE AGIP (2002). These two major unconformities represent important stratigraphic markers that help significantly in internal correlations, especially where data are scarce or insufficient.

Following the hydrostratigraphic sections by REGIONE EMILIA-ROMAGNA & ENI-AGIP (1998) and the conceptual model of AMOROSI & COLALONGO (2005) and AMOROSI *et alii* (2008), the surfaces chosen for stratigraphic subdivisions are placed at the generally abrupt facies shift from laterally extensive, amalgamated fluvial-channel bodies (aquifer systems I to IV) to overlying, organic-rich muddy units (figs. 4 to 9). This subdivision, which leads to identification of stratigraphic units with a lower, mudstone-dominated portion, and an upper interval characterized by increasing clustering of sand bodies, is here preferred from an operational point of view to depositional cycles bounded by channel-fill sand facies. Specifically, the tops of the aquifer systems can be physically traced throughout the basin and represent comparably smoother (and more easily mappable) surfaces than lower bounding surfaces. The latter show evidence of incision of up to several metres into the underlying substrate, and thus appear considerably more irregular.

Six sections (A to F in figs. 4 to 9) are shown. Sections A (58 km) and B (25 km), transversal to

the Apenninic chain, depict subsurface stratigraphy of the southern Po Plain, from proximal (alluvial fan) to distal (alluvial plain) depositional systems. Section C (28 km) shows stratigraphic architecture North of Po River. Section D (77 km) crosses the northern Po Plain, from the Alpine glacial deposits to the Po River, showing detailed stratigraphy of the Po channel belt. Section E (77 km) crosses the central Po Plain, parallel to Po River. Finally, Section F (56 km) represents the SE prolongation of Section E toward the Adriatic Sea.

Section A (fig. 4) crosses the Reggio Emilia and Mantua alluvial plain and is based upon 140 borehole data, including 10 continuously-cored boreholes performed by the Regione Emilia-Romagna Geological Survey. Between Montecchio Emilia and Guastalla, Section A has SW-NE direction, transversal to the Apenninic chain, while North of Po River it follows a SE-NW direction (fig. 1). The two major unconformities (yellow and red lines in fig. 4) diverge from the basin margin toward the depocentre. The lower boundary of Po Supersynthem (red line) displays a relatively flat geometry North of Castelnovo di Sotto, and is recorded around 500-600 m depth across 40 km. In contrast, the base of Upper Po Synthem (yellow line) has a concave-up geometry, with maximum depth of -330 m a.s.l. close to the intersection with Section E, and a depth of -180 m a.s.l. North of Po River, close to the intersection with Section C. Aquifer I and Aquifer II can be easily identified and tracked across most of the study area. Aquifer III and Aquifer IV can be identified uniquely at the section margins, while they are too deep in the depocentre to be reached by borehole data. In general, aquifers are very closely spaced in the Montecchio Emilia area (Enza alluvial fan) and beneath Oglio River, while they are separated by thicker muddy units in the depocentre (Po channel belt). In the Castelnovo di Sotto area, a 5 km wide succession of mud-prone alluvial plain deposits constitutes the physical separation between the Apenninic alluvial fan aquifers (to the South) and the Po channel belts (to the North).

Despite very close position to Section A (fig. 5), Section B shows striking differences in terms of lithology and facies architecture, being characterized by a remarkably low sand-to-mud ratio with a predominance of lens-shaped bodies. Scarcity of gravel and sand bodies along this section is due to the fact that Section B runs in an intermediate position between Enza and Secchia rivers (fig. 1). Coarse-grained bodies have poor lateral continuity, with a very low degree of inter-connectedness. The section is based upon 80 borehole data. Relatively continuous sand bodies,



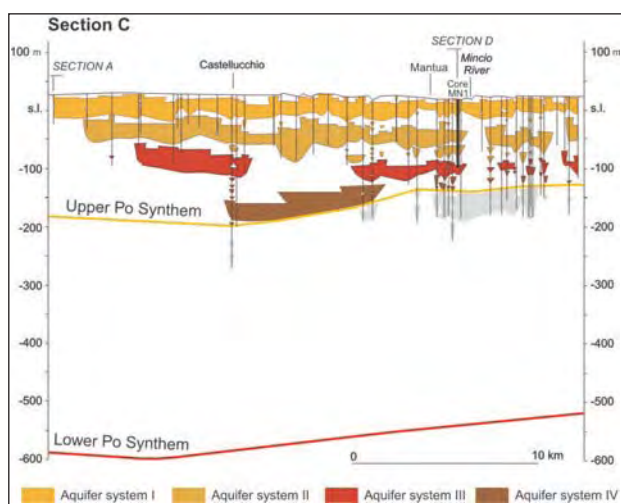


Fig. 6 - Stratigraphy of Po Supersynthem North of Po river (see figure 1, for location).

- *Stratigrafia del Supersintema Padano a Nord del Fiume Po (v. ubicazione in figura 1).*

corresponding to aquifer systems I and II, are identified in the Cadelbosco-Castelnovo area, close to the intersection with Section A. These aquifers are interpreted to represent the eastern termination of the Enza alluvial fan depositional system observed in Section A.

Section C (fig. 6) represents the prosecution of Section A in W-E direction (Mantua alluvial plain - fig. 1), and is based upon about 60 borehole data, including continuous core MN1. This core, 117 m long, has been recently characterized by a detailed, multi-proxy (sedimentological, gamma ray and pollen) investigation (AMOROSI *et alii*, 2008), and represents a fundamental tie point in the central Po Plain for the geometric characterization of aquifer systems I to III. Stratigraphic architecture is quite regular, as it can be observed by the geometry of the two major unconformities, which are gentle dipping to the West from -200 to -120 m a.s.l. (yellow line) and from -600 to -500 m a.s.l. (red line), respectively. Aquifer systems I and II display impressive lateral continuity and homogeneous thickness. The deepest stratigraphic data enable identification and correlation of the older aquifer systems (III and IV). Based upon seismic data interpretation (REGIONE LOMBARDIA & ENI DIVISIONE AGIP, 2002), Aquifer IV is interpreted to exhibit an onlapping contact onto the basal Upper Po Synthem unconformity (yellow line in fig. 6) and should not be in lateral continuity with coarse-grained bodies observed at the same depth, but is interpreted instead to represent the upper part of Lower Po Synthem. Tectonic deformation decreases from base to top, as documented by sub-horizontal geometry of Aquifers I to III.

Section D (fig. 7) was constructed on the basis

of 100 borehole data crossing the Mantua plain. Between Pozzolo and San Benedetto Po it has NW-SE direction, transversal to the Alpine chain, whereas East of S. Benedetto Po the section follows a WNW-ESE direction, roughly coincident with Po River. According to the overall basin geometry, which shows an increasing thickness of the Quaternary deposits from the basin margin to the central Po Plain (ORI, 1993), the two major unconformities (yellow and red lines) are progressively deeper moving from Garda Lake to the depocentre, and shallower when approaching the Ferrara folds, at the ESE termination of the section. It is remarkable that here the base of Po Supersynthem (red line) was identified at just -110 a.s.l., while the same surface is deeper than 500 m a.s.l. close to Mantua (fig. 7). With the exception of the Pozzolo-Marmirolo area, where only Aquifers I and II were identified, stratigraphic architecture along Po River, East of San Benedetto Po, is similar to that depicted by Section C, with a striking lateral continuity and sub-horizontal geometry of Aquifers I to III. The local presence of a fifth sedimentary bodies, of uncertain age attribution and provisionally attributed to Aquifer system IV, is suggested in the depocentre by correlation of two deep boreholes, among which ENEL Core SLS1.

Section E (fig. 8), based upon 75 borehole data, cuts the Mantua alluvial plain roughly parallel to Po River, following a W-E direction and providing a physical link between Section A (Core S10 at Villastrada - see fig. 1) and Section D (almost intersected in Poggio Rusco). East of Poggio Rusco, this section moves toward Ferrara, with NW-SE direction. Data density is relatively low, although several high-quality data are available for the uppermost 40 m. For the construction of this section, additional data derive from unpublished passive seismic interpretation (PIERI, 2008; PAVESI, 2009). Similarly to what observed in sections C and D, aquifer systems I, II and III display an impressive lateral continuity West of Poggio Rusco. Tectonic deformation, however, affects significantly aquifer architecture at the SE termination of the section, due to the presence of the Ferrara folds (fig. 8). Specifically, close to Casaglia, *i.e.* in coincidence of the Ferrara structural high, the lower boundary of Upper Po Synthem climbs up from -320 m to -50 m a.s.l. A very similar geometry is shown by the base of Po Supersynthem, which moves from -580 m a.s.l. to -170 m in the Ferrara area. Similarly to what observed in previous sections, aquifer systems II, III and IV display a likely onlapping geometry onto the lower bounding unconformity.



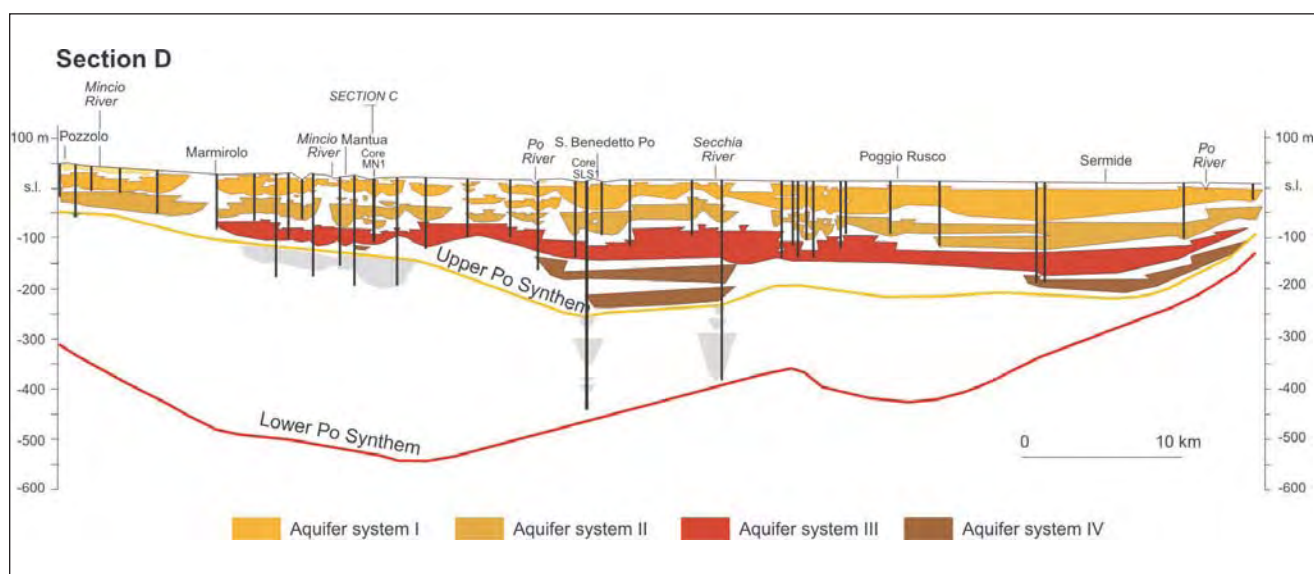


Fig. 7 - Stratigraphy of Po Supersynthem transversal from the Alpine glacial deposits to Po River (see figure 1, for location).  
- *Stratigrafia del Supersintema Padano dalla cerchia morenica alpina al Fiume Po (v. ubicazione in figura 1).*

Section F (fig. 9), representing the prolongation of Section E across the Ferrara coastal plain toward the Adriatic Sea, documents the stratigraphic relationships between the Quaternary fluvial deposits of the Po Basin and their distal (nearshore) counterparts. The subsurface of the Ferrara coastal plain has been depicted in detail by MOLINARI *et alii* (2007) through a number of geological cross sections, and for this reason will not be described here. The reader is referred to that paper for accurate reconstruction of stratigraphic architecture. Selected core data from MOLINARI *et alii* (2007), however, were incorporated in this section in order to enable correlation with their work. Subsurface strati-

graphy beyond the Ferrara folds mirrors the one depicted by Section E, with the lower boundary of Upper Po Synthem dipping toward SE, from -50 m to -350 m a.s.l. Alluvial sedimentation, however, displays remarkably different characteristics. In particular, the thick aquifer systems observed in Section E are replaced between Ferrara and Comacchio by a succession of distinct, relatively thinner and finer-grained sand bodies separated by thicker mud-dominated units. According to the sequence-stratigraphic model proposed by AMOROSI (2008) for the Po Basin, these sedimentary bodies are interpreted to represent two different facies associations (fig. 9): i) thinner and less extensive flu-

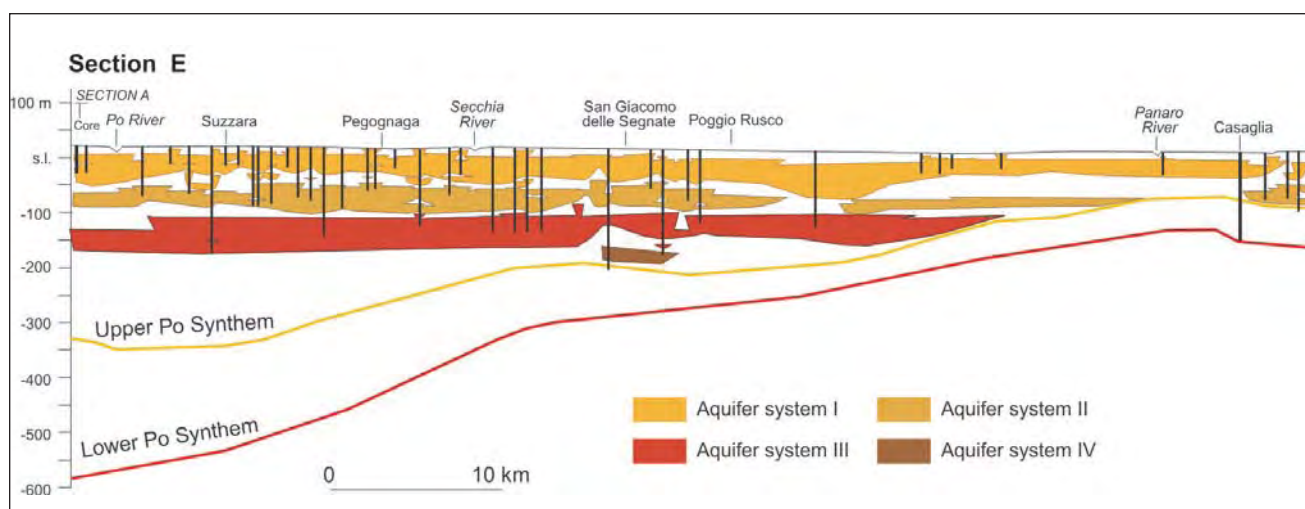


Fig. 8 - Stratigraphy of Po Supersynthem across the central Po Plain (see figure 1, for location).  
- *Stratigrafia del Supersintema Padano nella Pianura Padana centrale (v. ubicazione in figura 1).*

vial units than the aquifers of the Po channel belt, ii) prograding deltaic and coastal sand bodies, formed during phases of sea-level highstand. The characteristic wedge-shaped sand bodies identified from core correlations beneath the coastal plain (AMOROSI *et alii*, 1999b; 2004) are not apparent here, due to the fact that the transgressive shoreface sands are too thin and fine-grained to be detected by poor-quality borehole data.

## 5. – CONTROL OF CYCLIC FLUVIAL ARCHITECTURE

The cross sections of figures 4 to 9 allow to summarize the general features of Quaternary alluvial architecture across a significant portion of the Po Basin. The Po Supersynthem displays a maximum thickness of about 650 m in the depocentre, and typically wedges out either toward the basin margins, *i.e.* the Apenninic and Alpine foothills, or in coincidence of structural highs (e.g., Ferrara folds). The post-450 kyr unit (Upper Po Synthem) exhibits a maximum thickness of about 400 m (Sections E and F), although over wide areas (Sections C and D) is less than 250 m thick. Four major aquifer systems (I to IV), corresponding to units A1-A4 of REGIONE EMILIA-ROMAGNA & ENI-AGIP (1998), can be recognized and tracked in the Upper Po Synthem across the entire study area. In the central Po Plain, beneath the present Po River course, these comprise laterally extensive, high net-to-gross stacked channel belts, with excellent continuity, separated by laterally continuous mud-dominated permeability barriers. In contrast,

the aquifer systems tend to be amalgamated close to the basin margins, where fluvial sands are replaced by gravels formed in proximal alluvial-fan systems. Despite correlation and delineation of zones of generally high permeability may be relatively simple within the aquifer systems, internal correlation is difficult due to the lenticular shape of individual channel bodies, and sediment bodies are very likely to display a typical “jigsaw puzzle” pattern (WEBER & VAN GEUNS, 1990; GALLOWAY & SHARP, 1998).

The striking regularity shown by the middle-late Pleistocene record across a significant portion of the Po Plain indicates an allocyclic control as the driving mechanism for the observed cyclic facies architecture. Syn-depositional tectonics exerted a marked influence on facies and aquifer distribution over the last million years, through the continuous creation of accommodation, tectonic uplift, changes in sediment transport pathways, localisation of depocentres, and restriction of older aquifer systems to the resulting topographic lows.

Pronounced climatic fluctuations and, to a certain extent, sea-level oscillations, however, played a fundamental role in shaping stratigraphic architecture, leading to remarkable changes in sediment supply and in the type of sediment delivered to the basin. Although the influence of climate on fluvial succession is a still largely neglected issue, previous work on long-cored pollen successions of the Po Basin has shown that the distinctive cyclic facies architecture documented in this paper was paralleled by cyclic changes in vegetation patterns during the last hundred thousands of years (AMOROSI

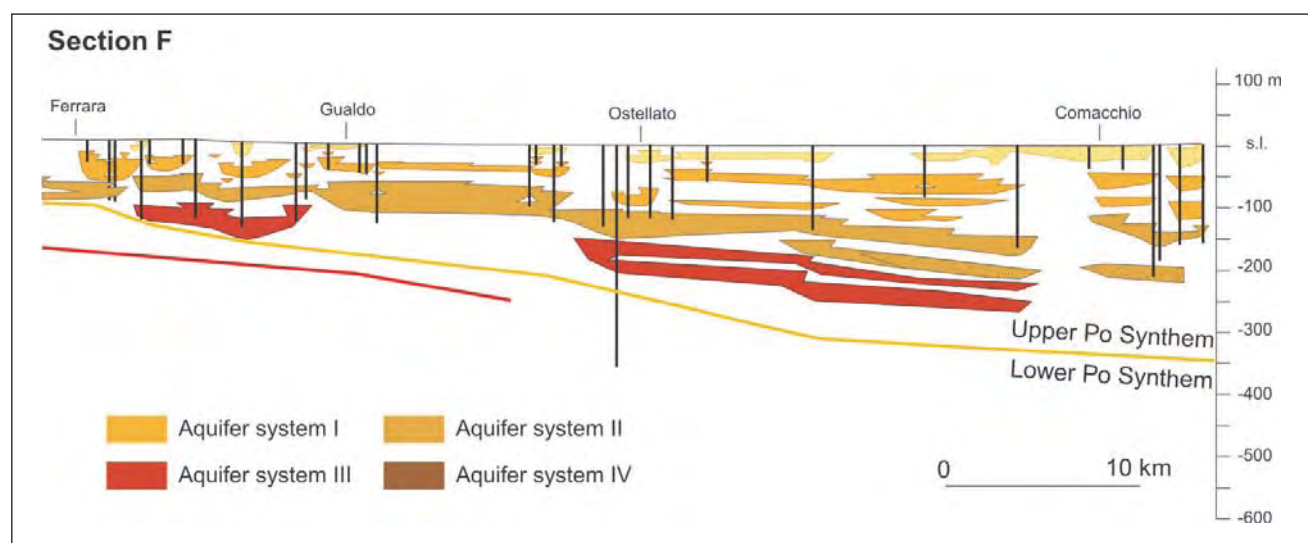


Fig. 8 - Stratigraphy of Po Supersynthem across the central Po Plain (see figure 1, for location).  
- *Stratigrafia del Supersintema Padano nella Pianura Padana centrale (v. ubicazione in figura 1).*

*et alii*, 2001, 2008). In particular, the laterally continuous muddy units that overlie the aquifer systems appear to be invariably associated with forest expansions. This indicates that major phases of channel abandonment, with generalized development of paludal areas and widespread floodplain aggradation, took place at the onset of warm-temperate (interglacial) climatic conditions, during phases of rapid sea-level rise.

Increased accommodation due to the combined effect of subsidence and sea-level rise allowed accumulation of conspicuous amount of fine-grained material, with preservation of small lenticular, poorly interconnected fluvial bodies on top of the aquifer systems. In terms of sequence stratigraphy, the laterally continuous permeability barriers can be interpreted as the transgressive systems tracts (TST) of 4<sup>th</sup>-order T-R sequences. The progressive decrease up-section in the relative proportion of overbank fines, which is accompanied by an increase in the thickness of fluvial-channel units, suggests decreasing accommodation during highstand conditions (HST). During very low-accommodation conditions, such as those related to forced regression (FST) and lowstand deposition (LST), overbank muds would rarely have survived fluvial erosion, favouring preservation of amalgamated sand sheets (SHANLEY & McCABE, 1993; OLSEN *et alii*, 1995; PLINT *et alii*, 2001). The channel belts (e.g., aquifer systems) are likely to have formed as incised-valley fills, following phases of channel incision and subsequent valley widening during prolonged lowstand phases (STRONG & PAOLA, 2006). It is still a debated problem whether fluvial sedimentation took place during lowstand phases, early transgressive conditions, or both.

## 6. – CONCLUSIONS

Detailed stratigraphic correlations based upon a large borehole dataset enable an improved understanding of stratigraphic architecture and aquifer distribution of the middle-late Pleistocene record of the Po Basin. Five vertically stacked, 4<sup>th</sup>-order, transgressive-regressive (T-R) sequences can be identified within the uppermost (post-450 kyr BP) 3<sup>rd</sup>-order depositional sequence, here referred to as Upper Po Synthem. The T-R sequences, recognized across alluvial fan, alluvial plain and coastal plain successions, define four geologically distinct aquifer systems (I to IV), few tens of metres thick, separated by laterally extensive permeability barriers. Aquifer systems consist of thick, amalgamated alluvial-fan gravel bodies close to the basin mar-

gins. In the depocentres, aquifer systems are re-presented by sandy channel belts, showing considerably high continuity and overall sheet-like geometry. Channel belts are separated by laterally continuous overbank deposits, acting as permeability barriers for each aquifer group. Despite this relatively simple picture of facies architecture, several heterogeneities are identified at both the lithofacies and facies association scale, with crevasse channels and splays, unconfined and non-channelized sandy units, and laterally continuous organic-rich horizons that may locally complicate the picture.

The vertically amalgamated multi-storey bodies that form the aquifer systems of the Po Basin have highly diachronous base. In contrast, the abrupt facies shifts from these laterally extensive sedimentary bodies to the overlying, organic-rich muds represent almost isochronous, easily mappable surfaces, and for this reason are taken as major bounding surfaces in building the hydrostratigraphic model. A multi-proxy data set enables recognition of a striking cyclicity with 100 kyr recurrence time within the middle-late Quaternary succession. Permeability barriers correlate with warm episodes and mark the onset of transgressive phases. On the other hand, the four major aquifer systems appear to have formed during phases of relatively low accommodation (lowstand periods and possibly early phases of transgression).

In summary, this study shows that accurate reconstruction of stratigraphic architecture and channel/overbank proportion in the Po Basin can help significantly in developing conceptual models that can be used to delineate aquifer connectivity and predict seal lithofacies distribution. In addition, availability of a common hierarchy of architectural units based on the physical characteristics of the depositional elements and their stratal bounding surfaces (MIALL, 1991) may facilitate correlation of events on a regional scale. Examining stratigraphic architecture of fluvial deposits through a sound sedimentological model and the use of sequence-stratigraphic concepts provide a very good basis for aquifer prediction and can be of interest for water-use planners.

## Acknowledgements

*This study is part of a PhD program (Marta Pavesi) carried out in conjunction with the Geological Survey of Emilia-Romagna and Lombardy. The authors are greatly indebted to Paolo Severi (Regione Emilia-Romagna) and Andrea Piccin (Regione Lombardia) for the access to their stratigraphic data base. The authors are indebted to B. Vigna and an anonymous reviewer for their comments and remarks.*



## REFERENCES

- AMOROSI A. (2008) – *Delineating aquifer geometry within a sequence stratigraphic framework: Evidence from the Quaternary of the Po River Basin, Northern Italy*. In: A. AMOROSI, B.U. HAQ & L. SABATO (Eds.), *Advances in Application of Sequence Stratigraphy in Italy*. GeoActa Spec. Publ. n. 1: 1-14.
- AMOROSI A., CAPORALE L., CIBIN U., COLALONGO M.L., PASINI G., RICCI LUCCHI F., SEVERI P. & VAIANI S.C. (1998) – *The Pleistocene littoral deposits (Imola Sands) of the northern Apennines foothills*. Giorn. Geol., **60**: 83-118.
- AMOROSI A. & COLALONGO M.L. (2005) – *The linkage between alluvial and coeval nearshore marine successions: evidence from the Late Quaternary record of the Po River Plain, Italy*. In: M.D. BLUM, S.B. MARRIOTT & S.F. LECLAIR (Eds.), *Fluvial Sedimentology VII*. Int. Assoc. Sedimentol. Spec. Publ. n. **35**: 257-275.
- AMOROSI A., COLALONGO M.L., DINELLI E., LUCCHINI F. & VAIANI S.C. (2007) – *Cyclic variations in sediment provenance from late Pleistocene deposits of the eastern Po Plain, Italy*. In: J. ARRIBAS, S. CRITELLI & M.J. JOHNSON (Eds.), *Sedimentary Provenance and Petrogenesis: Perspectives from Petrography and Geochemistry*. Geol. Soc. Am. Special Paper n. **420**: 13-24.
- AMOROSI A., COLALONGO M.L., FIORINI F., FUSCO F., PASINI G., VAIANI S.C. & SARTI G. (2004) – *Palaeogeographic and palaeoclimatic evolution of the Po Plain from 150-ky core records*. Global and Planetary Change, **40**: 55-78.
- AMOROSI A., COLALONGO M.L., FUSCO F., PASINI G. & FIORINI F. (1999a) – *Glacio-eustatic control of continental-shallow marine cyclicity from Late Quaternary deposits of the south-eastern Po Plain (Northern Italy)*. Q. Res., **52**: 1-13.
- AMOROSI A., COLALONGO M.L., PASINI G. & PRETI D. (1999b) – *Sedimentary response to Late Quaternary sea-level changes in the Romagna coastal plain (northern Italy)*. Sedimentology, **46**: 99-121.
- AMOROSI A. & FARINA M. (1995) – *Large-scale architecture of a thrust-related alluvial complex from subsurface data: the Quaternary alluvial succession of the Po Basin in the Bologna area (northern Italy)*. Giorn. Geol., **57**: 3-16.
- AMOROSI A., FORLANI L., FUSCO F. & SEVERI P. (2001) – *Cyclic patterns of facies and pollen associations from Late Quaternary deposits in the subsurface of Bologna*. GeoActa, **1**: 83-94.
- AMOROSI A., PAVESI M., RICCI LUCCHI M., SARTI G. & PICCIN A. (2008) – *Climatic signature of cyclic fluvial architecture from the Quaternary of the central Po plain, Italy*. Sediment. Geol., **209**: 58-68.
- BERSEZIO R., PAVIA F., BAIO M., BINI A., FELLETTI F. & RODONDI C. (2004) – *Aquifer architecture of the Quaternary alluvial succession of the southern Lambro basin (Lombardy-Italy)*. Il Quaternario, **17**: 361-378.
- CATUNEANU O., ABREU V., BHATTACHARYA J.P., BLUM M.D., DALRYMPLE R.W., ERIKSSON P.G., FIELDING C.R., FISHER W.L., GALLOWAY W.E., GIBLING M.R., GILES K.A., HOLBROOK J.M., JORDAN R., KENDALL C.G.St.C., MACURDA B., MARTINSEN O.J., MIAL A.D., NEAL J.E., NUMMEDAL D., POMAR L., POSAMENTIER H.W., PRATT B.R., SARG J.F., SHANLEY K.W., STEEL R.J., STRASSER A., TUCKER M.E. & WINKER C. (2009) – *Towards the standardization of sequence stratigraphy*. Earth-Sci Rev., **92**: 1-33.
- DALLA S., ROSSI M., ORLANDO M., VISENTIN C., GELATI R., GNACCOLINI M., PAPANI G., BELLI A., BIFFI U. & CITRULLO D. (1992) – *Late Eocene-Tortonian tectono-sedimentary evolution in the western part of the Padan basin (northern Italy)*. Paleontol. y Evol., **24-25**: 341-362.
- DONDI L. & D'ANDREA M.G. (1986) – *La Pianura Padana e Veneta dall'Oligocene superiore al Pleistocene*. Giorn. Geol., **48**: 197-225.
- DREYER T., SCHEIE A. & WALDERHAUG O. (1990) – *Minipermeability-based study of permeability trends in channel sand bodies*. Am. Ass. Petrol. Geol. Bulletin, **74**: 359-374.
- GALLOWAY W.E. & SHARP JR. J.M. (1998) – *Characterizing aquifer heterogeneity within terrigenous clastic depositional systems*. In: G.S. FRASER & J.M. DAVIS (Eds.), *Hydrogeologic Models of Sedimentary Aquifers*. Soc. of Econ. Pal. and Min. Concepts in Hydrogeology and Environmental Geology n. 1: 85-90.
- MIAL A.D. (1991) – *Hierarchies of architectural units in terrigenous clastic rocks, and their relationship to sedimentation rate*. In: A.D. MYALL & N. TYLER (Eds.), *The Three-Dimensional Facies Architecture of Terrigenous Clastic Sediments and Its Implications for Hydrocarbon Discovery and Recovery*. Soc. of Econ. Pal. and Min. Concepts in Sedimentology and Paleontology n. **3**: 6-12.
- MITCHUM JR. R.M., VAIL P.R. & THOMPSON III S. (1977) – *The depositional sequence as a basic unit for stratigraphic analysis*. In: C.E. PAYTON (Ed.), *Seismic Stratigraphy - Application to Hydrocarbon Exploration*, Am. Assoc. Petrol. Geol. Mem. n. **26**: 53-62.
- MOLINARI F.C., BOLDRINI G., SEVERI P., DUGONI G., RAPTI CAPUTO D. & MARTINELLI G. (2007) – *Risorse idriche sotterranee della Provincia di Ferrara*. In: G. DUGONI & R. PIGNONE (Eds.), *Risorse idriche sotterranee della Provincia di Ferrara*: 7-61.
- MUTTONI G., CARCANO C., GARZANTI E., GHIELMI M., PICCIN A., PINI R., ROGLEDI S. & SCIUNNACH D. (2003) – *Onset of major Pleistocene glaciations in the Alps*. Geology, **31**: 989-992.
- OLSEN T., STEEL R., HOGSETH K., SKAR T. & ROE S.L. (1995) – *Sequential architecture in a fluvial succession: sequence stratigraphy in the Upper Cretaceous Mesaverde Group, Price Canyon, Utah*. J. Sediment. Res., **B65**: 265-280.
- ORI G.G. (1993) – *Continental depositional systems of the Quaternary of the Po plain (northern Italy)*. Sediment. Geol., **83**: 1-14.
- PAVESI M. (2009) – *Architettura stratigrafica dei depositi medio e tardoquaternari del bacino padano, finalizzata alla caratterizzazione geometrica degli acquiferi*. PhD Thesis, Dipartimento di Scienze della Terra e Geologico Ambientali, University of Bologna, pp. 210.
- PIERI E. (2008) – *Stratigrafia con sismica passiva*. Thesis, Dipartimento di Scienze della Terra e Geologico Ambientali, University of Bologna, pp. 116.
- PIERI M. (1983) – *Three seismic profiles through the Po Plain*. Seismic Expression of Structural Styles. A Picture and Work Atlas. In: A.W. BALLY (Ed.), Am. Ass. Petr. Geol. Stud. Geol., **15**: 3.4.1/8-3.4.1/26.
- PIERI M. & GROPPI G. (1981) – *Subsurface geological structure of the Po Plain, Italy*. Publ. 414 P.F. Geodinamica, C.N.R., pp. 23.
- PLINT A.G., MCCARTHY P.J. & FACCINI U.F. (2001) – *Nonmarine sequence stratigraphy: Updip expression of sequence boundaries and systems tracts in a high-resolution framework, Cenomanian Dunvegan Formation, Alberta foreland basin, Canada*. Am. Assoc. Petrol. Geol. Bull., **85**: 1967-2001.
- REGIONE EMILIA-ROMAGNA & ENI-AGIP (1998) – *Riserve idriche sotterranee della Regione Emilia-Romagna*. A cura di G. DI DIO. S.E.L.C.A., Firenze, pp. 120.
- REGIONE LOMBARDIA & ENI DIVISIONE AGIP (2002) – *Geologia degli acquiferi Padani della Regione Lombardia*. A cura di C. CARCANO & A. PICCIN. S.E.L.C.A., Firenze, pp. 130.
- RICCI LUCCHI F., COLALONGO M.L., CREMONINI G., GASPERI G., IACCARINO S., PAPANI G., RAFFI I. & RIO D. (1982) – *Evoluzione sedimentaria e paleogeografica del margine appenninico*. In: G. CREMONINI & F. RICCI LUCCHI (Eds.), *Guida alla*



- geologia del margine appenninico-padano*. Guide Geologiche Regionali Soc. Geol. Ital., 17-46.
- SCARDIA G., MUTTONI G. & SCIUNNACH D. (2006) - *Subsurface magnetostratigraphy of Pleistocene sediments from the Po Plain (Italy): Constraints on rates of sedimentation and rock uplift*. Geol. Soc. Am. Bull., **118**: 1299-1312.
- SHANLEY K.W. & MC CABE P.J. (1993) - *Alluvial architecture in a sequence stratigraphic framework: a case study from the Upper Cretaceous of southern Utah, USA*. In: S.S. FLINT & I.D. BRYANT (Eds.), *The Geological Modelling of Hydrocarbon Reservoirs and Outcrop Analogues*. Int. Assoc. Sedimentol. Spec. Publ., **15**: 21-56.
- STRONG N. & PAOLA C. (2006) - *Fluvial landscapes and stratigraphy in a flume*. The Sedimentary Record, **4**: 4-8.
- WEBER K.J. (1986) - *How heterogeneity affects oil recovery*. In: L.W. LAKE & H.B. CARROLL (Eds.), *Reservoir characterization*. Academic Press, 487-544, New York.
- WEBER K.J. & VAN GEUNS L.C. (1990) - *Framework for constructing clastic reservoir simulation models*. Journal of Petroleum Technology, **42**: 1248-1253.

## Aquifer building and Apennine tectonics in a Quaternary foreland: the southernmost Lodi plain of Lombardy

*Origine degli acquiferi e tettonica appenninica in un avampaese quaternario: la pianura lodigiana meridionale in Lombardia*

BERSEZIO R. (\*)(\*\*), CAVALLI E. (\*), CANTONE M. (\*)

**ABSTRACT** - Syndepositional tectonics competes with climate and eustasy in shaping hydrostratigraphy of foreland basins. In the Po plain basin, Quaternary thrust-folding of the outer Apennine arcs contributed to alluvial evolution, both on the Apennine and the Alpine side. A N-S geological transect in Lombardy, from the former sites of the glacial mouths (North) to the present-day Po river (South), shows the competition of subsidence, glacial evolution and base-level dynamics in delineating aquifer building processes during the Quaternary. Surface geology and geomorphology, subsurface stratigraphy, age constraints from radiocarbon data and palynology, permitted to sketch the architecture and evolution of hydrostratigraphy, above the Lower Pleistocene marine shales that form the regional aquiclude in the Lodi area. Sub-surface mapping of the top boundary of the aquiclude shows that this erosion surface is gently folded and progressively lowered from SW to NE, in a sequence of *en-echelon* thrust-related folds. Transitional to alluvial sands and shales (Early to Middle Pleistocene in age) filled local depocentres in the intervening gentle hangingwall synclines, during the decline of folding and uplift rates. Growth of the northernmost and youngest WNW-ESE striking Apennine folds was accompanied by erosion at their flanks and hinges and regressive deposition in coastal to alluvial plain environments. The resulting aquifer bodies are wedges that pinch-out towards the uplifted marine aquicludes and fill incised valleys in their depocentres. The Middle Pleistocene alluvial succession was uplifted by the northernmost Apennine thrusts and locally crops out (San Colombano al Lambro, Zorlesco, Casalpusterlengo). It was eroded during the syn-glacial entrenchment of the river network. Fluvial sands, gravels and intervening mud, filled the local depocentres during three pulses of the Late Pleistocene glaciations. Summing up, the Early-Middle

Pleistocene Apennine tectonics acted to: 1) confine the aquifer systems into different depocentres, 2) raise buried hydrogeological divides, 3) force the erosion of hydrogeologic windows, shaping the lateral contacts between pervious alluvial bodies of different ages and 4) constrain aquitard/aquiclude building during the recovery stages of the river network.

**KEY WORDS:** aquifers, hydrostratigraphy, Lombardy Italy, Northern Apennines, Quaternary, sedimentation and tectonics.

**RIASSUNTO** - La tettonica sinsedimentaria contribuisce con l'evoluzione climatica ed eustatica a determinare l'architettura idrostratigrafica dei bacini di avampaese. Nel bacino del Po la progradazione verso Nord dei sovrascorimenti appenninici ha controllato la dinamica alluvionale su entrambi i margini strutturali del bacino. In Lombardia, un transetto N-S dagli anfitrioni glaciali settentrionali all'attuale posizione del Po, illustra la competizione tra subsidenza, dinamica dei livelli di base ed evoluzione glaciale nel delineare i processi genetici dell'idrostratigrafia durante il Quaternario. Geomorfologia, geologia di superficie e di sottosuolo, vincoli cronostratigrafici (date radiocarbonio) e analisi palinologiche consentono di descrivere l'architettura e l'evoluzione idrostratigrafica di un segmento di questo transetto nella pianura Lodigiana meridionale. I sedimenti fini del Pleistocene inferiore marino, costituiscono l'acquicludo basale della successione considerata. La ricostruzione nel sottosuolo del tetto dell'acquicludo mostra il blando piegamento di questa unità, che risulta erosa e progressivamente ribassata da Sud-Ovest a Nord-Est, in una sequenza di pieghe e sovrascorimenti disposti *en-echelon*. Sedimenti fini e sabbie da litorali ad alluvio-

(\*) Dipartimento Scienze della Terra – Università di Milano, via Mangiagalli 34, 20133 I-Milano  
(\*\*) CNR – IDPA Milano – Via Mangiagalli 34, 20133 I-Milano

nali (Pleistocene inferiore – medio), costituiscono il riempimento dei depocentri associati alle sinclinali di *hangingwall*, depositato durante le fasi di declino dei tassi di piegamento e sollevamento. La crescita delle pieghe appenniniche più settentrionali e recenti (Pleistocene medio) fu accompagnata da erosione dei fianchi e delle creste delle strutture, associata a regressione costiera e continentalizzazione. I corpi acquiferi che ne derivano sono cunei che terminano contro l'acquicludo basale piegato e sollevato e raggiungono i massimi spessori ove riempiono le valli incise ed i depocentri sinformi. La successione del Pleistocene medio fu sollevata dai sovrascorrimenti appenninici settentrionali ed affiora localmente (San Colombano, Zorlesco, Casalpusterlengo). Il susseguente approfondimento erosivo sin-glaciale del reticolo idrografico (Pleistocene superiore) determinò l'incisione di paleovalli, che furono colmate da sedimenti fluviali ghiaioso-sabbiosi durante diverse pulsazioni glaciali discrete, di cui tre almeno sono documentabili stratigraficamente. In sintesi, la tettonica appenninica del Pleistocene inferiore - medio contribuì a: 1) confinare i sistemi acquiferi in depocentri differenti, 2) sollevare spartiacque idrogeologici, deformando l'acquicludo basale, 3) forzare l'erosione di finestre idrogeologiche, originando contatti tra sistemi acquiferi di età differenti e 4) delimitare l'origine degli acquitardi/acquicludi alle sole fasi di recupero fluviale del reticolato idrografico.

**PAROLE CHIAVE:** acquiferi, Appennino settentrionale, idrostratigrafia, Lombardia, Quaternario, sedimentazione e tettonica.

## 1. - INTRODUCTION

In Quaternary foreland basins, building of alluvial aquifers is controlled by competing syn-depositional tectonics, glacial cycles and the dynamics of regional vs. local base-levels. The Po plain hydrostratigraphic basin is an important European example of this complex interplay. Since the Miocene, the basin represented the foredeep of the northward advancing Apennine thrusts, that loaded and down-flexured the former Southalpine foreland and thrust belt (PIERI & GROPPi, 1981) (fig. 1).

The influence of Plio-Quaternary Apennine tectonics on aquifer development has been recently illustrated by the regional reconstruction of hydrostratigraphy proposed by ENI-REGIONE EMILIA ROMAGNA (1998) and ENI-REGIONE LOMBARDIA (2002) in the central-eastern Po basin. In Lombardy, a N-S transect from Alps to Apennines clearly shows the interplay among Apennine syn-depositional thrusting, the inherited and active Alpine structures, glacial and base-levels dynamics (glacial pulses on the alpine side, isostatic response to glacial cycles, regression of the Adriatic coastline) (ARCA & BERETTA, 1985; BINI, 1997; CARMINATI *et alii*, 2003; MUTTONI *et alii*, 2003; BARLETTA *et alii*, 2006; SCARDIA *et alii*, 2006), sedimentation rates and sources.

The Quaternary hydrostratigraphic systems of Lombardy formed above the Southalpine thrusts and the interference zone between them and the northernmost Apennine fronts; only the southern-

most plain sits on the buried Apennine structures (fig.1). Sediment supply is mostly from the Alpine side and from the axial Po drainage system, the Apennine Quaternary sediments forming a narrow apron to this southern mountain belt (ORI, 1993).

Aiming to investigate the role of the different controls on aquifer building, we are studying a N-S transect from Lake Lario to Po river, encompassing the southern Adda valley and the Adda – Lambro interfluvium (PRIN 2007 Project: *Integrated geophysical, geological, petrographical and modelling study of alluvial aquifer complexes characteristic of the Po plain subsurface: relationships between scale of hydrostratigraphic reconstruction and flow models*).

Here we focus on the relationship between Apennine tectonics and the development of Quaternary Alpine-sourced depositional and hydrostratigraphic systems, based on the study of the Lodi segment of the regional transect, that is the region entirely belonging to the Apennine structural domain (fig.1).

The study is based on the traditional integration of surface geology (1:10.000 geomorphological and geological mapping, fig.2) with subsurface reconstruction (correlation of borehole and well data). Age constraints could be obtained from palynological analyses on a deep well close to Lodi, some radiocarbon datings on peat and wood fragments and from published archaeological findings and historical reports about recent hydrography.

## 2. - THE SOUTHERN LODI PLAIN

The southern Lodi plain is the region between Adda and Lambro rivers, bounded to the South by the present-day Po river course. The so-called “*Livello Fondamentale della Pianura*” Auct. (LFP) (CASTIGLIONI & PELLEGRINI, 2001, with references) is the widest morphological unit of the area. The Post-glacial to recent valleys of the major rivers (Adda, Lambro, Po) are entrenched within LFP, into a series of lowered terraces. The isolated relief of San Colombano al Lambro (fig. 1) elevates above LFP at the western end of the area. Together with the subdued relic relieves of Zorlesco and Casalpusterlengo, they correspond to structural culminations of different Apennine thrusts (DESIO, 1965; PIERI & GROPPi, 1981) (fig. 1). The San Colombano hill exposes the uplifted and gently folded marine Miocene and Lower Pleistocene units (Marne di S. Agata Fossili, Formazione di San Colombano; SERVIZIO GEOLOGICO D'ITALIA, 1967), unconformably overlain by the Middle Pleistocene alluvial deposits that form two gently tilted and partly suspended terraces (Invernino Unit and Cascina Parina Unit, in ascending

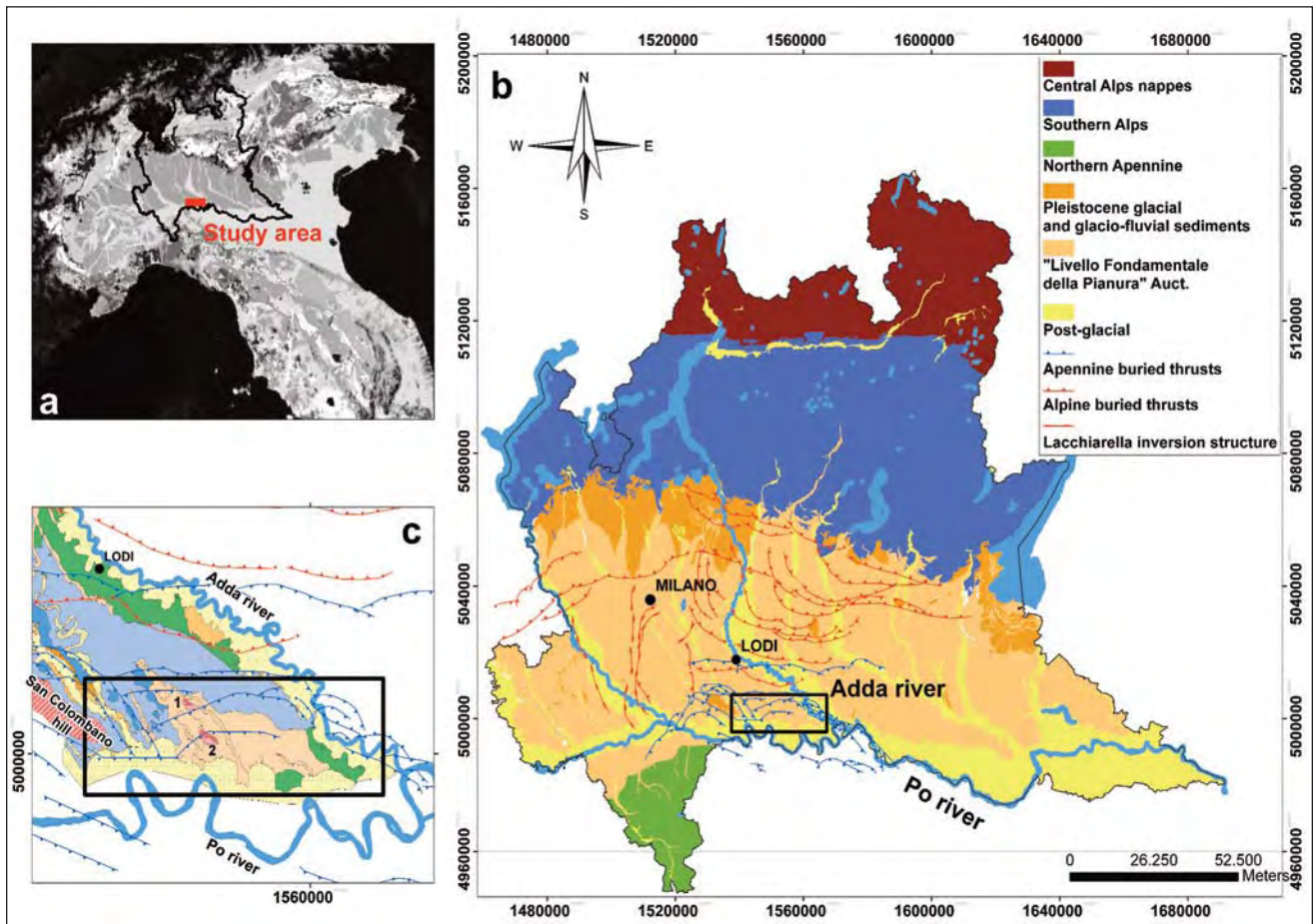


Fig. 1 – (a) Location map of the study area; (b) subsurface structural setting of the area (modified after BIGI *et alii*, 1992 and FANTONI *et alii*, 2004); (c) simplified structural map of the study area (subsurface structures after BIGI *et alii*, 1992 and FANTONI *et alii*, 2004); 1) Zorlesco relic relief; 2) Casalpusterlengo relic relief. Same legend as in figure 2(b).

– (a) Ubicazione dell'area in studio; (b) inquadramento strutturale dell'area (modificato da BIGI *et alii*, 1992 e FANTONI *et alii*, 2004); (c) carta strutturale semplificata dell'area in studio (strutture di sottosuolo da BIGI *et alii*, 1992 e FANTONI *et alii*, 2004); 1) dosso relitto di Zorlesco; 2) dosso relitto di Casalpusterlengo. La legenda dei colori è la stessa di figura 2(b).

order; PELLEGRINI *et alii*, 2003, with references). The Casalpusterlengo and Zorlesco gentle relieves expose deeply weathered Middle Pleistocene alluvial units ("Mindel" Auct.) with a loess cover (CREMASCHI, 1987). Hence, Quaternary uplift subsequent to Pliocene thrust-folding is documented by this structural and stratigraphic framework. The alluvial Middle to Upper Pleistocene succession covers and surrounds the relieves in the subsurface, resting above the Pliocene-Lower Pleistocene marine clays and sands ("Villafranchiano" Auct.). At the LFP surface, current literature reports LGM and post-glacial sediments (SERVIZIO GEOLOGICO D'ITALIA, 1967; CASTIGLIONI & PELLEGRINI, 2001; PELLEGRINI *et alii*, 2003) that have been named S.Cristina and Bissone Units by PELLEGRINI *et alii* (2003) in the southernmost sector surrounding the San Colombano hill. The low terraces within the major river valleys are formed by Holocene and recent alluvial deposits (SERVIZIO GEOLOGICO D'ITALIA, 1967; CASTIGLIONI & PELLEGRINI, 2001; PELLEGRINI *et alii*, 2003).

## 2.1. - SURFACE GEOLOGY

The new geomorphological and geological survey at 1:10.000 reveals the complex patchwork of morphological and stratigraphic units of the region (fig. 2). Based on cross-cut and elevation relations among fluvial traces and terrace scarps, six morphological units have been mapped, forming the LFP surface (LFP 1 to LFP 6 in ascending elevation order; fig. 2). In the same way, the alluvial valley terraces have been subdivided into ten terraced units, pertaining to the different major and minor river domains (fig. 2). Three different orders of relieves elevate above LFP: 1) the very low and deeply carved by human activity relic relieves of Maleo and Meleti (1-3 m above LFP), 2) the well known Casalpusterlengo and Zorlesco relic relieves (DESIO, 1965; CREMASCHI, 1987) and 3) the eastern termination of the San Colombano hill.

Combining the morphological features with sediment descriptions obtained at any exposure and with systematic mapping of surface soil tex-



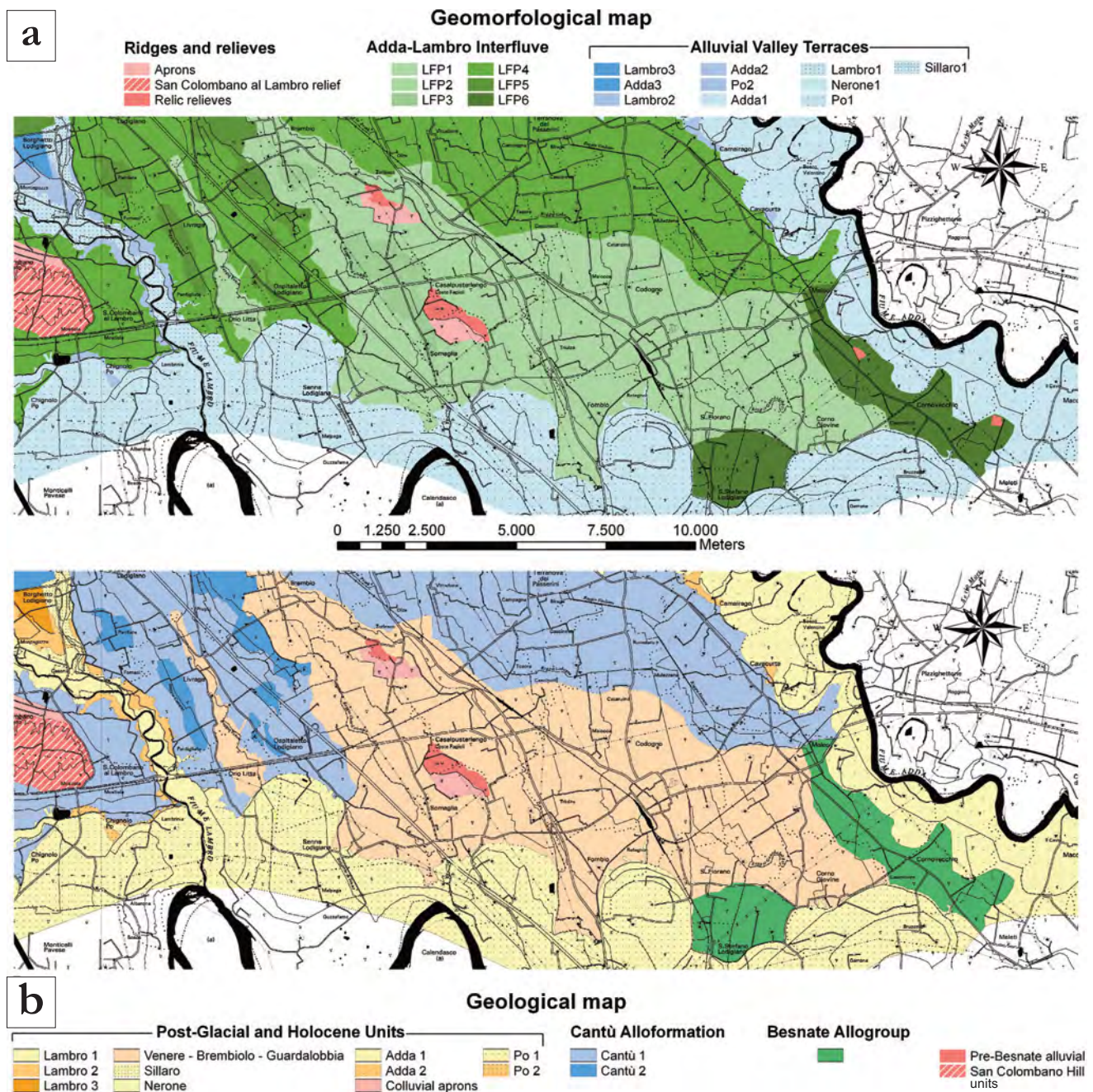


Fig. 2 – (a) Geomorphological map of the study area. Informal geomorphological units are mapped. LFP: “Livello Fondamentale della Pianura” Auct. (b) Geological map of the study area. The allostratigraphic classification has been adopted (regional allostratigraphic scheme after BINI, 1997).

– (a) Carta geomorfologica dell’area di studio; sono cartografate unità geomorfologiche informali. LFP: “Livello Fondamentale della Pianura” Auct. (b) Carta geologica dell’area di studio; è stata adottata una classificazione allostratigrafica (schema allostratigrafico regionale da BINI, 1997).

ture and Munsell colours, that were collected at every parcel, the frame of surface geological units has been reconstructed (fig. 2).

From the most ancient to the most recent we recognised:

1) San Colombano hill units (undifferentiated in the geological map), including The San Colombano Formation and the Cascina Parina Unit (SERVIZIO GEOLOGICO D’ITALIA, 1967; PELLEGRINI *et alii*, 2003);

2) pre-Besnate alluvial unit (Middle Pleistocene), with loess cover, that is exposed in the Casalpusterlengo and Zorlesco relic relieves (“Mindel” Auct.) (fig. 3). The loess weathered profile has been attributed to the last pleniglacial (LGM) by CREMASCHI (1987);

3) Besnate Allogroup (late Middle – Late Pleistocene), that forms two isolated areas cut by the Adda and Po terrace scarps, the former containing the relics of the very subdued relieves of Maleo





Fig. 3 – Exposure of weathered loess (LGM) overlaying deeply weathered alluvial sands (Middle Pleistocene). Casalpusterlengo relic relief (location in figure 2).  
 – Esposizione del profilo di alterazione del loess (LGM) che ricopre i sedimenti alluvionali profondamente alterati (Pleistocene medio) del dosso relitto di Casalpusterlengo (ubicazione in figura 2).

(Cascina Chiesiolo) and Meleti (fig. 2). Poorly preserved weathering profiles with 10YR Munsell colour characterize the top of this alluvial unit of trough cross-bedded sands with minor gravel bars and silty-clay flood plain lenses; very thin, weathered loess cover has been preserved at one site only;

4) Cantù Alloformation (Late Pleistocene, LGM), that represents the surface unit of the northern side of the area. It spreads out of the Sillaro *l.s.* palaeovalley (VEGGIANI, 1982; BERSEZIO, 1986), and flanks the Lambro entrenched course (fig. 2), forming two minor terraced units bounded by a very low scarp (< 1m). At the surface the Cantù Alloformation is made by very poorly weathered cross-bedded sands and sandy silts with clay layers;

5) the Post-Glacial and Holocene units (latest Pleistocene – Holocene and recent) include the terraced alluvial sediments (sands and recycled gravels) of the Lambro, Adda and Po river valleys, the most recent fluvial silts and sands of the Sillaro underfit stream, the veneer of silty and sandy fluvial deposits above the LFP, laid down by the minor

natural and agricultural hydrographic network, and the colluvial aprons of the isolated relieves.

The new geological and geomorphological maps show that the subdued complex morphology of the LFP corresponds to a patchwork of Pleistocene units (pre- and post-LGM) cut by the Post-glacial valleys, partly buried by very thin Post-glacial, Holocene and recent alluvial units, above which the uplifted relics of the Middle Pleistocene stratigraphy are elevated.

## 2.2. - SUBSURFACE ARCHITECTURE

Subsurface geology has been reconstructed and validated by correlation of borehole and well data (fig. 4), in combination with surface geology, adopting the following procedure: i) facies and compositional analysis of logs and cores, calibrated to outcrops and exposures; ii) assessment of vertical textural and compositional trends at each data point; iii) hierarchic classification of sedimentary units and bounding surfaces. An informal stratigraphic classification has been adopted in the sub-





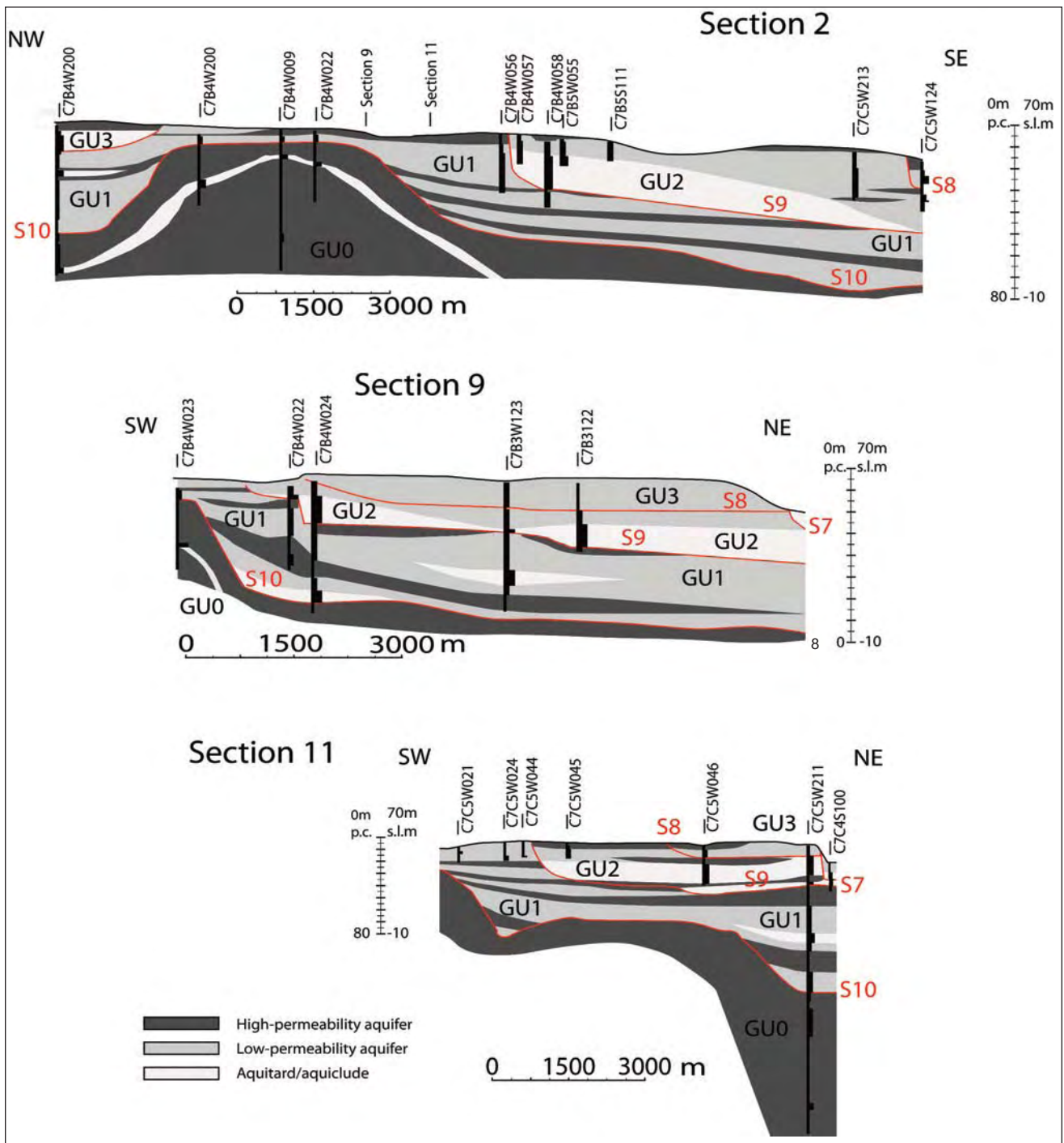


Fig. 5 – Three selected geological and hydrostratigraphic cross-sections in the Southern Lodi plain (location in fig. 4). S: bounding surfaces of maximum hierarchic order; GU informal subsurface geological units of maximum rank. The boundaries of the very thin topmost surface units, just below the ground surface, have been omitted for clarity.

– Tre sezioni geologiche ed idrostratigrafiche selezionate nella pianura lodigiana meridionale (ubicazione in fig. 4). S: limiti stratigrafici di ordine gerarchico massimo; GU: unità geologiche informali di sottosuolo, di ordine massimo. I limiti delle unità superficiali, molto sottili, sono stati omessi per chiarezza.

GU1. In the subsurface, within GU1, four sub-units have been recognised (fig. 5), each formed by a fining upwards trend from gravelly-sands to sands and sandy-silty clays. The uppermost sub-unit is exposed in the Casalpusterlengo relief (fig. 4). The lower three sub-units of GU1 wedge-out and lap onto both sides of the Casalpusterlengo

anticline, showing decreasing upwards mild deformation towards the limbs of the fold. The uppermost sub-unit smoothes the fold hinge, resting above a flat erosion segment of surface S10 (fig. 5 and 6). Based on outcrop and subsurface sedimentary features, we interpret GU1 as the alluvial succession that unconformably overlays the ma-



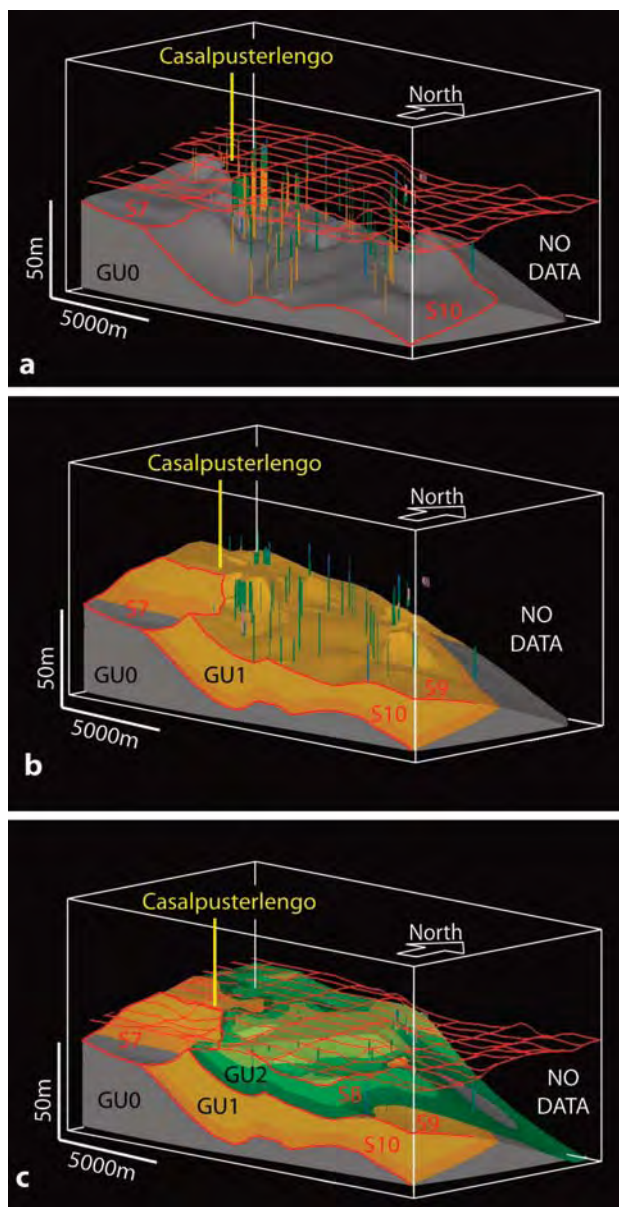


Fig. 6 – Three-dimensional models of subsurface geology of the Southern Lodi plain. Labels as in figure 5. Vertical dashes: well and borehole logs (location in figure 2). A recomputed DTM (based on 1:10.000 CTR Regione Lombardia topography, with dm vertical accuracy) is reported as a red grid in models (a) and (c).

– Modelli tridimensionali della geologia di sottosuolo della pianura lodigiana meridionale, corrispondente all'area di studio. Stile come in figura 5. Barre verticali: dati stratigrafici di sottosuolo (ubicazione in figura 2). Un DTM ricalcolato con precisione verticale 1 dm, sulla base della carta topografica CTR Regione Lombardia in scala 1:10.000, è riportato in rosso come griglia nei modelli (a) e (c).

rine Lower Pleistocene succession. Down-tracing of stratigraphy from outcrops of the San Colombano area permits to correlate parts of this unit to the Invernino and Cascina Parina units (Middle Pleistocene; PELLEGRINI *et alii*, 2003, with references therein). Palynological data from a well in the neighbourhoods of Lodi suggest to attribute the equivalent sandy gravel succession of the Lodi synformal depocentre to the Middle Pleistocene (RIGATO, 2007). These data help to attribute GU1

to the regional glacio-fluvial cycles of the Middle Pleistocene (MUTTONI *et alii*, 2003), plausibly equivalent to the Specola and/or Binago alloformations, following the classification of Pleistocene glacial and glacio-fluvial sediments proposed by BINI *et alii* (2004).

*Geological Unit 2* (GU2) partly fills a composite erosional depression, marked by surface S9 (fig. 5 and 6), that surrounds the San Colombano and Casalpusterlengo gentle anticlines. In the most complete successions, the stepped (*i.e.* terraced) S9 surface is covered by three gravel-to-sand, to silty clay with peat, fining upwards sub-units of alluvial environment. The uppermost one is exposed at the ground surface close to the Adda and Po terrace scarps, in the Maleo–Meleti area (Cascina Chiesio relic relief; fig. 2). Physical correlation in the sub-surface permits to correlate GU2 with the homonymous succession of the northern Lodi plain that was attributed to the Besnate Allogroup and dated as Middle p.p. - Late Pleistocene, by radiocarbon age determinations of the topmost sediments, palynology and stratigraphic position (BERSEZIO *et alii*, 2004). GU2 terminates against the terraced flanks of the mentioned anticlines, thickens away from them and attains its maximum thickness in the erosional depocentres that are located some kilometres eastward of these positive structures (fig. 6). Surface geology and subsurface correlations suggest that GU2 did not suffer active folding stages, representing the seal of the Pleistocene Apennine structures, eventually involved by differential uplift/subsidence after the end of active tectonic deformation.

*Geological Unit 3* (GU3) is soled by erosion surface S8 that truncates GU2 and GU1, carving some terraced valleys, the latest and most evident of which is at the southern end of the Sillaro palaeo-river (fig. 5 and 6). GU3 is characterized by different local successions in the different river valleys; as a general rule it is formed by at least two fining upwards sub-units, sandy gravel to sandy silt, interpreted as meandering river sediments and attributed to latest Pleistocene (LGM to initial post-Glacial) based on radiocarbon datings (BERSEZIO *et alii*, 2004; BERSEZIO *et alii*, 2007). GU3, that is exposed widely in the study area, has been correlated to the Cantù Alloformation (LGM) following the classification of BINI *et alii* (2004).

### 2.3. - SUMMARY OF GEOLOGICAL CONSTRAINTS TO HYDROSTRATIGRAPHY

The geological reconstruction indicates how Apennine active thrusting contributed to shape the shallow and subsurface geometry of sedimentary bodies. 1) Early p.p. to Middle p.p. Pleistocene



folding of the San Colombano and Casalpusterlengo very gentle thrust-related anticlines, raised the Lower Pleistocene marine succession (GU0), before and during deposition of the first alluvial units of the region (GU1). This evolution shaped the alluvial depocentres in the eastern sector of the study area and determined the lateral termination of the alluvial units against the uplifted marine substratum (fig. 6). 2) Middle p.p. to Late Pleistocene entrenchment of hydrography (terraced GU2 above S9, terraced GU3 above S8) occurred during differential uplift of positive structures vs. depocentral areas. This is testified also by the flat erosion surfaces carved at different elevations above the hinges and flanks of the folds (fig. 6). One exposed example is the erosion surface at the top of the relic relief of Casalpusterlengo, the origin of which can be constrained to the Late Pleistocene by superposition of an LGM loess profile (CREMASCHI, 1987) above the truncated topmost sub-unit of GU1. The Late Pleistocene sediments (GU2 and GU3) seal the previous deformation structures at different stratigraphic levels and elevations. 3) During the Post-glacial to recent entrenchment of the major river valleys (Adda, Lambro, Po) the existing stratigraphy was truncated. The relationship between the inherited structures and the location and trends of the terraced river valleys, and of the river courses within them, is apparent (fig. 1 and 2). During the same time span, a veneer of fine-grained alluvial deposits blanketed the Adda – Lambro interfluvium, corresponding to the LFP surface.

### 3. - HYDROSTRATIGRAPHY

The regional hydrostratigraphic framework of entire Lombardy has been recently sketched by ENI – REGIONE LOMBARDIA (2002). Four Aquifer Groups have been identified, named D to A in ascending order. Groups A and B are hosted by the Middle – Upper Pleistocene alluvial succession, groups C and D roughly correspond to the transgressive-regressive cycles (from open marine to coastal and alluvial) of the lower part of the Middle Pleistocene and Lower Pleistocene succession (including the “*Villafranchiano*” *Auct.*). The salt/freshwater interface occurs within the mostly marine and deepest Group D, rarely raising into the lowest part of transitional Group C.

The study area shows how complex might be the hydrostratigraphic reconstruction in the region subjected to the strong local control of active Apennine thrusts, combined with variable sediment supply from the northern sources during the Middle – Late Pleistocene cycles of glacial advance

and retreat. A qualitative attempt to classify the stratigraphic architecture in terms of hydrostratigraphy has been made, after textural parametrization of the sedimentary bodies, at their lowest hierarchic rank (minimum genetic sequences within sub-units). The result is displayed in figure 5, in which a rough threefold subdivision into high-permeability aquifers (mostly gravel), low permeability aquifers (mostly sand) and aquitards/aquicludes (mostly clays and silts with scattered sand-gravel lenses) has been adopted. In the study area, the unsaturated zone occupies the uppermost 5 – 10 m below ground surface, all the other aquifer units being saturated with freshwater. High concentrations of salt solutes have been detected in those parts of the aquifers that are adjacent to the San Colombano and Casalpusterlengo anticlines (ARIATI *et alii*, 1988; ALFANO & MANCUSO, 1996).

Dealing with the architectural component of hydrostratigraphy, that is the aim of this paper, we can observe that: i) the basal aquiclude (GU0, marine Lower Pleistocene) is uplifted by folding, forming hydrogeological divides between depocentres that collected the alluvial aquifers (fig. 5); ii) aquitard layers subdivide the deepest low-permeability aquifer hosted by GU1 into several aquifer systems (fig. 5), some of which host groundwater bearing a strong hydrochemical signature of mixing with marine connate waters (ARIATI *et alii*, 1988); iii) the depocentral areas, far-away from the uplifted structures, host the thickest and coarsest aquifers (uppermost GU1 and GU2; fig. 5), within wide and deeply entrenched palaeo-valleys, that contour the positive structures and wedge-out above erosion surfaces (S10 and S9); iv) in the LFP area (Adda – Lambro interfluvium) the vadose zone and the shallow phreatic surface are almost everywhere hosted by GU3 (LGM) and Post-glacial to Recent fine-grained and sandy sediments, but in the local exposure areas of GU2 (Besnate Allogroup) and GU1. Within the major river valleys, the unsaturated zone corresponds to the gravelly and/or sandy Post-glacial to recent deposits, mostly derived after recycling of the Pleistocene alluvial units.

### 4. - CONCLUSIONS

Surface geology and geomorphology, subsurface stratigraphy, age constraints from radiocarbon data and palinology, permitted to sketch the architecture and evolution of hydrostratigraphy, above the Lower Pleistocene marine shales (GU0) that form the regional aquiclude in the Southern Lodi plain. Subsurface mapping of the aquiclude (GU0) and of its top boundary (S10) shows that they are

gently folded and progressively lowered from SW to NE, in a sequence of en-echelon thrust-related folds (San Colombano, Casalpusterlengo). The growth of these northernmost and youngest WNW-ESE striking Apennine folds was accompanied by erosion at their flanks and hinges and regressive deposition in alluvial plain to alluvial environments. As a result, Middle Pleistocene alluvial sands and shales filled the depocentres hosted by the intervening gentle synclines, during the decline of folding rates, forming a group of at least partly confined aquifer systems (GU1). The resulting aquifer bodies are gently folded wedges that pinch-out towards the uplifted marine aquicludes and fill incised valleys in their depocentres. During the syn-glacial entrenchment of the river network (late Middle Pleistocene – Late Pleistocene), the major group of aquifer systems was built within deeply terraced valleys (GU2, Besnate Allogroup), under control of glacial pulses and differential uplift/subsidence of the depocentres vs. folded areas. The latest glacial cycle (LGM; GU3 and Post-glacial units) shaped the present-day geomorphology, building the vadose zone above terraced erosion surfaces (S8 and S7).

In summary, the Early-Middle Pleistocene Apennine tectonics acted to: 1) confine the aquifer systems into different depocentres, 2) raise buried hydrogeological divides, 3) force the erosion of hydrogeologic windows, shaping the lateral contacts between pervious alluvial bodies of different ages and 4) constrain aquitard/aquiclude building during the recovery stages of the river network.

#### Acknowledgements

*The Authors gratefully thank two anonymous Referees for revision of the manuscript. Financial support was provided by PRIN 2007 Project “Integrated geophysical, geological, petrographical and modelling study of alluvial aquifer complexes characteristic of the Po plain subsurface: relationships between scale of hydrostratigraphic reconstruction and flow models”, and by CNR – IDPA funds to R.B.*

#### REFERENCES

- ALFANO L. & MANCUSO M. (1996) – *Sull'applicabilità del metodo dipolo-polare continuo nelle ricerche idriche a media profondità in aree di pianura*. Acque sotterranee, **50** (2): 61–71, Italgrafica Segale (Segrate), Milano.
- ARCA S. & BERETTA G.P. (1985) – *Prima sintesi geodetico-geologica sui movimenti verticali del suolo nell'Italia settentrionale (1897-1957)*. Bollettino di Geodesia e Scienze Affini, **2**: 125-156, Firenze.
- ARIATI L., COTTA RAMUSINO S. & PELOSO L.G. (1988) – *La struttura del Colle di San Colombano al Lambro: riflessi idrogeologici e caratteristiche chimiche della falda freatica*. In: P. CASATI (Ed.) “Acque sotterranee di Lombardia”. Dipartimento Scienze della Terra e CNR – Centro di Studio per la stratigrafia e petrografia delle Alpi Centrali, 97-115, Milano.
- BARLETTA V. R., FERRARI C., DIOLAIUTI G., CARNIELLI T., SABADINI R. & SMIRAGLIA C. (2006) – *Glacier shrinkage and modeled uplift of the Alps*. Geophysical Research Letters, **33**, doi: 10.1029/2006 GL026490.
- BERSEZIO R. (1986) – *Studio fotogeologico e geofisico per la ricostruzione dell'andamento degli antichi alvei: prima ricostruzione dei paleoalvei della pianura tra Adda e Ticino*. Studi Idrogeologici sulla Pianura Padana, **2**: 3.1 – 3.25, CLUP, Milano.
- BERSEZIO R., PAVIA F., BAIO M., BINI A., FELLETTI F. & RODONDI C. (2004) – *Aquifer architecture of the Quaternary alluvial succession of the Southern Lambro Basin (Lombardy, Italy)*. Il Quaternario, **17** (2/1): 361-378.
- BERSEZIO R., GIUDICI M. & MELE M. (2007) – *Combining sedimentological and geophysical data for high resolution 3-D mapping of fluvial architectural elements in the Quaternary Po plain (Italy)*. Sedimentary Geology, **202**: 230-248.
- BIGI G., COSENTINO D., PAROTTO M., SARTORI D. & SCANDONE P. (1992) – *Structural Model of Italy*. Progetto Finalizzato Geodinamica CNR, 9 tavv., S.E.L.C.A., Firenze.
- BINI A. (1997) – *Problems and methodologies in the study of Quaternary deposits of the Southern side of the Alps*. Geologia Insubrica, **2** (2): 11-20, Lugano.
- BINI A., STRINI A., VIOLANTI D. & ZUCCOLI L. (2004) – *Geologia di sottosuolo dell'alta pianura a NE di Milano*. Il Quaternario, **17** (2/1): 343 – 354.
- CARMINATI E., MARTINELLI G. & SEVERI P. (2003) – *Influence of glacial cycles and tectonics on natural subsidence in the Po plain (Northern Italy): insights from <sup>14</sup>C ages*. Geochemistry, Geophysics, Geosystems, **4** (10): 1082, doi:10.1029/2002GC000481.
- CASTIGLIONI G.B. & PELLEGRINI G.B. (2001) – *Note illustrative della Carta Geomorfologica della Pianura Padana*. Supplementi di Geografia Fisica e Dinamica Quaternaria, **4**, pp. 209, Comitato Glaciologico Italiano, Torino.
- CREMASCHI M. (1987) – *Paleosols and vetusols in the central Po plain (Northern Italy)*. Collana Studi e Ricerche Sul Territorio, **28**, pp. 305, UNICOPLI, Milano.
- DESIO A. (1965) – *I rilievi isolati della pianura Lombarda ed i movimenti tettonici del Quaternario*. Rendiconti dell'Istituto Lombardo, A **99**: 881–894, Milano.
- ENI – REGIONE EMILIA ROMAGNA (1998) – *Riserve idriche sotterranee della Regione Emilia-Romagna*, pp. 120, S.E.L.C.A., Firenze.
- ENI – REGIONE LOMBARDIA (2002) – *Geologia degli acquiferi padani della Regione Lombardia*, pp. 130, S.E.L.C.A., Firenze.
- FANTONI R., BERSEZIO R. & FORCELLA F. (2004) – *Alpine structure and deformation chronology at the Southern Alps Po plain border in Lombardy*. Boll. Soc. Geol. It., **123** (3): 463-476, Roma.
- MUTTONI G., CARCANO C., GARZANTI E., GHIELMI M., PICCIN. A., PINI R., ROGLEDI S. & SCIUNNACH S. (2003) – *Onset of major Pleistocene glaciations in the Alps*. Geology, **31** (11): 989 – 992.
- ORI G.G. (1993) – *Continental depositional systems of the Quaternary of the Po plain (Northern Italy)*. Sedimentary Geology, **83** (1-2): 1-14. Amsterdam.
- PELLEGRINI L., BONI P. & CARTON A. (2003) – *Hydrographic evolution in relation to neotectonics aided by data processing and assessment: some examples from the Northern Apennines (Italy)*. Quaternary International, **101-102**: 211–217.
- PIERI M. & GROPPA G. (1981) – *Subsurface geological structure of the Po plain, Italy*. Progetto Finalizzato Geodinamica, Pubbl. 411, pp. 13, CNR, Roma.
- RIGATO V. (2007) – *Geologia degli acquiferi alluvionali della pianura lodigiana tra Lodi e Camairago*. Tesi di Laurea inedita, Università degli Studi di Milano, Dipartimento Scienze della Terra, pp. 243.
- SCARDIA G., MUTTONI G. & SCIUNNACH D. (2006) – *Subsurface magnetostratigraphy of Pleistocene sediments from the Po Plain (Italy): constraints on rates of sedimentation and rock uplift*. Geol. Soc. of America Bulletin, **118** (11/12): 1299–1312.
- SERVIZIO GEOLOGICO D'ITALIA – *Carta Geologica d'Italia alla scala 1:100.000, Foglio 160 Piacenza* (1967), II Edizione, Roma.
- VEGGIANI A. (1982) – *Variazioni climatiche e dissesti idrogeologici nell'alto medioevo in Lombardia e la rifondazione di Lodi*. Sibirium, **16**: 199-208, Varese.

## Assessment of groundwater availability in the Milan Province aquifers

*Stima della disponibilità idrica negli acquiferi della Provincia di Milano*

BONOMI T. (\*), DEL ROSSO F. (\*),  
FUMAGALLI L. (\*), CANEPA P. (\*)

**ABSTRACT** - Management programs often give less importance to groundwater because it is less visible than surface water, but this invisible resource, drawn from wells and springs, makes up about 10% of the requirements for irrigation and 95% of the water needed for civil use (drinking water, water for non-drinking purposes, fish-farming, etc.) in Lombardy. This study aims to provide a quantitative evaluation of the potential of the groundwater reservoir in the Milan province, through the integrated use of databases and models which permit the simultaneous management of large amounts of data. In fact, information on more than 7000 wells in the Milan province has been coded and stored in a special hydrogeological database, which permits a three-dimensional definition of the geometrical and hydrogeological characteristics of the subsurface system. The parameterisation of hydrogeological properties, such as effective porosity, helps to estimate the potential quantity of water stored in subsurface deposits throughout the whole provincial territory (approximately 34 billion cubic metres of water). Only a part of this is made up of mobile water, that is, the water that permeates medium and coarse materials (porosity over 17%), for a total of about 13-15 billion cubic metres of water. The variations of this groundwater reservoir depend on the piezometric level, the system's reaction to the static and dynamic characteristics of the hydrogeological system itself and make up the net balance of the system.

The estimation of the quantities of available both free and stored water volumes, is considered the best approach for simulating the effect of different impacts on resources, whether natural and/or man-made.

**KEY WORDS:** data bases, Groundwater, plains, pumping, stratigraphies, three-dimensional models.

**RIASSUNTO** - L'acqua sotterranea è spesso poco considerata nei programmi gestionali perché meno "evidente" rispetto a quella superficiale, ma questa risorsa invisibile, prelevata da pozzi e sorgenti, costituisce circa il 10% degli usi irrigui e il 95% di quelli civili (potabile, non potabile, piscicoltura, etc.) in Lombardia. Lo studio mira a dare una valutazione quantitativa della potenzialità idrica del serbatoio sotterraneo della provincia di Milano, mediante un uso integrato di banche dati e modelli, che consentono una gestione contemporanea di una mole elevata di dati. In una apposita banca dati idrogeologica sono stati infatti archiviati e codificati i dati di oltre 7000 pozzi per la provincia di Milano che consentono una definizione tridimensionale delle caratteristiche geometriche e, tramite quelli forniti di stratigrafia, anche delle caratteristiche idrogeologiche del sistema sotterraneo. La parametrizzazione delle proprietà idrogeologiche, come la porosità efficace, consente di stimare un potenziale quantitativo d'acqua stoccato all'interno dei sedimenti del sottosuolo (all'incirca 34 miliardi di m<sup>3</sup> d'acqua). Solamente una parte costituisce volumi d'acqua mobili, cioè quelli che permeano materiali medi e grossolani con classi di porosità media e medio alta (sopra il 17%), per un totale di circa 13-15 miliardi di metri cubi d'acqua, nell'intero territorio provinciale. Le oscillazioni di tale serbatoio sotterraneo dipendono dal livello piezometrico, risposta del sistema alle caratteristiche statiche e dinamiche del sistema idrogeologico stesso, e costituiscono il bilancio netto del sistema.

L'approccio di stimare quantitativamente i volumi idrici disponibili, liberi e stoccati, si ritiene possa essere la strada migliore per simulare variazioni negli impatti sulla risorsa, naturali e/o antropiche, all'interno di scenari logici e plausibili.

**PAROLE CHIAVE:** Acqua sotterranea, banca dati, modelli tridimensionali, pianura, prelievi, stratigrafie.

(\*) Dipartimento di Scienze dell'Ambiente e del Territorio, Università degli Studi di Milano-Bicocca, Piazza della Scienza 1, 20126 Milano



## 1. - INTRODUCTION

The groundwater of the Milan Province supplies the whole residential and commuter population, almost all industrial needs and part of agricultural requirements. This means that for the Milan province and for its capital, Milan, groundwater is currently the most important resource and will become even more so in the future. The conservation of this resource demands programs targeted to prevent quantitative and qualitative depletion. In order to be efficient, all measures aiming to save water resources must be based on accurate information: this refers to the entity of the reserves, their variations and their uses, as well as their quality. This means that it is essential to have detailed knowledge of the hydrogeological structure and the characteristics of groundwater aquifers, but also to have an efficient groundwater monitoring network and information on the volumes extracted throughout the territory.

Management programs often give less importance to groundwater because it is less visible than surface water, but this invisible resource drawn from wells and springs constitutes about 10% of the requirements for irrigation and 95% of the water needed for civil use (drinking water, water for non-drinking purposes, fish-farming, etc.) in the entire Lombardy region. (REGIONE LOMBAR DIA, 2006) (fig. 1).

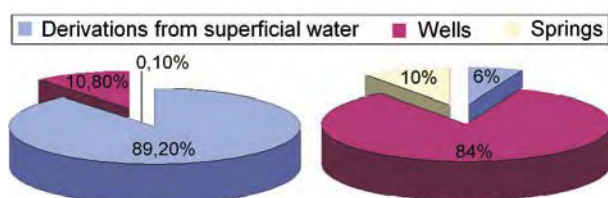


Fig. 1 - Water distribution for irrigation (left) and civil use (right) according to origin, in the Lombardy Region.

- Distribuzione dell'acqua per usi irrigui (a sinistra) e civili (a destra) in funzione della provenienza, in Regione Lombardia.

## 2. - STUDY AREA

The study area is located in the Po Plain in Italy (fig. 2), which is characterized by a very high density of urban, industrial and agricultural activities. The Milan Province, which covers 1989 km<sup>2</sup>, contains 189 municipalities, and 71% of the land is used for agriculture. The area also has a natural hydrographic network, as well as a man-made one. The natural network is made up of the Adda and Ticino rivers, the eastern and western boundaries, of the area respectively. Both rivers drain groundwater.

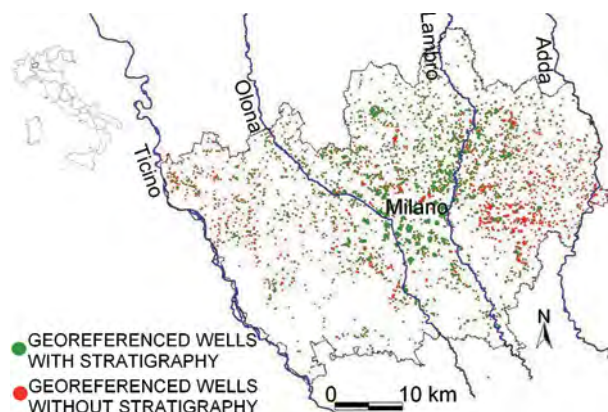


Fig. 2 - Location of Milan Province and wells georeferenced with stratigraphy (3493 in green) and wells georeferenced without stratigraphy (2114 in red).

- Ubicazione della Provincia di Milano e dei pozzi georeferenziati con stratigrafia (3493 in verde) e pozzi georeferenziati senza stratigrafia (2114 in rosso).

The main hydrogeological system consists of fluvial and fluvio-glacial deposits, mostly gravel and sand with discontinuous confining layers of silt and clay. From the hydrogeological point of view, an unconfined shallow aquifer is underlain by deeper semi-confined and confined aquifers (POZZI & FRANCAI, 1981; AVANZINI *et alii*, 1995; PROVINCIA DI MILANO *et alii*, 1995; PROVINCIA DI MILANO, 2001). The last description of the stratigraphical sequence of Pleistocene and Quaternary deposits separates them in four Aquifers Groups, on the basis of a multidisciplinary studies (REGIONE LOMBAR DIA, 2002), called A, B, C and D, from the youngest to the older. The Traditional Aquifer (A and B) consists of a hydrogeological system of the unconfined aquifer within a system of very heterogeneous layers, which has been traditionally used in the plain. The deep aquifers (C and D) have not been included in the study.

## 3. - UNDERGROUND SUPPLY SOURCES

Information concerning the aquifer systems in the Milan area is well documented (AVANZINI *et alii*, 1995; CAVALLIN *et alii*, 1984). In particular, research carried out by the Hydrogeology Unit at the Department of Environmental and Territorial Sciences at the Bicocca University in Milan aim to estimate groundwater availability through a 3D parameterisation of the subsurface. This research is performed through integrated use of databases and models which permit the simultaneous management of a large amount of data (BONOMI, 2009; BONOMI *et alii*, 2007).

The starting point is the collection of data concerning water wells, in particular the stratigraphic logs. Although these may not be accurate, they



have the advantage of providing large amounts of information. In the Lombardy Region, data pertaining to over 21.000 wells has been stored and processed in a special hydrogeological database for this purpose ([www.tangram.samit.unimib.it](http://www.tangram.samit.unimib.it), BONOMI *et alii*, 1995) (fig. 3).

The use of groundwater instead of surface water supplies dates back to the second half of the 19<sup>th</sup> century (1887) and is linked to the local abundance of groundwater resources. Since then, more than 10,000 well-drillings have been estimated in the province. During research work carried out in recent years, 7617 wells in the Province of Milan have been recorded in the database. Among them 5607 are georeferenced and 3493 have appropriately coded stratigraphic data (fig. 2). More than 5000 are private wells and the remaining 2100 are public (fig. 4). A large number of problems arising in recent decades, especially in relation to groundwater quality, have led to abandonment of about 30% of the wells. They are still an important measuring reference, but at the same time, may also be a possible contamination path towards the aquifers.

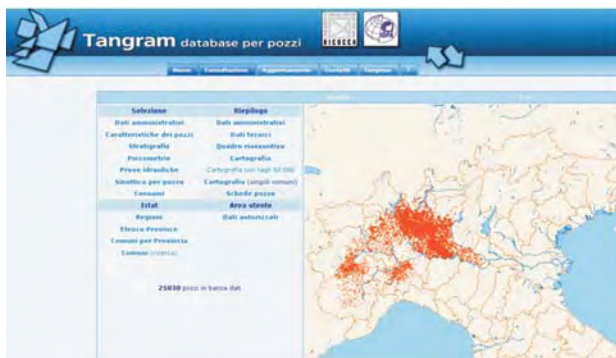


Fig. 3 - Home page of the Tangram hydrogeological database: [www.tangram.samit.unimib.it](http://www.tangram.samit.unimib.it). The screen capture shows data typology ("Selezione"), synopsis of data types and maps ("Riepilogo"), public data available ("ISTAT") and the users' site ("Area utente"). 25030 water wells are available in the database.

- Schermata dell'homepage della banca dati idrogeologica Tangram: [www.tangram.samit.unimib.it](http://www.tangram.samit.unimib.it). La schermata mostra la tipologia di estrazione ("Selezione"), sinossi della tipologia di dati e delle carte ("Riepilogo"), dati pubblici ("ISTAT") e la zona utente ("Area utente"). Nella banca dati disponibili 25030 pozzi per acqua.

#### 4. - 3-D PARAMETERIZATION OF THE GROUNDWATER RESERVOIR

The large amount of coded and georeferenced data enabled us to integrate previous work defining some relevant geometries (topographic surface and base of the phreatic aquifer system) and introducing the 3-D parameterisation of the groundwater reservoir (MARCHETTI, 2001; REGIONE LOMBARDIA, 2002). The geometries help to define the thickness of the groundwater reservoir (fig. 5),

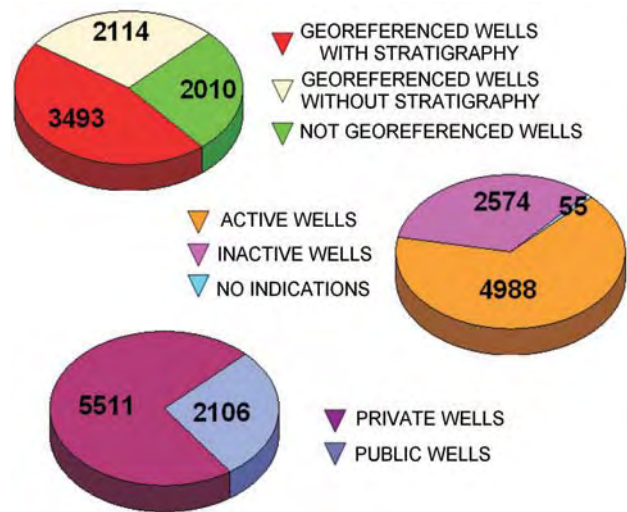


Fig. 4 - Breakdown of wells stored according to georeferencing, the presence of stratigraphy, status and type in the Milan Province.  
- Suddivisione dei pozzi archiviati secondo la georeferenziazione, la presenza di stratigrafia, lo stato e la tipologia, in Provincia di Milano.

which varies between a minimum of approximately 2 metres in the north-eastern zone and a maximum of approximately 190 metres to the south, and to calculate the volume of the aquifer that makes up the area, estimated at about 250 billion cubic metres of material.

Scientific literature recognises the importance of reconstructing the heterogeneity of the conceptual model when determining water flow, and has led to the development of methodologies, starting from extensive gathering of stratigraphic information, in order to achieve this purpose. MARTIN & FRIND (1998), MALLET J.L. (2002), used 3D geostatistics to reconstruct hydrogeological systems through the interpolation of the boundaries

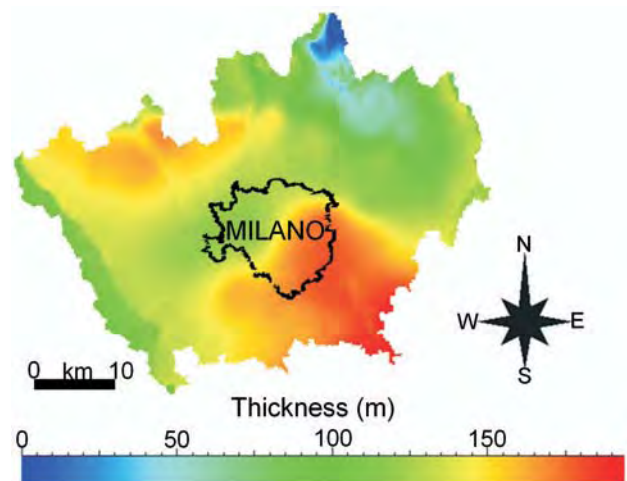


Fig. 5 - Thickness of the hydrogeological system under investigation (m), in the Milan Province.

- Spessore in metri del sistema idrogeologico in esame, in Provincia di Milano.

of the aquifer bodies and of their conductivity defined on the basis of stratigraphic and literature data

On the other hand FLECKENSTEIN *et alii* (2006) made a geostatistical analysis of the transition probabilities between the textural types characterized from conductivity data from scientific literature, and analysed the modelling results of different heterogeneity configurations.

In this work, parameterization is performed through the definition of a three-dimensional calculation grid into which the hydrogeological properties of the wells are entered, such as textural properties (coarse, medium and fine grain-size, BONOMI *et alii*, 2007) and hydrogeological properties (hydraulic conductivity and effective porosity).

It is possible to extract these characteristics from the database for selected depth intervals, using conversion textural – conductivity – effective porosity tables, previously entered in the reference database. Figure 6 shows the processing layout of the stratigraphic data, from the coding and storage stage, to the extraction stage.

The viewing of the point data, imported and

projected into the 3D space is shown in figure 7: a close-up of a portion of aquifer can be seen, and the wells are included within the two bounding surfaces (topographic surface in red and the aquifer base in grey); percentages of coarse terms are shown as an example. It can be easily noted that the abundance of coarse-grained units can vary between 40%-60% at the surface, and gradually decreases in depth, down to values of about 3%, with the exception of lenses with high relative abundance of coarse sediments corresponding to deep confined aquifers.

These textural quantitative evaluations constitute the base to obtain the quantitative estimation of groundwater resources.

A powerful software was used to construct the three-dimensional calculation grid (fig. 8): Gocad (Geological Object Computer Aided Design) developed by a Research Consortium (Gocad Research Consortium), currently composed of numerous university research centres and industrial companies (<http://gocad.ensg.inpl-nancy.fr/www/consortium/index.xhtml>).

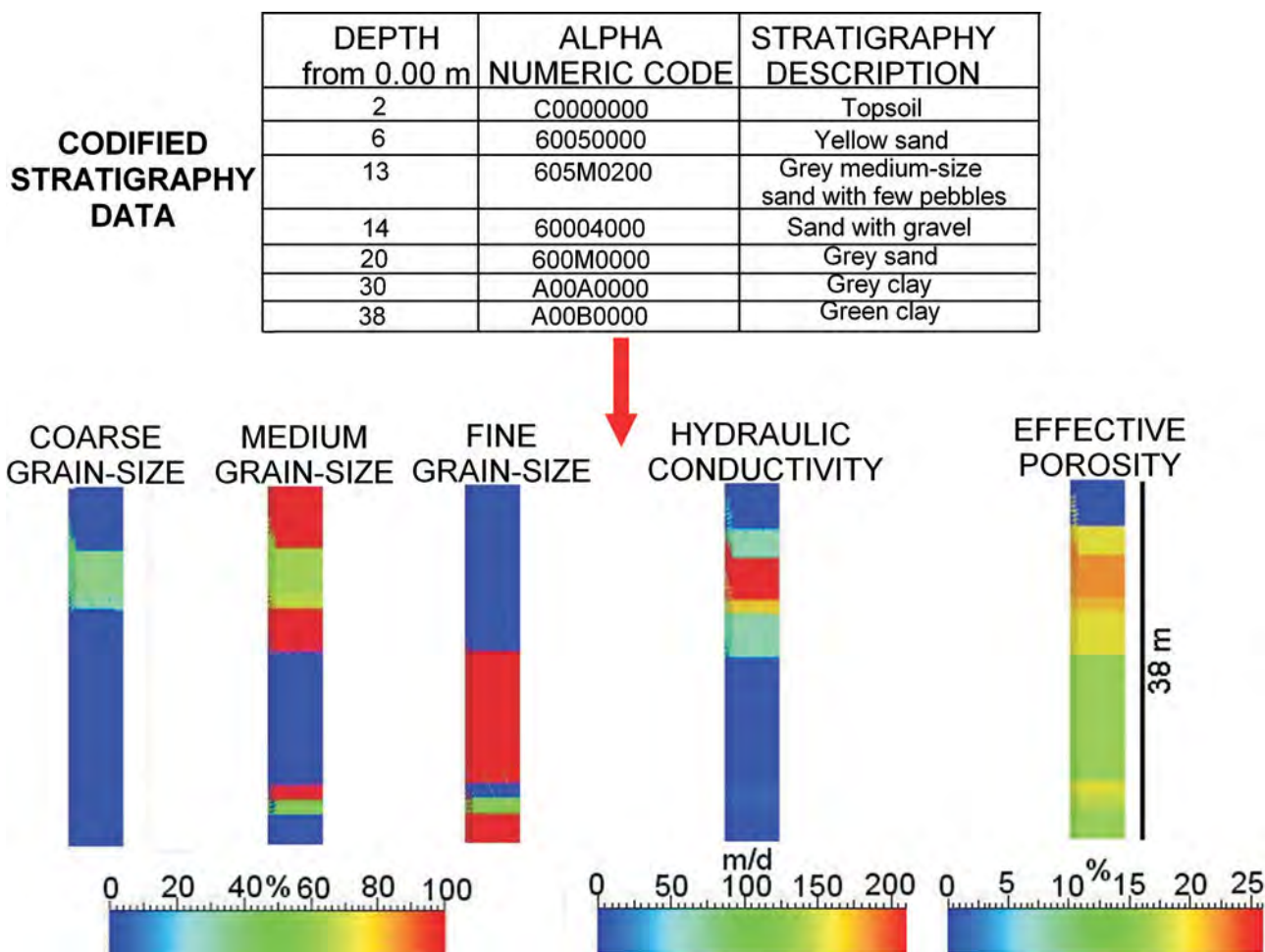


Fig. 6 - Parametrization of stratigraphic data codified in the database (table) and allocation of its textural and hydrogeological properties (columns).  
— Parametrizzazione dei dati stratigrafici nella banca dati (tabella) e attribuzione delle relative proprietà tessiturali ed idrogeologiche (colonne).



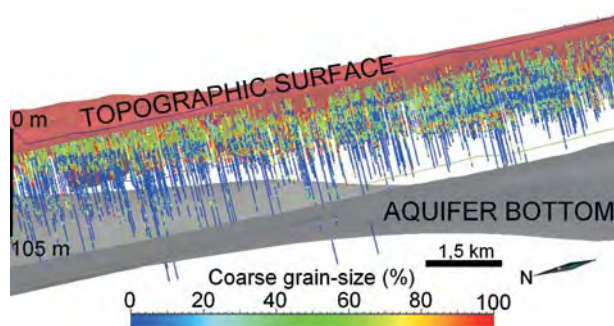


Fig. 7 - Close-up of a portion of the system: wells are shown between the topographic surface (pink) and the base of the aquifer (grey); gravel abundance (%) is shown.

- Zoom su una porzione del sistema in esame: pozzi visualizzati tra la superficie topografica (in alto, in rosso) e la base dell'aquifero (in basso, in grigio); come proprietà sono visualizzata i termini grossolani.

The grid was divided into 202 layers and is composed of 256 columns and 215 lines; each cell is 250 m x 250 m in size and has a thickness that varies around 2 metres since the grid was modified in proportion with the distance between the two surfaces. A total of 11,508,950 cells form the 3D calculation grid (fig. 8) and a property can be associated with each individual cell.

The data-points were interpolated by kriging; in this manner the properties are estimated in non-sampled points by means of a weighted linear combination of known values. The weights assigned to existing data are calculated by analysing the variogram relative to the initial in-

formation. In this way their correlation is examined according to distance and direction. The final result is a reconstruction of the textural characteristics and hydraulic parameters inside the total volume of the aquifer, aimed at reproducing vertical and areal heterogeneity, which is known to have a considerable influence on the flow direction as well as the contaminant transport (PECK *et alii*, 1988).

As an example, the distribution of effective porosity is shown (fig. 9), which varies in the sub-surface (between 6% and 26%) conditioning the sediment capacity to store and release water. In particular, figure 10 shows, for instance, the volumes that have an effective porosity of 12%, 14% and 22% inside the calculation grid.

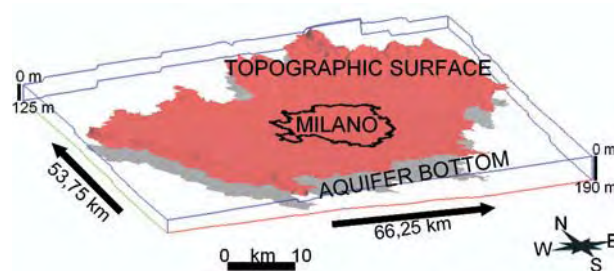


Fig. 8 - 3D computation grid: topography in red and basal aquiclude in grey (202 layers, 256 columns and 215 lines, cells 250m X 250m X 2m).

- Griglia 3D di calcolo, con all'interno le due superfici: in rosso il top e in grigio il bottom (202 strati, 256 colonne e 215 righe, celle 250m X 250m X 2m).

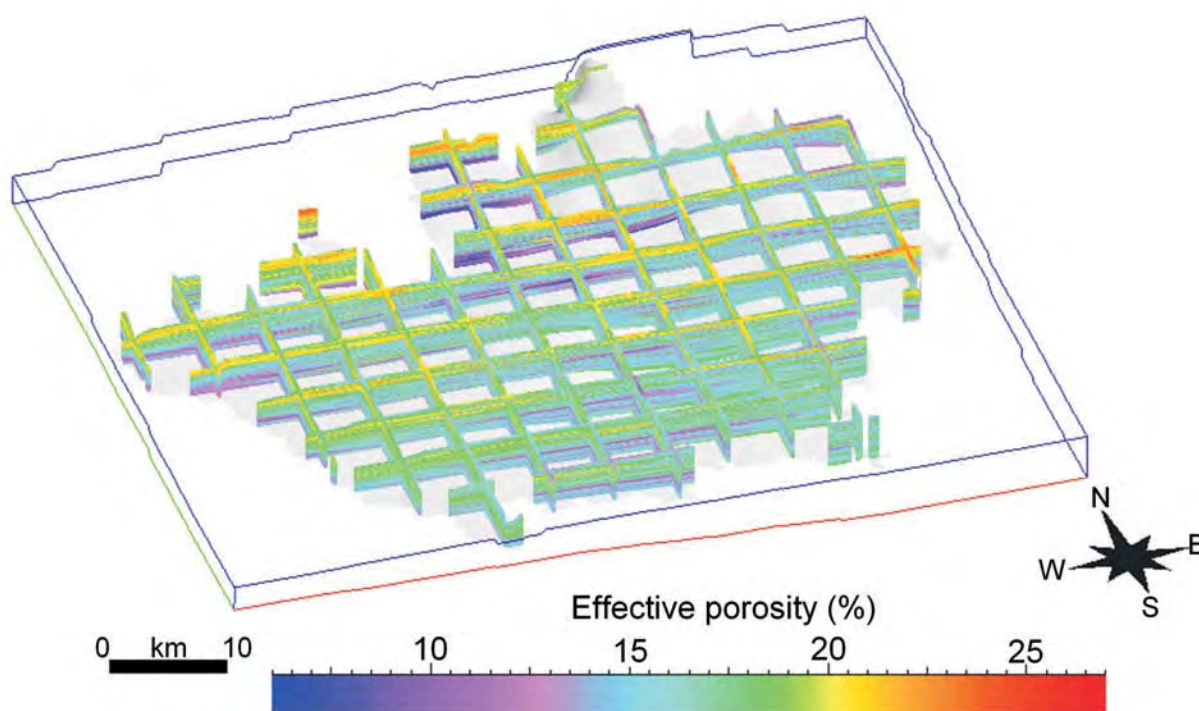


Fig. 9 - Cross-sections of effective porosity (%) distribution in the Milan Province. The scale ranges from a minimum of 5% (clay) to a maximum of 28% (coarse gravel).

- Sezioni incrociate della distribuzione della porosità efficace (%) nella Provincia di Milano. La scala varia da un minimo del 5% (argilla) ad un massimo del 28% (ghiaia grossolana).



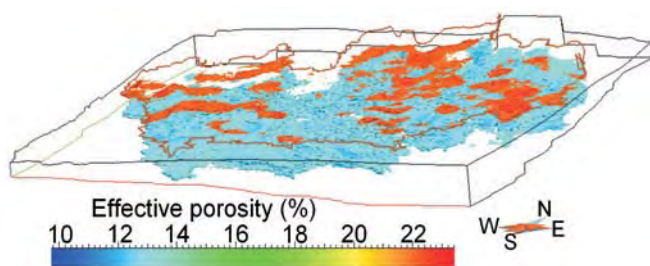


Fig. 10 - Volumetric representation of effective porosity: 12% (light cyan, 14% (dark cyan) and 22% (orange) are represented.  
- Volumi delle classi percentuali di porosità efficace del 12% (azzurro chiaro), 14% (azzurro scuro) e 22% (arancione).

## 5. - ESTIMATE OF GROUNDWATER AVAILABILITY

The evolution of the piezometric level shows how the system reacts to the water balance since its oscillations make up the net balance. The prevalent balance category in strongly urbanised impervious areas, like the city of Milan and its hinterland, is groundwater extraction, which has a strong influence on piezometric levels and water reserves when replenishment does not occur (BONOMI *et alii*, 2008). An example relative to an eastern zone in the city of Milan is shown in figure 11. If ex-

tractions were measured accurately, the correlation between them and levels on a provincial scale would provide an estimate of anthropogenic impact on groundwater resources. An evaluation of the history of this impact in relation to socio-economic development would help in setting up management programs.

A reconstruction of the piezometric areal evolution was performed for the 1979 – 2005 period, to determine the changes in water availability (fig. 12).

These changes are shown by variations in the saturated volume within the aquifer over a period of time, corresponding to a difference in water content resulting from changes in the effective porosity of the aquifer. Figure 13 shows modal classes of effective porosity; the value for sand and sandstone are between 15% and 19%. Furthermore, over the years the saturated pore volume of the aquifer was evidently subject to change, mainly for the highest values of porosity, concerning medium and coarse-grained deposits. In fact, these occur in the upper part of the aquifer where the height of the water table varies over time. On the other hand, the lowest porosity values (between 6% and 10%) relate to the finer deposits which occur at greater depths. Values between 23% and 26% are related to a very low saturated pore volume size.

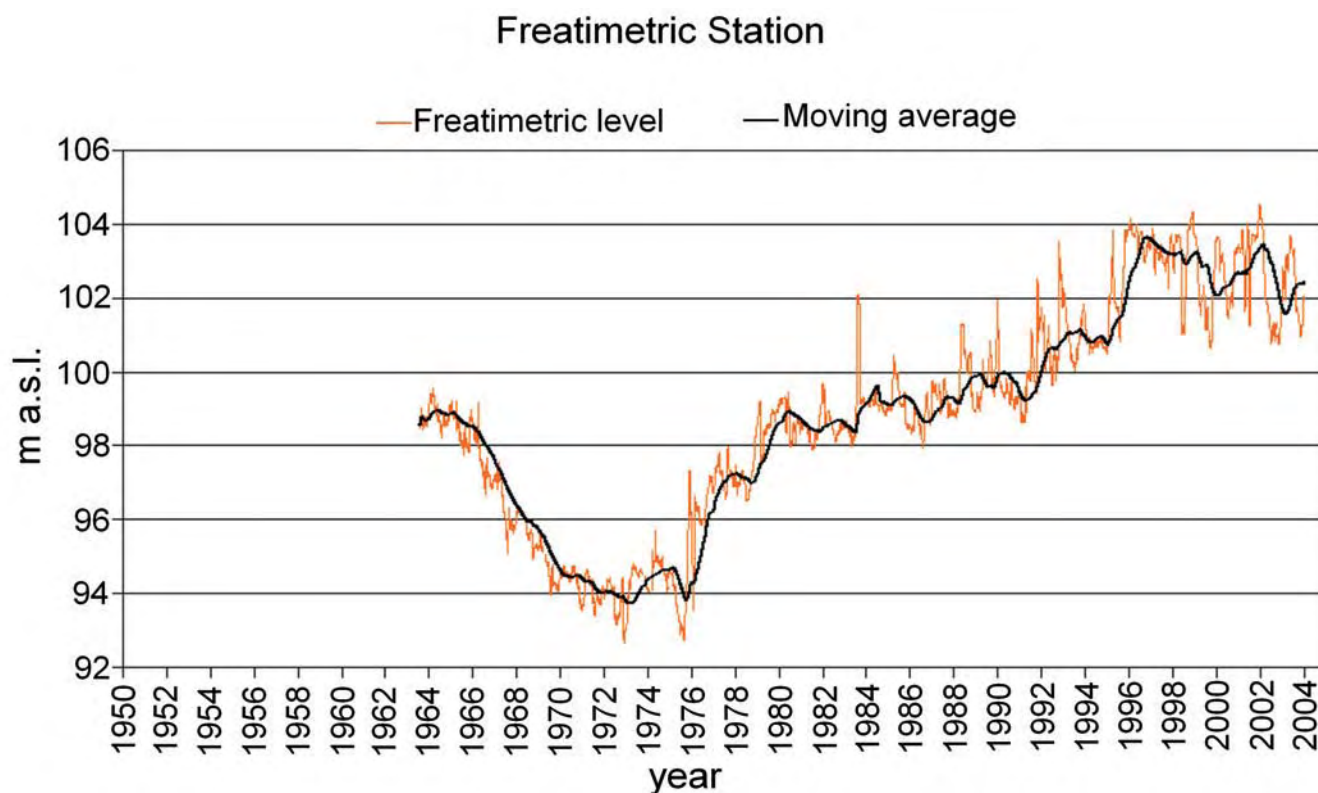


Fig. 11 - Historical evolution of the phreatic surface in a piezometer of the Milan municipal network, between 1964 and 2005. The moving average line over 12 months is shown in black.

- Andamento freatimetrico storico in un piezometro della rete comunale di Milano, dal 1964 al 2005. La linea nera indica la media mobile su 12 mesi.

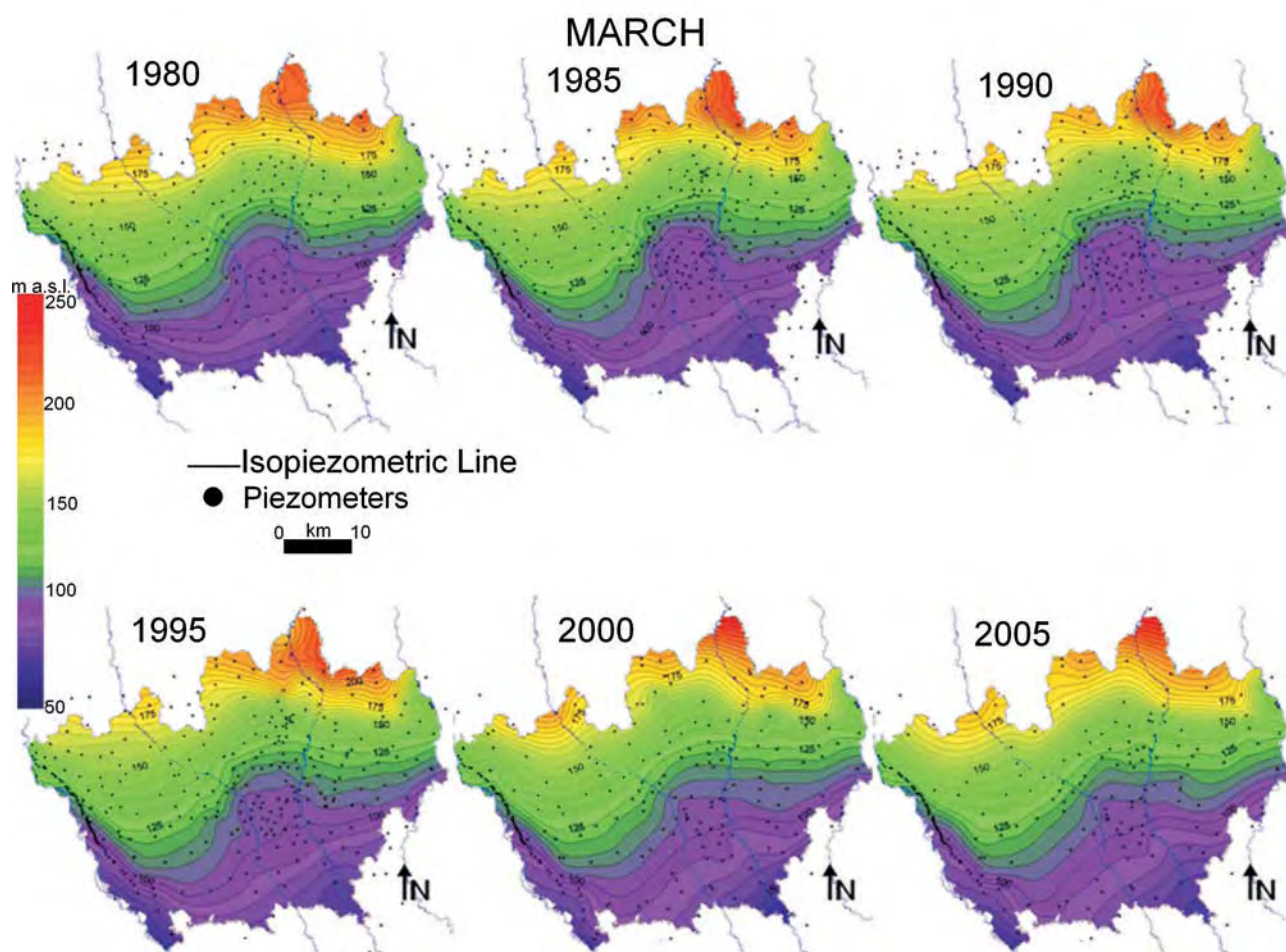


Fig. 12 - Piezometric surfaces in the Milan Province between 1980 and 2005 (m. a.s.l.), interpolating the data of the monitoring network.  
 - Ricostruzione piezometrica nella Provincia di Milano dal 1980 al 2005 (m s.l.m.), interpolando i dati della rete di monitoraggio.

The volumes of the aquifer have been calculated for each porosity classification and multiplied by the value of corresponding effective porosity to provide an estimate of the actual water volume available for the current year. Figure 14 shows the relative calculation of the saturated aquifer volume (brown bars) and the corresponding water volume it contains (blue bars) in relation to the period between 1979 and 2005.

The theoretical calculation of the water volume stored in the subsurface for the whole Milan province yields approximately 33-34 billion cubic metres (fig. 14). Only part of this volume is mobile water, which permeates medium and coarse-grained deposits (porosity over 17%) for a total of about 13-15 billion cubic metres of water. Naturally these volumes vary according to the evolution of the piezometric level which saturates or drains different portions of aquifer with varying water storage capacity (fig. 15).

The difference between these estimated annual values compared to the average in the period 1979-2005 (about 14.420.000 m<sup>3</sup>/y, red line in the figure 15), provides an idea of the variation of water

availability over a period of time. The oscillation represents the result between recharge and extraction. For example, provincial water withdrawal estimated in some publications is approximately 1 billion cubic metres of water (BERETTA *et alii*, 1985; BONOMI, 1995). A positive variation in water availability indicates that the replenishment of the system has succeeded not only in balancing the withdrawals, but also in providing a water surplus. A negative variation indicates that the replenishment has not been able to compensate the withdrawals, and the subsoil system is in deficit. Water availability estimation is a basic evaluation to be correlated with the evaluation of the minimum piezometric level sustainable by a system, which means the minimum water availability sustainable.

In the same area and for the same period, the aquifer recharge due to the precipitation has been estimated in about 370 million m<sup>3</sup>/year, varying between 830 million m<sup>3</sup> (1980) and 106-121 million m<sup>3</sup> (1981-2005); it represents about 1% of the total water reservoir and 2.7% of the mobile water, (FUMAGALLI, 2010, in press). The annual recharge rate is consistent with the groundwater oscillations,



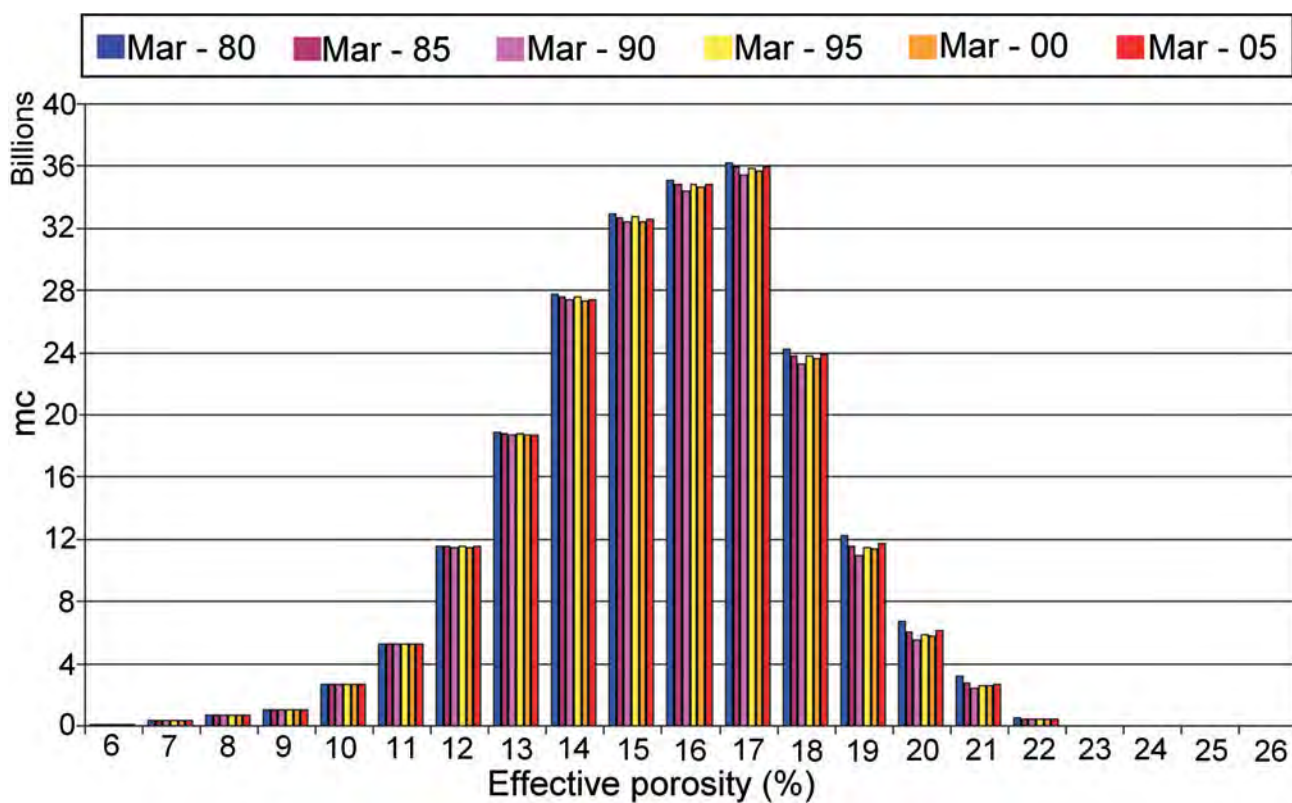


Fig. 13 - Histogram showing the saturated volumes for each effective porosity (%) classification over a period of time. The examples show values for the years: 1980, 1985, 1990, 1995, 2000 and 2005.

- Istogramma dei volumi saturi per ogni classe di porosità efficace (%) al variare del tempo. Come esempio sono riportati gli anni 1980, 1985, 1990, 1995, 2000 e 2005.

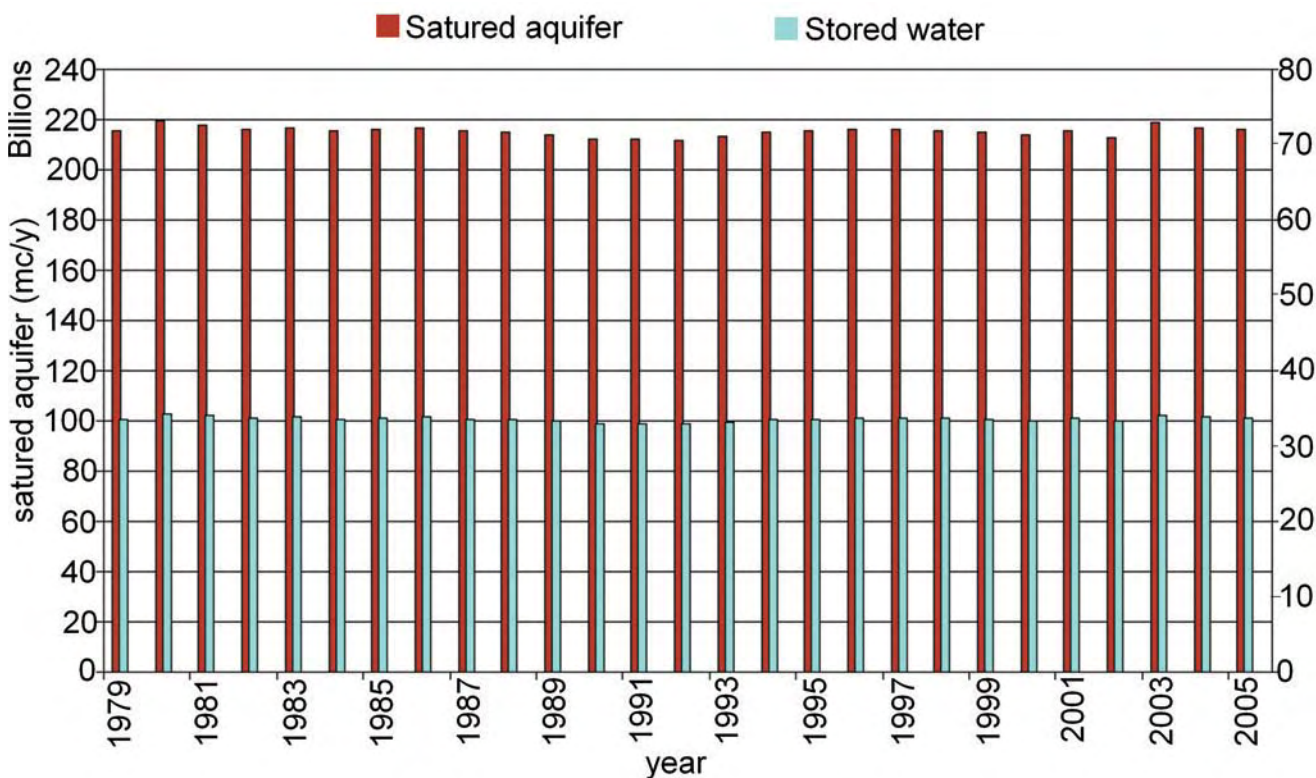


Fig. 14 - Histogram showing the saturated volume (brown bars) and the volume of stored water (blue bars) between 1979 and 2005 in the Milan Province.

- Istogramma della variazione nel tempo del volume saturo (barre marroni) e del volume d'acqua immagazzinata (barre blu) dal 1979 al 2005 in Provincia di Milano.



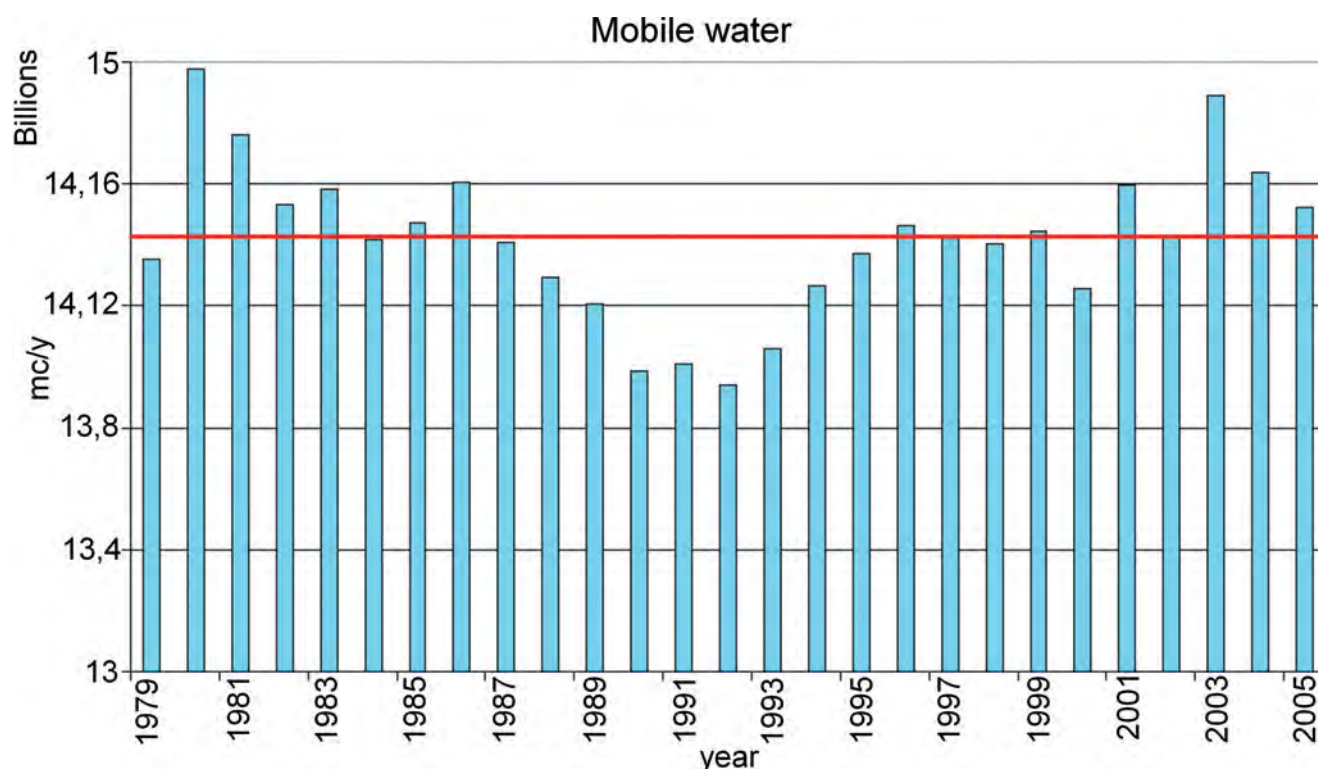


Fig. 15 - Histogram showing the volume of mobile water between 1979 and 2005 in the Milan Province (porosity over 17%). The red line shows the annual average over the period.

- Istogramma della variazione nel tempo dei volumi d'acqua mobile dal 1979 al 2005 in Provincia di Milano (porosità maggiore del 17%). La linea rossa indica la media annuale sul periodo considerato.

that are however delayed of some months.

These data refer to the results of soil water balance simulations (MACRO model, JARVIS, 1994) that have been done for the soil profiles of the province area, taking into account an average climatic and agricultural scenario and the waterproof urban area extension.

## 6. - FINAL REMARKS

The results of this study for resource management can be summarized as follows:

- quantification of the volume of water stocked in the Milan Province by estimating the effective porosity of the aquifers;
- estimates of the mobile water fraction according to the textural characteristics of the system.

There is no doubt that the groundwater reservoir is the best water reserve available and the best natural strategic storage throughout the territory. Variations between one year and the next represent the net water balance of the hydrogeological system, equal to the result between the recharge of the system (efficient rainfall, efficient irrigation, draining from canals and drainage systems, feeding from rivers, etc.) and withdrawal (well pumping, springs, feeding to rivers, etc.). If accurate

information concerning these factors were available, it would be possible to compute the groundwater balance and even water availability with good precision. Unfortunately, so far it has not been considered necessary to monitor the volume of water outflowing from the aquifer on a provincial scale.

The next step of the research will be the evaluation of the quantities that could be reasonably used according to sustainability parameters.

In this evaluation, another factor that must not be ignored is the porosity variation to which a sediment is subject due to variations of water content, and therefore it is necessary to introduce a corrective factor when attributing effective porosity to textural percentages.

The qualitative-quantitative information relative to this reservoir is a useful instrument at waterworks level (GIUDICI *et alii*, 2000; GIUDICI *et alii*, 2003), but it could be used to manage consumption increases, both continuous and sporadic also at a provincial level. The computation of the groundwater reservoir variations could be useful for Milan during Expo 2015, for example, when millions of tourists are expected. We consider that a quantitative estimate of available water volumes is an efficient approach for simulating the effect of diverse impacts on resources, both natural and/or anthropogenic.

## Acknowledgements

*The authors acknowledge the careful revision of the manuscript by Francani V. and an anonymous Referee.*

## REFERENCES

- AVANZINI M., BERETTA G.P., FRANCANI V. & NESPOLI A. (1995) – *Indagine preliminare sull'uso sostenibile delle falde profonde nella Provincia di Milano*. C.A.P., Consorzio per l'Acqua Potabile, Milano.
- BERETTA G.P., CAVALLIN A., FRANCANI V., MAZZARELLA S. & PAGOTTO A. (1985) – *Primi bilancio idrogeologico della Pianura Milanese*. Acque Sotteranee, nn. 2, 3, 4: pp. 35, (Ed.) Geograph, Segrate, Milano.
- BONOMI T. (2009) – *Database development and 3D modeling of textural variations in heterogeneous, unconsolidated aquifer media: application to the Milan plain*. Computers & Geosciences, 35, 134 – 145. DOI 10.1016/j.cageo.2007.09.006.
- BONOMI T., CANEPA P., DEL ROSSO F. & ROSSETTI A. (2008) – *Relazioni temporali pluridecennali di dati pluviometrici, idrologici e piezometrici nella pianura lombarda tra Ticino e Oglio*. Giornale di geologia applicata, 9 (2), pp. 227-248 ISSN: 1826-1256. doi:10.1474/GGA.2008-02.2-12.0242.
- BONOMI T., CAVALLIN A. & DE AMICIS M. (1995) – *Un database per pozzi: Tangram*. Quaderni Geologia Applicata, suppl. n. 3 1/95: 89-97.
- BONOMI T., CAVALLIN A., FUMAGALLI L. & PELLEGRINI M. (2007) – *Fluvial and fluvioglacial systems in the milan plain*. Mem. Descr. Carta Geol. d'It., 76, 67-78.
- BONOMI T., CAVALLIN A., STELLUTI G. & GUERRA G. (2002) – *3-D subsoil parameterisation in a plan region of North Italy*. Mem. Soc. Geol. It., 57 (2002): 543-550.
- CAVALLIN A., FRANCANI V. & MAZZARELLA S. (1983) – *Studio idrogeologico della pianura compresa tra Adda e Ticino*. Costruzioni, 1983, anno 32, nn. 326, 327, (Ed.) La Fiaccola, Milano: 65-84.
- FLECKENSTEIN J.H., NISWONGER R.G. & FOGG G.E. (2006) – *River-Aquifer Interaction, Geologic Heterogeneity, and Low-Flow Management*. Ground Water, 44(6), 837-852.
- FUMAGALLI L. – *Unsaturated Zone Modelling to Evaluate Groundwater Recharge*, Italian journal of engineering geology and environment, (in stampa).
- GIUDICI M., FOGLIA L., PARRAVICINI G., PONZINI G. & SINCICH B. (2000) – *A quasi three dimensional model of water flow in the subsurface of Milano (Italy): the stationary flow*, Hydrology and Earth System Sciences, 4, 113-124.
- GIUDICI M., PONZINI G., ROMANO, E. & VASSENÀ C. (2003) – *Caso applicativo: studio del flusso idrico sotterraneo nell'area metropolitana milanese con modelli di flusso a diverse scale*. In: R. BRATAN, F. LORUSSO, C. PONTREMOLI & A. SOANA (Eds.): <Modellizzazione applicata alle falde acquifere – bonifica dei siti contaminati e gestione delle risorse idropotabili>. Rapporti GSISR 145 – 05/03: 59-78.
- JARVIS N. (1994) – *The MACRO model (version 3.1). Technical description and sample simulations*. Reports and dissertations 19, Swedish University of Agricultural Sciences, Dept. of Soil Sciences, Uppsala.
- MALLET J.L. (1997) – *Discrete Modeling for Natural Object*. Journal of Mathematical Geology, 29(2): 199-219.
- MALLET J.L. (1992) – *Discrete Smooth Interpolation*. In: *Geometric Modeling Computer Aided Desing*, 24 (4): 177-191.
- MALLET J.L. (2002) – *Geomodeling. Applied Geostatistics*. Oxford University Press.
- MARCHETTI M. (2001) – *Fluvial, fluvioglacial and lacustrine forms and deposits. Illustrative Notes of the Geomorphological Map of the Po Plain*. Suppl. Geogr. Fis. Dinam. Quat., 4 (2001): 73-104.
- MARTIN P.J. & FRIND E.O. (1998) – *Modeling a Complex Multi Aquifer System: The Waterloo Moraine*. Ground Water, 36 (4): 679-690.
- PECK A., GORELICK S., DE MARSILY G., FOSTER S. & KOVALEVSKY V. (1988) – *Consequences of spatial variability in aquifer properties and data limitations for groundwater modeling practice*. IAHS Redbook Series, IAHS Press, Publication no. 175, 272.
- POZZI R. & FRANCANI V. (1981) – *Condizioni di alimentazione dalle riserve idriche del territorio milanese*. Estratto da: *Vie e trasporti*. La rivista della strada (Ed.), La Fiaccola, Milano anno XLIX, 467 – 470.
- PROVINCIA DI MILANO & POLITECNICO DI MILANO (1995) – *Le risorse idriche sotterranee nella Provincia di Milano*, 1: *Lineamenti idrogeologici*, pp. 128, Provincia di Milano.
- PROVINCIA DI MILANO (2001) – *La base dell'acquifero tradizionale*. Quaderni Direzione Centrale Ambiente, pp. 23, Provincia di Milano.
- REGIONE LOMBARDIA & ENI-DIVISIONE AGIP (2002) – *Geologia degli acquiferi padani della Lombardy Region*, CARCANO C. & A. PICCIN (Eds.), S.E.L.C.A., Firenze.
- REGIONE LOMBARDIA (2006) – *Usi e tutela delle acque in Lombardia. Linee strategiche, pianificazione e regole per un utilizzo razionale e sostenibile della risorsa*.

## A Google Map mashup for hydrogeochemical data of Emilia-Romagna Region

*Un Google map Mashup per i dati idrogeochimici della Regione Emilia-Romagna*

BONZI L. (\*), MARTINELLI G. (\*\*), SCIUTO P.F. (\*)

**ABSTRACT** - The present paper illustrates the Web 2.0 technology for the presentation of analytical data and results of the speciation calculation in groundwaters of the plain area of Emilia-Romagna region. Geographic data are viewed by means of a Web-GIS based application with Google map mashup technology, utilizing the functions offered by WEB 2.0. technology. The information content, consisting of hydrogeochemical data collected within the SINA (National Environmental Information System) network, while demanding in terms of IT resources, is nonetheless easily accessible. The dataset, comprising chemical analyses and speciation calculations, represents one of the few examples of data elaboration pertaining to sedimentary environments. The data is made available on the web in kmz format.

**KEY WORDS:** G.I.S, Google Map, hydrogeochemistry, KMZ, Emilia Romagna

**RIASSUNTO** - Il presente lavoro illustra la tecnologia Web 2.0 utilizzata per la rappresentazione dei dati analitici e dei risultati del calcolo di speciazione nelle acque sotterranee della zona di pianura della Regione Emilia-Romagna. I dati geografici sono stati messi su internet per mezzo di un Web-GIS, applicazione basata su tecnologia mashup con Google map, che utilizza le funzionalità offerte dalla tecnologia Web 2.0. Il contenuto informativo, costituito da dati idrogeochimici raccolti nell'ambito della rete SINA (Sistema Informativo Nazionale Ambientale), pur essendo esigente in termini di risorse IT, risulta comunque facilmente accessibile. Il set di dati, che comprende le analisi chimiche e calcoli di speciazione, rappresenta uno dei pochi esempi di elaborazione dati relativi agli ambienti sedimentari. I dati del sistema informativo Web 2.0 adottano il formato KMZ.

**PAROLE CHIAVE:** G.I.S, Google Map, Idrogeologia, KMZ, Emilia Romagna

### 1. - INTRODUCTION

The computer technology for the representation of geochemical data in a Web-GIS environment which began to appear at the end of the '90s, has to date developed in two different directions: chronologically, the first utilized standard proprietary products, while the second more recent technology availed of Open Source technology (i.e. WILLIAMS S., 2002). Looking at the cost/advantages relationship, proprietary products offer higher reliability and costs, while Open Source technology (i.e. openlayer, mapserver) requires greater investments in human resources. Both, in any case, require significant investments in terms of hardware (data and web servers, firewalls, etc.) and suitable premises for the necessary infrastructure. In more recent times (2005) the appearance of Web 2.0 has enabled a new approach which does not use specific hardware for network data management, instead using services offered virtually free of charge by Web 2.0 for storing, viewing and managing information, thus enhancing the investment in human resources. An additional benefit is that this latest approach is unaffected by physiological ageing of hardware technology; on the contrary the volume of data and management methods become through Web 2.0 progressively more efficient and effective. This present work has the dual purpose of studying Emilia Romagna

(\*) Regione Emilia-Romagna, Servizio Geologico, Sismico e dei Suoli, viale Silvani, 4/3, 40122 Bologna, Italy.

(\*\*) ARPA Emilia-Romagna, via Amendola 2, 42100 Reggio Emilia, Italy.



groundwater, applying in these speciation calculations with a view to studying the protection of aquifers, and, from a computational point of view, in consideration of the large volume of data processed, the possibility of using Web 2.0 technology for presenting results and maps in G.I.S..

## 2. - GEOCHEMISTRY

### 2.1. - THE UTILIZED DATA SET

Adopting a G.I.S approach, 395 wells characterized by depth in the range 60-400 m and by the presence of one filter only along the well tube were selected. The adopted criteria allows reliable representativity of groundwater geochemistry for mainly non-phreatic aquifers hosted in the Emilia-Romagna plain sediments. Each well has been sampled and analyzed for chemical and isotopic purposes. Available information allowed us to identify the hydrostratigraphic (REGIONE EMILIA-ROMAGNA-ENI, AGIP, 1998) localization of each well. In this way both hydrostratigraphic and technical characteristics may reduce uncertainties in geochemical data interpretation. Thus mineral-chemical equilibrium of groundwaters has been studied. The package adopted for the database and G.I.S mapping was ESRI ArcGis 9.2.

### 2.2. - DATA ELABORATION: SPECIATION CALCULATION

Speciation calculations were applied to the chemical analyses of 395 wells. This represents the most effective method for determining conditions of chemical equilibrium in aquifers. As established, for this type of data elaboration, for the dissolution of the mineral phase  $m$ , present in a rock, we consider the activity quotient  $Q_m$  expressed by the relationship

$$Q_m = \prod_i \frac{\alpha_{i,m}^{v_{i,m}}}{\alpha_m}$$

where  $\alpha_{i,m}$  is the activity and  $v_{i,m}$  is the stoichiometric coefficient of the mineral phase.

The free energy  $\Delta G$ , of the chemical reaction associated with the dissolution of the solid species is given by

$$\Delta G_m = \Delta G_{m,r}^0 + RT \ln Q_m$$

in conditions of equilibrium  $\Delta G_m = 0$

Since the relationship between the free energy of a standard partial molar reaction and the equilibrium constant  $K_m$  is

$$\ln K_m = \frac{\Delta G_{m,r}^0}{RT}$$

it follows that  $Q_m = K_m$  and  $\log \left( \frac{Q_m}{K_m} \right) = 0$  in

conditions of equilibrium. Conditions  $\log \left( \frac{Q_m}{K_m} \right) < 0$  and  $\log \left( \frac{Q_m}{K_m} \right) > 0$  correspond to conditions of

below and above saturation respectively for the phase examined. The general preference is to use  $\mathcal{S} = \log(Q/K)$  or the saturation index to indicate the state of equilibrium of the phase (i.e. REED & SPYCHER, 1984).

For the speciation calculation, the package SOLMIN.88PC/Shell (KHARAKA *et alii*, 1988; TALMAN, 1992) was adopted.

The large volume of data generated by the calculation is in itself a problem in terms of transfer and organization within a database. To computerize this procedure, an application called Chipmunk (fig. 1) was created in Microsoft Access: this enables the optimization of the procedure and slims down the data transfer process. A macro excel procedure enables spreadsheet data to be transformed into an input file for SOLMIN88. The package generates a verbose output of equilibria of solid phases and aqueous species which needs to be rearranged as records for a database. Chipmunk enables this process.

### 2.3. - SPECIATION RESULTS

The speciation calculation highlighted several unique characteristics of the sedimentary basins and revealed the limitations of this type of calculation. From a geochemical point of view, the sedimentary basins are significantly conditioned by the presence of clay and sand. From a mineralogical point of view, this is evident for types of mineral phases approaching equilibrium and aqueous species involved. The speciation calculation was therefore repeated in the case of variations in pH and Eh conditions so as to highlight the behaviour of water in conditions of water stress and/or in proximity to the coast with sea water ingress. The results allow us to describe hypothetical situations and therefore have a purely speculative value. In any case, the fact that the study focuses on wells of the SINA network, which are large-scale abstraction wells, highlights the fact that the chemical composition represents an average value based on the surrounding area; consequently this value cannot be used specifically, unless to pinpoint areas affected by certain processes and/or evolutive behavior.

For this reason the data was represented using two methods: a vector method, referring to the specific sampling point, and a range method using Thiessen polygons that extrapolate the punctual information to a surrounding area. THIESSEN (1911) polygons mathematically defined by the perpendicular bisectors of the lines between all



Fig. 1 - Chipmunk (Microsoft Access application): in the background main mask of the application, on right resulting tables.  
 - *Chipmunk* (applicazione in Microsoft Access): sullo sfondo maschera principale dell'applicazione, a destra le tabelle risultanti.

points, define individual areas of influence around each of a set of points. Thus, in terms of both the quantity and granularity of information generated, the cartographic representation of geochemical information is specifically suited to a G.I.S oriented environment. Geochemical evidence from speciation calculations confirms expected results.

The examples reported in figure 2 are a sort of paradigm of significance to the approach: both illustrate features of geology of Emilia-Romagna. Figure 2a represents the equilibrium condition of halite resulting from leaching phenomena by sediments enriched in marine ions and by possible saline intrusion phenomena. Figure 2b describes  $\text{SO}_4^{2-}$  abundance chiefly mobilized from evaporitic deposits of the Apennines and sometimes attributable to pollution phenomena.

The origin of halitic and evaporitic bearing groundwater in the Po sedimentary basin was reviewed by REGIONE EMILIA-ROMAGNA, ENI-AGIP (1998), by MARTINELLI *et alii* (1998) and by CONTI *et alii* (2000). Representation tools allow further control of geochemical data and multiply interpretative options.

## 2.4. - DATABASE MANAGEMENT

The obtained results were imported into the database of the Geological Survey of Emilia Romagna-Region and, purely as a prototype, a portion of the latter became part of a Google map mashup in order to explore the full potential of WEB 2.0.

Data available for Mashup were generated adopting KML format. The conversion the G.I.S package and KMZ (KML compressed) format was realized using the free package SHP2KML ([www.zonums.com](http://www.zonums.com)). This software allows the conversion from ESRI shapefile format to KML, a specific XML Google format for geographic information. KMZ files were stored on a Web 2.0 free area. This procedure has been adopted instead of a traditional client-server approach that entails the presence of a server and the activation of WMS (Web Map Service) for information management raster and/or WFS (Web Feature Service) to allow server and client dialogue.

This approach delivers easier data streaming on the net but can be critical with large dimension KMZ files.

This criticality was tested with the significant amount of hydrogeochemical data analysis and speciation results studied.

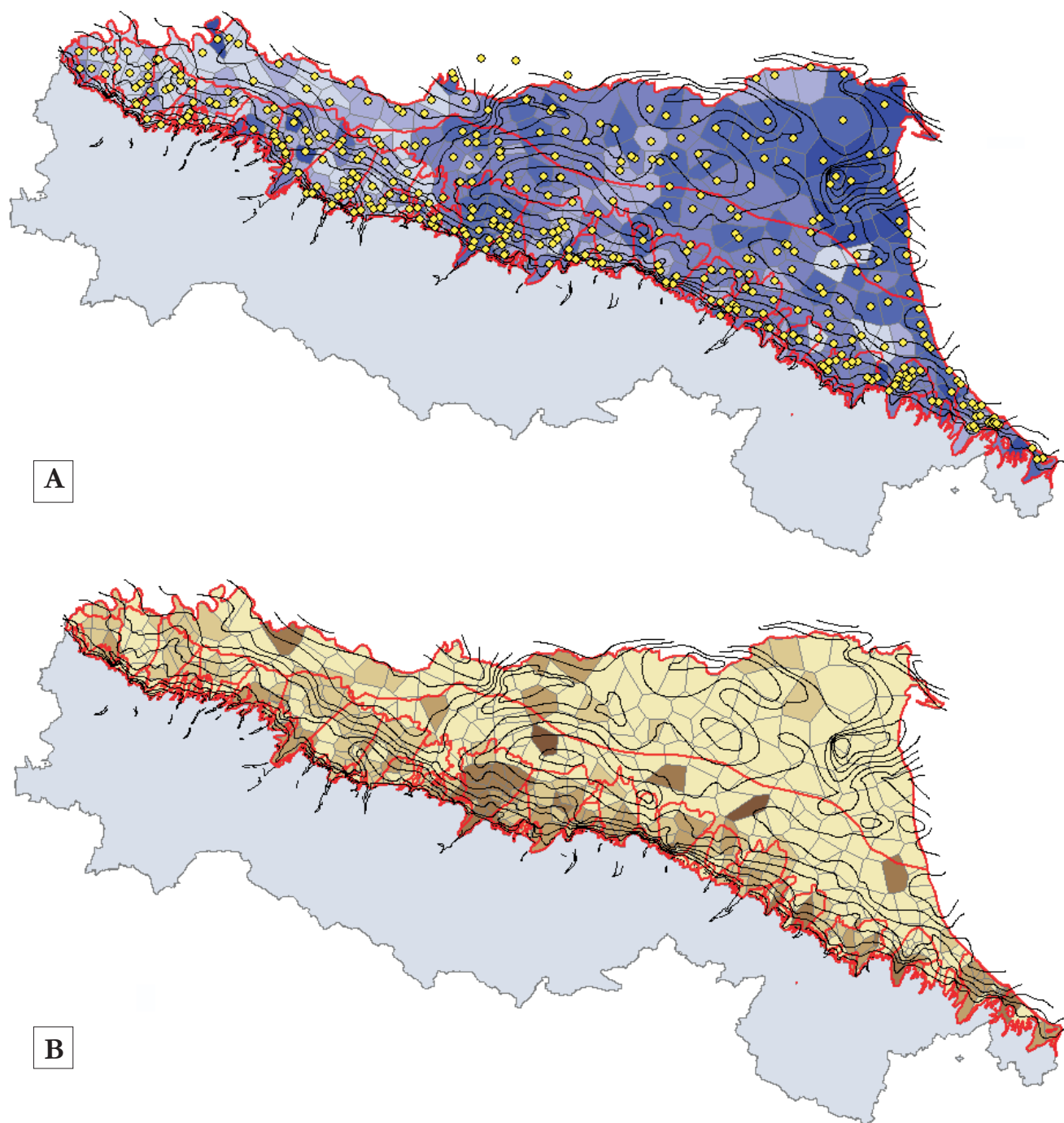


Fig. 2 - Speciation map results from SOLMIN88 (A) equilibria conditions ( $\log Q/K$ ) for halite solid phase (B) abundance of  $\text{SO}_4=$  specie. The gradation of colours in both figures indicates in the case of darker values, areas close to equilibrium while light colours are more distant.  
 - Mappe che illustrano i risultati della speciazione con SOLMIN88 (A) le condizioni di equilibrio ( $\log Q/K$ ) per la fase solida Halite (B) abbondanza della specie  $\text{SO}_4=$ . La gradazione dei colori in entrambe le mappe indicano con i valori più scuri, le aree prossime all'equilibrio, mentre i colori chiari le aree distali.

### 3. - WEB 2.0

#### 3.1. - WEB 2.0 TECHNOLOGY: AN INTRODUCTION

The term “Web 2.0” was coined by DI NUCCI (1999) to describe web development and web design that facilitates interactive information sharing, interoperability, user-centered design and collaboration on the World Wide Web. In essence, while

the traditional World Wide Web (retroactively referred to as Web 1.0) is based simply on availability of data from different sources, Web 2.0 allows utilization of resources and applications built specifically for collaborative purposes among Internet users and other users, content providers and enterprises. The Google search engine was a forerunner of these technologies first with an online translator and later with google docs (spreadsheet,



word editor) on line. A myriad of applications were subsequently built with programming languages such as Ajax and Ruby, specific for interoperability. There is no precise boundary that separates Web 1.0 from Web 2.0. but rather, a sort of progressive migration. One of the earliest Web 2.0 applications implemented in the geological geochemical field was the site created by <http://isobordat.jimdo.com/> Andreani, Adorni-Braccesi, Pennisi, Sciuto in 2007 when a collection of literature relating to isotopes of boron was managed entirely on the web adopting a free provider ([www.jimdo.com](http://www.jimdo.com)). In this case, database functionalities were encapsulated from [www.zoho.com](http://www.zoho.com), a suite of web-based programmes for small applications. The introduction of this technology grants numerous advantages in terms of saving resources, time and costs. It does not require specific hardware or operating systems, or people dedicated solely to the maintenance of the IT structure and there is no need to have dedicated server and firewall areas.

### 3.2. - GOOGLE MAP MASHUP

Mashup is a Web application that combines data or functionality from two or more sources into a single integrated application, hence realization of this Web 2.0 product requires familiarity with HTML, JavaScript, and the structure of Google API. The most common types of mashup use cartographic data from Google Maps, creating a new and distinct Web service not originally provided by either source (i.e. BROWN, 2006). Figure 3 illustrates the simple Google mashup proposed (the appendix details the source code). It is an AIO (all in one) application because it includes all the code necessary for its working in a single listing without external routines. The data are located on a Web 2.0 server in the Google kmz format and can be made available with a pop-up menu in the figure at the top right hand side. Viewing mode is full screen in order to offer maximum map area. We can see (also in figure 3) the controls for positioning (top left), place name search (bottom left), general view (bot-

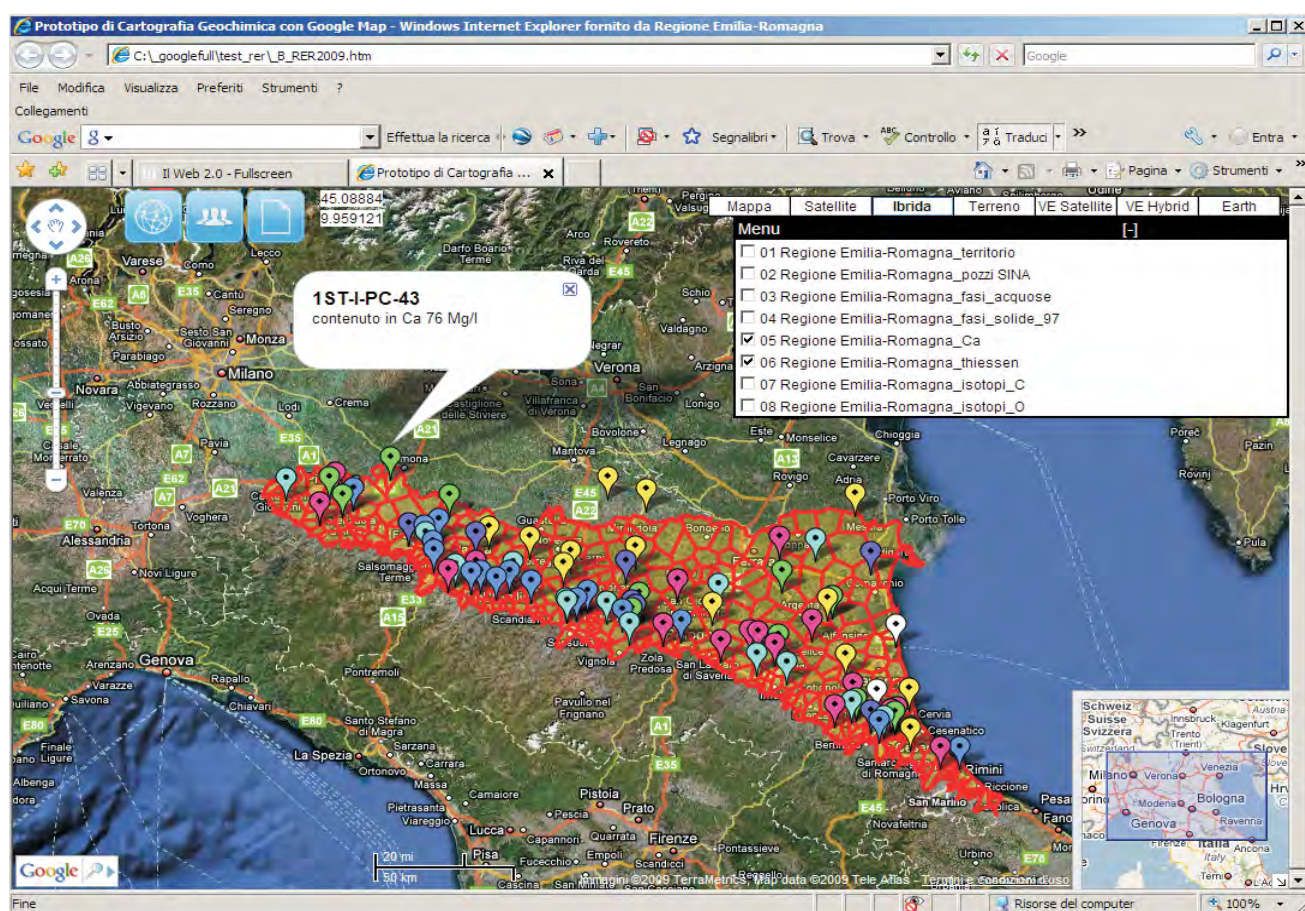


Fig. 3 - On top left: zoom controls of google map and hyperlink buttons to other applications, pages and pdf documents. On bottom left place name search. On top right management of google maps, google earth for google map, Virtual Earth controls and management of information layers with popup menus. On bottom right: general view map control.

- In alto a sinistra: controlli di zoom della mappa di Google e pulsanti di collegamento ad altre applicazioni, pagine e documenti PDF. In basso a sinistra Ricerca nome della località. In alto a destra: gestione di Google Maps, Google Earth per google map, Virtual Earth controlli e la gestione dei strati di informazioni con i menu popup. In basso a destra il controllo generale mappa.

tom right) and map (top right). The popup menu, together with the 3 buttons at the top right and the controls for the Microsoft Virtual Earth map (rival Google Map product) constitute the personalization available in this current prototype.

The prototype can be viewed with main browsers currently in use (Microsoft Explorer 7, Opera 9, Firefox 3, Google Chrome). The accuracy of the positioning of points resulting from the adopted map type and the degree of precision cannot in any case reflect the exact position attainable with commercial products. Nonetheless, discrepancies are being reduced thanks to progressive technological alignment of tools. Access to data is sufficiently rapid but depends in any case on available bandwidth. The mashup source code is detailed in the appendix.

#### 4. - DISCUSSION AND CONCLUSIONS

Hydrogeochemical data and speciation calculations for the 395 SINA network wells represented an excellent opportunity for studying groundwaters located in sedimentary basins and testing the potential of Web 2.0 for cartographic purposes.

The Thiessen approach constitutes an opportune representation of geochemical information because intrinsically it denotes information and its limitations. The volume of data elaborated provides a further boost to the already vast amount of geochemical information available in the Emilia-Romagna region. The provisional approach, considering not only measured pH Eh but also proximal range conditions, allows us to hypothesize different scenarios, emphasizing possible critical aspects of the hydrological environment. The use of Web 2.0 and Google mashup for viewing IT system data represents an increasingly valid alternative for the distribution of data within the technological network. In particular, we have observed that for functional management of the mashup with a network speed of 100 Mbps, the optimum size of each kmz files must be less than 1 Mb. Considering that the Google Map mashup has a size of 16 Kb and the total amount of all data is approximately 3 Mb (10 layers), data streaming is fluid. As regards data administration, the kmz format consists of layered information, so it does not

have the peculiarities of geodatabase which not support structured queries. This physiological limit, the result of a disproportionate use of KML standard for multitemporal meteorological data management, would appear to be circumvented by the imminent introduction of new Google API which allows greater flexibility. The chance to combine geochemical study with Web 2.0 proved to be a significant experiment, heralding new prospects for representation of geochemical, petrographic and geological data with low costs and high usability, making it a highly promising technology. Further technical data applications and source codes are available at the address <http://sciuto.yolasite.com>.

#### Acknowledgements

*The Authors acknowledge the careful revision of the manuscript by Antonio Longinelli and a second anonymous Referee.*

#### REFERENCES

- BROWN M.C. (2006) - *Hacking Google® Maps and Google® Earth*. pp. 408 Wiley Publishing, Inc. Hoboken, NJ, USA.
- CONTI A., SACCHI E., CHIARLE M., MARTINELLI G. & ZUPPI G.M. (2000) - *Geochemistry of the formation waters in the Po Plain (Northern Italy): an overview*. Applied Geochemistry, **15**: 51-65.
- DI NUCCI D. (1999) - *Fragmented Future*. Print, **53**: 32.
- KHARAKA Y.K. GUNTER. W.D., AGGARWAL P.K., PERKINS E.H. & DE BRAAL J.D. (1989) - *SOLMINEQ.88: a computer program for Geochemical Modelling Water-rock Interactions*. pp. 157, U.S. Geological Survey Water-Resources Investigations Report N° 88-4227, 420 pp.
- MARTINELLI G., MINISALE A. & VERRUCCHI C. (1998) - *Geochemistry of heavily exploited aquifers in the Emilia-Romagna region, Po Valley, northern Italy*. Environmental Geology. **36**: 195-206.
- REED M. & SPYCHER N. (1984) - *Calculation of pH and mineral equilibria in hydrothermal waters with application to geothermometry and studies of boiling and dilution*. Geochim. Cosmochim. Acta, **48**: 1479-1492.
- REGIONE EMILIA-ROMAGNA, ENI & AGIP (1998) - *Riserve idriche sotterranee della Regione Emilia-Romagna*. DI DIO G. (Ed.), Regione Emilia-Romagna - ENI & AGIP, pp. 120, S.E.L.C.A., Firenze.
- TALMAN S. (1992) - *User Manual for SOLMINEQ.88PC/Shell*. 250 pp. Alberta, Canada
- THIESSEN A.H. (1911) - *Precipitation averages for large areas*. Monthly Weather Review. **39**: 1082-1084
- WILLIAMS S. (2002) - *Free as in Freedom. Richard Stallman's crusade for free software*. O'Reilly Media, pp. 179, Inc. Sebastopol, CA, USA.



## APPENDIX – MASHUP CODE

```

<!DOCTYPE html PUBLIC "-//W3C//DTD XHTML 1.0 Strict//EN"
    "http://www.w3.org/TR/xhtml1/DTD/xhtml1-strict.dtd">
<html xmlns="http://www.w3.org/1999/xhtml">
<head>
<meta http-equiv="content-type" content="text/html; charset=UTF-8"/>
<title>Prototipo di Cartografia Geochimica con Google Map</title>
<script src="http://maps.google.com/maps?file=api&v=2.x&key=xxxxx"
    type="text/javascript"></script>
<!--<script src="java.js" type="text/javascript"></script>-->
<script type="text/javascript">
var ie4 = false; if(document.all) { ie4 = true; }
function getObject(id) { if (ie4) { return document.all[id]; } else { return document.getElementById(id); } }
function toggle(link, divId) { var lText = link.innerHTML; var d = getObject(divId);
if (lText == '+' ) { link.innerHTML = '-'; d.style.display = 'block'; }
else { link.innerHTML = '+'; d.style.display = 'none'; } }
</script>
<!-- flooble Expandable Content header end -->
<!-- Make the document body take up the full screen -->
<style type="text/css"> v\:* {behavior:url(#default#VML);} html, body {width: 100%; height: 100%;}
body {margin-top: 0px; margin-right: 0px; margin-left: 0px; margin-bottom: 0px;}
</style></head><body>
<!-- Declare the div, make it take up the full document body -->
<div id="map" style="width: 100%; height: 100%;"></div>
<div style="top:25px; left:600px; position:absolute; background-color:white; border:2px solid black;">
<table border="0" cellspacing="0" cellpadding="2" width="100%" style="background: #000000; color:
    #FFFFFF;FONT-FAMILY: arial;font-size:14px">
<tr><td>Menu</td><td align="left">
[<a title="show/hide" id="exp1231839082_link" href="javascript: void(0);" onclick="toggle(this,
    'exp1231839082');" style="text-decoration: none; color: #FFFFFF; ">-</a>]</td></tr></table>
<div id="exp1231839082" style="padding: 0px;FONT-FAMILY: arial;font-size:12px;">
<input type="checkbox" id="box1" onclick="boxclick01(this,'geolog')"/>01
    Regione Emilia-Romagna_pianura_schema_semplificato<br />
<input type="checkbox" id="box1" onclick="boxclick02(this,'kmzC97')"/>02 vuoto<br />
<input type="checkbox" id="box1" onclick="boxclick03(this,'kmzA97')"/>03 vuoto<br />
<input type="checkbox" id="box1" onclick="boxclick04(this,'kmzS97')"/>04 vuoto<br />
<input type="checkbox" id="box1" onclick="boxclick05(this,'kmzC98')"/>05 vuoto<br />
<input type="checkbox" id="box1" onclick="boxclick06(this,'kmzA98')"/>06 vuoto<br />
<input type="checkbox" id="box1" onclick="boxclick07(this,'kmzS98')"/>07 vuoto<br />
<input type="checkbox" id="box1" onclick="boxclick08(this,'kmzI98')"/>08 vuoto<br />
<input type="checkbox" id="box1" onclick="boxclick09(this,'ceolog')"/>09
    Regione Emilia-Romagna_anomalie_regionali<br />
<input type="checkbox" id="box1" onclick="boxclick10(this,'cmzC97')"/>10 vuoto<br />
<input type="checkbox" id="box1" onclick="boxclick11(this,'cmzA97')"/>11 vuoto<br />
<input type="checkbox" id="box1" onclick="boxclick12(this,'cmzS97')"/>12 vuoto<br />
<input type="checkbox" id="box1" onclick="boxclick13(this,'cmzC98')"/>13 vuoto<br />
<input type="checkbox" id="box1" onclick="boxclick14(this,'cmzA98')"/>14 vuoto<br />
<input type="checkbox" id="box1" onclick="boxclick15(this,'cmzS98')"/>15
    Regione Emilia-Romagna_Isotopia_pioggia<br />
<input type="checkbox" id="box1" onclick="boxclick16(this,'cmzI98')"/>16 vuoto<br />
<input type="checkbox" id="box1" onclick="boxclick17(this,'geolot')"/>17 vuoto<br />
<input type="checkbox" id="box1" onclick="boxclick18(this,'kmlC97')"/>18 vuoto<br />
<input type="checkbox" id="box1" onclick="boxclick19(this,'kmlA97')"/>19 vuoto<br />
<input type="checkbox" id="box1" onclick="boxclick20(this,'kmlS97')"/>20 vuoto<br />
<input type="checkbox" id="box1" onclick="boxclick21(this,'kmlC98')"/>21 vuoto<br />
<input type="checkbox" id="box1" onclick="boxclick22(this,'kmlA98')"/>22
    Regione Emilia-Romagna_grafici_a_torta <br />
<input type="checkbox" id="box1" onclick="boxclick23(this,'kmlS98')"/>23
    Regione Emilia-Romagna_grafici_a_barre<br />

```



```

<input type="checkbox" id="box1" onclick="boxclick24(this,'kmlI98')"/>24
    Regione Emilia-Romagna_grafici_a_cruscotto<br />
</div></div>
<!-- flooble Expandable Content box start -->
<div style="border: 1px solid #000000; padding: 0px; background: #EEEEEE;">
<table border="0" cellspacing="0" cellpadding="2" width="100%" style="background: #000000; color:
    #FFFFFF;">
<script language="javascript">toggle(getObject('exp1231839082_link'),'exp1231839082');</script>
</td></tr>
</table>
<noscript><b>JavaScript must be enabled in order for you to use Google Maps.</b>
However, it seems JavaScript is either disabled or not supported by your browser.
To view Google Maps, enable JavaScript by changing your browser options, and then
try again.
</noscript>
<script type="text/javascript">
//<![CDATA[
//virtual earth tiles
var msnVeTileA = function(a, b){
var sTile = '000000';
sTile += (parseInt(a.y.toString(2) * 2) +
parseInt(a.x.toString(2)));
sTile = sTile.substring(sTile.length - b, sTile.length);
s = 'http://a'
s += sTile.substring(sTile.length-1, sTile.length);
s += '.ortho.tiles.virtualearth.net/tiles/a'
s += sTile;
s += '.jpeg?g=1';
return s; };
//virtual earth tiles
//http://h0.ortho.tiles.virtualearth.net/tiles/h2100102010.jpeg?g=1
var msnVeTileH = function(a, b){
var sTile = '000000';
sTile += (parseInt(a.y.toString(2) * 2) +
parseInt(a.x.toString(2)));
sTile = sTile.substring(sTile.length - b, sTile.length);
s = 'http://h'
s += sTile.substring(sTile.length-1, sTile.length);
s += '.ortho.tiles.virtualearth.net/tiles/h'
s += sTile;
s += '.jpeg?g=1';
return s; };
//virtual earth oblique
var msnVeTileO = function(a,b){
var sTile = '000000';
sTile += (parseInt(a.y.toString(2) * 2) + parseInt(a.x.toString(2)));
sTile = sTile.substring(sTile.length - b, sTile.length);
s = 'http://c'
s += sTile.substring(sTile.length-1, sTile.length);
s += '.ortho.tiles.virtualearth.net/tiles/h'
s += sTile;
s += '.jpeg?g=77';
return s; }
//virtual earth tiles
var msnLayerA = new GTileLayer(new GCopyrightCollection(""),1,17);
msnLayerA.getTileUrl = msnVeTileA;
msnLayerA.getCopyright = function(a,b) {return 'MSN Virtual Earth';}
var msnLayerH = new GTileLayer(new GCopyrightCollection(""),1,17);
msnLayerH.getTileUrl = msnVeTileH;
msnLayerH.getCopyright = function(a,b) {return 'MSN Virtual Earth';}
//end virtual earth tiles

```

```

var map;
function doGenerateMarkerHtmlCallback(marker,html,result) {
html.innerHTML+="<b>Result Coordinates: "+result.lat+" "+result.lng+"</b><br>";
html.innerHTML+="<b>Marker Location: "+marker.getLatLng().toUrlValue()+"</b>";
return html;}
if (GBrowserIsCompatible()) {
map = new GMap2(document.getElementById("map"),{googleBarOptions:
{onGenerateMarkerHtmlCallback:doGenerateMarkerHtmlCallback}});
//{googleBarOptions:
//{onGenerateMarkerHtmlCallback:doGenerateMarkerHtmlCallback}
//});
map.setCenter(new GLatLng(44.310038, 11.040072), 8);
GEvent.addListener(map, 'click', function(overlay, point) {
if (point) {
document.getElementById('lat').innerHTML = "lat: "+point.y;
document.getElementById('long').innerHTML = "long: "+point.x; }});
GEvent.addListener(map, 'click', function(overlay) {
if (overlay) {
if (overlay instanceof GMarker) {
var point=overlay.getLatLng();
document.getElementById('lat').innerHTML = point.lat();
document.getElementById('long').innerHTML = point.lng();}}});
map.addControl(new GLargeMapControl3D());
map.addControl(new GMapTypeControl());
var topRight = new GControlPosition(G_ANCHOR_BOTTOM_LEFT, new GSize(300,7));
map.addControl(new GScaleControl(), topRight);
map.setMapType(G_SATELLITE_MAP);
map.addMapType(G_PHYSICAL_MAP);
map.setMapType(G_HYBRID_MAP);
var msnMapA = new GMapType([msnLayerA], G_SATELLITE_MAP.getProjection(), 'VE Satellite', {errorMessage:""});
var msnMapH = new GMapType([msnLayerH], G_SATELLITE_MAP.getProjection(), 'VE Hybrid',{errorMessage:""});
map.addMapType(msnMapA);
map.addMapType(msnMapH);
map.addMapType(G_SATELLITE_3D_MAP);
map.enableScrollWheelZoom();
map.enableContinuousZoom();
map.addControl(new GOverviewMapControl(new GSize(180,180)));
map.enableGoogleBar();
map.getDragObject().setDraggableCursor("crosshair");
var geolog = new GGeoXml("http://sciuto.yolasite.com/resources/xpianura_schema_semplificato.kmz");
var kmzC97=new GGeoXml("http://sciuto.yolasite.com/resources/vuoto");
var kmzA97=new GGeoXml("http://sciuto.yolasite.com/resources/vuoto");
var kmzS97=new GGeoXml("http://sciuto.yolasite.com/resources/vuoto");
var kmzC98=new GGeoXml("http://sciuto.yolasite.com/resources/vuoto");
var kmzA98=new GGeoXml("http://sciuto.yolasite.com/resources/vuoto");
var kmzS98=new GGeoXml("http://sciuto.yolasite.com/resources/vuoto");
var kmzI98=new GGeoXml("http://sciuto.yolasite.com/resources/vuoto");
var ceolog=new GGeoXml("http://sciuto.yolasite.com/resources/xanomalie_regionali.kmz");
var cmzC97=new GGeoXml("http://sciuto.yolasite.com/resources/vuoto");
var cmzA97=new GGeoXml("http://sciuto.yolasite.com/resources/vuoto");
var cmzS97=new GGeoXml("http://sciuto.yolasite.com/resources/vuoto");
var cmzC98=new GGeoXml("http://sciuto.yolasite.com/resources/vuoto");
var cmzA98=new GGeoXml("http://sciuto.yolasite.com/resources/vuoto");
var cmzS98=new GGeoXml("http://sciuto.yolasite.com/resources/xIsotopia_pioggia.kmz");
var cmzI98=new GGeoXml("http://sciuto.yolasite.com/resources/vuoto");
var geolot=new GGeoXml("http://sciuto.yolasite.com/resources/vuoto");
var kmlC97=new GGeoXml("http://sciuto.yolasite.com/resources/vuoto");
var kmlA97=new GGeoXml("http://sciuto.yolasite.com/resources/vuotoz");
var kmlS97=new GGeoXml("http://sciuto.yolasite.com/resources/vuoto");

```

```

var kmlC98=new GGeoXml("http://sciuto.yolasite.com/resources/vuoto");
var kmlA98=new GGeoXml("http://sciuto.yolasite.com/resources/torta.kmz");
var kmlS98=new GGeoXml("http://sciuto.yolasite.com/resources/quadrato.kmz");
var kmlI98=new GGeoXml("http://sciuto.yolasite.com/resources/cruscotto.kmz");
// display a warning if the browser was not compatible
else {alert("Sorry, the Google Maps API is not compatible with this browser");}
function doGenerateMarkerHtmlCallback(marker,html,result) {
html.innerHTML+="<b>Result Coordinates: "+result.lat+" "+result.lng+"</b><br>";
html.innerHTML+="<b>Marker Location: "+marker.getLatLng().toUrlValue()+"</b>";
return html;}
function showCoordinates(x, y) {
var coords = document.getElementById("_coords");
var google_map = document.getElementById("wmsMap");
google_map.appendChild(coords);
coords.style.zIndex = 100;
coords.style.position = 'absolute';
coords.style.top = y + "px";
coords.style.left = x + "px";
coords.style.visibility = 'visible'; }
function updateCoordinates(lon, lat) {var coords = document.getElementById("_coords");
coords.innerHTML = "Lon: " + lon + "&deg;W Lat: " + lat + "&deg;N"; }
function boxclick01(box,kml){if (box.checked){map.addOverlay(geolog);} else {map.removeOverlay(geolog);}}
function boxclick02(box,kml){if (box.checked){map.addOverlay(kmzC97);} else {map.removeOverlay(kmzC97);}}
function boxclick03(box,kml){if (box.checked){map.addOverlay(kmzA97);} else {map.removeOverlay(kmzA97);}}
function boxclick04(box,kml){if (box.checked){map.addOverlay(kmzS97);} else {map.removeOverlay(kmzS97);}}
function boxclick05(box,kml){if (box.checked){map.addOverlay(kmzC98);} else {map.removeOverlay(kmzC98);}}
function boxclick06(box,kml){if (box.checked){map.addOverlay(kmzA98);} else {map.removeOverlay(kmzA98);}}
function boxclick07(box,kml){if (box.checked){map.addOverlay(kmzS98);} else {map.removeOverlay(kmzS98);}}
function boxclick08(box,kml){if (box.checked){map.addOverlay(kmzI98);} else {map.removeOverlay(kmzI98);}}
function boxclick09(box,kml){if (box.checked){map.addOverlay(ceolog);} else {map.removeOverlay(ceolog);}}
function boxclick10(box,kml){if (box.checked){map.addOverlay(cmzC97);} else {map.removeOverlay(cmzC97);}}
function boxclick11(box,kml){if (box.checked){map.addOverlay(cmzA97);} else {map.removeOverlay(cmzA97);}}
function boxclick12(box,kml){if (box.checked){map.addOverlay(cmzS97);} else {map.removeOverlay(cmzS97);}}
function boxclick13(box,kml){if (box.checked){map.addOverlay(cmzC98);} else {map.removeOverlay(cmzC98);}}
function boxclick14(box,kml){if (box.checked){map.addOverlay(cmzA98);} else {map.removeOverlay(cmzA98);}}
function boxclick15(box,kml){if (box.checked){map.addOverlay(cmzS98);} else {map.removeOverlay(cmzS98);}}
function boxclick16(box,kml){if (box.checked){map.addOverlay(cmzI98);} else {map.removeOverlay(cmzI98);}}
function boxclick17(box,kml){if (box.checked){map.addOverlay(geolot);} else {map.removeOverlay(geolot);}}
function boxclick18(box,kml){if (box.checked){map.addOverlay(kmlC97);} else {map.removeOverlay(kmlC97);}}
function boxclick19(box,kml){if (box.checked){map.addOverlay(kmlA97);} else {map.removeOverlay(kmlA97);}}
function boxclick20(box,kml){if (box.checked){map.addOverlay(kmlS97);} else {map.removeOverlay(kmlS97);}}
function boxclick21(box,kml){if (box.checked){map.addOverlay(kmlC98);} else {map.removeOverlay(kmlC98);}}
function boxclick22(box,kml){if (box.checked){map.addOverlay(kmlA98);} else {map.removeOverlay(kmlA98);}}
function boxclick23(box,kml){if (box.checked){map.addOverlay(kmlS98);} else {map.removeOverlay(kmlS98);}}
function boxclick24(box,kml){if (box.checked){map.addOverlay(kmlI98);} else {map.removeOverlay(kmlI98);}}
//]]> </script>
<a target=new href='http://pfsciuto.googlepages.com/Gis2v5.htm' target='_blank' title='link' style='position: absolute; left: 93px; top: 2px'></a>
<a target=new href='http://www.regione.emilia-romagna.it/geologia' target='_blank' title='authors' style='position: absolute; left: 144px; top: 2px'></a>
<a target=new href='http://www.unisi.it' target='_blank' title='references' style='position: absolute; left: 195px; top: 2px'></a>
<span id="lat" style='position: absolute; left: 256px; top: 2px;font-size:12px;background-color: white;FONT-FAMILY: arial'>lat</span>
<span id="long" style='position: absolute; left: 256px; top: 20px;font-size:12px;background-color: white;FONT-FAMILY: arial'>long</span>
</body> </html>

```



## Hydrogeologic-hydrogeochemical multidisciplinary study of the confined gravelly aquifer in the coastal Pisan Plain between the Arno River and Scolmatore Canal (Tuscany)

*Studio multidisciplinare idrogeologico-geochimico dell'acquifero confinato in ghiaie nella fascia costiera pisana tra il Fiume Arno ed il Canale Scolmatore (Toscana)*

BUTTERI M. (\*), DOVERI M. (\*\*),  
GIANNECCHINI R. (\*\*\*), GATTAI P. (\*)

**ABSTRACT** - The gravelly horizon of the Pisa plain multilayered system, located at a depth between 50 and 100 m below the sea-level and about 10-20 m thick, is a confined aquifer tapped by a large number of wells. It contains a very important water resource for drinking, industrial and irrigable uses, although in some cases the groundwater is of poor quality.

In order to evaluate if in the coastal area between the Arno River and Scolmatore Canal this aquifer is interested by seawater intrusion and to understand the mixing mechanisms with fresh water, a multidisciplinary study was carried out by means of hydrostratigraphic correlations, water level collection and chemical and isotopic analysis. In particular, three on-site surveys were carried out in June and August 2008 and April 2009. In most of the measured points, piezometric values below the sea-level were collected; particularly depressed levels were registered in August 2008 near the coastline in the southern part of the study area (Calambrone zone) and in the internal part to North (S. Piero a Grado zone). Water-wells sampled along the coast, less than 1.5-2 km far from the coastline, show chemical composition and  $\delta^{18}\text{O}\text{‰}$  values indicative of seawater-fresh water mixing. This phenomenon, in agreement with piezometric conditions, is more evident in the southern zone, toward the Scolmatore Canal, where the fraction of salt water, calculated using the mass balance model of Cl, Br and  $\delta^{18}\text{O}\text{‰}$ , is about 7-8%.

Most of the other samples, collected up to 5 km from the coastline, were not interested by seawater; in these cases, groundwater shows the same characteristics found toward the internal part of the Pisa plain, with relatively low TDS and  $\delta^{18}\text{O}\text{‰}$  indicative of recharge average altitudes higher than local altitudes. Only two samples, collected in the North-

East portion near the Arno River, showed chemical and isotopic characteristics indicative of a seawater presence of about 8-9%. In these cases,  $\delta^{18}\text{O}\text{‰}$  values clearly show that the seawater intrusion does not directly occur in the gravelly aquifer, but through the shallow sandy aquifer, which in this zone is in contact with the gravel.

**KEY WORDS:** Hydrochemistry, Hydrogeology, Northern Tuscany, Piezometric condition, Seawater intrusion, Water isotopes.

**RIASSUNTO** - Il livello in ghiaie dell'acquifero multistrato della Pianura di Pisa, che si trova in generale ad una profondità compresa tra 50 e 100 m sotto il livello del mare ed è spesso circa 10-20 m, costituisce un acquifero confinato interessato da numerosi pozzi di emungimento. Esso contiene certamente una delle principali risorse idriche per approvvigionamento idropotabile, industriale e agricolo, sebbene, in diversi casi, l'acqua non sia di ottima qualità.

Al fine di valutare se nell'area costiera pisana meridionale, compresa tra il Fiume Arno e il Canale Scolmatore, tale importante acquifero sia interessato da fenomeni di intrusione marina, nonché per conoscere i meccanismi di miscelazione tra acque dolci e acqua di mare, è stato effettuato uno studio multidisciplinare mediante correlazioni idrostratigrafiche, rilevamento dei livelli piezometrici e analisi chimiche ed isotopiche delle acque. In particolare, sono state effettuate tre campagne di misura (Giugno e Agosto 2008 ed Aprile 2009).

In ciascun punto di misura è stato rilevato il livello piezometrico riferendolo al livello del mare; aree con superficie piezometrica particolarmente depressa sono state rinvenute

(\*) Geologist, external collaborator

(\*\*) Consiglio Nazionale delle Ricerche - Istituto di Geoscienze e Georisorse, Pisa

(\*\*\*) Dipartimento di Scienze della Terra - Università di Pisa

in Agosto 2008 nella parte più meridionale dell'area di studio (zona Calambrone) ed in quella più interna settentrionale (zona S. Piero a Grado). I campioni di acqua raccolti lungo costa, entro 1,5-2 km dalla linea di riva, mostrano composizione chimica e  $\delta^{18}\text{O}\text{‰}$  indicativi di mescolamento tra acque di falda e acqua di mare. Questo fenomeno, in accordo con le osservazioni piezometriche, risulta più marcato nel settore meridionale dell'area, verso il Canale Scolmatore, dove la frazione di acqua salata, valutata usando bilanci di massa di Cl, Br e  $\delta^{18}\text{O}\text{‰}$ , è intorno al 7-8%. La maggior parte degli altri campioni analizzati, raccolti fino a 5 km dalla linea di riva, non è interessata da fenomeni di intrusione marina; in questi casi, le acque sotterranee mostrano le stesse caratteristiche rinvenute nella parte interna della piana di Pisa, con un TDS relativamente basso e valori di  $\delta^{18}\text{O}\text{‰}$  indicativi di quote medie di ricarica maggiori delle quote locali. Soltanto due campioni, raccolti in prossimità dell'Arno nella parte più interna a Nord, mostrano caratteristiche chimiche ed isotopiche attribuibili alla presenza di acqua di mare in percentuali di circa 8-9%. In tali casi, i valori di  $\delta^{18}\text{O}\text{‰}$  mostrano chiaramente che l'intrusione di acqua di mare non avviene direttamente nell'orizzonte ghiaioso, ma attraverso gli acquiferi sabbiosi superficiali, che, in questa zona, sono in contatto diretto con le ghiaie più profonde.

PAROLE CHIAVE: Idrochimica, Idrogeologia, Intrusione marina, Isotopi dell'acqua, Piezometria, Toscana settentrionale.

## 1. - INTRODUCTION

The coastal plains usually represent preferential areas regarding the anthropic, industrial and agricultural settlements. This is due in particular to their easiness of access and transport, the water availability and the fertility of fields. In the world, more than 150 millions of people live below the altitude of 1 m a.s.l. and 250 millions live below the altitude of 5 m a.s.l. (UNESCO, 2007). Moreover, the tourist attitude which usually characterizes the coastal areas causes a significant seasonal increase of the population.

As a consequence, these regions are characterized by strong human pressure, which often lead to the deterioration of the environmental system, and in particular of the water resource. The pollution phenomena as well as the overexploitation of the groundwater cause a progressive qualitative and quantitative worsening of the water store. One of the most recurring effects is the variation of the natural equilibrium between fresh and sea waters, with consequent advancing of the seawater intrusion in the coastal aquifers (CUSTODIO, 2002). Recent studies (ERICSON *et alii*, 2006) moreover show that in many coastal regions in the world this process is accentuated by sea-level rise (up to 12.5 mm per year), mainly caused by a reduction of the supply of solid materials from the rivers (WALLING & FANG, 2003). However, other causes are represented by the subsidence phenomena, natural eustatic and climatic variations.

Many Italian coastal areas are involved in the seawater intrusion phenomenon (BARROCU, 2003; CAPACCIONI *et alii*, 2005; GIAMBASTIANI *et alii*, 2007; ANTONELLINI *et alii*, 2008); in Tuscany several critical situations linked to the salinization of the coastal aquifer have been highlighted by many authors (ROSSI & SPANDRE, 1994; BARAZZUOLI *et alii*, 1999; GRASSI & NETTI, 2000; GIMÉNEZ FORCATA *et alii*, 2001; GIANI *et alii*, 2001; PRANZINI, 2002; GRASSI *et alii*, 2007; DOVERI *et alii*, 2009).

In order to face the above mentioned problems regarding the interference between seawater and freshwater and to plan the water resource management, specific studies aimed at defining a detailed outline of the aquifer systems are needed. This study is included in a wide project that concerns the whole Versiliese-Pisana coastal plain which forms the Migliarino-San Rossore-Massaciuccoli Regional Park. This area has a high environmental value, due to its great variety of natural settings, ranging from dunes to sandy shores and from hygrophilous forests to marshlands.

In particular, in this study the occurrence of the seawater intrusion in the gravel confined aquifer (BALDACCI *et alii*, 1994) is analyzed in the area between the Arno River and the Scolmatore Canal (fig. 1a), with an extent of about 7-8 km from the coastline.

The problem was already approached by others authors (ROSSI & SPANDRE 1994; GRASSI & ROSSI 1996; SPANDRE *et alii*, 1999; FRONDINI *et alii*, 2001; GRASSI & CORTECCI, 2005). This aquifer is an important and strategic resource for the area, because it is the only able in providing a substantial volume of water in order to satisfy the request of the agricultural and zootechnical firms, tourist structures (in particular bathing establishments), and, not the last, the drinking use. Such human pressure could move forward the salt wedge in this aquifer.

In this work, the coastal aquifer salinization was analyzed by means of a multidisciplinary approach: integration of the hydrostratigraphic knowledge, verification of the piezometric conditions, analysis of chemical features and isotopic contents of the water sampled in three periods (June and August 2008, April 2009). In particular, this work is aimed at analyzing the present situation about the contamination of the first gravel aquifer of the Pisan coastal plain and at comprehending the mechanism of the fresh-salt water mixing. Referring to the last issue, the isotopic analysis represents a significant approach, also considering the availability of past isotopic surveys carried out in zones close to the studied area (GRASSI & CORTECCI, 2005) and in its surroundings (MUSSI *et alii*, 1998; DOVERI, 2004; DOVERI *et alii*, 2009).



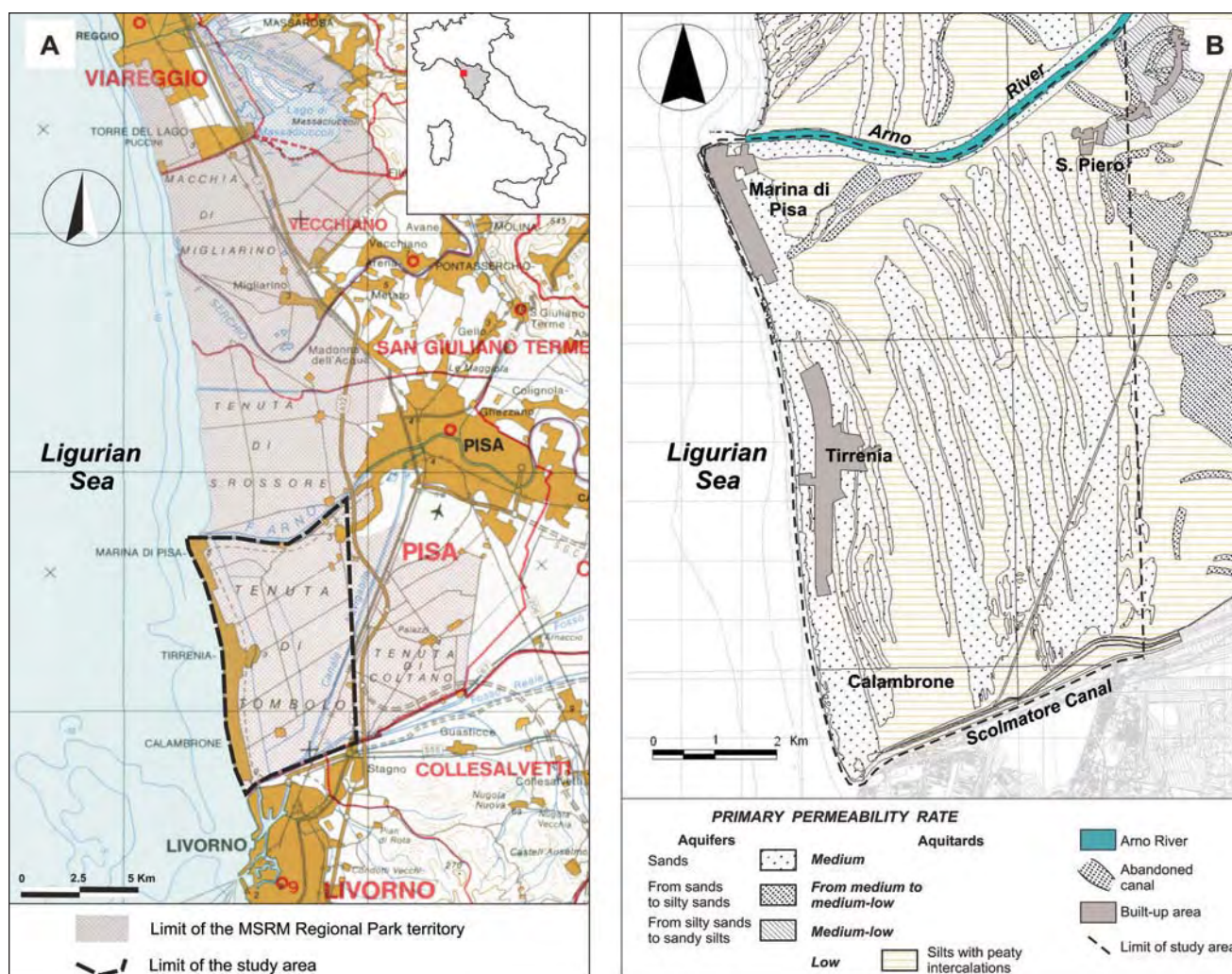


Fig. 1 - a) Location map of the study area (cartographic base by REGIONE TOSCANA, 1988). b) Permeability map, derived from the Provincia di Pisa (2005) geological map.  
 - a) Inquadramento geografico dell'area di studio (base cartografica da REGIONE TOSCANA, 1988). b) Carta della permeabilità, elaborata sulla base della carta geologica della Provincia di Pisa (2005).

## 2. - GEOLOGICAL AND GEOMORPHOLOGICAL SETTING

The Pisan coastal aquifers are included in a more complex depositional system, which constitutes the post-orogenic filling of the graben named Versiliese-Pisan Basin. This basin extends from the mouth of the Magra River to the North, to the surroundings of Pisa and Livorno to the South (MAZZANTI & PASQUINUCCI, 1983; FEDERICI, 1993). This structure is formed by a sub-triangular tectonic depression (direction NW-SE) and is delimited by the Apuan Alps, Oltre Serchio Mountains and Pisan Mountains to the East, the submerged Viareggio ridge to the West, and the Livornesi and Casciana Mountains to the South.

From Upper Miocene, the bedrock of the depression (characterized by formations of the Tuscan and Ligurian Units) was interested by deposition of marine, marine-transitional and continental inco-

herent sediments (GIANNINI & NARDI, 1965; RAU & TONGIORGI, 1974). The last mainly derive from the Magra, Serchio and Arno rivers basins.

Variations of the sea-level attributable to ice-age episodes are documented in the studied area during the Middle Pleistocene. The Würm II ne-gative one is particularly significant for the Pisan plain area. This phase is proved by clastic deposits of the ancient *Paleo-Arno* River, chiefly rich in pebbles coming from Pisan Mountains and Garfagnana area, which were transported by the ancient *Paleo-Serchio* River. In fact the latter, which drains the Garfagnana area, flowed in the past into the *Paleo-Arno* River through the Bientina depression (East of Pisan Mountains) (MAZZANTI & PASQUINUCCI, 1983). Afterwards, fluvial-lacustrine silt settled on these deposits, due to a reduced fluvial activity, probably linked to both the cessation of sea-level fall, and to a climatic drying up (DELLA ROCCA *et alii*, 1987). Above the fluvial-palustrine silt aeolian



sands lie.

The combined effect of formation of dunes and progressive sea-level rise prevented an easy coastal outlet of the main rivers, originating marshes and lagoons and the deposition of finer materials also containing peat and lignite (FANCELLI, 1984). This type of environment remained typical of the Pisan plain till historic present (DELLA ROCCA *et alii*, 1987).

### 3. - HYDROGEOLOGICAL FEATURES

In order to define the shallow hydrogeological conditions of the area included between the Arno River and the Scolmatore Canal, a permeability map was elaborated (fig. 1b). In particular, the available geological map of the area (PROVINCIA DI PISA, 2005) was converted into a permeability map on the basis of both literature information and of the grain size properties of the materials, in agreement with a previous classification of BALDACCI *et alii* (1994).

The hydrogeological units have been classified as aquifer and aquitards after parametrization with estimates of permeability ranges. The aeolian and shore deposits, constituted by medium-fine sand, have a medium permeability (about  $10^{-4}$ - $10^{-5}$  m/s, according to BALDACCI *et alii*, 1994). Sometimes, in the dune sands silt and peat levels occur, resulting in local lowering of permeability of the sands. The sandy deposits, belonging to ancient abandoned rivers, the “Sabbie e limi di Vicarello” formation (sand and silt) and the overlying alluvial deposits (silty sands) range in permeability from medium to low. The fluvial-palustrine materials have a low permeability, due to the presence of silt.

In the Pisan plain subsurface, below the discontinuous superficial phreatic aquifers, of poor practical interest, there is a complex multi-level confined aquifer that contains two major confined aquifers defined, from the top to the bottom, “1<sup>st</sup> sandy confined aquifer” and “1<sup>st</sup> gravelly confined aquifer” (BALDACCI *et alii*, 1994); the hydrostratigraphic, hydrodynamic, piezometric and hydrochemical features of such aquifers were defined and described by several authors (ROSSI & SPANDRE, 1994, 1995; BALDACCI, 1999; FRONDINI *et alii*, 2001; GRASSI & CORTECCI, 2005).

The roof depth of the 1<sup>st</sup> sandy confined aquifer changes from 20-30 m to the South of the Arno River, to 50-60 m in the Pisa area; then, it goes up again northward (BALDACCI *et alii*, 1994). It is prevalently constituted by sandy deposits (DINI, 1976). The recharge of this aquifer is mainly located in the coastal dune area between the Arno

and Serchio rivers, in the piedmont of the Pisan plain (where the sandy deposits are directly in contact with the fan gravelly materials), and through the alluvial deposits of the Serchio River at the Ripafratta Strait (SPANDRE *et alii*, 1999). This aquifer becomes phreatic close to the coastal area, because it is in hydraulic connection with the dune system (fig. 2).

The 1<sup>st</sup> gravelly confined aquifer is included in *Arno e Serchio da Bientina* conglomerates, represented by clastic fluvial deposits (pebbles of quartz, anagenite, limestone) with high permeability, which originated during the migration of the Serchio and Arno riverbeds (DELLA ROCCA *et alii*, 1987). According to BALDACCI *et alii*, 1994 (data obtained by pumping tests) the hydraulic conductivity of the gravelly aquifer is about  $10^{-3}$  m/s, and locally reaches  $10^{-2}$  m/s. The alluvial origin of such deposits implies some discontinuities in a bidimensional representation (see section 1 in fig. 2), which does not exclude possible hydraulic connections in the third dimension. However, these conglomeratic levels are connected to the sea at least in the mouth of the ancient *Paleo-Arno* river, individuated by SERGE (1955) and MAZZANTI & PASQUINUCCI (1983). In agreement with BALDACCI *et alii* (1994) the recharge of this aquifer is principally due to the direct infiltration on the Vicarello hills, through the pebbly bodies which lie in the piedmont areas and in the intermountain valley of the Pisan Mountains, and through the alluvial deposits of the Bientina area.

The analysis of many stratigraphic logs of the coastal area, provided by the Province of Pisa Administration, allowed us to integrate previous studies (BALDACCI *et alii*, 1994, 1998; BALDACCI, 1999), describing the hydrostratigraphic structure of the study area by means of two longitudinal and three cross-sections (fig. 2). The gravelly level seems more continuous in the SW area, among Tirrenia, Tombolo and Calambrone villages (fig. 2, sections 2, 3, 4, 5). As cited above (fig. 2, sections 1, 4), the gravel horizon is characterized by several lenticular alluvial bodies, partly overlapped. In the S. Piero a Grado zone (fig. 2, section 1), the discontinuous gravelly levels are interposed between the main sandy aquifer (fed also by the dune system) and the deeper gravelly aquifer. Hydraulic connections are also possible between the two main aquifers by vertical exchange phenomena through the semi-permeable thin horizons which separate such aquifers (BALDACCI, 1999). In general, the principal gravelly levels are less than 10 m thick and are located at 50 m below the land surface in the southern part of the study area and at about 100 m northward (fig. 2, section 4).

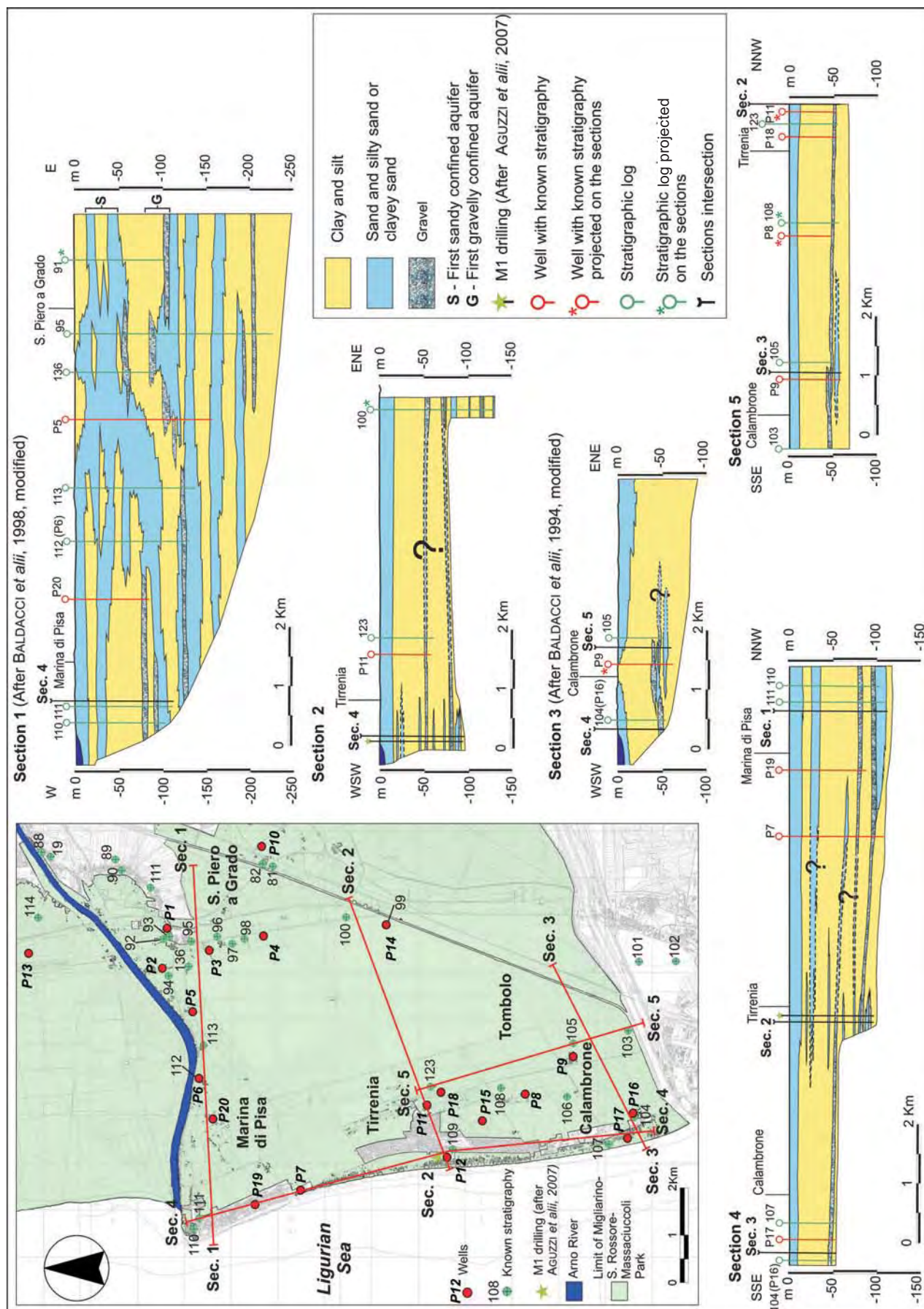


Fig. 2 - Hydrostratigraphic cross-sections of the southern coastal Pisan plain. - *Sezioni idrostratigrafiche della porzione meridionale della pianura costiera pisana.*



This hydrostructural outline generally confirms the model of the local groundwater circulation proposed by BALDACCI *et alii* (1994) and ROSSI & SPANDRE (1994, 1995), with two main aquifers (sandy and gravelly) sometimes composed by more levels in hydraulic connection among them and with the sea floor.

#### 4. - ON-SITE SURVEYS AND ANALYTICAL METHODS

The research was carried out by several steps. Firstly, in order to obtain piezometric data, the water wells which intercept the gravelly aquifer were chosen (fig. 3) by means of existing hydrogeological documents and on-site surveys. For each well, the absolute elevation (in m a.s.l.) of the topographic surface was obtained using a specific planimetric-altimetric survey with a double-frequency instrument Leica GPS 1200 Series (planimetric precision in mm  $\pm 10 + 1$  ppm; altimetric precision in mm  $\pm 20 + 1$  ppm) in RTK (Real Time Kinematics) modality, with correction from single station (nearest site).

Three field surveys were carried out in June and August 2008 and April 2009, respectively. With regard to the first one, the piezometric level, temperature and electric conductivity were measured and the chloride concentrations were determined on a selection of water-wells.

In the subsequent surveys, the alkalinity (through titration with HCl 0,1M) and pH were measured in addition to the others data. Some water samples (raw and filtered-acidified) were collected for chemical and isotopic analysis. Sampling was done in 20 wells tapping the gravelly aquifer, and in one point of the Arno River (only in April 2009) at two different depths (1 and 4 m under water level). The determination of the anions  $\text{Cl}^-$ ,  $\text{SO}_4^{2-}$ ,  $\text{Br}^-$ ,  $\text{NO}_3^-$  was obtained by ion chromatography, while the cations  $\text{Na}^+$ ,  $\text{K}^+$ ,  $\text{Ca}^{2+}$ ,  $\text{Mg}^{2+}$  were analyzed by means of optical ICP. The  $\delta^{18}\text{O}\text{‰}$  and  $\delta^2\text{H}\text{‰}$  (FRITZ & FONTES, 1980) were determined by means of mass spectrometry in gas phase, after sample preparation using vacuum lines and isotopic equilibration at 25°C with  $\text{CO}_2$  ( $\delta^{18}\text{O}\text{‰}$ ) and at 460 °C with Mg ( $\delta^2\text{H}\text{‰}$ ). The used reference isotopic standard is V-SMOW (HOEFS, 2004) and the standard error is  $\pm 0.1 \text{ ‰}$  and  $\pm 1 \text{ ‰}$  for  $\delta^{18}\text{O}\text{‰}$  and  $\delta^2\text{H}\text{‰}$  respectively.

The use of environmental isotopes in this type of study yields more useful information than classic chemical elements do. In fact, the isotopic contents are not influenced by interaction processes between water and solid matrix in normal temperature conditions. This implies that the isotopes

preserve information about the origin of the infiltration water and, referring to the coastal aquifer, permit to discriminate if the water salinity is really attributable to the seawater-fresh water mixing or if it is attributable to dissolution phenomena in sea deposits, which are present in the study area.

The piezometric and physical-chemical data obtained on site are shown in table 1, while the results of the chemical and isotopic analysis are shown in table 2.

#### 5. - PIEZOMETRIC LEVELS AND ELECTRIC CONDUCTIVITY (EC)

Because of the random distribution of water-wells and of the absence of data for some wells, the piezometric maps shown in figure 4 are only representative of the broad piezometric configuration and are not aimed to describe the flow patterns in detail. These maps substantially evidence the presence of water levels generally below the sea-level on most of the territory and of two local piezometric depressions, in the S. Piero a Grado (wells P1-P2-P3) and Calambrone (wells P8-P9) zones respectively.

Further considerations are possible taking into account the seasonal variations of the water level and the existing relationship between water level (figs. 3, 4 and 5) and the groundwater electric conductivity (EC) (figs. 3 and 5). Referring to the June and August 2008 surveys, all the piezometric data show values below the sea-level, with a relative drawdown in August more than 1 m in comparison with the June data. Such a drawdown (maximum in the wells P2 and P3, S. Piero a Grado area), of about -1.40/-1.50 m, is mainly related to the intense pumping which is typical of the summer period for the study area. An exception is represented by the well P1, probably due to the pumping before June 2008, which could have significantly influenced the measured piezometric level. As regards the April 2009 survey, despite the measured piezometric levels are still below the sea-level, we can note a general raising of more than 1 m with respect to the two previous surveys. The major rise of the water level was individuated in the wells P2 and P10, with 1.96 m and 2.25 m respectively in comparison with the August 2008 situation. This might result from the combination of abundant rainfall from autumn 2008 to winter and spring 2009 and significant pumping reduction during the same period.

With regard to the wells P15, P16, P17, P18 and P20, only April 2009 data are available, thus the comparison with the previous surveys is not possible. What's more, only in these water-wells, ex-



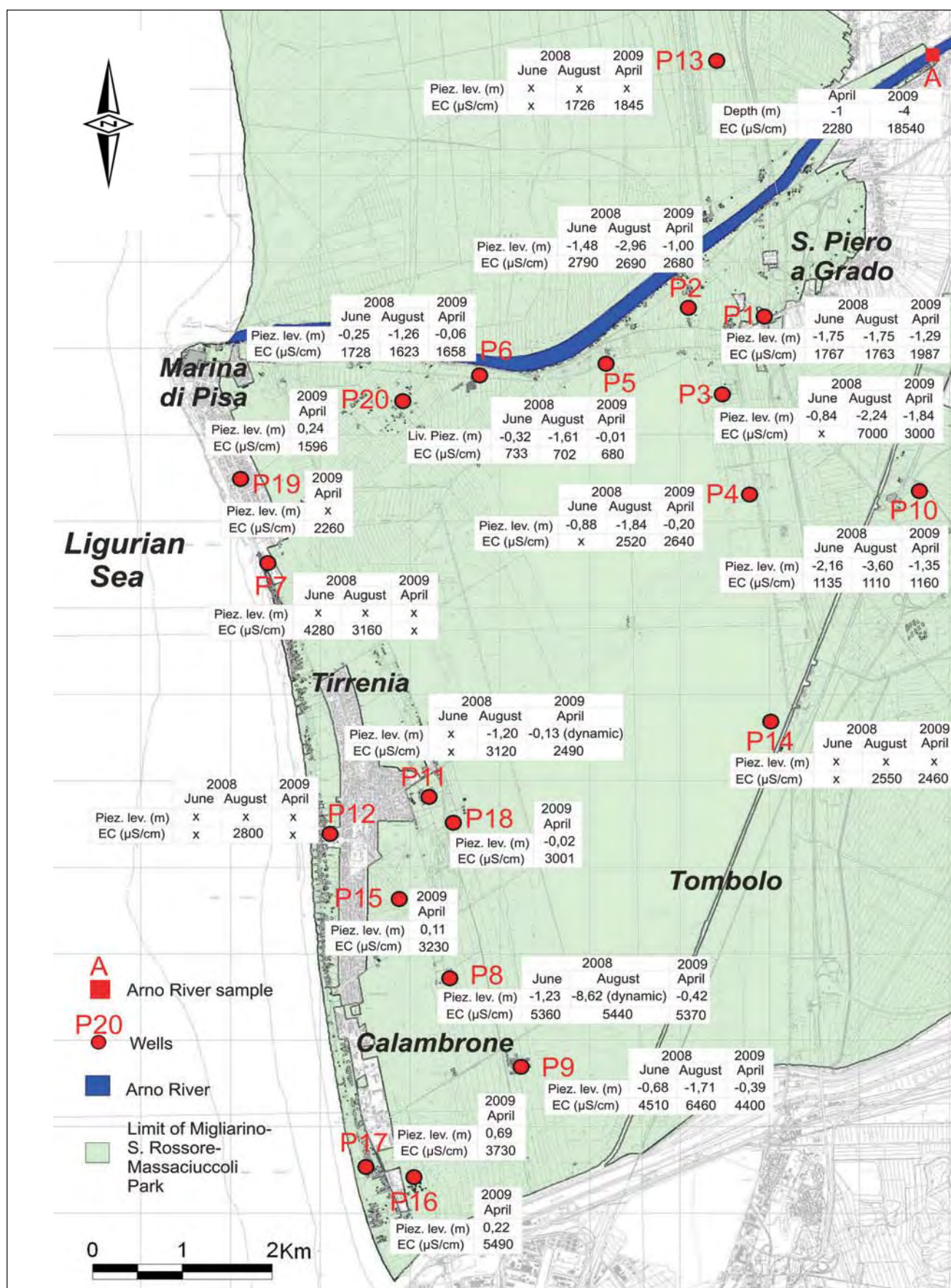


Fig. 3 - Location of the water sampling points and piezometric and electric conductivity (EC) data.  
 - Ubicazione dei punti d'acqua campionati e dati piezometrici e di conducibilità elettrica.

Tab. 1 - *Piezometric and physical-chemical data collected on site* (^: sampling depth from water level; \*: dynamic level; n.m.: not measured; location of sampling points in figure 3).

- Dati piezometrici e chimico-fisici ottenuti in sito (^: profondità di campionamento rispetto alla quota del pelo libero dell'acqua; \*: livello dinamico; n.m.: non misurato; ubicazione dei punti di campionamento in figura 3).

Water point	Well depth (m)	JUNE 2008			AUGUST 2008				APRIL 2009			
		Piezometric level (m a.s.l.)	Conductivity ( $\mu\text{S}/\text{cm}$ at 25°C)	T (°C)	Piezometric level (m a.s.l.)	Conductivity ( $\mu\text{S}/\text{cm}$ at 25°C)	pH	T (°C)	Piezometric level (m a.s.l.)	Conductivity ( $\mu\text{S}/\text{cm}$ at 25°C)	pH	T (°C)
P1	100	-1.75	1767	18,6	-1,75	1945	6,83	19,1	-1,29	1987	6,82	18,2
P2	105	-1.48	2790	17,7	-2,96	2640	7,25	17,7	-1,00	2680	7,25	17,6
P3	97	-0.84	n.m.	n.m.	-2,24	8750	7,52	17,1	-1,84	3000	6,98	15,2
P4	101	-0.88	n.m.	n.m.	-1,84	2530	6,57	18,5	-0,43	2640	6,74	18,7
P5	154	-0.32	733	15,4	-1,61	723	10,30	16,1	-0,01	680	9,97	14,8
P6	131	-0,25	1728	20,6	-1,26	1762	7,19	20,0	-0,06	1658	6,86	18,1
P7	110	n.m.	4280	20,9	n.m.	3400	7,16	20,0	n.m.	n.m.	n.m.	n.m.
P8	50	-1.23	5360	19,5	-8.62*	5560	7,33	20,5	-0,70	5370	7,09	19,8
P9	54	-0.68	4510	20,7	-1,71	6460	7,20	19,5	-0,39	4400	6,78	17,0
P10	72	n.m.	1135	17,6	-3,60	1190	7,27	17,8	-1,35	1160	6,94	17,9
P11	55	n.m.	n.m.	n.m.	-1,20	3120	7,16	20,0	-0.13*	2490	6,99	20,6
P12	80	n.m.	n.m.	n.m.	n.m.	2800	6,78	20,6	n.m.	n.m.	n.m.	n.m.
P13	100	n.m.	n.m.	n.m.	n.m.	2040	6,55	20,0	n.m.	1845	6,68	19,0
P14	60	n.m.	n.m.	n.m.	n.m.	2550	6,90	16,80	n.m.	2460	6,96	16,9
P15	55	n.m.	n.m.	n.m.	n.m.	n.m.	n.m.	n.m.	0,11	3200	6,91	17,6
P16	43	n.m.	n.m.	n.m.	n.m.	n.m.	n.m.	n.m.	0,22	5490	6,86	15,3
P17	55	n.m.	n.m.	n.m.	n.m.	n.m.	n.m.	n.m.	0,69	3730	7,24	17,6
P18	70	n.m.	n.m.	n.m.	n.m.	n.m.	n.m.	n.m.	-0,02	3100	6,92	18,6
P19	92	n.m.	n.m.	n.m.	n.m.	n.m.	n.m.	n.m.	n.m.	2260	6,92	17,5
P20	85	n.m.	n.m.	n.m.	n.m.	n.m.	n.m.	n.m.	0,24	2596	7,08	17,0
Arno River (depth 1 m)	1^	n.m.	n.m.	n.m.	n.m.	n.m.	n.m.	n.m.	n.m.	2280	6,93	16,6
Arno River (depth 4 m)	4^	n.m.	n.m.	n.m.	n.m.	n.m.	n.m.	n.m.	n.m.	18540	7,06	16,1

cept one (P18), we recorded water levels above the sea-level (maximum +0.69 m a.s.l. in P17).

After all, considering all the data collected, in two areas (S. Piero a Grado and the area between Tombolo and Calambrone, figs. 3, 4 and 5) the piezometric level is particularly depressed below the sea-level. On the other hand, in these areas the main farms are present. Such a piezometric situation was already highlighted by ROSSI & SPANDRE (1994) and BALDACCINI *et alii* (1999).

In the water-wells belonging to these areas we also recorded higher EC values (7,000 and 6,460  $\mu\text{S}/\text{cm}$ , in P3 and P9 respectively in August 2008). However, we can observe in general high values of EC (frequently more than 3,000  $\mu\text{S}/\text{cm}$ ) in all the wells close to the coastline between Marina di Pisa and Calambrone villages, with a tendency to raise southward. With the exception of P2, P3 and P4 (S. Piero a Grado area), almost all the water sampled in the well of inland zones are characterized by electric conductivity relatively low, often minor than 2,000  $\mu\text{S}/\text{cm}$ .

From June 2008 to April 2009 we can observe significant variations of EC only at P3 and P9, with higher values in August 2008, corresponding to the lower piezometric level. The maximum EC (18,500  $\mu\text{S}/\text{cm}$ ) was recorded for the Arno River close to the bottom of the bed (-4 m from the surface of the water). This is clearly attributable to the sea-water which goes upstream for several kilometres, as documented for this area by various authors (LA RUFFA & PANICHI, 2000; CORTECCI *et alii*, 2002).

## 6. - CHEMICAL AND ISOTOPIC CHARACTERISTICS OF THE WATER

Figure 6 shows that most samples of ground-water are usually characterized by an intermediate chemical composition  $\text{Ca-Na}/\text{HCO}_3\text{-SO}_4$ ,  $\text{Ca-Na}/\text{HCO}_3\text{-SO}_4\text{-Cl}$  or  $\text{Ca-Na}/\text{HCO}_3\text{-Cl}$ . Among the remaining samples, P10 is  $\text{Ca}/\text{HCO}_3$ , P13  $\text{Ca}/\text{SO}_4$ , while P2-P8-P16-P17 and P3-P9 sampled in August 2008 have a composition  $\text{Na}/\text{Cl}$  (see fig. 3 for the location of the water sampling points).

In general, we can observe that up to middle values of TDS (fig. 7) the salinity is mainly regulated by  $\text{HCO}_3^-$  and sometimes by  $\text{SO}_4^{2-}$ . On the contrary, high values of TDS depend on Cl contents.

Regardless of the TDS values, some water samples show particularly low values in  $\text{SO}_4^{2-}$ , due to the phenomenon of reduction by bacteria, as highlighted by GRASSI & CORTECCI (2005) during studies on the internal portion of the Pisan Plain.

After all, the chemical composition points out that in the study area the gravelly aquifer is characterized by a water circulation with prevalently  $\text{Ca}/\text{HCO}_3^-$ - $\text{SO}_4^{2-}$  composition, which evolves towards  $\text{Na}/\text{Cl}$  composition caused by seawater mixing. This process is confirmed by the fact that the samples with high Cl contents have  $\text{Na}/\text{Cl}$  and

$\text{Br}/\text{Cl}$  ratios comparable to those of the seawater (figs. 8 and 9).

The significant influence of sulphate in the groundwater chemical features, not involved in seawater mixing, is attributable to a feeding component from the Mesozoic calcareous aquifer, in hydraulic connection with the gravel aquifer (GRASSI & CORTECCI, 2005). In fact, this calcareous aquifer outcrops on the hills close to the Pisan Plain and constitutes its bedrock as well. The water circulating in this aquifer is mainly characterized by  $\text{Ca}-\text{SO}_4^{2-}$ , as demonstrated by chemical analyses of some springs located in the Pisan Mountains edge (GRASSI *et alii*, 1994).

In agreement with the electric conductivity and piezometric level, the chemical features show that the seawater-freshwater mixing is particularly evi-

Tab. 2 - Chemical and isotopic data (n.d.: not determined; location of sampling points in figure 3).  
- Dati chimici e isotopici (n.d.: non determinato; ubicazione dei punti di campionamento in figura 3).

Sampling period	Water point	$\text{Ca}^{2+}$ (mg/l)	$\text{Mg}^{2+}$ (mg/l)	$\text{Na}^+$ (mg/l)	$\text{K}^+$ (mg/l)	$\text{Cl}^-$ (mg/l)	$\text{NO}_3^-$ (mg/l)	$\text{SO}_4^{2-}$ (mg/l)	$\text{HCO}_3^-$ (mg/l)	$\text{Br}^-$ (mg/l)	$\delta^{18}\text{O}\text{‰}$	$\delta^2\text{H}\text{‰}$
JUNE 2008	P2	n.d.	n.d.	n.d.	n.d.	507,1	n.d.	n.d.	n.d.	n.d.	n.d.	n.d.
	P6	n.d.	n.d.	n.d.	n.d.	220,4	n.d.	n.d.	n.d.	n.d.	n.d.	n.d.
	P8	n.d.	n.d.	n.d.	n.d.	1256,3	n.d.	n.d.	n.d.	n.d.	n.d.	n.d.
	P9	n.d.	n.d.	n.d.	n.d.	780,4	n.d.	n.d.	n.d.	n.d.	n.d.	n.d.
AUGUST 2008	P1	176,5	49,7	145,3	7,8	159,0	0,4	408,8	482,0	0,5	-6,60	-41,5
	P2	89,3	35,6	401,7	9,6	479,3	6,6	208,5	518,6	1,7	-6,02	-36,4
	P3	140,1	136,2	1019,1	38,9	1926,9	25,8	142,8	671,1	5,9	-5,37	-34,9
	P4	291,4	73,7	179,9	12,4	186,7	<0,2	546,9	707,7	0,6	-6,82	-38,7
	P6	156,6	45,6	145,6	6,5	177,8	<0,2	263,0	457,6	0,6	-6,55	-39,4
	P7	248,7	76,1	314,2	16,6	452,4	6,7	370,8	762,7	1,9	-6,59	-38,6
	P8	119,6	71,5	892,9	24,0	1395,2	<0,2	23,6	875,5	6,1	-6,18	-36,6
	P9	137,0	160,1	969,9	41,4	1542,6	0,8	62,9	1421,6	6,1	-6,25	-39,4
	P10	93,5	25,3	110,4	5,7	114,5	0,3	82,3	408,8	0,4	-6,60	-41,1
	P11	259,5	85,0	292,8	17,5	352,5	27,6	487,4	799,3	1,5	-6,87	-39,8
	P12	246,0	77,5	256,6	14,0	331,9	1,7	445,2	780,0	1,4	-6,65	-40,0
	P13	236,2	49,9	119,1	14,7	110,7	14,0	553,5	451,5	0,3	-6,86	-42,9
	P14	263,5	95,1	185,1	10,9	199,2	<0,2	509,8	841,0	0,6	-6,79	-41,1
	P1	193,2	51,8	182,5	9,5	190,1	n.d.	454,4	488,1	0,6	-6,62	-38,1
APRIL 2009	P2	77,5	34,1	440,2	9,7	424,6	n.d.	235,8	494,2	1,6	-6,01	-32,8
	P3	88,9	42,9	210,4	7,7	295,6	n.d.	79,3	482,0	1,2	-5,96	-32,8
	P4	203,4	70,9	287,1	17,7	282,1	n.d.	378,3	677,2	1,0	-6,40	-37,1
	P6	149,8	44,1	151,4	5,8	172,0	n.d.	260,6	457,6	0,7	-6,52	-37,0
	P8	114,7	67,2	923,5	21,9	1332,5	n.d.	22,3	915,2	5,8	-6,25	-37,0
	P9	149,0	129,5	622,5	25,4	821,0	n.d.	83,4	1446,0	3,4	-6,72	-38,6
	P10	93,3	24,7	116,6	5,0	114,5	n.d.	81,9	457,6	0,4	-6,59	-38,9
	P11	127,8	75,3	301,1	16,0	318,2	n.d.	361,3	567,4	1,3	-6,68	-40,3
	P13	234,2	48,2	128,7	14,8	115,3	n.d.	554,9	457,6	0,3	-6,79	-39,9
	P14	248,5	85,5	188,5	9,0	182,4	n.d.	512,2	793,2	0,5	-7,03	-38,9
	P15	170,7	82,8	385,5	19,9	521,0	n.d.	209,7	890,8	1,7	-6,75	-37,6
	P16	282,3	96,5	712,3	18,1	1406,0	n.d.	237,9	640,6	6,3	-5,88	-36,2
	P17	195,1	61,0	490,0	14,0	847,0	n.d.	147,7	488,1	3,5	-6,09	-35,0
	P18	253,6	82,3	308,1	18,1	395,0	n.d.	461,1	848,1	1,5	-6,71	-40,3
	P19	212,9	51,1	200,7	7,9	282,3	n.d.	238,0	665,0	0,8	-6,53	-36,7
	P20	130,5	32,8	148,5	7,9	195,6	n.d.	60,8	500,3	0,6	-6,29	-40,0
	Arno River (depth 4 m)	n.d.	n.d.	3450,2	127,9	6223,0	n.d.	879,8	298,0	19,6	-4,13	-23,1
	Arno River (depth 1 m)	n.d.	n.d.	311,9	12,9	289,0	n.d.	138,2	256,3	0,9	-6,40	-38,2



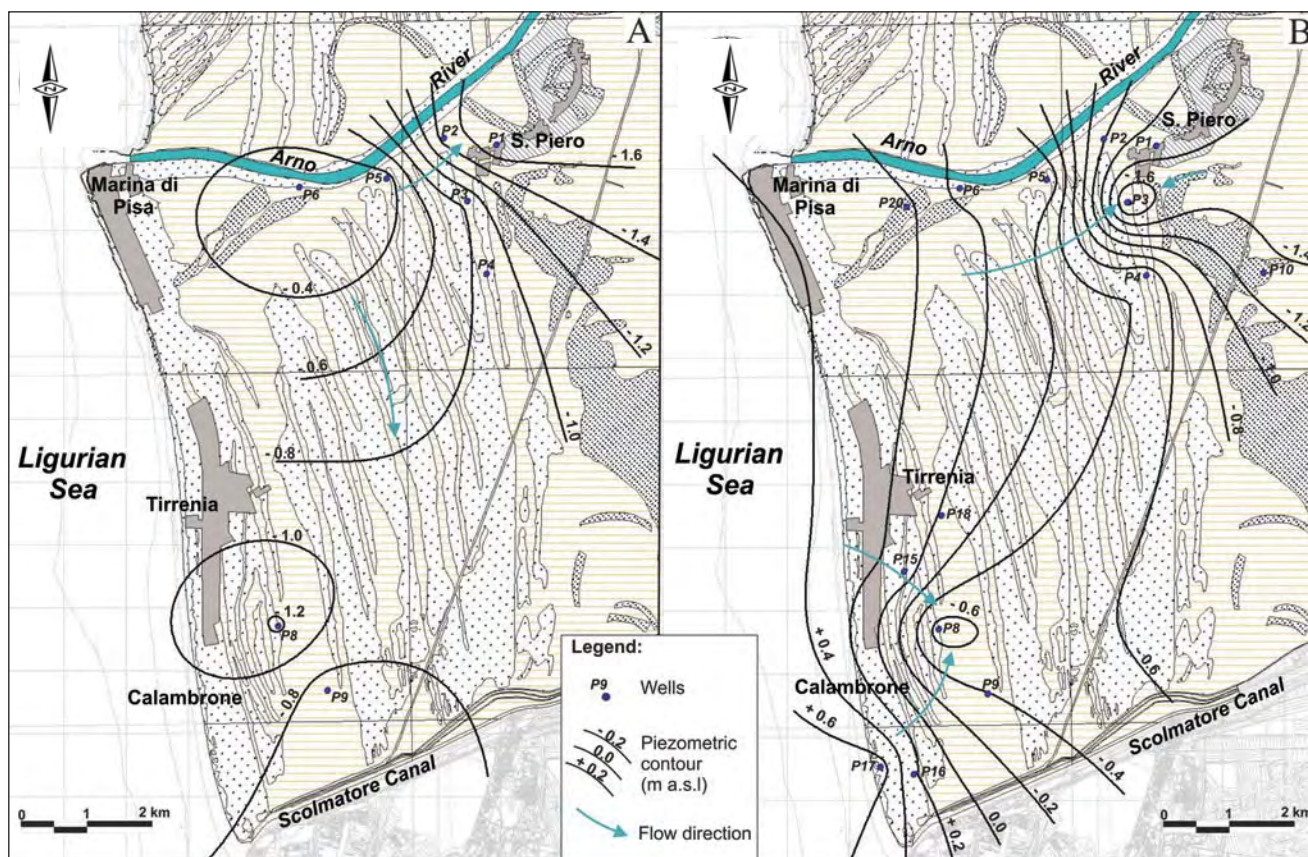


Fig. 4 - Piezometric sketch map of the confined gravelly aquifer: A) June 2008, B) April 2009 (see fig. 1b for the legend of the base map).  
 - Carte piezometriche schematiche relative all'acquifero ghiaioso confinato: A) Giugno 2008; B) Aprile 2009 (vedi fig. 1b per la legenda della cartografia di base).

dent in the S. Piero a Grado area (P2, P3) and in the southern portion of the study area, between Tombolo and Calambrone (P8, P9, P16, P17). As shown in figure 6, such mixing in many cases is not conservative and this is principally caused by the mentioned phenomenon of sulphate reduction which includes the removal of  $\text{SO}_4$  and a relative enrichment of  $\text{HCO}_3$  in solution.

The analysis of the Cl contents permits to individuate some groundwater samples (P1, P6, P10, P13, P14, P20) with concentration ranging 110-200 mg/l, in agreement with the observations of GRASSI & CORTECCI (2005) about the gravelly aquifer in the internal portion of the plain. Such values could reasonably represent the "Cl background value" in the groundwater of the gravelly aquifer reaching in the coastal plain. In the other sampling points, higher Cl values were registered from more than 300 mg/l up to more than 1900 mg/l (P3 in August), depending the seawater-freshwater mixing degree.

Considering the wells sampled in two of three surveys at least (fig. 10), we can observe that the groundwater with lower Cl concentration show a general stability with time of this element. On the

contrary, a pronounced variability is recognizable in the wells that show higher values (in particular P3 and P9). From a quantitative point of view, this indicates that seawater mixing depends on the different seasonal conditions in terms of both recharge and pumping. In fact, higher values of Cl concentration is present in August, namely in the period characterized by low recharge amount and high withdrawal, which determine the lower piezometric levels.

On the basis of Br and Cl contents, the max percentage of seawater in samples is about 8-9% in S. Piero a Grado area (P3 in August) and 7-8% in the area between Tombolo and Calambrone (P9 in August, P8 in August and April).

As regards the isotopic contents, the diagram in figure 11 shows that most groundwater samples are grouped into values of  $\delta^{18}\text{O}\text{‰}$  and  $\delta^2\text{H}\text{‰}$  of about -6.5/-6.8 and -37/-40, respectively. Such values are typical of the water circulating in the confined gravelly aquifer of the internal portion of the Pisan Plain (GRASSI & CORTECCI, 2005) and are representative of recharge altitude higher than the plain. Actually, the rainfall at Pisa has  $\delta^{18}\text{O}\text{‰}$  medium yearly contents in the order of -5.3 and -

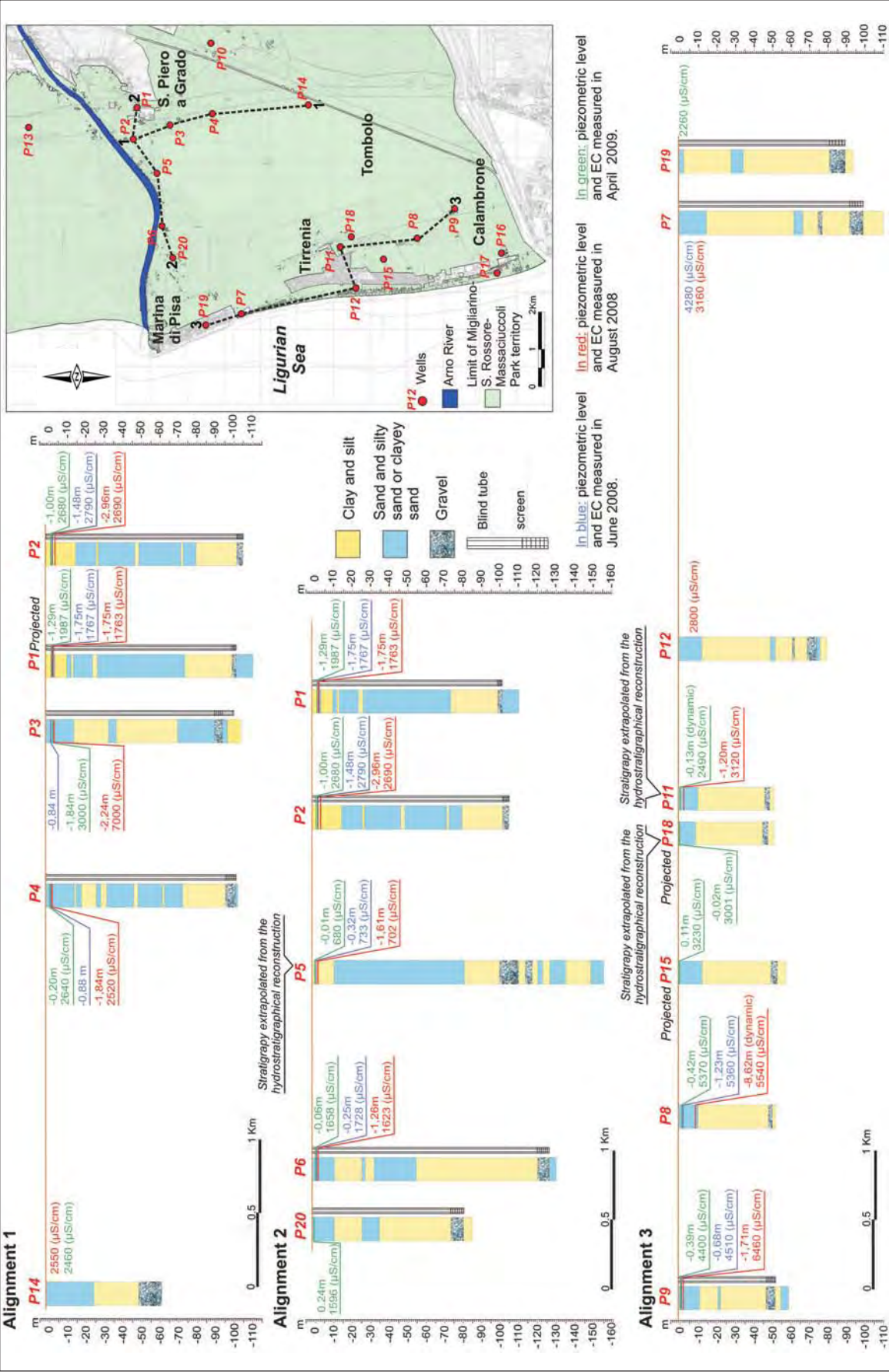


Fig. 5 - Stratigraphic outline of the water wells with piezometric and electric conductivity data (location of wells in figure 3).  
- Schema stratigrafico dei pozzi con relativi dati piezometrici e conduttività (l'ubicazione dei pozzi è riportata in figura 3).



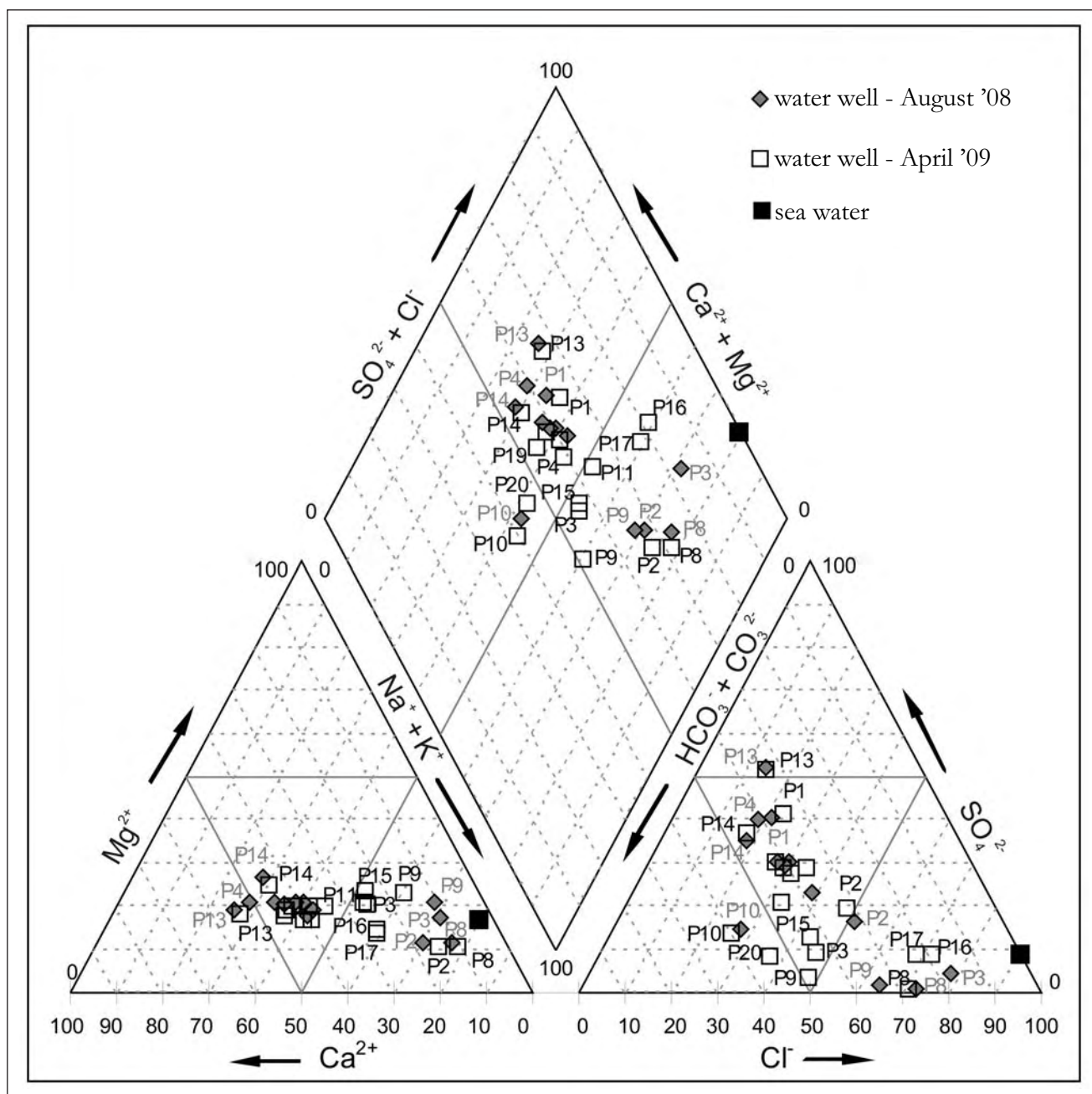


Fig. 6 - Piper diagram (PIPER, 1994).  
- Diagramma di Piper (PIPER, 1944).

5.8 (IAEA/WMO, 2001; MUSSI *et alii*, 1998). Such values are generally found also in the unconfined aquifers of the Versiliese-Pisan coast (DOVERI *et alii*, 2009; DOVERI, 2004; BALDACCI & DOVERI, 2008). The lower values that characterize most of the water samples collected in the confined gravelly aquifer highlight a negligible or absent supply linked to the direct infiltration of rainfall in the Pisan Plain. Corroborating the chemical analysis, the isotopic data indicate the contribute from the Mesozoic calcareous aquifer ( $\delta^{18}\text{O}\text{‰}$  at Pisan

Mountains springs of about -6.5; GRASSI *et alii*, 1994) in addition to the Pisan hills, Lucca Plain and Arno River Plain. The shifting of isotopic ratios for samples P2, P3, P8, P9, P16, P17 and P20 from the main group toward higher values of  $\delta^{18}\text{O}\text{‰}$  and  $\delta^2\text{H}\text{‰}$  (fig. 11) is compatible with both local connections between sandy aquifer (with higher isotopic contents) and gravelly aquifer and with a fresh water-seawater mixing. On the other hand, the sample collected in the Arno River is clearly influenced by seawater intrusion, with isotopic con-



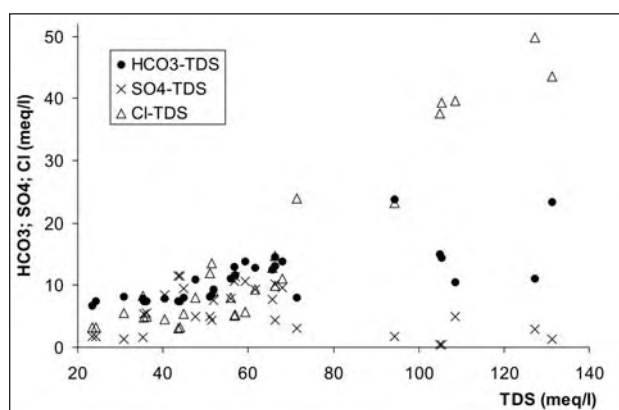


Fig. 7 - Binary diagram HCO<sub>3</sub>, SO<sub>4</sub>, Cl vs. TDS.  
- Diagramma binario HCO<sub>3</sub>, SO<sub>4</sub>, Cl vs. TDS.

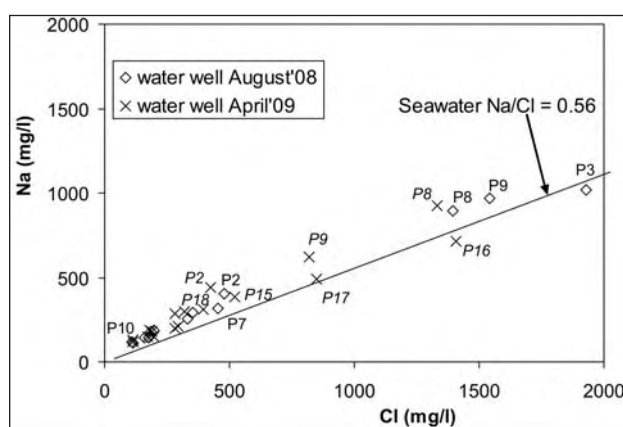


Fig. 8 - Binary diagram Na vs. Cl.  
- Diagramma binario Na vs. Cl.

centration even higher than the rainfall at sea altitude.

Comparing the  $\delta^{18}\text{O}\text{‰}$  and Cl contents (fig. 12), we can conclude that the samples interested by seawater intrusion, with different percentage, are included within 2 km from the shoreline (P7, P8, P9, P11, P12, P15, P16, P17, P18, P19) and P2-P3 close to S. Piero a Grado. However, this process occurs in different ways. In fact, the direct capture of the seawater in the gravel aquifer is probable only for the wells nearer to the coast. As regards P2 and P3 (S. Piero a Grado area), fig. 12 shows that in addition to the seawater there is a mixing with the water of the Arno River and/or of the sandy aquifer, which is in connection with the surface in this area. Moreover, considering that between P2 and P3 and the coastline there are other wells that intercept the gravel horizon showing low values of  $\delta^{18}\text{O}\text{‰}$  and Cl, we can state that the seawater fraction individuated in P2 and P3 is not due to the hydraulic connection between sea and gravelly aquifer, but is related to

the Arno River or the sandy aquifer. In fact, in this area the two aquifers could be in hydraulic connection, due to the lack or thickness reduction of the silty-clayey aquiclude/aquitard that usually separates them (fig. 2, section 1). However, we can not exclude that the hydraulic connection between the two aquifers is due by technical features of the wells, with water extraction both from the sandy and the gravelly aquifer. This is the most probable cause of the limited shift from the linear mixing *gravel groundwater-seawater* (GG-SW) showed by P16 and P17 samples (fig. 12), collected near the coastline in the southern part of the area.

## 7. - CONCLUSIONS

The confined gravelly aquifer, belonging to the Pisan Plain multi-level system aquifer, presents certain continuity in the coastal area at a depth of

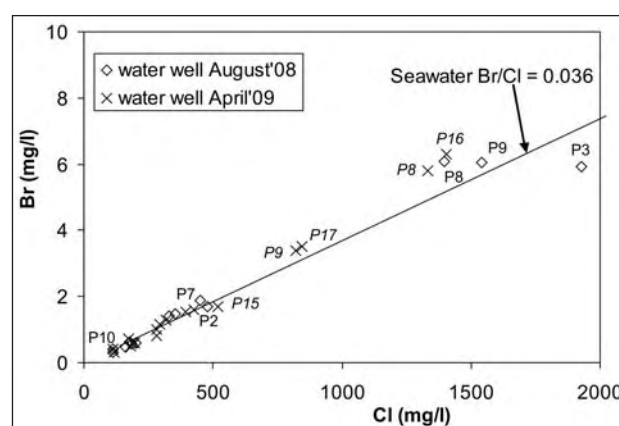


Fig. 9 - Binary diagram Br vs. Cl.  
- Diagramma binario Br vs. Cl.

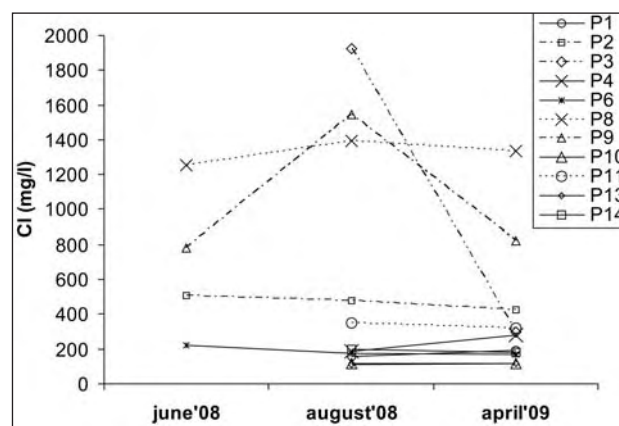


Fig. 10 - Cl concentration in the different sampling periods (location of wells in fig. 3).  
- Concentrazione di Cl nei diversi periodi di campionamento (ubicazione dei pozzi in fig. 3).

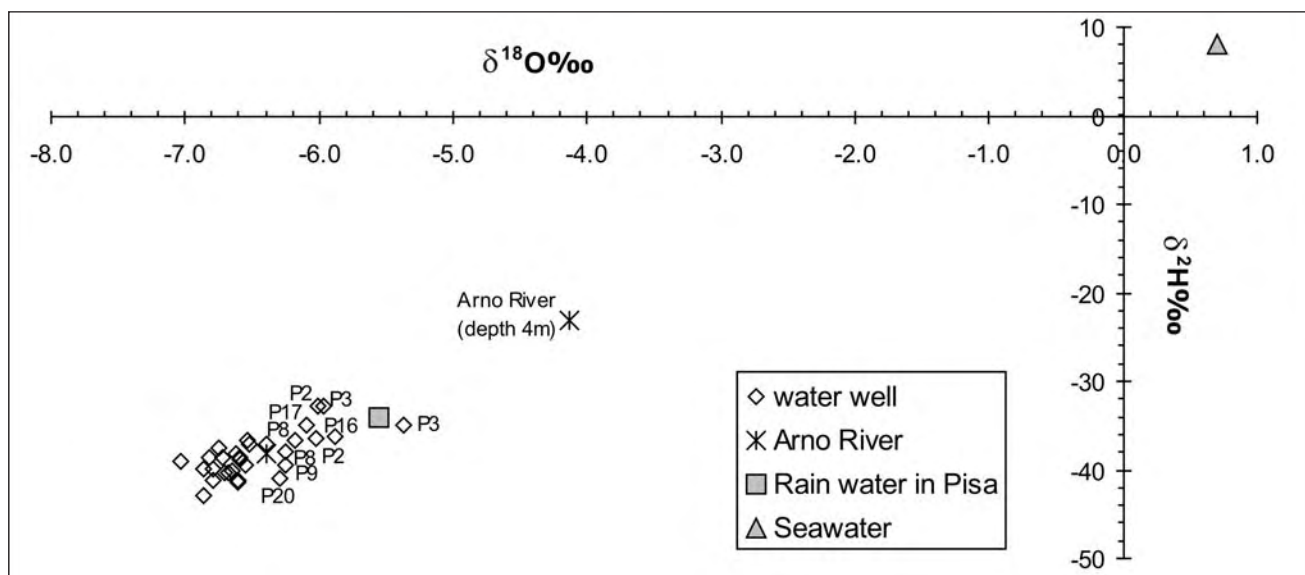


Fig. 11 - Relationship between  $\delta^{18}\text{O}\text{‰}$  and  $\delta^2\text{H}\text{‰}$ . - *Relazione tra  $\delta^{18}\text{O}\text{‰}$  e  $\delta^2\text{H}\text{‰}$ .*

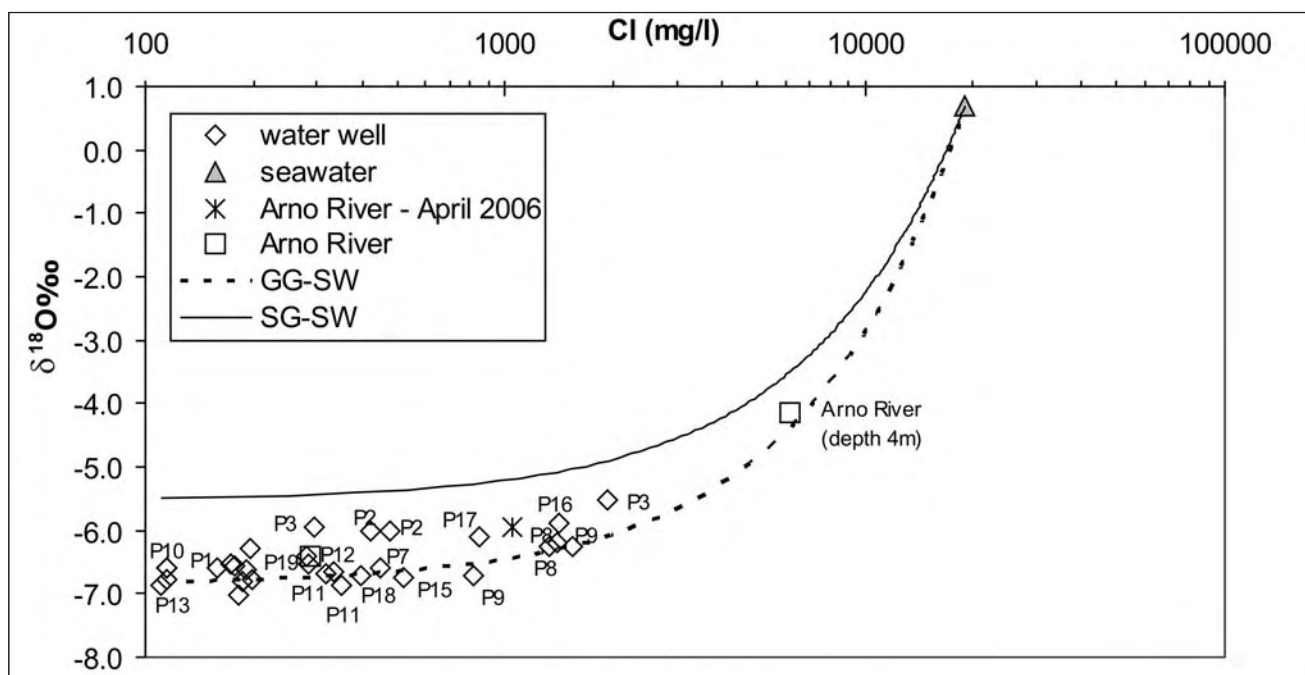


Fig. 12 - Binary diagram  $\delta^{18}\text{O}\text{‰}$  vs. Cl (Arno River-April 2006 after BALDACCI & DOVERI, 2008; GG-SW: gravel groundwater-seawater mixing; SG-SW: sand groundwater-seawater mixing).  
- *Diagramma binario  $\delta^{18}\text{O}\text{‰}$  vs. Cl (Arno River-April 2006 da BALDACCI & DOVERI, 2008; GG-SW: mixing tra falda delle ghiaie e acqua di mare; SG-SW: mixing tra falda delle sabbie e acqua di mare).*

about 50 m below the land surface. In several zones there are discontinuous gravelly horizons at different depths (higher and lower than 50 m). Across the study area the gravelly level is substantially separated from the overlying sandy aquifer, but locally (e.g. S. Piero a Grado) some in hydraulic connection could exist, due to absence or thickness reduction of the silty-clayey aquiclude/aquitard that usually separates them.

The piezometric level is lower than the sea-level in almost all the survey points (with the exception of some water points of the April 2009 survey). In the southern coastal area (Calambrone) and in the S. Piero a Grado area, the maximum depression of piezometry occurs because of intense pumping related to agricultural and tourist activity. In these zones, the groundwater, usually characterized by relatively low salinity ( $\text{EC} < 2,000 \mu\text{s}/\text{cm}$  at  $25^\circ\text{C}$ )

and chemical facies  $\text{Ca}/\text{HCO}_3\text{-SO}_4$ , shows high EC,  $\delta^{18}\text{O}\text{‰}$ , Br and Cl values. This clearly indicates the freshwater-seawater mixing in the order of about 9% as showed by the mass balance based on the Br and Cl contents.

The contemporaneous use of chemical and isotopic data enabled us to highlight two different origins of such a mixing. In particular, up to 1.5-2 km from the southern coastline (Calambrone area) and in a restricted area close to the coastline to the North, the seawater intrusion directly develops in the confined gravelly horizon in contact with the sea floor. In the S. Piero a Grado area the mixing with seawater is controlled by the seawater intrusion that interests the Arno River-phreatic sandy aquifer system and by the hydraulic connection between the last and gravelly aquifer.

Future developments of this research will better identify the relations between aquifers of the plain and among them and the Arno River, in order to evaluate the vulnerability of the main water horizon (gravelly aquifer) and to control the withdrawal.

#### Aknowledgement

*The authors are grateful to the Referees, T. Bonomi and M. Masetti, and to R. Bersezio, whose comments and suggestions effectively improved this paper.*

#### REFERENCES

- AGUZZI M., AMOROSI A., COLALONGO M.L., RICCI LUCCHI M., ROSSI V., SARTI G. & VAIANI, S.C. (2007) - *Late Quaternary climatic evolution of the Arno coastal plain (Western Tuscany, Italy) from subsurface data*. Sediment. Geol., **202**: 211-229.
- ANTONELLINI M., MOLLEMA P., GIAMBASTIANI B., BISHOP K., CARUSO L., MINCHIO A., PELLEGRINI L., SABIA M., ULAZZI E. & GABBIANELLI G. (2008) - *Salt water intrusion in the coastal aquifer of the southern Po Plain, Italy*. J. Hydrogeol., **16**: 1541-1556.
- BALDACCIO F. (1999) - *Struttura e piezometria del "primo acquifero artesiano in ghiaie" della Pianura Pisana*. Atti Soc. Tosc. Sci. Nat. Mem., ser. A, **106**: 90-101, Pisa.
- BALDACCIO F., BELLINI L. & RAGGI G. (1994) - *Le risorse idriche sotterranee della Pianura Pisana*. Atti Soc. Tosc. Sci. Nat. Mem., ser. A, **101**: 241-322, Pisa.
- BALDACCIO F., BELLINI L. & RAGGI G. (1998) - *Sistema Acquifero della Pianura di Pisa (Sap) - Carta della permeabilità delle rocce*. Atti Soc. Tosc. Sci. Nat. Mem., ser. A, **105**, 1 tav., Pisa.
- BALDACCIO F. & DOVERI M. (2008) - *L'intrusione marina nella fascia costiera versiliese-pisana: Studio Idrogeologico-geochimico degli acquiferi freatici nelle zone Canale Burlamacca-Fosso della Bufalina e Fiume Arno-Fiume Serchio*. Rapporto tecnico-scientifico, CNR-IGG/UNIPI-DST/Parco Regionale MSRM, pp. 111.
- BARAZZUOLI P., BOUZELBOUDJEN M., CUCINI S., KIRALY L., MENICORI P. & SALLEOLINI M. (1999) - *Olocenic alluvial aquifer of the River Cornia coastal plain (southern Tuscany, Italy): database design for groundwater management*. Environ. Geol., **39**: 123-143.
- BARROCU G. (2003) - *Seawater intrusion in the coastal aquifers of Italy*. In: J. CALAFERRA (Ed.): «*State of seawater intrusion in coastal aquifers of the Mediterranean Coast*». SWIM-SWICA: 207-223, Alicante, Spain.
- CAPACCIONI B., DIDERO M., PALETTA C. & DIDERO L. (2005) - *Saline intrusion and refreshing in a multilayer coastal aquifer in the Catania Plain (Sicily, southern Italy): dynamics of degradation processes to the hydrochemical characteristics of groundwater*. J. Hydrol., **307**: 1-16.
- CORTECCI G., DINELLI E., BENCINI A., ADORNI-BRACCESI, A. & LA RUFFA, G. (2002) - *Natural and anthropogenic  $\text{SO}_4$  sources in the Arno River catchment, northern Tuscany, Italy; a chemical and isotopic reconnaissance*. Appl. Geochem., **17**: 79-92.
- CUSTODIO E. (2002) - *Coastal aquifers as important natural hydrogeological structures*. In: E. BOCANEGRA, D. MARTÍNEZ & H. MASSONE (Eds.) «*Groundwater and Human Development*»: 1905-1918, Bremerhaven, Germany.
- DELLA ROCCA R., MAZZANTI R. & PRANZINI E. (1987) - *Studio geomorfologico della pianura di Pisa*. Geog. Fis. Dinam. Quat., **10**: 56-84.
- DINI I. (1976) - *La prima falda artesianica della zona di Pisa*. Provincia - Comune di Pisa.
- DOVERI M. (2004) - *Studio idrogeologico e idrogeochimico dei sistemi acquiferi del bacino del Torrente Carrione e dell'antistante piana costiera*. PhD Dissertation, Università di Pisa: pp. 178.
- DOVERI M., GIANNECCHINI R., GIUSTI G. & BUTTERI M. (2009) - *Studio idrogeologico-geochimico dell'acquifero freatico nella zona compresa tra il Canale Burlamacca ed il Fosso della Bufalina (Viareggio, Toscana)*. Proc. 3° AIGA Congress. Accepted Giorn. Geol. Appl., **12**, 103-119.
- ERICSON J.P., VÖRÖSMARTY C.J., DINGMAN S.L., WARD L.G. & MEYBECK M. (2006) - *Effective sea-level rise and deltas: causes of change and human dimension implications*. Global Planet Change, **50**: 63-82.
- FEDERICI P.R. (1993) - *The Versilian transgression of the Versilia area (Tuscany, Italy) in the light of the drillings and radiometric data*. Mem. Soc. Geol. It., **49**: 217-225.
- FANCELLI R. (1984) - *Tentativo di ricostruzione dell'andamento della falda artesianica tra i -30 ed i -50 m di profondità nel sottosuolo di Pisa e dintorni*. Rapporto CNR - Ist. Int. Ric. Geotermiche, Pisa.
- FRITZ P. & FONTES J.C.H. (1980) - *Introduction*. In: P. FRITZ & J.C.H. FONTES (Eds.), «*Handbook of Environmental Isotope Geochemistry*»: 1-19, Elsevier Scientific Publishing Company, Amsterdam-Oxford-New York.
- FRONDINI F., ZANZARI A. & GIAQUINTO S. (2001) - *Salt water intrusion in Pisa the coastal plain (Central Italy)*. In: R. CIDU (Ed.), «*Proc. Tenth International Symposium on Water-Rock Interaction 2001*», **1**: 513-516, Balkema, Lisse.
- GIAMBASTIANI B.M.S., ANTONELLINI M., OUDE ESSINK G.P. & STUURMAN R.J. (2007) - *Saltwater intrusion in the unconfined coastal aquifer of Ravenna (Italy): a numerical model*. J. Hydrol., **340**: 91-104.
- GIANI P., BELLUCCI L., PANICHI C. & PODDA F. (2001) - *Studio sulla presenza di acqua di mare nel tratto terminale del Fiume Arno con metodologie chimico-isotopiche*. Atti Soc. Tosc. Sci. Nat. Mem., ser. A: 53-60.
- GIANNINI E. & NARDI R. (1965) - *Geologia nella zona nord occidentale del Monte Pisano e dei Monti d'oltre Serchio (Provincia di Pisa e Lucca)*. Boll. Soc. Geol. It., **13**: 210-233.
- GIMÉNEZ FORCATA E., BENCINI A. & PRANZINI G. (2001) - *Salinization in coastal plain of Grosseto: Hydrochemical study*. In: R. CIDU (Ed.), «*Proc. Tenth International Symposium on Water-Rock Interaction 2001*», **1**: 517-520, Balkema, Lisse.
- GRASSI S. & CORTECCI G. (2005) - *Hydrogeology and Geochemistry of multilayered confined aquifer of the Pisa Plain*. Appl. Geochem., **20**: 41-54.
- GRASSI S., GIANELLI G. & TORO B. (1994) - *Studies of Low-Temperature Hydrothermal Systems: San Giuliano Prospect (Pisa, Italy)*. Energ. Source, **16**: 401-423.



- GRASSI S., CORTECCI G. & SQUARCI P. (2007) - *Groundwater resource degradation in coastal plains: the example of the Cecina area (Tuscany - Central Italy)*. Appl. Geochem., **22**: 2273-2289.
- GRASSI S. & NETTI R. (2000) - *Sea water intrusion and mercury pollution of some coastal aquifers in the province of Grosseto (Southern Tuscany-Italy)*. J. Hydrol., **237**: 198-211.
- GRASSI S. & ROSSI S. (1996). *Il cloro delle acque sotterranee della Pianura di Pisa*. Atti Soc. Tosc. Sci. Nat. Mem., ser. A, **103**: 135-142.
- HOEFS J. (2004) - *Stable isotope geochemistry*: 5<sup>th</sup> edition, Springer Verlag, Berlin, pp. 244.
- IAEA/WMO (2001) - *Global Network of Isotopes in Precipitation*. Available by: <<http://isohis.iaea.org>>.
- LA RUFFA G. & PANICHI C. (2000) - *Caratterizzazione chimico isotopica delle acque fluviali: il caso del fiume Arno*. In: «Caratterizzazione chimico isotopica delle acque fluviali: il caso del fiume Arno»: 1-101, Istituti Editoriali e Poligrafici Internazionali, Pisa-Roma.
- MAZZANTI R. & PASQUINUCCI M. (1983) - *L'evoluzione del litorale lunense-pisano fino alla metà del XIX secolo*. Boll. Soc. Geogr. It., **12**: 603-628.
- MUSSI M., LEONE G. & NARDI I. (1998) - *Isotopic geochemistry of natural water from the Alpi Apuane-Garfagnana area, Northern Tuscany, Italy*. Miner. Petrogr. Acta, **41**: 163-178.
- PIPER A.M. (1944) - *A graphic procedure in the geochemical interpretation of water analyses*. Am. Geophys. Un. Trans., **25**: 914-923.
- PRANZINI G. (2002) - *Groundwater salinization in Versilia (Italy)*. Proc. SWIM 17<sup>th</sup>: 412-421, Delft, Holland.
- PROVINCIA DI PISA (2005) - *La Geologia della Provincia di Pisa - Cartografia, Geositi e Banche Dati*. Provincia di Pisa, Area Governo del Territorio-Servizio Difesa del Suolo.
- RAU A. & TONGIORGI M. (1974) - *Geologia dei Monti Pisani a sud-est della valle del Gnappero*. Mem. Soc. Geol. It., **13** (3): 227-408.
- REGIONE TOSCANA (1988) - *Carta Generale del Territorio*. Ed. S.EL.CA., Firenze.
- ROSSI S. & SPANDRE R. (1994) - *L'intrusione marina nella falda artesiaiana in ghiaia nel litorale pisano*. Acque Sotterranee, **43**: 51-58.
- ROSSI S. & SPANDRE R. (1995) - *Caratteristiche idrochimiche della prima falda artesiaiana in sabbia nei dintorni di Pisa*. Acque Sotterranee, **48**: 27-48.
- SERGE A. (1955) - *Nota sulla idrografia continentale e marina*. In: «Note illustrative della Carta Geologica d'Italia, scala 1:100.000, Foglio 111 Livorno». Serv. Geol. d'It., Roma.
- SPANDRE R., CERAGIOLI M. & SPINICCI A. (1999) - *Realizzazione di una carta di vulnerabilità degli acquiferi della Pianura pisana compresa tra la linea di costa, il Canale Scolmatore, il Fosso della Bufalina e la città di Pontedera*. Provincia di Pisa, Settore Pianificazione del Territorio.
- UNESCO (2007) - *Global sea-level: past, present and future*. Reprint from IOC Annual Report 2006: pp. 8.
- WALLING D.E. & FANG D. (2003) - *Recent trends in the suspended sediment loads of the World's Rivers*. Global Planet Change, **39**: 111-126.

## Sedimentology, stratigraphic architecture and preliminary hydrostratigraphy of the Metaponto coastal-plain subsurface (Southern Italy)

*Sedimentologia, architettura stratigrafica e idrostratigrafia preliminare del sottosuolo della piana costiera metapontina (Italia meridionale)*

CILUMBRIELLO A. (\*), SABATO L. (\*), TROPEANO M. (\*),  
GALLICCHIO S. (\*), GRIPPA A. (\*), MAIORANO P. (\*),  
MATEU-VICENS G. (\*\*), ROSSI C.A. (\*\*\*), SPILOTRO G. (\*\*\*\*),  
CALCAGNILE L. (\*\*\*\*\*), QUARTA G. (\*\*\*\*\*)

**ABSTRACT** - The stratigraphic and hydrostratigraphic architecture of the Metaponto coastal plain subsurface (Southern Italy) was obtained from a data set composed of twenty continuously cored boreholes and over 350 drills, 50-120 m deep. In particular, sedimentological, biostratigraphical and chronostratigraphical analyses were performed on four continuously cored boreholes. Further more, some profiles, parallel and transversal to the present-day shoreline, permitted correlations between the stratigraphic logs obtained from all boreholes. The overall obtained data allowed the distinction of four types of depositional systems of Middle Pleistocene-Holocene age, including eight facies associations in turn subdivided in seventeen lithofacies.

Thanks to the recognition of two discontinuity surfaces of regional extent, the late Quaternary Metaponto buried succession may be subdivided into three units, each made up of different lithofacies. The middle-upper (?) Pleistocene lower unit ("substratum"), at least 60 m thick, is made up of silty and clayey-silty shelf-transition deposits passing upward and landward to sandy and sandy-gravelly deltaic deposits. The upper boundary of this lower unit is represented by a very irregular surface which locally deepens up to 90 m and this can be related to incised valleys formed during time spans of sub-aerial exposition induced by relative fallings and low-stands of the sea level. These "palaeovalleys", mainly filled by estuarine deposits, developed during two time spans comprised between the Marine Isotope Stage 4 (MIS 4) and the

Last Glacial Maximum (LGM). The middle unit, called unit MP1 (Metaponto Plain 1), lying on the substratum discontinuously, is late Pleistocene in age and has a thickness of 15 m. However, this thickness reaches 60 m when a palaeovalley is filled. The unit MP1 is composed in the first case of sandy-gravelly fluvial and/or deltaic deposits; in the second case, the palaeovalley is filled with silty-sandy estuarine to deltaic deposits. The upper unit, called unit MP2 (Metaponto Plain 2), lying either on the unit MP1 or on the substratum, is late Pleistocene and Holocene in age. The unit MP2 has a thickness of 30 m. However, when palaeovalleys are filled, thickness may reach 90 m. In the first case it is made up of silty-clay offshore-transition deposits passing upward to silty-sandy deltaic deposits and then finally to sandy fluvial deposits; in the second case, the palaeovalley fill, is composed of sandy-gravelly fluvial deposits passing upward to silty and sandy estuarine deposits.

This stratigraphic frame permits us to sketch the hydrostratigraphic picture of the buried Metaponto succession, where units MP1 and MP2, as a whole, correspond to a multilayered aquifer lying on the clayey substratum. Inside each incised valley, this aquifer appears to be laterally confined and vertically partitioned where permeable deposits alternate with low-permeable ones.

**KEY WORDS:** hydrogeology, Metaponto Plain, Quaternary, Southern Italy, stratigraphy.

(\*) Dipartimento di Geologia e Geofisica, Università degli Studi di Bari "Aldo Moro", 70125 Bari, Italy

(\*\*) MARUM - Universität Bremen, Germany

(\*\*\*) Dipartimento di Scienze Geologiche, Università degli Studi della Basilicata, 85100 Potenza, Italy

(\*\*\*\*) Dipartimento di Strutture, Geotecnica, Geologia Applicata all'Ingegneria, Università degli Studi della Basilicata, 85100 Potenza, Italy

(\*\*\*\*\*) CEDAD - Centro DATazione e Diagnostica - Dipartimento di Ingegneria dell'Innovazione, Università di Lecce, Cittadella della Ricerca, 72100 Brindisi

**RIASSUNTO** – Al fine di proporre una prima interpretazione idrostratigrafica dei depositi sepolti della piana costiera metapontina (Golfo di Taranto - Italia meridionale), un'area che ricade nell'estrema propaggine meridionale della Fossa bradanica, sono stati analizzati venti sondaggi a carotaggio continuo aventi profondità variabili da 50 m fino ad un massimo di 120 m. Lungo quattro carote dei venti sondaggi (quelle per le quali è stata possibile la conservazione presso il Dipartimento di Geologia e Geofisica dell'Università di Bari) sono state condotte analisi di facies di dettaglio ed analisi biostratigrafiche e cronostratigrafiche (datazioni con il metodo del radiocarbonio) di tipo mirato su campioni ritenuti utili. Altre informazioni di carattere esclusivamente litostratigrafico provenienti da oltre 350 sondaggi svolti dall'Ente Irrigazione della Regione Basilicata, di cui non è stato possibile analizzare le carote (ormai perdute) ma solo reinterpretare le stratigrafie di perforazione, ed informazioni indirette di tipo geofisico (*gamma ray logs*) hanno completato il *data set* di partenza. Il riconoscimento di due superfici di discontinuità di significato regionale, ottenuto tramite correlazioni stratigrafiche effettuate lungo profili sia paralleli che trasversali alla linea di costa attuale, ha permesso di suddividere la successione sepolta dell'area metapontina in tre unità sovrapposte, di cui solo la più alta affiorante, ognuna delle quali composta da più litofacies. Il dettagliato studio sui caratteri di facies dei depositi attraversati, sui rapporti latero-verticali delle stesse facies e sull'organizzazione stratigrafica delle loro associazioni ha permesso di distinguere all'interno dei depositi analizzati quattro tipi di sistemi deposizionali: sistema fluviale, sistema deltizio dominato dalle onde, sistema estuarino dominato dalle onde, e sistema di transizione alla piattaforma. Depositati riferibili ad uno o più di tali sistemi costituiscono ognuna delle tre unità, per cui tipi litologici simili, a seconda della loro posizione rispetto alle superfici di discontinuità regionale, possono essere ricondotti ad unità differenti.

L'unità inferiore è stata incontrata a partire da una profondità minima di almeno 40 m sotto il livello del mare; costituisce il substrato della successione attraversata dai sondaggi ed è stata perforata per almeno 60 m senza che la base sia stata raggiunta. Tale unità è costituita da depositi prevalentemente siltosi e siltoso-argillosi di ambienti riferiti a sistemi di transizione alla piattaforma, passanti verso terra e verso l'alto a depositi sabbiosi e sabbioso-ghiaiosi di ambienti riferiti a sistemi deltizi dominati dalle onde. Da considerazioni di carattere geologico regionale, l'unità viene attribuita al Pleistocene medio e, dubitativamente, superiore; inoltre, la parte siltoso-argillosa dell'unità può essere considerata come la porzione più recente della formazione delle argille subappennine, facente parte del ciclo di riempimento della Fossa bradanica. Il tetto dell'unità inferiore è rappresentato da una superficie molto irregolare ed articolata, localmente caratterizzata da bruschi approfondimenti che vengono riferiti ad incisioni vallive prodottesi in intervalli di tempo di esposizione subaerea dell'area e correlati a fasi di caduta e stazionamento basso del livello relativo del mare. Il loro riempimento sarebbe avvenuto prevalentemente ad opera di sistemi deposizionali estuarini dominati dalle onde sviluppatisi durante intervalli di tempo di risommersione dell'area correlati a fasi di risalita del livello relativo del mare. Un primo ciclo di caduta e risalita relativa del livello del mare, riferito ad un intervallo di tempo compreso fra il MIS 4 (*Marine Isotope Stage* 4) e il LGM (*Last Glacial Maximum*) e quindi al Pleistocene superiore, avrebbe permesso prima lo sviluppo e successivamente l'erosione al tetto dell'unità intermedia, definita "unità MP1" (*Metaponto Plain* 1). Questa costituisce un corpo discontinuo e a geometria irregolare il cui tetto può essere riconosciuto ad una profondità di circa 30 m. L'unità MP1 presenta uno spessore di 15 m che aumenta bruscamente fino

ad un massimo di 60 m dove riempie una paleovalle; nel primo caso si tratta di depositi sabbioso-ghiaiosi di ambienti riferiti a sistemi fluviali e/o deltizi, nel secondo caso di depositi siltoso-sabbiosi di ambienti riferiti a sistemi estuarini passanti verso l'alto a depositi siltoso-sabbiosi di ambienti riferiti a sistemi deltizi. Un secondo ciclo di caduta e risalita relativa del livello del mare avrebbe determinato prima l'incisione di una nuova serie di valli fluviali su entrambe le unità precedenti e successivamente il loro riempimento da parte di depositi di ambienti riferiti a sistemi estuarini; il colmamento delle valli sarebbe stato seguito dall'aggradazione di depositi siltoso-argillosi di ambienti riferiti a sistemi di transizione alla piattaforma che passano verso l'alto a depositi siltoso-sabbiosi di ambienti riferiti a sistemi deltizi ed infine a depositi sabbiosi di ambienti riferiti a sistemi fluviali, questi ultimi costituenti l'attuale piana metapontina. L'insieme di questi depositi costituisce l'unità superiore, definita "unità MP2" (*Metaponto Plain* 2) e riferita ad un intervallo di tempo compreso fra il LGM e l'attuale (parte alta del Pleistocene superiore e Olocene). A causa della base irregolare l'unità MP2 mostra spessori variabili da 30 m fino ad un massimo di 90 m nei riempimenti delle paleovalle.

I caratteri stratigrafici riconosciuti e le caratteristiche di facies riscontrate permettono di considerare i depositi siltosi e siltoso-argillosi dell'unità più bassa, cioè quelli riferiti alla formazione delle argille subappennine, come il substrato dei depositi del sottosuolo della piana metapontina. La superficie di tetto di tale substrato, articolata dalla presenza delle profonde paleoincisioni vallive, corrisponde all'acquitrando di un unico acquifero multistrato ospitato nelle due unità stratigraficamente sovrastanti il substrato. Alla luce dell'architettura stratigrafica riconosciuta nelle due unità sovrastanti il substrato, nei riempimenti delle incisioni vallive l'acquifero si approfondisce ed è confinato lateralmente dai depositi del substrato che costituivano i fianchi delle paleovalle successivamente riempite. Verticalmente l'acquifero risulta partizionato, con falde in pressione presenti nei corpi più porosi ospitati nel riempimento delle paleovalle e falde freatiche, non confinate lateralmente, nei corpi porosi ospitati nella porzione più alta della successione che caratterizza il sottosuolo della piana metapontina.

**PAROLE CHIAVE:** idrogeologia, Italia Meridionale, Piana di Metaponto, Quaternario, stratigrafia.

## 1. - INTRODUCTION

To suggest correct land-uses and management of present-day coastal and alluvial plains it is necessary to continuously increase the knowledge regarding the hydrogeologic set-up of sedimentary successions located below the topographic surface of these plains. Therefore, both detailed data regarding subsurface stratigraphy as well as models of spatial distributions of analysed facies are needed. However, these kinds of information cannot be obtained without the knowledge of both sedimentary dynamics of depositional systems and their response to relative sea-level/base-level changes.

Thanks to data interpretation of several cores and following the above outlined approach, this paper represents the first attempt to detail through



a sequence-stratigraphy frame the hydrogeologic structure of the buried late Pleistocene to Holocene succession of the Metaponto coastal area (Taranto Gulf, Southern Italy). Interpretation of stratigraphic and sedimentological features allowed us to suggest 2D geometric reconstructions of facies distribution and stratigraphic architectures of late Quaternary buried bodies. This may represent the starting point for a further, more detailed and better constrained picture of the hydrogeologic structure and so for better aquifer-management.

## 2. - GEOLOGICAL SETTING

The studied succession lies below the Metaponto coastal plain (fig. 1a, b), a wide and flat area facing the Ionian Sea in the Taranto Gulf (Southern Italy). The elevation of this plain reaches no more than 15 m above sea level. In this area, five main rivers (from the south to the north: Sinni, Agri, Cavone, Basento, and Bradano rivers – fig. 1b) run more or less parallel to each other before reaching the shoreline. Regionally, the Metaponto coastal plain represents the most recent exposed sector of the Southern Apenninic foredeep (the Bradanic Trough) (fig. 1a), a foreland basin that, at least since middle Pleistocene times, is in uplift (CIARANFI *et alii*, 1983; DOGLIONI *et alii*, 1994; 1996). Inland, this active uplift allowed us to ob-

serve stratigraphic and sedimentological features of the upper part of the infill succession of the Bradanic Trough. The outcropping part of this succession is made up of lower and middle Pleistocene offshore silty clays (Argille subappennine formation) (CIARANFI *et alii*, 1996) followed by coarse-grained coastal and continental deposits known as “regressive coastal deposits of the Bradanic Trough” (PIERI *et alii*, 1996). These regressive deposits diachronously developed onto the Argille subappennine formation (TROPEANO *et alii*, 2002), forming the well-known staircase of marine-terraced deposits of the Metaponto area (*i.e.* CILUMBRIELLO *et alii*, 2008, and references therein), in the southernmost sector of the Bradanic Trough. Studies about the Metaponto coastal plain, starting from COTECCHIA & MAGRI (1967), mostly concerned the geomorphological features or focused on the development of a narrow litoral strip facing the sea (COTECCHIA *et alii*, 1971; COCCO *et alii*, 1975; BONORA *et alii*, 2002; among others). Only recently, as regards the sedimentological characters of the whole plain, lithologies and other facies features of the outcropping deposits were mapped in detail and referred to environments belonging mainly to alluvial or delta/beach systems (PESCATORE *et alii*, 2009).

As regards the buried succession, firstly it was described by VEZZANI (1967) as being made up of post-Tyrrhenian siliciclastic deposits, up to 40 m thick, overlying Calabrian clays (the Argille subap-

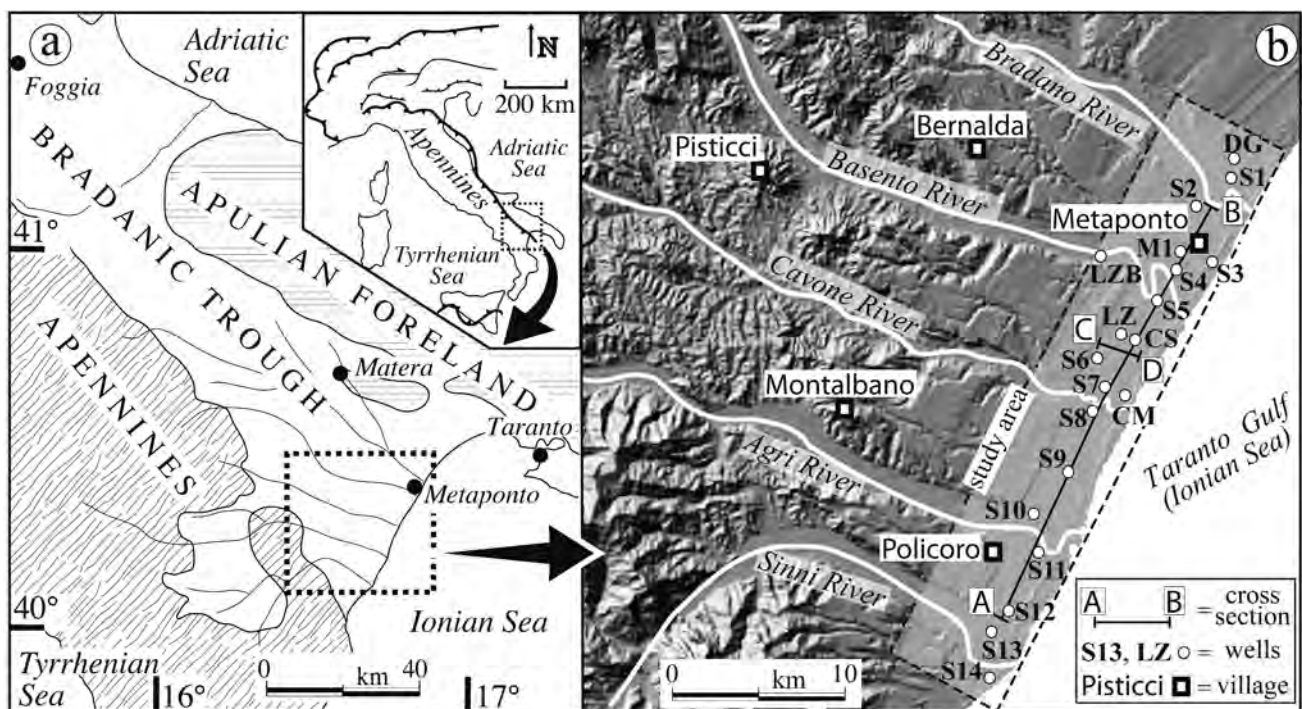


Fig. 1 - a) Schematic geological map of the Southern Italy; b) study area with location of the wells analyzed in this work and trace of cross-sections in figures 4 and 5.  
- a) Carta geologica schematica dell'Italia meridionale; b) area di studio con ubicazione dei sondaggi analizzati in questo lavoro e traccia delle sezioni geologiche nelle figure 4 e 5.

pennine formation). Later, COTECCHIA *et alii* (1969) obtained a  $^{14}\text{C}$  age of  $11.700 \pm 160$  years BP at about 50 m of depth below the Sinni river (fig. 1b), whilst BOENZI *et alii* (1987) suggested the age of the upper part of the buried succession of the Metaponto plain, at about 3 m of depth, thanks to archaeological remains dated between the 7<sup>th</sup> and the 3<sup>rd</sup> century BC.

As regards the stratigraphy of the buried succession, thanks to some wells and following a sequence stratigraphic approach, CAPRETTO (2003) recognized the Holocene Transgressive Systems Tracts (TST), below, and the Highstand Systems Tracts (HST), above, in a 50 m thick succession. In the same year, POLEMIO *et alii* (2003a), after a preliminary study of POLEMIO & RICCHETTI (1991) and thanks to a data set of more than one thousand boreholes, proposed a schematic geolithological 2D view of the buried deposits of the Metaponto coastal area. According to POLEMIO *et alii* (2003a), four units, each of them displaying different thicknesses moving either along dip or along strike, characterize the Metaponto subsurface. The upper unit is made up of clays, from a few centimetres up to 10 m thick. The second unit is made up of gravelly sands with thin silty clayey and clayey layers; this unit, whose bottom may reach 45–50 m of depth, is characterized by a variable thickness. The third unit, often only touched by drills, consists of silty clays and clays whose drilled thickness may reach up to over 30 m. The fourth unit, rarely reached by drilling, consists of either fine- or coarse-grained grey sands. From a hydrogeologic point of view the same Authors recognized in the plain two different types of aquifers: one type encloses aquifers constituted by alluvial deposits of present-day rivers; the other type of aquifer is a coastal multilayered one and corresponds to the second unit of the coastal plain. According to POLEMIO *et alii* (2003b), this coastal aquifer is laterally widespread but its transversal continuity is partially reduced by the deep riverbeds of the different rivers flowing into the Ionian Sea.

Later, SPILOTRO (2004), proposing a simplified 2D stratigraphic reconstruction of the buried Metaponto succession, provided a different interpretation of the depth and size of the multilayered aquifer, whose lower boundary corresponds to an erosional profile cutting a “basement” made up of “blue clays”. According to this Author, below the present-day shoreline and in correspondence to present-day river mouths, this boundary deepens at about 100 m below the sea level, recording the base level reached by rivers during the Last-Glacial Maximum (LGM) and so the coastal multilayered aquifer of the Metaponto plain comprises the sedimentary fill of these paleovalleys.

A more detailed stratigraphic interpretation of the subsurface of Metaponto coastal plain was recently proposed by PESCATORE *et alii* (2009). The authors drew some geological sections normal to the present-day shoreline and located away from paleovalleys axes; they subdivide the buried succession in three units which, from the bottom to the top, are: a middle and upper Pleistocene first unit, which represents the substratum and corresponds to the Argille subappennine formation passing landward to sandy and gravelly sandy deposits; an upper Pleistocene second unit, bounded by unconformities and which represents an up to 20 m thick buried coarse-grained coastal wedge, and an upper Pleistocene and Holocene third unit, which erosionally overlies both the previous units and is made up of a coarse-grained coastal wedge passing seaward to shelf-transition deposits up to about 50 m thick.

### 3. - METHODS AND DATA SET

The study of subsurface of alluvial and/or coastal plains needs many integrated data coming from different methodological approaches ranging from core-drilling to seismic analysis and well logs (spontaneous potential logs, gamma ray logs and so on). Moreover, according to AMOROSI (2006), this kind of study requires experience and expertise, since both a good facies reading and the application of sequence stratigraphy may lead to suggest correct 3D interpretations also from either random or apparently ambiguous data.

As regards the buried succession of the Metaponto coastal plain the used data set consists of: i) detailed stratigraphies and sedimentological data derived from four continuously cored boreholes (CS, LZ, CM, LZB) (figs. 1b, 2 and 3) with depths varying from about 50 m up to 120 m. These cores were stored in the “Dipartimento di Geologia e Geofisica” of Bari University (Italy); ii) core stratigraphy of other sixteen continuously cored boreholes reaching a maximum depth of about 120 m (M1, DG, S1–S14) (fig. 1b); samples and some stratigraphic/sedimentological data were collected during drilling even though the cores could not be stored; iii) gamma-logs obtained from several of the studied wells; iv) absolute age on 6 samples represented by valves of marine invertebrates and by organic material ( $^{14}\text{C}$  radiocarbon uncalibrated dates performed at CEDAD, University of Lecce, Italy); v) palaeoecology and biostratigraphy obtained by macro- and micropaleontological analysis from samples coming both from stored and not stored cores; vi) a simplified stratigraphic description derived from hundreds of wells (num-



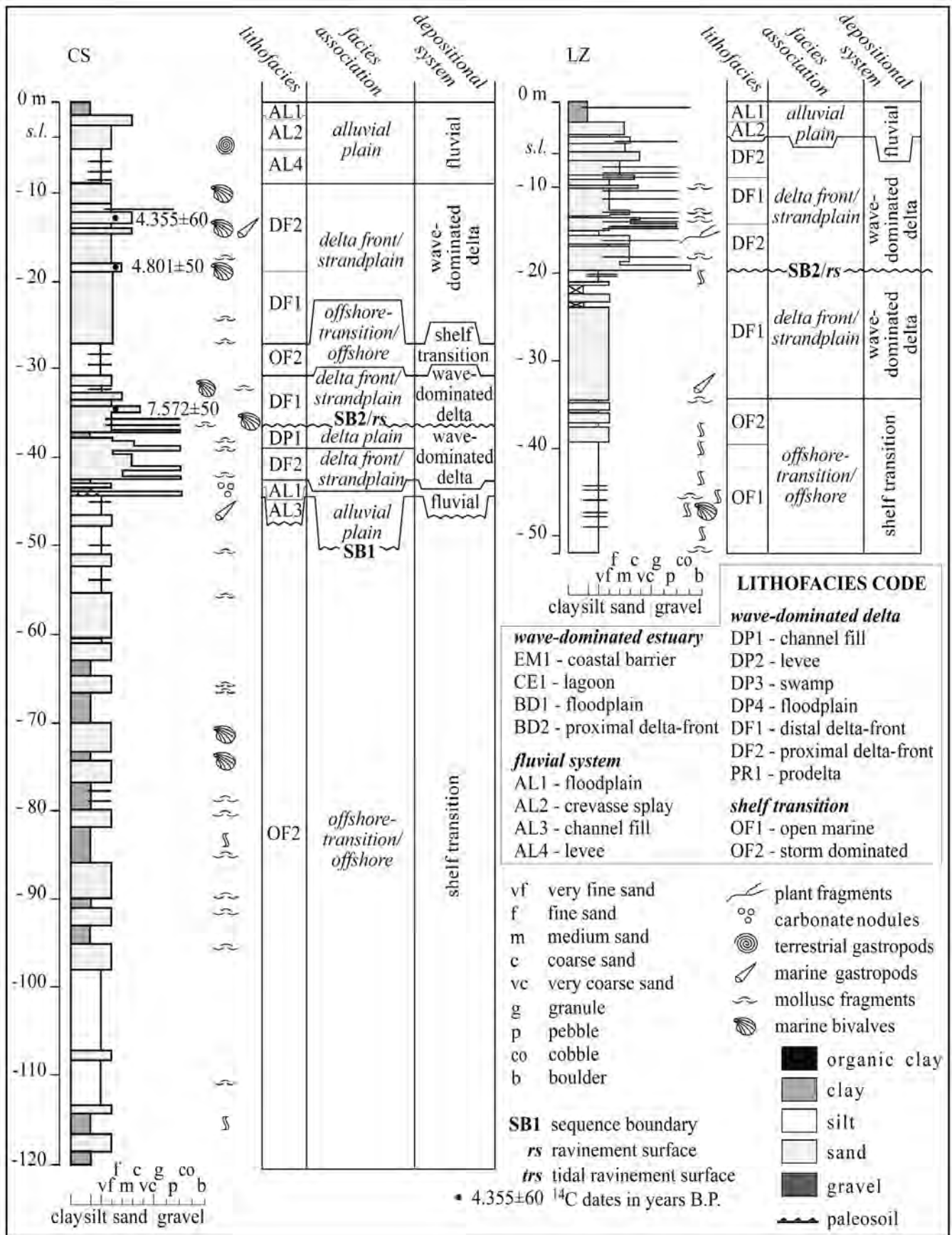


Fig. 2 – Stratigraphy and interpretation of facies associations of cores CS and LZ.  
 – Stratigrafia delle carote di sondaggio CS e LZ con indicazione dei principali caratteri di facies.



bered from 1010 to 1367) drilled at different times by various regional public bodies.

In order to calibrate the stratigraphic data coming from the complete wells set and to propose facies interpretation of each continuously cored borehole, a detailed facies analysis was performed on the four stored cores; this analysis was subsequently used to interpret data coming from the other wells. 2D correlations along both dip and strike with respect to the present-day shoreline, which may be considered more or less parallel to late Quaternary paleoshorelines, also contributed to provide a stratigraphic interpretation of data. Finally, sequence stratigraphy was used to interpret the stacking pattern of the middle Pleistocene to Holocene buried succession of the Metaponto coastal plain.

#### 4. - DEPOSITIONAL SYSTEMS AND FACIES ASSOCIATIONS

In order to suggest a stratigraphic interpretation of the succession drilled in the Metaponto coastal plain, our study started with a careful description of facies features of the four stored cores from the wells CS, LZ, CM and LZB (figs. 1, 2 and 3). Facies were differentiated according to the following features: thickness, lithology, grain size, texture, sedimentary structures, kind of boundary, fossil content. Facies analysis allowed us to recognize several lithofacies (whose vertical relationships result to be either gradational, sharp or erosional), and were used to refine data coming from other 16 wells (M1, DG, and S1-S14) (figs. 1b and 5). Accordingly, the buried stratigraphic succession of the Metaponto coastal plain results basically made up of siliciclastic lithofacies, whose grain size varies from silty clay to gravel and facies associations may be referred to depositional environments varying from fully marine to continental. Previous similar works performed along Italian coastal plains and some concepts deriving from sequence stratigraphy helped us to better constrain our environmental and stratigraphic interpretations. Present-day Italian coastal plains developed after the sea-level rise which followed the Last-Glacial Maximum (LGM), and, before this rise, continental shelves were exposed and subjected to subaerial and fluvial erosion (TORTORA *et alii*, 2001). Exposed shelves were incised by deep river-valleys in response to up to 100 m of sea level fall linked to the LGM, and this morphology, now buried below a thick sedimentary succession, was recognized below both Tyrrhenian and Adriatic coastal plains (BELLOTTI *et alii*, 1994, 1995; AGUZZI *et alii*, 2005; AMOROSI *et alii*, 2008a; 2008b;

MILLI *et alii*, 2008), and also below the Metaponto coastal plain (SPILOTRO, 2004). The post-LGM succession began to develop soon after the onset of the deglaciation phase, when a sea-level rise with a growth rate higher than the rate of sediment supply took place (*i.e.* PIRAZZOLI, 1997). According to sequence-stratigraphy principles and studies, river-valleys deeply cut shelves which become exposed as a consequence of a lowering of the sea level; during transgression due to sea-level rise following this phase of sea-level fall and low-stand, valleys are flooded by the sea (POSAMENTIER & VAIL, 1988) and mainly estuarine systems develop inside previous incisions (DALRYMPLE *et alii*, 1992; ZAITLIN *et alii*, 1994). When, during rise, the sea level reaches margins of flooded valleys, paleointerfluvial areas are drowned and shelf environments develop, whereas, when sea level decreases and stops rising, up to a relative still stand, coastal plain progradation takes place on the previous shelf deposits and aggrading to prograding fluvial and wave-dominated delta depositional systems develop (POSAMENTIER & VAIL, 1988). According to these depositional steps, several facies, belonging to different depositional systems, spanning from shelf, delta, estuarine and alluvial systems, should be encountered during drilling of the Metaponto coastal plain. In accordance with this idea, our data demonstrate that the buried stratigraphic succession of the Metaponto coastal plain comprises facies associations belonging to these depositional systems. In order to avoid repetitions and to make the illustration of the buried succession easier, the depositional systems are described first; interpretation of facies and facies associations previously made following the main literature regarding facies analysis and its application to sequence stratigraphy (*i.e.* VAN WAGONER *et alii*, 1990; WALKER & JAMES, 1992; READING, 1996; POSAMENTIER & ALLEN, 1999; CATUNENANU, 2006; POSAMENTIER & WALKER, 2006; among others) is proposed inside the description of each depositional system, whose definition was obtained also in accordance with logs correlations. The different systems are described from continental to fully marine ones.

##### 4.1. - FLUVIAL SYSTEM

As suggested by POSAMENTIER & VAIL (1988), along basin margins recording sea-level changes, fluvial deposition may be described as “wide-spread” or “incised-valley fill”. The first type characterizes deposition during eustatic highstand of the sea level, when progradation rather than aggradation takes place. Deposits of these fluvial systems show a good lateral continuity and often are

linked to meandering rivers. On the contrary, the second type of fluvial deposition basically develops during late lowstand and early transgression of eustatic sea-level variations, and characterizes both the lowermost and the landward parts of incised-valley fills (DARLIMPLE *et alii*, 1992; ZAITLIN *et alii*, 1994). Deposits of these fluvial systems are confined within incised-valleys, show an along dip (along incised valley) continuity, and may be linked either to meandering or braided rivers.

Without making differentiations between the two types of fluvial deposition, four lithofacies (AL1, AL2, AL3 and AL4) (fig. 2 and well log LZB in fig. 3), often in relationship to each other and belonging to alluvial plain facies association, were recognized in the drilled deposits.

Lithofacies AL1 is made up of clayey silts and/or massive grey clays rich in organic material (plant fragments). These deposits form up to 10 m thick successions. Yellowish and reddish-brown alteration-colours and pedogenic structures, such as carbonate nodules, often characterize and pervade these deposits. Macropaleontological content is represented by terrestrial gastropods, such as *Helicidae*, while micropaleontological content is formed by ostracods and abundant algae (*Characea* oogonia). This monotonous succession of clays and clayey silts, showing features that testify to phases of subaerial exposure, is interpreted as the result of the deposition from suspension in low-energy subaqueous depositional environments such as ponds or abandoned channels. For these reasons, this lithofacies can be related to flood-plain deposits. Lithofacies AL2 consists of sandy silts, which form lenticular bodies up to about 5 m thick, that locally show a coarsening-upward trend, from very fine to medium sands. This lithofacies displays the same macro- and micropaleontological content observed within lithofacies AL1. Based on geometry, macro- and micropaleontological content and coarsening upward tendencies, this lithofacies can be referred to crevasse splay deposits. Lithofacies AL3 is made up of gravels, gravelly sands and sands, which compose erosionally based successions whose thickness varies from 1 m to about 3 m (well log LZB in figure 3, where lithofacies AL3 repeats itself forming an about 10 m thick succession). These deposits form narrow and continuous bodies, mainly elongated perpendicularly to the paleoshoreline. Thicker successions show a fining-upward trend and basically are distinguished in two parts: the lower part is made up of clast-supported and poorly-sorted gravels with angular clasts, composed either of small pebbles and/or pebbles/cobbles; the upper part is mainly made up of poorly sorted and massive sands containing rare and a few decimetres

thick gravelly layers. A few decimetres thick dark clays cap the succession. Pedogenic structures, such as carbonate nodules, also characterize this lithofacies. Moreover, terrestrial small gastropods, such as *Helicidae*, were observed. The geometry, texture, fining-upward trend, paleontological content, and erosional base of AL3 lithofacies are characteristics of fluvial channel-fill deposits. The lithofacies AL4 is made up of rhythmical alternation of silty sands and silty clay layers, a few centimetres thick, and commonly shows a brownish colouring. These facies features permit us to refer the lithofacies AL4 to levee deposits.

#### 4.2. - WAVE-DOMINATED DELTA SYSTEM

Along microtidal coasts fed by river sedimentary discharge, where waves energy exceeds river-capacity to build a prominent delta, wave-dominated delta systems develop. These depositional systems consist of a set of laterally continuous beach ridges (delta front/strandplain), landward passing to a delta plain (simulating a widespread fluvial system) and seaward passing to prodelta settings. According to sequence stratigraphy concepts, wave-dominated delta systems mainly develop and aggrade during slow rises of the sea level, for example during eustatic high stands (POSAMENTIER & VAIL, 1988).

Three facies associations belonging to wave-dominated delta systems were recognized within drilled deposits: delta plain, delta front/strandplain and prodelta facies associations.

The delta plain facies association is composed of four lithofacies: DP1, DP2, DP3 and DP4 (well log CS in fig. 2 and fig. 3). Lithofacies DP1 is characterized by up to 4 m thick sandy-silty deposits, showing an erosional basal surface coupled with a basal channel lag and a fining-upward trend. These deposits generally form isolated bodies and this involves a scanty correlation with the adjacent cores. Based on geometry, grain size tendencies and erosional base, this lithofacies can be attributed to channel-fill deposits. Lithofacies DP2 is made up of a few centimetres thick silty sands and silty clay layers, showing a rhythmical alternation, up to 4 m thick. Some layers show a yellow shading caused by subaerial alteration. Locally these deposits present a fining-upward trend. On the basis of facies features, this lithofacies can be referred to levee deposits. Lithofacies DP3 is basically made up of up to 50 cm thick intensively bioturbated dark clays with abundant plant fragments. These deposits are the result of sedimentation in stagnant environments and so are interpreted as swamp deposits. Lithofacies DP3 generally alternates with lithofacies DP4. The latter is made up of grey clays and

silty clays which display characteristic yellow and brown colours, due to the presence of iron and manganese oxides, and form up to 6-7 m thick successions. These kinds of features can indicate floodplain deposits.

The delta front/strandplain facies association forms up to 25 m thick and laterally continuous bodies and consists of two major lithofacies: DF1 and DF2 (fig. 2 and well log CM in figure 3). Lithofacies DF1 is made up of about 15 m thick successions of well-sorted and thin laminated fine sands and silts with intercalations of very-fine sand layers, up to 1 m thick. Indeterminable shell fragments are abundant throughout this lithofacies. Based on these facies features, lithofacies DF1 is interpreted as the lower part of delta front/strandplain facies association and represents the distal delta front/lower shoreface deposits. Lithofacies DF2 is made up of up to about 10 m thick successions of fine sands with thin pebbly layers, passing upward to fine- to coarse-sands and pebbly sands. This lithofacies contains assemblages of marine molluscs, such as *Tellina* sp., *Spisula subtruncata*, *Chamelea gallina*, *Cerithium* sp. and *Fissidentalium rectum*, in addition to abundant indeterminable shell fragments (LA PERNA, 2010, *pers. comm.*). On the basis of sedimentary features and fossil content, the lithofacies DF2 can be referred to proximal delta front/upper shoreface deposits.

The micropaleontological content of samples coming from both distal delta front/lower shoreface (lithofacies DF1) and proximal delta-front/upper shoreface deposits (lithofacies DF2) is scanty: benthic foraminifers are mainly represented by relatively deep species (*Euvigerina peregrina*, *E. mediterranea*, *Lenticulina* sp.) often included in Low-Oxygen Foraminiferal Assemblages (LOFA *sensu* BERNHARD & GUPTA, 1999); planktonic foraminifers are very scarce and reworked.

The prodelta facies association forms up to about 10 m thick successions whose thickness decreases moving landward. Within this facies association, one lithofacies (PR1) (well log CM in figure 3) was recognized and it is made up of rhythmic alternation of silts and very fine-grained sands. Abundant marine molluscs, such as *Tellina* sp. and *Fissidentalium rectum*, besides indeterminate fragments of bivalves, scaphopods, serpulids, and gastropods, were found. The micropaleontological content includes foraminifera assemblages represented by *Ammonia beccarii*, *Elphidium macellum*, *Lachlanella* sp., *Pseudotriloculina oblonga*, *Textularia* sp., *Nonion* sp., *Sigmoilina schlumbergeri*. The described facies features, and macro- and micropaleontological content are typical of relatively deep, oxygen-poor and high-organic matter environments such as those of prodelta.

#### 4.3. - WAVE-DOMINATED ESTUARY SYSTEM

This depositional system typifies flooded incised-valleys (BOYD *et alii*, 2006, and references therein) and related successions aggrade in these valleys during transgressions induced by eustatic sea-level rises following a main phase of relative sea-level fall and lowstand. Within this system three facies associations were recognized: bayhead delta, central estuary and estuary-mouth complex facies associations (according to settings standardized by DARLYMPLE *et alii*, 1992, and to terminology recently introduced by CATUNEANU, 2006). Also in the studied logs, sediments related to a wave-dominated estuary system characterize incised-valley fill successions that can reach up to 65 m of thickness.

The bayhead-delta facies association forms up to about 10 m thick successions, and is represented by two lithofacies: BD1 and BD2 (well log LZB in fig. 3). Lithofacies BD1 is basically represented by up to about 9 m thick grey silty-clayey deposits, showing yellow and brown mottles, due to iron and manganese oxides and pedogenic phenomena. Moreover, these deposits contain abundant plant debris. These facies features allowed us to refer BD1 lithofacies to floodplain deposits. Lithofacies BD2 is made up of very fine and medium sandy deposits showing occasionally a coarsening upward trend. Remains of plants are present. These deposits form sandy bodies interpreted as delta front deposits.

The central estuary facies association is composed of up to about 20 m thick monotonous successions, within which only one lithofacies was recognized: CE1 (fig. 3). This lithofacies is made up of silts and organic clays with intercalations of thin (from a few centimetres to some decimetres) parallel-laminated sand layers. Paleontological analyses, performed on these deposits, show a highly bioclastic content which includes, besides foraminifers, ostracids, gastropods, echinoids, and *Ditrupa* sp., also fragments of bivalves, rare fragments of bryozoans and echinoids, and very rare fish teeth. Foraminiferal assemblage is dominated by *Ammonia beccarii*, *Elphidium crispum* and, less abundant, *Valvulineria bradyana*. The latter has been documented in LOFA and tolerates dysoxic conditions (MURRAY, 2006). *Ammonia beccarii* also belongs to the LOFA, and tolerates a wide range of salinity and temperature. Other taxa, such as Boliviniids and Buliminids, along with Textulariids and Nonionids, also indicate low-oxygen contents (BERNHARD & GUPTA, 1999); other observed species correspond to low-oxygen tolerant taxa, along with other forms typically from *Posidonia oceanica* meadows (*i.e.* *Pseudotriloculina*/*Triloculina* spp., *Quinqueloculina vulgaris*, *Lobatula lobatula*, *Textu-*



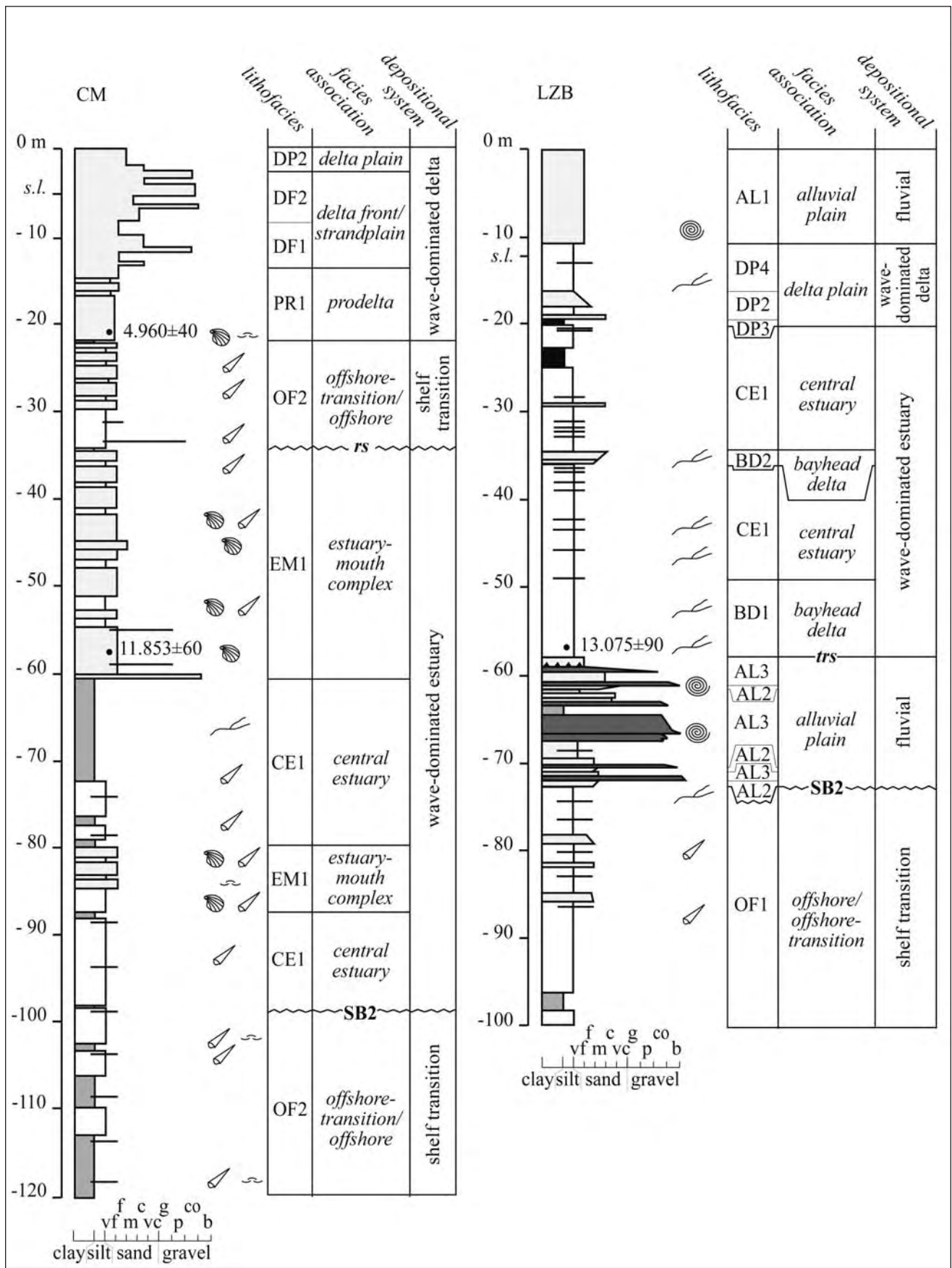


Fig. 3 - Stratigraphy and interpretation of facies associations of cores CM and LZB. Key as in figure 2.  
- Stratigrafia delle carote di sondaggio CM e LZB con indicazione dei principali caratteri di facies. Per la legenda vedi figura 2.

*laria gramen*). Also *Elphidium crispum*, *Elphidium macellum* and Miliolids (*Pseudotriloculina trigonula*) and Textularids (*Textularia communis*, *Textularia gramen*) can be related to *Posidonia oceanica* meadows. Reworked planktonics are also present (genera *Globigerinoides* sp. and *Globigerina* sp.). Fine sediments, sedimentary structures, presence of organic matter and micropaleontological content are relative to low energy environments, such as lagoon deposits in estuarine context.

The estuary-mouth complex facies association forms up to over 25 m thick successions and is composed of one lithofacies: EM1 (fig. 3). This lithofacies is made up of silty sands to well-sorted and thinly laminated fine sands, with intercalation of silty layers. Locally, thinner pebbly layers can be observed. Many fragments of molluscs are present and among these, it is possible to recognize *Turritella communis*. These facies features and their location in the studied successions allowed us to refer EM1 lithofacies to a sandy barrier (coastal-barrier deposits) aggrading during short still-stands of the relative sea-level characterizing a major relative sea-level rise.

#### 4.4. - SHELF-TRANSITION SYSTEM

Shelf-transition system corresponds to widespread settings located both seaward of clastic shorelines and below main wave-base level. According to sequence stratigraphy concepts, shelf deposits may be cyclically exposed and cut by rivers (incised valleys) during main eustatic sea-level falls and lowstands. In the studied successions, shelf-transition system deposits were diffusely drilled below suites of deposits belonging to the previously described depositional systems, but they also represent facies of shallow-marine settings located seaward of either wave-dominated delta systems or wave-dominated estuary systems.

The shelf-transition system forms laterally extensive and up to 75 m thick sedimentary bodies. One facies association was recognized (offshore transition/offshore facies association) and two lithofacies were distinguished (OF1 and OF2) (figs. 2 and 3). Lithofacies OF1 is made up of silty and clayey deposits, commonly constituted by massive strata, locally homogenized by an intense bioturbation. This lithofacies shows facies characteristics typical of open-marine deposits. Lithofacies OF2 is made up of an alternation of either beds or bedsets made up of silts, clays and very fine-grained sands. Silts and clays are massive or thinning laminated; the sands are very sorted and laminated, and are organized in layers forming up to 5 m thick bedsets bounded both at the base and top by erosional/sharp surfaces. Sands may contain very thin

intercalations of grey silty clays. Marine macrofossils are abundant and commonly constitute assemblages of *Ditrupa aretina*, *Turritella communis*, and *Corbula gibba*. The characteristics of lithofacies OF2 are representative of deposits developing below the mean fairweather wave base when storm events cause the accumulation of sandy deposits inside silty and clay deposits which form, on the contrary, during fairweather conditions (storm-dominated deposits).

## 5 - STRATIGRAPHY OF CORES CS, LZ, CM AND LZB

### 5.1. - CORE CS

Core CS (fig. 2) was drilled about 2.5 km inland from the present-day shoreline (fig. 1b), starting from 4 m a.s.l., and reaching 120 m in length. According to the presence of two main erosional surfaces, the drilled stratigraphic succession shows a 75 m thick lower portion, made up of shelf-transition deposits, an 8 m thick middle portion made up of fluvial and wave-dominated delta deposits, and finally a 37 m thick upper portion, mainly composed of either wave-dominated delta or fluvial deposits (fig. 2).

The lower portion is characterized by very-fine sand, clay and silt offshore-transition/offshore deposits (storm-dominated lithofacies OF2). As regards the middle and upper portions, they form a vertical stack of two transgressive-regressive cycles. The first cycle, about 8 m thick, lies on an erosional surface and starts with clay, sand and gravel alluvial plain deposits (channel-fill lithofacies AL3) passing upward to floodplain lithofacies AL1). Sand and gravel deposits of delta front/strandplain (proximal delta front/upper shoreface lithofacies DF2) overlay with a sharp contact the alluvial plain unit; these lithofacies pass upwards to clay, sand and gravel deposits of the delta plain (channel-fill lithofacies DP1). The second cycle, about 37 m thick, opens with silt, sand and gravel delta front/strandplain deposits (distal delta front/lower shoreface lithofacies DF1) passing upward to silt and sand offshore-transition/offshore deposits (storm-dominated lithofacies OF2). The succession continues again with mainly sandy delta front/strandplain deposits (distal delta front/lower shoreface lithofacies DF1) passing upward to proximal delta front/upper shoreface lithofacies DF2) passing upward to clay, silt and sand alluvial plain deposits (levee, crevasse splay and floodplain respectively lithofacies AL4, AL2 and AL1).

Each cycle is bounded by important unconformity surfaces. The base of the first cycle (about 45

m of depth) is represented by a subaerial erosional surface, since fluvial deposits with paleosoils lie onto marine clays. Stratigraphic correlations with others cores (fig. 4) allowed us to interpret it as a sequence boundary (SB1 in figs. 2 and 4). The boundary between the first and the second cycle, located at about 37 m of depth, is represented by an erosional surface along which delta plain deposits below and delta front/strandplain deposits above come in contact (fig. 2). This contact records a ravinement process which occurred in the studied area, and, thanks to stratigraphic correlations with others cores, it is interpreted as being part of a sequence boundary locally reworked during a transgression (SB2/*rs* in figs 2 and 4).

Moreover, radiocarbon analyses were performed on mollusc samples coming from deposits of the second cycle. In particular, the samples yielded these results: a  $^{14}\text{C}$  uncalibrated age of  $7.572 \pm 50$  years B.P. at 35 m core depth (sample

C6), a  $^{14}\text{C}$  uncalibrated age of  $4.801 \pm 50$  years B.P. at 19 m core depth (sample C3), and a  $^{14}\text{C}$  uncalibrated age of  $4.355 \pm 60$  years B.P. at 13 m core depth (sample C2).

## 5.2. - CORE LZ

Core LZ, 52 m long, was recovered about 3.5 km inland from the present-day shoreline (fig. 1b), starting from 6 m a.s.l. According to the presence of a main erosional surface the core LZ has been subdivided into two portions (fig. 2). The lower portion is 33 m thick and is made up of shelf-transition deposits passing upward to wave-dominated ones; the upper portion, 19 m thick, is composed of wave-dominated deposits passing upward to fluvial ones.

In particular, the lower portion is characterized by silt and very fine sand offshore-transition/offshore deposits (open-marine lithofacies OF1 and

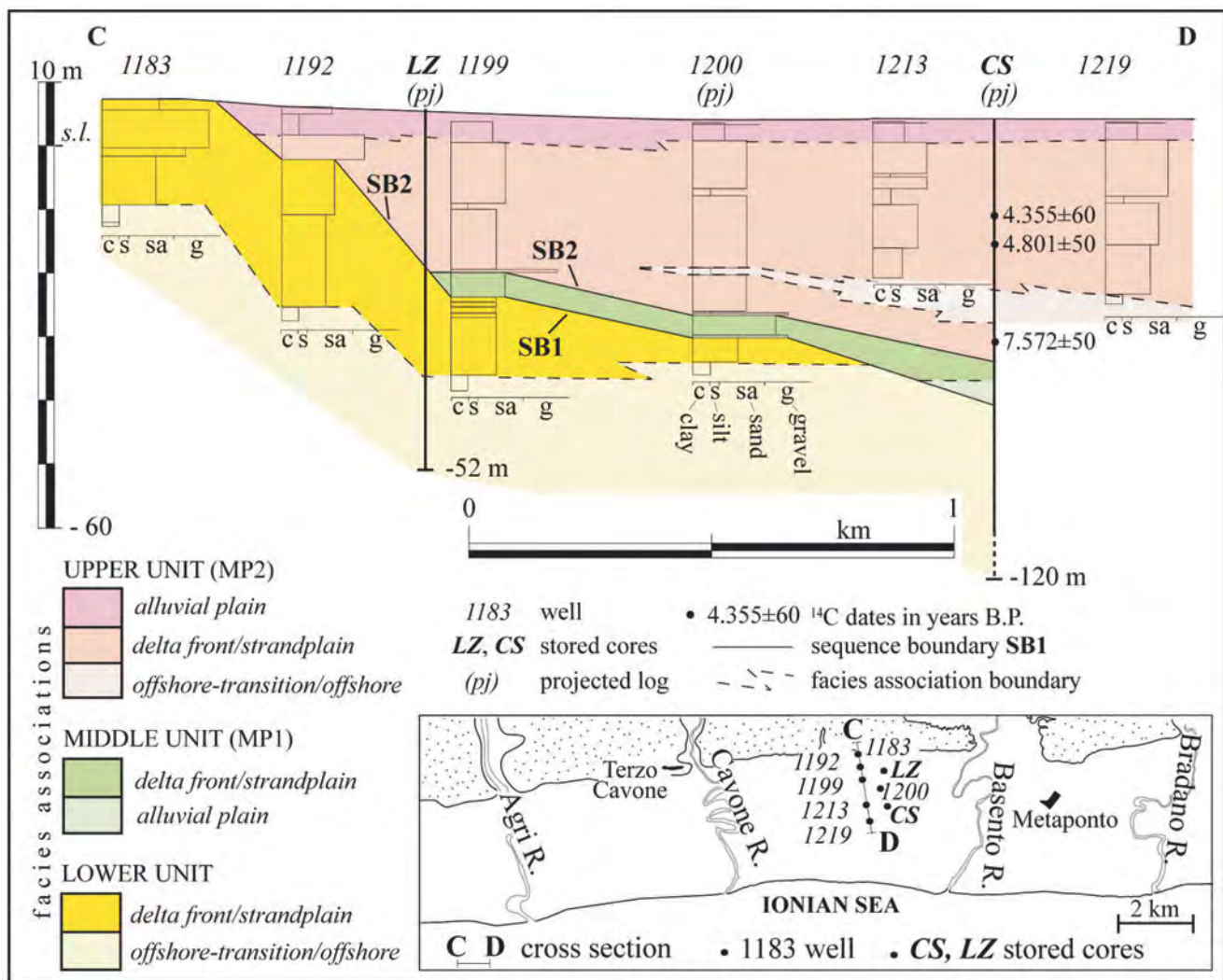


Fig. 4 – Cross section transversal to the present-day shoreline in interfluve areas.  
– Sezione geologica perpendicolare all'attuale linea di costa nelle aree di interfluvio.



storm-dominated lithofacies OF2) passing to very fine sand delta front/strandplain deposits (distal delta front/lower shoreface lithofacies DF1). On these deposits lies the upper portion, consisting of a transgressive-regressive cycle. This cycle is formed mostly by very fine to medium sand and thin gravel delta front/strandplain deposits (proximal delta front/upper shoreface lithofacies DF2, distal delta front/lower shoreface lithofacies DF1, and finally lithofacies DF2 again) passing upward to fine sand and clay alluvial plain deposits (crevasse splay lithofacies AL2 and floodplain lithofacies AL1). The base of this cycle is characterized by an erosional surface overlain by a lag deposit, that can be interpreted as a ravinement surface (*rs*). Stratigraphic correlation with other cores (fig. 4) allowed us to interpret this surface as a part of a sequence boundary which was later and locally reworked by a transgression (SB2/*rs* in figures 2 and 4).

### 5.3. - CORE CM

Core CM (fig. 3) was recovered about 920 m inland from the present-day shoreline (fig. 1b), starting from 5 m a.s.l. and reaching 120 m in length. Thanks to the presence of a main erosional surface, the drilled succession may be subdivided into a lower part made up of shelf-transition deposits, and an upper part mainly made up of wave-dominated estuary passing upward to wave-dominated delta deposits (fig. 3).

The lower part of the core, about 21 m thick, is represented by clay, silt and very thin sand offshore-transition/offshore deposits (storm-dominated lithofacies OF2). The upper part of the drilled succession is instead characterized below by a vertical stack of transgressive-regressive cycles formed by alternating clay/silt central estuary deposits and silt/very fine sand estuary-mouth complex deposits (respectively lagoon lithofacies CE1 and coastal barrier lithofacies EM1), about 64 m thick. Above these cycles develops a 35 m thick succession made up of: i) silt and very fine sand offshore-transition/offshore deposits (storm-dominated lithofacies OF2), ii) very fine sand prodelta deposits (lithofacies PR1), iii) sand to gravel delta front/strandplain deposits (distal delta front/lower shoreface lithofacies DF1 and proximal delta front/upper shoreface lithofacies DF2) and iv) fine sand delta plain deposits (levee lithofacies DP2).

Two important surfaces characterize the entire stratigraphic succession. The first surface, located at about 99 m of depth (fig. 3), represents a sharp and erosional contact, also recognized thanks to gamma log analyses. Along this surface offshore-

transition/offshore deposits and central estuary deposits come into contact. Thanks to stratigraphic correlations with other cores, this surface is interpreted as a sequence boundary (SB2 in figures 3 and 5a). Moreover, two radiocarbon data were obtained from this core, since molluscs fragments sampled at 58 m (sample CM2 in figure 3) and at 21 m (sample CM1 in figure 3) of depth indicated respectively a  $^{14}\text{C}$  uncalibrated age of  $11.853 \pm 60$  years B.P. and of  $4.960 \pm 40$  years BP. These ages allowed us to interpret the sequence boundary SB2 as related to the sea-level fall linked to the Last Glacial Maximum (LGM). Another significant surface is observed at about 35 m of depth (fig. 3). Along this surface estuary-mouth complex deposits and offshore-transition/offshore deposits come into contact. This surface is also underlined by the occurrence of scattered pebbles and is interpreted as a ravinement surface (*rs* in fig. 3).

### 5.4. - CORE LZB

Core LZB, drilled about 6.8 km inland from the present-day shoreline (fig. 1b), starts at 12 m a.s.l. and reaches 100 m of length. The stratigraphic succession is composed of two portions, separated by a disconformity surface, located at about 72 m below the core head (fig. 3). The lower portion consists of about 26 m thick shelf-transition deposits, while the upper 74 m thick portion is made up of fluvial to wave-dominated estuary deposits, passing upward to wave-dominated delta, and finally to fluvial deposits again.

In particular, the lower portion displays silt, fine sand and clay offshore-transition/offshore deposits (open-marine lithofacies OF1). The upper portion forms a transgressive-regressive cycle lying on the previous deposits through an erosional surface. At the base, this cycle includes about 16 m thick alluvial plain deposits (gravel with sand and clay) represented by an alternation of crevasse splay deposits (lithofacies AL2) and fluvial-channel deposits (lithofacies AL3). These fluvial deposits are capped by a palaeosol on which the upper part of the cycle, about 58 m thick, lies. The first 38 m are mainly comprised of a series of high-frequency transgressive-regressive cycles. These cycles are formed by alternation of silt and sand bayhead delta deposits (delta front lithofacies BD1 and floodplain lithofacies BD2) and silt and organic clay central estuary deposits (lagoon lithofacies CE1). The last 20 m are made up of silt and sand delta plain deposits (levee lithofacies DP2, swamp lithofacies DP3 and floodplain lithofacies DP4) passing upward to very fine sand alluvial plain deposits (floodplain lithofacies AL1).

Two important surfaces are recognizable along the succession LZB. A first surface is located at about 74 m of depth (fig. 3) and can be assigned to a subaerial erosional surface, since fluvial deposits lie onto marine clays. This surface is interpreted as a sequence boundary (SB2 in figure 3). At about 58 m of depth a second surface is observed; it represents a sharp surface along which alluvial plain deposit below and bayhead delta deposits above come into contact. This surface can be referred to a flooding surface (a tidal ravinement surface *sensu* ZAITLIN *et alii*, 1994) (*trs* in fig. 3).

Finally, an important radiocarbon age determination was obtained from this core, since plant fragments sampled at 58 m of depth (sample LZ5 in fig. 3) yielded a  $^{14}\text{C}$  uncalibrated age of  $13.075 \pm 90$  years B.P.

## 6. - STRATIGRAPHY AND HYDROSTRATIGRAPHY OF BURIED METAPONTO COASTAL PLAIN DEPOSITS

The detailed stratigraphy and facies analysis of the four stored cores were used to calibrate stratigraphic and lithological data coming from the other wells. All these data allowed us to make bi-dimensional correlations and to propose a preliminary “sequential” interpretation of the stratigraphic organization of the buried deposits of the Metaponto coastal plain. Correlations were made along two geological profiles which cross each other: one runs for about 2 km perpendicularly to the coast (fig. 4), the second runs for about 24.5 km parallel to the coast (about 2.5 km inland) (fig. 5a). A preliminary hydrostratigraphic interpretation was also obtained thanks to these profiles (fig. 5b).

### 6.1. - LITHOSTRATIGRAPHICAL SUBDIVISION

Both the geological profiles show that the buried succession can be vertically divided into three units (figs. 4 and 5a), which will be described from bottom to top.

#### 6.1.1. - *The lower unit*

The lower unit, whose bottom was not reached by the studied wells, is bounded at the top by a very irregular surface. This surface (SB1 in figures 4 and 5a), in the section running parallel to the coast, is mainly located at 40-45 m of depth but, locally it sharply deepens up to about 90 m (logs S4 and CM; fig. 5a) or at least up to about 60 m in those wells where the top of the lower unit was not reached by drillings (logs S3, S9 and S11; fig. 5a).

Along the same geological section, this unit re-

sults to be basically made up of clayey-silty shelf-transition deposits, while, along the geological profiles drawn perpendicularly to the coast, the clayey-silty deposits pass landward to sandy-gravelly delta front/strandplain deposits (fig. 4). Micropaleontological analyses performed on samples of this unit (coming from S1, S8, S12, CS and LZ cores) indicate that calcareous nannofossil assemblages are often poorly preserved and characterized by several reworked *taxa*. The most significant *taxa* are represented by: *Gephyrocapsa oceanica* (> 4 micron), rare to common *Pseudoemiliania lacunosa*, and very rare and possibly reworked specimens of *Gephyrocapsa omega*. This content suggests an age not older than the Middle Pleistocene, between the upper part of *Pseudoemiliania lacunosa* zone and *Gephyrocapsa oceanica* zone of RIO *et alii* (1990). The Last Occurrences of *Gephyrocapsa omega* and *Pseudoemiliania lacunosa*, which represent valuable Middle Pleistocene bioevents in the Mediterranean record according to the scheme of RIO *et alii* (1990), cannot be identified with certainty due to reworking. In accordance with the interpretation proposed in the geological sheet 508 “Policoro” (SABATO *et alii*, in prep.) of the New Geological Map of Italy (CARG Project), this unit represents the “substratum” (“basement” in SPILOTRO, 2004) of the buried succession of the Metaponto coastal plain.

Clayey-silty deposits observed along the section parallel to the shoreline may be interpreted as the youngest part (middle and, dubitatively, upper Pleistocene) of the Argille subappennine formation. When the top of this unit deepens, it indicates the presence of paleoincisions, which, thanks to interpretation of natural gamma radioactivity profiles, were for the first time regionally recognized by SPILOTRO (2004).

#### 6.1.2. - *The middle unit*

The middle unit, here called MP1 (Metaponto Plain 1), is a discontinuous body lying on the substratum; in the section parallel to the coastline, the MP1 unit shows a thickness of about 15 m (logs CS, S5, and S12; fig. 5a), with boundaries (unconformities locally represented by erosional surfaces due to ravinement processes) located between 30 m (top) and 45 m (bottom) below the Metaponto coastal plain. Locally, the lower boundary deepens to 90 m of depth and the unit reaches a thickness of about 60 m (log S4; fig. 5a). According to sequence stratigraphy interpretations, this deepening is interpreted as related to a valley incision which occurred during a phase of falling and early low-stand of the relative sea-level; differently where the lower boundary is found at about 45 m of depth, it represents the exposed surface (palaeotopogra-

phy) in the interfluvial areas during the same time span. Accordingly, the lower boundary of the MP1 unit represents a sequence boundary (SB1). Above the SB1, estuarine deposits (log S4 in fig. 5a) developed in the paleovalley during rise of the relative sea-level; when the relative sea-level reached interfluvial areas, alluvial plain deposits (fluvial-channel, levee, and crevasse splay lithofacies) followed by wave-dominated delta deposits (delta front/strandplain facies associations) developed both above the SB1 in the interfluvial areas, and above the incised-valley fill deposits in correspondence of the paleovalley. According to sequence stratigraphy concepts and to environmental interpretation and superimposition of drilled deposits, estuarine deposits filling the paleoincision are interpreted to be part of the Transgressive System Tract (TST) of a sequence (whose age and hierarchy will be defined below); also fluvial deposits and, partly, the wave-dominated delta deposits (both extending beyond the margins of the incised valley and above it) belong to this TST. The upper part of the wave-dominated delta and the overlying fluvial deposits represent the Highstand Systems Tract (HST) of the same sequence. The upper boundary of the MP1 unit corresponds to the base (lower boundary) of the uppermost unit (see the following paragraph).

#### 6.1.3. - The upper unit

The upper unit, here called MP2 (Metaponto Plain 2), develops from about 30 m of depth up to the topographic surface (logs CS, S4, S5, and S12; fig. 5a) but locally the lower boundary sharply deepens to 90 m in depth (log CM; fig. 5a) (paleoincisions). The deepening of this boundary may be observed in four wells and corresponds to the occurrence of four different incised valleys (logs S11, S9, CM and S3; fig. 5a). Again, according to sequence stratigraphy concepts, where the boundary is found at about 30 m of depth, it is interpreted as the exposed surface in the interfluvial areas during a fall and early lowstand of relative sea-level, which led to the deep incision of the four paleovalleys. These paleovalleys roughly correspond to the present-day river courses. Accordingly, also the lower boundary of the MP2 unit represents a sequence boundary (SB2). In the incised valleys, above the SB2 (in the geological section running parallel to the coastline), bayhead delta, central estuary and estuary-mouth complex deposits were drilled. Landward, in the same incised valleys, fluvial deposits (alluvial plain facies associations) lie on the SB2 below estuary-system deposits (well log LZB; fig. 3). Both fluvial and estuarine deposits developed during the relative sea-level rise. When the

relative sea-level reached interfluvial areas, wave-dominated delta (delta front/strandplain facies associations), passing upward to shelf-transition systems, developed (offshore-transition/offshore facies association) above both the SB2 in the interfluvial areas and the incised-valley fill deposits in correspondence of paleovalleys (fig. 5a). At the end of the transgression, a depositional regression took place since, on previous deposits, progradational wave-dominated delta deposits developed (figs. 4 and 5). The oldest buried sediments linked to this depositional regression were found at least about 7 km landward from the present-day shoreline (well log LZB; fig. 3).

According to sequence stratigraphy concepts, environmental interpretation and superimposition of drilled deposits, fluvial and estuarine deposits that fill paleoincisions together with overlying wave-dominated delta deposits passing to shelf-transition deposits are to be interpreted as the TST of a sequence. Wave-dominated delta deposits passing upward to fluvial-system deposits (the present-day Metaponto alluvial plain), which developed due to a depositional regression, represent part of the HST (the present-day systems-tract in progress) of the same sequence.

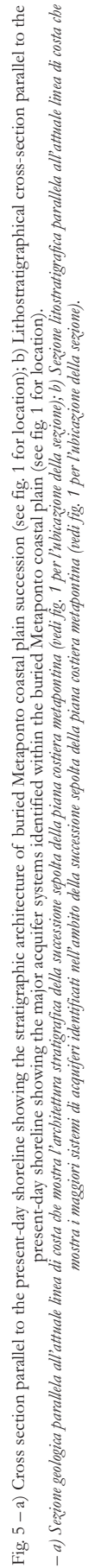
Radiocarbon dating allowed us to assign the MP2 unit to late Pleistocene and Holocene time. In particular, six  $^{14}\text{C}$  uncalibrated dates were obtained from fragments of shells collected in the upper 60 m of cores CM, LZB and CS (see position of samples and ages obtained in figures 2 and 3). As regards biostratigraphical data, calcareous nannofossil content was generally very poor and represented by *Coccolithus pelagicus*, *Reticulofenestra* spp., small *Gephyrocapsa* and scattered specimens of *Gephyrocapsa oceanica* (> 4 micron) and *Emiliania huxleyi*. The occurrence of the latter taxa, found in samples coming from the uppermost 10 m of the upper unit in the S3 core, may be considered in good agreement with the age obtained by radiometric data.

#### 6.2. - AGE AND SEQUENTIAL HIERARCHY OF MP1 AND MP2 UNITS

As suggested on first approximation, the two units above the substratum correspond to systems tracts of two sequences (or to parts of them).

The MP2 unit is the uppermost unit of the buried Metaponto coastal deposits and its upper part corresponds to the outcropping coastal plain deposits. It is bounded below by an unconformity surface (sequence boundary SB2) which sharply deepens from about 30 m up to 90 m in depth (fig. 5a). According to radiocarbon age obtained for deposits belonging to the MP2 unit and to quoted li-





temperature on development of other coastal plains in Italy, these paleovalleys were incised during the last falling and early low stand of the relative sea-level, namely during the LGM. Therefore, the MP2 unit developed after the LGM, and its age is late Pleistocene and Holocene. Palaeovalleys filling was mainly due to backstepping of depositional systems whose deposits, characterized by a deepening-upward trend, record a “long term” late Pleistocene to early Holocene transgression. At the end of the transgression, a depositional regression took place since, on previous deposits, progradational wave-dominated delta deposits developed (figs. 4 and 5). According to sequence stratigraphy concepts, the whole transgressive phase, recorded in the MP2 unit before the depositional regression, corresponds to the last Quaternary TST (the post-LGM TST), the age of which spans from no more than about 18ky B.P. (according to the interpretation of the origin of the sequence boundary below the MP2 unit) up to about 5.5ky B.P. (according both to literature data and to collected radiocarbon ones). The regressive phase of the MP2 unit, according to sequential interpretations, corresponds to the last Quaternary HST (late Holocene in age and post 5.5ky B.P., following radiocarbon data) and is the still-active phase in the Metaponto coastal area. Both thickness and age span of the MP2 unit suggest to ascribe it to a high-frequency sequence (a 5<sup>th</sup> order sequence); according to late Quaternary cyclicity (*i.e.* WAELBROECK *et alii*, 2002) and in accordance with interpretations made by BELLOTTI *et alii* (1995) for coeval and similar deposits, the MP2 unit may be considered also the initial part of the 4<sup>th</sup> order sequence that developed since the LGM. Therefore the SB2, *i.e.* the lower boundary of the MP2 unit, represents contemporaneously both a 5<sup>th</sup> and a 4<sup>th</sup> order sequence-boundary.

Unit MP1 discontinuously lays between the substratum and the MP2 sequence. Also the MP1 unit is characterized by the filling of a paleovalley. This paleoincision developed during a phase of fall and early lowstand of the relative sea-level. Since the sequence boundary below the MP2 unit cut the MP1 unit, this phase of fall and early lowstand was older than that which led to the incision at the base of the MP2 sequence. According to sequence stratigraphy concepts, age of the MP1 unit could be indirectly obtained, since this unit developed between a relative sea-level fall and a subsequent one; therefore, since MP2 unit formed after the LGM, corresponding to the Marine Isotope Stage (MIS) 2, the sea-level fall preceding the LGM corresponds to MIS 4, and, accordingly, the top of the MP1 unit most likely developed around the MIS 3 (late Pleistocene in age).

Thickness and age of MP1 suggest to ascribe it to a high-frequency sequence (a 5<sup>th</sup> order sequence); following the cyclicity and sea-level changes proposed for the Late Pleistocene (*i.e.* WAELBROECK *et alii*, 2002), the MP1 unit should represent a 5<sup>th</sup> order sequence punctuating a Falling Stage System Tract (FSST) of a 4<sup>th</sup> order sequence, namely the FSST of the 4<sup>th</sup> order sequence that followed the MIS5 (post Tyrrhenian in age) and that preceded the LGM. Accordingly, the SB1, namely the lower boundary of the MP1 unit, corresponds to a 5<sup>th</sup> order sequence boundary, while, in accordance with the FSST definition proposed by PLINT & NUMMENDAL (2000), the SB2, bounding on top the same unit, corresponds to a 4<sup>th</sup> order sequence boundary (as suggested before), locally coinciding with a 5<sup>th</sup> order sequence boundary.

### 6.3. - HYDROSTRATIGRAPHY

Thanks to the complete wells database, to decades of piezometric measurements, and to the stratigraphic interpretation of the buried Metaponto coastal plain succession (fig. 5a), it is possible to make a preliminary hydrostratigraphic interpretation of this succession, even though, considering the alternance between less and more permeable sedimentary bodies, the hydrostratigraphic architecture appears to be very complex (fig. 5b). As a whole, on a first approximation, the MP1 and MP2 units correspond to a multilayered aquifer, in accordance with the definition of POLEMIO *et alii* (2003a; 2003b) and with the size (considering paleovalleys infills) suggested by SPILOTRO (2004). The aquifer lies on clays and silty clays of the Argille subappennine formation (the lower unit of the lithostratigraphic subdivision of drilled deposits), and almost the whole thickness of the aquifer lies below the sea level and is confined by fine-grained sediments toward the coast.

Close to the coast, in an along-strike section, the lower part of the aquifer system is laterally partitioned; each partition corresponds to a paleovalley infill and is laterally confined by clays and silty clays deposits, belonging to the argille subappennine formation, which were cut during sea-level falls and exposed along flanks of paleoincisions. Each of these partitions of the aquifer system is, in turn, vertically partitioned, given that water permeates sandy silty and sandy gravelly layers which alternate with mainly silty layers (fig. 5b). Moving landward, inside paleovalleys, sandy-silty and sandy-gravelly layers are elongated along dip and become thicker and thicker, gradually passing to a more vertically continuous porous body made up mainly of sands (deposits of the inner part of estuary systems) and sandy gravels (deposits of fluvial systems feeding

marine-transitional systems). On the contrary, moving seaward and according to both facies and depositional systems interpretation, the same sandy-silty and sandy-gravelly layers should become thinner and thinner up to the termination within shelf-transition clays and silty clays. Accordingly, inside paleovalleys and close to the coast, the multilayered aquifer shows artesian features, since inland it is fed by flows running along buried fluvial deposits and seaward it is characterized by thinning confined layers enclosed in low-permeable sediments.

Above paleovalleys fills and below the present-day Metaponto coastal plain, up to about 30-40 m of depth, the multilayered aquifer becomes a phreatic one; fresh water splits into several horizons with a low inclination, the shallowest of which is characterized by free piezometric oscillations. Also in this case, water flowing along coarse-grained deposits inside valleys (note that, inland, paleovalleys coincide with present-day valleys) feeds the coastal multilayered aquifer, but, according to POLEMIO *et alii* (2003a; 2003b), also water coming from coarse-grained deposits cropping out inland in the interfluvial areas (terraced marine-deposits) may feed this part of the multilayered aquifer system.

## 7. - CONCLUSIONS

A new view of the subsurface stratigraphy/hydrostratigraphy of the Metaponto coastal plain is proposed. This view was obtained combining lithological criteria in the interpretation of a large number of wells drilled in the last few decades with the contribution that both a modern sedimentological/stratigraphic approach and the wide literature on late Quaternary development of coastal plains may offer to the topic. The new stratigraphic picture of the Metaponto coastal-plain subsurface shows a complex architecture governed either by lateral and vertical variations of facies within a depositional system or by the overlap of different depositional systems through time, in accordance with changes of the relative sea-level. Thanks to the distinction of two main boundaries (two erosional surfaces of regional extent), three units were recognized in the drilled Quaternary deposits of the plain (up to about 120 m in depth): a lower unit, mainly formed by clays and silty clays, that represents the substratum of the middle and upper units formed by a complex alternation between coarse- and fine-grained facies. Both the middle and upper units host a multilayered aquifer basically located below the present-day sea-level. The aquifer locally reaches about 100 m in depth, given that the buried deposits of either the middle or the

upper unit may fill paleovalleys cut in the clayey and silty-clayey substratum. Paleovalleys developed at least twice, during phases of relative sea-level fall and lowstand linked to the MIS 4 and the LGM; fluvial and mainly estuarine deposits filled paleovalleys, while shallow-marine deposits followed by coastal-plain deposits developed after filling of incised valleys.

## Acknowledgments

*Cilumbriello and Sabato supervised facies analysis and depositional systems interpretation; Cilumbriello and Tropeano supervised stratigraphic interpretations.*

*Discussions with Amorosi, Caporale, La Perna, Mallardo e Pieri regarding the research theme were very useful. Critical reviews by the Referees F. Felletti and S. Milli were very appreciated.*

*Research funds were provided to Sabato by Bari University ("Fondi di Ateneo - ex 60%" 2005-2009) and MIUR (PRIN-Cofin 2003).*

## REFERENCES

- AGUZZI M., AMOROSI A. & SARTI G. (2005) - *Stratigraphic architecture of Late Quaternary deposits in the lower Arno Plain (Tuscany Italy)*. *Geologica Romana*, **38**: 1-10.
- AMOROSI A. (2006) - *Reading late Quaternary stratigraphy from cores: a practical approach to facies interpretation*. *GeoActa*, **5**: 61-78.
- AMOROSI A., FONTANA A., ANTONIOLI F., PRIMON S. & BONDESAN A. (2008a) - *Post-LGM sedimentation and Holocene shoreline evolution in the NW Adriatic coastal area*. *GeoActa*, **7**: 41-67.
- AMOROSI A., SARTI G., ROSSI V. & FONTANA A. (2008b) - *Anatomy and sequence stratigraphy of the late Quaternary Arno valley fill (Tuscany, Italy)*. In: A. AMOROSI, B.U. HAQ & L. SABATO (Eds.): "Advances in Application of Sequence Stratigraphy in Italy". *GeoActa, Spec. Publ. n° 1*: 55-66.
- BELLOTTI P., CHIOCCI F.L., MILLI S., TORTORA P. & VALERI P. (1994) - *Sequence stratigraphy and depositional setting of the Tiber delta: integration of high resolution seismics, well logs, and archaeological data*. *Journ. Sed. Res.*, **B64**, 3: 416-432.
- BELLOTTI P., MILLI S., TORTORA P. & VALERI P. (1995) - *Physical stratigraphy and sedimentology of the Late Pleistocene-Holocene Tiber Delta depositional sequence*. *Sedimentology*, **42**: 617-634.
- BERNHARD J.M. & B.K.S. GUPTA (1999) - *Foraminifera of oxygen-depleted environments*. In: B.K.S. GUPTA (Ed.): "Modern Foraminifera". Kluwer Academic Publishers: 201-216.
- BOENZI F., CHERUBINI C. & GIASI C. (1987) - *Dati e considerazioni sull'evoluzione recente e sui caratteri idrogeologici della piana costiera metapontina compresa tra il F. Bradano ed il F. Basento (Basilicata)*. *Geogr. Fis. Dinam. Quat.*, **10**: 34-46.
- BONORA N., IMMORDINO F., SCHIAVI C., SIMEONI U. & VALPRED A. (2002) - *Interaction between catchment basin management and coastal evolution (Southern Italy)*. *Journ. Coast. Res.*, Sp. Issue **36**: 81-88.
- BOYD R., DARLYMPLE R.W. & ZAITLIN B.A. (2006) - *Estuarine incised-valley facies models*. In: H.W. POSAMENTIER & R.G. WALKER (Eds.): "Facies models revisited". *Soc. of Econ. Pal. and Min., Spec. Publ. n° 84*: 171-235.
- CAPRETTO G. (2003) - *I depositi olocenici della piana costiera di Metaponto in Basilicata (Italia meridionale). Studi di sedimentologia e mineralogia*. PhD Thesis, Università degli Studi del Sannio: pp. 360.
- CATUNEANU O. (2006) - *Principles of sequence stratigraphy*. Else-



- vier: pp. 375.
- CIARANFI N., GHISETTI F., GUIDA M., IACCARINO G., LAMBIASE S., PIERI P., RAPISARDI L., RICCHETTI G., TORRE M., TORTORICI L. & VEZZANI L. (1983) - *Carta neotettonica dell'Italia meridionale*. Prog. Fin. Geod. del CNR, **515**: pp. 62.
- CIARANFI N., MARINO M., SABATO L., D'ALESSANDRO A. & DE ROSA R. (1996) - *Studio geologico stratigrafico di una successione infra e mesopleistocenica nella parte sudoccidentale della Fossa Bradanica (Montalbano Ionico, Basilicata)*. Boll. Soc. Geol. It., **115**: 379-391.
- CILUMBRIELLO A., TROPEANO M. & SABATO L. (2008) - *The Quaternary terraced marine-deposits of the Metaponto area (Southern Italy) in a sequence-stratigraphic perspective*. In: A. AMOROSI, B.U. HAQ & L. SABATO (Eds.): "Advances in Application of Sequence Stratigraphy in Italy". GeoActa, Spec. Publ. n° 1: 29-54.
- COCCO E., CRAVERO E., DI GERONIMO S., MEZZADRI G., PAREA G.C., PESCATORE T., VALLONI R. & VINCI A. (1975) - *Lineamenti geomorfologici e sedimentologici del litorale alto ionico (Golfo di Taranto)*. Boll. Soc. Geol. It., **94**: 993-1051.
- COTECCHIA V., DAI PRA G. & MAGRI G. (1969) - *Oscillazioni tirreniane ed oloceniche del livello del mare nel Golfo di Taranto, corredate da datazioni col metodo del radiocarbonio*. Geol. Appl. e Idrog., **4**: 93-148.
- COTECCHIA V., DAI PRA G. & MAGRI G. (1971) - *Morfogenesi litorale olocenica tra Capo Spulico e Taranto nella prospettiva della protezione costiera*. Geol. Appl. e Idrog., **6**: 65-78.
- COTECCHIA V. & MAGRI G. (1967) - *Gli spostamenti delle linee di costa quaternarie del Mar Ionio fra Capo Spulico e Taranto*. Geol. Appl. e Idrog., **2**: 1-25.
- DALRYMPLE R.W., ZAITLIN B.A. & BOYD R. (1992) - *Estuarine facies models: conceptual basis and stratigraphic implications*. Journ. Sed. Petr., **62**: 1130-1146.
- DOGLIONI C., MONGELLI F. & PIERI P. (1994) - *The Puglia uplift (SE-Italy): an anomaly in the foreland of the Apenninic subduction due to buckling of a thick continental lithosphere*. Tectonics, **13**: 1309-1321.
- DOGLIONI C., TROPEANO M., MONGELLI F. & PIERI P. (1996) - *Middle-late Pleistocene uplift of Puglia: an "anomaly" in the Apenninic foreland*. Mem. Soc. Geol. It., **51**: 101-117.
- MILLI S., MOSCATELLI M., PALOMBO M.R., PARLAGRECO L. & PACIUCCI M. (2008) - *Incised valley, their filling and mammal fossil record: a case study from Middle-Upper Pleistocene deposits of the Roman Basin (Latium, Italy)*. In: A. AMOROSI, B.U. HAQ & L. SABATO (Eds.): "Advances in Application of Sequence Stratigraphy in Italy". GeoActa, Spec. Publ. n° 1: 67-87.
- MURRAY J. W. (2006) - *Ecology and Applications of Benthic Foraminifera*. Cambridge Univ. Press, Cambridge: pp. 426.
- PESCATORE T., PIERI P., SABATO L., SENATORE M.R., GALLICCHIO S., BOSCAINO M., CILUMBRIELLO A., QUARANTIello R. & CAPRETTO G. (2009) - *Stratigrafia dei depositi pleistocenico-olocenici dell'area costiera di Metaponto compresa fra Marina di Ginosa ed il Torrente Cavone (Italia meridionale): Carta Geologica in scala 1:25.000*. Il Quaternario (It. Journ. Quatern. Sc.), **22**(2): 307-323.
- PIERI P., SABATO L. & TROPEANO M. (1996) - *Significato geodinamico dei caratteri deposizionali e strutturali della Fossa bradanica nel Pleistocene*. Mem. Soc. Geol. It., **51**: 501-515.
- PIRAZZOLI P.A. (1997) - *Sea-Level changes, the last 20.000 years*. Wiley: pp. 211.
- PLINT A.G. & NUMMEDAL D. (2000) - *The falling stage systems tract: recognition and importance in sequence stratigraphic analysis*. In: D. HUNT & R.L. GAWTHORPE (Eds.): "Sedimentary responses to forced regressions". Geol. Soc. Sp. Publ., **172**: 1-17.
- POLEMIO M., DRAGONE V., LIMONI P.P., MITOLO D. & SANTALOIA F. (2003b) - *Caratterizzazione idrogeologica della Piana di Metaponto, qualità e rischi di degrado delle acque sotterranee*. Acque sotterranee, **83**: 35-49.
- POLEMIO M., LIMONI P.P., MITOLO D. & SANTALOIA F. (2003a) - *Characterization of the ionian-lucanian coastal plain aquifer (Italy)*. Boletín Geológico y Minero, **114**: 225-236.
- POLEMIO M. & RICCHETTI E. (1991) - *Caratteri idrogeologici dell'acquifero della piana costiera di Metaponto (Basilicata)*. Convegno Nazionale Giovani Ricercatori in Geologia Applicata, Gargnano (BS), Italy: 417-426.
- POSAMENTIER H.W. & ALLEN G.P. (1999) - *Siliciclastic sequence stratigraphy - Concepts and applications*. Soc. of Econ. Pal. and Min., Concepts in Sedimentology and Paleontology N° 7: pp. 210.
- POSAMENTIER H.W. & VAIL P.R. (1988) - *Eustatic controls on clastic deposition II - sequence and systems tract models*. In: C.K. WILGUS, B.S. HASTINGS, C.G.St.C. KENDALL, H.W. POSAMENTIER, C.A. ROSS & J.C. VAN WAGONER (Eds.): "Sea-level changes: an integrated approach". Soc. of Econ. Pal. and Min., Spec. Publ. n° 42: 125-154.
- POSAMENTIER H.W. & WALKER R.G. (Eds.) (2006) - *Facies models revisited*. Soc. of Econ. Pal. and Min., Spec. Publ. n° 84: pp. 527.
- READING H.G. (Ed.) (1996) - *Sedimentary Environments: Processes, Facies and Stratigraphy (third edition)*. Blackwell Science: pp. 688.
- RIO D., RAFFI I. & VILLA G. (1990) - *Pliocene-Pleistocene calcareous nannofossil distribution patterns in the Western Mediterranean*. In: KASTENS K.A., MASELE J. et alii (Eds.), Proc. Oc. Drill. Prog., Sci. Res., **107**: 513-533, College Station, Texas.
- SABATO L. & CILUMBRIELLO A., con contributi di: BERTINI A., GALLICCHIO S., LA PERNA R., MAIORANO P., PIERI P., SPILOTRO G. & TROPEANO M. (in prep.) - *Note illustrative della Carta Geologica d'Italia alla scala 1:50.000, Foglio 508 "Pollicoro"*: pp. 61, CARG Project, Basilicata, III SAL.
- SPILOTRO G. (2004) - *Erosion profile of the Blue Clay bedrock along the Ionian coast of the Basilicata Region*. Quaternaria Nova, **8**: 247-261.
- TORTORA P., BELLOTTI P. & VALERI P. (2001) - *Late-Pleistocene and Holocene deposition along the coasts and continental shelves of the Italian peninsula*. In: G.B. VAI & I.P. MARTINI (Eds.): "Anatomy of orogen: the Apennines and Adjacent Mediterranean Basins". Kluwer Academic Publisher: 455-477.
- TROPEANO M., SABATO L. & PIERI P. (2002) - *Filling and cannibalization of a foredeep: the Bradanic Trough (Southern Italy)*. In: S.J. JONES & L.E. FROSTICK (Eds.): "Sediment Flux to Basins: Causes, Controls and Consequences". Geol. Soc. of London, Spec. Publ. n° 191: 55-79.
- VAN WAGONER J.C., MITCHUM R.M.J., CAMPION K.M. & RAHMANIAN V.D. (1990) - *Siliciclastic sequence stratigraphy in well logs, cores and outcrops*. AAPG Methods in Exploration Series, **7**: pp. 55.
- VEZZANI L. (1967) - *I depositi plio-pleistocenici del litorale ionico della Lucania*. Atti Acc. Gioenia Sc. Nat. in Catania s. 6, **18**: 159-180.
- WAELEBROECK C., LABEYRIE L., MICHEL E., DUPLESSY J.C., McMANUS J.F., LAMBECK K., BALBON E. & LABRACHERIE M. (2002) - *Sea-level and deep water temperature changes derived from benthic foraminifera isotopic records*. Quaternary Science Reviews, **21**: 295-305.
- WALKER R.G. & JAMES N.P. (Eds.) (1992) - *Facies models-response to sea level changes*. Geological Association of Canada: pp. 454.
- ZAITLIN B.A., DALRYMPLE R.W. & BOYD R. (1994) - *The stratigraphic organization of incised valley systems associated with relative sea-level change*. In: R.W. DALRYMPLE, B.A. ZAITLIN & R. BOYD (Eds.): "Incised valley systems: origin and sedimentary sequences". Soc. of Econ. Pal. and Min., Spec. Publ. n° 51: 45-60.

## Simulation of heterogeneity in a point-bar/channel aquifer analogue

*Simulazione dell'eterogeneità in un analogo di acquifero fluviale meandriforme (sistema barra puntiforme/canale)*

DELL'ARCIPRETE D. (\*), BERSEZIO R. (\*), FELLETTI F. (\*),  
GIUDICI M. (\*), VASSENA C. (\*)

**ABSTRACT** - The aim of the study is the geostatistical simulation of fine-scale heterogeneities of a gravelly sand aquifer analogue from a quarry exposure in the Lambro River valley.

Three different simulation methods have been used and compared. The analogue consists of two superimposed bar-channel units of sand and subordinate gravel that formed in two different meander loops of the Roman-Medieval Lambro River. We developed an architectural hierarchical model based on the data obtained from direct inspection of 5 quarry exposures, that have been mapped and logged during excavation. In the analysed volume (approximately 30000 m<sup>3</sup>) four operative hydrofacies have been recognised: very fine sand and silt; sand; gravelly sand; open framework gravel. Transition-probability and variographic analysis of the operative hydrofacies were computed both for the entire dataset and for the individual depositional elements, after discretization of the facies maps with square cells (spacing 0.05 m). This analysis was aimed to obtain the correlation length of each hydrofacies along different directions. The geostatistical simulations have been conditioned to: i) the discretized facies maps, ii) the measured logs and iii) the facies proportions. Several equiprobable realizations were computed for a test volume of approximately 400 m<sup>3</sup> and for the entire volume using three different simulation techniques: 1) Sequential Indicator Simulation (SISIM), 2) Transition Probability Geostatistics (T-ProGS) and 3) Multiple Point Simulation (MPS).

From the comparison of the different simulations, the following consideration can be pointed out: i) with every method the geological model is best reproduced when the simulations are realised separately for each highest rank depositional element and subsequently merged; ii) the three methods yield different images of the volume. In particular MPS is efficient in mapping the geometries of the most represented hydrofacies, whereas SISIM and T-ProGS can account for the distribution of the less represented facies.

**KEY WORDS:** aquifers, geostatistics, Multiple Point Simulation MPS, Sequential Indicator Simulation SISIM, T-ProGS.

**RIASSUNTO** - Viene presentato il risultato della simulazione geostatistica a piccola scala di un analogo di acquifero ghiaioso-sabbioso proveniente da un'esposizione in cava nella valle del Fiume Lambro. Sono stati impiegati tre differenti metodi di simulazione e i cui risultati sono stati successivamente confrontati. L'analogo comprende due elementi deposizionali barra-canale sovrapposti, composti da sabbia con subordinata ghiaia e formati in due cicli evolutivi di età storica (Romano e Medioevale) del Fiume Lambro. È stato sviluppato un modello gerarchico basato sui dati ottenuti dall'osservazione di 5 fronti di cava, che sono stati cartografati e misurati durante lo scavo. Sono state calcolate le probabilità di transizione ed i variogrammi, sia sull'intera base di dati che sui singoli elementi deposizionali, dopo la discretizzazione delle mappe di facies con celle quadrate (lato 0.05 m). Questa analisi è stata effettuata principalmente per ottenere la distanza di correlazione di ogni idrofacies nelle diverse direzioni.

Il volume analizzato, di circa 30000 m<sup>3</sup> (47 m×75 m×8.6 m), è stato simulato distribuendo nello spazio 4 idrofacies operative (sabbia molto fine e limo, sabbia, sabbia ghiaiosa, ghiaia con struttura aperta). Le simulazioni sono state condizionate a: i) mappe di facies discretizzate, ii) sezioni stratigrafiche di dettaglio misurate, iii) proporzioni di facies. Sono state ottenute diverse simulazioni equiprobabili sia per un volume di prova di circa 400 m<sup>3</sup> che per l'intero volume. Sono state utilizzate tre differenti tecniche di simulazione: 1) simulazione sequenziale delle variabili indicatrici (SISIM), 2) simulazione con le probabilità di transizione (T-ProGS) e 3) simulazione multi-punto (MPS).

Dal confronto delle differenti simulazioni si evidenzia che: con qualunque metodo si ottengono risultati più realistici quando gli elementi deposizionali di più alto rango vengono

(\*) Dipartimento di Scienze della Terra "A.Desio", Università degli Studi di Milano, via Mangiagalli 34, 20133 Milano (Italy)

simulati separatamente e quindi composti; i tre metodi utilizzati mostrano diversa efficacia nel riprodurre differenti caratteristiche del volume: MPS è più efficiente nel simulare le geometrie delle idrofacies più abbondanti, SISIM e T-ProGS forniscono risultati più soddisfacenti di MPS nella distribuzione delle facies meno rappresentate.

PAROLE CHIAVE: acquiferi, geostatistica, Multiple Point Simulation MPS, Sequential Indicator Simulation SISIM, T-ProGS.

## 1. - INTRODUCTION

The hydrogeological properties of alluvial sediments are determined by textural variations within the hierarchic arrangement of depositional units, from individual strata to depositional systems, and by the geometry of these units at different scales (JORDAN & PRIOR, 1992; LUNT *et alii*, 2004; BRIDGE & LUNT, 2006; RUBIN *et alii*, 2006). This complex heterogeneity, which is characterized by multiple scale lengths, affects groundwater flow and contaminant transport. Reliable flow and transport numerical models can be developed when this complexity is sufficiently well-known and eventually reproduced by geostatistical simulations. Because it is not always feasible to map the fine-scale heterogeneity in the subsurface (meters to sub-meters), several studies have been devoted to the analysis of outcropping reservoir/aquifer analogues as well as of modern analogues (LIU *et alii*, 1996; ANDERSON, 1997; HUGGENBERGER & AIGNER, 1999; HEINZ *et alii*, 2003; HEINZ & AIGNER, 2003; LUNT *et alii*, 2004; FELLETTI *et alii*, 2006). Exposed aquifer analogues allow to test the results of different simulation techniques at different scales.

Many geostatistical grid-based approaches are available for distributing facies heterogeneities through space. For a discussion about their applicability in practical situations see DE MARSILY *et alii* (2005) and FALIVENE *et alii* (2007). In this work lithofacies distribution was simulated using Sequential Indicator Simulation (SISIM; GOOVAERTS, 1997;

DEUTSCH & JOURNAL, 1992), Transition-probability geostatistics (T-ProGS; CARLE & FOGG, 1996) and Multiple Point Simulation (MPS; STREBELLE, 2002; LIU *et alii*, 2005), which simulate the different facies in the form of coded indicator-type variables where each value corresponds to a given facies.

SISIM has been applied at different scales in a variety of depositional settings such as alluvial (JOURNAL *et alii*, 1998; SEIFERT & JENSEN, 1999; ZAPPA *et alii*, 2006; FELLETTI *et alii*, 2006; FALIVENE *et alii*, 2007), deltaic (CABELLO *et alii*, 2007), aeolian (SWEET *et alii*, 1996), and turbiditic (JOURNAL & GÓMEZ-HERNÁNDEZ, 1993; FALIVENE *et alii*, 2007).

T-ProGS has been used to model facies distribution in braided river deposits (FELLETTI *et alii*, 2006) and in alluvial fans (FOGG *et alii*, 1998; CARLE *et alii*, 1998; WEISSMANN *et alii*, 1999; WEISSMANN & FOGG, 1999).

MPS has been used to reconstruct turbiditic reservoirs using 3D training images and conditioning data from boreholes and geophysics (STREBELLE *et alii*, 2003) and to make 3D reconstructions starting from 2D training images at the pore scale (OKABE & BLUNT, 2004).

The results from the three above mentioned techniques of geostatistical simulation are compared with each other; the case study is an aquifer analogue, exposing two composite point bar-channel depositional elements of a meandering river depositional system.

### 1.1. - CASE HISTORY

Excavation of gravel and sand in the Po alluvial plain offers several ephemeral exposures of aquifer analogues of different fluvial types. For this study we had the opportunity to investigate the historical sediments of the Lambro River at a quarry site south of Milan (fig. 1). In this sector, the Lambro River is a meandering river, flowing since the post-glacial age within a narrow valley encased into

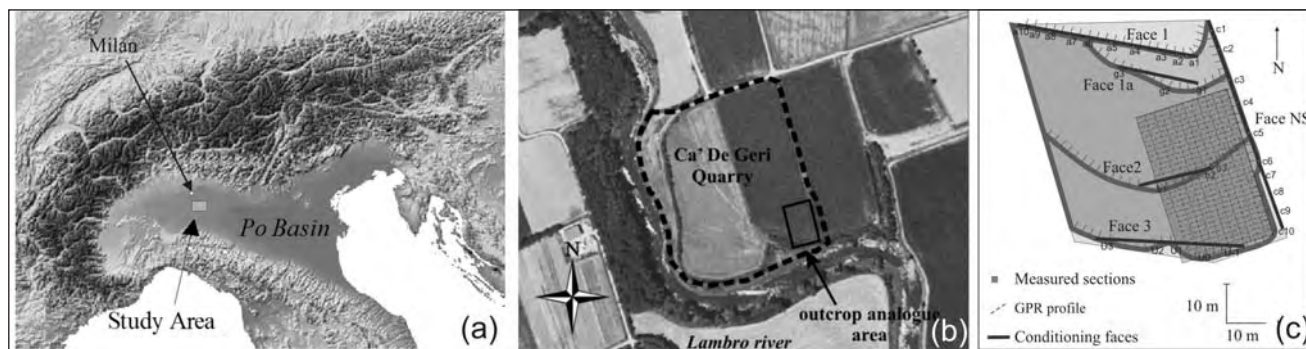


Fig. 1 - Location of the southern Lambro Valley (a) and of the studied quarry site (b); scheme of the study site. The location and orientation of the pit wall exposures (Face NS, Face 1, 2 and 3), of the 31 measured sections and of the GPR profiles is drawn (c).

- Ubicazione della valle meridionale del Fiume Lambro (a) e del sito in studio (b); schema del sito di studio, con segnalate le posizioni degli spaccati misurati, delle 31 sezioni stratigrafiche di dettaglio e del rilievo GPR eseguito (c).



the Upper Pleistocene sandur of the Lecco glacial amphitheatre. The quarry site exposes three superimposed depositional units formed by sands, gravels and subordinate silt and clay, which could be attributed to an historical age, as it was proved by the findings of Roman to Middle Age and Renaissance Age artifacts (bricks, tiles, ceramics), imbricated within dunes and bars (DELL'ARCIPRETE, 2005; BERSEZIO *et alii*, 2007). Two units correspond to the exposed parts of two composite point bars and channels with minor channel fills on top. We named them respectively unit A (the lower, with Roman-Middle Age findings) and unit B (the upper, with Renaissance Age findings). Unit A shows the lateral transition from a composite point bar to main channel fill, unit B is mostly represented by a composite point bar, with chute channel scour and fills on top. The erosion surface between them, tapered by lag deposits, is the  $\alpha$  surface (fig. 2). A younger channel (unit C, bounded by erosion surface  $\beta$  and partly anthropogenic) eroded part of unit B and will not be considered here because of the very scarce observations. Together with units A and B, it is cut by the modern and present-day courses of the Lambro River. Units A and B are formed by a hierarchic arrange-

ment of depositional units, from the 2<sup>nd</sup> order of bed-sets to the 5<sup>th</sup> order of the bar/channel systems, which determines the architectural heterogeneity of the aquifer analogue.

## 1.2. - PURPOSE

The goals of this study are the multi-scale reconstruction of the aquifer heterogeneity by the integration of geological and sedimentological, geophysical, geostatistical and numerical modelling methods and the evaluation of the efficiency of different geostatistical simulation techniques, as SISIM, MPS and T-ProGS. The problem is how these techniques can reproduce complexity, at different simulations scales, and in the extremely heterogeneous case of meandering river sediments.

## 2. - WORK PLAN AND METHOD

We have analysed a volume of approximately 30000 m<sup>3</sup> (47 m×75 m×8.6 m). We have studied (1) the entire volume and (2) a test volume of about 400 m<sup>3</sup> (11.4 m×11.4 m×2.85 m) cut into the whole volume.

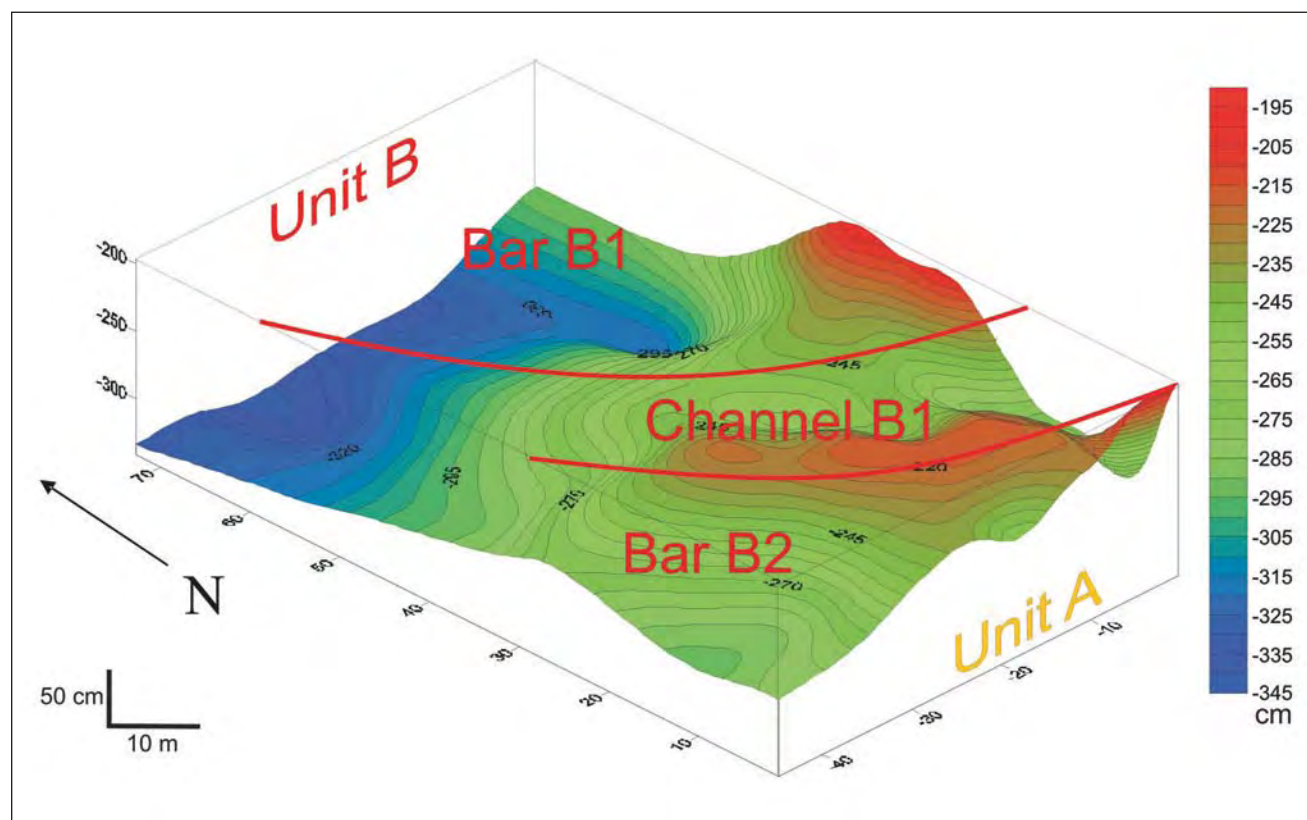


Fig. 2 - Kriged map of the erosional surface  $\alpha$  between unit A and B obtained by GPR survey and stratigraphic logs. The colour scale indicates the depth of the  $\alpha$  surface below the ground surface.

- Mappa della superficie erosionale  $\alpha$  di separazione fra le unità A e B, ottenuta per kriging dei punti quotati da rilievi GPR e sezioni stratigrafiche. La scala indica la profondità della superficie a rispetto al piano campagna.

The data set consists in: i) images of five, almost orthogonal, quarry faces; ii) 31 vertical sedimentological logs with cm-scale resolution; iii) grain-size, porosity and permeability data of 5 facies classes (28 samples); iv) Ground Penetration Radar (GPR) and Vertical Electrical Sounding (VES) images of the volume.

At first, the geological and hydrostratigraphic model was elaborated, starting from the stratigraphical, sedimentological and geophysical analysis of the quarry volume. Facies mapping was performed in the field by measurement and sampling of the 31 detailed sedimentological logs and was supported by the analysis of the photo-composition of the quarry faces. In this way plan-view and vertical maps of the geometry, hierarchy and internal architecture of the sedimentary bodies were obtained. This model includes: i) the geometry and the hierarchic arrangement of the depositional units and of their bounding surfaces at different scales; ii) the distribution of the facies and the hydrofacies within the hierarchical arrangement of the stratigraphic units; iii) the hydrostratigraphical characterisation of the hydrofacies and the hydrofacies groups (porosity, permeability, continuity and connectivity); iv) the interpretation of the ge-

nesis and the evolution of the sedimentary bodies.

Then the volume was simulated with SISIM, T-ProGS and MPS. Conditioning data were taken from the vertical facies maps of the quarry faces (fig. 1c). For modelling purposes four hydrofacies were used, based on the analysis of  $K$  values obtained by samples: least permeable (F, very fine sand and silt-clay respectively from topmost channel-fill, silt/clay plugs, drapes and balls), low permeable (S, sand from point-bar and channel fill bedforms), medium permeable (SG, sandy gravel and gravelly sand from point bars) and most permeable (G, open framework gravels from the lower parts of the lateral accreted units). See table 1 for further details. The facies maps were discretized with square cells (0.05 m spacing) and variographic and transition probability description of correlation of hydrofacies were performed on the discretized domains.

The 3-D facies simulation was run on the entire volume, with “big cells” (0.4 m×0.4 m×0.1 m, coarse grid) and “small cells” (0.2 m×0.2 m×0.05 m, fine grid) and on the test volume with the fine grid. This test volume has been chosen in an area with many conditioning data, from two orthogonal faces, and covers part of the three units A, B and C (fig. 3).

Tab. 1 - *Facies classification adopted in this study, correlative hydrofacies and estimated permeability values.*

- Classificazione di facies adottata in questo lavoro, idrofacies operative e valori di permeabilità stimati.

Facies Class	Facies	Interpretation	Estimated K values (m/s)	Operative hydrofacies		
F	Fm,	Clay plug, mud balls	$1 \cdot 10^{-9} \div 1 \cdot 10^{-6}$	F/fS		
	Fl	Clay drapes				
S	Sh	Low-relief bedwaves, upper flow regime	$5 \cdot 10^{-5} \div 5 \cdot 10^{-4}$			
	Sm	Channel fills, lower flow regime				
	Sr	Ripples				
	St	3D sand dunes	$1 \cdot 10^{-4} \div 1 \cdot 10^{-3}$			
	Sp	2D sand dunes				
	Sl	Sand drape				
SG	SGm	Avalanching (scroll bars and channel fills)	$5 \cdot 10^{-4} \div 1 \cdot 10^{-2}$	SG-GS		
	SGt	3D gravelly sand dunes				
	SGp	2D gravelly sand dunes				
	SGh	Traction carpet, upper flow regime				
	SGl	Bedload sheets				
GS	GSm	Avalanching (scroll bars and channel fills)				
	GSt	3D gravelly sand dunes				
	GSp	2D gravelly sand dunes				
	GSh	Traction carpets, upper flow regime				
	GSl	Bedload sheets				
G	Gm	Avalanching (scroll bars and channel fills)	$1 \cdot 10^{-2} \div 5 \cdot 10^{-2}$	G		
	Gt	Migration of 3D gravel dunes				
	Gp	Migration of 2D gravel dunes				
	Gh	Bedload sheets, upper flow regime				

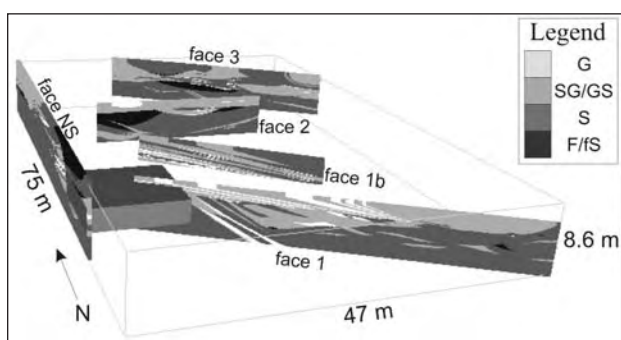


Fig. 3 - Vertical facies maps of the quarry faces. The test volume is drawn at the northern end of face NS.

- Mappe di facies verticali della cava. Lungo la faccia NS è riportato il volume test utilizzato per le prove a scala molto fine.

In order to evaluate efficiency and pitfalls of the different simulation techniques, at different operative scales, we have modelled the entire volume in two different ways: either simulating the undivided entire volume or simulating separately the units, then merging the simulations through the kriged  $\alpha$  boundary between A and B.

Semivariogram computation and sequential-indicator simulations were performed using GSLib (DEUTSCH & JOURNAL, 1992); markov chains analysis and transition-probability simulation were computed with T-ProGS (CARLE, 1999) and multi-point- simulations were performed with CtMainMPSimListLDI code, developed by Straubhaar, Comunian and Renard (University of Neuchatel – CH).

Figure 4 shows an example of the computed semivariograms, of the transition probabilities graphs and of the training images.

At last we could compare the outcomes of several equiprobable realizations obtained by the different methods to each other and to the geological model, applied to different domains and at different scales. In this case quantitative objective validation was impossible. In fact hydraulic tests or tracer tests could not be performed on this aquifer analogue, located in an active quarry area. Therefore, the comparison between the geological model and the simulations was made by visual inspection and image analysis on the vertical facies maps and on sections cut through the simulated volume.

### 3. - RESULTS

In figure 5 the geological model is presented.

The results of the simulations obtained with the different methods applied to the entire volume, to the separate units and to the test volume, are exemplified in figures 6, 7, 8. On the test vo-

lume 50 equiprobable simulations were obtained with each method (fig. 6). On the entire volume we performed 10 realizations for each method using big cells (depositional elements scale, figure 7) and one realization for each method using small cells, for the whole volume and for the units A and B separately (fig. 8).

The observation of semivariograms and experimental transition probabilities, computed for the four hydrofacies on the entire dataset, shows a good correspondence between the semivariogram ranges and the experimental transition probabilities. This good correspondence occurs because both semivariograms and transition probability curves quantify the lateral continuity of the hydrofacies and our analysis is performed on several thousands of data continuously sampled along the vertical and horizontal directions in our indicator database. This dataset does not include the multiple sources of error typical of the databases consisting only of borehole logs (bias in estimates of facies proportion and spurious lateral indicator correlation, respectively due to clustering and sparse and non-random distribution of logs).

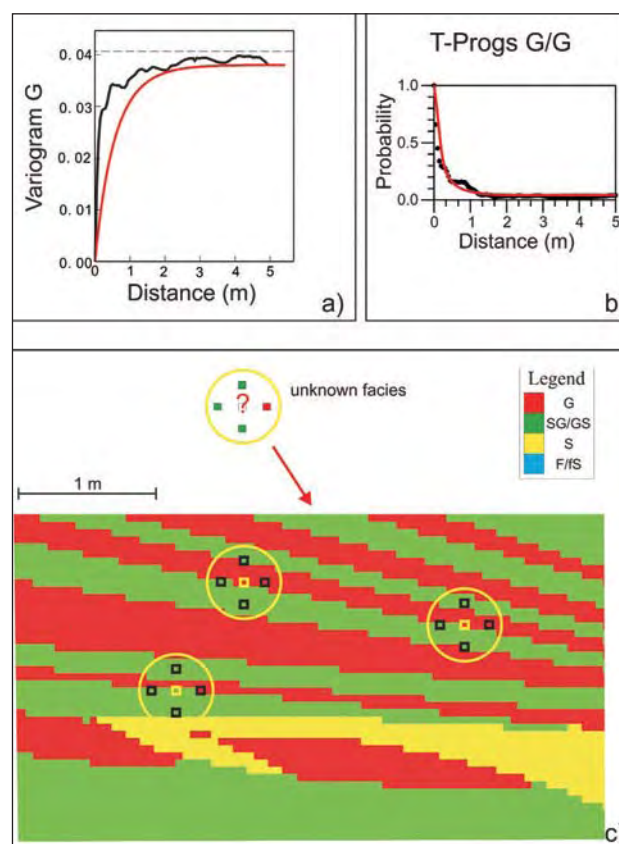


Fig. 4 - Example of semivariograms (a) and transitional probabilities (b) for the hydrofacies G (gravel) in the vertical direction; in black the experimental curves, in red the fitted models. (c) Example of training image.

- Esempio di semivariogramma (a) e probabilità di transizione (b) per l'idrofacies G nella direzione verticale; in nero le curve sperimentali, in grigio le curve relative ai modelli adattati. (c) Esempio di training image.



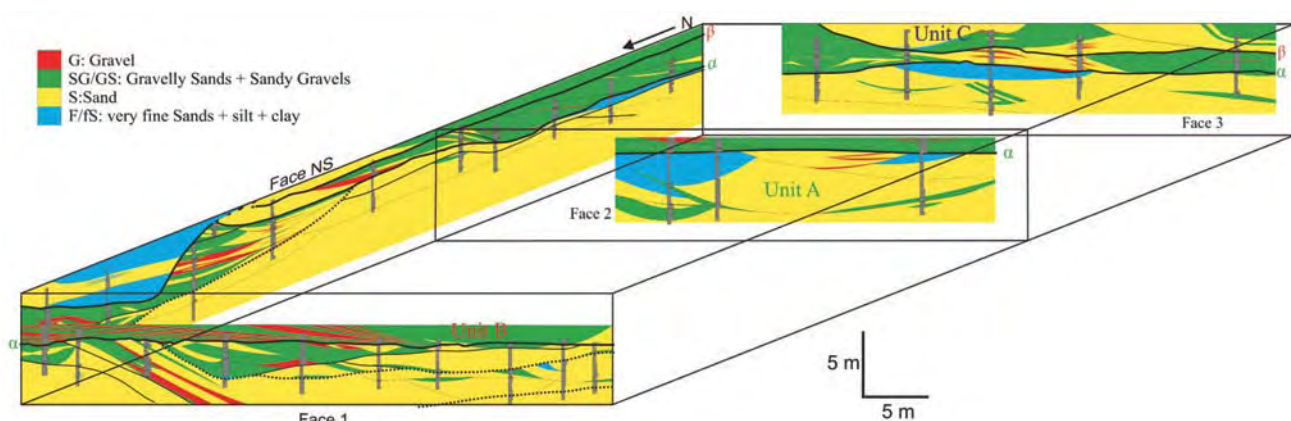


Fig. 5 - Geological model, that includes the shape and hierarchy of the depositional units and the distribution of the 4 operative hydrofacies (G: Open Framework Gravels; SG: Gravelly Sands and Sandy Gravels; S: Clean Sands and F: Sandy Silts and Clays).  
 - Modello geologico. Esso include la forma e la gerarchia delle unità deposizionali e la distribuzione delle 4 idrofaccie operative (G: Ghiaie a trama aperta; SG: Ghiaie sabbiose e Sabbie ghiaiose; S: Sabbia pulita e F: Sabbia siltosa e argilla).

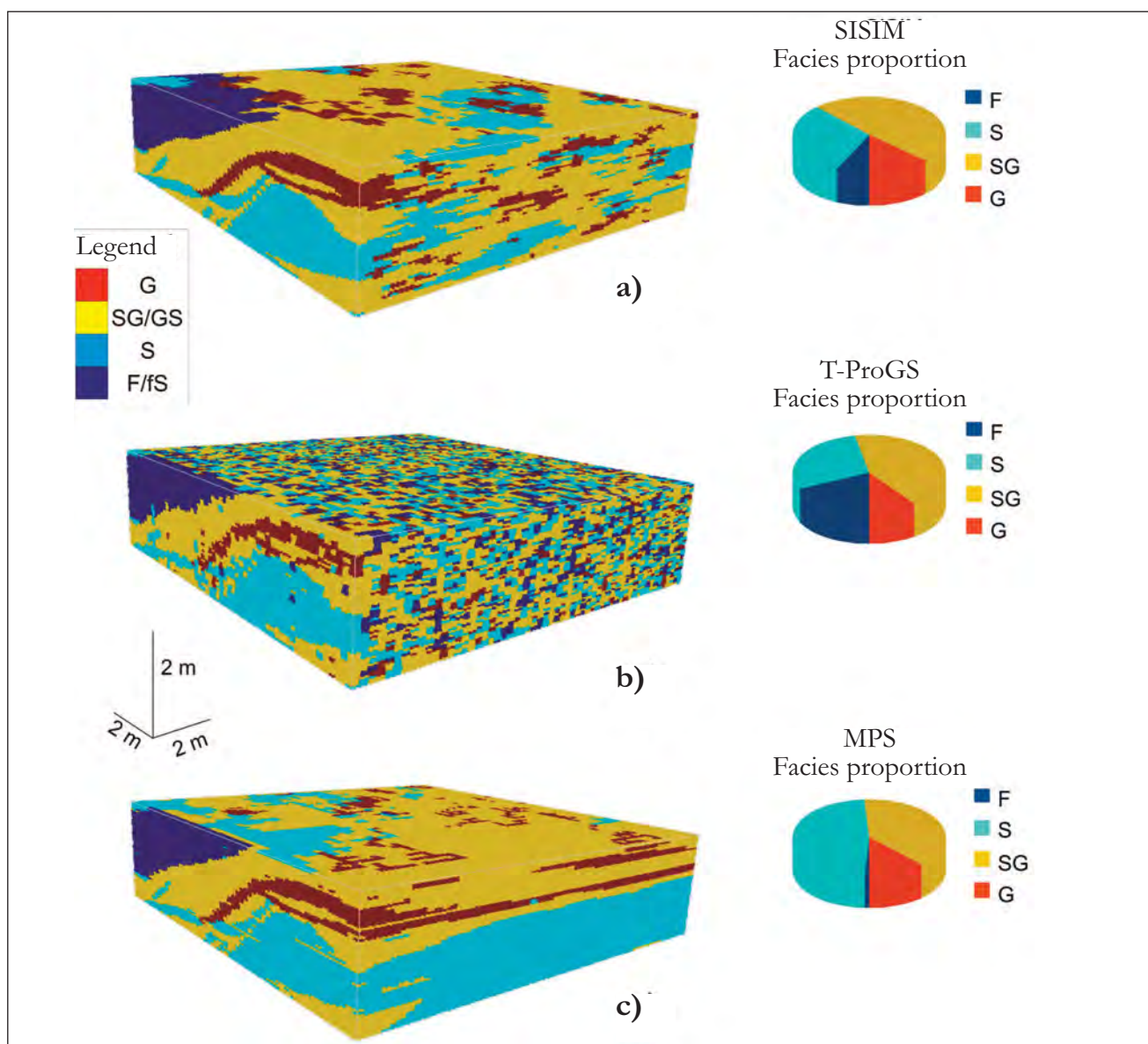


Fig. 6 - Equiprobable simulation number 1 of 50, computed in the test volume with (a) SISIM (b) T-ProGS and (c) MPS.  
 - Risultati della simulazione equiprobabile numero 1 di 50, ottenuta nel volume di prova con (a) SISIM (b) T-ProGS e (c) MPS.

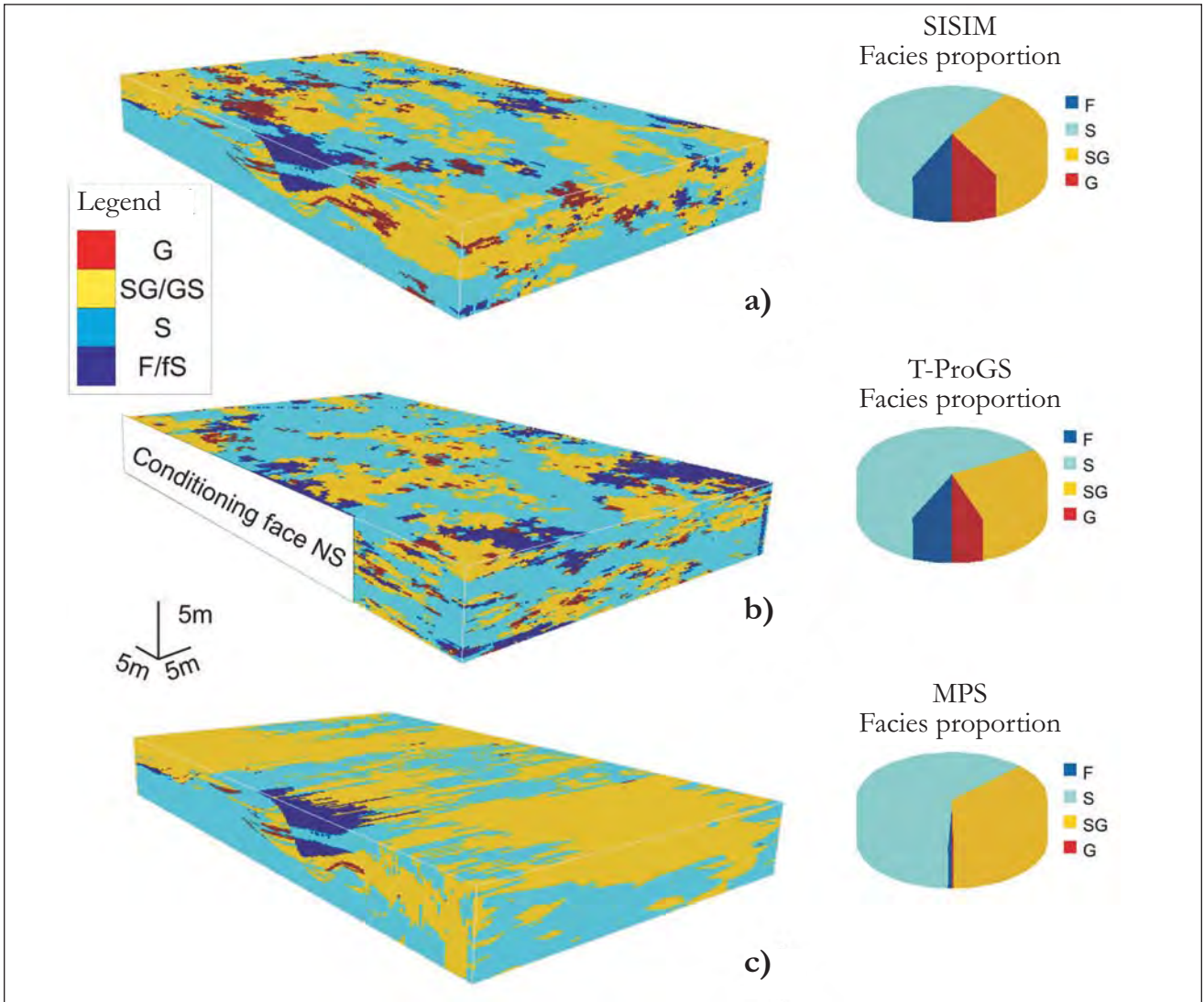


Fig. 7 - Equiprobable simulation number 1 of 10, computed in the entire volume ( $0.4 \text{ m} \times 0.4 \text{ m} \times 0.1 \text{ m}$  cells) with (a) SISIM (b) T-ProGS and (c) MPS.  
 - Risultati della simulazione equiprobabile numero 1 di 10, ottenuta nel volume intero (celle di  $0.4 \text{ m} \times 0.4 \text{ m} \times 0.1 \text{ m}$ ) con (a) SISIM (b) T-ProGS e (c) MPS.

## 4. - DISCUSSION

### 4.1. - COMPARISONS AMONG DIFFERENT REALIZATIONS

#### 4.1.1. - *Depositional elements scale*

Probability of occurrence of each facies has been computed from the 10 realizations of the entire volume with each method (fig. 9). A connectivity analysis was also performed and applied to support the comparisons between simulations. In this study we used a connectivity parameter (total connectivity) that measures the probability that pairs of connected points belong to a subset characterised by a given property, e.g., texture or hydraulic conductivity, as proposed in VASSENA *et alii* (2009) (fig. 10). We have computed total connectivity for the test volume and for the entire volume both for small and big cells. For the simulations

realized in entire volume with small cells, we have computed the connectivity indicators for moving blocks of  $57 \times 57 \times 57$  cells, to produce a moving average of the connectivity values.

The visual inspection and the connectivity analysis show that T-ProGS simulations generate a background of S hydrofacies voxels, connected in the whole volume, through which the other hydrofacies are sparse with low connectivity. On the contrary MPS simulations yield well connected volumes of SG hydrofacies bodies that alternate with the S hydrofacies bodies (fig. 11).

#### 4.1.2. - *Facies scale*

The probability of occurrence for each facies have been computed from the 50 equiprobable simulations of the test volume (fig. 12). At this scale the following results can be highlighted:



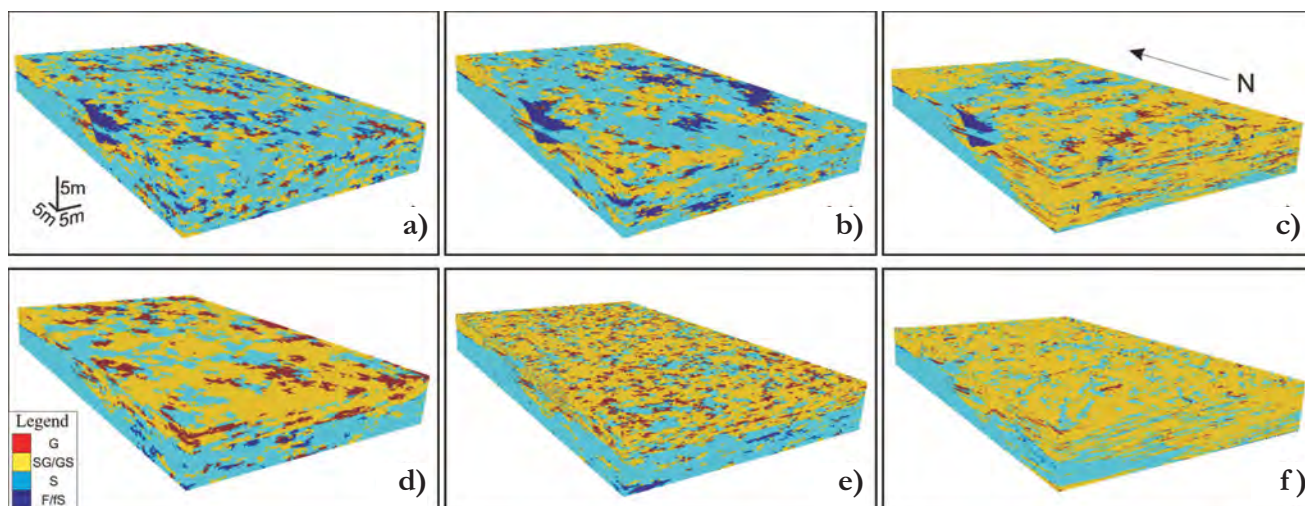


Fig. 8 - Simulations of the undivided entire volume ( $0.2 \text{ m} \times 0.2 \text{ m} \times 0.05 \text{ m}$  cells) computed with (a) SISIM (b) T-ProGS and (c) MPS. Simulations of units A and B computed separately using (d) SISIM (e) T-ProGS and (f) MPS.

- Simulazioni realizzate nel volume totale indiviso (celle di  $0.2 \text{ m} \times 0.2 \text{ m} \times 0.05 \text{ m}$ ) con (a) SISIM (b) T-ProGS e (c) MPS; simulazioni realizzate simulando separatamente le unità A e B con (d) SISIM (e) T-ProGS e (f) MPS.

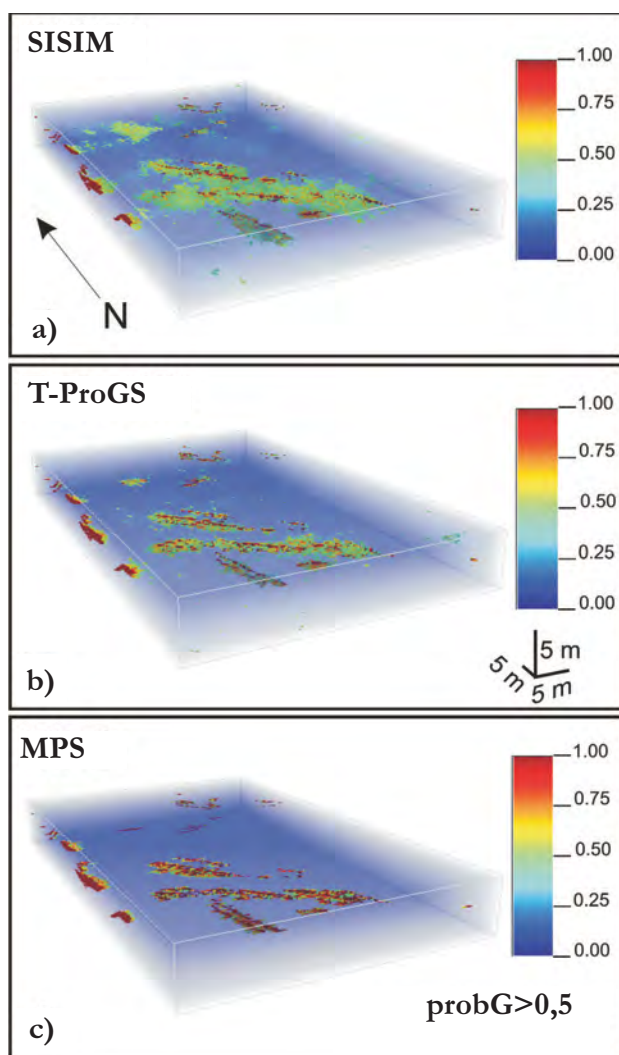


Fig. 9 - Probability > 50% to find facies G in each cell of the simulated entire volumes with (a) SISIM (b) T-ProGS and (c) MPS.

- Probabilità > 50% di trovare la facies G in ciascuna cella dei volumi totali simulati con (a) SISIM (b) T-ProGS e (c) MPS.

It was almost impossible find a Markov Chain model fitting the transition probabilities statistics computed on the conditioning faces of the test volume, therefore T-ProGS simulations are unsatisfactory for all facies at this scale. At this scale, in fact, there are few repetitions of the facies bodies, therefore transition probabilities statistics are inadequate.

MPS simulations produce continuous facies bodies for the S, SG and G facies, that are the most abundant in the conditioning faces used to derive the training images; on the other hand the same simulations cannot take into account the geometry and distribution of the F facies bodies, that are present only in one of the orthogonal training images.

SISIM yields a good spatial continuity for all the facies bodies, but different equiprobable realizations lead to significantly different results.

#### 4.2. - COMPARISONS TO THE GEOLOGICAL MODEL

Simulations obtained with different methods were compared to the geological model obtained from the analysis of the quarry exposures and yields the following results.

Visual inspection and comparison with field observations show that, for the simulations with fine grid of the entire volume, SISIM and T-ProGS yielded unrealistic results for the whole volume of units A and B. The realizations obtained by separate simulation of the two units were by far more realistic. On the contrary for MPS, the simulation of the undivided volume is more realistic than the simulation for the Units A and B separately. MPS method, in fact, can take in account the differences between units that are evident in training images.

To compare different simulations we performed



a 2-D image analysis of the hydrofacies bodies, considering different parameters computed over the conditioning faces 1 and NS and on four sections cut into the SISIM- and T-ProGS- simulated volumes, parallel to the conditioning faces at increasing separation distances (DELL'ARCIPIRETE *et alii*, 2009). The image analysis shows that when units A and B are simulated separately every technique underestimates the continuity and size of the low-rank geological elements (hydrofacies bodies). MPS simulations generate a quite smaller number of connected objects (i.e. hydrofacies bodies) than T-ProGS and SISIM for the simulations on the coarse grid. MPS too produces fragmented objects when applied to the fine grid.

The distribution of hydrofacies G (open framework gravels along the lower part of the inclined bed-sets of the composite bars) and F (meter-sized lenses of very fine sand and mud at the top of minor channel elements and decimeter-size mud clasts at their base) is not reproduced by T-ProGS simulations, that yield a scattered pattern of small

clusters, within a “matrix” of facies S and SG. MPS yields better results for background hydrofacies than for the least abundant facies. Simulations by SISIM reproduced rather efficiently the size, shape, distribution and orientation (sloping features of lateral and frontal accreted elements) of these low-hierarchy elements.

The geological model shows a polarity of transition from GS and G hydrofacies association to S and less abundant F hydrofacies towards the western and southern part of the volume, where the bar to channel-fill transitions occur. This trend is only partially reproduced by simulations. Visual inspection of the simulated volumes reveals periodical repetitions of the most permeable facies G, at a separation distance that is multiple of the variogram range in the case of the SISIM, and of the minimum of transition probability in the case of T-ProGS. MPS yields repetitions of S and SG bodies, imitating their shape in the training images. In summary, all the simulation methods do not account for the non-stationary architecture of composite bars and channels and are not capable to reproduce their real spatial trends.

SISIM and T-ProGS do not reproduce the elements of the architectural complexity, like minor channels, erosion bases, etc. This problem affects many pixel-oriented methods of simulation and, in our case, it arises from the fact that the semi-variogram and correlation matrix are a bivariate isotropic measure (two-point autocorrelation), and therefore any non-linear correlation structure (e.g., curved surfaces) cannot be reproduced. MPS, on the contrary, can reproduce the shape of the curved structures, but cannot reproduce their internal features at this scale. Moreover, vertical tendencies at the scale of the bed-sets and bed-set groups (2–4 m), which are evident in the cross-variogram and in the off-diagonal vertical transition-probability plots of the facies maps, are partially lost in the 3D simulation. The representation of such non-stationary periodicities is still an open issue and cannot be resolved using “classical stationary” semivariogram or Markov chain models (FELLETTI *et alii*, 2006).

Observing the differences between the simulations performed on small and big cells we can notice that the use of small cells do not significantly improve the results. On the contrary in MPS the shape and the dimension of S and SG hydrofacies bodies are partly lost.

Connectivity analysis shows that the differences between units A and B are caught by connectivity indicators. For instance in unit B it is possible to observe the presence of oblique layers of connected open framework gravel (G) that were not simulated in unit A, consistently with the geological observations.

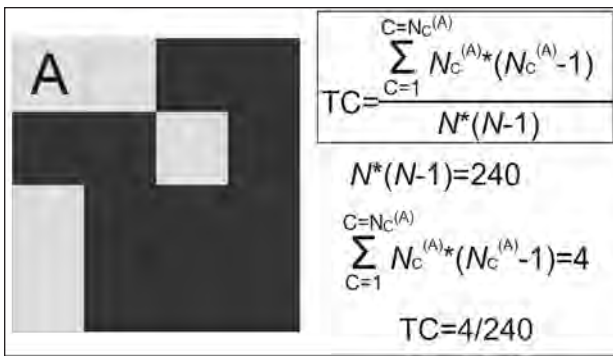


Fig. 10 - Total connectivity computation, according to VASSENA *et alii* (2009), where  $NC(A)$  is the number of connected points belonging to facies A;  $N$  is the number of points in the domain and  $TC$  is the total connectivity.  
- Calcolo della connettività totale, secondo VASSENA *et alii* (2009), con  $NC(A)$  numero di punti connessi appartenenti alla facies A;  $N$  numero di punti appartenenti al dominio e  $TC$  connettività totale.

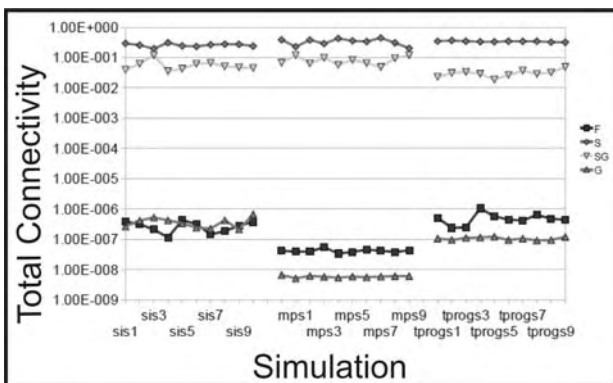


Fig. 11 - Total Connectivity computed in the entire volume ( $0.4 \text{ m} \times 0.4 \text{ m} \times 0.1 \text{ m}$  cells) with SISIM, MPS and T-ProGS.  
- Connettività totale calcolata nel volume totale (celle di  $0.4 \text{ m} \times 0.4 \text{ m} \times 0.1 \text{ m}$ ) con SISIM, MPS e T-ProGS.

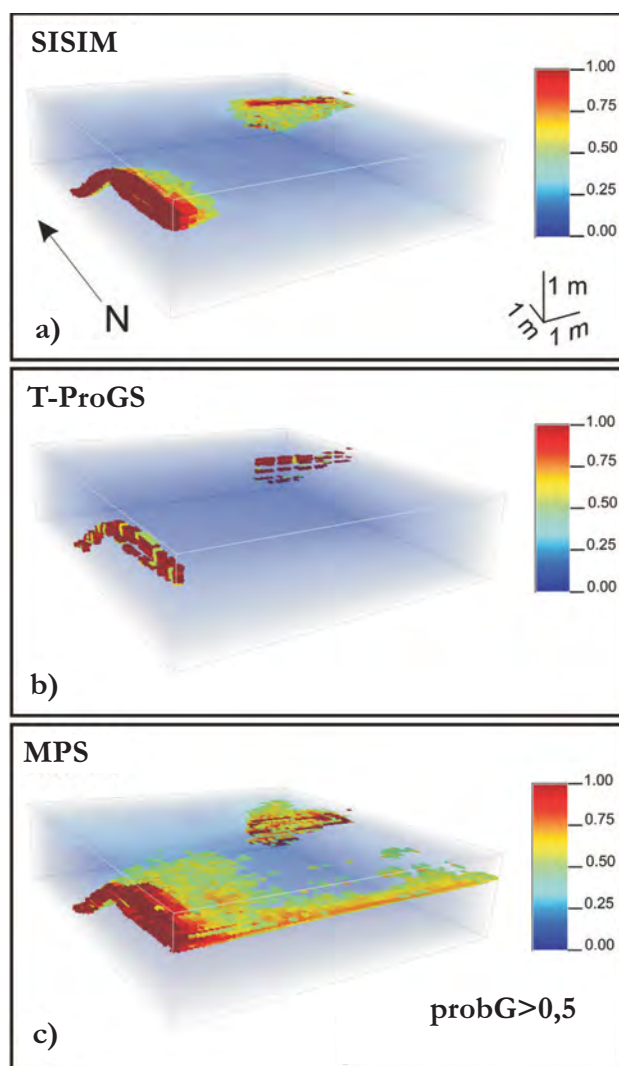


Fig. 12 - Probability > 50% to find facies G in each cell of the simulated test volumes with (a) SISIM (b) T-ProGS and (c) MPS.  
 - Probabilità > 50% di trovare la facies G in ciascuna cella dei volumi di prova simulati con (a) SISIM (b) T-ProGS e (c) MPS.

## 5. - CONCLUSIONS

Simulation of fine-scale heterogeneity of aquifer analogues characterized by high textural and structural complexity is possible, but realistic results are by far difficult to obtain yet. However our attempts yielded realizations that show many similarities with the geological model. SISIM revealed itself more prone to reproduce size, continuity and shape of the low-rank elements of the sedimentary architecture (bed-sets or hydrofacies bodies) than T-ProGS. MPS can reproduce size, continuity and shape of the elements that are well represented in the orthogonal training images, but completely misses the poorly represented facies.

Simulations of the undivided volume, obtained by SISIM, T-ProGS and MPS, are unrealistic because units A and B are characterized by very dif-

ferent statistical properties (frequency and correlation of hydrofacies). In fact realistic simulations can be obtained if statistical properties do not vary significantly throughout the studied domain (FALIVENE *et alii*, 2007). Therefore, at any scale, a preliminary detailed delimitation of the hydrofacies bodies to be reproduced is a primary need.

Both the studied composite bar and channel systems are characterized by facies trends that introduce non-stationarity. All methods we used reproduce non-stationary features only in an indirect way, accounting for facies proportions of the conditioning faces. How to account for depositional trends that are associated with periodicities at different scales, as is the case of point-bar complexes, looks to be an open problem in such a case.

## Acknowledgements

The authors warmly acknowledge the careful revision by the referees M. BIANCHI and L. GUADAGNINI.

Financial support to this work derived from the MIUR and the University of Milano through the research project of national interest "Integrated geophysical, geological, petrographical and modelling study of alluvial aquifer complexes characteristic of the Po plain subsurface: relationships between scale of hydrostratigraphic reconstruction and flow models" (PRIN 2007: PI M. GIUDICI). The "Ca' de Geri" quarry property is warmly acknowledged for kindness and hospitality.

## REFERENCES

- BERSEZIO R., GIUDICI M. & MELE M. (2007) - *Combining sedimentological and geophysical data for high resolution 3-d mapping of fluvial architectural elements in the Quaternary Po plain (Italy)*. *Sedimentary Geology*, **202**: 230-247.
- BRIDGE J.S. & LUNT I.A. (2006) - *Depositional models of braided rivers*. In: G.S. SAMBROOK SMITH *et alii* (Eds.), «Braided Rivers» Int. Assoc. Sedimentol. Spec. Publ., **36**: 11-50.
- CABELLO P., CUEVAS J.L. & RAMOS E. (2007) - *3D modelling of grain size distribution in quaternary in deltaic plain deposits (Lobregat Delta, NE Spain)*. *Geologica Acta*, **5**: 231-244.
- CARLE S.F. (1999) - *T-ProGS: Transition Probability Geostatistical Software version 2.1*. University of California, Davis.
- CARLE S.F. & FOGG G.E. (1996) - *Transition probability-based indicator geostatistics*. *Mathematical Geology*, **28**: 453-477.
- CARLE S.F., LABOLLE E.M., WEISSMANN G.S., VAN BROCKLIN D. & FOGG G.E. (1998) - *Conditional Simulation of Hydrofacies Architecture: A Transition Probability/Markov Approach*. In: G.S. FRASER & J.M. DAVIS (Eds.) «Hydrogeologic models of sedimentary aquifers». SEPM Special Publication, Concepts in Hydrogeology and Environmental Geology, 147-170.
- DELL'ARCIPRETE D. (2005) - *Caratterizzazione di un analogo di acquifero fluviale meandriforme*. Università degli Studi di Milano, Tesi di Laurea, p. 226.
- DELL'ARCIPRETE D., FELLETTI F. & BERSEZIO R. (2009) - *Simulation of fine-scale heterogeneity of meandering river aquifer analogues: comparing different approaches*. *GeoENV VII, Geostatistics for Environmental applications*, Springer, in press.
- DE MARSILY G., DELAY F., GONÇALVES P.R.J., TELES V. & VIOLETTE S. (2005) - *Dealing with spatial heterogeneity*. *Hydrogeology Journal*, **13**: 161-183.

- DEUTSCH C. & JOURNAL A. (1992)- *GSLIB: Geostatistical Software Library*. Oxford Univ. Press.
- FALIVENE O., CABRERA L., MUÑOZ J.A., ARBUÉS P., FERNÁNDEZ O. & SÁEZ A. (2007) - *Statistical grid-based facies reconstruction and modelling for sedimentary bodies. Alluvial-palustrine and turbiditic examples*. *Geologica Acta*, **5**: 199-230.
- FELLETTI F., BERSEZIO R. & GIUDICI M. (2006) - *Geostatistical simulation and numerical upscaling to model groundwater flow in a sandy-gravel, braided river aquifer analogue*. *Journal of Sedimentary Research*, **76** (11): 1215-1229.
- FOGG G.E., NOYES C.D. & CARLE S.F. (1998) - *Geologically based model of heterogeneous hydraulic conductivity in an alluvial setting*. *Hydrogeology Journal*, **6** (1): 131-143.
- GOOVAERTS P. (1997) - *Geostatistics for Natural Resources Evaluation*. Oxford University Press, Oxford.
- HEINZ J. & AIGNER T. (2003) - *Three dimensional GPR analysis of various Quaternary gravel-bed braided river deposits (south-western Germany)*. In: C.S. BRISTOW & H.M. JOL (Eds.), «Ground Penetrating Radar in Sediments» Geological Society Spec. Publ., **211**: 99-110.
- HEINZ J., KLEINEDAM S., TEUTSCH G. & AIGNER T. (2003) - *Heterogeneity patterns of Quaternary glacio-fluvial gravel bodies (SW Germany): application to hydrogeology*. *Sedimentary Geology*, **158**: 1-23.
- JORDAN D.W. & PRYOR W.A. (1992) - *Hierarchical levels of heterogeneity in a Mississippi River meander belt and application to reservoir systems*. *AAPG Bull* **76**: 1601-1624.
- JOURNAL A.G. & GÓMEZ-HERNÁNDEZ J.J. (1993) - *Stochastic Imaging of the Wilmington Clastic Sequence*. Society of Petroleum Engineers Formation Evaluation March: 33-40.
- JOURNAL A.G., GUNDESO R., GRINGARTEN E. & YAO T. (1998) - *Stochastic modelling of a fluvial reservoir: a comparative review of algorithms*. *Journal of Petroleum Science and Engineering*, **21**: 95-121.
- KNUDBY C. & CARRERA J. (2005) - *On the relationship between indicators of geostatistical, flow and transport connectivity*. *Adv. Water Resour.* **28**: 405-421.
- LIU Y., HARDING A., GILBERT R. & JOURNAL A. (2005) - *A Workflow for Multiple-point Geostatistical Simulation*. In: «Geostatistic Banff 2004»: 245-254.
- LUNT I.A., BRIDGE J.S. & TYE R.S. (2004) - *Development of a 3-D depositional model of braided river gravels and sands to improve aquifer characterization*. In: *Aquifer Characterization*, J.S. BRIDGE & D. HYNDMAN (Eds.) Spec. Publ. SEPM Soc. Sediment. Geol., **80**: 139-169.
- OKABE H. & BLUNT M. (2004) - *Multiple-point Statistics to Generate Pore Space Images*. In: «Geostatistics Banff 2004». 763-768, Springer Netherlands.
- RITZI R.W. (2000) - *Behavior of indicator variogram and transition probabilities in relation to the variance in lengths of hydrofacies*. *Water Resources Research*, **36**: 3375-3381.
- RUBIN Y., LUNT I.A. & BRIDGE J.S. (2006) - *Spatial variability in river sediments and its link with river channel*. *Water Resources Research*, **42**, w06d16, doi:10.1029/2005wr004853.
- SEIFERT D. & JENSEN J.L. (1999) - *Using Sequential Indicator Simulation as a tool in reservoir description: Issues and Uncertainties*. *Mathematical Geology*, **31**: 527-550.
- STREBELLE S. (2002) - *Conditional simulation of complex geological structures using multiple point statistics*. *Mathematical Geology*, **34** (1): 1-22.
- STREBELLE S., PAYRAZIAN K. & CAERS J. (2003) - *Modeling of a deepwater turbidite reservoir conditional to seismic data using principal component analysis and multiple-point geostatistics*. *SPE Journal*, **8** (3): 227-235.
- SWEET M.L., BLEWDEN C.J., CARTER A.M. & MILLS C.A. (1996) - *Modeling heterogeneity in a low-permeability gas reservoir using geostatistical techniques, Hyde Field, Southern North Sea*. *AAPG Bulletin*, **80** (11): 1719-1735.
- VASSENA C., CATTANEO L. & GIUDICI M. (2009) - *Assessment of the role of facies heterogeneity at the fine scale by numerical transport experiments and connectivity indicators*. *Hydrogeology Journal*, in press. Online version available: doi:10.1007/s10040-009-0523-2.
- WEISSMANN G.S. & FOGG G.E. (1999) - *Multi-scale alluvial fan heterogeneity modeled with transition probability geostatistics in a sequence stratigraphic framework*. *Journal of Hydrology*, **226**: 48-65.
- WEISSMANN G.S., CARLE S.F. & FOGG G.E. (1999) - *Three-dimensional hydrofacies modeling based on soil surveys and transition probability geostatistics*. *Water Resources Research*, **35**: 1761-1770.
- ZAPPA G., BERSEZIO R., FELLETTI F. & GIUDICI M. (2006) - *Modeling aquifer heterogeneity at the facies scale in gravel-sand braided stream deposits*. *Journal of Hydrology*, **325**: 134-153.



## Hydrogeological implication of the Pliocene-Pleistocene torrential and debris flow succession around the Lanzo Ultramafic Massif (Western Alps)

*Significato idrogeologico della successione torrentizia e di debris flow al margine del Massiccio Ultrabásico di Lanzo (Alpi Occidentali)*

FORNO M.G. (\*), DE LUCA D.A. (\*),  
FIORASO G. (\*\*), GIANOTTI F. (\*)

**ABSTRACT** - A thick succession of deposits associated with torrential and debris flow processes preserved around the Lanzo Ultramafic Massif is described in this study. It represents the oldest Pliocene-Quaternary complex of continental sediments locally outcropping close to the inner margin of the Western Alps.

These sediments, observed into the deepest fluvial incisions, show prevalent gravel facies with clast supported texture and trough cross bedding. The decimetric clasts are derived locally because of the reworking of peridotite substratum. The matrix consists of a mixture of sand, silt and clay. Both the sedimentological features and the distribution into the watercourse incisions indicate torrential and debris flow genesis. In the sectors not incised by watercourses the succession is instead prevalently constituted by angular or poorly rounded clasts, derived from the local supply, with a scarce matrix and a stratification parallel to the slope. These features are a significant evidence that here the gravitative facies prevail. Silty sediments are observed locally, either without clasts or containing small peridotite fragments, with a bedding parallel to slope. These sediments are connected to colluvial processes and supplied by the reworking of mature soils developed at the expense of peridotite bedrock.

The definite stratigraphic position of the torrential and debris flow succession, located at the base of the different sedimentary Pliocene-Pleistocene units, and the strong weathering of sediments, indicated by their argillification and cementation by iron oxides, reflect an ancient age. This assessment is in agreement with the local interfingering with the Lower Complex of "villafranchian succession" (CARRARO Ed., 1996) that is related to the Middle Pliocene. The strong weathering of this succession produces the peculiar hydrogeological significance.

The hydrogeological conceptual model of the area is described. In the different areas some springs linked to permeability contrast and piezometric surface emergence are

signalled. These springs are prevalently used for drinking water, irrigation or domestic purpose.

Some examples of springs around the Lanzo Ultramafic Massif are presented in a detailed geological map. The springs result from the difference in permeability between the ancient torrential and debris flow succession and the glacial, outwash and detrital cover. In these areas the ancient torrential and debris flow sediments have the hydrogeological role of a separation element between the shallow aquifer in the glacial, glaciofluvial and detrital deposits and the deep aquifer in the fracture network of the crystalline rocks.

**KEY WORDS:** debris flow, fluvial sediments, hydrogeology, Lanzo Massif, Pleistocene, Pliocene.

**RIASSUNTO** - Viene segnalata la presenza di una potente successione, connessa essenzialmente con fenomeni torrentizi e di *debris flow*, conservata ai margini del Massiccio Ultrabásico di Lanzo: costituisce il termine pliocenico-quaternario continentale più antico affiorante a ridosso del rilievo alpino occidentale, in corrispondenza delle incisioni fluviali più profonde.

Questi depositi sono caratterizzati da una facies prevalente ghiaiosa, con tessitura *clast supported* e un accenno di stratificazione incrociata concava: i ciottoli, di dimensioni decimetriche, sono di apporto locale derivando esclusivamente dallo smantellamento del substrato peridotitico; la matrice è costituita da percentuali di sabbia, silt e argilla estremamente variabili. L'insieme delle caratteristiche sedimentologiche e la distribuzione entro le incisioni modellate dal reticolato idrografico suggeriscono l'origine essenzialmente torrentizia. Nei settori privi di incisioni fluviali questi sedimenti contengono numerosi elementi angolosi, con una scarsa matrice e un accenno di stratificazione parallela al versante, indicativi di una genesi prevalentemente detritica. Ancora più localmente affiorano invece sedimenti essenzialmente siltoso-argillosi, di origine prevalentemente colluviale.

(\*) Dipartimento di Scienze della Terra, Università di Torino, via Valperga Caluso 35, 10125 Torino

(\*\*) C.N.R. - Istituto di Geoscienze e Georisorse, Unità Operativa di Torino, via Valperga Caluso 35, 10125 Torino

La posizione stratigrafica, alla base delle diverse unità pliocenico-pleistoceniche affioranti, e l'alterazione molto spinta della successione descritta, caratterizzata da un elevato grado di argillificazione e cementazione da parte degli ossidi di ferro, è indicativa dell'età antica: l'interdigitazione, localmente osservabile, con i depositi "villafranchiani" del Complesso Inferiore (CARRARO Ed., 1996), suggerisce come la deposizione sia iniziata a partire dal Pliocene medio. La notevole alterazione è responsabile della permeabilità molto modesta di questi sedimenti, che determina particolari modalità nella circolazione idrica sotterranea.

È stato inoltre prodotto un modello geologico concettuale. Nelle diverse aree sono segnalate alcune sorgenti per contrasto di permeabilità e per emergenza della superficie piezometrica, utilizzate prevalentemente per usi idropotabili, agricoli o domestici.

Sono infine presentati alcuni esempi di sorgenti localizzate ai margini del Massiccio Ultrabasico di Lanzo, per i quali sono state realizzate carte geologiche di dettaglio. Le sorgenti esaminate sono connesse con differenze di permeabilità tra l'antica successione torrentizia e di *debris flow* e la copertura glaciale, fluvioglaciale e detritica: in queste aree gli antichi depositi torrentizi e di *debris flow* hanno il ruolo di elemento di separazione tra gli acquiferi superficiali, ospitati nei depositi glaciali, fluvioglaciali e detritici, e gli acquiferi profondi ospitati nel substrato cristallino.

PAROLE CHIAVE: colata di detrito, idrogeologia, Massiccio di Lanzo, Pleistocene, Pliocene, sedimenti fluviali.

## 1. - INTRODUCTION

During the surveying for the 1:50.000 "Torino Ovest" 155 Sheet of the CARG (Geological Map of Italy) project, the diffuse presence of a particular sedimentary complex on the slopes of the Lanzo Ultramafic Massif appeared. This succession is preserved in wide and very thick relicts. They were disregarded in the previous geological maps and exclusively described in the magnesite mineralization studies of the lower Susa Valley.

This succession consists of different facies and various age deposits and is extensively weathered. The strong argillification and cementation of these sediments produce their peculiar hydrogeological significance. Some springs localised around the Lanzo Ultramafic Massif are present at the top of these sediments and conditioned by their presence.

## 2. - GEOLOGY OF THE LANZO ULTRAMAFIC MASSIF

The Lanzo Ultramafic Massif (LUM) is localised in the internal part of the high-pressure, low-temperature metamorphic belt of the Western Alps between the lower Susa Valley and Viù Valley, 35 km North-West of Turin (fig. 1) (DAL PIAZ *et alii*, 1990). It represents one of the largest outcrops of peridotites in the world. This massif is well

known because of the freshness of its rocks, in which ancient mantle and oceanic lithological associations are clearly observable (NICOLAS, 1974; BOUDIER, 1978; BODINIER *et alii*, 1986; PICCARDO *et alii*, 2007).

The LUM is interpreted as a slide of lithospheric subcontinental mantle, deeply transformed by asthenospheric melt impregnation and melt/rock interaction during the early rift evolution of the Jurassic Ligurian Tethys oceanic lithosphere (PICCARDO *et alii*, 2007).

The LUM is commonly divided into a southern body (55 km<sup>2</sup>), a central body (90 km<sup>2</sup>) and a northern body (5 km<sup>2</sup>), which are separated by two broad mylonitic and serpentized shear zones with a NW-SE direction (BOUDIER & NICOLAS, 1972; ELTER *et alii*, 2005; BALESTRO *et alii*, 2009b).

The core of the three bodies of the LUM is mainly composed of massive weakly serpentized plagioclase peridotite with minor granular harzburgite and spinel peridotite. These rocks are frequently cut by gabbroic veins and dykes and sometimes by basalt. In the peripheral areas of the LUM the peridotite gradually becomes more serpentized until it becomes massive serpentinite due to the Alpine high-pressure/low-temperature eclogitic metamorphic imprint (KIENAST & POGNANTE, 1988; LAGABRIELLE *et alii*, 1989; PELLETIER & MÜNTENER, 2006).

The peridotite preserves an ancient pervasive magmatic foliation and is cross-cut by three regularly spaced joint sets (0.5-1.5 m), isolating approximately equidimensional blocks with a typical cubic, prismatic or rhombohedral shape.

The LUM is bounded by high-pressure ophiolite and calcschist (Piemontese Zone *Auct.*) in the west and by continental units of the Sesia-Lanzo Zone in the north. In the east the LUM is covered by a thick Middle Pleistocene fluvial fan succession of the Stura di Lanzo River (Unità di Fiano). This latter deposit rests above a fluvio-lacustrine "villafranchian" succession Middle Pliocene to Lower Pleistocene in age (BALESTRO *et alii*, 2009a; FORNO *et alii*, 2009). Along the south-eastern edge of the LUM a succession of torrential and debris flow fans links the slopes of the peridotitic massif to the fluvial plain. Finally, in the south the LUM is bounded by the Rivoli-Avigliana Morainic Amphitheatre, situated at the mouth of the Susa Valley. The glacial and outwash deposits that form the amphitheatre were built during the various expansions of the Dora Riparia glacier. Two groups of moraines have been referred to the Middle Pleistocene glaciations, whereas the third group of moraines has been interpreted as the Late Pleistocene glacial expansion (PETRUCCI, 1970; CARRARO *et alii*, 2005; BALESTRO *et alii*, 2009b).

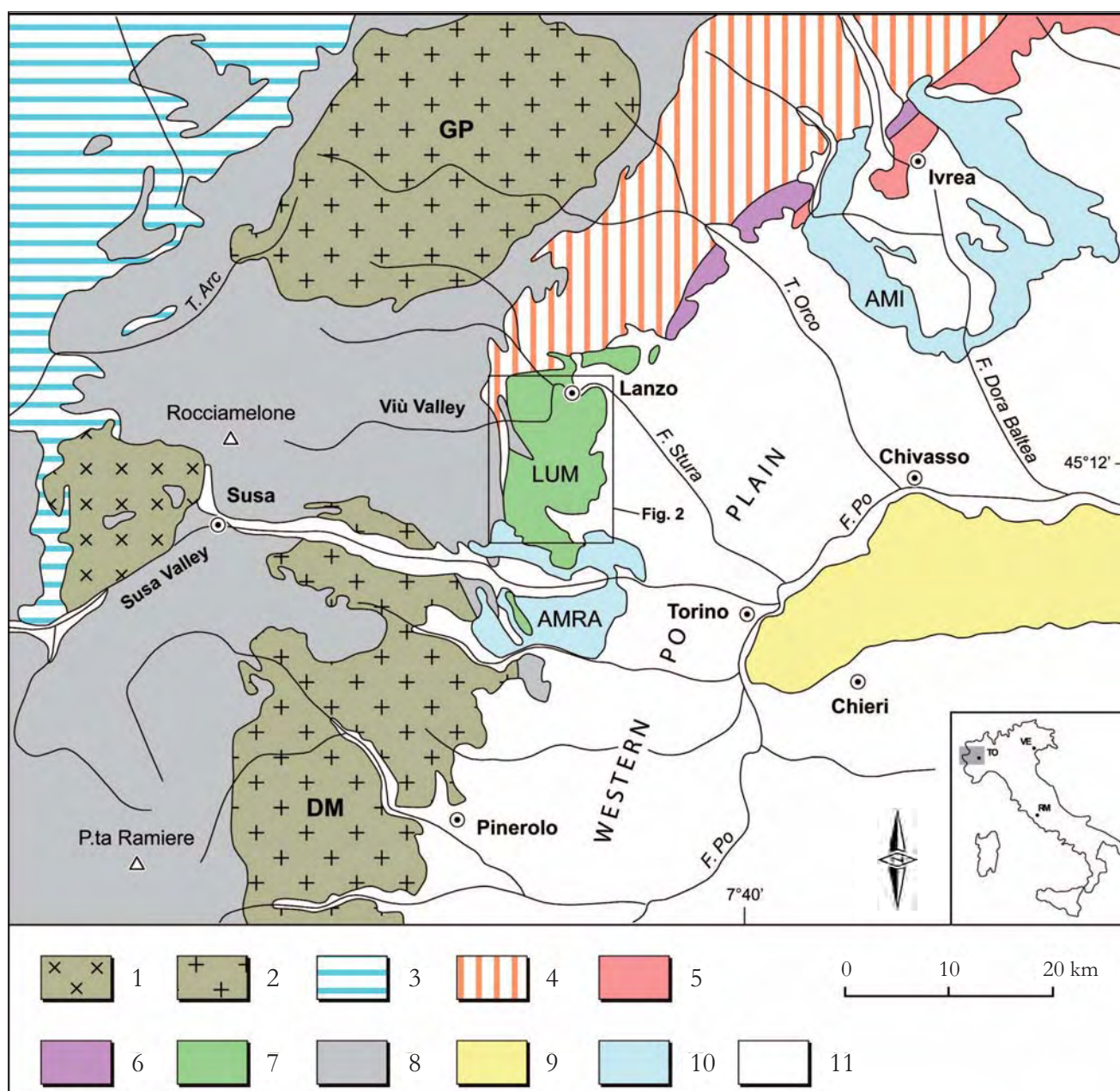


Fig. 1 - Structural sketch map of the Italian Western Alps (from DAL PIAZ *et alii*, 1990, modified). 1: Ambin Massif (Penninic Domain). 2: internal crystalline massifs of the Penninic Domain (GP = Gran Paradiso; DM = Dora-Maira). 3: Grand St. Bernard Zone (Penninic Domain). 4: Sesia-Lanzo Zone (Austroalpine Domain). 5: Ivrea-Verbano Zone (Southalpine Domain). 6: Canavese Zone. 7: Lanzo Ultramafic Massif (LUM). 8: ophiolite-bearing calcschist of the Piedmontese Zone. 9: Oligo-miocene succession of the Monferrato - Torino Hill (Piedmont-Ligurian Tertiary Basin). 10: Pleistocene glacial deposits (AMRA = Rivali-Avigliana Morainic Amphitheatre; AMI = Ivrea Morainic Amphitheatre). 11: Quaternary fluvial and glaciofluvial deposits of the Western Po Plain.

- Schema strutturale delle Alpi Occidentali (modificato da DAL PIAZ *et alii*, 1990). 1: Massiccio d'Ambin (Dominio Penninico). 2: massicci cristallini interni del Dominio Penninico (GP = Gran Paradiso; DM = Dora-Maira). 3: Zona del Gran S. Bernardo (Dominio Penninico). 4: Zona Sesia-Lanzo (Sistema Austroalpino). 5: Zona Ivrea-Verbano (Dominio Sudalpino). 6: Zona del Canavese. 7: Massiccio Ultrabasico di Lanzo (LUM). 8: calciscisti ofiolitici della Zona Piemontese. 9: successione oligo-miocenica del Monferrato - Collina di Torino. 10: depositi glaciali pleistocenici (AMRA = Anfiteatro Morenico di Rivali-Avigliana; AMI = Anfiteatro Morenico di Ivrea). 11: depositi fluviali e fluvio-glaciali quaternari della Pianura Padana occidentale.

The rocks of the LUM are involved in intense and deep-seated chemical-physical weathering phenomena, particularly developed where peridotite crops out. This peridotite has high susceptibility to weathering due to the abundant presence of olivine, which constitutes about 60% of the whole rock volume. Weathering is caused by chemical processes such as hydration, hydrolysis, oxidation

and leaching of femic minerals (olivine and pyroxene) occurring in the ultramafic rocks. Characteristics and degree of weathering are spatially heterogeneous relative to the local morphologic context of the LUM. On the watersheds and along steep slopes, erosive phenomena, related to the outflow of the meteoric waters, prevail and remove weathering products, exposing the bedrock. Lo-



cally, an eluvio-colluvial 1-2 m thick cover is present. This cover prevents gelifraction but allows weathering processes to develop along the fracture network sometimes at depths of about 8-12 m.

At the base of slopes, where erosion processes are less effective, weathering phenomena occur in depth and involve slope deposits (mainly mud-debris flow deposits and colluvial cover) and underlying bedrock at depths of tens of metres (e.g., Caselette and Val della Torre quarries). On the whole, weathered covers show a yellowish and reddish colouring with a mean colour index ranging between 7.5YR and 10R (Munsell Soil Colour Charts). Moreover weathering phenomena are responsible for widespread magnesite mineralisation (associated with minor dolomite, aragonite, opal and quartz), distributed in the peridotite bedrock and secondly in the torrential and debris flow deposits that mantle the base of slopes (NATALE, 1972; MIÈ & NATALE, 1978).

Weathering phenomena has been interpreted as a result of a long-term processes developed mainly during past sub-tropical climates before the Pleistocene glacial phases that were characterised by high temperature and abundant rainfall (NATALE, 1972; MIÈ & NATALE, 1978; FIORASO & SPAGNOLO, 2009).

### 3. - THE ANCIENT TORRENTIAL AND DEBRIS FLOW SUCCESSION

Around the Lanzo Ultramafic Massif (LUM), a torrential and debris flow succession is present (fig. 2). This succession is very particular with regard to its geologic and hydrogeological features. The main outcropping areas of these sediments are localised in the right lateral sector of the Lanzo alluvial fan (between Vallo and Givoletto, A4÷A12 in figure 2), in the lower Viù Valley (between Maddalene and Germagnano, A13 and A14 in figure 2) and in the lower Susa Valley (between Rubiana and Rivera, A1÷A3 in figure 2).

The strong deepening of the watercourses produced deep incisions (fig. 3), which allowed us to

observe the deposits in great detail. Within the entire outcrop area, the complex lies on the substratum of the LUM (peridotite and serpentinitized peridotite) or, locally, on the Piemontese Zone (ophiolite-bearing calcschists). It shows a definite stratigraphic position at the base of the different sedimentary Pliocene-Pleistocene units, and has strong weathering that is responsible for the peculiar hydrogeological significance. Because of these elements the complex can be referred to as the most ancient of the Pliocene-Quaternary continental succession outcropping along the inner margin of the western Alps.

In various areas the ancient torrential and debris flow succession is covered by different sedimentary bodies: the Lanzo alluvial Fan deposits (basal Middle Pleistocene Fiano Unit in FORNO *et alii*, 2009) (fig. 4); the Rivoli-Avigliana Amphitheatre glacial sediments (Middle-Late Pleistocene Magnoletto, Frassinere and Bennale Units in BALESTRO *et alii* (2009a); a peculiar facies of Lower Pleistocene to Holocene detrital sediments (block streams in FIORASO & SPAGNOLO, 2009); and more recent torrential and debris flow sediments (fig. 2).

The weathered torrential and debris flow succession is composed by numerous metres-thick overlapped lenticular bodies. The paucity of sub-surface data does not allow us to evaluate the extension and the maximum thickness of this succession (estimated as 50-60 m). The lack of these sediments in the alluvial plain suggests that they are limited to the edge of the alpine chain.

Facies associations change from place to place. At the valleys' mouths, a coarse conglomerate prevails (fig. 5). It consists of decimetre-size angular to well-rounded elements and mixed with a variously abundant matrix. It shows alternating coarsening and fining-upward structures. The matrix is formed by a mixture of sand, silt and clay, with variable percentage within the same outcrop. Rare levels contain boulders over 1 m<sup>3</sup> in size.

These sediments have a clast supported texture and, only locally, a matrix-supported texture. They often show trough cross bedding (fig. 5). In some outcrops the imbricate structure of some elements

Fig. 2 - Geological map of the Lanzo Ultramafic Massif. a: "Gneiss minuti" (Sesia-Lanzo Zone). b: lherzolites, harzburgites and dunites (Lanzo Ultramafic Massif). c: serpentinites and serpentinitized peridotites (Piemontese Zone and Lanzo Ultramafic Massif). d: metabasites (Piemontese Zone). e: calcschists (Piemontese Zone). f: weathered and cemented torrential, debris flow and detrital-colluvial deposits (Middle Pliocene to Lower Pleistocene?); number refers to the localities quoted in the text (A1 = Rubiana; A2 = Almese; A3 = Miosia; A4 = Givoletto; A5 = Rivasacco; A6 = Truc Miola; A7 = S. Biagio; A8 = Baratonina; A9 = Varisella; A10 = S. Maria della Neve; A11 = Rio l'Adrit; A12 = Vallo; A13 = Germagnano; A14 = Maddalene). g: Stura di Lanzo ancient fluvial deposits (Middle to Late Pleistocene). h: glaciofluvial deposits (Middle to Upper Pleistocene). i: undifferentiated glacial deposits of the Rivoli-Avigliana Morainic Amphitheatre (Middle to Late Pleistocene). l: torrential and debris flow deposits (Late Pleistocene). m: recent fluvial deposits (Holocene). n: springs listed in table 2. See figure 1 for location of the area.

- Schema geologico del Massiccio Ultrabasic di Lanzo. a: "Gneiss minuti" (Zona Sesia-Lanzo). b: lherzoliti, harzburgiti e duniti (Massiccio Ultrabasic di Lanzo). c: serpentiniti e peridotiti serpentinitezzate (Zona Piemontese e Massiccio Ultrabasic di Lanzo). d: metabasiti (Zona Piemontese). e: calciscisti (Zona Piemontese). f: depositi torrentizi, di debris flow e detritico-colluviali alterati e cementati (Pliocene medio - Pleistocene inferiore?); i numeri si riferiscono alle località citate nel testo (A1 = Rubiana; A2 = Almese; A3 = Miosia; A4 = Givoletto; A5 = Rivasacco; A6 = Truc Miola; A7 = S. Biagio; A8 = Baratonina; A9 = Varisella; A10 = S. Maria della Neve; A11 = Rio l'Adrit; A12 = Vallo; A13 = Germagnano; A14 = Maddalene). g: depositi fluviali antichi della Stura di Lanzo (Pleistocene medio). h: depositi fluvio-glaciali (Pleistocene medio-superiore). i: depositi glaciali indifferenziati dell'Amfiteatro morenico di Rivoli-Avigliana (Pleistocene medio-superiore). l: depositi torrentizi e di debris flow (Pleistocene superiore). m: depositi fluviali recenti (Olocene). n: sorgenti elencate in tabella 2. Si veda la figura 1 per l'ubicazione dell'area.

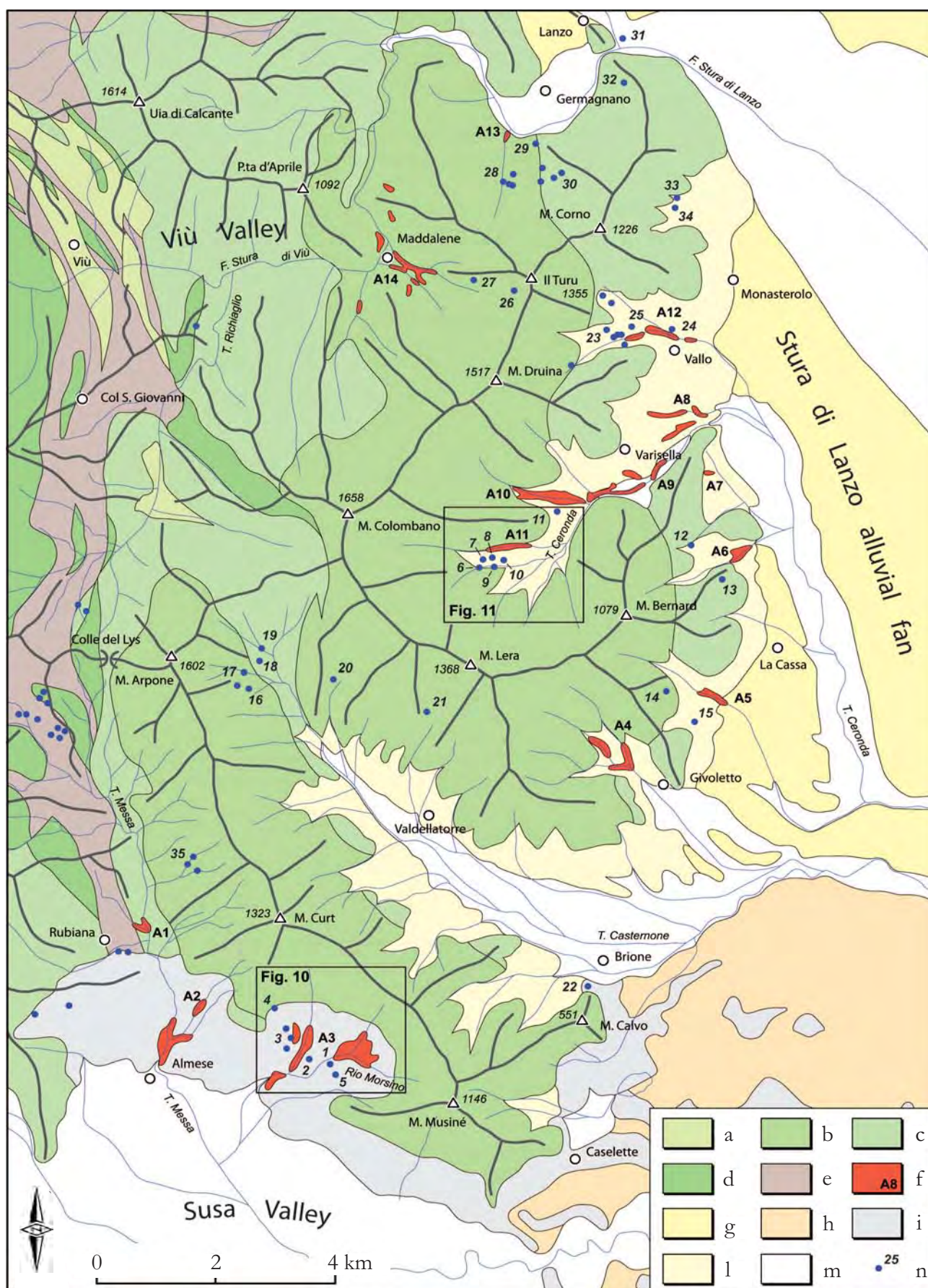






Fig. 3 - Wide outcrop of the torrential and debris flow succession (T. Ceronda incision, SW of Varisella).  
 - Esteso affioramento della successione torrentizia e di debris flow (incisione del T. Ceronda a SW di Varisella).

is evident. Sandy lenticular bodies with trough cross bedding, 10-40 cm thick, develop locally. Clasts are constituted by peridotite, serpentinized peridotite and serpentinite, with rare prasinite and meta-gabbrous, suggesting a local supply from the basins shaped in the LUM.

The sedimentologic features of these sediments and their distribution at the valleys' mouths suggest a prevalent torrential and debris flow genesis connected to a fan environment.

At the base of the slopes, in the sectors not incised by watercourses (Givoletto, La Cassa) these sediments are mainly constituted by angular clasts and show a poor bedding parallel to the slopes (fig. 6). The scarce matrix is composed of a sand, silt and clay mixture. In these sediments the detrital elements, supplied by physical crumbling of the slope, prevail. The clast petrographic composition indicates the local supply.

Locally, at least in the sheltered from erosion sectors (Rivera, Germagnano), silty sediments are observed, without clasts or containing small peri-

dotite fragments, with a bedding parallel to the slope (fig. 7). These sediments are connected to colluvial processes and supplied by the reworked soils developed on peridotite.

The various facies constituting the ancient torrential and debris flow succession show an interfingering relationship. Moreover, they form wide torrential fans distributed at the base of the LUM slopes.

The succession is affected by a weathering that produces a strong argillification, responsible for continuous and thick clay patinas developed around the clasts and into the fractures. Clay aggregates, some centimetres in size, also diffusely develop.

Sometimes the weathering is so strong that peridotite clasts become entirely loose. Exclusively coarse and serpentinite elements are partially preserved. In the strongly weathered peridotite clasts in which there are the olivine crystals totally transformed to a clayey aggregate, the original rock structures are preserved. The strong weathering is related to the presence of peridotite substratum, highly sensitive to weathering in the hot-wet con-



ditions prevailing before the Middle-Upper Pleistocene glaciations.

The weathering phenomena also produce a strong oxidation of Fe, responsible for the matrix's dark red colour (10R 4/4,6 - 2.5 YR 5/6), that appears throughout the whole thickness of the deposits (fig. 8). These sediments are also affected by the oxidation of Mn, which produces aggregates and continuous black patinas around the clasts.

These processes are responsible for the diffuse cementation of the sediments.

The strong cementation, providing resistance to erosion, allows for good preservation of these ancient sediments, even in sectors (e.g. Almese) subjected to further glacial exaration.

The described succession, which includes more different facies, also comprises overlapped bodies with decreasing grades of weathering, suggesting a sedimentation over a long period. The torrential and debris flow deposits are locally interfingered

with the Lower Complex of the “villafranchian succession” (CARRARO Ed., 1996) (Unità di La Cassa in BALESTRO *et alii*, 2009a,b), that is dated to the Middle Pliocene (MARTINETTO, 1994; MARTINETTO *et alii*, 2006). This evidence indicates sedimentation during this period. The overlapping of Middle Pleistocene fluvial sediments (Fiano Unit in FORNO *et alii*, 2009) suggests that the sedimentation potentially continued during the Lower Pleistocene.

In the silty-clayey facies, fractures systems develop locally (Germagnano). These fractures, decimetric to metric in extension, show a discontinuous distribution. They are prevalently connected to contraction phenomena. Sometimes, fault systems with metric to some decametric length and different strike directions, connected to glaciotectionic deformation, are observed (Almese). In other places, local fault systems connected to gravitative collapses are observed (Vallo).



Fig. 4 - Irregular erosional surface between torrential and debris flow sediments, that are supplied from a local source, and the overlapped fluvial sediments connected with the Stura di Lanzo River (Fiano Unit).

- Superficie di erosione, articolata nel dettaglio, che separa i depositi torrentizi e di debris flow, di alimentazione locale, e i depositi fluviali legati al bacino del T. Stura di Lanzo (Unità di Fiano).





Fig. 5 - Trough cross bedded torrential sediments (T. Ceronda incision, SW of Varisella).  
 - *Stratificazione incrociata concava dei depositi torrentizi affioranti lungo l'incisione del T. Ceronda, a SW di Varisella.*

#### 4. - HYDROGEOLOGICAL CONCEPTUAL MODEL

The hydrogeological conceptual model applied to the Lanzo Ultramafic Massif includes four hydrogeological units (tab. 1 and fig. 9).

*Complex (1).* This complex corresponds to glacial deposits that are essentially flow till (Almese), glaciofluvial and fluvial deposits (Almese, Germano), debris flow deposits (Varisella), block deposits with open-work texture (block streams) and gravitative deposits (diffusely distributed). These are porous sediments, with medium (flow till and debris flow deposits) to high (glaciofluvial deposits) and very high (block stream deposits) permeability. This complex constitutes a shallow aquifer.

*Complex of the weathered torrential and debris flow succession (2).* This complex consists of originally coarse deposits whose weathering produced an abundant fine matrix and chemical decomposition of clasts. The complex presents a permeability value from low to very low, comparable with the permeability

of a very clayey silty sand. Such a complex represents an aquiclude forming the impermeable substratum of the overlying Complex 1.

*Complex of the fractured crystalline rocks (3).* The surface layer of the peridotite bedrock is often very fractured for some metres in depth (locally for about ten metres). This layer shows a medium permeability. It can host a shallow aquifer where it outcrops or is covered by Complex 1 deposits. Otherwise it represents a confined aquifer where it is buried by Complex 2 deposits.

*Complex of the poorly fractured crystalline rocks (4).* This complex forms the main reliefs and the substratum of the Plio-Quaternary sedimentary succession. It consists of magmatic intrusive ultramafic rocks, such as lherzolite, harzburgite and dunite, and metamorphic rocks, principally serpentinite. The basement has a very low fissure permeability and it represents the basal aquiclude.

The shallow aquifer represented by Complex 1 feeds a set of springs conditioned by the morphology of its basal surface (top of the weathered



Tab. 1 - *Facies and features of the four hydrogeological complexes of the LUM.*  
 - *Facies e caratteristiche dei quattro complessi idrogeologici del LUM.*

Complex	Lithologic features	Hydraulic conductivity (m/s)	Primary or secondary porosity	Hydrostratigraphy	Estimated thickness (m)
1	glacial, glaciofluvial, fluvial, debris flow, block stream and gravitative deposits	from medium to high ( $10^{-1} \div 10^{-4}$ )	primary	aquifer	10-40
2	weathered torrential and debris flow deposits	from low to very low ( $10^{-6} \div 10^{-8}$ )	primary	aquiclude	20-60
3	fractured crystalline rocks	from medium to high ( $10^{-4} \div 10^{-2}$ )	secondary	aquifer	<10
4	poorly fractured crystalline rocks	low ( $10^{-5} \div 10^{-6}$ )	secondary	aquitard	>100



Fig. 6 - Sediments with angular clasts indicative of the prevalent detrital supply (Germagnano).  
 - *Sedimenti caratterizzati dalla presenza di clasti angolosi, indicativa di prevalenti apporti detritici (Germagnano).*





Fig. 7 - Lenticular silty body connected with colluvial supply (T. Ceronda incision, SW of Varisella).  
 - *Corpo lenticolare siltoso legato a locali apporti colluviali (incisione del T. Ceronda a SW di Varisella).*

torrential and debris flow succession) and the topographic surface (tab. 2). This surface shows an irregular morphology because it was dissected by watercourses.

Depending on the nature of the bedrock and sedimentary cover and their relationships, permeability of deposits, position of the water table and local topography, at least three types of springs developed in the study area: barrier springs (A in figure 9), contact springs (B and C in figure 9) and for piezometric surface emergence (D in figure 9).

The discharge trend of these springs is strongly influenced by the volumetric extension and permeability of the feeding aquifer.

Where the aquifer is wide, spring discharge is relatively high and it can be equal to some l/s (A and D in figure 9). In case of the spring located in position A, it is fed by direct infiltration waters in the aquifer and by snow melt and runoff coming from the highest sectors of the basin shaped in the substratum. This evidence ensures that the aquifer feeding the spring has a bigger and more continu-

ous recharge over time. Some of these springs show a high variable discharge, especially where most of the aquifer is constituted by very high permeability sediments like block stream deposits. In this case, the discharge of the springs can vary from less than one to about 25 l/s in a period of a few hours, especially after particularly intense rain events.

Where the aquifer has a limited volumetric extension because it is dissected by watercourses (B and C in figure 9), spring discharge is low (mean discharge lower than 1 l/s), with a high variability index. These springs are often temporary; i.e., they undergo an interruption in connection with periods characterised by poor or null recharge to the aquifers.

Most of the described springs are used for drinking water (for example Fusalas, Rul, Lil and Falasca in Varisella commune; Listelli, Morsino Alto and Fontana Fredda in Almese commune), irrigation, or non drinking domestic use (tab. 2).

The supplying works typologies are represented above all by holding spoils, but also by burdened drainage.





Fig. 8 - Dark red colour (10 R 4/4) and strong cementation connected with weathering of the torrential succession (T. Ceronda incision, SW of Varisella).  
 - Colore rosso intenso (10 R 4/4) e sensibile cementazione della successione torrentizia, connessi con l'alterazione pedogenetica (incisione del T. Ceronda a SW di Varisella).

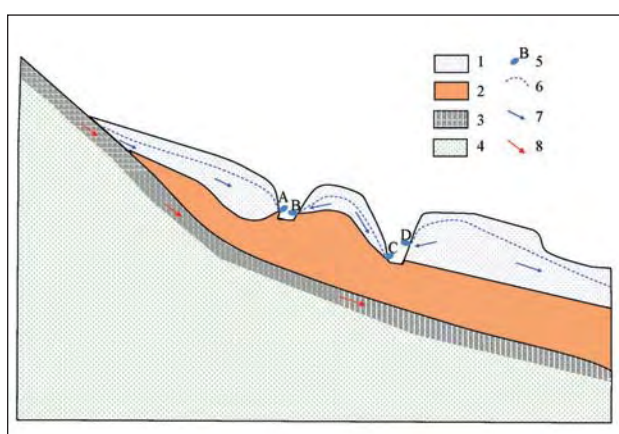


Fig. 9 - Conceptual hydrogeological scheme: 1: Complex of the glacial and glaciofluvial deposits; 2: Complex of the weathered torrent and debris flow deposits; 3: Complex of the fractured crystalline rocks; 4: Complex of the poorly fractured crystalline rocks; 5: springs with labels; 6: profile of the piezometric surface; 7: direction of flow into the shallow aquifer; 8: ground-water flow path into the fractured bedrock. A, B, C, D: springs.

- Schema concettuale dell'assetto idrogeologico e della circolazione idrica sotterranea. 1: Complesso dei depositi glaciali e fluvioglaciali; 2: Complesso dei depositi torrentizi e di debris flow alterati; 3: Complesso delle rocce cristalline fratturate; 4: Complesso delle rocce cristalline scarsamente fratturate; 5: sorgenti e relativa sigla; 6: profilo piezometrico della falda idrica; 7: linea di flusso nella falda idrica superficiale; 8: direzione di flusso della rete acquifera delle rocce cristalline fratturate. A, B, C, D: sorgenti.

The aquifer represented by Complex 3, developed in the first metres of the fractured crystalline bedrock, do not show significant springs. Part of Complex 3 can feed the block stream deposits aquifer; part of it is covered by the Complex of the weathered torrential and debris flow deposits creating a confined aquifer. In this last case, the Complex 2 of the weathered torrential and debris flow deposits has the hydrogeological role of a separation element between the shallow aquifer located in the glacial and outwash deposits and the deep aquifer in the fractured peridotite bedrock network.

## 5. - HYDROGEOLOGICAL FEATURES OF SOME SPRINGS RELATED TO WEATHERED TORRENTIAL AND DEBRIS FLOW SEDIMENTS

To explain the relationship between springs and the weathered torrential and debris flow deposits, two examples are considered: the Almese area (out-

Tab. 2 - *List of the springs of the LUM (from Provincia di Torino Archive and surveys of the authors). Numbers are referred to the springs mapped in figure 2. Commune and main catchment, discharge (l/s) and water use are indicated. Complex 1 is the main aquifer, formed by glacial, glaciofluvial, alluvial, debris flow, gravitative and block stream deposits. The asterisks (\*) indicate springs mainly linked to block stream deposits. Complex 2 is the main aquiclude formed by weathered and cemented torrential and debris flow deposits. Discharge values are prevalently taken from Provincia di Torino Archive; some values are directly measured by the authors (+). In the Germagnano area the discharges of linked-to-block stream springs\* range from 2-5 to 15-25 l/s (FIORASO & SPAGNOLO, 2009).*

- Elenco delle sorgenti del LUM (dall'Archivio della Provincia di Torino e dai rilevamenti degli autori). I numeri rimandano alle sorgenti rappresentate in figura 2. Sono indicati comune e bacino idrografico, portata e utilizzo dell'acqua. Il Complesso 1 è l'aquifero principale, costituito da depositi glaciali, fluvio-glaciali, fluviali, di *debris flow*, gravitativi e di *block stream*. Gli asterischi (\*) indicano le sorgenti strettamente legate ai depositi di *block stream*. Il Complesso 2 è l'aquiclude principale, costituito da depositi torrentizi e di *debris flow* alterati e cementati. I valori di portata provengono prevalentemente dall'Archivio della Provincia di Torino; sono contrassegnati (+) i valori direttamente misurati dagli autori. Nel territorio di Germagnano le portate delle sorgenti alimentate dai depositi di *block stream* variano da 2-5 a 15-25 l/s (FIORASO & SPAGNOLO, 2009).

commune / catchment	n°	spring name	discharge l/s	aquifer	aquifer substrate	use
Almese / Rio Morsino	1	Morsino Alto	2	Complex 1	Complex 2	drinking
	2	Fontanafredda 1	1	Complex 1	Complex 2	drinking
		Fontanafredda 2	1.05	Complex 1	Complex 2	drinking
	3	Listelli 1	0.04	Complex 1	Complex 2	drinking
		Listelli 2	0.07	Complex 1	Complex 2	drinking
		Listelli 3	0.06	Complex 1	Complex 2	drinking
		Listelli 4	0.04	Complex 1	Complex 2	drinking
		Listelli 5	0.07	Complex 1	Complex 2	drinking
	4	Bunino	0.08	Complex 1	peridotites	drinking
Varisella / T. Ceronda	5	Miosa	0.08	Complex 1	Complex 2	drinking
	6	Rul 1	1.11	Complex 1*	Complex 2	drinking
	7	Rul 2	1.04	Complex 1*	Complex 2	drinking
	8	Lil	0.08	Complex 1*	Complex 2	drinking
	9	Rio del Lupo	5 <sup>+</sup>	Complex 1*	Complex 2	untapped
	10	Fusalas 1	0.5 / 0.29 <sup>+</sup>	Complex 1	Complex 2	drinking
		Fusalas 2	0.5 / 0.22 <sup>+</sup>	Complex 1	Complex 2	drinking
	11	Falasca	5.4 / 4.8 <sup>+</sup>	Complex 1	Complex 2	drinking
La Cassa / T. Ceronda	12	Valceronda	1.05	Complex 1	serpentinites	irrigation
Givoletto / Rio Risalto	13	Pra Maria	/	Complex 1	serpentinites	irrigation
	14	La Douce	/	Complex 1	serpentinites	irrigation
Val della Torre/T. Casternone	15	Mousset	/	Complex 1	serpentinites	irrigation
	16	Fontanafredda 1	1	Complex 1	peridotites	drinking
		Fontanafredda 2	2	Complex 1	peridotites	drinking
	17	Arpone	2.05	Complex 1	peridotites	drinking
	18	Riva d'la Mena	4	Complex 1	serpentinites	drinking
	19	Codra	3	Complex 1	serpentinites	drinking
	20	Fontanabruna	2.05	Complex 1	peridotites	drinking
	21	Roch	2.05	Complex 1	peridotites	drinking
	22	Truc del Brione	0.05	Complex 1	peridotites	drinking
	23	Benna (8 springs)	total 8	Complex 1	Complex 2	drinking
Vallo Torinese/Rio Tronta	24	Galinverno	0.09	Complex 1	Complex 2	drinking
	25	Lupo	0.08	Complex 1	Complex 2	drinking
	26	Lenciassa	1	Complex 1	peridotites	drinking
Germagnano/T. Stura di Lanzo	27	Cugno	1.34	Complex 1	peridotites	drinking
	28	Gurba (4 springs)	total 4.5	Complex 1*	peridotites	drinking
	29	Stura	4.04	Complex 1*	peridotites	drinking
	30	Cerre, Griva, Vecchia, Freda (4 springs)	total 13.45	Complex 1*	serpentinites	drinking
	31	Via Cafasse	2	alluvial dep.		pisciculture
Lanzo Torinese/T. Stura di Lanzo	32	Croassere	/	Complex 1	serpentinites	/
Cafasse/T. Stura di Lanzo	33	Rio Proglio	/	Complex 1	serpentinites	irrigation
	34	Montebasso	/	Complex 1	serpentinites	irrigation
Rubiana / T. Messa	35	Oliva (3 springs)	total 4.8	Complex 1	peridotites	drinking



crop A3 in figure 2 and geological map and cross-section in figure 10) and the Varisella area (outcrop A11 in figure 2 and geological map and cross-section in figure 11).

Listelli, Fontana Fredda and Morsino Alto springs (tab. 2) are located in the Almese commune (left side of the lower Susa Valley), between 460 and 470 m a.s.l., at the south-western side of the LUM (fig. 10). During the Last Glacial Maximum, this sector was covered by the Dora Riparia Glacier. Here the main aquifer (Complex 1) is represented by Late Pleistocene flow till and glaciofluvial deposits lying on the ancient torrential and debris-flow succession. Small bodies of subglacial deposits are covered by the other glacial deposits. Because of their very low permeability, subglacial deposits are referred to as hydrogeological Complex 2. The springs are placed along the deepest incisions modelled into glaciofluvial deposits, like Fontana Fredda spring hosted by an abandoned riverbed.

Fus alas spring is located in the Varisella commune at the eastern side of the LUM. It is picked up by two adjacent supplying works, between Rio dell'Adrit and Rio del Lupo, into a left tributary incision of the Rio del Lupo at 730 m a.s.l. (fig. 11).

This sector of the LUM was not involved in the Pleistocene glaciations because it is at a low elevation and is not connected with the main glacial valleys (Susa and Stura di Lanzo). Here, the weathered and cemented torrential succession (Complex 2) outcrops continuously along the Rio dell'Adrit incision. This unit is covered by debris flow sediments that are several metres thick, with low permeability because of their fine texture and strong weathering.

Extremely permeable block stream deposits rest on this unit in the high sector of the basin. Block stream deposits contain an aquifer with high transmissivity. They feed directly some springs localised at the distal edge of block streams, with intermittent discharges variable from dozens of l/s to less than 1 l/s, and strictly linked to rain water and snow supply (Rio del Lupo spring in tab. 2). In contrast, all of the caught springs linked to Varisella aqueduct, show rather constant and low (less than 1 l/s) discharges. They are distributed along the block stream lateral sides but they are localised into the debris flow deposits (Rul and Lil springs in tab. 2). These data are in agreement with the presence of an aquifer hosted by the debris flow deposits with low permeability and high water retention, recharged mainly by the high permeable aquifer in the block streams. The springs are probably located some metres above the contact between ancient torrential deposits and the debris flow cover. This location is due to the difference of permeability between these three kinds of deposits.

The low electrolytic conductivity values of the

analysed spring waters of Varisella sector (Rul: 76  $\mu\text{S}/\text{cm}$ ; Fus alas: 99  $\mu\text{S}/\text{cm}$ ; Falasca: 95  $\mu\text{S}/\text{cm}$ ) indicate a low mineralisation of waters connected to the monotonous peridotite composition of the local bedrock and its detrital cover, without carbonatic and sulphatic lithotypes. This feature is also linked to their brief standing into the aquifer because of the short distance between the block streams edges and these springs (from some metres to some hundreds of metres).

The higher electrolytic conductivity of the analysed spring waters of the Almese sector (Listelli: 266  $\mu\text{S}/\text{cm}$ ; Fontana Fredda: 310  $\mu\text{S}/\text{cm}$ ; Morsino Alto: 256  $\mu\text{S}/\text{cm}$ ) is, instead, connected to the various lithological composition of the aquifer. It is represented by glacial deposits from Susa Valley and constituted by carbonate and silicate rock fragments.

## 6. - CONCLUSIONS

In this study we describe a wide-extensive and thick succession of torrential and debris flow deposits of Middle Pliocene-Lower Pleistocene age that had been disregarded in previous literature. These deposits lie on the peridotite bedrock of the Lanzo Ultramafic Massif.

The ancient succession is affected by weathering with strong argillification and iron oxidation. These secondary processes imparted comparable permeability values to different facies and produced an impermeable body that is very significant to the hydrogeological structure of the area.

The distribution of springs in the outcrop area of the torrential and debris flow succession was mapped in this study (fig. 2). Many springs are linked to the weathered deposits, interpreted as the main aquiclude (Complex 2) (tab. 1). This aquiclude bounds different shallow aquifers, hosted by the overlying permeable sediments (Complex 1). The latter consists of different facies if we compare the areas that were occupied by the Pleistocene glaciers (Almese) with the non-glaciated areas (Varisella). These facies (flow till, glaciofluvial, fluvial, debris flow, block stream and gravitative deposits) show variable permeability, from medium to very high (tab. 1). The presence of the low-permeability torrential and debris flow succession in the shallow subsurface causes water emergences where the topography is close to, or cuts across, the aquifer/aquiclude interface. The spring discharges are generally very low (1 l/s or less; tab. 2).

Only the springs fed directly by block stream deposits reach high discharges (25 l/s) but the discharge regime is highly variable in phase with the meteorological events.



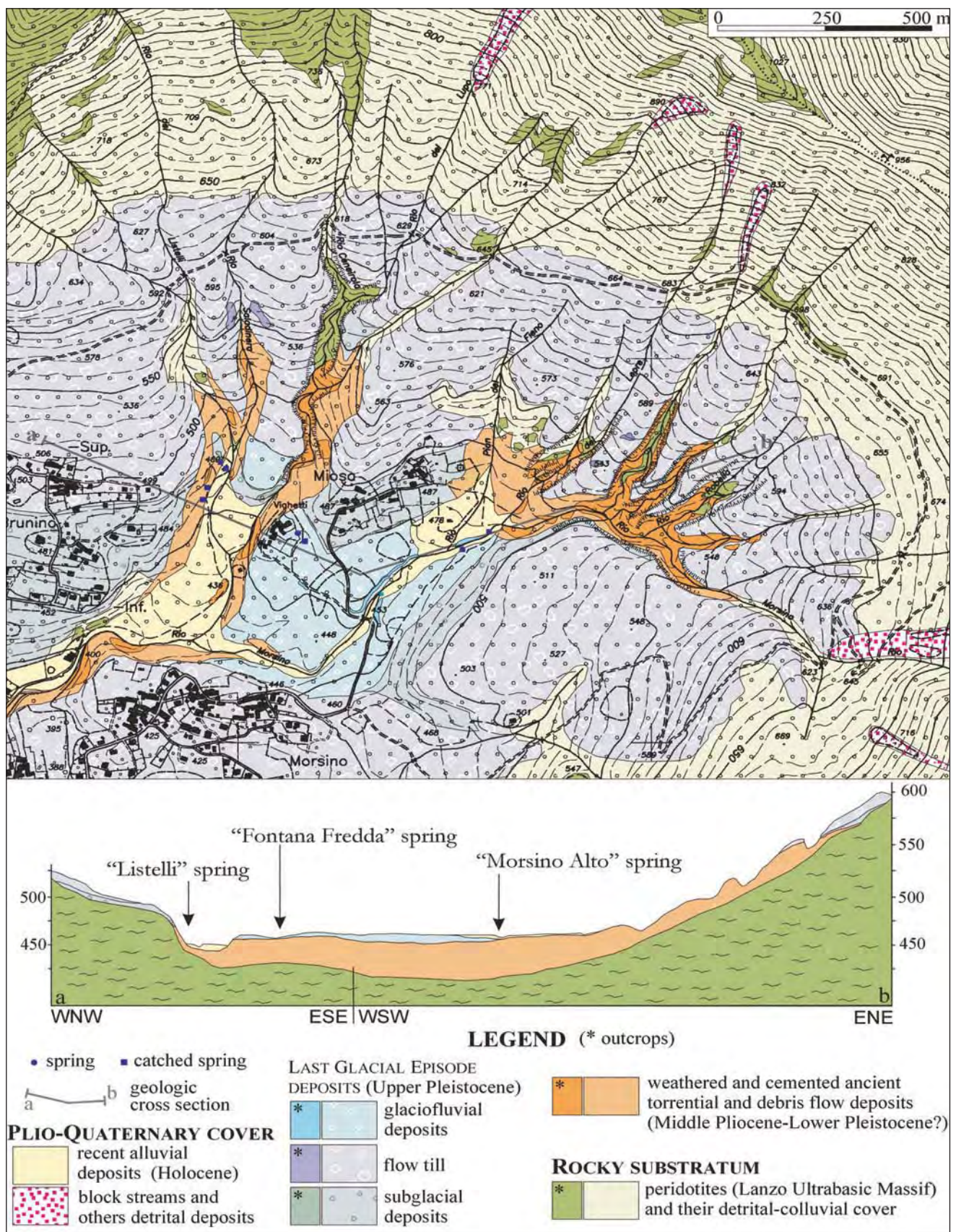


Fig. 10 - Geological map and cross section of the Almese, Morsino and Listelli springs (Almese, lower Susa Valley; see figure 2 for location of the area); vertical exaggeration in cross section is about 2,5.

- Carta geologica e profilo geologico dell'area delle sorgenti Almese, Morsino and Listelli (Almese, bassa Val di Susa; si veda figura 2 per l'ubicazione dell'area); l'esagerazione verticale nel profilo è di circa 2,5.



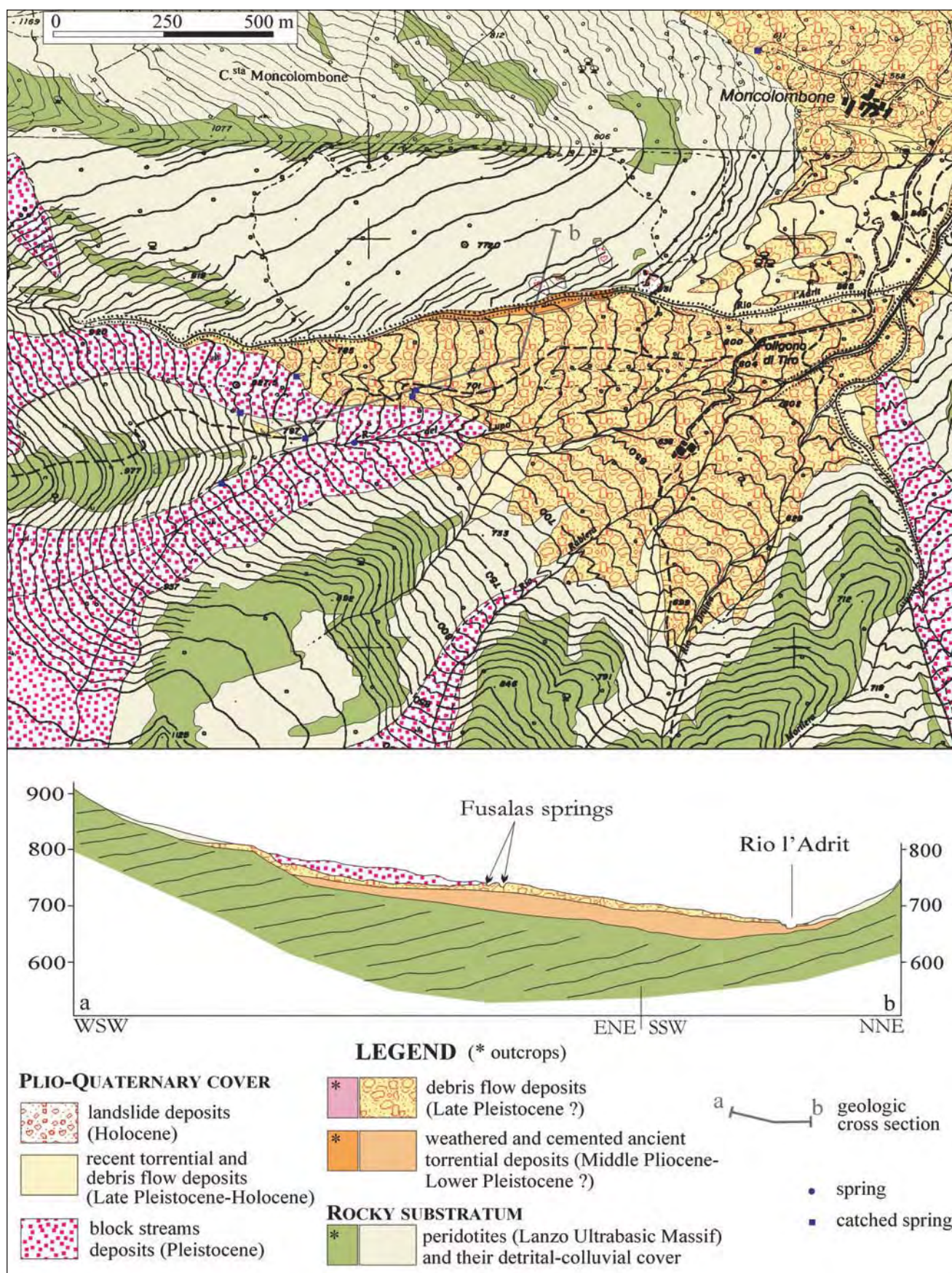


Fig. 11 - Geological map and cross section of the Fusalas springs (Varisella, Val Ceronza; see figure 2 for location of the area); vertical exaggeration in cross section is about 1,5.  
 - Carta geologica e profilo geologico dell'area delle emergenze Fusalas (Varisella, Val Ceronza; si veda figura 2 per l'ubicazione dell'area); l'esagerazione verticale nel profilo è di circa 1,5.



## Acknowledgments

The authors are especially grateful to the Provincia di Torino managers G. Massazza e V. Latagliata for consulting of the Servizio Gestione Risorse Idriche archive and to the Mayor G. Ossola for his availability and assistance in accessing to sources of Varisella Municipality. We thank A. Bini, an anonymous reviewer and R. Bersezio for their numerous helpful suggestions.

## REFERENCES

- BALESTRO G., CADOPPI P., PICCARDO G.B., POLINO R., SPAGNOLO G., TALLONE S., FIORASO G., LUCCHESI S. & FORNO M.G. (2009a) - Note illustrative del F. 155 "Torino Ovest" della Carta Geologica d'Italia alla scala 1:50.000. APAT, Servizio Geologico d'Italia - Dipartimento Difesa del Suolo, pp. 160, Roma.
- BALESTRO G., SPAGNOLO G., LUCCHESI S., FIORASO G., FORNO M.G., CADOPPI P., TALLONE S., PICCARDO G.B. & POLINO R. (2009b) - Carta Geologica d'Italia alla scala 1:50.000 - Foglio n. 155 Torino Ovest. APAT, Servizio Geologico d'Italia - Dipartimento Difesa del Suolo, Roma.
- BODINIER J.L., GIRAUD M., DUPUY C. & DOSTAL J. (1986) - Geochemistry of basic dykes in the Lanzo Massif (W.A.). Tectonophysics, **128**: 77-95.
- BOUDIER F. (1978) - Structure and petrology of the Lanzo peridotite massif (Piedmont Alps). Geol. Soc. Am. Bull., **89**: 1574-1591.
- BOUDIER F. & NICOLAS A. (1972) - Fusion partielle gabbroïque dans la lherzolite de Lanzo (Alpes piémontaises). Schweiz. Min. Petrogr. Mitt., **52**: 39-56.
- CARRARO F. (Ed.) (1996) - Revisione del Villafranchiano nell'area-tipo di Villafranca d'Asti. Atti del Convegno: "Il significato del Villafranchiano nella stratigrafia del Plio-Pleistocene", (Peveragno (CN), Villafranca d'Asti (AT), 20-24 giugno 1994). Il Quaternario It. Journ. Quatern. Sc., **9** (1): 5-120.
- CARRARO F., FIORASO G., LUCCHESI S. & GIARDINO M. (2005) - L'Amphithéâtre morainique de Rivoli-Avigliana. In: P. DELINE, M. GIARDINO & G. NICOU D (Eds.): "Le Quaternaire des Vallées Alpines". Cahiers de Géographie, **3**: 153-166.
- DAL PIAZ G.V., CASTELLARIN A., BOCCALETTO M., AGIP MINERARIA & SARTORI R. (Coord.) (1990) - Structural Model of Italy. Sheet 1. Consiglio Nazionale delle Ricerche.
- ELTER F.M., PICCARDO G.B., POLINO R., ZANETTI A., SPAGNOLO G., POGGI E. & BALBI P. (2005) - Structural and compositional features of the Mt. Musinè peridotites (Lanzo Massif, Western Alps, Italy). Ofioliti, **30** (2): 161-173.
- FIORASO G. & SPAGNOLO G. (2009) - I block stream del Massiccio Peridotitico di Lanzo (Alpi Nordoccidentali). Il Quaternario It. Journ. Quat. Sc., **22** (1): 3-22.
- KIENAST J.R. & POGNANTE U. (1988) - Chloritoid-Bearing Assemblages in Eclogitized Metagabbros of the Lanzo Peridotite Body (Western Italian Alps). Lithos, **21** (1): 1-11.
- FORNO M.G., GREGORIO L. & VATTERONI R. (2009) - La successione stratigrafica del settore destro del Conoide di Lanzo e il suo significato per l'utilizzo del territorio. Convegno Nazionale AIGeo: "Ambiente geomorfologico e attività dell'uomo: risorse, rischi, impatti". Torino 28-30 marzo 2007, Riv. Geografica It., **87** (1-2): 237-247.
- LAGABRIELLE Y., FUDRAL S. & KIENAST J.R. (1989) - La couverture océanique des ultrabasites de Lanzo (Alpes Occidentales): arguments lithostratigraphiques et pétrologiques. Geodynamica Acta, **3** (2): 43-55.
- MARTINETTO E. (1994) - Analisi paleocarpologica dei depositi continentali pliocenici della Stura di Lanzo. Boll. Mus. Reg. Sc. Nat. Torino, **12** (1): 251-286.
- MARTINETTO E., SCARDIA G. & VARRONE D. (2006) - Magnetostratigraphy of the Stura di Lanzo Fossil Forest Succession (Piedmont, Italy). Riv. It. Paleont. Strat., Milano, **1**: 109-125.
- MIE R. & NATALE P. (1978) - Fenomeni di alterazione paleoclimatica nel Massiccio Ultrabassico di Lanzo. Boll. Ass. Min. Sub., **15** (3-4): 1-47.
- NATALE P. (1972) - Nuove osservazioni sull'origine dei giacimenti di magnesite delle Alpi Occidentali. Boll. Ass. Min. Sub., **9** (1-2): 107-124.
- NICOLAS A. (1974) - Mise en place des péridotites de Lanzo (Alpes piémontaises). Relation avec tectonique et métamorphisme alpins: conséquences géodynamiques. Schweiz. Mineral. Petrogr. Mitt., **54**: 449-460.
- PELLETIER L. & MÜNTENER O. (2006) - High pressure metamorphism of the Lanzo peridotite and its oceanic cover, and some consequences for the Sesia-Lanzo zone (northwestern Italian Alps). Lithos, **90**: 111-130.
- PETRUCCI F. (1970) - Rilevamento geomorfologico dell'Anfiteatro morenico di Rivoli-Avigliana (Prov. Torino). Mem. Soc. It. Sc. Nat., **18** (3): 95-124.
- PICCARDO G.B., MÜNTENER O., ZANETTI A., BRUZZONE S., POGGI E., ROMAIRONE A. & SPAGNOLO G. (2004) - The Lanzo South peridotite: melt/peridotite interaction in the mantle lithosphere of the Jurassic Ligurian Tethys. Ofioliti, **29** (1): 51-76.
- PICCARDO G.B., ZANETTI A. & MÜNTENER O. (2007) - Melt/Peridotite interaction in the Lanzo South peridotite: field, textural and geochemical evidence. Lithos, **94**: 181-209.

## Modeling water flow and solute transport in alluvial sediments: scaling and hydrostratigraphy from the hydrological point of view

*Modellazione del flusso idrico e del trasporto di soluti in sedimenti alluvionali: i passaggi di scala e l'idrostratigrafia dal punto di vista idrologico*

GIUDICI M. (\*)

**ABSTRACT** - The sustainable management and the protection and remediation of water resources often require that geoscientists study ground water flow and solute transport in alluvial aquifers. Modeling approaches differ according to the scales relevant for the specific practical problems and also the geological structures can be described with different approaches. The scales of interest can be identified with the horizontal and vertical domain lengths and resolutions. The scale lengths span a wide range from the dimension of water molecules to the typical size of sedimentary basins. Therefore the study of ground water flow and solute transport in alluvial sediments requires many different exploration and interpretation methods, including geochemistry, petrography, sedimentology, stratigraphy, geophysical prospecting, in order to map geological structures and to describe geological and physical processes at different scales. In this paper it is proposed a revised classification of the relevant scales, discussing the corresponding physical processes, flow and transport models, geological objects, investigation methods. In fact a proper characterization of alluvial sediments might help to correctly setup flow and transport numerical models.

**KEY WORDS:** alluvium aquifers, ground water, hydrology, mathematical models, prospecting, water resources.

**RIASSUNTO** - La gestione sostenibile, la protezione e la bonifica delle risorse idriche richiedono spesso lo studio del flusso idrico sotterraneo e del trasporto di soluti negli acquiferi alluvionali. Gli approcci modellistici si distinguono in base alle scale a cui vanno sviluppati per risolvere i problemi concreti e anche le strutture geologiche possono essere descritte con diversi approcci. Le scale di interesse possono essere identificate con le lunghezze caratteristiche dei domini e con le risoluzioni, che in generale sono diverse lungo le direzioni orizzontali e verticali. Queste scale co-

prono un ampio intervallo di dimensioni, da quelle delle molecole d'acqua a quelle dei bacini sedimentari. Pertanto lo studio del flusso idrico sotterraneo e del trasporto di soluti nei sedimenti alluvionali richiede l'applicazione di molte e diverse tecniche di esplorazione e interpretazione, tra le quali la geochimica, la petrografia, la sedimentologia, la stratigrafia, la geofisica applicata. In questo modo è possibile identificare le strutture geologiche e descrivere i processi geologici e fisici a diverse scale. In questo lavoro viene presentata una classificazione delle scale rilevanti, per le quali vengono discussi i principali processi fisici, i tipi di modelli di flusso e trasporto, gli oggetti geologici e le principali tecniche di indagine. Una caratterizzazione appropriata dei sedimenti alluvionali può aiutare a impostare in modo corretto i modelli numerici di flusso e trasporto.

**PAROLE CHIAVE:** acqua sotterranea, falda in alluvioni, idrologia, modelli matematici, prospezione, risorse idriche.

### 1. – INTRODUCTION

The sustainable management and the protection and remediation of water resources require decision support tools whose basic engines are numerical models of water flow and solute transport. In order to face practical problems, the development and application of numerical models should take into account the goals of the models, i.e. the actual problems to be solved, the relevant processes and the corresponding space and time scales (GIUDICI, 2001).

(\*) Università degli Studi di Milano, Dipartimento di Scienze della Terra "A. Desio", Sezione di Geofisica, via Cicognara 7, 20129 Milano, Mauro.Giudici@unimi.it

It is questionable to apply the same conceptual and mathematical model to compute water balance for ground water management policies at the basin scale and to study flow and transport at the local scale, e.g. for assessing the environmental impact of a landfill or for the remediation of a contaminated site. Different models should be used and different parameterisations of the geometry and of the heterogeneity of the subsurface are required: as a consequence, modelers need different types and details of geological information for different purposes.

The aim of this paper is to discuss the relationship between the geological information (hydrostratigraphy and aquifer sedimentology) and the ground water flow and solute transport models at different scales in alluvial aquifers. These sedimentological systems are considered in this paper because they host a lot of fresh water bodies exploited for drinkable purposes both in Italy and worldwide.

In the second section a brief review of scaling problems in modeling is given: it includes an improved characterization of the scales relevant for practical problems.

The classification scheme proposed in this paper is a revision of those proposed by HEINZ & EIGNER (2003) and by FALIVENE *et alii* (2007), whose work is mainly based on hierarchical dynamic stratigraphy; here the classification starts from hydrological aspects. In the third section the link between the hydrostratigraphic and the modeling approach to scaling is discussed.

In the last section some conclusive remarks are given.

All these topics are examined with examples taken from case studies of the Pleistocene sediments in the Po plain.

## 2. – THE SCALES AT WHICH GROUND WATER FLOW AND SOLUTE TRANSPORT ARE MODELLED

The goal of this section is to show how scaling issues arise from hydrological study to answer to practical questions related to the management and protection of water resources.

For instance, one of the questions that water management agencies, regional governments and local administrations pose to professionals is: which is the sustainable amount of water that can be extracted from an aquifer? In general this query is debatable (SOPHOCLEOUS, 1997; BEAR, 1979; ALLEY & LEAKE, 2004; SOPHOCLEOUS, 2005), but any tentative answer needs the identification of the

terms of the water balance at the scale of an hydrographic basin. Therefore the study area could be larger than thousands of square kilometres and the typical horizontal length of the domain,  $H$ , could be greater than 10 km. At this scale hydrologists deal with the large scale aquifer structures down to depths of few hundred meters ( $V > 100$  m). Since the ratio  $H/V$  is very large and therefore vertical components of flow can be often neglected, the ground water flow is usually modeled with a 2D or quasi-3D approach. The relevant horizontal and vertical resolution lengths ( $b$  and  $v$ , respectively), i.e., the spacing of the grid used for numerical models, are  $b > 100$  m,  $v \approx 100$  m. At this scale the modelers consider the main aquifer groups, which are the result of the basin fill. In some cases it is necessary to map the horizontal and vertical continuity of the alternation of aquifers and aquitards produced by the climatic control on fluvio-glacial dynamics and deposition, in order to identify the capture zones of deep wells and to assess the degree of protection of deep water resources.

Of course these basin-scale models introduce strong simplifications of the geological complexity and some drastic approximations of processes occurring at finer scales. For instance the quantification of exchanges between ground and surface water bodies requires a finer resolution. This is also the case for models aimed at studying flow and transport in areas of limited extension, e.g. for the risk analysis of a contaminated site or the environmental impact assessment of a landfill. In these cases  $100 \text{ m} < H < 1 \text{ km}$ ,  $10 \text{ m} < V < 100 \text{ m}$ ,  $1 \text{ m} < b < 10 \text{ m}$ ,  $0.1 \text{ m} < v < 1 \text{ m}$  and the vertical components of flow and transport cannot be neglected. Therefore, at this local scale, 3D flow and transport models require the distribution of permeable and poorly conductive sediments, in order to capture the effects of preferential flow paths or impermeable barriers. The heterogeneity at the local scale is controlled by the facies bodies created by the dynamics of the environmental system.

The hydrodynamic and hydrodispersive parameters at the local scale depend upon the heterogeneity of the depositional elements and of the lithological strata for which the classical concept of representative elementary volume can be defined. Finer scales (the microscopic – pores and grains – scale and the molecular scale) are important for transport phenomena, because they are the proper scales at which hydrogeochemical processes take place. Notice that at these scales the horizontal and vertical resolution length can be identified with the size of the measurement support (CUSHMAN, 1986), i.e. the length over which physical quantities are averaged and as-



sumed representative.

The synthetic description given above can be summarized in table 1, where a tentative ranking of scales is given. This is a refinement of the schemes originally proposed by HEINZ & EIGNER (2003) and by FALIVENE *et alii* (2007); the classifications proposed by these Authors were mainly based on the concept of hierarchical dynamic stratigraphy, whereas here the classification is mainly based on hydrological aspects, but the link between the two approaches is apparent in the sequel of this paper. Simplified schemes of scale classification have also been proposed, e.g., by DAGAN (1989), LUNATI *et alii* (2001), GIUDICI *et alii* (2007). The distinction between regional and local flow is given also in several textbooks, e.g., BEAR (1979) and FREEZE & CHERRY (1979).

### 3. – THE LINK BETWEEN HYDROSTRATIGRAPHY AND MODELLING OF FLOW AND TRANSPORT AT DIFFERENT SCALES

The different scales, at which flow and transport in alluvial sediments are studied, are now examined in more detail, with reference to the relevant physical quantities and processes. Moreover, the analytical methods, the sedimentary structures and the hydrological processes that are relevant at the different scales are listed.

It is important to stress that the classification

proposed here, like any classification scheme, could appear too rigid in specific cases. In fact there is no natural sharp distinction between different scales; in real world applications, professionals deal with a mixture of scales. However a classification scheme can be useful to fix ideas and concepts, to properly plan the investigation work and to identify the conceptual model.

#### 3.1. – MOLECULAR SCALE

The finest scale at which a porous medium can be studied is the molecular scale ( $h \cong v \cong 10^{-10}$  m). At this scale the relevant interactions are molecular forces, acting among the molecules constituting the fluid (liquid or gas) and the solid phases.

#### 3.2. – MICROSCOPIC SCALE

At the characteristic scale considered in classical fluid dynamics, the relevant physical quantities (velocity, density, fluid pressure, solid stress, temperature, etc.) are averages of the physical quantities at the molecular scale over statistically significant volumes, that include a large number of molecules, but are nevertheless so small as to provide a point value. We refer to this scale as the microscopic scale (pore-grain scale,  $10^{-5}$  m  $\leq h \cong v \leq 10^{-3}$  m). The interactions between the pore fluid (water and solutes) and the porous matrix at this scale might be important to characterize some transport phe-

Tab. 1 - *Scale lengths at which ground water flow can be studied.*  
- Lunghesse di scala a cui può essere studiato il flusso idrico sotterraneo.

Scale	Scale length		Resolution		Objects	Hydrological models
	Horizontal	Vertical	Horizontal	Vertical		
Terascopic	$10^4$ m	$10^2$ m to $10^3$ m	$10^2$ m to $10^3$ m	10 m to $10^2$ m	Basins	2D or quasi-3D models
Gigascopic	$10^3$ m to $10^4$ m	10 m to $10^2$ m	10 m to $10^2$ m	1 m to 10 m	Aquifer complexes	Quasi-3D models
Megascopic	10 m to $10^3$ m	10 m to $10^2$ m	1 m to 10 m	0.1 m to 10 m	Facies bodies	3D models
Macroscopic	1 m to $10^2$ m	1 m to $10^2$ m	$10^{-2}$ m to 1 m	$10^{-2}$ m to 1 m	Depositional elements	3D models
Mesosopic			$10^{-3}$ m to $10^{-1}$ m	$10^{-3}$ m to $10^{-1}$ m	Strata, hydrofacies	Phenomenological (Darcy, Fick, Fourier) laws
Microscopic			$10^{-5}$ m to $10^{-3}$ m	$10^{-5}$ m to $10^{-3}$ m	Pores and grains	Classical continuum physics
Molecular			$10^{-10}$ m	$10^{-10}$ m	H <sub>2</sub> O molecule, clay particles, minerals	

nomena (e.g., adsorption/desorption).

The characteristics of the porous medium at the microscopic scale are studied mainly with geochemistry and petrographical analyses. In particular the sediments petrography provides information on the grain minerals and therefore on the provenance and the origin of the sediments.

### 3.3. – MESOSCOPIC SCALE

A further step yields to the mesoscopic scale, the scale at which the representative elementary volume is defined ( $10^{-3} \text{ m} \leq h \leq v \leq 10^{-1} \text{ m}$ ). At this scale the physical quantities (porosity, Darcy's velocity, solute concentration, volumetric water content, etc.) are representative of the physics of the porous medium, in the sense that they take into account the presence of several phases (gas, liquid, and solid phases) and possibly several constituents within each phase. This is the scale relevant for soil physics and for studies related to unsaturated flow and transport: this is the scale at which phenomenological laws (among which Darcy's, Fick's, Fourier's laws) are introduced and experimentally validated. The methods of investigation include laboratory experiments on samples and field tests involving small volumes.

The geological structures which are relevant at this scale are strata characterized by homogeneous features in terms of sedimentary properties (grain-size distribution, texture, fabric). These lithofacies are then differentiated according to sedimentary properties, which affect the hydrodynamic properties, namely the hydraulic conductivity. As a consequence, at this scale lithofacies can be grouped in hydrofacies, i.e. hydrogeological units which are relatively homogeneous, but possibly anisotropic (if the grains have an ellipsoidal shape or are deposited along preferential directions) with respect to the hydraulic conductivity. The sedimentological analysis of samples and of the outcropping sediments is one of the principal geological means of investigation at this scale.

### 3.4. – MACROSCOPIC SCALE

The visual inspection of outcrops clearly shows that lithofacies types, and therefore hydrofacies, are organized in sedimentary bodies at a macroscopic scale characterised by  $10^{-1} \text{ m} \leq V < 10 \text{ m}$  and  $1 \text{ m} \leq H < 100 \text{ m}$ . For sediments belonging to an alluvial depositional system, the individual architectural elements include channels, levees, floodplains, etc. The present day geometry of the depositional elements is the effect of their formation and evolution and determines the distribution

of the hydraulic conductivity, the correlation length and the connectivity of permeable units (see KNUDBY & CARRERA, 2005, and VASSENA *et alii*, 2009, for definitions and further references). The heterogeneity at mesoscale determines the effective hydrodynamic and hydrodispersive properties at the macroscopic scale. Moreover, the presence and the connectivity of permeable bodies introduces preferential flow paths, which are very important also for the fate of contaminant transport. This can be analysed with techniques of geostatistical simulation and three dimensional numerical modelling of flow and convective (possibly reactive) transport. In fact the link between meso- and macroscopic scales is sometimes performed with studies on aquifer analogues, i.e., outcropping sediments which are representative of the burden water reservoirs (see, e.g., JUSSEL *et alii*, 1994; RITZI *et alii*, 1995; WITTAKER & TEUTSCH, 1996; HUGGENBERGER & AIGNER, 1999; BERSEZIO *et alii*, 1999; ANDERSON *et alii*, 1999; ZAPPA *et alii*, 2006). The study at this scale is conducted not only with sedimentological analysis of samples and outcropping sediments, but also with geophysical exploration methods (e.g. ground penetrating radar) and with hydraulic field and laboratory tests (e.g., infiltration or permeametric tests).

The heterogeneous conductivity field, which is mapped at the macroscopic scale on the basis of the hydrofacies distribution, is upscaled to find equivalent parameters of the porous medium at the macro- or megascopic scale. Thorough reviews on upscaling are given by WEN & GÓMEZ-HERNÁNDEZ (1996), RENARD & MARSILY (1997), CUSHMAN *et alii* (2002), SÁNCHEZ-VILA *et alii* (2006).

The transition from the molecular scale to the microscopic and mesoscopic scales requires new physical quantities and physical laws (from molecular interactions to basic equations of fluid dynamics to Darcy's law). On the other hand, the upscaling from the meso- to the macroscale or to even larger scales (see section 3.5 below) is often performed in such a way that the same equations are applied, but the values of the physical parameters change. The geometrical regularity of the structures at the fine scales often yields anisotropy of the equivalent parameters at the coarser scales.

Also the meaning of some physical parameters is modified during the change of scale. For instance, the transport at the macroscopic scale is often modeled as purely convective and the irregularities of the flow field within pores are neglected or accounted for with small dispersivities. The transport at coarser scales is modeled with advective/dispersive equations which include the effects of the heterogeneity of the flow field related to the

heterogeneity of the conductivity field at the macroscopic scale by means of the tensor of hydrodynamic dispersion.

Examples of upscaling flow parameters from the meso- to the macroscopic or coarser scales in alluvial sediments of the Po plain are given by BERSEZIO *et alii* (1999), FELLETTI *et alii* (2006) and ZAPPA *et alii* (2006). The equivalent conductivity tensors have been computed from the distribution of the hydraulic conductivity at the mesoscopic scale. GIUDICI & VASSENA (2007) show that the method applied for this upscaling guarantees the symmetry of the equivalent conductivity tensor; furthermore VASSENA & GIUDICI (2007) show some effects of the discretisation on the computed equivalent conductivity tensor. In a recent work VASSENA *et alii* (2010) perform some numerical experiments of conservative transport on the blocks of sediments previously analyzed by ZAPPA *et alii* (2006) and they relate the hydrodispersive parameters to different types of connectivity indicators, namely: (1) the connectivity function (ALLARD & HERESIM GROUP, 1993; ALLARD, 1994; WESTERN *et alii*, 2001); (2) flow, transport and statistical connectivity indicators (KNUDBY & CARRERA, 2005); (3) original (intrinsic, normal and total) indicators of facies connectivity. VASSENA *et alii* (2010) show that some of these transport and statistical connectivity indicators are correlated with dispersivity and the joint analysis of the three indicators of facies connectivity permits to emphasize the fundamental geometrical features that control transport.

### 3.5. – MEGASCOPIC SCALE

Local field problems ( $1\text{ m} \leq h \leq 10\text{ m}$ ,  $0.1\text{ m} \leq v \leq 1\text{ m}$ ,  $10\text{ m} \leq H \leq 10^3\text{ m}$ ,  $10\text{ m} \leq V \leq 10^2\text{ m}$ ) can be studied at the megascopic scale. This is the scale at which pumping tests are usually performed and analysed; it is also the typical scale at which 3D models of flow and transport are developed and applied for the characterization and remediation of contaminated sites or for environmental impact assessment during the design of landfills, buildings, dams, bridges, mines, etc.

From the sedimentological point of view at this scale the assemblage of depositional elements builds facies bodies and produces compartments within alluvial sediments. In fact, facies bodies can be characterised as permeable aquifer or less permeable aquitard structures, which influence both local and regional ground water flow and transport. Field tests are among the main investigation techniques at this scale, together with well log data. They are integrated with geophysical techniques,

as DC electrical methods, electromagnetic methods (mainly in the frequency domain), refraction seismics or studies with surface waves.

Again upscaling studies are often conducted at this scale and are devoted, e.g., to the comprehension of the effect of connected permeable aquifer bodies on the results of well pumping tests and on the contaminant transport (FOGG, 1986; SCHAD & TEUTSCH, 1994; MEIER *et alii*, 1999; FERNÁNDEZ GARCIA *et alii*, 2002; CORTIS & KNUDBY, 2006; KNUDBY & CARRERA, 2005; MARTINEZ-LANDA & CARRERA, 2005; SÁNCHEZ-VILA *et alii*, 2006; FLECKENSTEIN & FOGG, 2008; TRINCHERO *et alii*, 2008; KERROU *et alii*, 2008).

Examples of analysis at this scale in restricted areas of the Po plain are given by BERSEZIO *et alii* (1999), who combine facies analysis and numerical modelling for a pro-glacial delta environment, and by BERSEZIO *et alii* (2007), who combine sedimentological and geophysical survey for a detailed 3D reconstruction of fluvial architectural elements.

### 3.6. – GIGA- AND TERASCOPIC SCALES

Finally, regional aquifer systems are studied at the giga- and terascopic scale ( $10\text{ m} \leq h \leq 10^3\text{ m}$ ,  $1\text{ m} \leq v \leq 10^2\text{ m}$ ,  $10^3\text{ m} \leq H \leq 10^4\text{ m}$ ,  $10\text{ m} \leq V \leq 10^2\text{ m}$ ), to develop engines of decision support tools for resource management and regional planning.

We refer to gigascale for the genetic sequences created by aquifer dynamics. In other words, we refer to the aquifer complexes which consist of aquifer/aquitard couples with a good lateral continuity and created by the alternation of different climatic conditions.

For these sequences the flow and transport processes are usually studied with quasi-3D models, i.e. assuming that the water flow is essentially horizontal in the aquifers and vertical in the aquitards.

Basin dynamics is instead controlled by long-term glacial and climatic cycles, as well as by tectonics. The assemblage of aquifer complexes yields aquifer groups, whose structure is characterised by basin-wide correlation of well data, interpolation of the results of well tests, geophysical prospecting (DC, TDEM and FDEM, reflection seismics). At this scale the thickness of the volume under study is much smaller than its horizontal extension, so that water flow can be approximated as two-dimensional.

## 4. – SUMMARY AND CONCLUSIONS

The answers to practical problems related to the management, protection and remediation of ground water resources require modelling water flow and



transport at different scales. The numerical models should be simple enough to permit the numerical solution of the balance equations, the calibration and validation of the model. On the other hand they should be complex enough to describe the effects that heterogeneities at the fine scale can have on the processes occurring at the model scale.

From the point of view of a modeller, the physical parameters at the model coarse scale depend upon the heterogeneity at the finer scales, the link between the parameters at the fine and coarse scales is conceptually given by upscaling and the best values of the model parameters are often obtained with inverse methods (YEH, 1986; CARRERA, 1988; GINN & CUSHMAN, 1990; SUN, 1994; GIUDICI, 2001; CARRERA *et alii*, 2005).

Professionals can provide reliable forecasts of the behaviour of such heterogeneous natural systems as alluvial aquifers, if they clearly define the scale at which flow and transport are modelled, the types of sedimentary structures, the required data. The classification scheme proposed with this paper provides a revised description of the scales at which water flow and solute transport in alluvial aquifers are studied. Such scheme relates hydrological aspects to the structures studied with hierarchical dynamic stratigraphy and therefore is a contribution to the comprehension of the scaling issues and to the joint of the points of view of different experts: the geologists and the hydrologists, the sedimentologists and the modellers, the hydrogeologists and the geophysicists.

## Acknowledgements

*This work was financially supported by the MIUR and the University of Milano through the research projects of national interest "Integrating geophysical and geological data for modeling flow in some aquifer systems of alpine and apenninic origin between Milano and Bologna" (PRIN 2005) and "Integrated geophysical, geological, petrographical and modelling study of alluvial aquifer complexes characteristic of the Po plain subsurface: relationships between scale of hydrostratigraphic reconstruction and flow models" (PRIN 2007). The author is the Principal Investigator of both projects.*

*Sincere thanks are offered to dott. Chiara Vassena and two reviewers (prof. Alberto Guadagnini and an anonymous one) for their useful comments and suggestions.*

## REFERENCES

- ALLARD D. (1994) - *Simulating a geological lithofacies with respect to connectivity information using the truncated Gaussian model*. In: M. ARMSTRONG & P.A. DOWD (Eds.): «*Geostatistical Simulations: Proceedings of the Geostatistical Simulation Workshop*». 197-211, Kluwer Acad., Norwell (MA).
- ALLARD D. & HERESIM GROUP (1993) - *On the connectivity of two random set models: The truncated Gaussian and the Boolean*. In: A. SOARES (Ed): «*Geostatistics Troia '92*». 467-478, Kluwer Acad., Norwell (MA).
- ALLEY W.M. & LEAKE S.A. (2004) - *The journey from safe yield to sustainability*. Ground Water, **42**: 12-16.
- ANDERSON M.P., AIKEN J.S., WEBB E.K. & MICKELSON D.M. (1999) - *Sedimentology and hydrogeology of two braided stream deposits*. Sedimentary Geology, **129**: 187-199.
- BEAR J. (1979) - *Hydraulics of groundwater*, McGraw-Hill, New York.
- BERSEZIO R., BINI A. & GIUDICI M. (1999) - *Effects of sedimentary heterogeneity on groundwater flow in a quaternary proglacial delta environment: joining facies analysis and numerical modeling*. Sedimentary Geology, **129**: 327-344.
- BERSEZIO R., GIUDICI M. & MELE M. (2007) - *Combining sedimentological and geophysical data for high resolution 3-D mapping of fluvial architectural elements in the Quaternary Po plain (Italy)*. Sedimentary Geology, **202**: 230-248, doi:10.1016/j.sed-geo.2007.05.002.
- CARRERA J., ALCOLEA A., MEDINA A., HIDALGO J. & SLOOTEN L.J. (2005) - *Inverse problems in hydrogeology*. Hydrogeol. J., **13**: 206-222.
- CARRERA J. (1988) - *State of art of the inverse problem applied to the flow and solute transport equations*. In: E. CUSTODIO *et alii* (Eds.): «*Groundwater flow and quality modelling*». 549-583, Reidel, Dordrecht.
- CORTIS A. & KNUDBY C. (2006) - *A continuous time random walk approach to transient flow in heterogeneous porous media*. Water Resour. Res., doi:10.1029/2006WR005227.
- CUSHMAN J.H. (1986) - *On measurement, scale, and scaling*. Water Resour. Res., **22**: 129-134.
- CUSHMAN J.H., BENNETHUM L.S. & HU B.X. (2002) - *A primer on upscaling tools for porous media*. Adv. in Water Resour., **25**: 1043-1067.
- DAGAN G. (1989) - *Flow and Transport in Porous Formations*, Springer-Verlag, New York.
- FALIVENE O., CABRERA L., MUÑOZ J.A., ARBUÉS P., FERNÁNDEZ O. & SÁEZ A. (2007) - *Statistical grid-based facies reconstruction and modelling for sedimentary bodies. Alluvial-palustrine and turbiditic examples*. Geologica Acta, **5**: 199-230.
- FELLETTI F., BERSEZIO R. & GIUDICI M. (2006) - *Geostatistical simulation and numerical upscaling, to model groundwater flow in a sandy-gravel, braided river, aquifer analogue*. J. Sediment. Res., **76**: 1215-1229, doi:10.2110/jsr.2006.091.
- FERNÁNDEZ - GARCIA D., SANCHEZ - VILA X. & ILLANGASEKARE T.H. (2002) - *Convergent-flow tracer tests in heterogeneous media: combined experimental-numerical analysis for determination of equivalent transport parameters*. J. Contam. Hydrol., **57**: 129-145.
- FLECKENSTEIN J.H. & FOGG G.E. (2008) - *Efficient upscaling of hydraulic conductivity in heterogeneous alluvial aquifers*. Hydrogeol. J., doi:10.1007/s10040-008-0312-3.
- FOGG G.E. (1986) - *Groundwater flow and sand body interconnectedness in a thick, multiple-aquifer system*. Water Resour. Res., **22**: 679-694.
- FREEZE R.A. & CHERRY J.A. (1979) - *Groundwater*, Prentice-Hall, Englewood Cliffs (NJ).
- GINN T.R. & CUSHMAN J.H. (1990) - *Inverse methods for subsurface flow: a critical review of stochastic techniques*. Stochastic Hydrol. Hydraul., **4**: 1-26.
- GIUDICI M. & VASSENA C. (2007) - *About the Symmetry of the Upscaled Equivalent Transmissivity Tensor*. Mathematical Geology, doi:10.1007/s11004-007-9101-0.
- GIUDICI M. (2001) - *Development, calibration and validation of physical models*. K.C. CLARKE, B.O. PARKS & M.C. KRANE (Eds.): «*Geographic Information Systems and Environmental Modelling*». 100-121, Prentice-Hall, Upper Saddle River (NJ).
- GIUDICI M., PONZINI G., ROMANO E. & VASSENA C. (2007) - *Some lessons from modelling ground water flow in the metropoli-*

- tan area of Milano (Italy) at different scales. Mem. Descr. della Carta Geol. d'It., **76**: 207-218.
- HEINZ J. & AIGNER T. (2003) - Hierarchical dynamic stratigraphy in various Quaternary gravel deposits, Rhine glacier area (SW Germany): implications for hydrostratigraphy. Int. J. Earth Sci., **92**: 923-938, doi:10.1007/s00531-003-0359-2.
- HUGGENBERGER P. & AIGNER T. (1999) - Introduction to the special issue on *Aquifer Sedimentology: problems, perspectives and modern approaches*. Sedimentary Geology, **129**: 179-186.
- JUSSEL P., STAUFFER S. & DRACOS T. (1994) - Transport modeling in heterogeneous aquifers, 1. Statistical description and numerical generation of gravel deposits. Water Resour. Res., **30**: 1803-1817.
- KERROU J., RENARD P., HENDRICKS FRANSSSEN H.J. & LUNATI I. (2008) - Issues in characterizing heterogeneity and connectivity in non-multiGaussian media. Adv. Water Resour., doi:10.1016/j.advwatres.2007.07.002.
- KNUDBY C. & CARRERA J. (2005) - On the relationship between indicators of geostatistical, flow and transport connectivity. Adv. Water Resour., doi:10.1016/j.advwatres.2004.09.001.
- LUNATI I., BERNARD D., GIUDICI M., PARRAVICINI G. & PONZINI G. (2001) - A numerical comparison between two up-scaling techniques: non-local inverse based scaling and simplified renormalization. Adv. Water Resour., **24**: 913-929.
- MARTINEZ-LANDA L. & CARRERA J. (2005) - An analysis of hydraulic conductivity scale effects in granite (Full-scale Engineered Barrier Experiment (FEBEX), Grimsel, Switzerland). Water Resour. Res., doi:10.1029/2004WR003458.
- MEIER P.M., CARRERA J. & SÁNCHEZ-VILA X. (1999) - A numerical study on the relationship between transmissivity and specific capacity in heterogeneous aquifers. Ground Water, **37**: 611-617.
- RENARD PH. & DE MARSILY G. (1997) - Calculating effective permeability: a review. Adv. Water Resour., **20**: 253-278.
- RITZI R.W., DOMINIC D.F., BROWN N.R., KAUSCH K.W., MC ALLENNEY P.J. & BASIAL M.J. (1995) - Hydrofacies distribution and correlation in the Miami Valley aquifer system. Water Resour. Res., **31**: 3271-3281.
- SÁNCHEZ-VILA X., GUADAGNINI A. & CARRERA J. (2006) - Representative hydraulic conductivities in saturated groundwater flow. Rev. Geoph., doi:10.1029/2005RG000169.
- SCHAD H. & TEUTSCH G. (1994) - Effects of the investigation scale on pumping tests results in heterogeneous porous aquifers. J. Hydrol., **159**: 61-77.
- SOPHOCLEOUS M.A. (1997) - Managing water resources systems: Why safe yield is not sustainable. Ground Water, **35**: 561.
- SOPHOCLEOUS M.A. (2005) - Groundwater recharge and sustainability in the high plains aquifer in Kansas, USA. Hydrogeol. J., **13**: 351-365.
- SUN N.Z. (1994) - Inverse problems in groundwater modelling, Kluwer, Norwell.
- TRINCHERO P., SÁNCHEZ-VILA X. & FERNÁNDEZ-GARCÍA D. (2008) - Point-to-point connectivity, an abstract concept or a key issue for risk assessment studies? Adv. Water Resour., doi:10.1016/j.advwatres.2008.09.001.
- VASSENA C. & GIUDICI M. (2007) - Application of integrated finite differences to compute symmetrical upscaled equivalent conductivity tensor. In: A.A. MAMMOLI & C.A. BREBBIA (Eds.): «Computational Methods in Multiphase Flow IV». Wessex Institute of Technology Transactions on Engineering Sciences, **56**:153-161, WITPress.
- VASSENA C., CATTANEO L. & GIUDICI M. (2010) - Assessment of the role of facies heterogeneity at the fine scale by numerical transport experiments and connectivity indicators. Hydrogeol. J., **18**: 651-668, doi:10.1007/s10040-009-0523-2.
- WEN X.-H. & GÓMEZ-HERNÁNDEZ J.J. (1996) - Upscaling hydraulic conductivity in heterogeneous media: an overview. Hydrol. J., **183**: ix-xxxii.
- WESTERN A., BLOSCHL G. & GRAYSON R.B. (2001) - Toward capturing hydrologically significant connectivity in spatial patterns. Water Resour. Res., **37**: 83-97.
- WITTAKER J. & TEUTSCH G. (1996) - The simulation of subsurface characterization methods applied to a natural aquifer analogue. In: K. KOVAR & P. VAN DER HEIJDE (Eds.): «Calibration and Reliability in groundwater modeling». International Association of Hydrological Sciences Publication, **237**: 425-434.
- YEH W.-G.W. (1986) - Review of parameter identification procedures in groundwater hydrology: the inverse problem. Water Resour. Res., **22**: 95-108.
- ZAPPA G., BERSEZIO R., FELLETTI F. & GIUDICI M. (2006) - Modeling heterogeneity of gravel-sand, braided stream, alluvial aquifers at the facies scale. J. Hydrol., doi:10.1016/j.jhydrol.2005.10.016.

## Modeling dissolution experiments and heavy metals competition in porous media

*Modellazione ed interpretazione di processi di dissoluzione e di assorbimento competitivo di metalli pesanti in mezzi porosi*

GUADAGNINI A. (\*), RIVA M. (\*) GUADAGNINI L. (\*)

**ABSTRACT** - We present a synthetic review of some key modeling aspects associated with (a) precipitation / dissolution reactions in carbonate systems and (b) competitive behavior of heavy metals compounds in a well characterized porous system. We start by reviewing some recent advances in theoretical and numerical modeling of complex reactive transport problems, resulting in a methodology conducive to a simple exact expression for the distribution of reaction rates in the presence of homogeneous or heterogeneous reactions under chemical equilibrium (DE SIMONI *et alii*, 2005, 2007). We then focus on a set of laboratory-scale experiments and show how this methodology can be used to describe the global (integral) reaction rate occurring in a relatively complex, geochemically-active system under the assumption of chemical equilibrium. We model three calcium carbonate dissolution experiments reported in SINGURINDY *et alii* (2004, 2005), in which saltwater and freshwater were mixed in different proportions. The experimental results are also used to examine the performance of a Darcy-scale flow and reactive transport numerical model, based on the advection-dispersion-reaction equation, to reproduce measured global reaction rates. We then present a comparative analysis of the ability of four alternative models to interpret the set of batch experiments presented by SRIVASTAVA *et alii* (2006), involving competitive binary-component adsorption studies of cadmium (Cd(II)) and nickel (Ni(II)) ions onto bagasse fly ash (BFA). We use formal model selection criteria to associate each of these four models with a weight, or posterior probability, representing the relative degrees of likelihood of each model. When the Kashyap's information criterion (KASHYAP, 1982) is adopted, some of the weights are large enough so that it may not be justified adopting one of the four models at the exclusion of all others.

**KEY WORDS:** adsorption, geochemistry, ground-water, hydrogeology, precipitation.

**RIASSUNTO** - Si presentano alcuni recenti sviluppi relativi alla modellazione di processi di trasporto di soluti reattivi in mezzi porosi. Si pone l'accento sull'analisi di alcuni aspetti caratterizzanti (a) processi di precipitazione / dissoluzione in sistemi carbonatici e (b) adsorbimento competitivo di metalli pesanti su mezzi porosi ben caratterizzati. A valle della presentazione della complessa formulazione generale di un problema di trasporto reattivo, si espone la metodologia proposta da DE SIMONI *et alii* (2005, 2007), che consente il calcolo diretto dei tassi di reazione associati a scenari di trasporto multi-specie mediante il disaccoppiamento del sistema di equazioni che descrive l'evoluzione dei soluti nel dominio. Questa formulazione viene applicata per l'interpretazione di tre esperimenti di dissoluzione presentati da SINGURINDY *et alii* (2004, 2005) e condotti in un sistema carbonatico omogeneo alla scala di laboratorio, in cui si induce il mescolamento di acqua dolce e salata. Si illustrano possibilità e prospettive di applicazione della metodologia investigata. Si presenta, quindi, una analisi delle potenzialità di diversi modelli matematici nell'interpretazione degli esperimenti presentati da SRIVASTAVA *et alii* (2006) e relativi a studi di adsorbimento competitivo di ioni metallici (cadmio, Cd(II), e nickel, Ni(II)) su matrice porosa completamente satura. I singoli modelli sono valutati sulla base di criteri formali di discriminazione. A ciascun modello è associato un peso, o probabilità a posteriori, che ne rappresenta la capacità predittiva.

**PAROLE CHIAVE:** acque sotterranee, adsorbimento, geochimica, idrogeologia, precipitazione.

(\*) Dipartimento di Ingegneria Idraulica, Ambientale, Infrastrutture Viarie, Rilevamento (DIIAR), Politecnico di Milano, Piazza L. Da Vinci, 32, 20133, Milano, Italy.



## 1. - INTRODUCTION

Understanding and modeling reactive transport processes is crucial for the prediction of the complex chemical/physical evolution of Earth systems. Amongst the various reactive transport scenarios which can take place in natural systems, here we focus on the analysis of some aspects associated with (a) precipitation / dissolution reactions in carbonate systems and (b) competitive behavior of heavy metals compounds in soils. Both processes are relevant for the assessment of the quality of the subsurface environment and are characterized by unique conceptual, interpretation and modeling challenges.

Because of their complexity and ubiquity, mixing-driven processes governing the geochemistry of carbonate systems, within which precipitation / dissolution reactions take place, have been extensively studied [*e.g.*, SANFORD & KONIKOW, 1989; SINGURINDY *et alii*, 2004; REZAEI *et alii*, 2005, STEEFEL *et alii*, 2005 and references therein]. The relevance of mixing in these processes is well documented. Mixing occurring at various scales governs chemical speciation in aquatic systems and the distribution of pollutant concentrations in transition regions where surface and subsurface waters interact. It is therefore not surprising that characterization of precipitation / dissolution scenarios relies heavily on the concept of mixing and that major efforts have been devoted to the inclusion of these effects into a series of mathematical formulations. Precipitation / dissolution reactions occurring at interfaces between waters with different chemical compositions lead to modifications in physical-geo-chemical properties of aquifers, such as porosity, hydraulic conductivity and distribution coefficient [SINGURINDY & BERKOWITZ, 2004; REZAEI *et alii*, 2005; KATZ *et alii*, 2010]. This has relevant implications in management practices of natural aquifers and reliable approaches are needed to describe changes in macroscale parameters of the groundwater system.

Another problem which is rapidly becoming of pressing concern is the reactive transport scenario associated with the presence of heavy metals in groundwater systems. Heavy metals are a key constituent in a wide variety of industrial and domestic products, processes and applications (including fertilizers, limiting materials, sewage sludge, and compost). Road networks, vehicular emission, housing and emission from municipal waste incinerators are also main sources of metals in urban areas. The subsequent release of these metals to the environment has already caused widespread contamination of soil and water resources. Therefore, heavy metal reactions, in a competi-

tive system, are important to determine heavy metal availability to plants and their mobility throughout the soil. These problems, found worldwide, are especially dramatic in several EU countries. Italy is not immune to this. Critical situations are reported in the northern (*e.g.*, in the sediments of the Lagoon of Venice; see BERNARDELLO *et alii* (2006)), central (*e.g.*, in urban soils of coastal Tuscany; see BRETZEL & CALDERISI (2006)), and southern (*e.g.*, sites West of the city of Naples; see ADAMO *et alii* (2002)) regions. Heavy metals, such as chromium, nickel, lead, molybdenum, and vanadium are commonly used in industrial processes that include the production of electronic components, paint, leather tanning, timber processing, and plating of metals, as well as in preparation of many cosmetics and pharmaceuticals. Interconnections between surface waters and groundwater allow heavy metals to migrate into the subsoil and to undergo complex (and mostly unknown) bio-geo-chemical processes in the heterogeneous water-soil system.

The hydro-geo-chemical processes described above involve multiple reactive species and are generally analyzed using advanced numerical codes. Modeling is a challenging problem, necessary for understanding the fate of pollutants and geo-chemical processes occurring in diverse highly heterogeneous environments such as aquifers, rivers, estuaries and oceans. Unfortunately, development of realistic models is complex, both conceptually and mathematically. The governing equations describing reactive transport in porous media are based on (1) conservation of energy, (2) conservation of solid, fluid and solute mass, (3) conservation of momentum (Navier-Stokes equation at the pore scale and Darcy's Law at some meso- or macro-scale), and (4) constitutive laws for key parameters (including, amongst others, fluid density, viscosity, permeability). The nature of participating species and reactions leads to a broad range of possible different behaviors of the system. These ingredients render the system of governing equations complex and highly non linear. Basically two types of interpreting approaches can be considered: pore scale and continuum (macroscale) models. If it were possible to model flow and reactive transport at the pore scale over any observation scale of interest (*e.g.*, basin scale) there would be no need to consider other approaches. Unfortunately this is not the case. In groundwater sciences it is practically impossible to solve the Navier-Stokes equations at the pore scale for the problems of common interest (at the laboratory and field scale). Flow and (conservative or reactive) transport phenomena are traditionally described by macroscale

models based on a continuum interpretation of the underlying microscale processes. Since (many) of the physical and chemical processes take place at the pore (and sub-) scales the development of approaches to translate information from this scale to larger scales is essential.

The complete analysis of a reactive transport problem typically involves specification of a large number of aqueous and non-aqueous species. An excellent recent review on the topic is offered by STEEFEL *et alii* (2005). Here, we focus only on some recent key modeling aspects. A common method to estimate spatial distributions of chemical species concentrations and associated reaction rates is to resort to numerical modeling. A series of mathematical formulations are available in the literature (*e.g.*, RUBIN, 1990; YEH & TRIPATHI, 1991; FRIEDLY & RUBIN, 1992; RUBIN, 1992; LICHTNER, 1996; STEEFEL & MAC QUARRIE, 1996; CLEMENT *et alii*, 1998; SAALTINK *et alii*, 1998, 2001; TEBES-STEVENSON *et alii*, 1998; ROBINSON *et alii*, 2000; MOLINS *et alii*, 2004), which are included in a variety of codes. All these methodologies are based on the idea that the reactive transport problem can be reformulated in terms of a subset of conservative transport scenarios. The methodology typically consists of the following steps: (a) defining conservative components, which are usually linear combinations of reactive species concentrations, and decouple the solution of the equations associated with the chemical reactions from the mass balance of chemical compounds; (b) solving the transport equations for the conservative components by means of standard Eulerian or Lagrangian methods; (c) performing speciation calculations to obtain the concentration of aqueous species from the space-time distribution of components; and (d) substituting the latter into the transport equations to evaluate numerically reaction rates. This approach is appealing for its simplicity and can be applied when the concentrations of the reacting species stand in algebraic relationship to each other, the coefficients describing physical mixing in the system coincide for all compounds, and all aqueous species are advected by the same (meso-scale) velocity. The first requirement is met by systems either in local chemical equilibrium or instantaneous, complete, irreversible reactions (*e.g.*, LIEDL *et alii*, 2005) and can also be used for specific cases of kinetic reactions (CIRPKA & VALOCCHI, 2007; MOLINS *et alii*, 2004).

A methodology to compute directly homogeneous and heterogeneous reaction rates under instantaneous equilibrium has been presented recently by DE SIMONI *et alii* (2005, 2007). It allows to calculate the rate of the reactions as a

function of quantities such as the concentration of components, the equilibrium constants, and the dispersion coefficients, without the need to calculate the concentration of the dissolved species. The results of DE SIMONI *et alii* (2007) suggest that the problem of assessing reaction rates in a reactive system involving a relatively high number of aqueous and constant activity species can be decoupled into a transport problem posed in terms of mixing ratios plus a speciation term. Their general expression for the reaction rates illustrates that mixing processes control equilibrium reaction rates. The methodology has then been extended (SANCHEZ-VILA *et alii*, 2010) to include a scenario where the geochemical system can be described by an arbitrary number of equilibrium (fast) reactions and one kinetic (slow) reaction, in the absence of non-constant activity immobile species. As compared to formulations proposed previously in the literature (*e.g.*, MOLINS *et alii*, 2004; RUBIN, 1990, 1992; SAALTINK *et alii*, 1998, 2001), this method is simpler and more concise and conducive to an analytical expression for the reaction rates that includes the model of PHILLIPS (1991) as a particular case. In essence, it allows the direct evaluation of the distribution of reaction rates of a complex multispecies reactive transport problem by solving two independent problems: (a) the transport of one or more conservative species, and (b) chemical speciation. The method can only be applied when the mineral is present for all mixing ratios, which can not always be the case. While in general the calculation of the reaction rates is performed numerically, in some cases, typically in the context of uniform systems in the presence of uniform seepage flow and specific types of solute injection, it is possible to obtain closed-form analytical solutions (DE SIMONI *et alii*, 2005, 2007). The approach has been used by GUADAGNINI *et alii* (2008) in conjunction with laboratory-scale  $\text{CaCO}_3$  dissolution experiments reported in SINGURINDY *et alii* (2004, 2005) to describe the spatial distribution of reactions rates in a homogeneous flow cell.

A number of recent observations and findings show that multicomponent reactive transport behavior and its link to the geochemical properties of the aquifer and to the phenomena involved at the pore scales are far from being completely understood. For example, DE SIMONI *et alii* (2005) analyzed the spatial distribution of the total precipitation rate for a typical precipitation/dissolution problem. The authors observed that the location of the center of the plume does not coincide with the position of the maximum precipitation rate. KATZ *et alii* (2010) performed conservative

and reactive transport experiments in a quasi-two-dimensional laboratory flow cell, filled with homogeneous and heterogeneous porous media. Conservative experiments were performed by injecting solutions containing sodium chloride and calcium chloride into the domain. In reactive transport experiments, inlet solutions of calcium chloride and sodium carbonate were injected in parallel. The reactive transport experiments featured the formation of a calcium carbonate mineral phase within the mixing zone between the two solutions, which controlled the spatial evolution of calcium carbonate in the domain. Numerical simulations performed on high resolution grids for both the homogeneous and heterogeneous porous systems underestimated clogging of the system. Although qualitative agreement between model results and experimental observations was obtained, accurate model predictions of the spatial evolution of calcium concentrations at sample points within the flow cell could not be achieved. Phenomena such as chelation and simultaneous presence of several metals add to the list.

Notwithstanding the above concerns and research efforts, only over the last years has the impact of competitive behavior of heavy metals in solute transport been recognized (*e.g.*, MAYES *et alii*, 2000; GOMES *et alii*, 2001; SAHA *et alii*, 2002; FONTES & GOMES, 2003; SRIVASTAVA *et alii*, 2005). Most of the studies that analyze the problem of metal competition are performed under batch conditions. SAHA *et alii* (2002) found that the competition between Cd and Zn increases with the initial concentration of the metals on Montmorillonite (Mt), Hydroxylaluminium-Mt (HyA-Mt) and Hydroxylaluminosilicate-Mt (HAS-Mt). When the initial concentration is less than  $5 \times 10^{-5}$  M, the addition of a second metal has little effect on the adsorption of a given metal, which suggests that each metal preferentially binds to different sites (*i.e.*, their preferred binding sites do not overlap each other). Similarly, FONTES & GOMES (2003) found that, in soils of tropical and sub-tropical area (Oxisols, Ultisols, Alfisols) heavy metals (Ni, Zn, Cd, Cr, Cu, Pb) are adsorbed proportional to their relative molar concentration at the lowest concentration applied in their experiments. As the concentration increases, competition starts to occur and the proportion of the stronger competitors (Cr, Cu, Pb) increases, as compared with the weakest ones (Ni, Zn, Cd). SRIVASTAVA *et alii* (2005) considered the competitive adsorption of heavy metals on kaolinite for varying pH conditions. The adsorption behavior of Cd, Cu, Pb and Zn in single- and multi-element system differs. The selectivity sequence is  $\text{Cu} > \text{Pb} > \text{Zn} > \text{Cd}$  in a single element system

and  $\text{Pb} > \text{Cu} > \text{Zn} > \text{Cd}$  in a multi-element system. These results can be relevant to the analysis of the potential of strongly contaminated soils to adsorb and retain heavy metals during groundwater remediation activities. In addition to batch experiments, only a limited set of flow-through experiments has been performed (*e.g.*, VOEGELING *et alii*, 2001; CHANG *et alii*, 2001; TSANG & LO, 2006; ANTONIADIS *et alii*, 2007). The Freundlich model has been found to describe monometal sorption satisfactorily. Various alternative models have been proposed to predict metal sorption in competitive systems. These include (a) a modification of the Freundlich model introduced by SHEINDORF *et alii* (1981), referred to as the SRS model, (b) a modified competitive Langmuir isotherm (BELLOT & CONDORET, 1993), and (c) an extended Langmuir model (YANG, 1987). Examining the applicability of existing multi-component adsorption isotherm equations to the competitive adsorption equilibria of the metals in a multi-component system is still an open problem.

Following the brief literature review presented, our aim is to present some aspects associated with the interpretation of reactive multi-component transport in porous media. In Section 2 we start by illustrating the main theoretical aspects underlying the general formulation of a reactive transport problem. For ease of discussion, we focus on equilibrium reactions. Section 3 describes some of the key results obtained by GUADAGNINI *et alii* (2009), who presents a modeling study of the dissolution laboratory-scale experiments performed by SINGURINDY *et alii* (2004, 2005). Finally, Section 4 presents a comparative analysis of the ability of some alternative models to interpret the competitive bi-metal sorption batch experiments presented by SRIVASTAVA *et alii* (2006).

## 2. - THEORETICAL BASIS

Modeling reactive transport involves describing mass balances of species and reactions among species. The basic equations, an ADRE (Advective-Dispersive-REactive) formulation, and the strategy adopted to solve them, are described below.

### 2.1. - SPECIES TRANSPORT EQUATIONS

A species mass balance can be written as

$$\frac{\partial(\mathbf{m})}{\partial t} = \mathbf{ML}(\mathbf{c}) + \mathbf{f} \quad (1)$$



Here, vector  $\mathbf{m}$  contains the moles of species per unit volume of porous medium and vector  $\mathbf{c}$  contains species concentrations in mol/mass of liquid ( $m_i = \phi \rho c_i$  for the  $i$ -th mobile species in a system of porosity  $\phi$  and liquid density  $\rho$ ). Matrix  $\mathbf{M}$  is diagonal and its diagonal terms are unity when a species is mobile and zero otherwise;  $\mathbf{f}$  is a source/sink term, which we use to represent chemical reactions. Here we define the linear operator  $L(c_i)$  in (1) as  $L(c_i) = -\nabla \cdot (\phi \rho \mathbf{v} c_i) + \nabla \cdot (\phi \rho \mathbf{D} \nabla c_i)$ , where  $\mathbf{D}$  is the diffusion/dispersion tensor and  $\mathbf{v}$  is the fluid velocity,  $\mathbf{v} = \mathbf{q}/\phi$ ,  $\mathbf{q}$  being Darcy's flux vector. In the application presented in Section 3, we assume that all mobile species are characterized by the same coefficients depicting physical mixing, along the lines of, e.g., SAALTINK *et alii* (1998) and MOLINS *et alii* (2004). This condition requires that hydrodynamic dispersion dominates over pore-scale diffusion in the relevant mixing process.

## 2.2. - EQUILIBRIUM REACTIONS

Reactions can be considered at equilibrium when the time scales involved in the various chemical reactions occurring in the system are small with respect to typical diffusive and advective time scales. In our application we only consider aqueous reactions and precipitation-dissolution of minerals. We define  $\mathbf{f} = \mathbf{S}_e^T \mathbf{r}$ , where  $\mathbf{r}$  is the vector of reaction rates (expressed per unit volume of medium) and  $\mathbf{S}_e$  is the stoichiometric matrix of the chemical system (*i.e.*,  $\mathbf{S}_e$  is an  $N_r \times N_s$  matrix,  $N_r$  and  $N_s$  being the number of reactions and of chemical species, respectively). Equilibrium is described by the mass action law, which can be written as  $\mathbf{S}_e \log \mathbf{a} = \log \mathbf{K}$ , where  $\mathbf{K}$  is the vector of chemical equilibrium constants and  $\mathbf{a}$  is the vector of species activities. In the following we adopt the notation of SAALTINK *et alii* (1998), and DE SIMONI *et alii* (2005, 2007).

The mass action law can be written such that the activities of  $N_r$  secondary species can be calculated from the activities of  $N_s - N_r$  primary species (STEEFEL & MACQUARRIE, 1996; SAALTINK *et alii*, 1998; MOLINS *et alii*, 2004; DE SIMONI *et alii*, 2005). Following DE SIMONI *et alii* (2005), we choose as primary species the  $N_c$  constant activity species plus  $N_s - N_r - N_c$  aqueous species. All secondary species are aqueous, as mineral species are considered to have constant activities. Vector  $\mathbf{a}$  is split as  $\mathbf{a} = (\mathbf{a}_c \ \mathbf{a}'_a \ \mathbf{a}''_a)^T$  where  $\mathbf{a}_c$  contains the activities of the  $N_c$  constant activity species,  $\mathbf{a}'_a$  contains the  $N_\mu (= N_s - N_r - N_c)$  activities of aqueous primary species, and  $\mathbf{a}''_a$  is composed by the  $N_r$  activities of secondary species. Likewise,  $\mathbf{S}_e$  is subdivided into three parts,

*i.e.*,  $\mathbf{S}_e = (\mathbf{S}_{ec} | \mathbf{S}'_{ea} | \mathbf{S}''_{ea})$ , where  $\mathbf{S}_{ec}$ ,  $\mathbf{S}'_{ea}$  and  $\mathbf{S}''_{ea}$  correspond, respectively, to the stoichiometric coefficients of constant activity, primary and secondary species. It is always possible to redefine the chemical system so that  $\mathbf{S}_e = (\mathbf{S}_{ec} | \mathbf{S}'_{ea} | -\mathbf{I})$ ,  $\mathbf{I}$  being the identity matrix. This allows explicit calculation of secondary species activities from mass action laws. In term of concentrations,  $\mathbf{c} = (\mathbf{c}_c \ \mathbf{c}_a)^T = (\mathbf{c}_c \ \mathbf{c}'_a \ \mathbf{c}''_a)^T$  (where  $\mathbf{c}'_a$  and  $\mathbf{c}''_a$  are the concentrations of primary and secondary species, respectively), one can write the concentration of secondary species as

$$\log \mathbf{c}''_a = \mathbf{S}'_{ea} \log \mathbf{c}'_a - \log \mathbf{K}^*, \quad (2)$$

where  $\mathbf{K}^*$  is a vector of equivalent equilibrium constants defined as

$$\log \mathbf{K}^* = \log \mathbf{K} - (\mathbf{S}'_{ea} | -\mathbf{I}) \log \boldsymbol{\gamma}_a, \quad (3)$$

$\boldsymbol{\gamma}_a$  being the vector of activity coefficients. The latter are typically calculated in terms of the ionic strength,  $I$ , through the extended Debye-Hückel equation (HELGERSON & KIRKHAM, 1974)

$$\log \gamma_i = -\frac{A z_i^2 \sqrt{I}}{B + a_i \sqrt{I}} + b_i I. \quad (4)$$

Here,  $z_i$  and  $a_i$  are, respectively, the valence and the ionic radius of aqueous species  $i$ ;  $b$ ,  $A$  and  $B$  are temperature-dependent parameters, and  $I = 0.5 \sum z_i^2 c_i$ . A reactive transport process is fully described once concentrations of the  $N_s$  species are obtained, together with the  $N_r$  reactions rates ( $N_s + N_r$  unknowns). In our case, this requires solution of the  $N_s$  coupled mass balance equations (1) and the  $N_r$  equilibrium equations (2).

## 2.3. - COMPONENTS

Solution of a reactive transport problem can be simplified upon defining components by introducing an auxiliary component matrix,  $\mathbf{U}$ .

Following DE SIMONI *et alii* (2005, 2007), we define  $\mathbf{U}$  so that  $\mathbf{U} \mathbf{S}_e^T = (\mathbf{S}_{ec}^T \ \mathbf{0})^T$ .

Multiplying (1) by  $\mathbf{U}$  leads to

$$\frac{\partial(\mathbf{m}_c)}{\partial t} = \mathbf{M}_c L(\mathbf{m}_c) + \mathbf{S}_{ec}^T \mathbf{r}, \quad (5)$$

$$\frac{\partial(\phi \mathbf{u})}{\partial t} = L(\mathbf{u}) \quad (6)$$

where vector  $\mathbf{m}_c$  contains the mass of constant activity species and  $\mathbf{u}$  is a vector of  $N_\mu$  (aqueous) components defined as

$$\mathbf{u} = \mathbf{U}_a \mathbf{c} = \mathbf{c}'_a + (\mathbf{S}'_{ea})^T \mathbf{c}''_a. \quad (7)$$

Equation (6) represents  $N_\mu$  transport equations. Vector  $\mathbf{u}$  contains only aqueous species so that we can leave out matrix  $\mathbf{M}$  in (6), while  $\mathbf{M}_c$  in (5) is the part of  $\mathbf{M}$  referring to constant activity species. As  $\mathbf{S}'_{ea}$  may vary in time and space,  $N_c$ ,  $N_\mu$  and matrix  $\mathbf{U}$ , may vary as well.

If the definition of the chemical system does not change, the easiest way to solve (6) is to first solve  $\mathbf{u}$  (with appropriate boundary and initial

conditions). Then, (aqueous) solute concentrations are obtained from the expression of  $\mathbf{u}$  in terms of concentrations of species (7) and the mass action law (2). Equilibrium reaction rates are then calculated, e.g., from transport equations (1) of secondary species as

$$\mathbf{r} = L(\mathbf{c}_a'') - \frac{\partial(\phi \mathbf{c}_a'')}{\partial t} \quad (8)$$

The mass evolution of the constant activity species is finally obtained upon substituting  $\mathbf{r}$  into (5).

#### 2.4. - MODIFICATION OF MEDIUM PROPERTIES

Dissolution/precipitation processes may lead to changes in medium properties, specifically porosity and hydraulic conductivity, which have a major influence on groundwater velocity. To assess the importance of these effects, porosity variability needs to be included in the numerical simulations of experiments. Permeability ( $k$ ) updating can be performed for each time step on the basis of, e.g., the Kozeny relationship

$$k = k_0 \frac{\phi^3}{(1-\phi)^2} \frac{(1-\phi_0)^2}{\phi_0^3} \quad (9)$$

where  $k_0$  and  $\phi_0$  denote initial permeability and initial porosity, respectively. The porosity is calculated from the concentrations of minerals as

$$\frac{\partial \phi}{\partial t} = - \sum_m v_m \frac{\partial n_m}{\partial t} \quad (10)$$

where subscript  $m$  refers to a mineral and  $v$  is the molar volume.

#### 2.5. - ANALYTICAL EXPRESSION OF REACTION RATES

The analyses presented above clearly shows that  $\mathbf{c}_a''$  is a function of the space-time distribution of components,  $\mathbf{u}$ , as well as chemical equilibrium constants, i.e.,  $\mathbf{c}_a'' = f(\mathbf{u}, \mathbf{K}_{eq})$ , where  $f(\cdot)$  represents a functional relationship described on the basis of (2) and (7). DE SIMONI *et alii* (2005) derived a general analytical expression rendering the space-time distribution of reaction rates. When chemical equilibrium parameters are uniform in space and time, the rate of the  $m$ -th reaction is given by the following expression (DE SIMONI *et alii*, 2005) where, for simplicity, we did not adopt a vectorial notation

$$r_m = \phi \sum_{i=1}^{N_s} \sum_{j=1}^{N_s} \frac{\partial^2 c_{am}''}{\partial u_i \partial u_j} \nabla^T u_i \mathbf{D} \nabla u_j \quad (11)$$

DE SIMONI *et alii* [2007] have extended (11), developing a formulation which provides reaction rates in terms of the mixing ratios of waters with different chemical signatures in the presence of precipitation / dissolution reactions under equilibrium conditions. In this context, one starts by

identifying the different waters taking part in the observed processes. A vector of mixing ratios,  $\boldsymbol{\beta} = (\beta_1, \dots, \beta_N)$ , is then introduced. Here,  $\beta_i$  is the volumetric proportion of the  $i$ -th ( $i = 1, \dots, N$ ) water in a sample. Mixing of  $N$  waters originates  $(N - 1)$  independent variables as mixing ratios sum up to unity. Mixing ratios are conservative quantities, the evolution of which is described by nonreactive transport equations

$$\frac{\partial \beta_i}{\partial t} = L(\beta_i) \quad (12)$$

with given initial and boundary conditions. DE SIMONI *et alii* (2007) derived the following formulation, expressing reaction rates in terms of mixing ratios

$$\mathbf{r} = \phi \sum_i \frac{\partial^2 \mathbf{c}_a''}{\partial \beta_i^2} (\nabla^T \beta_i \mathbf{D} \nabla \beta_i) \quad (13)$$

On these bases, it is clear that reaction rates can be calculated directly, without the need to solve the complete reactive transport problem. Several alternatives are available to compute the first term appearing on the RHS of (13). In simple cases,  $\partial^2 c_{am}'' / \partial \beta_i^2$  ( $c_{am}''$  is the concentration of the  $m$ -th secondary species) can be evaluated analytically or numerically. In general, chemical speciation routines capable of providing the functional dependence of  $\mathbf{c}_a''$  on  $\beta_i$  are a standard option of codes such as *PHREEQC* (PAKHURST & APPELO, 1999), *RETRASO* (SAALTINK *et alii*, 2004), or *CHEPROO* (BEA *et alii*, 2009).

### 3. - MODELING OF LABORATORY-SCALE DISSOLUTION EXPERIMENTS

Here we present the main results obtained by applying the modeling techniques illustrated in Section 2 to analyze  $\text{CaCO}_3$  dissolution experiments performed in a homogeneous laboratory flow cell and presented by SINGURINDY *et alii* (2004, 2005). The experiments are modeled on the basis of (a) the numerical solution of the complete system of equations describing the reactive transport problem and (b) the decoupled methodology of DE SIMONI *et alii* (2005, 2007), which allows calculating directly the rate of the reactions occurring in the system.

#### 3.1. - SYNTHETIC DESCRIPTION OF THE EXPERIMENTS

The experimental set-up described in SINGURINDY *et alii* (2004, 2005) consisted of a  $16 \times 16 \times 1 \text{ cm}^3$  flow cell packed with  $\text{CaCO}_3$  particles, to produce a uniform porous system. The cell was connected to two inlet reservoirs: one containing 40 g/L NaCl dissolved in double

deionized water (hereafter called “saltwater”) and the other containing only double deionized water (“freshwater”). Before injection into the cell, both waters were brought into contact with calcite and with  $\text{CO}_2$  at a partial pressure of 1 atm until conditions of chemical equilibrium were obtained. Further details regarding the set-up are reported by SINGURINDY *et alii* (2004). The dissolution experiments we consider differ from each other in terms of the ratio between fresh and saltwater flow inlet rates, the total volumetric flow rate,  $Q$ , comprising both fresh water and salt water, being the same in all three experiments ( $Q=1.44 \times 10^{-3} \text{ m}^3 \text{ day}^{-1}$ ). On the basis of measurements of cumulative differences between inlet and outlet  $\text{Ca}^{2+}$  concentrations, SINGURINDY *et alii* (2004, 2005) calculated a global dissolution rate for the system. Key data and experimental results are reported in table 1. Experimental results are associated with a pseudo-steady state condition, in which aqueous species concentrations do not vary in time while mineral ( $\text{CaCO}_3$ ) concentrations do. This condition is frequently used in the analysis of the evolution of carbonate systems in coastal aquifers (*e.g.*, SANFORD & KONIKOW, 1989; REZAEI *et alii*, 2005).

Tab. 1 - *Flow rates, flow ratios and experimental dissolution rates in the experiments of SINGURINDY et alii (2004, 2005). Here,  $R_{f-s}$  is the ration between fresh and salt water adopted in the experiments;  $Q_{in,f}$  and  $Q_{in,s}$  are the inlet fresh and salt water flow rates, respectively; and  $R_{TOT,1}$  and  $R_{TOT,2}$  are the experimental global reaction rates respectively relative to the mixing volume  $V_e$  (defined by SINGURINDY et alii, 2004) and to the total volume of the flow cell,  $V_{cell}$ .*

- Portate volumetriche e tassi di dissoluzione relativi agli esperimenti di SINGURINDY *et alii* (2004, 2005);  $R_{f-s}$  è il rapporto tra le portate di acqua dolce e salata adottate negli esperimenti;  $Q_{in,f}$  e  $Q_{in,s}$  sono le portate di acqua dolce e salata;  $R_{TOT,1}$  e  $R_{TOT,2}$  sono i tassi di dissoluzione globali rispettivamente relativi al volume di mescolamento,  $V_e$  (come definito da SINGURINDY *et alii*, 2004) e al volume totale della cella di flusso,  $V_{cell}$ .

Experiment	$R_{f-s}$	$Q_{in,f}$	$Q_{in,s}$	$R_{TOT,1}$	$R_{TOT,2}$
	(%/%)	[ $\text{m}^3 \text{ d}^{-1}$ ]	[ $\text{m}^3 \text{ d}^{-1}$ ]	[ $\text{kg m}^{-3} \text{ d}^{-1}$ ]	[ $\text{kg m}^{-3} \text{ d}^{-1}$ ]
1	50/50	$7.2 \times 10^{-4}$	$7.2 \times 10^{-4}$	0.18	0.157
2	30/70	$4.3 \times 10^{-4}$	$10.1 \times 10^{-4}$	0.13	0.057
3	70/30	$10.1 \times 10^{-4}$	$4.3 \times 10^{-4}$	0.73	0.277

### 3.2. - MODELING APPROACH BASED ON THE SOLUTION OF THE FULL GEOCHEMICAL SYSTEM

We start by using the code *PHREEQC* (PAKHURST & APPELO, 1999) to calculate the chemical composition of the two inflowing waters used in the experiments under the assumption of equilibrium with respect to calcite and a partial  $\text{CO}_{2(g)}$  pressure of 1 atm. *PHREEQC* also provides the relevant aqueous complexation reactions. The complete chemical system is formed by 19 chemical species and 13 reactions. All reactions and their equilibrium constants are displayed in table 2. The flow and reactive transport problem

Tab. 2 - *Chemical reactions with their log equilibrium constants,  $\log K_{eq}$ , used in the reactive transport simulations.*

*A uniform temperature,  $T=23^\circ\text{C}$ , is assumed.*

- Reazioni chimiche e relative costanti di equilibrio,  $\log K_{eq}$ , utilizzate nelle simulazioni numeriche del fenomeno di trasporto reattivo. Si assume che gli esperimenti siano condotti a temperatura uniforme  $T=23^\circ\text{C}$ .

Reaction	$\log K_{eq}$
$\text{CaCl}^+ = \text{Ca}^{2+} + \text{Cl}^-$	0.6938
$\text{CaCl}_{2(aq)} = \text{Ca}^{2+} + 2\text{Cl}^-$	0.6283
$\text{CaHCO}_3^+ = \text{Ca}^{2+} + \text{HCO}_3^-$	-1.0606
$\text{CaOH}^+ + \text{H}^+ = \text{Ca}^{2+} + \text{H}_2\text{O}$	12.9321
$\text{CO}_{2(aq)} + \text{H}_2\text{O} = \text{HCO}_3^- + \text{H}^+$	-6.3636
$\text{CO}_3^{2-} + \text{H}^+ = \text{HCO}_3^-$	10.3524
$\text{OH}^- + \text{H}^+ = \text{H}_2\text{O}$	14.0707
$\text{HCl}_{(aq)} = \text{H}^+ + \text{Cl}^-$	0.6693
$\text{NaCl}_{(aq)} = \text{Na}^+ + \text{Cl}^-$	0.7811
$\text{NaCO}_3^- + \text{H}^+ = \text{Na}^+ + \text{HCO}_3^-$	9.8145
$\text{NaHCO}_{3(aq)} = \text{Na}^+ + \text{HCO}_3^-$	-0.1715
$\text{NaOH}_{(aq)} + \text{H}^+ = \text{Na}^+ + \text{H}_2\text{O}$	14.2479
$\text{CaCO}_{3(s)} + \text{H}^+ = \text{Ca}^{2+} + \text{HCO}_3^-$	1.8789

is modeled with the numerical code *RETRASO* (SAALTINK *et alii*, 2004), following the methodology illustrated in Section 2. The complete numerical solution of the reactive transport problem entails: (a) solving 4 conservative ADEs, (b) performing speciation calculations, consisting in the solution of a nonlinear system of 17 algebraic equations, and finally (c) calculating numerically the reaction rates by solving the 13 transport



equations with the format of (1) satisfied by the secondary species. Steady-state flow within a homogeneous, two-dimensional porous domain is modeled. A uniform intrinsic permeability of  $k = 3.975 \times 10^{-10} \text{ m}^2$  (SINGURINDY & BERKOWITZ, 2003) was adopted. Inflow boundaries are modeled by imposing a constant volumetric flux, uniformly distributed along the inlet boundaries according to the data presented in table 1.

A constant head equivalent to atmospheric pressure is imposed at the outflow boundaries. Porosity,  $\phi$ , was set to the measured value of 0.33 (SINGURINDY *et alii*, 2004). Transport parameters, *i.e.*, dispersivities, are calibrated for the experiments by comparing the calculated total rates to experimental rates (reported in table 1). The latter are derived on the basis of the available experimental data, which consist of the overall dissolved calcite concentrations,  $C_{\text{CaCO}_3}^t$ , evaluated at times  $t$ , and computed by mass balance from the inflow and outflow  $\text{Ca}^{2+}$  concentrations. The domain was discretized into square finite elements of uniform size  $\Delta = 0.133 \text{ cm}$ , *i.e.*,  $120 \times 120$  elements. For simplicity, and due to lack of sensitivity of the model results to longitudinal dispersivity,  $\alpha_L$ , the diffusion-dispersion process has been modeled as isotropic, and we set  $\alpha_L = \alpha_T = \alpha$  as the only fitting parameter. The calibration procedure to match the experiments resulted in the following values of dispersivities: (a)  $\alpha = 0.0010 \text{ m}$  for the 50/50 experiment (Experiment 1 in table 1); and (b)  $\alpha = 0.0040 \text{ m}$  for the 70/30 experiment (Experiment 3 in table 1). Due to software constraints, it was not possible to adopt a grid refinement compatible with very low dispersivity values which would have been needed in order to obtain a good calibration of the 30/70 experiment (Experiment 2 in table 1). We note that the isotropic dispersivity providing the best agreement against experimental results tends to decrease as the proportion of salt water increases. Factors which might contribute to this behavior include sensitivity of the model to the chemical composition of the inlet waters, and temperature effects that could influence the activity coefficients.

### 3.3. - MODELING APPROACH BASED ON THE DIRECT CALCULATION OF LOCAL REACTION RATES

Since only two end-members are present, the chemical problem is characterized completely by a single mixing ratio,  $\beta$ . Assuming that solute transport can be properly described by means of an advection-dispersion (or advection-diffusion) equation, DE SIMONI *et alii* (2007) provided an explicit expression for the computation of local reaction rates  $r$  in terms of  $\beta$

$$r = \phi \underbrace{\frac{\partial^2 c_{\text{Ca}}}{\partial \beta^2}}_A \underbrace{\nabla \beta^T \mathbf{D} \nabla \beta}_B \quad (14)$$

where  $r$  is expressed in  $\text{mol kg}^{-1} \text{ s}^{-1}$ . Here,  $c_{\text{Ca}}$  in (15) corresponds to total aqueous concentration of calcium. Mixing ratios,  $\beta$ , can be obtained from any conventional transport or random walk particle tracking code. The nonlinear chemistry-related factor,  $A$ , in (14) can be calculated by plotting the total aqueous calcium concentration,  $c_{\text{Ca}}$ , versus mixing ratio,  $\beta$ , for a suite of arbitrary mixing scenarios. To this end, an existing speciation codes, such as *PHREEQC*, can be used. We calculate the local distribution of rates under pseudo-steady-state transport conditions at constant temperature according to (14), and then integrate it over the flow cell volume to obtain the total reaction rate within the system. Dispersivities are then calibrated for each of the three experiments by comparing the calculated total rates to experimental rates (reported in table 1). Dispersivities values providing the best match between experimental and computed global reaction rates coincide with those obtained by means of the fully numerical geochemical modeling approach for the 50/50 and 70/30 experiments. A good calibration of the 30/70 experiment against numerical modeling results was obtained by adopting the isotropic dispersivity value  $\alpha = 0.0002 \text{ m}$ . It is remarked that the calibrated (isotropic) dispersivity values are of the order of the pore size of the porous rock, thus being (in principle) suitable for describing mixing at the molecular scale. Although all calibrated values are within an order of magnitude, the variability in the values cannot be explained solely on the basis of error measurements and uncertainty. This may be due to the use of an ADRE-based continuum model in the presence of pore-scale reactions. As noted by TARTAKOVSKY *et alii* (2008, and references therein) and further discussed by KATZ *et alii* (2010), several scale separation conditions must be maintained (*e.g.*, the characteristic length associated with the pore space geometry must be much smaller than the characteristic length of the averaging volume) to allow use of the ADRE. These conditions are often violated in transport processes that involve mixing, and might contribute to explain the results obtained.

## 4. - MODELING OF LABORATORY-SCALE COMPETITIVE ADSORPTION EXPERIMENTS

This Section is devoted to the interpretation of the competitive adsorption of cadmium ( $\text{Cd(II)}$ ) and nickel ( $\text{Ni(II)}$ ) ions onto bagasse fly ash (BFA) performed by SRIVASTAVA *et alii* (2006).

#### 4.1. - OVERVIEW OF THE EXPERIMENTS

SRIVASTAVA *et alii* (2006), performed a series of batch experiments involving mono- and binary-component adsorption studies of cadmium (Cd(II)) and nickel (Ni(II)) ions onto bagasse fly ash (BFA). Experimental details on the preparation and characterization of the BFA samples, the chemical composition of the solutions adopted in the experiments, and the protocols adopted to measure Cd(II) and Ni(II) concentrations are presented in SRIVASTAVA *et alii* (2006). For single metal systems, initial metal ion concentration was varied from 10 to 100 mg/l. In binary metal ion mixtures, for each initial concentration of Cd(II) solution, *i.e.*, 10, 20, 30, 50 and 100 mg/l, the nickel concentration was varied in the range of 10–100 mg/l (*i.e.*, 10, 20, 30, 50 and 100 mg/l). In all cases, the pH of the solution was maintained at 6.0. Experiments were carried out until equilibrium conditions were attained. The complete data-set of 50 individual and total adsorption equilibrium uptakes and yields measured in the experiments at different cadmium(II) concentrations in the absence and presence of increasing concentrations of nickel(II) ions are presented by SRIVASTAVA *et alii* (2006).

Single-component isotherms have been modeled by Freundlich, Langmuir and R-P models. Bi-component isotherms were interpreted by several models. These include the Sheindorf–Rebuhn–Sheintuch (SRS) model (SHEINDORF *et alii*, 1981)

$$q_{e,j} = K_{F,j} C_{e,j} \left( \sum_{j=1}^N q_{e,j} C_{e,j} \right)^{n_j-1} \quad (15)$$

the modified competitive Langmuir isotherm (BELLOT & CONDORÉ, 1993)

$$q_{e,j} = \frac{q_{m,j} K_{L,j} (C_{e,j} / \eta_j)}{1 + \sum_{j=1}^N (C_{e,j} / \eta_j)} \quad (16)$$

the extended Langmuir isotherm (YANG, 1987)

$$q_{e,j} = \frac{q_{max} K_i C_{e,j}}{1 + \sum_{j=1}^N K_j C_{e,j}} \quad (17)$$

and the extended Freundlich model

$$q_{e,1} = \frac{K_{F,1} C_{e,1}^{a_1+1}}{C_{e,1}^{a_1} + y_1 C_{e,2}^{a_1}}; \quad q_{e,2} = \frac{K_{F,2} C_{e,2}^{a_2+1}}{C_{e,2}^{a_2} + y_2 C_{e,1}^{a_2}} \quad (18)$$

Here,  $N$  is the number of metals involved in the competitive experiment (in our case  $N = 2$ );  $q_{m,j}$  and  $K_{L,j}$  are the parameters of the individual Langmuir isotherm models;  $K_{F,j}$  and  $n_j$  are the Freundlich parameters determined from the single-component equilibrium adsorption data; the isotherm parameters  $\eta_j$ ,  $q_{max}$ ,  $K_i$ ,  $x_1$ ,  $y_1$ ,  $z_1$ ,  $x_2$ ,  $y_2$ ,  $z_2$ , and  $a_{jp}$  are determined upon a best-fit procedure against the experimental data. SRIVASTAVA *et alii* (2006) assessed the quality of the fit of the

different models analyzed on the basis of the minimized Marquardt's percent standard deviation. On these bases, they conclude that the binary adsorption of Cd(II) and Ni(II) ions by BFA can be represented satisfactorily and adequately by the extended Freundlich isotherm (18).

#### 4.2. - INTERPRETATION BASED ON MULTIMODEL APPROACH

Hydrogeochemical processes taking place in complex subsurface environments are prone to multiple interpretation and mathematical descriptions. As a consequence, adopting only one of these might lead to statistical bias and underestimation of uncertainty. In the spirit of NEUMAN (2003) we adopt formal model selection (discrimination, information) criteria to select the best amongst the different competing models (15) - (18). We associate each of these four models with a weight, or posterior probability, representing their relative degrees of likelihood.

Let  $\beta$  be a vector of unknown model parameters. We wish to obtain a maximum likelihood (ML) estimate  $\hat{\beta}$  of  $\beta$  based on  $N$  measurements of adsorbed ions concentration at equilibrium,

$$q_{e,j}^* = q_{e,j} + \varepsilon_j^* \quad j = 1, 2, \dots, N \quad (19)$$

where  $q_{e,j}$  is the unknown true value of adsorbed ion concentration corresponding to given values of initial ( $C_0$ ) and equilibrium ( $C_e$ ) concentrations and  $j^*$  is a corresponding zero-mean measurement error. We designate the vectors of adsorbed ion concentration measurements and corresponding measurement errors by  $\mathbf{q}^*$  and  $\boldsymbol{\varepsilon}^*$ , respectively. Following the rationale of CARRERA & NEUMAN (1986a,b) we treat the prior error vectors as being multivariate Gaussian, an assumption that can be validated a posteriori by a statistical analysis of the corresponding residuals  $\boldsymbol{\varepsilon}^* \simeq \hat{\mathbf{q}} - \mathbf{q}^*$ ,  $\hat{\mathbf{q}}$  being a vector of adsorbed ion concentrations predicted using parameter estimates  $\hat{\beta}$ . For simplicity and without loss of generality, we assume that measurement error statistics lack correlation. Then a ML estimate of  $\beta$  is obtained by minimizing the negative log likelihood criterion (support function)

$$NLL = (N + N_p) \ln(2\pi) + \ln |\mathbf{S}_q| + (\mathbf{q}^* - \hat{\mathbf{q}})^T \mathbf{S}_q^{-1} (\mathbf{q}^* - \hat{\mathbf{q}}) \quad (20)$$

with respect to  $\beta$ . Here,  $N_p$  is the number of model parameters,  $\mathbf{S}_q = \sigma_\varepsilon^2 \mathbf{V}_q$  is a diagonal covariance matrix of measurement errors,  $\boldsymbol{\varepsilon}_j^*$ , where  $\mathbf{V}_q$  is the identify matrix and is determined upon minimization of (20) though it may have an estimated prior value. If the prior estimate of  $\sigma_\varepsilon^2$  is considered reliable and is fixed, then the minimization of (20) reduces to minimization of the generalized

sum of squares criterion. We minimize (20) using the iterative Levenberg-Marquardt algorithm implemented in the public domain code PEST (DOHERTY, 2002). The minimization algorithm computes an updated parameter estimate  $\hat{\mathbf{q}}$  of the (unknown) true vector  $\mathbf{q}$  and a Cramer-Rao lower bound approximation for the covariance matrix,  $\mathbf{Q}$ , of the corresponding estimation errors; the latter is evaluated according to

$\mathbf{Q} = \sigma_\varepsilon^2 [\mathbf{J}^T \mathbf{V}^{-1} \mathbf{J}]^{-1}$  here  $\mathbf{J}$  is a Jacobian matrix of derivatives of the adsorbed ion concentrations with respect to  $\beta$ , evaluated at  $\hat{\beta}$ . We repeat the parameter estimation procedure for each of the interpretive models described in Section 4.1 and then we select an optimum model based on how sharply it corresponds to a minimum of any of the following model selection (discrimination, information) criteria

$$AIC = NLL + 2N_p \quad (21)$$

$$AIC_c = NLL + 2N_p + \frac{2N_p(N_p + 2)}{N - 1} \quad (22)$$

$$BIC = NLL + N_p \ln(N + N_p) \quad (23)$$

$$HIC = NLL + 2N_p \ln(\ln(N + N_p)) \quad (24)$$

$$KIC = NLL + N_p \ln\left(\frac{N + N_p}{2\pi}\right) - \ln|\mathbf{Q}| \quad (25)$$

$AIC$  is due to AKAIKE (1974),  $AIC_c$  to HURVICH & TSAI (1989),  $HIC$  to HANNAN (1980),  $BIC$  to SCHWARTZ (1978), and  $KIC$  to KASHYAP (1982).

Following YE *et alii* (2004) we translate the values of (21) - (25) into posterior model weights for model  $M_k$  (in our case, we have  $k = 4$  alternative models),  $p(M_k | \mathbf{q})$ , which represent posterior model probability conditioned on the vector  $\mathbf{q}$  of measures. We compute posterior model weights using an approach proposed by TSAI & LI (2008) according to which

$$p(M_k | \mathbf{q}) = \frac{\exp\left(-\frac{1}{2} \alpha \Delta IC_k\right) p(M_k)}{\sum_{i=1}^K \exp\left(-\frac{1}{2} \alpha \Delta IC_i\right) p(M_i)} \quad (26)$$

where  $\Delta IC_k$  is the difference between the model information criterion  $IC$  (it can be  $AIC$ ,  $AIC_c$ ,  $BIC$ ,  $HIC$  or  $KIC$ ) of model  $k$  and the minimum value of the model selection criterion over all the 4 models,  $p(M)$  is the prior model probability (which we take to be equal for all models, *i.e.*,  $p(M) = 1/4$ ) and

$$\alpha = \frac{s_1}{s_2 \sigma_D} \quad (27)$$

is a scaling factor. In (27),  $s_1$  is  $\Delta IC_k$  corresponding to a given significance level in Occam's window and

$s_2$  is the width of a variance window, in units of  $\sigma_D$ , where  $\sigma_D^2 = 2N$  is the variance of  $IC_k$ . A significance level of 5 % corresponds to  $s_1 = 6$  and a window size of  $4\sigma_D$ , *i.e.*,  $s_2 = 4$  and thus  $\alpha = 0.15$ . Table 3 lists the values of the selection criteria (21) - (25) associated with each of the models (15) - (18), together with the corresponding model weights. All five criteria in table 3 rank the extended Freundlich model (18) as best, the SRS model (15) as second best, the modified competitive Langmuir (16) as third, the extended Langmuir isotherm (17) as worst among these four models.

Tab. 3 - *Values of the selection criteria (12)-(25) associated with each of the models (15) - (18). The corresponding model weights are reported in parenthesis.*

- Valori assunti dai criteri di discriminazione (21) - (25) e associati ai modelli (15) - (18). In parentesi sono riportati i pesi a posteriori corrispondenti.

	Eq. (15)	Eq. (16)	Eq. (17)	Eq. (18)
$AIC$	40.02 (0.022)	54.72 (0.007)	58.47 (0.005)	-10.47 (0.965)
$AIC_c$	40.34 (0.025)	55.05 (0.008)	59.08 (0.006)	-8.51 (0.961)
$BIC$	43.92 (0.039)	58.62 (0.013)	64.38 (0.009)	1.68 (0.939)
$HIC$	41.51 (0.028)	56.23 (0.009)	60.74 (0.007)	-5.76 (0.957)
$KIC$	45.25 (0.210)	62.85 (0.056)	82.31 (0.013)	28.83 (0.720)

$AIC$ ,  $AIC_c$ ,  $BIC$ , and  $HIC$  assign a weight of about 96 % to the extended Freundlich model (18).  $KIC$  assign a weight of about 73% to (18), 20% to (15) and virtually 0 % to (16) and (17). We note that Kashyap's criterion favors the model that is least probable (in an average sense) of being incorrect. Stated otherwise, the criterion minimizes the average probability of selecting the wrong model among a set of alternatives. The Fisher information term, which is proportional to  $\mathbf{Q}$ , imbues  $KIC$  with desirable model selection properties not shared by other criteria, such as  $BIC$ , as it has the ability to discriminate between models on the basis not only on their goodness-of-fit to available observations and number of parameters but also on the quality of the available data and of the parameter estimates. According to  $KIC$ , the results of table 3 imply that whereas models based on (16) and (17) can validly be eliminated as being inferior to the other two models, there is no justification for adopting any one of the latter two models (the extended Freundlich (18) and the SRS model (15)) at the exclusion of the remaining one. Instead, there is uncertainty about each of these two models and their parameters. A possibility to account for this uncer-



tainty is to average predictions of competitive adsorption of Cd(II) and Ni(II) ions by BFA rendered by (15) and (18) using the weights in table 3, and to assess the corresponding predictive uncertainty accordingly, using, *e.g.*, maximum likelihood Bayesian model averaging (MLBMA) as described in NEUMAN (2003), YE *et alii* (2004, 2008) and TSAI & LI (2008).

## 5. - CONCLUSIONS

We have presented a synthetic review of recent modeling developments associated with the interpretation of reactive transport problems. We then present the salient results of modeling studies of (a) dissolution experiments performed in a laboratory-scale porous medium, and (b) binary-component adsorption analyses of cadmium and nickel ions onto bagasse fly ash (BFA). Our work highlights the following key conclusions.

As shown by GUADAGNINI *et alii* (2009), it is possible to use a simple methodology of the kind recently presented by DE SIMONI *et alii* (2005, 2007) to interpret relatively complex dissolution processes at the laboratory scale.

The performance of four popular models describing heavy metals competition in batch experiments has been analyzed against a set of published data. With the aid of formal model selection criteria we associate each of these four models with a weight, or posterior probability, representing their relative degrees of likelihood. When the Kashyap's information criterion (KASHYAP, 1982) is adopted, some of the weights are large enough so that it may not be justified adopting one of the four models at the exclusion of all others. This suggests that predictions of competitive adsorption of Cd(II) and Ni(II) ions by BFA can be best performed in the context of a multimodel approach, such as maximum likelihood Bayesian model averaging.

## Acknowledgement

*The work has been partly supported by the Marie Curie Initial Training Network "Towards Improved Groundwater Vulnerability Assessment (IMV/UL)". We thank the two anonymous reviewers and the Associate Editor, Mauro Giudici, for their constructive comments to our manuscript.*

## REFERENCES

ADAMO P., ARIENZO M., BIANCO M.R., TERRIBILE F. & VIOLANTE P. (2002) - Heavy metal contamination of the soils used for stocking raw materials in the former ILVA iron-steel industrial plant of Bagnoli (southern Italy). *Sci. Total Environ.*, **295**: 17–34.

AKAIKE H. (1974) - *A new look at statistical model identification*. IEEE Trans. Autom. Control, **AC19**: 716–723.

ANTONIADIS V., MCKINLEY J.D. & ZUHAIRI W.Y.W. (2007) - *Single-element and competitive metal mobility measured with Column Infiltration and Batch Tests*. J. Environ. Qual., **36**: 53–60. doi:10.2134/jeq2006.0134.

BEA S.A., J. CARRERA, C. AYORA, F. BATLLÉ & SAALTINK M.W. (2009) - *CHEPROO: A Fortran 90 object-oriented module to solve chemical processes in Earth Science models*. Comput. Geosci., **35** (6): 1098–1112.

BELLOT J.C. & CONDORET J.S. (1993) - *Modelling of liquid chromatography equilibrium*. Process Biochem., **28**: 365–376.

BERNARDELLO M., SECCO T., PELLIZZATO A., CHINELLATO M., SFRISO A. & PAVONI B. (2006) - *The changing state of contamination in the Lagoon of Venice Part 2: Heavy metals*. Chemosphere, **64**: 1334–1345.

BRETZEL F. & CALDERISI M. (2006) - *Metal contamination in urban soils of coastal Tuscany*. Environ. Monit. Assess., **118**: 319–335. doi: 10.1007/s10661-006-1495-5.

CARRERA J. & NEUMAN S.P. (1986a) - *Estimation of aquifer parameters under transient and steady state conditions: 1. Maximum likelihood method incorporating prior information*. Water Resour. Res., **22** (2): 199–210.

CARRERA J. & NEUMAN S.P. (1986b) - *Estimation of aquifer parameters under transient and steady state conditions: 2. Uniqueness, stability, and solution algorithms*. Water Resour. Res., **22** (2): 211 – 227.

CHANG C.M., WANG M.K., CHANG T.W., LIN C. & CHEN Y.R. (2001) - *Transport modeling of copper and cadmium with linear and nonlinear retardation factors*. Chemosphere, **43**: 1133–1139.

CIRPKA O.A. & VALOCCHI A.J. (2007) - *Two-dimensional concentration distribution for mixing-controlled bioreactive transport in steady state*. Adv. Water Resour., **30** (6-7): 1668–1679.

CLEMENT T.P., SUN Y., HOOKER B.S. & PETERSEN J.N. (1998) - *Modeling multispecies reactive transport in ground water*. Ground Water Monit. Remed., **18** (2): 79 – 92.

DE SIMONI M., CARRERA J., SANCHEZ-VILA X. & GUADAGNINI A. (2005) - *A procedure for the solution of multicomponent reactive transport problems*. Water Resour. Res., **41**, W11410, doi:10.1029/2005WR004056.

DE SIMONI M., SANCHEZ-VILA X., CARRERA J. & SAALTINK M.W. (2007) - *A mixing ratios-based formulation for multicomponent reactive transport*. Water Resour. Res., **43**, W07419: 1–16. doi:10.1029/2006WR005256.

DOHERTY J. (2002) - *PEST: Model Independent Parameter Estimation, User Manual (5th ed.)*, pp. 279, Watermark Numerical Computing, Brisbane, Queensland, Australia.

FONTES M.P.F. & GOMES P.C. (2003) - *Simultaneous competitive adsorption of heavy metals by the mineral matrix of tropical soils*. Appl. Geochem., **18**: 795–804.

FRIEDLY J.C. & RUBIN J. (1992) - *Solute transport with multiple equilibrium-controlled or kinetically controlled chemical reactions*. Water Resour. Res., **28** (6): 1935–1953.

GOMES P.C., FONTES M.P.F., DA SILVA A.G., MENDONÇA E.D. & NETTO A.R. (2001) - *Selectivity sequence and competitive adsorption of heavy metals by Brazilian soils*. Soil Sci. Soc. Am. J., **65** (4): 1115–1121.

GUADAGNINI A., SANCHEZ-VILA X., SAALTINK M.W., BUSSINI M. & BERKOWITZ B. (2009) - *Application of a mixing-ratios based formulation to model mixing-driven dissolution laboratory experiments*. Adv. Water Resour., **32**: 756–766.

HANNAN E.S. (1980) - *The estimation of the order of an ARMA process*. Ann. Stat., **8**: 1971–1981.

HELGERSON H.C. & KIRKHAM D.H. (1974) - *Theoretical prediction of the thermodynamic behaviour of aqueous electrolytes at high pressure and temperature: II Debye-Hückel parameters for activity coefficients and relative partial molar properties*. Am. J. Sci., **274**: 1199–1261.

- HURVICH C.M. & TSAI C.L. (1989) - *Regression and time series model selection in small sample*. *Biometrika*, **76** (2): 99-104.
- KASHYAP R.L. (1982) - *Optimal choice of AR and MA parts in autoregressive moving average models*. *IEEE Trans. Pattern Anal. Mach. Intel. (TPAMI)*, **4** (2): 99-104.
- KATZ G.E., BERKOWITZ B., GUADAGNINI A. & SAALTINK M.W. (2010) - *Experimental and modeling investigation of multicomponent reactive transport in porous media*. *J. Contam. Hydrol.*, doi:10.1016/j.jconhyd.2009.11.002.
- LICHTNER P. (1996) - *Continuous formulation of multicomponent-multiphase reactive transport*. In: P.C. LICHTNER, C.I. STEEFEL & E.H. OEKLEERS (Eds.): «*Reactive transport in porous media*». *Miner. Soc. Amer., Rev. Mineral.*, **34** Washington D.C.
- LIEDL R., VALOCCHI A.J., DIETRICH P. & GRATHWOHL P. (2005) - *Finiteness of steady state plumes*. *Water Resour. Res.*, **31** (12): W12501, doi:10.1029/2005WR004000.
- MAYES M.A., JARDINE P.M., LARSEN I.L., BROOKS S.C. & FENDORF S.E. (2000) - *Multispecies transport of metal-EDTA complexes and chromate through undisturbed columns of weathered fractured saprolite*. *J. Contam. Hydrol.*, **45** (3-4): 165-372.
- MOLINS S., CARRERA J., AYORA C. & SAALTINK M.W. (2004) - *A formulation for decoupling components in reactive transport problems*. *Water Resour. Res.*, **40** (10): W10301, doi:10.1029/2003WR002970.
- NEUMAN S.P. (2003) - *Maximum likelihood Bayesian averaging of alternative conceptual-mathematical models*. *Stoch. Environ. Res. Risk Assess.*, **17** (5): 291-305.
- PAKHURST D.L. & APPELO C.A.J. (1999) - *User's guide to PHREEQC (Version 2) - A computer program for speciation, batch-reaction, one-dimensional transport, and inverse geochemical calculations*. U.S. Geological Survey Water-Resources Investigations Report 99-4259: pp. 310.
- PHILLIPS O.M. (1991) - *Flow and Reactions in Permeable Rocks*, pp. 280, Cambridge Univ. Press, New York.
- REZAEI M., SANZ E., RAEISI E., VÁZQUEZ-SUÑÉ E., AYORA C. & CARRERA J. (2005) - *Reactive transport modeling of calcite dissolution in the salt water mixing zone*. *J. Hydrol.*, **311**: 282-298.
- ROBINSON B.A., VISWANATHAN H.S. & VALOCCHI A.J. (2000) - *Efficient numerical techniques for modeling multicomponent ground-water transport based upon simultaneous solution of strongly coupled subsets of chemical components*. *Adv. Water Resour.*, **23** (4): 307-24.
- RUBIN J. (1990) - *Solute transport with multisegment, equilibrium-controlled reactions: a feed forward simulation method*. *Water Resour. Res.*, **26** (9): 2029-2055.
- RUBIN J. (1992) - *Solute transport with multisegment, equilibrium-controlled classical reactions: problem solvability and feed forward method's applicability for complex segments of at most binary participants*. *Water Resour. Res.*, **28** (6): 1681-1702.
- SAALTINK M.W., AYORA C. & CARRERA J. (1998) - *A mathematical formulation for reactive transport that eliminates mineral concentrations*. *Water Resour. Res.*, **34** (7): 1649-1656.
- SAALTINK M.W., CARRERA J. & AYORA C. (2001) - *On the behavior of approaches to simulate reactive transport*. *J. Contam. Hydrol.*, **48**: 213-235.
- SAALTINK M.W., BATLLE F., AYORA C., CARRERA J. & OLIVELLA S. (2004) - *RETRASO, a code for modeling reactive transport in saturated and unsaturated porous media*. *Geol. Acta*, **2** (3): 235-251.
- SAHA U.K., TANIGUCHI S. & SAKURAI K. (2002) - *Simultaneous adsorption of cadmium, zinc, and lead on hydroxyl-aluminum- and hydroxyl-aluminosilicate-montmorillonite complexes*. *Soil Sci. Soc. Am. J.*, **66**: 117-128.
- SANCHEZ-VILA X., DONANDO L.D., GUADAGNINI A. & CARRERA J. (2010) - *A solution for multicomponent reactive transport under equilibrium and kinetic reactions*. *Water Resour. Res.*, in press.
- SANFORD W.E. & KONIKOW L.F. (1989) - *Simulation of calcite dissolution and porosity changes in saltwater mixing zones in coastal aquifers*. *Water Resour. Res.*, **25**: 655-667.
- SCHWARZ G. (1978) - *Estimating the dimension of a model*. *Ann. Stat.*, **6** (2): 461-464.
- SHEINDORF C., REBHUM M. & SHEINTUCH M. (1981) - *A Freundlich-type multicomponent isotherm*. *J. Colloid Interface Sci.*, **79**: 136-142.
- SINGURINDY O. & BERKOWITZ B. (2003) - *Evolution of hydraulic conductivity by precipitation and dissolution in carbonate rock*. *Water Resour. Res.*, **39** (1): 1-14.
- SINGURINDY O. & BERKOWITZ B. (2004) - *Dedolomitization and flow in fractures*. *Geophys. Res. Lett.*, **31**: L24501. doi:10.1029/2004GL021594.
- SINGURINDY O., BERKOWITZ B. & LOWELL R.P. (2004) - *Carbonate dissolution and precipitation in coastal environments: Laboratory analysis and theoretical consideration*. *Water Resour. Res.*, **40**: W04401. doi:10.1029/2003WR002651.
- SINGURINDY O., BERKOWITZ B. & LOWELL R.P. (2005) - *Correction to "Carbonate dissolution and precipitation in coastal environments: Laboratory analysis and theoretical consideration"*. *Water Resour. Res.*, **41**: W11701. doi:10.1029/2005WR004433.
- SRIVASTAVA P., SINGH B. & ANGOVE M. (2005) - *Competitive adsorption behavior of heavy metals on kaolinite*. *J. Colloid Interface Sci.*, **290**: 28-38.
- SRIVASTAVA V.C., MALL I.D. & MISHRA I.M. (2006) - *Equilibrium modelling of single and binary adsorption of cadmium and nickel onto bagasse fly ash*. *Chem. Eng. J.*, **117**: 79-91.
- STEEFEL C.I. & MACQUARRIE K.T.B. (1996) - *Approaches to modelling reactive transport*. In *Reactive transport in porous media*. *Rev. Mineral.*, **34**: 83-129.
- STEEFEL C.I., DE PAOLO D.J. & LICHTNER P.C. (2005) - *Reactive transport modeling: An essential tool and a new research approach for the Earth sciences*. *Earth Planet. Sci. Lett.*, **240**: 539-558.
- TARTAKOVSKY A.M., REDDEN G., LICHTNER P.C., SCHEIBE T.D. & MEAKIN P. (2008) - *Mixing-induced precipitation: Experimental study and multiscale numerical analysis*. *Water Resour. Res.*, **44**: W06S04. doi:10.1029/2006WR005725.
- TEBES-STEVENS C., VALOCCHI A.J., VAN BRIESEN J.M. & RITTMANN B.E. (1998) - *Multicomponent transport with coupled geochemical and microbiological reactions: model description and example simulations*. *J. Hydrol.*, **209** (1-4): 8-26.
- TSAI F.T.-C. & LI X. (2008) - *Inverse groundwater modeling for hydraulic conductivity estimation using Bayesian model averaging and variance window*. *Water Resour. Res.*, **44**: W09434. doi:10.1029/2007WR006576.
- TSANG D.C.W. & LO I.M.C. (2006) - *Competitive Cu and Cd sorption and transport in soils: a combined batch kinetics, Column, and Sequential Extraction Study*. *Environ. Sci. Technol.*, **40**: 6655-6661.
- YANG R.T. (1987) - *Gas Separation by Adsorption Processes*, pp. 352, Butterworths, Boston, MA.
- YE M., NEUMAN S.P. & MEYER P.D. (2004) - *Maximum Likelihood Bayesian averaging of spatial variability models in unsaturated fractured tuff*. *Water Resour. Res.*, **40** (5): W05113. doi:10.1029/2003WR002557.
- YE M., MEYER P.D. & NEUMAN S.P. (2008) - *On model selection criteria in multimodel analysis*. *Water Resour. Res.*, **44**: W03428. doi:10.1029/2008WR006803.
- YEH G.T. & TRIPATHI V.S. (1991) - *A model for simulating transport of reactive multispecies components: model development and demonstration*. *Water Resour. Res.*, **27** (12): 3075-3094.
- VOEGELIN A., VULAVA V.M. & KRETZSCHMAR R. (2001) - *Reaction-based model describing competitive sorption and transport of Cd, Zn, and Ni in an acidic soil*. *Environ. Science Technol.*, **35**: 1651-1657.

## Hydrostratigraphy of the late Messinian-Quaternary basins in southern Piedmont (northwestern Italy)

*Idrostratigrafia dei bacini messiniano-quaternari del Piemonte meridionale (Italia nord-occidentale)*

IRACE A. (\*), CLEMENTE P. (\*\*), PIANA F. (\*), DE LUCA D.A. (\*\*),  
POLINO R. (\*), VIOLANTI D. (\*\*), MOSCA P. (\*),  
TRENKWALDER S. (\*), NATALICCHIO M. (\*\*),  
OSSELLA L. (\*), GOVERNA M. (\*\*\*),  
PETRICIG M. (\*\*\*)

**ABSTRACT** - An integrated stratigraphic approach has been adopted to define the 3D hydrostratigraphic regional framework of the fresh-water aquifers of the Savigliano and Alessandria Basins, in southern Piedmont.

In the present work, the Aquifer Groups represents the “fundamental” hydrostratigraphic units, since they physically correspond to synthems, that have been recognized both in the subsurface and outcrops.

Each Aquifer Group is characterized by Hydrogeologic Units (HU) defined on the basis of lithofacies associations that display homogeneous hydrogeologic properties (e.g. permeability ratio, storage coefficient). Four main typologies of Hydrogeologic Units have been distinguished, on the basis of their hydrogeologic characteristics: HU I) unconfined aquifers, HU II) multi-layered “discontinuous” aquifers, HU III) multi-layered “continuous” aquifers, HU IV) aquitards/aquicludes.

It has been assumed in this work that, due to its peculiar stratigraphic architecture (i.e. internal stratal organization) each Aquifer Group has a distinctive response to the regional groundwater flow system. In this sense, each main type of Hydrogeologic Unit will present a peculiar and distinctive instance in each single Aquifer Group. Consequently, the Aquifers Groups can be subdivided into lower rank hydrostratigraphic units, here defined as “Synthemetic Hydrogeologic Units”. These units, although encompassed in the four main typologies of Hydrogeologic Units, do inherit the peculiar architectural properties of the Aquifer Group they belong to. In this sense, each main type of Hydrogeologic Unit will present its own instance within the different Aquifer Groups. Following these criteria, nineteen Synthemetic Hydrogeologic Units, grouped into seven Aquifer Groups were recognized within the Savigliano and Alessandria Basins.

The reconstruction of the hydrostratigraphic model allowed to portray, for the first time, the geometry and archi-

tecture of the Aquifer Groups of the whole upper Messinian-Quaternary successions in southern Piedmont and to reconstruct the regional distribution and characteristics of potentially exploitable aquifers.

Moreover, the use of stratigraphic constraints (i.e. distribution of depositional systems and lithofacies associations) led to the reconstruction of the geometry of the fresh-salt water interface, also in those areas with scarce well data, and to better estimate the maximum thickness of deep fresh-aquifers that, up to date, are still unexploited.

The hydrostratigraphic reconstruction here proposed constitutes a forward step with respect to the previous knowledge on Piedmont subsurface hydrogeology, and cast the bases for future development of water exploitation and water flow modeling.

**KEY WORDS:** Aquifer Groups, Fresh-salt water interface, Hydrogeologic Synthemetic Units, Hydrostratigraphy, Messinian-Quaternary Piedmont Basins, Physical stratigraphy, Synthems.

**RIASSUNTO** - È stato utilizzato un approccio stratigrafico integrato per definire il quadro idrostratigrafico a scala regionale degli acquiferi permeati da acqua dolce dei Bacini di Savigliano ed Alessandria, nel Piemonte meridionale.

In questo lavoro, i Gruppi Acquiferi rappresentano le unità idrostratigrafiche “fondamentali”, dal momento che essi corrispondono ai sintemi che sono stati riconosciuti sia nel sottosuolo che in affioramento.

Ogni Gruppo Acquifero è caratterizzato da Unità Idrogeologiche (HU), definite sulla base delle associazioni di litofacies, che mostrano proprietà idrogeologiche omogenee (per es. grado di permeabilità, coefficiente di immagazzinamento). Sulla base del loro ruolo idrogeologico sono state riconosciute quattro tipologie principali di Unità Idrogeo-

(\*) CNR, IGG-Istituto di Geoscienze e Georisorse, Via Valperga Caluso 35, Torino.

(\*\*) Dipartimento di Scienze della Terra, Università degli Studi di Torino, Via Valperga Caluso 35, Torino

(\*\*\*) Regione Piemonte, Direzione Ambiente, Via Principe Amedeo 17, Torino



giche: HU I) acquifero monostrato, HU II) acquifero multistrato “discontinuo”, HU III) acquifero multistrato “continuo”, HU IV) acquitarzo/acquitudo.

Nel presente lavoro si è assunto che, a scala regionale, ogni Gruppo Acquifero mostri un comportamento distintivo in risposta al sistema di flusso sotterraneo, a causa della sua peculiare architettura stratigrafica (ovvero organizzazione stratale interna). Secondo tale assunto, ogni tipologia principale di Unità Idrogeologica presenterà caratteristiche uniche e contestuali all'interno di ogni singolo Gruppo Acquifero. Di conseguenza, i Gruppi Acquiferi possono essere suddivisi in unità idrostratigrafiche di rango inferiore, qui definite come “Unità Idrogeologiche di Sintema”. Nonostante tali unità siano sempre inquadrabili all'interno di una delle tipologie principali di Unità Idrogeologiche sopra definite, esse ereditano le caratteristiche architettoniche del Gruppo Acquifero di appartenenza. In tal senso, ogni tipologia principale di Unità Idrogeologica presenterà la sua particolare istanza all'interno dei diversi Gruppi Acquiferi.

Seguendo tali criteri, nei Bacini di Savigliano ed Alessandria sono state riconosciute diciannove “Unità Idrogeologiche di Sintema”, raggruppate in sette Gruppi Acquiferi.

La ricostruzione del modello idrostratigrafico ha consentito di ritrarre, per la prima volta, la geometria e l'architettura interna dei Gruppi Acquiferi dell'intera successione di età messiniana superiore-quaternaria nel Piemonte meridionale e di ricostruire a scala regionale la distribuzione e le caratteristiche degli acquiferi potenzialmente sfruttabili.

Inoltre, l'utilizzo di vincoli stratigrafici (quali la distribuzione dei contesti deposizionali e delle associazioni di litofacies) ha permesso di ricostruire la geometria dell'interfaccia acqua dolce-salata, anche in quelle aree con dati di pozzo scarsi o mancanti, e di stimare quindi con maggior precisione lo spessore massimo di acquiferi profondi dolci, che finora non erano stati studiati e che tuttora non sono ancora sfruttati.

La ricostruzione idrostratigrafica proposta rappresenta un miglioramento delle precedenti conoscenze sull'idrogeologia del sottosuolo piemontese e getta le basi per lo sviluppo futuro di modelli di potenziale di sfruttamento e modelli di flusso.

**PAROLE CHIAVE:** Bacini messiniano-quaternari piemontesi, Gruppi Acquiferi, Idrostratigrafia, Interfaccia acqua dolce-salata, Sintemi, Stratigrafia fisica, Unità Idrogeologiche di Sintema.

## 1. - INTRODUCTION

The knowledge on Piedmont subsurface hydrogeologic systems mainly regards, up to date, only the uppermost portion of the Pliocene-Quaternary sedimentary pile, namely the first 200-300 m from the ground level. This knowledge essentially derives from hydrogeologic reconstructions, based on simple lithostratigraphic correlations of poor-quality well data, often reducing the reliability of the hydrogeologic models themselves.

Only few studies in Piedmont (BOTTINO *et alii*, 1994a; VIGNA, 1996) have described in detail the aquifer architecture of Pliocene-Quaternary deposits, through the application of a hydrostratigraphic approach, that considers the definition of the actual genetic relationships and geometries of

sedimentary bodies as the essential step to elaborate reliable hydrogeologic and flow system models. Unfortunately, these studies have focused only on local scale.

Owing to the increasing demand of groundwater and the necessity of the Regional Administration (Regione Piemonte) to have a reliable tool for a comprehensive knowledge of all fresh-groundwater resources, a regional hydrostratigraphic study on fresh-water aquifers of the whole upper Messinian-Quaternary successions has been carried out in the southern sector of the Piedmont region. This study focuses on the two main fresh-water reservoirs in southern Piedmont, the Savigliano and Alessandria Basins, and enlarges the investigations up to those depths (namely ca. 1500-2000 m), that were still unexplored for fresh water research purposes.

The aims of this paper are:

- to present the integrated approach used to elaborate the hydrostratigraphic model;
- to illustrate the hydrostratigraphic framework of the Savigliano and Alessandria Basins, by describing the architectural elements of recognised Aquifer Groups;
- to estimate the maximum thickness of potentially exploitable aquifers, illustrating the distribution of the fresh-salt water interface.

## 2. - GEOLOGICAL SETTING

The investigated area is subdivided into three principal domains: the Savigliano Basin, the Alessandria Basin and the interposed Asti area. For the sake of simplicity, in the chapters focusing on stratigraphic and hydrostratigraphic architecture, they will be illustrated as a whole.

The Savigliano Basin shows a dominant N-S elongated shape and is laterally bounded by Alpine Basement units to the west and south, by the Tertiary Piedmont Basin (TPB) succession to the east, and by Torino Hill Tertiary sediments and relative western subsurface prolongation to the north.

The Alessandria Basin displays a prevalent ellipsoidal shape with a NW-SE striking major axis. It is bounded by TPB successions to the south and by the Monferrato successions and relative eastern subsurface prolongation to the north (fig. 1A).

In the Savigliano and Alessandria Basins the Messinian-Quaternary basin fill defines two regional synforms (PIERI & GROPPi, 1981; BELLO & FANTONI, 2002; MOSCA, 2006) and displays maximum thickness of 2000-2500 m in depocentral zones, that are roughly located in the central sectors of the basins (figg. 1B, 3). From the buried depocentral areas, the Messinian-Quaternary succes-

sion progressively thins toward its present-day borders. In the Asti area, placed between the Savigliano and Alessandria Basins, the Messinian-Quaternary succession displays reduced sediment thickness (ca. 800-1000 m) and depicts a gentle antiform.

On the western border of the Savigliano Basin, the thick pile of Messinian-Quaternary deposits is generally sub-horizontal and displays progressive onlap terminations onto older Oligocene-Miocene deposits or on the Alpine Basement, as already illustrated by previous reconstructions (e.g. PIERI & GROPPi, 1981); such a configuration clearly indicates that the western border of the Savigliano Basin represents a preserved original margin (figg. 1, 3). Toward the eastern border of Alessandria Basin, Messinian-Quaternary successions wedge onto older Oligocene-Miocene deposits or on Ligurian units of the Apennines (figg. 1, 3).

The Savigliano and Alessandria Basins developed onto an Oligo-Miocene tectonic belt at the junction between Alps and Apennine systems. The main tectonic structures of this belt have been active also during the Messinian, Pliocene and Pleistocene, controlling the sedimentary evolution of the studied basins and displacing them along major thrust or fault zones. These mainly consist in buried north-verging thrust systems and high-angle strike-slip faults (PIERI & GROPPi, 1981; GHIELMI *et alii*, 2002; MOSCA 2006).

In the Savigliano Basin, the major tectonic features are: (i) E-W striking thrust fronts developed along its southern border, (ii) the Saluzzo-Sommariva del Bosco faulted anticline ("SDB" in fig. 1A) located in the central sector and (iii) the western subsurface prolongation of Torino Hill-Monferrato thrust front, in the northern part.

In the Alessandria Basin, the major tectonic features correspond to complex NW-SE reverse faults and related structural highs, well developed in its north-eastern sector.

The Asti area corresponds to a fault-bounded structural high (hereafter indicated as Asti high; "AH" in figure 1A), placed in between the two basins (MOSCA, 2006).

In the following, the stratigraphic approach followed to delineate a 3D reconstruction of the hydrostratigraphic architecture of the Savigliano and Alessandria Basins is described.

### 3. - STRATIGRAPHIC ANALYSIS

Stratigraphic analysis has been carried out through the integration of subsurface and surface data. A grid of 17 seismic reflection lines (fig. 1C), partially published in MOSCA *et alii* (2009) and ROSSI *et alii* (2009), has been re-interpreted for a

linear coverage of about 750 km. The seismic grid has been analyzed to ca. 2s TWT.

Ten stratigraphic logs of exploration wells (published in AGIP, 1972; AGIP, 1994), have provided a general calibration for seismic interpretation even if, due to the lack of informations on interval-velocities, time-depth conversion has been achieved by using average values of 1600-1800 m/s for Quaternary successions, 1800-2000 m/s for Pliocene successions and 2500-3500 m/s for Messinian successions.

Because of poor resolution of seismic data in the uppermost 100-200 m, the analysis of uppermost Quaternary deposits has been carried out through the stratigraphic correlations of about 6000 shallow wells, that have been made available by the Department of Earth Sciences-Torino University and Regione Piemonte.

Correlation between subsurface and surface geology has been based on local field observations performed along the southern border of the studied basins and integrated with new biostratigraphic analyses, as well as on a critical review of some sheets of the geological maps of Italy: F67 Pinerolo, F80 Cuneo, F56 Torino, F68 Carmagnola, F 57 Vercelli, F58 Mortara, F70 Alessandria, F69 Asti, F71 Voghera at 1:100.000 scale (SERVIZIO GEOLOGICO D'ITALIA, 1913, 1931, 1969a, 1969b, 1969c, 1969d; 1970a, 1970b, 1971) and at 1:50.000 scale, F157 Trino (SERVIZIO GEOLOGICO D'ITALIA, 2003).

In this study, seismic stratigraphic analysis has been used as fundamental tool to reconstruct a reliable 3D stratigraphic reference frame of basins fill and to better characterize the major tectonic structures.

Seismic profiles have been analysed on the basis of conventional seismo-stratigraphic criteria (MITCHUM *et alii*, 1977; BADLEY, 1987). The analysis of reflection terminations has allowed the identification of discontinuity surfaces of regional extent and the subdivision of basins fill into major synthems.

Interpretation of seismic facies has led to identification of major internal patterns and then to preliminary delineation of major depositional systems and lithofacies associations.

The calibration of seismic data with exploration well logs and outcrop features has allowed tracing of those discontinuity surfaces that are not clearly imaged in seismic profiles and defining the distributions of depositional systems and lithofacies associations.

The discontinuity surfaces and synthems have been dated according to the ages proposed by AGIP (1972; 1994) in the exploration wells, as well as those based on biostratigraphic analyses.



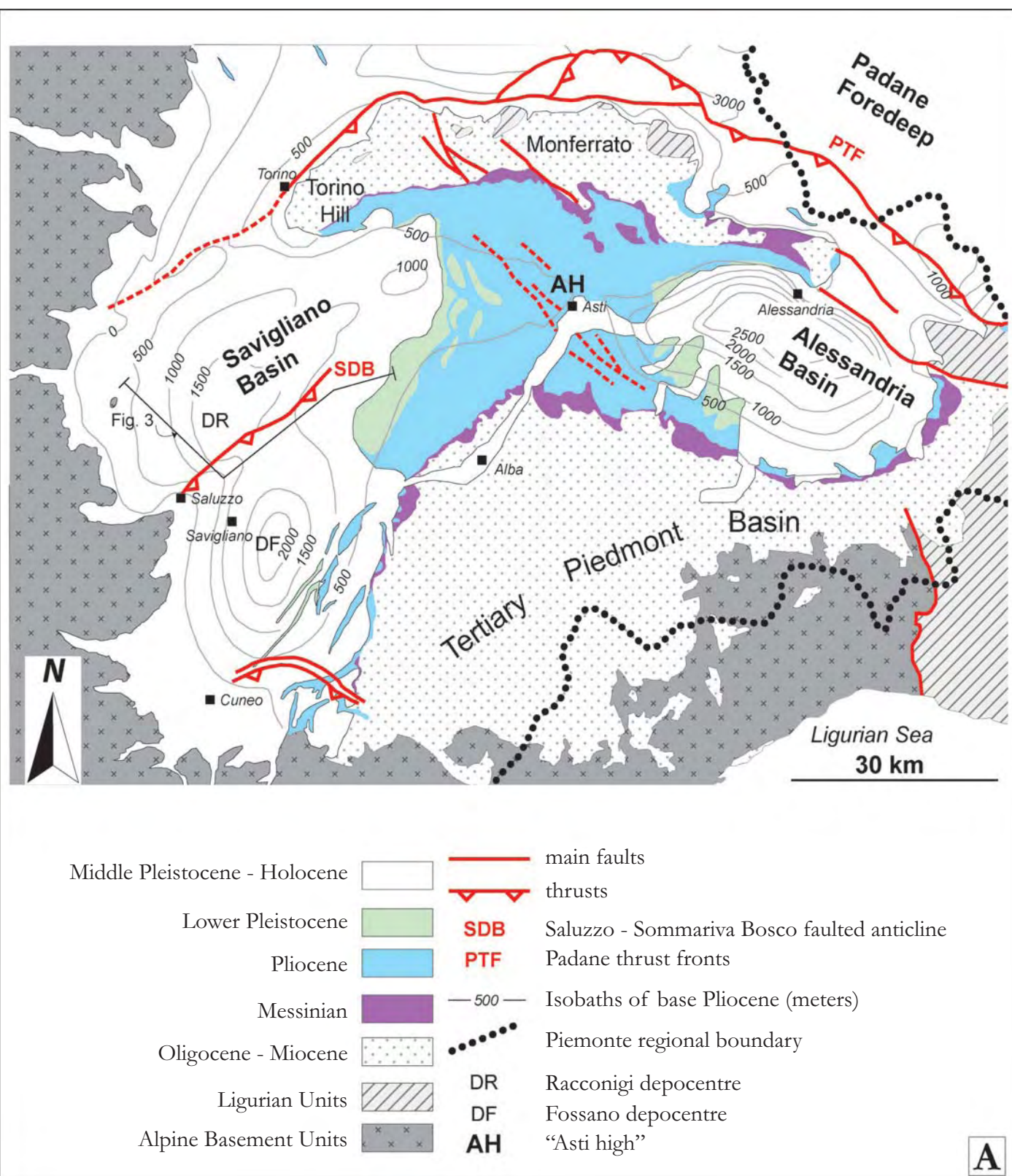
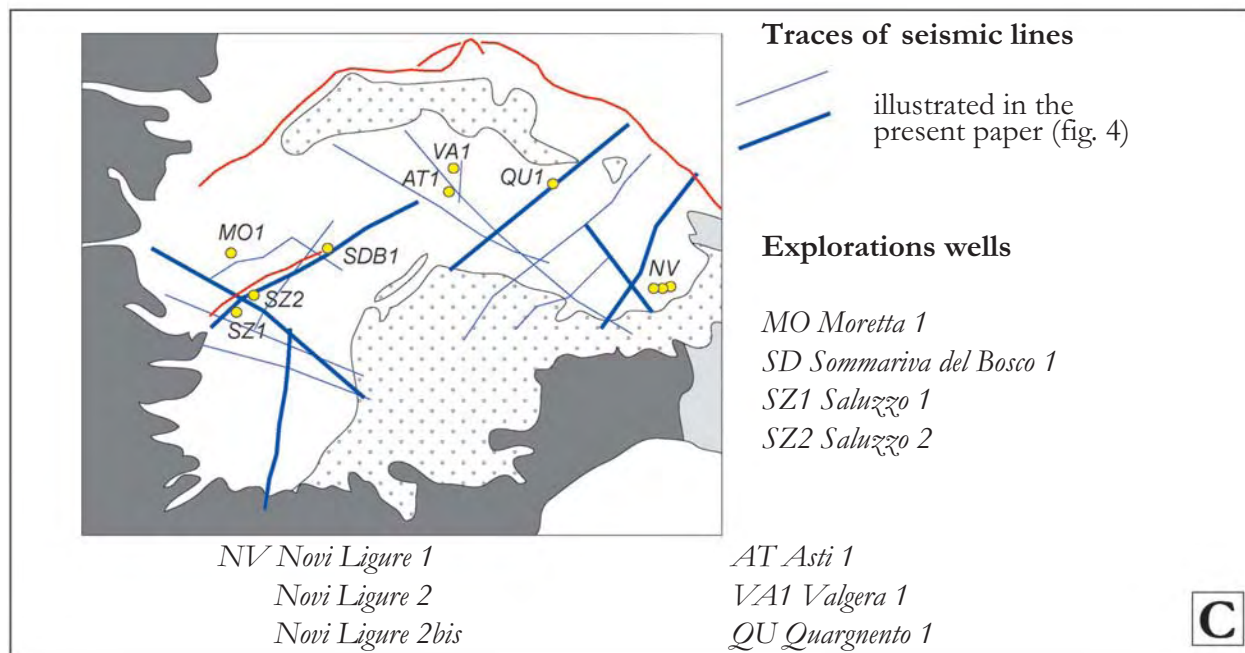
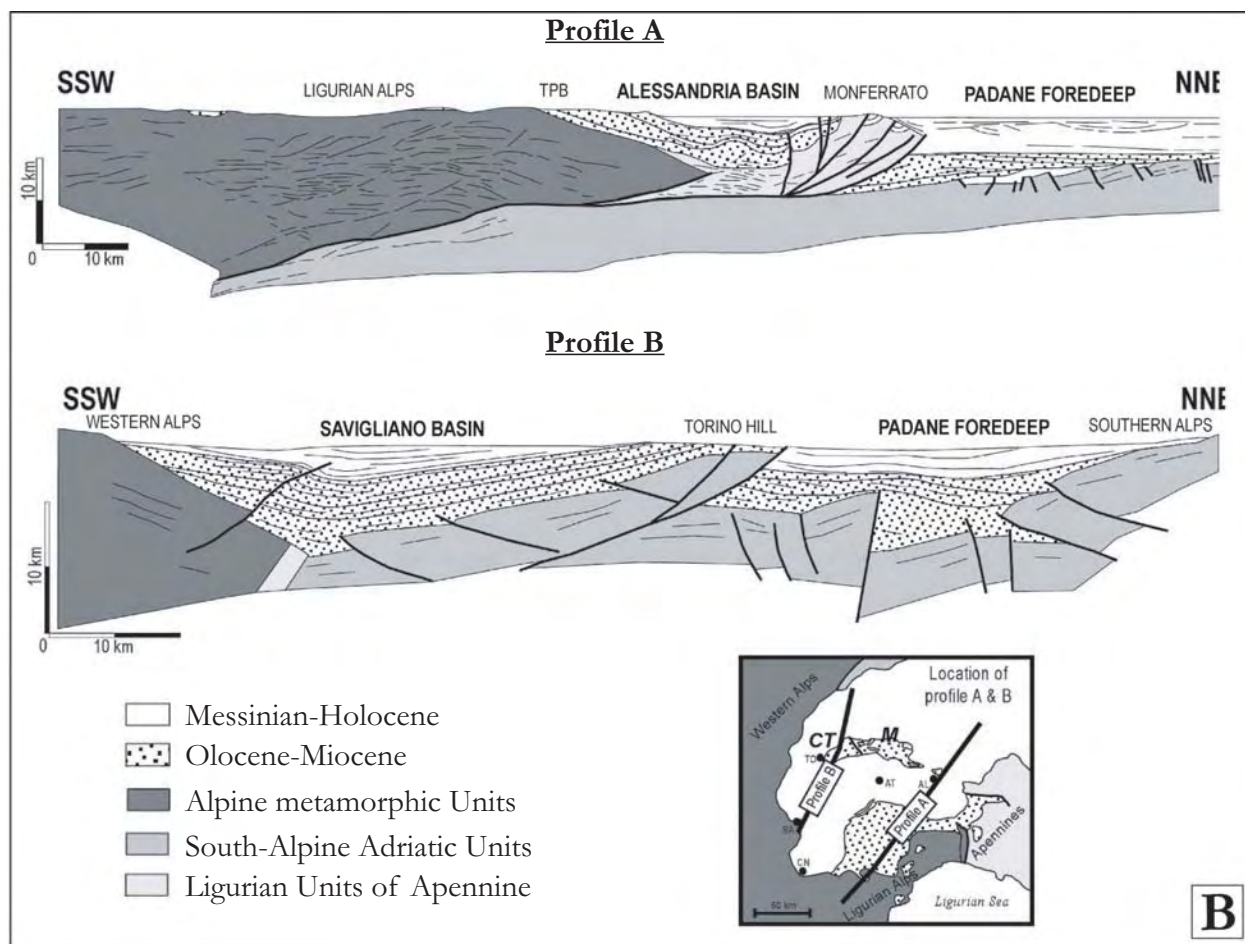


Fig. 1 - (A) Schematic geologic map of southern Piedmont showing the distribution of Alpine metamorphic Units, Ligurian Units of the Apennines, outcrops of Oligocene-Miocene, Pliocene and Quaternary successions and buried Pliocene-Quaternary depocentres, which represent the major fresh-water reserves of this area (modified from BIGI *et alii*, 1990). (B) Regional geologic profiles across main structural domains of Western Po Plain, showing the Alessandria and Savigliano synforms, that can be considered as "piggy back" basins, overthrust onto the Padane Foredeep (modified from CASSANO *et alii*, 1986; FALLETTI *et alii*, 1995; MOSCA, 2006). (C) Location of seismic reflection lines and exploration wells used in this study.





— (A) Schema geologico semplificato del Piemonte meridionale in cui sono rappresentati: le unità metamorfiche della catena alpina, le unità Liguri-Appenniniche, le successioni oligocenico-mioceniche, plioceniche e quaternarie affioranti e i depocentri plio-quaternari sepolti, in cui risiedono i principali acquiferi della regione (modificato da BIGI et alii, 1990). (B) Profili geologici schematici attraverso i principali elementi strutturali della Pianura Padana occidentale: essi mostrano le sinclinali regionali di Alessandria e Savigliano, che a grande scala costituiscono bacini di "piggy-back" sovrascorsi verso nord sulle successioni dell'Avanfossa Padana (modificato da CASSANO et alii, 1986; FALLETTI et alii, 1995; MOSCA, 2006). (C) Ubicazione delle linee sismiche e dei pozzi esplorativi utilizzati nel presente lavoro.

The stratigraphic analysis has allowed to reconstruct a regional depositional framework of the Savigliano and Alessandria Basins that will be briefly illustrated below.

### 3.1. - STRATIGRAPHIC FRAMEWORK OF SAVIGLIANO AND ALESSANDRIA BASINS AND OF THE ASTI AREA

The Messinian-Quaternary succession has been subdivided into 7 unconformity bounded stratigraphic units, corresponding to synthem (CHANG, 1975), that can be correlated across the entire studied area (figg. 2, 3). They include, in stratigraphic order, synthem M1 (upper Messinian), synthem M2 (upper Messinian), synthem P1 (lower Pliocene), synthem P2 (lower-middle Pliocene), synthem P3 (middle-upper Pliocene), synthem Q1 (lower Pleistocene) and synthem Q2 (middle Pleistocene-Holocene).

A complete discussion of the sedimentary and tectonic evolution of the investigated area is well beyond the scope of this paper, which is mainly focused on hydrostratigraphy. Therefore, these topics will be treated only in their general aspects.

The vertical stacking of these synthem represents the product of a large scale regressive-transgressive-regressive cycle, that resulted from the complex interaction between tectonics, relative sea-level variations and climatic changes. Essentially, the basin fill records periods of intense subsidence in depocentral areas (that remained roughly fixed in the central portions of the basins) concomitant with strong tectonic uplift along basin margins (now mainly eroded) and periods of general subsidence (also along the margins) both in the Alessandria and Savigliano Basins and in the interposed Asti area.

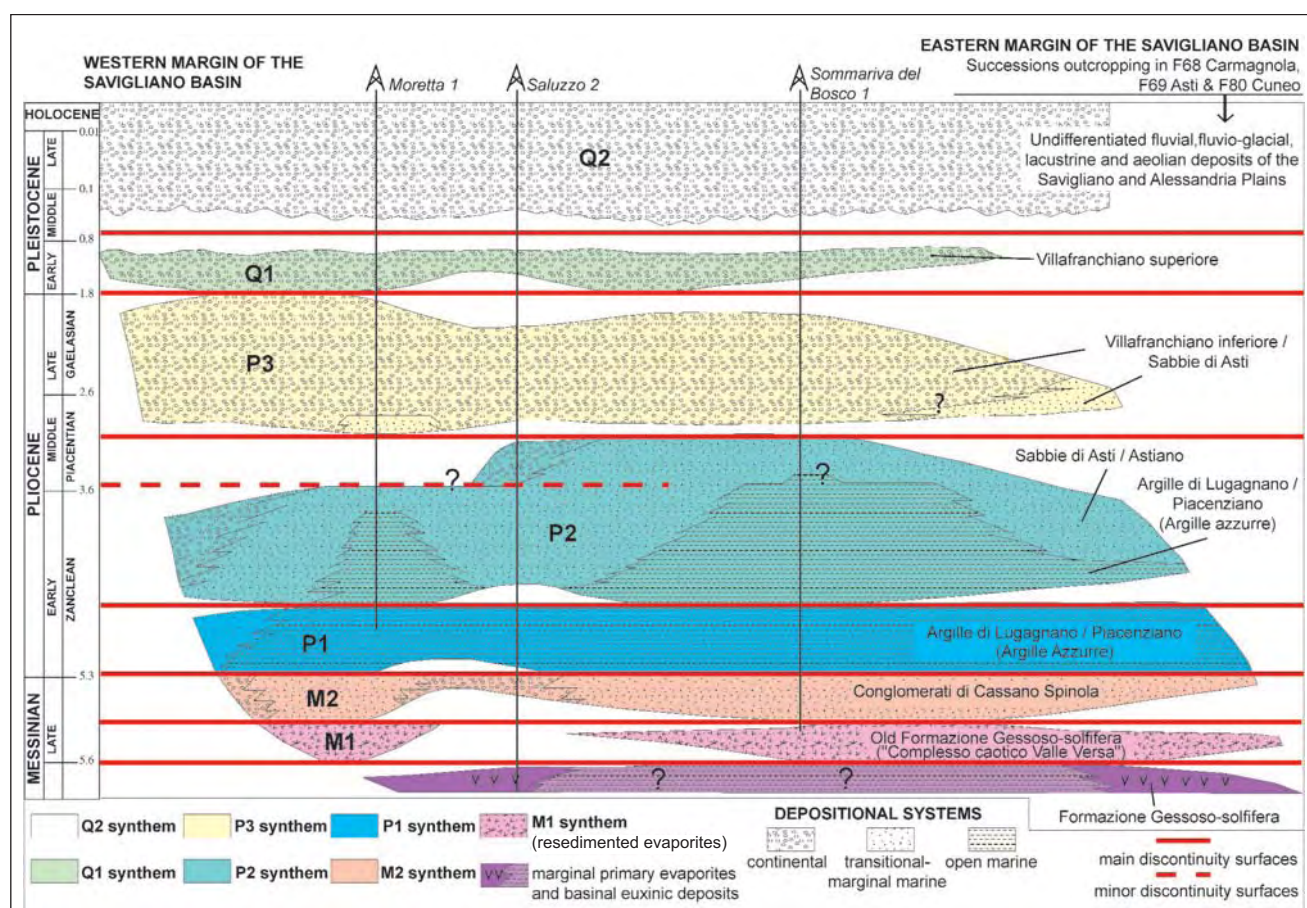


Fig. 2 - Roughly W-E striking chronostratigraphic framework of the Savigliano Basin, connecting its western margin, the depocentral area, and the present-day eastern border (see location in figure 1). Distribution of main depositional systems is illustrated within each synthem. On the right, classic formational names of *Carta Geologica d'Italia* at 1:100,000 scale are indicated for sediments that crop out along the eastern border of the basin. In the present work, continental deposits of P2 are correlated to the lower portion of the "Villafranchiano" in the sheet n. 80 Cuneo (Savigliano Basin). The SZ2 well is located on the Saluzzo-Sommariva del Bosco faulted anticline.

- *Quadro cronostatigrafico del Bacino di Savigliano, elaborato lungo un transetto orientato circa W-E (l'ubicazione è indicata in figura 1), congiungente il margine occidentale sepolto, l'area depocentrale settentrionale e l'attuale margine orientale. All'interno di ogni sintema è illustrata la distribuzione dei principali contesti deposizionali. Sulla destra sono indicati i classici nomi formazionali utilizzati nella Carta Geologica d'Italia alla scala 1:100.000 per le successioni affioranti lungo il margine orientale del bacino. Nel presente lavoro i depositi continentali del sintema P2 sono correlati alla porzione inferiore delle successioni cartografate come "Villafranchiano" nel Foglio n. 80 Cuneo (Bacino di Savigliano). Il pozzo SZ2 è ubicato sull'anticlinale fagliata di Saluzzo-Sommariva del Bosco.*



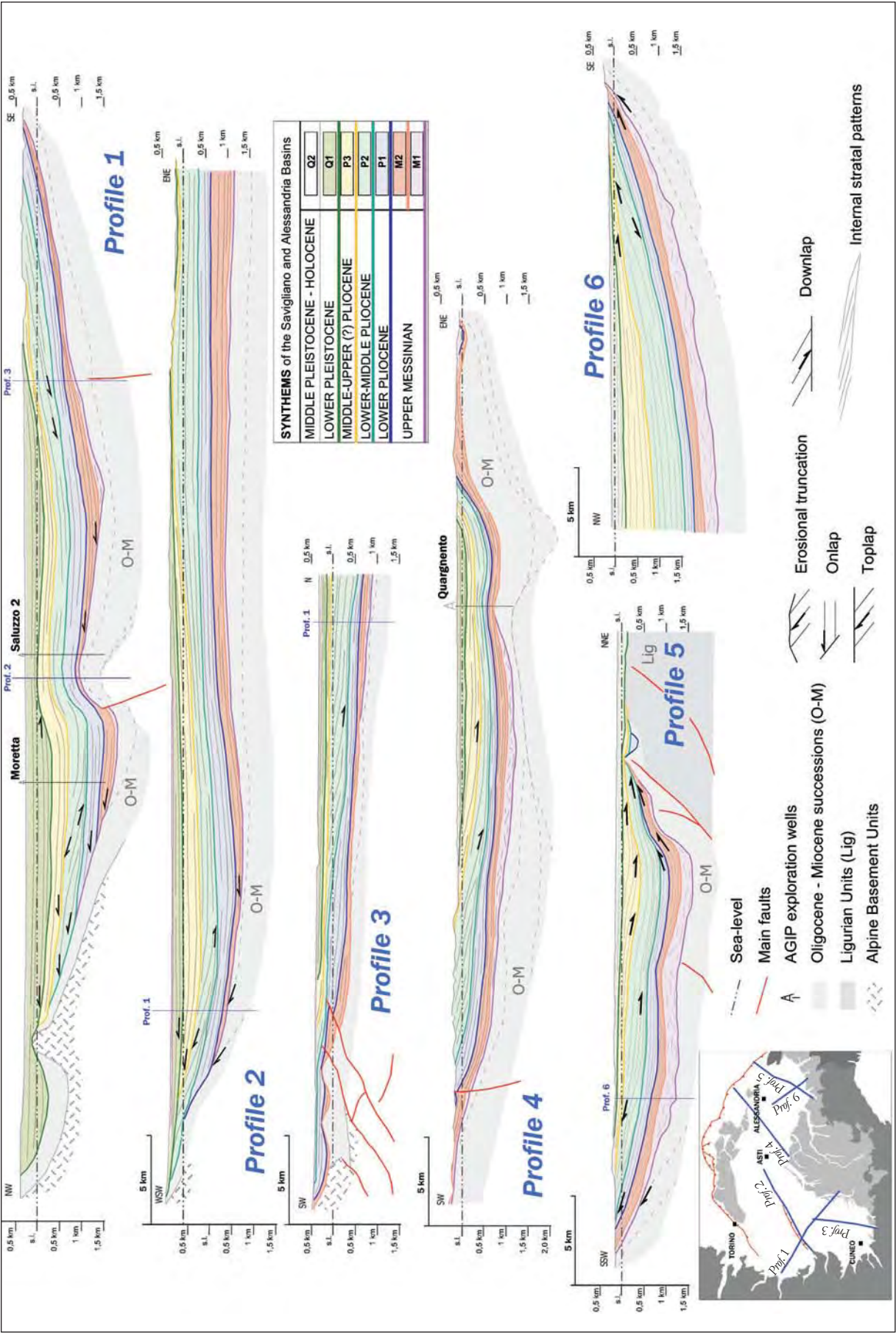


Fig. 3 - Geologic cross-sections showing thickness changes, external geometries and internal configurations of synthems recognized in the Savigliano and Alessandria Basins. Geologic profiles 1 to 6 derive from the seismic stratigraphic analysis of the grid shown on the lower left.

- Profili geologici interpretativi, in cui sono illustrati lo spessore, la geometria esterna e l'architettura interna dei sistemi riconosciuti nei Bacini di Savigliano ed Alessandria. Questi profili derivano dall'analisi sismico-stratigrafica della maglia di profili sismici mostrata in basso a sinistra.



Synthem M1 records a major phase of tectonic uplift (“intra-Messinian tectonic phase”; e.g. GELATI *et alii*, 1987; ROVERI *et alii*, 2003) and erosion of marginal primary evaporites resulting in emplacement of huge complex of resedimented evaporites, the major accumulations of which are located in depocentral areas (figg. 2, 3 - profiles 1,4-6).

Synthem M2 records a relative sea-level rise (i.e. transgressive phase) linked to a period of enhanced subsidence and basin widening (ROVERI *et alii*, 1998). This is documented by the deposition of backstepping wedges of fluvio-deltaic deposits, overlapping against basin margins, which were subject to local tectonic uplift (figg. 2, 3 - profiles 1, 2, 5). The transgressive trend culminated with the sharp deposition of open marine P1 sediments, that mark the re-establishment of fully marine conditions in the Mediterranean, at the end of the Messinian salinity crisis (IACCARINO *et alii*, 1999).

Synthem P2 records periods of renewed sediment flux related to southernmost margins uplift and a strongly increasing volume of sediment supply from the southern areas, through the northward progradation (“forced regression”, see also GHIELMI *et alii*, 2002) of basin-margin and deltaic systems (figg. 2, 3).

Synthem P3 (fig. 2) appears to represent a period of general tectonic subsidence and minor uplift of the margins, concomitant with a progressively increasing supply and aggradation of continental deposits, that were probably fed by the uplift of most internal sectors of the Alps.

Synthem Q1 is introduced by a tectonic pulse responsible for accelerated uplift along basin margins (see also CARRARO, 1996) as well as Asti high (sharp basal angular unconformity in most of profiles of fig. 3), but mainly records a period of general tectonic subsidence (suggested by strong aggradational patterns) and final transition to continental conditions (fig. 2).

Synthem Q2 marks the “closure” of the regressive evolution and records multiple events of continental sedimentation and erosion (BOTTINO *et alii*, 1994b; CAVALLI & VIGNA, 1995).

In the Savigliano Basin, sedimentation was strongly controlled by the Saluzzo-Sommariva del Bosco faulted anticline (fig. 1A; fig. 3 - profile 1, 2). Continued growth of the anticline was coeval with Messinian-Pleistocene regional subsidence, as it is clearly shown by thinning of synthem at the anticlinal crest and by the occurrence of distinct depocentral areas to the north and the south of this structure (“DR” e “DF” in figure 1A).

Thrust fronts to the south also exerted an important control on sedimentation. The growth of these structures caused the sudden uplift of the southern margin of the basin that led to the infill

of northern depozones with widespread progradational systems (synthem P2; fig. 3 - profile 3).

In the Alessandria Basin, sedimentation was strongly controlled by NW-SE reverse faults and related structural highs, that constantly bounded the basin in its northern-east sector (fig. 3 - profile 5). The continued growth of these structures is clearly indicated by progressive syn-tectonic angular unconformities, with local erosional truncation, and by the overall geometry wedging of synthem to the east.

The Asti area was characterized during the Late Messinian, and during the Middle Pliocene and Pleistocene by the growth of a “high” (the “Asti high”) acting as an intrabasinal divide between the Savigliano Basin to the west and Alessandria Basin to the east (fig. 1A). The growth of this high during Pliocene-Pleistocene is strongly supported by the progressive lateral thickening of synthem P2 and Q1 from the “Asti high” toward the central sectors of the Savigliano and Alessandria Basins (fig. 3 - profiles 2,4).

#### 4. - HYDROSTRATIGRAPHY

In this work, due to the poor quality of available subsurface data (e.g. low number of deep cores and absence of core samples; low resolution seismic profiles) as regards the regional scale and the great depths of investigation, it has been assumed that the synthem represents the “operational unit” of the hydrostratigraphic model (fig. 4).

A synthem is a complex sedimentary prism bounded above and below by discontinuity surfaces of regional extent and composed of genetically related strata-sets with variable lithology and geometry, conformably deposited in different but adjoining depositional systems. Internal bedding surfaces can touch but can not intersect the bounding discontinuity surfaces (CHANG, 1975).

##### 4.1. - HYDROSTRATIGRAPHIC VALUE OF SYNTHEMS

Here it has been assumed that the hydrostratigraphic value of synthem mainly depends on their stratigraphic architecture and lithofacies associations (fig. 4).

The stratigraphic architecture is defined by the internal geometry (i.e. internal stratal patterns, imaged by seismic reflectors) of synthem, including for example parallel/aggradational, divergent, progradational or chaotic patterns (for a complete discussion see MITCHUM *et alii*, 1977 and BROWN & FISHER, 1980). A generic hydrostratigraphic value has been assigned to the stratigraphic architecture, since it is known that internal stratal pattern re-pre-

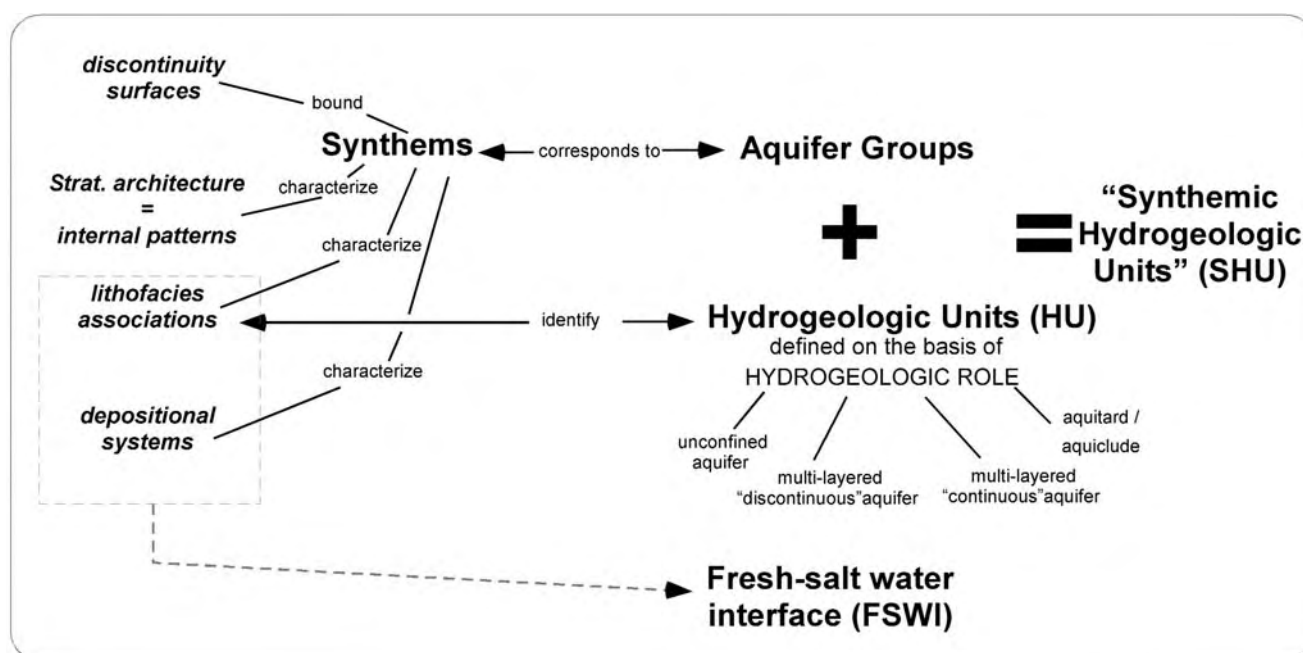


Fig. 4 - Scheme of the relationships between geologic and hydrogeologic concepts adopted for the reconstruction of the hydrostratigraphic framework of the Savigliano and Alessandria Basins.

- Schema delle relazioni tra i concetti geologici e idrogeologici utilizzato per definire il quadro idrostratigrafico dei Bacini di Savigliano ed Alessandria.

sents a prominent factor in controlling main regional groundwater flow directions.

Lithofacies associations (fig. 5) are volumes of sediments, that show homogeneous lithologic properties such as grain size, composition and bedding style.

Eight different lithofacies associations (lf 1 to lf 8) have been defined on the basis of two criteria:

- grain-size ratio, that is the relative percent of coarse grained (sands and gravel) and fine grained (silts and clays/marls) sediments forming the lithofacies association;

- the degree of lateral persistence of sedimentary bodies (both fine and coarse grained), in alternations (lf 2 to lf 7 in fig. 5); lithologic bodies that are more than 2 kilometers long have been considered as “continuous”, whereas those less than 2 kilometers long have been considered as “discontinuous”.

In addition, two lithofacies associations have been recognized (lf 9 and lf 10), that are typical features of synthem M1 and consist of resedimented evaporite complexes.

The lithofacies associations (or group of lithofacies associations), have been subdivided into 4 main typologies of “Hydrogeologic Units” (HU; (1)) (fig. 5), distinguished on the basis of their hydrogeologic characteristics, in the sense that they

represent rock bodies with different water exploitation potential. The four main HU types are: HU1) unconfined aquifers, HU2) multi-layered “discontinuous” aquifers, HU3) multi-layered “continuous” aquifers, HU4) aquitards/aquicludes that have progressively minor water exploitation potential.

#### 4.2. - AQUIFER GROUP AND SYNTHETIC HYDROGEOLOGIC UNIT

In order to elaborate the hydrostratigraphic scheme, it has been assumed that each synthem is conceptually equivalent to an “Aquifer Group” (concept already used in REGIONE EMILIA ROMAGNA & ENI-AGIP, 1998 and in REGIONE LOMBARDIA & ENI-AGIP, 2002) that in this work has been considered as an unconformity bounded sedimentary body (figg. 4, 6), the hydrostratigraphic properties of which are determined by its Hydrogeologic Units, that are in turn dependent on lithofacies associations, and their peculiar stratigraphic architecture.

According to this assumption, hereafter we will use the term “Aquifer Group” instead of “synthem”.

At basin scale, an Aquifer Group will show a distinctive hydrogeologic behaviour (that is: a peculiar response to the regional groundwater flow system)

(1) According to the definition of FRANCANI (1985), in the present work, an Hydrogeologic Unit corresponds to a lithofacies association or group of lithofacies associations that shows homogeneous hydrogeologic properties (e.g. permeability ratio, storage coefficient) at regional scale.

		Lithofacies associations (If)	Main typologies of Hydrogeologic Units (HU)	HYDROGEOLOGIC ROLES
"DISCONTINUOUS" ALTERNATIONS		<b>If 1</b> sands & gravels with subordinate silty-clayey interbeds (silty-clays 0-20%, sands+gravels 80-100%)	<b>HU I</b>	<b>UNCONFINED AQUIFERS</b>
		<b>If 2</b> discontinuous alternations of prevailing sands and gravels, and silty-clays (silty-clays 20-40%, sands+gravels 60-80%)		
		<b>If 3</b> discontinuous alternations of silty-clays, sands & gravels (silty-clays 40-60%, sands+gravels 40-60%)	<b>HU II</b>	<b>MULTI-LAYERED "DISCONTINUOUS" AQUIFERS</b>
		<b>If 4</b> discontinuous alternations of prevailing silty-clays, and sands & gravels (silty-clays 60-80%, sands+gravels 20-40%)		
"CONTINUOUS" ALTERNATIONS		<b>If 5</b> continuous alternations of prevailing sands and gravels, and silty-clays (silty-clays 20-40%, sands+gravels 60-80%)	<b>HU III</b>	<b>MLTI-LAYERED "CONTINUOUS" AQUIFERS</b>
		<b>If 6</b> continuous alternations of silty-clays, sands & gravels (silty-clays 40-60%, sands+gravels 40-60%)		
		<b>If 7</b> continuous alternations of prevailing silty-clays, and sands (clays 60-80%, sands 20-40%)		
		<b>If 8</b> clays with subordinate sandy and gravelly interbeds (clays 80-100%, sands 0-20%)	<b>HU IV</b>	<b>AQUITARDS / AQUICLUDES</b>
		<b>If 9</b> chaotic deposits consisting of gypsum and carbonate blocks, floating in a clayey matrix (silty-clays 60-70%)		
		<b>If 10</b> alternations of gypsarenites-rudites and silty-clays (60-70%)		

Fig. 5 - Scheme showing the relationships between lithofacies associations (or group of lithofacies associations) and four main typologies of Hydrogeologic Units (HU), that are defined on the basis of their hydrogeologic characteristics. HU I represents an unconfined aquifer with high permeability; HU II & HU III are multilayered aquifers, with median values of permeability (these 2 typologies are differentiated on the basis of the vertical conductivity: good to moderate in HU II and very low in HU III); HU IV represents an aquitard or rarely an aquiclude.

- Schema illustrante le corrispondenze fra associazioni di litofacies (o gruppi di associazioni di litofacies) e le quattro principali tipologie di Unità Idrogeologiche (HU), che sono definite sulla base del loro ruolo idrogeologico. La tipologia HU I rappresenta un acquifero libero, caratterizzato da buona permeabilità; le tipologie HU II e HU III sono acquiferi multistrato, con valori intermedi di permeabilità (queste due tipologie sono state distinte sulla base della diversa conducibilità idraulica verticale: da buona a media per HU II e molto bassa per HU III); la tipologia HU IV ha ruolo di acquitardo o, in casi meno frequenti, di acquicludo.

in comparison with other Aquifer Groups, since each one of them has its own stratigraphic architecture, that strongly control the flow directions.

As a consequence, it is necessary to assume that, within each Aquifer Group, the same Hydrogeologic Unit does present peculiar and contextual properties. In other words, the same typology of Hydrogeologic Unit will display partially different hydrogeologic features, depending on the characteristics of the Aquifer Group it belongs to.

For example, the HU1) main typology will display peculiar features (e.g. stratigraphic architecture, compaction and cementation degree) and then will show a different behaviour as regards the regional groundwater flow, depending on whether it belongs to a shallower aquifer group (e.g. B Aquifer Group) or it belongs to a deeper aquifer group (e.g. D Aquifer Group). For these reasons we coined a new concept labelled as "Synthetic Hydrogeologic Unit" (fig. 4; hereafter SHU). Each SHU will be indicated with an acronym, composed by the capital letter of the Aquifer Group it belongs to and by a roman numeral referred to the main typology of Hydrogeologic Unit it derives from (figg. 6, 7).

The choice of the "Aquifer Group" as a key concept to elaborate the hydrostratigraphic model,

is supported by the well known fact that, at basin scale, groundwater flow paths are mainly parallel to internal bedding surfaces (at least for what concerns lateral flow paths, according to the model of TOTTH, 1963), and therefore, these flows remain mostly confined within the same Aquifer Group, although vertical exchanges among different aquifer groups can locally take place.

In this sense the concept of "Aquifer Group" has a similar but not equal meaning to that proposed by REGIONE EMILIA-ROMAGNA & ENI-AGIP (1998). In the present work in fact the "Aquifer Group" is defined only on the basis of its bounding discontinuities and internal architecture, whilst in the reconstruction of REGIONE EMILIA-ROMAGNA & ENI-AGIP (1998), the occurrence of regionally extended fine-grained interval (that can guarantee the hydraulic insulation between vertically stacked Aquifer groups) was assumed as key discerning factor.

#### 4.3. - CRITERIA TO IDENTIFY THE FRESH-SALT WATER INTERFACE

The surface that separates fresh- from deeper salt (2)-groundwaters (for brevity fresh-salt water

(2) According to AGIP (1994), salt waters are here considered those showing concentrations of soluted ions heavier than 1 g/l, and then also the brackish waters.



interface; FSWI) is another fundamental key factor that governs the location of groundwater resources.

The reconstruction of geometry and positioning of FSWI is of extreme importance, since it corresponds to the lower boundary of freshwater aquifers that are potentially exploitable for drinking, municipal and agricultural purposes.

The recognition of large scale position and geometry of this surface in Piedmont region subsurface was based, up to date, on core and spring data correlations (BORTOLAMI *et alii*, 1982; ABATUCCI *et alii*, 2005), performed regardless of complex spatial heterogeneity of sedimentary bodies in the Messinian-Quaternary basins.

In the present work the reconstruction of the distribution and geometry of FSWI was based on the integration of core data and geologic interpretations (i.e.: depositional systems, lithofacies associations and present day position of Aquifer Groups) and it was not supported by hydrogeologic data.

In this study, the concept of depositional system (fig. 4) was used, that is believed to hold, together with the lithofacies associations, a

fundamental role on 3D distribution of fresh- and salt- groundwaters. The knowledge of the depositional system is a reliable tool for prediction of FSWI subsurface geometrical trend and distribution, also in those areas with scarce constraints on saltwaters location at depth.

Integrated analysis of available data set made it possible to recognize only major groups of depositional systems, that are: continental systems (co), transitional-marginal marine systems (tm) and open marine systems (om) (fig. 2, 7).

Although transitional-marginal marine sediments are originally permeated by salt-water during deposition, they can be permeated by fresh-water in a second time (REGIONE EMILIA-ROMAGNA & ENI-AGIP, 1998). These sediments in fact can receive, directly from continental areas, great amount of recharge (meteoric and alluvial) fresh water, that is able to displace the connate saltwaters.

Moreover, it is known that saltwaters displacement can be more effective during forced regressions (REGIONE EMILIA-ROMAGNA & ENI-AGIP, 1998), when FSWI is forced to follow the downward shift of sea-level.

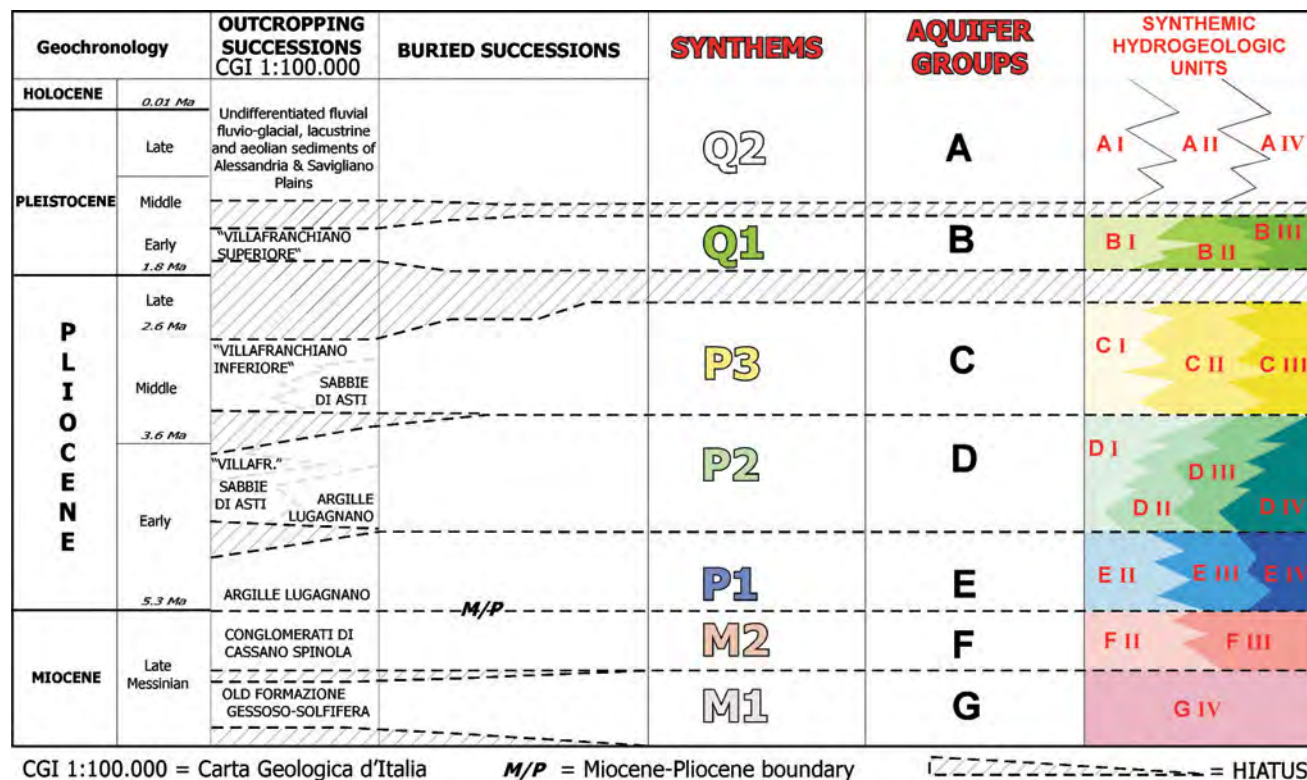


Fig. 6 - Simplified hydrostratigraphic framework of the Savigliano and Alessandria Basins showing the links between synthems, Aquifer Groups and Synthetic Hydrogeologic Units. On the left, classic formational names of *Carta Geologica d'Italia* at 1:100.000 scale are indicated for outcropping successions. Note that, according to present work, the successions mapped as "Villafranchiano" are split by 2 discontinuity surfaces and belong to 3 different synthems: P2, P3 and Q1. - Quadro idrostratigrafico riassuntivo dei Bacini di Savigliano e Alessandria, in cui sono illustrate le corrispondenze tra sintemi, Gruppi Acquiferi ed Unità Idrogeologiche di Sintema. Sulla sinistra sono indicati i classici nomi formazionali utilizzati, nella Carta Geologica d'Italia alla scala 1:100.000, per le successioni affioranti. Si noti che, secondo il presente lavoro, le successioni "Villafranchiane" s.l. sono suddivise da 2 superfici di discontinuità, venendo così ad appartenere a tre differenti sintemi: P2, P3 e Q1.

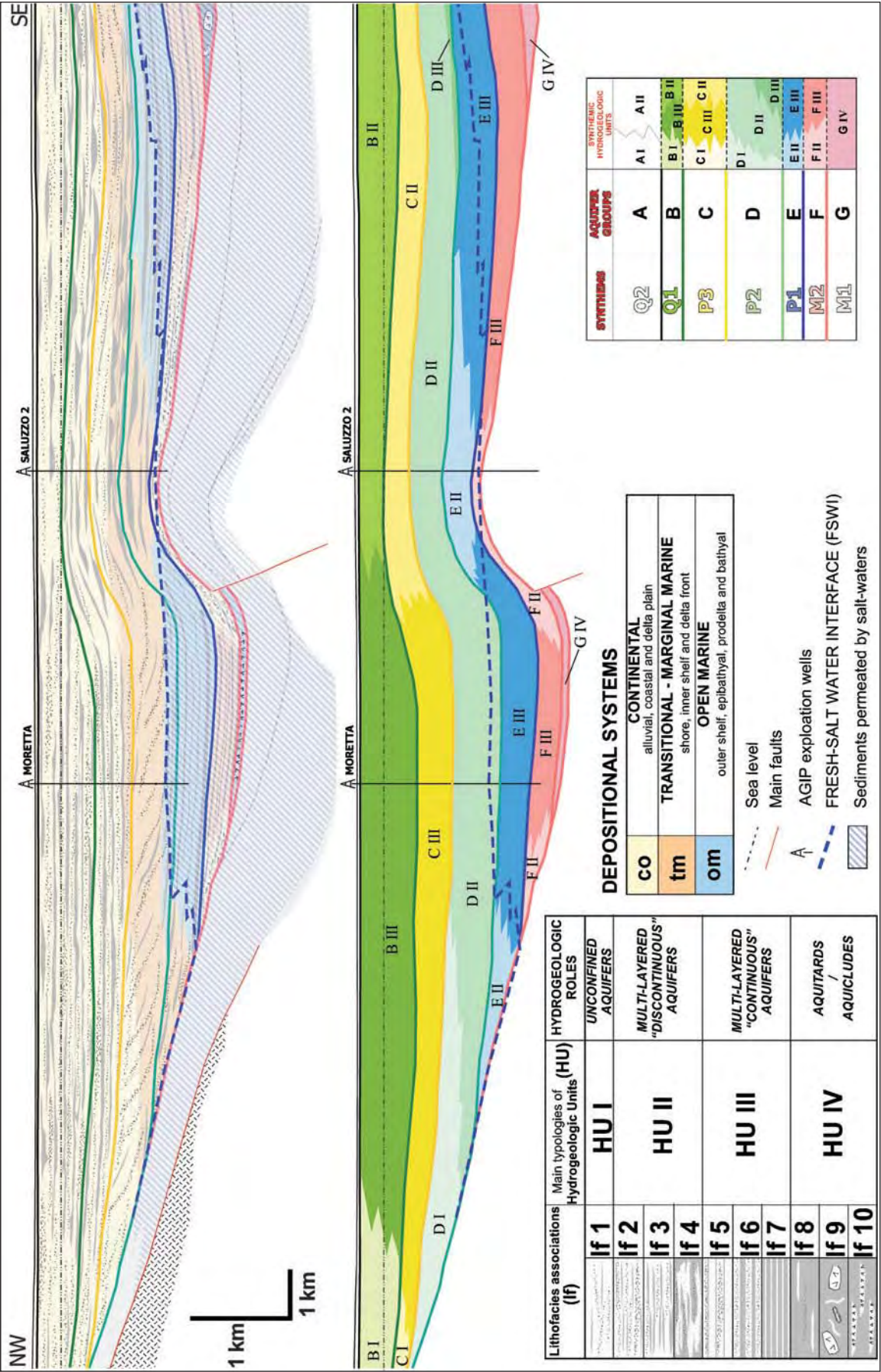


Fig. 7 - Detailed geologic (upper part) and hydrostratigraphic (lower part) section across the Savigliano Basin, portraying the central segment of profile 1 in figure 4. Internal patterns of synthems as well as the spatial distribution of lithofacies associations and depositional systems are illustrated. Note the lateral and vertical stacking patterns of Synthetic Hydrogeologic Units within each Aquifer Group. Note also the "saw-tooth"-like inferred geometry of the fresh-salt water interface (dashed blue line) on the left, where no one constraint on saltwaters location was available.

- Sezione geologica (parte superiore) ed idrostratigrafica (parte inferiore) di dettaglio del Bacino di Savigliano, raffigurante la porzione centrale del profilo 1 di figura 4. Sono illustrate la geometria interna dei sintemi, la distribuzione delle associazioni di litofacies dei contesti deposizionali. Si notino gli schemi di impilamento laterale e verticale delle Unità Idrogeologiche di Sistema all'interno dei Gruppi Acquiferi. Si noti inoltre verso sinistra l'andamento ipotizzato a "denti di sega" dell'interfaccia Acqua dolce-salata (tratteggio blu). Tale geometria è stata ipotizzata in base ai vincoli stratigrafici forniti dai contesti deposizionali.



For these reasons, it has been operatively assumed that the position of FSWI should be located within open marine settings or at the boundary between marginal marine and open marine settings.

As above mentioned, the distribution of the lithofacies associations (fig. 4) also play an important role on saltwater distribution. In this study, they have been therefore carefully considered in delineating FSWI position. Specifically, since saltwaters appear to be mainly confined in fine grained strata, it has been operatively assumed to trace FSWI within fine-grained lithofacies associations or close to the boundary between fine-grained lithofacies associations and coarse-grained lithofacies ones, which are more water-transmissive and then they are likely permeated by freshwater.

It is important to stress that the above assumptions are reliable only as regard the depocentral zones, whereas they gradually lose validity toward the margins of the basins, in which the original (i.e. syn-depositional) distribution of connate saltwaters could be very likely modified by post-depositional tectonic factors. Specifically, along these margins, tectonics may have caused tilting, uplift and erosion of open marine successions, allowing displacement of connate saltwaters (REGIONE EMILIA-ROMAGNA & ENI-AGIP, 1998). Therefore, along marginal areas devoid of resolution core and spring data, it is not always possible to infer the distribution of FSWI, whose positioning is necessarily interpretative.

## 5. - HYDROSTRATIGRAPHIC ARCHITECTURE

It is here presented the hydrostratigraphic architecture of the Savigliano and Alessandria basins and of the Asti area, in which 7 Aquifer Groups have been defined and labelled with capital letters from G to A, that is from the oldest to youngest one (figg. 6, 7).

It is worth noting that Aquifer Groups A, B, C and D do not physically correspond with the Aquifer Groups A, B, C and D recognized in the adjoining areas (i.e. Regione Emilia Romagna and Regione Lombardia).

In the next sections, the Aquifer Groups are described by (i) their overall stratigraphic architecture and geometry (ii) and their general pattern of distribution of thickness, depositional systems and Synthemic Hydrogeologic Units.

However, the map distribution of all these characters will be portrayed only for one Aquifer Group (i.e. D Group; fig. 8).

### 5.1. - AQUIFER GROUP G (SYNTHEM M1)

Aquifer Group G is characterized by a chaotic (fig. 3) stratigraphic architecture. It reaches maximum thickness of 400 m in the central portion of the Alessandria Basin (fig. 3, profiles 5,6) and 150 m in the northern sector of the Savigliano Basin.

From depocentral zones, G Group progressively tapers toward the present-day basin margins. It wedges out toward the western margin of the Savigliano Basin as well as on the Asti high. It thins out below the overlying F Aquifer Group, towards the eastern border of the Alessandria Basin.

Aquifer Group G is entirely composed by slope and basin resedimented evaporites, that consist of chaotic sediments (Alessandria B.) and subordinate stratified sediments (central belt of Savigliano B.). Chaotic sediments are made up of m to hm-sized blocks of evaporite rocks (including primary selenite, microcrystalline gypsum and gypsarenites/gypsrudites) and carbonate rocks, randomly distributed in a fine-grained matrix. Stratified sediments consist of laterally discontinuous strata of gypsarenite/gypsrudite, embedded into clayey deposits.

These units can be correlated to the chaotic successions that, in the outcrops, have been historically included (along with in place primary evaporite) into the “Formazione Gessoso-solfifera”, but they actually form a younger stratigraphic interval, that has been recently ascribed to the “Complesso caotico della Valle Versa” (DELA PIERRE *et alii*, 2003; IRACE, 2004; IRACE *et alii*, 2005) (figg. 2, 6).

These deposits can thus be considered as time equivalent to the resedimented evaporites recently recognized in most of circum-Mediterranean Messinian basins (ROVERI *et alii*, 2008) and can be referred to the lower part of the post-evaporitic interval (p-ev1 *sensu* ROVERI *et alii*, 2003).

Group G only consists of SHU GIV that, at regional scale, represents an aquitard/aquiclude (figg. 6, 7). By contrast marked permeability, owing to karstification, can locally characterize the large scale evaporite blocks exposed on present day margins (FIORASO *et alii*, 2004).

### 5.2. - AQUIFER GROUP F (SYNTHEM M2)

Aquifer Group F is characterized by a parallel to basinward-divergent stratigraphic architecture (fig. 3).

It shows maximum thickness of 400m both in the central-northern sector of the Savigliano Basin and in the western area of the Alessandria Basin, close to the eastern side of the Asti high deformational zone. On the latter minor thickness (ca. 150



m) is preserved. Moving from the buried areas to the present-day northern and southern margins, Aquifer Group F progressively thins, up to 100 m, displaying local onlap terminations on the underlying Aquifer Group G (fig. 3). It thins out both toward the western margin of the Savigliano Basin and the eastern border of the Alessandria Basin, through progressive onlap terminations onto older Oligocene-Miocene successions (fig. 3, profiles 1, 5). To the north-east it is also truncated by the erosional unconformity at the base of Aquifer Group D.

Aquifer Group F mainly consists of transitional deposits, represented by regular alternations of sands and clays, that are widespread in depocentral areas. Whereas towards the margin of the Savigliano Basin as well as the northern and southern regions of the Alessandria Basin these facies laterally pass to time-equivalent fan deltas deposits (e.g. GHIBAUDO *et alii*, 1985) that, in the outcrops, have been classically mapped as “Conglomerati di Casano-Spinola” (fig. 3, 6). All these units can be referred to the “Lago-Mare” interval (p-ev2 *sensu* ROVERI *et alii*, 2003).

Most of Group F consists of SHU FIII (figg. 6, 7), that plays the role of multi-layered “continuous” aquifer, whereas SHU FII, that represents a multi-layered “discontinuous” aquifer, occurs along the western margin of Savigliano Basin and the southern border of Alessandria Basin.

### 5.3. - AQUIFER GROUP E (SYNTHEM P1)

Aquifer Group E is characterized by a predominant parallel stratigraphic architecture and by aggradational geometries (fig. 3).

Major accumulations are in the order of 400 m in the central-northern part of the Savigliano Basin. They gradually decrease to 300 m on the Asti high, up to 200 m in the central sector of the Alessandria Basin. From depocentral areas, Group E thins toward present day northern and southern margins (fig. 3, profiles 1,3,5,6), where average thickness are of about 100 m. It displays an abrupt thinning out to the north-east (fig. 3, profile 5), being truncated by the basal erosional surface (associated to an angular unconformity) of overlying Aquifer Group D. Moreover, group E wedges out also at the western border of the Savigliano Basin, onlapping onto Oligocene- Miocene successions.

The bulk of the Aquifer Group E consists of open marine (fine to coarse-grained) deposits that, in the outcrops, have been classically ascribed to the “Argille di Lugagnano” or “Piacenziano”, and recently to the “Argille Azzurre” (figg. 2, 6).

However, along the western margin of the Savigliano Basin, open marine deposits laterally grade into time equivalent transitional deposits (figg. 2, 7),

recognized in the exploration wells sections.

Group E mainly consists of SHU EIII (figg. 6, 7), that represents a multi-layered “continuous” aquifer. In the Asti area as in southern regions of Alessandria Basin and eastern sector of Savigliano Basin, SHU EIV occurs, with the role of aquiclude. Instead, in western margin of SB, Group E comprises SHU EII, that represent a multi-layered “discontinuous” aquifer.

### 5.4. - AQUIFER GROUP D (SYNTHEM P2)

Aquifer Group D is characterized by a progradational stratigraphic architecture, that originated from progradation of basin-margin and deltaic systems from southern and south-western margins, toward the north/north-east.

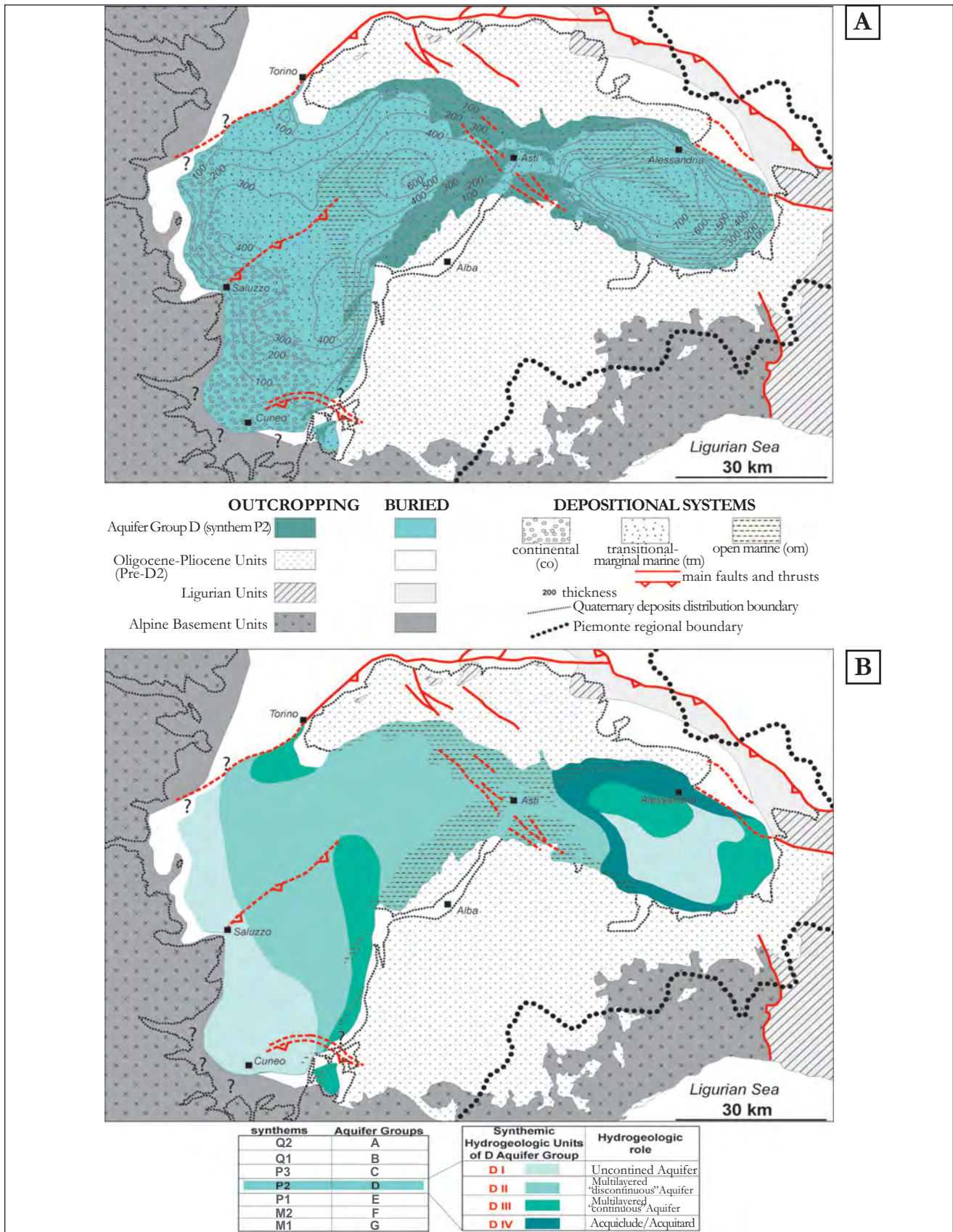
Sub-horizontal topset packages (figg. 3, 7) are excellently preserved only in the subsurface of Savigliano Basin (southwestern margin). They consist of coarse-grained delta plain deposits (figg. 7, 8A) that are correlatable to continental successions exposed in the southernmost region of the Savigliano Basin (figg. 2, 6; lower portion of the “Villafranchiano” in the sheet F80 Cuneo (SERVIZIO GEOLOGICO D'ITALIA, 1931) also described by CAVALLI & VIGNA (1995).

Foreset packages (figg. 3, 7) are well-developed throughout the distribution area of Aquifer Group D and consist of marginal marine deposits (fig. 8A). These units can be correlated with sand-rich successions that, in the outcrops, have been classically referred to the “Sabbie di Asti” or “Astiano” (figg. 2, 6).

Foreset packages frontally pass to bottomset strata (figg. 3, 7), which consist of open marine deposits. These sediments are mostly buried in depocentral zones (fig. 8A), but they are locally exposed along southern present-day margins, where they correspond to the uppermost portion of clayey and sandy successions, known as “Argille di Lugagnano” or “Piacenziano” (figg. 2, 6) in the literature (now “Argille Azzurre”).

Group D reaches maximum thickness (fig. 8A) on the order of 600-700 m in the north eastern part of the Savigliano Basin, close to the western border of the Asti high and in the central area of the Alessandria Basin. Maximum thickness of 400 m are preserved to the south and to the north of the SDB faulted anticline. On the Asti high, Group D displays thickness of about 200 m. Generally, Group D deposits thin moving from buried depocentral areas to the present day borders (fig. 3, profiles 2, 6; fig. 8A), however considerable thickness can also be locally observed along the margins (e.g. fig. 3, profile 4).

Along the western border of the Savigliano





Basin, Group D wedges out onlapping onto older Oligocene-Miocene deposits (fig. 3, profiles 1,2). Toward the eastern margin of the Alessandria Basin Group D progressively thins out onlapping, through an angular unconformity, on southwestward tilted Aquifer Groups E and F and Miocene deposits (fig. 3, profile 5).

The articulated stratigraphic architecture of Aquifer Group D gives rise to a quite composite distribution of synthem hydrogeologic units (fig. 8B).

The SHU DI (with the role of unconfined aquifer) occurs both along western margin of Savigliano Basin and in the central area of Alessandria Basin, and, more specifically, it is distributed in the upper part of the Aquifer group. The SHU DII (with the role of multi-layered “discontinuous” aquifer) is distributed in large part of Savigliano Basin and in the Asti area. The SHU DIII (with the role of multi-layered “continuous” aquifer) occurs both along eastern margin of Savigliano Basin as well as in the central and eastern areas of Alessandria Basin, and, more specifically, in the lower part of the Aquifer Group D. The SHU DIV (with the role of aquiclude) can be found along most of present-day borders of Alessandria Basin.

#### 5.5. - AQUIFER GROUP C (SYNTHEM P3)

At regional scale, Aquifer Group C shows a characteristic divergence of strata packages toward depocentral areas and has an internal aggradational organization, that strongly contrasts with the clinostratified geometry of underlying Aquifer Group D (fig. 3). Only in the Alessandria Basin minor progradational patterns are recognizable (fig. 3, profile 4,5).

Group C reaches maximum thickness of 500 m in the central and northern part of Savigliano Basin (fig. 3, profiles 1,2) and 700 m in the Alessandria Basin (fig. 3, profile 6). From depocentral areas, Group C markedly tapers toward present day northern and southern margins, where thickness are in the order of 100 m. Group C thins out towards the western border of the Savigliano Basin and the eastern border of the Alessandria Basin (fig. 3, profiles 1,2,5), through progressive onlap terminations onto underlying Aquifer Group D and older Miocene strata. On the Asti high, only some tens of meters of Group C successions are preserved, owing to the superimposition of syn-tectonic condensation and post-depositional erosion.

In the Savigliano Basin, Group C consists of peat-rich continental deposits (fig. 7), that progressively pass to transitional sediments in the Asti high and Alessandria Basin. These units can be correlated to the continental lagoon and deltaic successions that, in the outcrops, have been ascribed

to the “Villafranchiano inferiore” (figg. 2, 6).

Aquifer Group C is made up of three synthem hydrogeologic units (fig. 6, 7). SHU CI (unconfined aquifer) occurs in north-western margin of Savigliano Basin, in all the Asti zone and in southern regions of Alessandria Basin. SHU CII (multi-layered “discontinuous” aquifer) constitutes all southern area of Savigliano Basin and also forms a narrow belt in the Alessandria Basin depocenter. SHU CIII (multi-layered “continuous” aquifer) can be found in the northern depocentral zone of Savigliano Basin (fig. 7), and it is also present along Alessandria Basin northern margin.

#### 5.6. - AQUIFER GROUP B (SYNTHEM Q1)

Aquifer Group B is characterized by parallel-aggradational internal geometries and in the investigated basins forms two large scale lenticular bodies, separated by the Asti high deformational zone.

In the Savigliano Basin, Group B displays maximum thickness of 500-600 m to the south and to the north of the SDB faulted anticline (fig. 3, profile 1), whereas in the Alessandria Basin depocenter it shows maximum thickness of about 300 m (fig. 3, profiles 4, 6).

From depocentral areas, Group B progressively thins towards present day northern and southern margins, where thickness are in the order of 50-100 m. Towards the western margin of the Savigliano Basin, Group B markedly wedges out and unconformably rests, through progressive onlap terminations, onto underlying Aquifer Groups C and D, older miocene strata and also directly onto basement units (fig. 3, profiles 1, 2). At the eastern border of the Alessandria Basin Group B unconformably rests on Ligurian units of the Apennines, and then it become thicker moving to the NE (fig. 3, profile 5).

In most of Savigliano and Alessandria Basins, Group B consists of continental deposits (fig. 7), correlatable to fluvial successions that, in the outcrops, have been referred to the “Villafranchiano superiore” (figg. 2, 6). These deposits grade into transitional (coastal?) facies toward the Alessandria depocenter.

Group B mainly consists of SHU BII. It represents a multi-layered “discontinuous” aquifer, that characterizes all the Alessandria Basin area, as well as the northern margin and a large part of the southern depocenter of Savigliano Basin. SHU BI, corresponding to an unconfined aquifer, constitutes a wide belt along western margin of Savigliano Basin. SHU BIII with the role of multi-layered “continuous” aquifer is restricted to the northern depocenter of Savigliano Basin (fig. 7).



### 5.7. - AQUIFER GROUP A (SYNTHEM Q2)

It is the shallowest Aquifer Group recognized. It entirely consists of continental deposits, and groups fluvial/fluviog-lacial, lacustrine and aeolian sediments, on which the present day Savigliano and Alessandria Plain areas rest (figg. 2, 6).

Aquifer Group A shows maximum thickness of about 60-80 m in western and southern borders of the Savigliano Plain and in southern zones of the Alessandria Plain (axial part of alluvial fans and channel belts). It thins up to few meters toward their central and northern areas.

Aquifer Group A mainly consists of (fig. 6) SHU AI (unconfined aquifer) and SHU AII (multi-layered "discontinuous" aquifer) and secondarily of SHU AIV (aquitard/aquiclude). SHU AI is well developed in the central-southern areas of Savigliano Basin and in the central sector of Alessandria Basin. SHU AII occurs in the northern part of Savigliano Basin and in most of Alessandria Basin.

SHU AIV is relegated to the northern borders of the basins.

### 6. - THE FRESH-SALT WATER INTERFACE

On a large scale, the FSWI displays a regular distribution, that appears to mime the synformal geometry of the sedimentary fill in the Savigliano and Alessandria Basins and the gentle antiformal geometry in the Asti area (fig. 9). In general, it results deeper in the depocentral areas, from which it progressively becomes shallower toward present-day borders (structural highs included), along which, the positioning of FSWI is often hampered

by the insufficiency of data.

In the Savigliano Basin, the FSWI displays maximum depths from the ground level of about 1800 m in the depocentral zones, while it reaches minimum depths of 70 m, toward the eastern margin.

Along the western margin it usually holds depth in the order of 600-800 m, except on the western culmination of the Saluzzo-Sommariva del Bosco faulted anticline, where it occupies a very shallow depth.

In the Alessandria Basin, the FSWI displays maximum depths from the ground level of about 1500 m in the depocentral area, while it reaches minimum depths of 100 m, both in the southwestern border and along the northern margin.

Very low depths are recognizable on the Asti Area.

By excluding the thickness (i.e. 200-300 m) of currently used superficial aquifers, it is therefore possible to estimate the overall thickness of deep fresh aquifers, that have still to be exploited: maximum thickness are in the order of 1200 m in the Alessandria Basin depocenter and 1500 in the central sector of the Savigliano Basin. From these areas, thickness progressively reduces up to some tens/hundreds of meters as regard the present-day margins.

### 7. - CONCLUDING REMARKS

The proposed reconstruction of the geological setting of the southern Piedmont subsurface Messinian-Quaternary basins represents an improvement of the geological knowledge on the distribution of the main sedimentary bodies and their mutual genetic relations, as well as the pre-

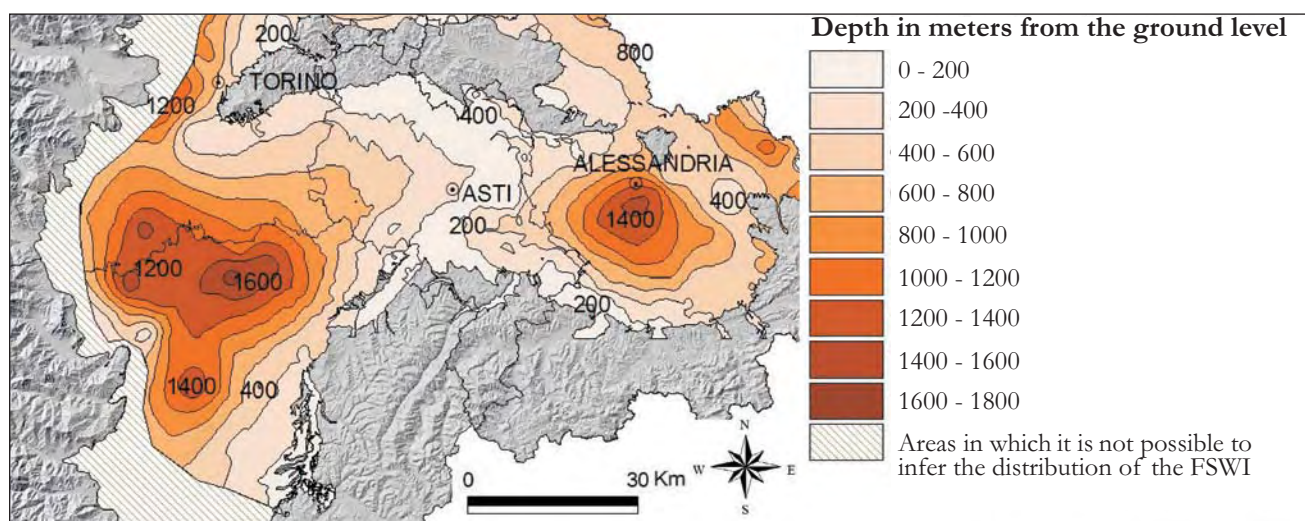


Fig. 9 - Subsurface distribution of the fresh-salt water interface in the Savigliano and Alessandria Basins.  
- Distribuzione della superficie di interfaccia acqua dolce-salata nei Bacini di Savigliano ed Alessandria.

sence of the main tectonic features. Although the resulting framework led to a better definition of the subsurface hydrostratigraphy, the suitability of the model is strictly dependent on the project assumptions, namely the choice of delimiting the Aquifer Groups by discontinuity surfaces and basin scale internal patterns, instead of on the occurrence of regionally extended permeability barriers.

The project assumptions were imposed to contextual factors such as the poor quality of available subsurface data and constrained by the detail of the investigation, conducted at regional scale.

These considerations must be carefully taken into account in using the proposed hydrostratigraphic model as a source of input data for further water exploitation evaluations and water flow modeling.

#### Acknowledgments

*We thank the Referees A. AMOROSI and P. SEVERI for the revision of the manuscript and for their fruitful suggestions.*

#### REFERENCES

- ABATUCCI G., CLEMENTE P., DE LUCA D.A., LASAGNA M. & MASCIOTTO L. (2005) - *Deep groundwater resources individuation in Piemonte plane (Northern Italy)*. Proceedings of the 6<sup>th</sup> International Conference "Sharing a common vision of our water resources", Menton, France, 7-10 September 2005, Paper EWRA066b, pp. 25.
- AGIP (1972) - *Acque dolci sotterranee*. Inventario dei dati raccolti dall'AGIP durante la ricerca di idrocarburi in Italia: pp. 914.
- AGIP (1994) - *Acque dolci sotterranee*. Inventario dei dati raccolti dall'AGIP durante la ricerca di idrocarburi in Italia: pp. 515.
- BADLEY M.E. (1987) - *Practical seismic interpretation*. AGIP: pp. 274.
- BELLO M. & FANTONI R. (2002) - *Deep oil play in Po Valley: deformation and hydrocarbon generation in a deformed foreland*. AAPG Hedberg Conference "Deformation History, Fluid Flow and Reservoir Appraisal in Foreland Fold and Thrust Belts", May, 14-18, Palermo (Italy): 1-4.
- BIGI G., COSENTINO D., PAROTTO M., SARTORI R. & SCANDONE P. (1990) - *Structural Model of Italy*. Geodynamic project, scale 1:500.000, sheet 1, C.N.R., S.EL.CA., Firenze.
- BORTOLAMI G., DI MOLFETTA A. & VERGA G. (1982) - *Il contributo della geotermia al risparmio energetico in Piemonte: il progetto Geotorino*. Estratto da: "Sistemi Urbani", rivista quadrimestrale di scienze della città e del territorio, anno IV, 1/2: 162-181.
- BOTTINO G., CAVALLI C. & VIGNA B. (1994a) - *L'analisi di facies nella prospezione idrogeologica*. Geol. Rom., 30: 515-524.
- BOTTINO G., CAVALLI C., EUSEBIO A. & VIGNA B. (1994b) - *Stratigrafia ed evoluzione plio-quadernaria del settore sud-orientale della pianura cuneese*. Atti Tic. Sc. Terra, ser. spec. 1: 153-166.
- BROWN L.F. & FISHER W.L. (Ed.) (1980) - *Seismic stratigraphic interpretation and petroleum exploration*. Am. Ass. Petrol. Geol., Continuing Education Course Note, Series 16, Bureau of Economic Geology: pp.181, University of Texas at Austin.
- CAVALLI C. & VIGNA B. (1995) - *Il "Villafranchiano" nel sottosuolo della pianura cuneese*. Il Quaternario, 8 (2): 423-434.
- CARRARO F. (Ed.) (1996) - *Revisione del Villafranchiano nell'area tipo di Villafranca d'Asti*. Il Quaternario, 9 (1): pp. 119.
- CASSANO E., ANELLI L., FICHERA R. & CAPPELLI V. (1986) - *Pianura Padana: interpretazione integrata di dati geofisici e geologici*. AGIP, 73° Congr. Soc. Geol. It., 29 settembre-4 ottobre, Roma: 1-27.
- CAVALLI C. & VIGNA B. (1995) - *Il "Villafranchiano" nel sottosuolo della pianura cuneese*. Il Quaternario, 8 (2): 423-434.
- CHANG K.H. (1975) - *Unconformity bounded stratigraphic units*. GSA Bull., 86: 1544-1552.
- DELA PIERRE F., PIANA F., FIORASO G., BOANO P., BICCHI E., FORNO M.G., VIOLANTI D., CLARI P. & POLINO R. (2003) - *Note illustrative della Carta Geologica d'Italia alla scala 1:50.000. Foglio 157 "Trino"*. APAT, Dipartimento Difesa del Suolo: pp. 147, Litografia GEDA, Nichelino (To).
- FALLETTI P., GELATI R. & ROGLEDI S. (1995) - *Oligo-Miocene evolution of Monferrato and Langhe, related to deep structure*. In: R. POLINO, R. SACCHI (Eds.) - Atti Convegno Rapporti Alpi-Appennino, Peveragno (1994), Acc. Naz. Sc., 14: 1-19.
- FIORASO G., BICCHI E., IRACE A. & BOANO P. (2004) - *Manifestazioni carsiche nelle evaporiti messiniane del Monferrato e della Collina di Torino (Italia nord-occidentale): analisi dei meccanismi genetici nel quadro dell'evoluzione pliocenico-quadernaria del Bacino Terziario Piemontese*. Il Quaternario, 17 (2/2): 453-476.
- FRANCANI V. (1985) - *Geologia applicata 4. Idrogeologia generale*. CLUP: pp. 316, Milano.
- GELATI R., ROGLEDI S. & ROSSI M.E. (1987) - *Significance of the Messinian unconformity-bounded sequences in the Apenninic margin of the Padan foreland basin, northern Italy*. Mem. Soc. Geol. It., 39: 319-323.
- GHIBAUDO G., CLARI P.A. & PERELLO M. (1985) - *Litostratigrafia, sedimentologia ed evoluzione tettonico-sedimentaria dei depositi miocenici del margine Sud-Orientale del Bacino Terziario Ligure-Piemontese (Valli Borbera, Scrivia e Lemme)*. Boll. Soc. Geol. It., 104: 349-397.
- GHIEMI M., ROGLEDI S., VIGNA B. & VIOLANTI D. (2002) - *Evoluzione tettono-sedimentaria della successione plio-pleistocenica nel settore del Piemonte centro-meridionale*. 81° Riun. Est. Soc. Geol. It., Riass.: 201-202.
- IACCARINO S., CASTRATORI D., CITA M.B., DI STEFANO E., GABOARDI S., MC KENZIE J.A., SPEZZAFERRI S. & SPROVIERI R. (1999) - *The Miocene-Pliocene boundary and the significance of the earliest Pliocene flooding in the Mediterranean*. Mem. Soc. Geol. It., 54: 109-131.
- IRACE A. (2004) - *Il Messiniano Piemontese: nuovi dati da due aree campione*. PhD Thesis: pp. 167, Torino University.
- IRACE A., DELA PIERRE F. & CLARI P. (2005) - *Normal and chaotic deposits in the Messinian Gessoso-solfifera Fm. At the north-eastern border of the Langhe domain (Tertiary Piedmont Basin)*. Boll. Soc. Geol. It., vol. spec. 4: 77-85.
- MITCHUM R.M., VAIL P.R. & SANGREE J.B. (1977) - *Seismic stratigraphy and global changes of sea-level, part 7: stratigraphic interpretation of seismic reflection patterns in depositional sequences*. In: Seismic Stratigraphy—Applications to Hydrocarbon Exploration. Mem. Am. Ass. petr. Geol., 26: 135-144.
- MOSCA P. (2006) - *Neogene basin evolution in the Western Po Plain (NW Italy)*. PhD Thesis: pp. 190, Vrije Universiteit Amsterdam.
- MOSCA P., POLINO R., ROGLEDI S. & ROSSI M. (2009) - *New data for the kinematic interpretation of the Alps–Apennines junction (Northwestern Italy)*. Int. J. Earth Sci. (Geol. Rundsch), DOI 10.1007/s00531-009-0428-2.
- PIERI M. & GROPPI P. (1981) - *Subsurface Geological Structure of the Po Plain, Italy*. Quad. CNR, Progetto finalizzato Geodinamica, 414: pp.13, Roma.
- REGIONE EMILIA ROMAGNA & ENI – AGIP (1998) - *Riserve idriche sotterranee della Regione Emilia Romagna*. A cura di G. DI DIO: pp. 120, S.EL.CA., Firenze.
- REGIONE LOMBARDIA & ENI DIVISIONE AGIP (2002) - *Geolo-*

- gia degli acquiferi Padani della Regione Lombardia*. A cura di C. CARCANO & A. PICCIN: pp. 130, S.EL.CA., Firenze.
- ROSSI M., MOSCA P., POLINO R., ROGLEDI S. & BIFFI U. (2009) - *New outcrop and subsurface data in the Tertiary Piedmont Basin (NW-Italy): unconformity-bounded stratigraphic units and their relationships with basin-modification phases*. Riv. It. Pal. Strat., **115** (3): 305-335.
- ROVERI M., MANZI V., BASSETTI M.A., MERINI M. & RICCI LUCCHI F. (1998) - *Stratigraphy of the Messinian post-evaporitic stage in eastern-Romagna (northern Apennines, Italy)*. Giorn. Geol., **60**: 119-142.
- ROVERI M., MANZI V., RICCI LUCCHI F. & ROGLEDI S. (2003) - *Sedimentary and tectonic evolution of the Vena del Gesso basin (Northern Apennines, Italy): Implications for the onset of the Messinian salinity crisis*. Geol. Soc. Amer. Bull., **115**(4): 387-405.
- ROVERI M., LUGLI S., MANZI V. & SCHREIBER C. (2008) - *The shallow- to deep-water record of the Messinian salinity crisis: new insight from Sicily, Calabria and Apennine basins*. In: F. BRIAND (Ed.) CIESM 2008, "The Messinian Salinity Crisis mega-deposits to microbiology - A consensus report". CIESM Workshop Monographs, **33**: 73-82.
- SERVIZIO GEOLOGICO D'ITALIA (1913) - *Carta Geologica d'Italia alla scala 1:100.000 - Foglio n. 67 Pinerolo*, I edizione, Roma.
- SERVIZIO GEOLOGICO D'ITALIA (1931) - *Carta Geologica d'Italia alla scala 1:100.000 - Foglio n. 80 Cuneo*, I edizione, Roma.
- SERVIZIO GEOLOGICO D'ITALIA (1969a) - *Carta Geologica d'Italia alla scala 1:100.000 - Foglio n. 56 Torino*, II edizione, Roma.
- SERVIZIO GEOLOGICO D'ITALIA (1969b) - *Carta Geologica d'Italia alla scala 1:100.000 - Foglio n. 68 Carmagnola*, II edizione, Roma.
- SERVIZIO GEOLOGICO D'ITALIA (1969c) - *Carta Geologica d'Italia alla scala 1:100.000 - Foglio n. 57 Vercelli*, II edizione, Roma.
- SERVIZIO GEOLOGICO D'ITALIA (1969d) - *Carta Geologica d'Italia alla scala 1:100.000 - Foglio n. 58 Mortara*, II edizione, Roma.
- SERVIZIO GEOLOGICO D'ITALIA (1970a) - *Carta Geologica d'Italia alla scala 1:100.000 - Foglio n. 70 Alessandria*, II edizione, Roma.
- SERVIZIO GEOLOGICO D'ITALIA (1970b) - *Carta Geologica d'Italia alla scala 1:100.000 - Foglio n. 69 Asti*, II edizione, Roma.
- SERVIZIO GEOLOGICO D'ITALIA (1971) - *Carta Geologica d'Italia alla scala 1:100.000 - Foglio n. 71 Voghera*, II edizione, Roma.
- SERVIZIO GEOLOGICO D'ITALIA (2003) - *Carta Geologica d'Italia alla scala 1:50.000 - Foglio n. 157 Trino*, APAT, Dipartimento Difesa del Suolo, Litografia GEDA, Nichelino (To).
- TOTH J. (1963) - *A theoretical analysis of groundwater flow in small drainage basins*. J. Geoph. Res., **68**: 4785-4812.
- VIGNA B. (1996) - *Il contributo dell'analisi sedimentologica nella valutazione della vulnerabilità degli acquiferi*. Atti 2° Convegno Nazionale sulla protezione e gestione delle acque sotterranee: metodologie, tecnologie e obiettivi, Nonantola (Modena) 17-19 Maggio 1995, Quad. Geol. Appl., suppl. 4: 129-141.



## Isotope geochemistry and the water cycle: a short review with special emphasis on Italy

*La geochimica isotopica ed il ciclo delle acque: un breve sguardo  
retrospettivo con particolare riferimento all'Italia*

LONGINELLI A. (\*), SELMO E. (\*)

**ABSTRACT** - The growth of stable isotope hydrology started at the end of the second world war and reached its full development in the seventies. Its use for hydrological studies became more and more important through time and the IAEA in Vienna gave a vital impetus to the development of these studies. The basic principles of this relatively new branch of hydrology are briefly summarized, bypassing the physical and mathematical principles, to draw attention on the practical meaning and the possible interpretation of the isotopic data that may be obtained. The overall distribution of the isotopic values of precipitation in Italy is briefly reported as well as some anomalous results. These results, that sometimes seem to be in sharp contrast with the relationships that are generally accepted and normally found between the isotopic composition of precipitation and other variables, may be normally explained even though, in some case, they are not yet fully understood. First, the well known relationship between the isotopic composition of precipitation and the surface temperature is considered and some anomalies are reported. Then, the isotopic vertical gradient is considered and the results obtained from several pluviometers throughout Italy are reported. Some anomalous results obtained in northern Italy in the south Alpine area, not far from Trento, are also discussed and, at least partially, explained. However, the large number of variables affecting this value often prevent a correct interpretation of the measured values. A didactic example of the relationship existing between the isotopic composition and the amount of precipitation is also shown. Some examples of stable isotope studies applied to different hydrological problems are reported as well as a brief discussion on the existing relationship between the isotopic composition of groundwater and the isotopic composition of local precipitation.

**KEY WORDS:** Hydrogen isotopes, Italy, Oxygen isotopes, vertical isotopic gradients, water cycle.

**RIASSUNTO** - Sono ormai diversi decenni che la geochimica isotopica è entrata prepotentemente nel campo degli studi idrologici. Purtroppo, in Italia questa innovativa disciplina non ha incontrato il grande successo che, nel resto del mondo, ha caratterizzato la sua crescente utilizzazione. Vengono qui brevemente riassunti i principi di base di questa particolare branca dell'idrologia, trascurando gli aspetti più prettamente matematici e fisici, per mettere in evidenza il significato pratico e le possibili interpretazioni dei dati isotopici ottenuti studiando il ciclo delle acque. Si riporta una mappa con la distribuzione dei valori isotopici delle precipitazioni in Italia, essendo le precipitazioni il punto di riferimento per lo studio di qualsiasi acquifero, sia superficiale che profondo. La distribuzione generale dei valori è praticamente controllata dalla presenza della catena appenninica, almeno a livello della penisola, la pianura padana costituendo un corpo a sé sul quale il rilievo appenninico non ha in pratica alcuna influenza. La distribuzione dei valori isotopici sulla pianura padana è invece controllata, in buona parte, dai venti orientali che spingono verso ovest masse d'aria che trasportano vapore acqueo di origine adriatica. Non incontrando rilievi montuosi di qualche entità lungo il percorso da est a ovest, queste masse d'aria determinano precipitazioni relativamente poco negative che consentono di tracciare questo effetto fino quasi alla longitudine di Milano. Altra caratteristica apparentemente anomala è rappresentata dalla quasi costanza dei valori isotopici delle precipitazioni costiere dalla Sicilia alla Liguria, nonostante le sostanziali differenze climatiche latitudinali. Questo dato non è del tutto chiaro ma una possibile concausa può essere la relativa omogeneità latitudinale di temperatura superficiale del Tir-

(\*) University of Parma, Department of Earth Sciences, Viale G.P.Usberti 157/A, 43100 Parma, Italy

reno che può influire, in maniera sensibile, sulle precipitazioni strettamente litorali. La relazione positiva normalmente esistente tra composizione isotopica delle precipitazioni e temperatura al suolo viene esemplificata graficamente. Vengono anche discussi alcuni valori medi annui ponderati di composizione isotopica delle precipitazioni che sembrano contraddire tale correlazione. In particolare, si riportano i valori apparentemente anomali riscontrati nel corso del 2003 (anno con temperature estive eccezionalmente elevate). L'apparente anomalia viene spiegata tenendo conto dell'ammontare stagionale delle precipitazioni e dei relativi valori isotopici medi ponderati. Vengono riportati anche i valori dei gradienti isotopici verticali misurati in Italia da nord a sud e viene messa in evidenza la limitata ma sostanziale differenza tra la maggior parte di questi valori ed il valore medio, generalmente ottenuto nell'ambito del bacino mediterraneo. In particolare, si riportano valori anomali dei gradienti isotopici verticali riscontrati nell'area alpina in prossimità di Trento dati che, in buona parte, possono essere spiegati con l'effetto "ombra" determinato da rilievi montuosi di una certa entità. Si riporta anche un caso di particolare chiarezza ed evidenza che mette in relazione la composizione isotopica delle precipitazioni con periodi di piovosità particolarmente intensa. Vengono anche brevemente discussi alcuni esempi che dimostrano la diretta correlazione tra composizione isotopica di un acquifero e composizione isotopica delle precipitazioni nell'area di ricarica dell'acquifero stesso. Un ultimo aspetto di rilevante interesse è quello della rilevazione di infiltrazioni, in acquiferi di importanza particolare, di acque inquinate di origine superficiale (principalmente fiumi o altri corsi d'acqua). Le misure isotopiche permettono in genere di evidenziare chiaramente tali apporti: vengono riportati alcuni esempi pratici di particolare interesse. Inoltre, si discutono i risultati ottenuti da un dettagliato studio isotopico degli acquiferi del Carso triestino, risultati che hanno permesso di verificare l'inconsistenza delle ipotesi generalmente accettate sull'origine di queste acque e sul loro deflusso sotterraneo. E' stato anche possibile mettere in evidenza l'apporto, pressochè sistematico nel corso dei mesi di Maggio/Giugno di ogni anno, di acqua dal fiume Isonzo che in quel periodo riceve le acque di fusione della copertura di neve del suo bacino alpino.

PAROLE CHIAVE: Ciclo delle acque, gradienti isotopici verticali, isotopi dell'idrogeno, isotopi dell'ossigeno, Italia.

## 1. - INTRODUCTION

Nine different stable isotope water species occur in natural waters but only three of them are of importance for hydrological studies and are amenable to accurate analytical assay:  $H_2^{16}O$ ,  $H_2^{18}O$ , and  $HD^{16}O$ . The first dedicated studies on the isotopic variations in natural waters were developed more than fifty years ago (EPSTEIN & MAYEDA, 1953; CRAIG, 1961; DANSGAARD, 1954; 1961; 1964; CRAIG & GORDON, 1965): besides the first sets of isotopic data, these studies suggested models for the evaporation, mixing, and precipitation processes. From that time a number of dedicated studies were developed on the use of stable isotope abundance in hydrological studies so that a few years later the need of summarizing the work carried out was

already felt by the scientific community (FIDEL, 1976). More papers were published, particularly in the eighties, to fully understand the temporal and spatial distribution of the isotopic composition of precipitations and the relationship between ground waters and precipitations (e.g. GAT, 1980; SIEGENTHALER & OESCHGER, 1980; ROZANSKI *et alii*, 1982; FÖRSTEL & HÜTZEN, 1982; JOUSSAUME *et alii*, 1984; ROZANSKI, 1985; etc.). We must recall the deserving effort of the international organizations that designed the global IAEA/WMO precipitation network in order to provide worldwide basic data for hydrological applications as well as an averaged climatic characterization of precipitation, based on the study of monthly composite samples. Nowadays, specific hydrological problems are studied by several national agencies by means of stable isotope surveys but, unfortunately, our country is again very late in this field taking into account the intensive isotopic study of precipitations and of surface and deep aquifers carried out by different countries all over the world.

## 2. - MAIN FEATURES OF THE ISOTOPE DATA

The prominent features of the isotope data that are of importance for hydrological studies can be summarized as follows taking into account that mean weighted monthly samples are generally used to study precipitations:

1) the isotopic composition of a water sample is reported in terms of delta units where delta ( $\delta$ ) is defined by:

$$\delta = [(R_{\text{sample}} - R_{\text{standard}}) / R_{\text{standard}}] \times 1000$$

where R is the abundance ratio between the heavy and the light isotope:  $R = {}^{18}O/{}^{16}O$  or  $D/H$ ;

2) the delta values of atmospheric precipitation from all the studied countries cluster along the so-called global meteoric water line (CRAIG, 1961) whose equation is:

$$\delta D = 8 \delta {}^{18}O + 10 \quad 1)$$

3) in the Mediterranean area precipitations often show a deuterium excess considerably larger than that given by equation 1): (this variable is defined by:  $d_{\text{excess}} = \delta D - 8 \delta {}^{18}O$ );

4) a good correlation between the mean isotopic composition of precipitation and the mean surface temperature is generally found at various sites; the best results are obtained comparing yearly mean isotopic values with mean yearly temperature even though good correlations can be obtained also at the monthly level;

5) in the case of semi-arid and arid regions regional precipitation lines have a slope of less than 8 on the  $\delta D$  versus  $\delta {}^{18}O$  diagram; this effect is explained with kinetic evaporation processes

affecting the rain drops during their fall;

6) heavy isotope species are depleted in precipitation relative to the ocean water source. This is the result of the isotopic fractionation taking place during evaporation from the sea-surface (preferential loss of isotopically light water molecules) and of the isotopic fractionation that takes place during the condensation of liquid water from vapour (preferential condensation of isotopically heavy water molecules). The former fractionation is generally kinetic while the latter fractionation is closely related to the temperature of condensation;

7) it follows that precipitations collected at different elevations in the same area show vertical isotopic gradients in the case of both oxygen and hydrogen: the average value of this gradient in Italy is of about  $-0.15\text{‰}/100$  metres in the case of oxygen (LONGINELLI & SELMO, 2003), slightly higher than the mean value measured in the Mediterranean basin (about  $-0.20\text{‰}/100$  m).

We can now consider in some detail these issues and briefly discuss some of the experimental results obtained in Italy so far.

Equation 1) was confirmed by YURTSEVER & GAT (1981) and by ROZANSKI *et alii* (1993) who considered all the isotopic results obtained from the IAEA/WMO network and calculated the following equation:

$$\delta D = (8.20 \pm 0.07)\delta^{18}O + (11.27 \pm 0.65) \quad 2)$$

when weighted mean values were used. LONGINELLI & SELMO (2003) plotted all the weighted monthly  $\delta^{18}O$  versus the  $\delta D$  values obtained from 80 stations all over Italy and calculated the following equation:

$$\delta D = 7.61 \delta^{18}O + 9.21 \quad 3)$$

not far from the global meteoric water line.

However, considering separately the mean monthly values obtained in northern Italy, in central Italy, and in southern Italy, three different equations were obtained, the differences being of importance when we study local hydrological problems. The three equations are the following:

$$\text{Northern Italy } \delta D = 7.709 \delta^{18}O + 9.403 \quad 4)$$

$$\text{Central Italy } \delta D = 7.047 \delta^{18}O + 5.608 \quad 5)$$

$$\text{Southern Italy } \delta D = 6.970 \delta^{18}O + 7.316 \quad 6)$$

The differences are even larger when we consider individual stations. The slopes of the equations obtained from individual stations range from 5.7 to 8.9 and the deuterium excess is also quite variable ranging from 9.2 to 19.1. These variations should be taken into account when studying relatively small areas where rather large variations may be found, related either to the morphology of the area or to its geographical position or to the main trajectory of atmospheric perturbations.

### 3. - OVERALL DISTRIBUTION OF THE ISOTOPIC VALUES IN ITALY

Rather large differences are found between the western and the eastern side of Italy, the Apennine ridge acting as a north-south barrier that separates this geographic area into two different sections. The section of Italy west of the Apennine barrier is mainly interested by westerly winds carrying water vapour from the Balearic basin and the Tyrrhenian basin. The Adriatic section is mainly interested by north-easterly winds from continental areas and/or by south-easterly winds carrying water vapour from the central and the eastern Mediterranean. The effect of this situation is clearly shown in figure 1 where the contour lines report the overall variability of the mean oxygen isotopic composition of precipitation in Italy, calculated for the period of this survey, variable for different stations from a couple of years to about ten years. The marked effect of the different conditions existing West and East of the Apennines and the importance of

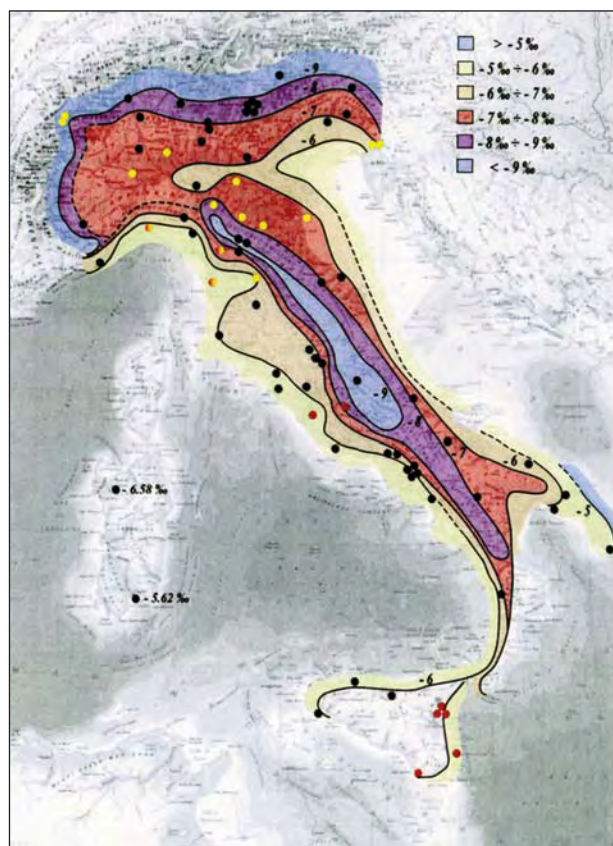


Fig. 1 – Contour lines reporting the overall variability of the mean oxygen isotopic composition of precipitation in Italy. Black and yellow dots are stations controlled by the authors; red dots are stations controlled by other colleagues (modified from figure 2 in LONGINELLI & SELMO, 2003).  
- Curve ipsometriche relative ai valori medi di composizione isotopica dell'ossigeno nelle precipitazioni sull'Italia. I punti neri e gialli si riferiscono a stazioni pluviometriche controllate dagli autori; i punti rossi si riferiscono a stazioni controllate da altri colleghi (modificata dalla figura 2 di LONGINELLI & SELMO, 2003).



this barrier from the hydrological point of view are shown by some peculiar distribution of the contour lines. The largest of these effects is the -6.0 and -7.0 ‰ contour lines entering deep inside the Po plane. This is the result of the inflow of water vapour from the Adriatic, carried by the north-easterly and easterly winds prevailing over the northern Adriatic.

If we compare the isotopic composition of precipitations at locations at the same latitude along the central section of the Adriatic and the Tyrrhenian coastal areas the former locations show mean isotopic values considerably lower (up to about 2 ‰) than those in the Tyrrhenian section. This is at least partially due to the “shadow” effect of the Apennines that strongly affects the distribution of the isotopic values along the whole Italian peninsula, with a marked elevation effect, particularly in the central section. The less negative isotopic values in the southeastermost section of Italy (Apulia) are probably the effect of the frequency in this area of the warm southeasterly wind. It is noteworthy that, despite the latitudinal extension of the Tyrrhenian coast no latitudinal isotopic gradient was observed despite some obvious temperature gradients between different sections of this coast. This peculiar behaviour may be, at least partially, related to differences between seasonal amounts of precipitation and to the homogeneous surface temperatures of the Tyrrhenian sea that may affect in some way the most littoral precipitations. A last remark should be made on the shadow effect of the Alps that is considerably smaller than expected.

#### 4. - RELATIONSHIP BETWEEN ISOTOPIC VALUES AND SURFACE TEMPERATURE

Several studies were carried out to show the positive relationship existing between the isotopic composition of precipitation and the surface temperature. This relationship was first demonstrated by DANSGAARD (1964); YURTSEVER (1975) and YURTSEVER & GAT (1981) clearly showed the existence of a time variation in monthly  $\delta^{18}\text{O}$  and temperature ( $^{\circ}\text{C}$ ) data from the Vienna IAEA station as well as from a group of 39 IAEA/WMO network stations with a minimum of six years of continuous monthly data. In the majority of the stations analyzed there is only a 12-month cycle in the  $\delta^{18}\text{O}$ -time series with lighter isotopic values (both oxygen and hydrogen) during winter and heavier isotopic values during summer. These isotopic variations are characteristic of most of the studied areas and their amplitude is directly related to the amplitude of the seasonal temperature

gradients: a huge amplitude is normally found in polar areas and a very small one in tropical areas. However, it was demonstrated that the best coupling of these two variables usually occurs for annual mean values. Several stations among which Bamaho, Kinshasa, Reykjavik, Tokio, Midway Island and Hilo-Hawaii showed either shorter cycles superimposed on the 12-month cycle or no distinct variations in their  $\delta^{18}\text{O}$ -time series. These anomalous behaviours were related to local climatological conditions and/or to different effects super-imposed on each other (YURTSEVER & GAT, 1981).

In Italy, we generally observed quite normal  $\delta^{18}\text{O}/t$  relationships as was the case e.g. with the Aosta pluviometer during 2002-2004 (fig. 2).

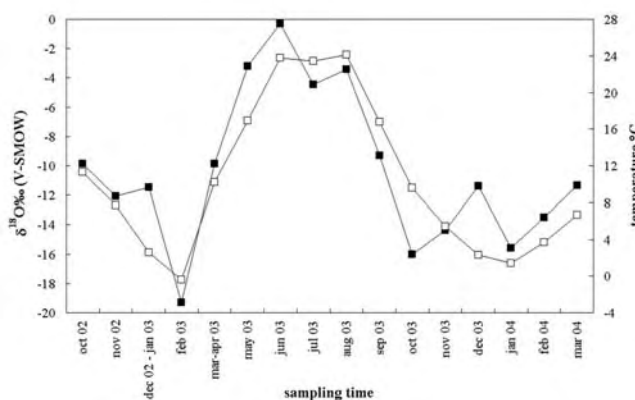


Fig. 2 – Mean monthly temperatures ( $^{\circ}\text{C}$ , open squares) and  $\delta^{18}\text{O}$  (full squares) of the mean monthly samples of precipitation at Aosta (north-western Italy) between October 2002 and March 2004.

– Temperature medie mensili ( $^{\circ}\text{C}$ , quadrati bianchi) e  $\delta^{18}\text{O}$  (quadrati neri) dei campioni medi mensili di precipitazioni ad Aosta tra l'Ottobre del 2002 ed il Marzo del 2004.

However, in a few cases anomalous results were obtained as was the case with the Basovizza pluviometer (north-eastern Italy, near the border with Slovenia, 397 m.a.s.l.) during 1998 (fig. 3). This is a very short period however, at Basovizza, the lack of a direct relationship between  $\delta^{18}\text{O}$  and surface temperature is not exceptional: between November 1999 and October 2001 the overall range of  $\delta^{18}\text{O}$  values was only 1.5 ‰, despite the normal seasonal temperature changes. During the same periods at the Trieste pluviometer, only a few kilometres away from Basovizza, the  $\delta^{18}\text{O}/t$  relationship was normally respected. We have no plausible interpretation of the reported anomalous behaviour. However, we should point out that, during about a decade of isotopic measurements in Italy, very few anomalous behaviours were detected. In a general way, as demonstrated by MERLIVAT & JOUZEL (1979), there is a good relationship between the isotopic

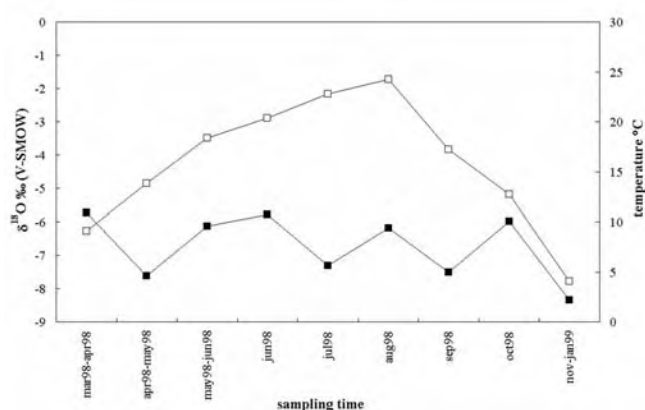


Fig. 3 - Mean monthly temperatures (°C, open squares) and  $\delta^{18}\text{O}$  (full squares) of the mean monthly samples of precipitation at Basovizza (Trieste, north-eastern most Italy) between March 1998 and January 1999. - Temperature medie mensili (°C, quadrati bianchi) e  $\delta^{18}\text{O}$  (quadrati neri) dei campioni medi mensili di precipitazioni a Basovizza (Trieste) tra il Marzo 1998 ed il Gennaio 1999.

composition of precipitations (both oxygen and hydrogen) and climatic conditions.

A very interesting feature which could be erroneously interpreted as an anomaly to the  $\delta^{18}\text{O}/t$  relationship was observed between 2002 and 2004 when exceptionally high temperatures were experienced, particularly during summer 2003. During this period Italy, as well as almost all Europe, recorded summer temperatures among the most elevated of the last 200 years. Accordingly, one could expect a shift of the mean isotopic values of precipitation towards less negative results. On the contrary, weighted mean yearly values resulted considerably more negative than “normal” values almost all over Italy. As examples of the results obtained we report the mean monthly values measured at two stations in northern Italy, Milano and Parma (tab. 1) (LONGINELLI *et alii*, 2006). At Milano the mean yearly temperature of 2003 was higher than the 2002 and the 2004 temperatures by about one degree centigrade, the highest temperature anomaly taking place between May and September 2003. During these five months the amount of precipitation was only 213 mm, about 25% of the amount during the same period in 2002; however, the amount of precipitation between January and April was also considerably lower than normal. As a result, the weighted yearly mean  $\delta^{18}\text{O}$  value of 2003 was heavily affected by the amount of precipitation during the last three months of the year and by their negative isotopic values. Consequently, despite the increase in the isotopic summer values, the 2003 weighted mean isotopic values resulted considerably more negative than those of the previous year. If we now consider the 2004 isotopic values they look even more anomalous

since the yearly mean temperature was quite normal while the yearly weighted mean  $\delta^{18}\text{O}$  values were more negative than the 2003 values. This is clearly due to the small amount of summer precipitation (identical to that of the previous year), to the large amount of precipitation during the first four months, with very negative isotopic values, and to the very negative isotopic values of the precipitation during the last three months of 2004. In this case the weighted mean isotopic values would misrepresent the climatic situation suggesting drastically decreasing mean yearly temperatures.

The results obtained at Parma (tab. 1) are only slightly different from those obtained at Milano. Also at Parma the 2003 summer precipitations were extremely reduced and their  $\delta^{18}\text{O}$  substantially shifted towards less negative values. However, the very negative isotopic composition of winter, spring and fall precipitations caused a marked decrease of the weighted mean yearly values. A large amount of precipitations during

Tab. 1 - Mean  $t$  values, amount of precipitation and weighted mean isotopic values.

- Valori medi di  $t$ , quantità di precipitazioni e valori isotopici medi ponderati.

Period	mean $y$ , t°C	mean $t$ °C	mm rain	mean $\delta^{18}\text{O}$	mean $\delta\text{D}$	w. $\delta^{18}\text{O}$	w. $\delta\text{D}$
<b>Milano</b>							
01/04/02		9.0	430	-7.13	-48.9		
05/09/02	14.9	22.0	815	-6.88	-46.7	-6.99	-46.9
10/12/02		10.8	460	-7.05	-45.6		
01/04/03		8.8	112	-8.94	-61.6		
05/09/03	15.9	25.5	213	-5.22	-33.1	-8.36	-54.2
10/12/03		9.5	430	-9.76	-62.8		
01/04/04		8.3	424	-10.28	-72.2		
05/09/04	14.8	22.5	218	-5.68	-39.3	-9.23	-64.2
10/12/04		10.5	250	-10.53	-72.3		
<b>Parma</b>							
01/04/02		6.9	225	-7.19	-45.0		
05/09/02	14.4	21.2	372	-6.27	-41.8	-7.79	-51.8
10/12/02		9.4	382	-9.63	-65.5		
01/04/03		5.8	198	-13.09	-96.6		
05/09/03	14.9	23.5	120	-4.50	-26.8	-10.18	-69.4
10/12/03		7.9	317	-10.51	-68.6		
01/04/04		6.5	432	-11.47	-80.4		
05/09/04	14.1	21.5	310	-5.83	-36.4	-9.61	-64.7
10/12/04		10.0	336	-10.70	-70.5		

The isotopic values are reported in ‰ versus VSMOW

2004 and quite negative isotopic values of winter, spring and fall precipitations determined a negative weighted yearly mean value while the mean yearly temperature of 2004 was only slightly lower than normal. In this case, the yearly mean isotopic values alone could lead to a distorted interpretation of the climatic conditions.

## 5. - AMOUNT EFFECT AND EVAPORATION EFFECT

Another peculiar feature that could be erroneously considered an anomaly in the  $\delta^{18}\text{O}/t$  relationship while it is related to different causes, is the so-called “amount effect”. This effect on the isotopic composition of precipitation (isotopic results lighter than those expected for the recorded temperature in the case of very heavy rain) was recognized long ago by DANSGAARD (1964). The mechanism of this effect is not yet fully understood, however it has been at least partially explained considering that during a precipitation the isotopic composition of water vapour in the lower air layers is continuously modified by exchange processes with rain water drops. Consequently, it is brought isotopically closer to the following rain, the duration and the amount of rain affecting, as an additional parameter, the isotopic composition of precipitation. Not many quantitative examples of such an effect were reported in the Mediterranean area. We have a really didactic example observed in 1997 while studying the isotopic composition of precipitation at some stations in the southern pre-Alps for applied hydrological purposes. During June, July and August 1997 at the station of Boario Terme (about 50 km North of Brescia) anomalous  $\delta^{18}\text{O}$  mean monthly values were measured, between two and four per mil more negative than expected (fig. 4). It must be pointed out that during these three summer months the amount of rain was 785 mm, (296, 352, and 137 mm respectively) about three times higher than the mean value of precipitation during the same period.

Normally, rain represents the cloud base composition only in the case of humid climates. In the case of arid or semi-arid areas when the air below the cloud is relatively dry, rain drops partially evaporate during their fall. The effect of this non-equilibrium fractionation is a final increase of the heavy-isotope content of the drops reaching the ground level and a decrease of the value of the deuterium excess. In Italy this effect can be sometimes observed during summer, particularly in southern Italy, but normally it does not seriously affect the weighted mean isotopic values that are

used for hydrological applications, also because of the relatively small amount of summer precipitation. However, evaporation and isotope exchange between rain drops and water vapour are probably at least partially responsible for values lower than 8 of the coefficient in equation 1) as is the case with equations 5) and 6) for central and southern Italy.

## 6. - VERTICAL ISOTOPIC GRADIENTS

Hydrological applications of stable isotope measurements are strictly related to an accurate knowledge of the vertical isotopic gradients that are generally used to calculate the mean elevation of the recharge area of aquifers. Air masses, raising at progressively higher elevations, expand adiabatically: subsequent fractional condensations of water vapour take place at decreasing temperatures from a water vapour that is progressively depleted in heavy molecules. This composite effect causes isotopically lighter precipitations with increasing elevations and is generally referred to as “vertical isotopic gradient”. In Italy we measured this variable at 26 different stations all over the country (fig. 5 and tab. 2) (LONGINELLI & SELMO, 2003) and found that, on average, the mean value of this variable is close to  $-0.15\text{‰}/100$  metres, slightly higher than the  $-0.2\text{‰}/100$  metres generally considered a reliable mean value, frequently found in the Mediterranean area. Normal or quasi-normal values had been repeatedly found in this area, e.g. in Sicily by HAUSER *et alii* (1980), at the island of Vulcano, along the Tyrrhenian coast of Sicily by CAPASSO *et alii* (1990), and along the eastern side

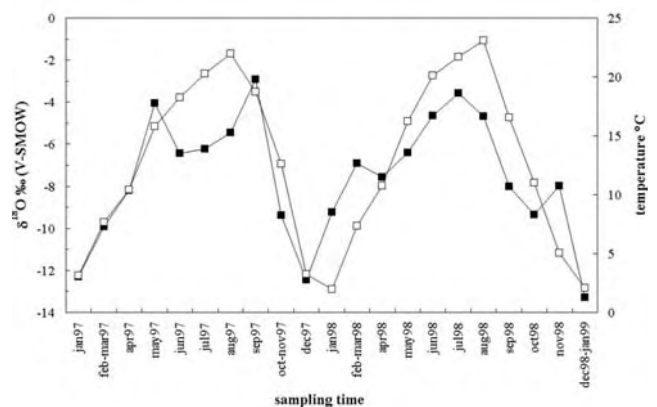


Fig. 4 – Isotopic amount effect at the pluviometric station of Boario (northern Italy, southern pre-Alps) during June, July and August, 1997. Open squares are temperatures and full squares are  $\delta^{18}\text{O}$  (from LONGINELLI & SELMO, 2003).

- Effetto isotopico della quantità di precipitazioni alla stazione pluviometrica di Boario durante i mesi di Giugno, Luglio ed Agosto 1997. I quadrati bianchi si riferiscono alla temperatura ed i quadrati neri ai valori di  $\delta^{18}\text{O}$  (da LONGINELLI & SELMO, 2003).





Fig. 5 – Location and number of pluviometers at which the vertical isotopic gradients were measured (from LONGINELLI & SELMO, 2003).  
 - Posizione e numero di pluviometri utilizzati per la misura dei gradienti isotopici verticali (da LONGINELLI & SELMO, 2003).

of the Apennines by CONVERSINI & TAZIOLI (1993); slightly lower gradients were calculated by MUSSI *et alii* (1998) for the Apennines and the Apuane Alps. Several anomalous values were found, particularly in Northern Italy, in the Alpine area around Trento where five stations at different elevations were monitored for about two years (BORSATO *et alii*, 2000). The results obtained (tab. 3) show that, at the yearly level, large negative and positive anomalies are found either between stations at very close elevations (e.g. Rifugio Graffer and Paganella) or between stations with moderate differences in elevations (e.g. Campo C. Magno and Andalo) or between stations with large differences in elevation (e.g. Paganella and Trento). The problem of the variability of the vertical isotopic gradient, particularly in Alpine areas, was already discussed; STICHLER *et alii* (1997) suggested a variability between  $-0.1\text{‰}/100\text{ m}$  and  $-0.3\text{‰}/100\text{ m}$ , mainly related to the position of the mountains with respect to the direction of the prevailing wind, i.e. with the prevailing trajectory of the rain-clouds front. In the case of the Trento area the calculated vertical gradients (tab. 3) largely exceed the values suggested by STICHLER *et alii* (1997) ranging from -

Tab. 2 - Vertical isotopic gradients measured in Italy. Pluviometers Gallo, Vairano and Valle Agricola are reported in figure 5 as Vairano pluviometers.

- Gradienti isotopici verticali misurati in Italia. I pluviometri Gallo, Vairano e Valle Agricola sono riportati in figura 5 come pluviometri di Vairano.

Collecting station	Elevation m.a.s.l.	$\delta^{18}\text{O}$ (VSMOW)	Collecting station	Elevation m.a.s.l.	$\delta^{18}\text{O}$ (VSMOW)	$\Delta\delta^{18}\text{O}/100\text{m}$ (‰)
Basovizza	400	-7.36	Trieste	10	-6.60	-0.19
Passo Presolana	1290	-8.75	Darfo-Boario	208	-7.66	-0.10
Passo Presolana	1290	-8.75	Sarnico	197	-7.70	-0.10
Graniga	1100	-9.04	Pallanza	208	-7.40	-0.18
Fanano 1	1280	-8.50	Fanano 3	660	-7.57	-0.15
Fanano 1	1280	-8.50	Fanano 2	935	-8.46	-0.01
Monte T. Maggiore	1000	-7.29	San Gemini	350	-6.39	-0.14
Roccamonfina	620	-6.64	Riardo	110	-6.03	-0.12
Roccamonfina	620	-6.64	Campagnola	350	-6.33	-0.11
Campagnola	350	-6.33	Riardo	110	-6.03	-0.13
Gallo	825	-6.85	Vairano 2	135	-5.96	-0.14
Gallo	825	-6.85	Valle Agricola	680	-7.13	0.19
Valle Agricola	680	-7.13	Vairano 1	155	-5.72	-0.27
Etna 3	950	-8.23	Etna 2	570	-7.18	-0.28
Etna 3	950	-8.23	Etna 1	2	-5.49	-0.29
Etna 2	570	-7.18	Etna 1	2	-5.49	-0.30

Tab. 3 - *Vertical isotopic gradients ( $\Delta\delta^{18}\text{O}/100\text{m}$ ): Trento area.*  
 - Gradienti isotopici verticali ( $\Delta\delta^{18}\text{O}/100\text{m}$ ): area di Trento.

Collecting stations and elevation	Period	$\Delta\delta^{18}\text{O}/100\text{m}$
		(‰)
Paganella (2125m) - Trento (312m)	10/1997- 09/1999	-0.05
Campo C. Magno (1685m) - Andalo (1005m)	10/1997- 09/1999	-0.21
Paganella (2125m) - Campo C. Magno (1685m)	10/1997- 09/1999	0.30
Rifugio Graffer (2263m) - Paganella (2125m)	10/1997- 09/1999	-1.46
Paganella (2125m) - Andalo (1005m)	10/1997- 09/1999	-0.009

1.46 ‰/100 m to +0.30 ‰/100 m. This anomalous behaviour can be at least partially explained. The eastern face of the Paganella mountain is mainly exposed to southern winds blowing along the river Adige valley. This elevated wall causes a marked “shadow effect”, particularly in the direction of the town of Andalo, only a few kilometres north-west of the Paganella mountain. The other two stations (Rifugio Graffer and Campo Carlo Magno) are located north-west of the Paganella and are exposed to a prevailing wind direction from the western quadrant. Before reaching these two stations rain-clouds are forced to climb over high mountains where repeated fractional condensations affect the pristine isotopic values of the atmospheric moisture.

We know that, in the case of vertical gradients, several different variables, besides the dynamic of air masses, may interfere and modify these values, such as atmospheric pressure, atmospheric

humidity, etc. However, it is of interest to point out that the measured anomalies are not found only at the yearly level but also at the monthly and even at the daily level, as shown by the results reported in table 4. The results reported on the left side of the table [gradients between Paganella (2125 m.a.s.l.) and Andalo (1005 m.a.s.l.)] clearly show that during winter and spring of 1998 the mean monthly values reversed the vertical effect showing more negative isotopic values at the lower station. The results reported on the right side of the table show the anomalies that were found (in this case, far away from the Mediterranean) between high mountain stations in the Tianshan Mountains, Xinjiang Autonomous region, westernmost China (GU WEIZU & LONGINELLI, 1993). The reported vertical gradients refer to the isotopic values of daily samples of precipitation collected at the reported stations. In this case, a huge range of values was

Tab. 4 - *Anomalies in the vertical isotopic gradient ( $\delta^{18}\text{O}$  vs. VSMOW).*  
 - Valori anomali di gradienti isotopici verticali ( $\delta^{18}\text{O}$  vs. VSMOW).

Samples	Paganella* 2125 masl	Andalo* 1005 masl	Samples	Tianshan Mts.** stations (m.a.s.l.)	$\Delta\delta^{18}\text{O}/100\text{m}$ (‰)
Oct. 1997	-11.43	-10.20	06/15/1989	A 3693 - B 3539	-0.66
Nov. 1997	-12.27	-11.38	06/19/1989	A 3693 - C 2650	-0.37
Dec. 1997	-15.10	-15.01	06/30/1989	C 2650 - F 2336	<b>1.02</b>
Jan. 1998	-10.13	-11.00	06/30/1989	B 3539 - C 2650	-0.64
Feb. 1998	-11.74	-12.39	07/13/1989	C 2650 - F 2336	<b>0.11</b>
Mar. 1998	-3.31	-6.99	07/30/1989	B 3539 - F 2336	-0.24
Apr. 1998	-4.69	-10.19	08/12/1989	K 3805 - B 3539	-0.93
May. 1998	-8.90	-10.03	08/12/1989	B 3539 - C 2650	<b>0.32</b>
June.1998	-6.87	-5.96	08/20/1989	A 3693 - B 3539	-3.59
July. 1998	-6.86	-5.47	08/24/1989	K 3805 - A 3693	<b>1.87</b>
weighted mean values (2 years)	<b>-9.36</b>	<b>-9.26</b>			

\* Italian Alps, Trento area

\*\* Xinjiang Autonomous region, Western China

obtained, from  $-3.59\text{ ‰}/100$  metres to  $+1.87\text{ ‰}/100$  metres. Strangely enough, inverse isotopic gradients were found for the same precipitation event when snow was collected at higher stations and rain at lower stations. Some of these vertical gradients clearly show that small differences in elevation often yield anomalous results.

## 7. - RELATIONSHIP BETWEEN PRECIPITATION AND GROUNDWATER

The European Community recommended long ago the use of stable isotope studies to support the hydrological research and several European countries produced a commendable effort in this direction. Detailed maps of the isotopic composition of precipitation and of the main surface and deep aquifers were produced, German and Israel agencies being particularly active in this field. In Italy nothing has been done at the nation level and only a few agencies have produced relatively large sets of data, among which the Emilia-Romagna region is one of the most active in this field. Several commercial enterprises performed detailed isotope studies on relatively small areas, particularly to define the catchment basin of aquifers exploited for mineral water sale. However, we are still far away from a nationwide systematic survey that would be particularly welcome in a country whose hydrological systems are deeply related to geological and geomorphological conditions.

The study of the origin of groundwaters has been a very successful area of application of natural stable isotope variations. This is mainly due to the conservative nature of the stable isotope composition of water in an aquifer: the original isotopic composition of a groundwater is normally preserved over extremely long periods and, consequently, the isotopic composition of meteoric groundwater is often found to match reasonably the mean isotopic composition of precipitation over the recharge area. Consequently, shallow and locally derived groundwaters are often used to characterize the isotopic content of meteoric waters when, for some reason, the drawn-out process of precipitation sampling is avoided. This was the case with a study carried out by MUSSI *et alii* (1998) in northern Tuscany (Alpi Apuane-Garfagnana area) that enabled a useful reconstruction of the local distribution of the isotopic composition of rainfall starting from the measurement of surface and spring waters and using a limited number of samples per single station.

Under arid conditions an evaporative heavy isotope enrichment of groundwater may easily

take place, in parallel with a decrease in the value of the deuterium excess. Changes in the isotopic composition of groundwater may also result from mixing of groundwaters from different points of origin, mixing with fossil water bodies, and interactions and isotope exchange between water and the rock matrix. Particularly large interactions take place in deep aquifers at rather elevated temperatures. This process is specific of geothermal areas. It should be pointed out that in the first half of the twentieth century, the origin of steam in geothermal areas, and particularly at Larderello, was related to the emission of magmatic (and/or “juvenile”) water from a deep granite intrusion. The measurement of the isotopic composition of steam from Larderello (CRAIG, 1963) clearly demonstrated the meteoric origin of the steam whose oxygen isotopic composition was deeply modified by high temperature exchange processes with limestones (systematically  $^{18}\text{O}$  enriched when compared with meteoric water) while the hydrogen isotopic composition preserved its meteoric signature, mainly because of the lack of hydrogen rich materials in the geological sequence involved. Similar results were also obtained from other geothermal areas like the Geysers, Lassen Park and Steamboat Springs in the USA (CRAIG, 1963).

The meteoric origin of waters whose chemical composition was drastically modified by water-rock mass transfer can be demonstrated by the preservation of the rain water isotopic signature also when no thermal anomaly affected the hydrological system. This was the case with a survey of spring waters from the Genova province ranging from neutral  $\text{Mg-HCO}_3$  waters to some high-pH,  $\text{Ca-OH}$  waters found in association with serpentinites (BRUNI *et alii*, 2002).

In the case of alluvial deposits like the Po plain, the recharge of aquifers by infiltration from rivers is of great importance. BORTOLAMI *et alii* (1973) studied in some detail the origin of groundwaters in the plain of Venice by means of stable isotope measurements. This investigation clearly showed that phreatic aquifers in the middle and upper part of the plain underwent marked infiltration from the Brenta and Piave rivers. The oxygen isotopic composition of these aquifers was quite negative (around  $-10\text{ ‰}$ ) and very close to that of the rivers, far away from the isotopic composition of local precipitation whose average value was close to  $-7\text{ ‰}$ .

A completely different situation was found in the case of the Karst area where the dissolution processes of limestone formations and the resulting morphological features deeply affect the hydrological processes. In the classical Karst area



of Trieste, a sort of metropolitan tale (often accepted also by local hydrologists) says that the water discharged in the Gulf of Trieste at the mouth of the Timavo river comes from the so called "upper Timavo river" which disappears underground in the S. Canziano caves, about 35 km south-east of the "Timavo mouth" near Monfalcone. From the S. Canziano cave a sort of sealed pipe would carry the water to the river mouth, crossing directly the Karst area. Results of tracing experiments (ERIKSSON *et alii*, 1963) already proved that the contribution of the "Upper Timavo water" to the outflow was only of a few units per cent. To confirm these results, a long and detailed study of the isotopic composition of waters from several springs and rivers in the Karst area was carried out from 1985 to 1988 (LONGINELLI, 1988; FLORA *et alii*, 1990). A marked seasonal isotopic inversion with heavier isotopic values in winter becoming progressively lighter through spring and summer is apparent (fig. 6). The isotopic disturbances at the end of 1986 should be probably related to marked disturbances in the meteorological trend with very heavy rain in October.

The dramatic seasonal inversion may be explained as follows. The isotopic composition of the outflow of the Timavo river in winter is identical to the mean isotopic composition of precipitation on the coastal Karst section; it follows that, during winter, this outflow comes from a reservoir which is basically fed by local atmospheric precipitation. The isotopic evolution from the winter to

the summer values (normally followed by a decrease in the outflow) is the effect of a variable mixing of water of this reservoir with an isotopically lighter water that may come only from the internal (slovenian) section of the Karst area with mean elevations of about 900/1000 metres a.s.l. Coastal rain water should prevail during winter (high hydraulic pressure) while internal water should prevail during summer when the hydraulic pressure of the local system is reduced by output and reduced precipitation. A third minor component may come from the Isonzo river, essentially according to the hydraulic pressure gradients between different aquifers. This contribution is suggested by the minor negative variations recorded in May/June by the Timavo water when the Isonzo river reaches its highest flow and its most negative isotopic values related to the snow melting in its alpine basin. The old hypothesis of a direct connection between the "Upper Timavo" and the "Timavo mouth" is clearly contradicted by the isotopic results obtained.

#### Acknowledgements

In this paper table 1 is reprinted from: LONGINELLI A. et alii, *Isotopic composition of precipitation in northern Italy: reverse effect of anomalous climatic events*. J. of Hydrol., 329: 471-476, (p. 474), copyright 2006, with kind permission of the Copyright Clearance Center, Inc.; tables 2 and 3 and figures 4 and 5 are reprinted from: LONGINELLI A. & SELMO E., *Isotopic composition of precipitation in Italy: a first overall map*. J. of Hydrol., 270: 75-88, (p. 82, 83, 85), copyright 2003, with kind permission of the Copyright Clearance Center, Inc.

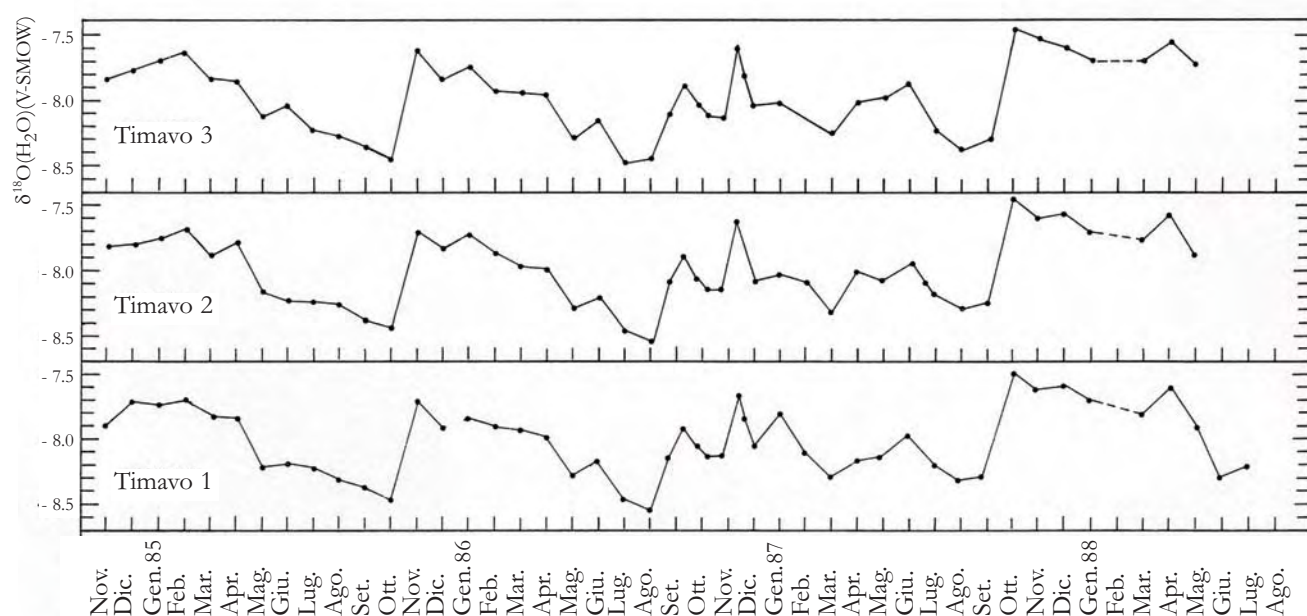


Fig. 6 - Oxygen isotopic composition of monthly water samples from the three main Timavo mouths.

- Valori della composizione isotopica dell'ossigeno di campioni mensili di acqua prelevati da quelle che vengono considerate le tre bocche principali del Timavo.

## REFERENCES

- BORSATO A., FRISIA S., CORRADINI F., LONGINELLI A., ARTIOLI G.F. *et alii* (2000) - *Acquiferi carsici in Trentino: caratteristiche fisico-chimiche, vulnerabilità e inquinamento*. Rapporto Interno Provincia Autonoma di Trento, Dipartimento dell'Ambiente, 280 pp.
- BORTOLAMI G., FONTES J.CH. & PANICHI C. (1973) - *Isotopes du milieu et circulations dans les aquifères du sous-sol Vénétien*. Earth Planet. Sc. Letters, **19**: 154-160.
- BRUNI J., CANEPA M., CHIODINI G., CIONI R., CIPOLLI F., LONGINELLI A., MARINI L., OTTONELLO G. & VETUSCHI ZUCCOLINI M. (2002) - *Irreversible water-rock mass transfer accompanying the generation of the neutral, Mg-HCO<sub>3</sub> and high-pH, Ca-OH spring waters of the Genova province, Italy*. Applied Geochem., **17**: 455-474.
- CAPASSO G., DONGARRÀ G., FAVARA R., HAUSER S. & VALENZA M. (1990) - *Composizione isotopica delle piogge, dell'acqua dei pozzi e del vapore fumarolico dell'isola di Vulcano*. CNR, Pubblicaz. Istituto Geochim. dei Fluidi, Palermo, pp. 38-52.
- CONVERSINI P. & TAZIOLI G.S. (1993) - *Indagini idrogeologiche nella media e alta valle del fiume Menotre, Umbria orientale*. Atti Ticin. Sci. Terra, **36**: 153-164.
- CRAIG H. (1961) - *Isotopic variations in meteoric waters*. Science, **133**: 1702-1703.
- CRAIG H. (1963) - *The isotopic geochemistry of water and carbon in geothermal areas*. In: E. TONGIORGI (Ed.): «Nuclear geology in geothermal areas». CNR, Pisa, 17-53.
- CRAIG H. & GORDON L.I. (1965) - *Deuterium and oxygen-18 variations in the ocean and the marine atmosphere*. In: E. TONGIORGI (Ed.): «Stable isotopes in oceanographic studies and paleotemperatures». CNR, Pisa, pp. 9-130.
- DANSGAARD W. (1954) - *The <sup>18</sup>O abundance in fresh water*. Geochim. Cosmochim. Acta, **6**: 241-252.
- DANSGAARD W. (1961) - *The isotopic composition of natural waters*. Medd. om Grönland, **165** (2): 1-120.
- DANSGAARD W. (1964) - *Stable isotopes in precipitation*. Tellus, **16**: 436-468.
- EPSTEIN S. & MAYEDA T. (1953) - *Variation of <sup>18</sup>O content of waters from natural sources*. Geochim. Cosmochim. Acta, **4**: 213-224.
- ERIKSSON E., MOSETTI F., HODOŠČEK K. & OSTANEK L. (1963) - *Some new results on the karstic hydrology with the employ of tritiated water as a tracer*. Boll. Geof. Teor. Appl., **5**: 18-32.
- FIDEL R. (1976) - *Bibliography of hydrogen and oxygen stable isotope hydrology*, The Hebrew University of Jerusalem.
- FLORA O., GALLI G., NEGRINI L. & LONGINELLI A. (1990) - *Studio geochimico-isotopico di alcune sorgenti carsiche: un nuovo modello idrologico*. Atti e Mem. Commiss. Grotte "E. BOEGAN", **29**: 83-102.
- FÖRSTEL H. & HÜTZEN H. (1982) - *<sup>18</sup>O/<sup>16</sup>O ratios of ground-water at the Federal Republic of Germany*. In: H.L. SCHMIDT, H. FÖRSTEL. & K. HEINZINGER (Eds.): *Stable isotopes, Analytical Chemistry Symposium Series*, **11**: 173-178, Elsevier, Amsterdam.
- GAT J.R. (1980) - *The isotopes of hydrogen and oxygen in precipitation*. In: P. FRITZ & J.CH. FONTES (Eds.): *Handbook of environmental isotope geochemistry*, **1**, The terrestrial environment, pp. 21-47, Elsevier Publ. Co., Amsterdam.
- GU WEIZU & LONGINELLI A. (1993) - *A case study on the hydrological significance of stable isotope data on alpine catchments with snow cover and glaciers, Xinjiang, China*. In: W. LAURIER (Ed.): *Proceedings of the ISSGH Katmandu Conference*. IAHS Publication, **218**: 371-383.
- HAUSER S., DONGARRÀ G., FAVARA R. & LONGINELLI A. (1980) - *Composizione isotopica delle piogge in Sicilia. Riferimenti di base per studi idrogeologici e relazioni con altre aree mediterranee*. Rend. Soc. Ital. Mineral. Petrol., **36**: 671-680.
- JOUSSAUME S., SADOURNY R. & JOUZEL J. (1984) - *A general circulation model of water isotope cycles in the atmosphere*. Nature, **311**: 24-29.
- LONGINELLI A. (1988) - *Stable isotope hydrology of the classical Karst area, Trieste, Italy*. In: F. BARBERI, F. INNOCENTI, M. LEONE & F.P. SASSI (Eds.): *Special volume in memory of M. Carapezza*, Rend. Soc. Ital. Mineral. Petrol., **43**: 1175-1183.
- LONGINELLI A., ANGLESIO E., FLORA O., IACUMIN P. & SELMO E. (2006) - *Isotopic composition of precipitation in Northern Italy: reverse effect of anomalous climatic events*. J. of Hydrol., **329**: 471-476.
- LONGINELLI A. & SELMO E. (2003) - *Isotopic composition of precipitation in Italy: a first overall map*. J. of Hydrol., **270**: 75-88.
- MERLIVAT L. & JOUZEL J. (1979) - *Global climatic interpretation of the deuterium-oxygen-18 relationship for precipitation*. J. Geoph. Res., **84**: C, 5029-5033.
- MUSSI M., LEONE G. & NARDI I. (1998) - *Isotopic geochemistry of natural waters from the Alpi Apuane-Garfagnana area, Northern Tuscany, Italy*. Mineral. Petrogr. Acta, **41**: 163-178.
- ROZANSKI K. (1985) - *Deuterium and Oxygen-18 in European groundwaters - links to atmospheric circulation in the past*. Chem. Geol., **52**: 349-363.
- ROZANSKI K., ARAGUÁS-ARAGUÁS L. & GONFIANTINI R. (1993) - *Isotopic patterns in modern global precipitation*. AGU, Geophys. Monogr., **78**: 1-36.
- ROZANSKI K., SONTAG C. & MÜNNICH K.O. (1982) - *Factors controlling stable isotope composition of European precipitation*. Tellus, **34**: 142-150.
- SIEGENTHALER U. & OESCHGER H. (1980) - *Correlation of <sup>18</sup>O in precipitation with temperature and altitude*. Nature, **285**: 314-316.
- STICHLER W., TRIMBORN P., MALOSZEWSKI P., RANK D., PAPESCH W. & REICHERT B. (1997) - *Isotopic investigations*. Acta Carsologica, **26** (1): 213-259.
- YURTSEVER Y. (1975) - *Worldwide survey of stable isotopes in precipitation*. Internal report IAEA, Vienna.
- YURTSEVER Y. & GAT J. (1981) - *Atmospheric waters*. In: J.R. GAT & R. GONFIANTINI (Eds.): *Stable isotope Hydrology: Deuterium and Oxygen-18 in the water cycle*, IAEA, Techn. Rep. Ser., **210**: 103-142. IAEA, Vienna, Austria.

## Stratigraphic revision of Brindisi-Taranto plain: hydrogeological implications

*Revisione stratigrafica della piana Brindisi-Taranto  
e sue implicazioni sull'assetto idrogeologico*

MARGIOTTA S. (\*), MAZZONE F. (\*),  
NEGRI S. (\*)

**ABSTRACT** - The studied area is located at the eastern and western coastal border of the Brindisi-Taranto plain (Apulia, Italy). In these pages, new detailed cross-sections are presented, based on surface surveys and subsurface analyses by borehole and well data supplied by local agencies or obtained by private research and scientific literature, integrated with new ERT surveys. The lithostratigraphic units identified in the geological model have been ascribed to the respective hydrogeologic units allowing for the identification of the main aquifer systems:

- a deep aquifer that lies in the Mesozoic limestones, made of fractured and karstic carbonates, and in the overlying Lower Pleistocene calcarenite;
- a shallow aquifer that is formed by the middle-upper Pleistocene marine calcarenitic and sandy deposits overlying the lower Pleistocene clays, holding a phreatic ground water body.

The Brindisi sands are part of the shallow aquifer, constituting its lower hydrogeologic unit. The identification of this body permits the modification of previous models. The results of this research indicate the importance of the detailed geological mapping of the Brindisi – Taranto area particularly in order to clarify the stratigraphy and hydrostratigraphy of the Pleistocene successions. ERT data proved itself to be indispensable in the definition of the different hydrogeological units.

**KEY WORDS:** Brindisi – Taranto plain, Electrical Resistivity Tomography (ERT), Hydrogeologic units, Shallow aquifer, Stratigraphy.

**RIASSUNTO** - In questo articolo si propone una revisione stratigrafica delle unità della piana Brindisi – Taranto e se ne evidenziano le implicazioni sull'assetto idrogeologico. Rilievi geologici di superficie e del sottosuolo, sia attraverso l'osservazione diretta di carote di perforazioni sia mediante indagini ERT, hanno permesso di delineare gli assetti geologici e di reinterpretare i numerosi dati di sondaggi a disposizione. Definito il modello geologico sono state individuate le unità idrogeologiche che costituiscono i due acquiferi principali. Il primo, profondo, soggiace tutta l'area di studio ed è costituito dai Calcari di Altamura mesozoici, permeabili per fessurazione e carsismo, e dalle Calcareniti di Gravina pleistoceniche, permeabili per porosità. Il secondo superficiale, è costituito dai depositi pleistocenici calcarenitici e sabbiosi permeabili per porosità, ed è sorretto dalle argille anch'esse pleistoceniche. L'identificazione all'interno di questo secondo acquifero, della unità delle Sabbie di Brindisi, che ne costituisce la parte inferiore, consente di modificare i precedenti modelli geologici ed idrogeologici. Le ricerche effettuate mettono comunque in evidenza la necessità di maggiori studi di dettaglio con particolare riferimento ai depositi pleistocenici. A questo scopo, a causa dell'estensione nel sottosuolo di queste unità, quasi ovunque mascherate dalle coperture continentali recenti, indispensabile sarà l'uso e lo sviluppo delle metodologie ERT che si sono dimostrate altamente affidabili e risolutive.

**PAROLE CHIAVE:** Acquifero superficiale, piana Brindisi – Taranto, Stratigrafia, Tomografia Geoelettrica (ERT), Unità idrogeologiche.

(\*) Dipartimento di Scienza dei Materiali, Università del Salento, via per Monteroni, 73100 Lecce



## 1. - INTRODUCTION AND PREVIOUS WORKS

The studied area is located at the eastern and western coastal border of the Brindisi - Taranto plain (fig. 1), that is part of the Apulian foreland. This is the emerged area of the Apulian Plate, consisting of a thick basement made of Mesozoic limestones (SELLI, 1962; D'ARGENIO *et alii*, 1973; D'ARGENIO, 1974; RICCHETTI, 1980; CIARANFI *et alii*, 1983). They are covered by Plio-Pleistocene deposits, resulting from the sedimentary cycle of the Bradanic foredeep (RICCHETTI *et alii*, 1988; RICCHETTI, 1967, 1980; DOGLIONI *et alii*, 1999). Gravina Calcarenite (yellowish calcarenites of Early Pleistocene) and subapennine Clays (grey-blue silty clays of Early Pleistocene) represent the litho-stratigraphic units of this cycle in the studied area (CIARANFI *et alii*, 1992). These deposits are covered by marine terraced bioclastic deposits (Middle-Late Pleistocene) (BENTIVENGA *et alii*, 2004) and by Holocene to recent continental deposits. In accordance with this geological model a deep regional karsic aquifer in mesozoic carbonate rocks and a shallow aquifer in Terraced Deposits have been identified (COTECCHIA, 1977; CHERUBINI *et alii*, 1987; RICCHETTI & POLEMIO, 1996).

Detailed biostratigraphical (COPPA *et alii*, 2002) studies have assigned to Early and Middle Pleistocene a sequence of yellowish muddy sands cropping up along the Brindisi sea-cliff about one kilometre south of our study site. The Authors do not identify contact with the overlying and underlying units and indicate the uncertain and discordant ascriptions of this sequence in literature (DI GERONIMO, 1969; GENTILE *et alii*, 1996) to formal lithostratigraphic units.

In the Taranto area, also BELLUOMINI *et alii* (2002) describe a transgressive clayey - sandy unit (about 4m thick) overlying the subapennine Clay Formation that is attributable to the Middle Pleistocene age; lack of borehole log data do not permit the assessment of the extension and thickness of this unit in the subsurface.

Our purpose is to clarify the geological and geophysical features of the subsoil for hydrogeologic purpose. This work has been carried out in five distinct phases. The first is the geological study that was organized in surveys of the surface and of the subsoil via direct observation of borehole cores (figg. 1, 2, 3); the second is characterized by the identification of existing wells in the area, collection of stratigraphical data (about 1000, figure 1 and 3) drawn from borehole cores and supplied by local agencies, from private research and from scientific literature (RADINA, 1968; TEDESCHI, 1969). The distribution of the data deriving from the well

stratigraphic logs is homogeneous in the Brindisi - Taranto plain (fig. 1) but, in the Brindisi area numerous borehole and piezometer logs have been carried out to assess the contamination from some industrial sites (fig. 2). In the third phase these data have been processed taking into account the geological model. The collated data have been inserted in input to a Geographical Information System (GIS). In this phase, also the hydrological and geotechnical data (piezometric levels, flow, permeability of the various formations, physical and granulometric characteristics) available from private research and scientific publications (CHERUBINI *et alii*, 1987) have been processed. In the fourth phase, ERT surveys were carried out in particular selected areas in order to clarify the features of the shallow aquifer. The Electrical Resistivity Tomography (ERT) is widely used in the detection and investigation of shallow-depth targets. ERT has been applied with great success in solving geological (LEUCCI *et alii*, 2004, CARDARELLI, 2006) and hydrogeological (FURMAN *et alii*, 2004, MARGIOTTA & NEGRI, 2005) problems. In the fifth phase, the hydrogeologic units and the main aquifer systems have been defined and parametrized.

## 2. - MORPHOLOGICAL SETTING

The morphology of the area is characterized, both on the Adriatic and the Ionian coast, by a broad plain, slightly sloping towards the sea, in many places marked by a drainage network made of small natural and/or man-made channels. The altitude is between 30 and 40m asl, decreasing towards the coastal zone. The Adriatic coastline in the surrounding area of "Cerano" power station is composed of a vertical cliff that reaches a maximum height of 15m. Cliff height decreases northward until it gives place to a number of coastal depressions whose bottom is bsl (e.g. the "Salina Vecchia").

The drainage system in the area is well developed. It is characterized by numerous shallow channels that in many cases run directly into the sea (e.g. "Fiume Grande", "Foggia Rau", "Fiume Piccolo", "Canale Palmarini - Patri", "Canale Cil-larese"). Some of them are cut by the present cliff whereas the lower course of main streams has been submerged due to Holocene sea level rise, forming narrow inlets like the "Canale Pigonati", "Seno di Levante" and "Seno di Ponente", which form the natural port of Brindisi.

Watersheds are hard to identify. Numerous smaller channels flow into broad depressions which are very prone to flooding. There is a broad marshy area near the mouth of the "Canale di Scarico".

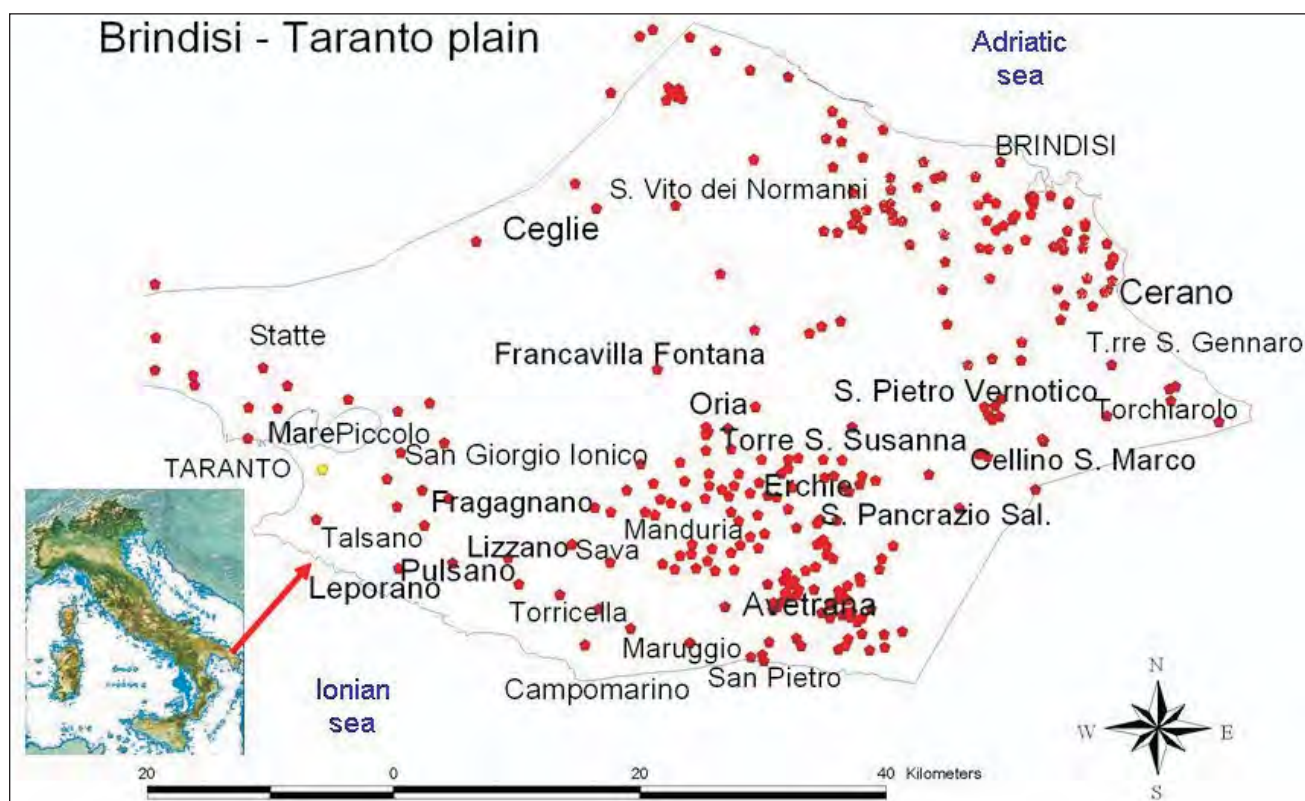


Fig. 1 – Collected well data in the studied area.

– Area di studio con ubicazione dei dati a disposizione provenienti da carote di perforazione.

On the Ionian coast, the area is marked by wet zones, dune belts, lagoon areas and coastal springs (fig. 4). The drainage system, in this area, is well-developed but, in many places, it has a temporary character; as usual in karst areas, it is of secondary importance compared to the ground water circulation. Infiltration of water through the most fractured zones in the carbonate rock mass enhanced the development of karstic phenomena as sinkholes. At these sites, rapid infiltration of surface water in the subsoil is prevailing.

This area has been strongly influenced by human activity. Especially over the last few decades, reclamation works have strongly modified the drainage network and have been responsible for the filling of the main depressions which marked the area.

### 3. - STRATIGRAPHY

The geological surveys integrated with borehole data (figg. 1, 2) have allowed us to define the geological models of the area (fig. 3, fig. 6), to determine the thickness of stratigraphic units (fig. 5), to realize numerous two-dimensional cross sections (figg. 7, 8) and to identify under-investigated areas.

Altamura Limestone (Late Cretaceous) outcrops

corresponding to the Murge hills, immediately to the west of the Brindisi area, and to the east of the Taranto one; the succession is made of alternating limestones and dolomitic limestones, both micritic, compact and tenacious, whitish, light grey or hazel in colour, in layers from a few centimetres to about 1m thick. In places, the layers appear densely laminar; flakes may be easily broken off pieces of the rock. The outcrops have a thickness of a few metres only, in places covered by topsoil. Greater thickness (up to 30-40m) is visible in the quarries located near the area under study, some of which are still in use while others are used as waste dumps. In many places layers are fractured and disjointed. There are few macrofossils, characterized by fragments of rudist, with smaller amounts of coral and bivalves. The top of the carbonatic basement is found at variable depths in nearby areas, due to the presence of NW-SE striking faults with offsets of several decametres. In general, the top of this formation deepens moving from the “Murge” hills, where the Cretaceous limestones outcrop out at elevations of about 35–40m, towards the sea. Along the Ionian coast, the top of this formation is at about 280 m (fig. 5) bsl while, on the eastern side (fig. 8), the top of the formation deepens from the south of the investigated zone (Cerano power station, where the top is 20 m

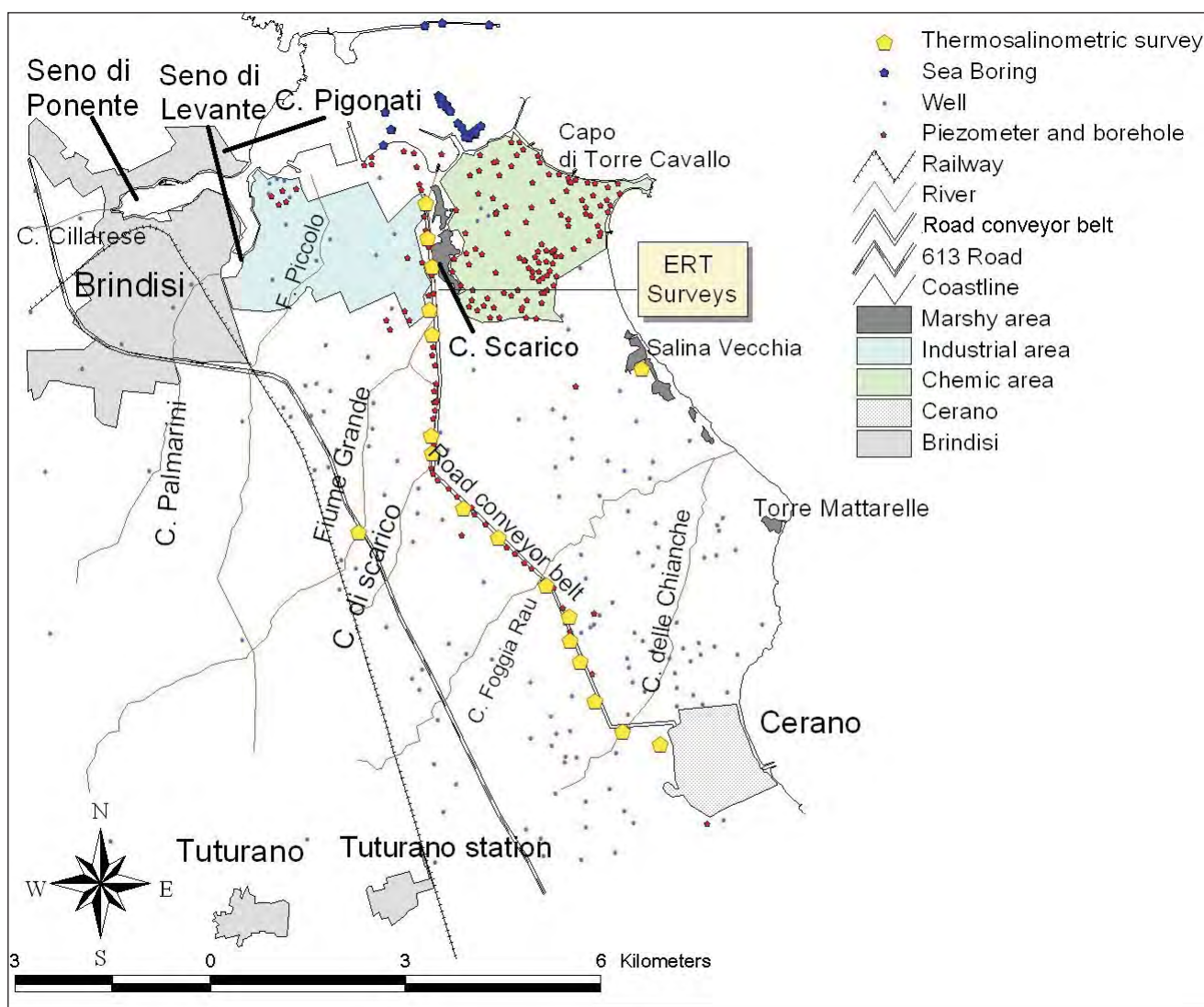


Fig. 2 – Brindisi area with location of the piezometer and borehole logs available.  
 – Area di Brindisi con ubicazione dei dati a disposizione provenienti da sondaggi e piezometri.

bsl) towards the north (Brindisi port, where the top is 90 m bsl).

A unit of whitish – greyish micritic limestone interbedded with centimetre-scale layers of whitish limestone and laminated yellowish calcareous marls, silt and clays, with paleosols and lignite layers was recognized in a borehole log near Talsano. It has been correlated with the Galatone Formation (Late Oligocene), that was recently formalized by BOSSIO *et alii* (1999) in the nearby Salento Leccese area. The permeability of Galatone Formation is variable, due to the different lithological types.

Gravina Calcarenite is the most ancient of the Early Pleistocene formations of the area. This unit outcrops in the inner part of the study area and can be observed in the quarries near Avetrana, Manduria and Sava, on the western side of southern Apulia, because the rock is used as building material. It overlies, with angular unconformity, the

Cretaceous basement, and consists of yellow coarse-grained calcarenite with abundant fossils. The thickness of the formation varies considerably and reaches maximum values of more than 30 m at the eastern coast and 45m at the western one.

The subapennine Clays (Early Pleistocene) formation is made of clays and grey-blue sandy clays, rich in fossils. These deposits can be defined as sands with clay; nevertheless, there is considerable variation in the dimensions of the grains. The percentage of sand varies from 2% to 55%, that of silt about 10%; the average carbonate content is 31%; this value increases moving towards the underlying Gravina Calcarenite. Inside the formation, whose thickness is never less than several decameters, there are sandy layers of a grey-blue colour whose lateral and vertical extension is not easily measurable. The stratigraphical transition to the underlying Gravina Calcarenite has never been ob-



served in outcrop. Along the eastern coast, the thickness of this formation varies greatly from a few metres to over 50 m. Specifically, the thickness increases moving from the “Cerano” power station (average 20 m), placed at the southern limit of the investigated area, to the port of Brindisi, which is at the northern limit (average 45 m). Moving from west to east, the tops of the Mesozoic limestones and of the overlying Pleistocene calcarenite deepens, and the thickness of the subapennine Clays, which overlie the Pleistocene calcarenite, increases.

The top of the subapennine Clays is above sea level in the zone near the “Cerano” power station, while elsewhere the top is found at a maximum elevation of 29 m bsl. Along the western side, two distinct intervals can be distinguished: the upper is made of grey to yellow-light brown, fine-grained sands with abundant diagenetic concretions. Moving downwards, there is an enrichment of the silty-clayey fraction, interlayered with sands from a few millimetres to centimetres thick. Overall thickness of this interval is about 10 m. The lower interval of the subapennine Clays can be defined as

clays and grey-blue sandy clays. Within this interval, whose thickness is never less than several decameters, there are grey-blue sandy layers whose lateral and vertical extension is not easily measurable. This formation outcrops along several cliff faces along the Ionian coast. Along this side, the total thickness of the subapennine Clays increases, moving from the Murge towards the coast, reaching a maximum of 230 m in the subsoil (fig. 5).

The provisional and informal term of Brindisi sands is used by MARGIOTTA *et alii* (2008) to refer to sandy and silty-clayey deposits found in places between the Middle – Upper Pleistocene Terraced Deposits and the subapennine Clays along the coast of Brindisi. The type-section of this formation is located on the cliff near the “Cerano” power station (fig. 9) where it is about 12 m thick. The transition between the Terraced Deposits and this formation is characterized by an abrupt lithological variation (from diagenetic calcarenite to sands). The erosional contact with the underlying subapennine Clays is also visible here. In terms of granulometry, moving downwards, the transition

## Geological Map

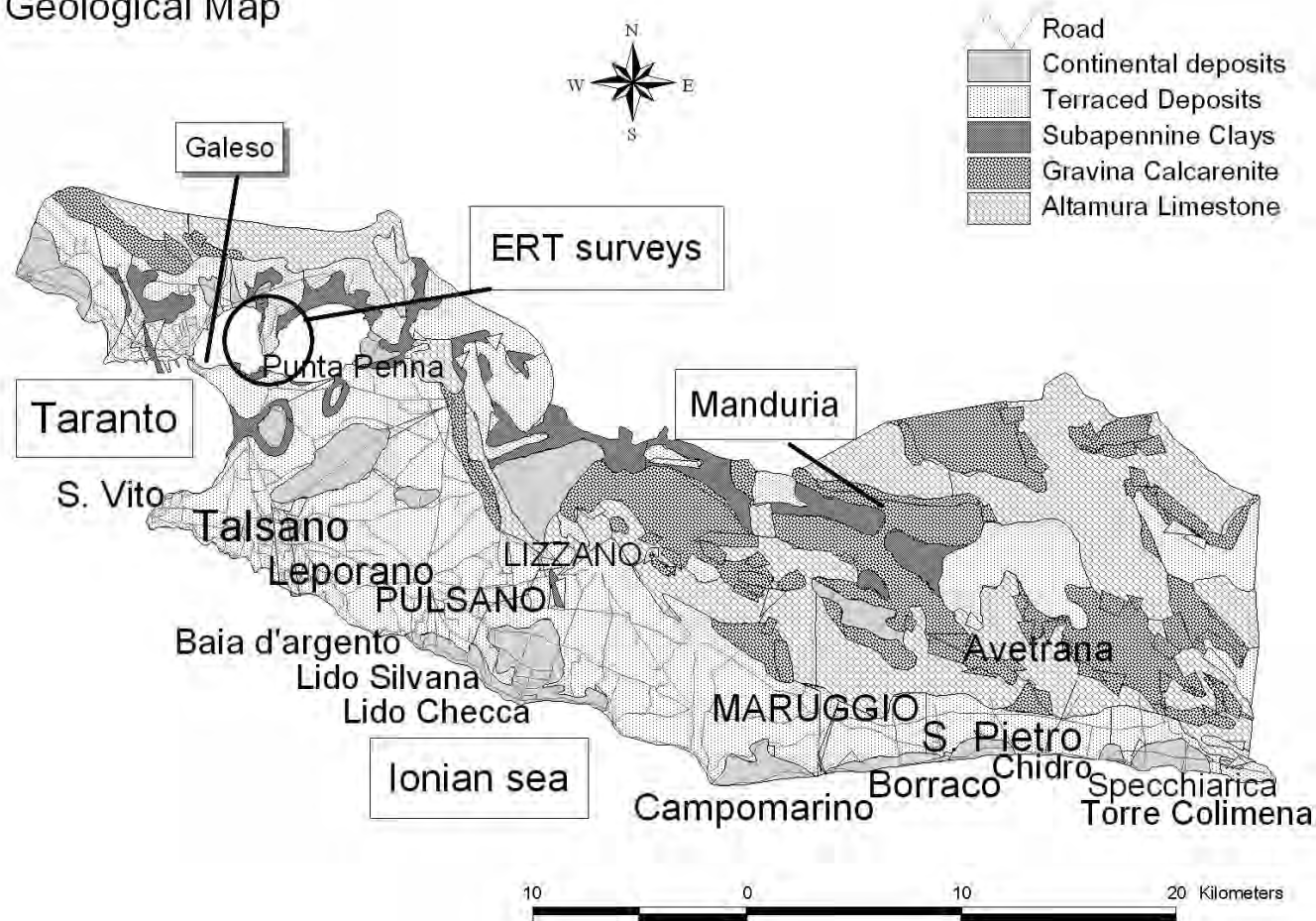


Fig. 3 – Schematic geological map of Taranto area.  
– Carta geologica schematica dell'area di Taranto.

involves an enrichment of the silty-clayey fraction, interleaved with sandy layers a few millimetres or centimetres thick. The Brindisi sands are composed of fine-grained sands whose colour shifts from grey to yellow-light brown moving upwards; these sands contain abundant diagenetic concre-



Fig. 4 – Example of spring phenomena, the Chidro spring.  
– Esempio di manifestazione sorgentizia (Chidro).

tions that are aligned in the upper part and become scattered moving downwards. The lower part of this formation is made up of clayey-sandy silts of grey colour, with carbonaceous fragments. In mineralogical terms, the grains of the sandy fraction are mainly made up of carbonate and quartz fragments. The clayey and sandy fractions comprise 35% to 38% of the lower part of the layer. The stratification is indistinct. The thickness of this formation varies from a few decimetres to 20 m. The mean thickness is about 13 m - 14 m. The age, according to its stratigraphic position, is Early-Middle Pleistocene.

The Middle-Upper Pleistocene formation of the Terraced Deposits is lithologically composed of yellowish coarse-grained biocalcarenites with sandy layers or layers of organogenic limestones varying in thickness from a few centimetres to 15cm; in places, near the contact with the subapennine Clays, layers of very compact and tenacious limestones, a few decimetres thick, are present. The sandy facies is composed mainly of quartz grains, feldspars and carbonatic material of detritic and bioclastic origin; mica crystals are rare.

Grain-size of the sandy facies varies greatly de-

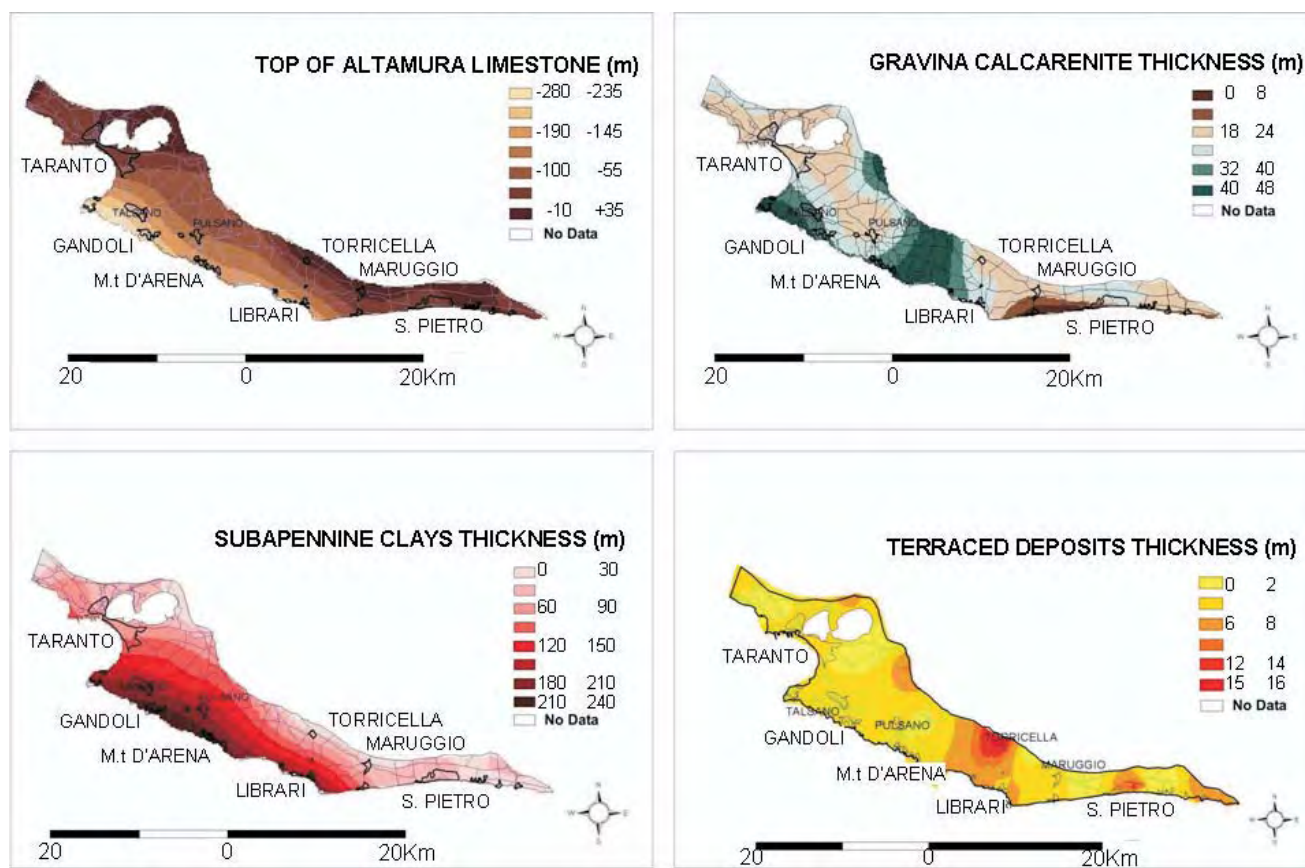


Fig. 5 – Thickness of the lithostratigraphical units and elevation map of the Altamura Limestone top in the Taranto area.  
– Spessori delle unità litostatigrafiche e mappa del tetto del Calcare di Altamura nell'area tarantina.



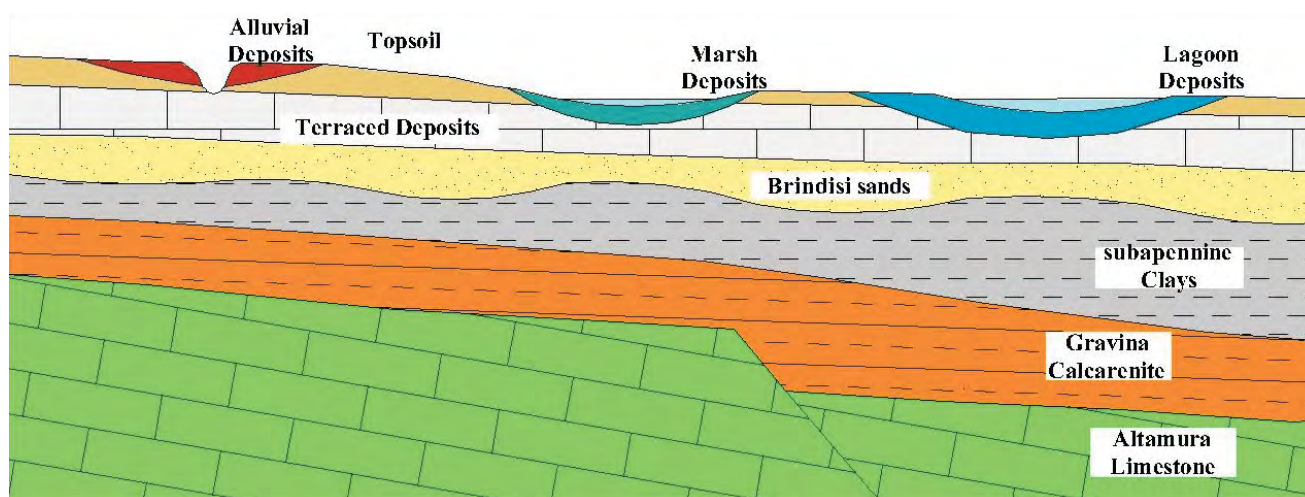


Fig. 6 – Stratigraphic scheme in Brindisi area.  
– Schema stratigrafico nel Brindisino.

pending on the stratigraphical level (gravel: 0%-28%, sand: 3%-84%, silt: 2%-75%). The upper portion of the middle Pleistocene succession (Terraced Deposits) consists of marine sands and conglomerates forming several orders of terraces. These in turn are linked to sea level changes caused by the primarily glacio-eustatic phenomena that occurred in the Middle-Late Pleistocene age and/or to tectonic movement. The transition to the underlying subapennine Clays is in some places direct and in others through the interposition of Brindisi sands as described before (fig. 9). The contact of Terraced Deposits with the underlying subapennine Clays is characterized by an abrupt lithological variation (from diagenetic calcarenite to sands); this transition can be frequently observed in detail on the cliff of the western coast (fig. 10) near the “T.S. Vito, Leporano, Punta Penna, Baia d’Argento, Lido Silvana, Lido Checca” and inside some channels (for example S. Nicola channel). At Torre Castiglione and at the base of the Murge hillside, the contact with the Altamura Limestone is visible, characterized by evident angular discordance. It may be assumed that this formation extends discontinuous across the whole of the studied area. The thickness varies considerably, from a few decimetres to about 20 m, although the most frequent values are in the range of 5-6 m.

Continental deposits are constituted by marsh (maximum thickness of 25 m and degree of saturation very close to 100%), eluvial (maximum thickness of about 6.2 m and saturation level not high), alluvial (thickness between 40 cm and 8 m and saturation of 100%) and lagoon deposits (thickness between 60 cm and 9.6 m and degree of saturation of about 95%). Top soil lies over almost all the area under examination.

#### 4. – ELECTRICAL RESISTIVITY TOMOGRAPHY (ERT)

Geoelectrical prospecting was conducted in different places of the two studied areas aiming to determine the electrical properties of the units and to clarify the mechanism of formation of the spring phenomena. In this section we show two of the most important profiles conducted on the eastern side of the Brindisi-Taranto plain, near two boreholes whose logs and stratigraphies were well-known and helpful for calibration of the geophysical model (fig. 2).

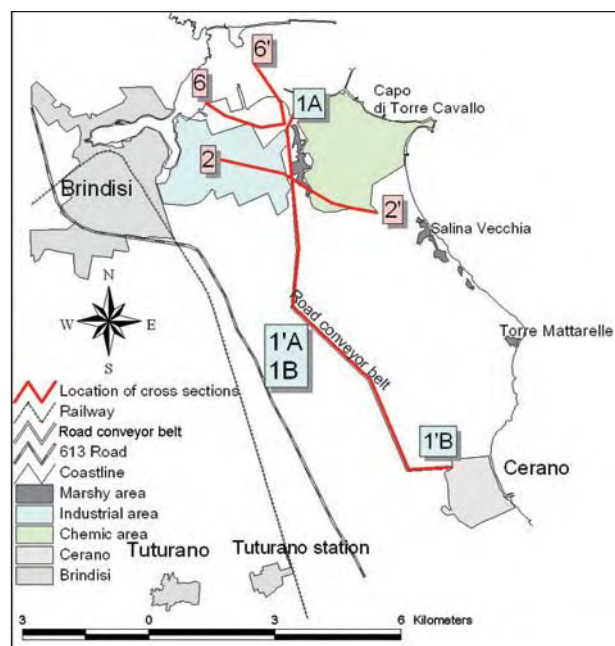


Fig. 7 – Location of the cross sections in the Brindisi area.  
– Ubicazione delle tracce delle sezioni geologiche del Brindisino.



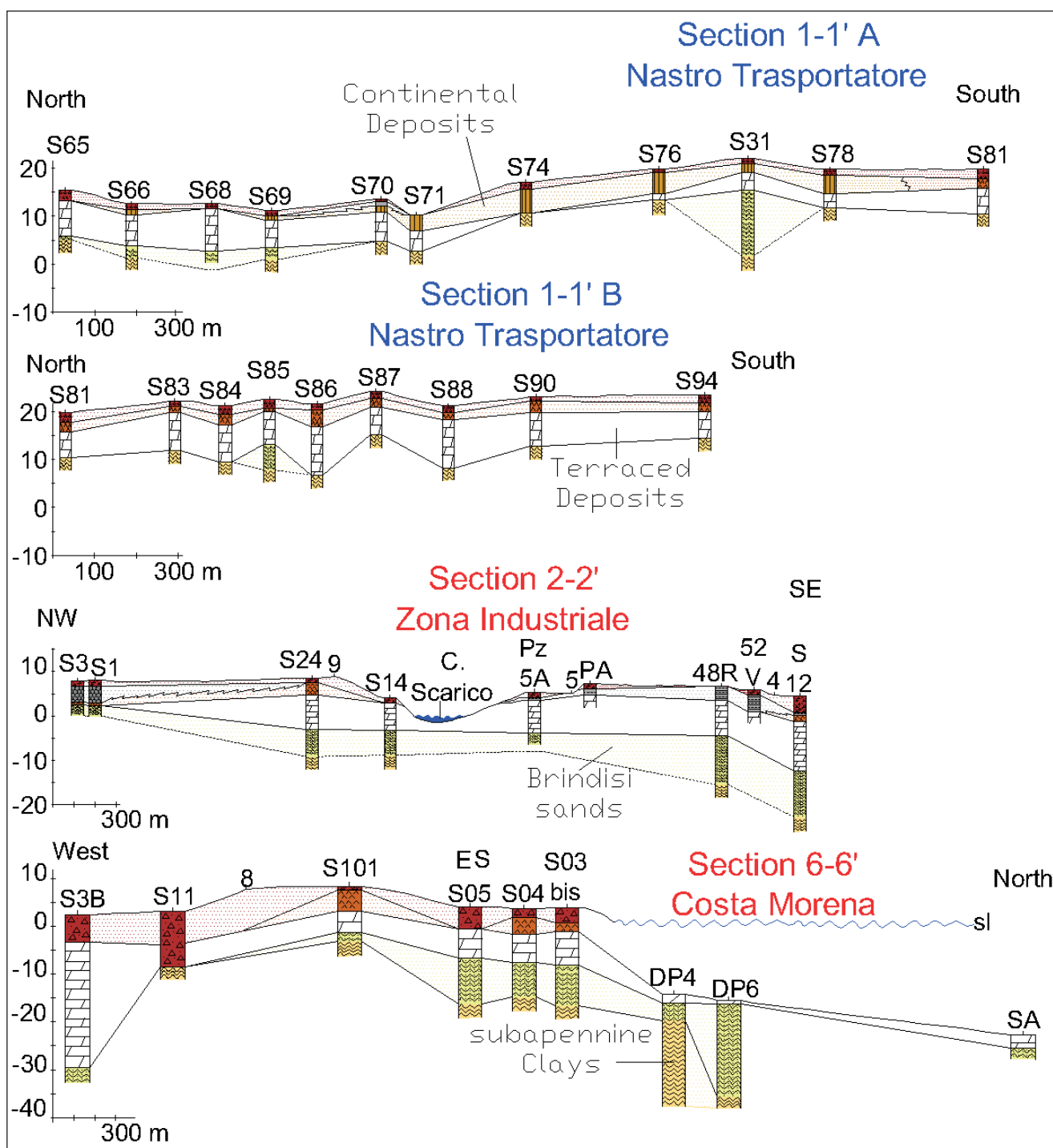


Fig. 8 – Cross sections in the Brindisi area.  
– Sezioni geologiche del Brindisino.

Apparent-resistivity data were collected using a Syscal-R1 (manufactured by Iris instruments), in multielectrode configuration. To obtain 2D resistivity models, the measured data were processed using the smoothness constrained least square method. The finite-difference and finite-elements method was applied in order to calculate forward response of the geoelectrical models while Gauss–Newton optimization method was used to solve

the inverse resistivity problem. The two software packets used were, in order, TomoLab, produced by Geostudi Astier s.r.l. and LOKE (2004) produced by Geotomo Software. The ERT results were compared with geological and hydrogeological data existing in the study area (boreholes S14 and S17).

The most significant ERT 2D models are shown in figure 10 related profile P5 and P6. The survey carried out for P5 and P6 using array dipole–dipole

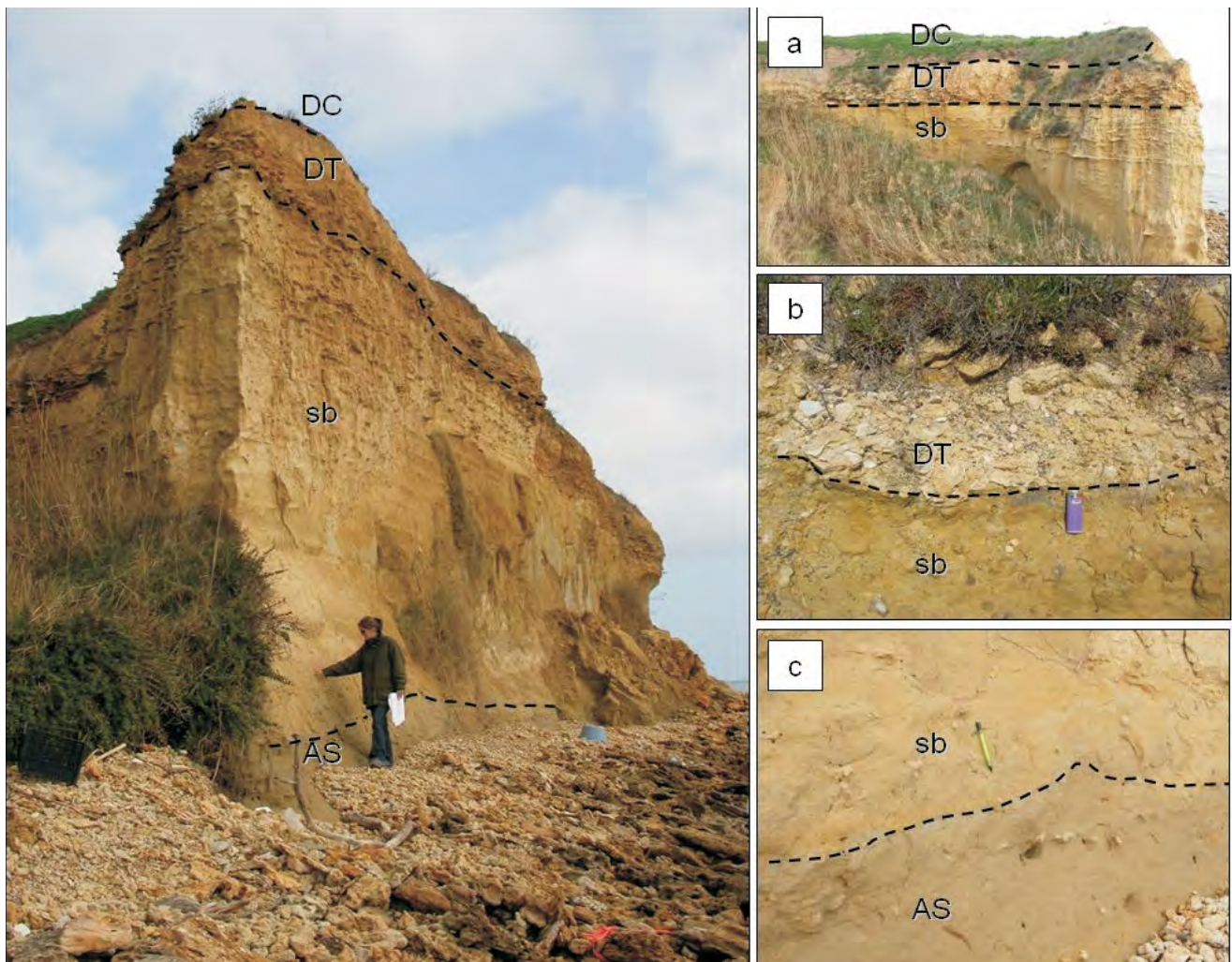


Fig. 9 – Cerano power station (cliff) type section of Brindisi sands. (a) contact between continental Deposits (DC), Terraced Deposits (DT) and Brindisi sands (sb), (b) contact between Terraced Deposits (DT) and Brindisi sands (sb), (c) contact between Brindisi sands (sb) and subapennine Clays (AS).  
 – Sezione-tipo delle Sabbie di Brindisi presso la Falesia in località Cerano. (a) contatto tra i Depositi continentali (DC), quelli di Terrazzo (DT) e le Sabbie di Brindisi (sb), (b) contatto tra gli stessi Depositi di Terrazzo (DT) e le Sabbie di Brindisi (sb), (c) contatto tra le Sabbie di Brindisi (sb) e le Argille subappennine (AS).

with 48 electrodes and the distance between electrodes along the lines was also 3 m. The subsoil can be subdivided into the following four distinct electro-layers (moving downwards from the surface):

Electro-layer 1: the thickness of this layer varies between 1 and 3m and its resistivity values between 10 and 20ohm\*m. This layer is attributable to infill material at the surface;

Electro-layer 2: the resistivity of this layer varies between 50 and 200ohm\*m, and its thickness from 6 to 8 m. In P5 the bottom of this layer lies at a depth of approximately 10.5 m. This layer is attributable to water-saturated calcarenite of the Terraced Deposits. These interpretations are supported by existing lithological and hydrogeological data;

Electro-layer 3: the thickness of this layer varies between 5 and 7m; the bottom lies at a depth of 18m and its resistivity values range from 8 to 20ohm\*m. This electro-layer may geologically be

associated with saturated Brindisi sands;

Electro-layer 4: the resistivity of this last electro-layer is characterized by values below 5ohm\*m. This layer corresponds to the subapennine Clays. The resistivity values decrease with depth and this is certainly due, in the absence of vertical lithological variations, to the increasing salinity of the water content.

The ERT models are in accordance with the geological and hydrogeological data obtained from specific points (boreholes S14 and S17).

Another profile, conducted in the western side, near “Mar Piccolo” is shown (fig. 3 and 12). The survey was carried out using array dipole–dipole with 71 electrodes and the distance between electrodes along the lines was also 5 m. The electrical profile, conducted transversally to a spring (fig. 12) in an area near the shoreline, permits the clarification of the site geology. In this case, according to the geological surveys, the subsoil can be subdivi-





Fig. 10 – Contact between the impervious subapennine Clays (AS) and the permeable Terraced Deposits (DT) along the coast near Lido Silvana.  
 – Contatto tra le Argille subappennine (AS), impermeabili, ed i Depositi di Terrazzo (DT), permeabili, lungo la costa Tarantina in località Lido Silvana.

vided into the following three distinct electro-layers (moving downwards from the surface):

1. a superficial electro-layer with a depth of about 0–12m and resistivity values of 1-5ohm\*m. This layer is attributable to subapennine Clays;

2. an electro-layer with a depth of about 12–20m and resistivity values of 5-20ohm\*m. This layer is attributable to water-saturated calcarenite of the Gravina Calcarenite;

3. an electro-layer whose top is about 40m depth and resistivity values of 25-40ohm\*m. This electro-layer may geologically be associated with saturated Altamura limestone. It is important to

note that this electro-layer has a discontinuous top surface probably due to a fault. In correspondence of this discontinuity, where Subapennine Clays layers obstruction is interrupted, there is a spring.

## 5. – THE AQUIFER SYSTEMS OF THE BRINDISI – TARANTO PLAIN

On the basis of the previously described stratigraphic models and of ERT researches, several aquifer systems have been identified in the studied area. Both the eastern and the western areas con-



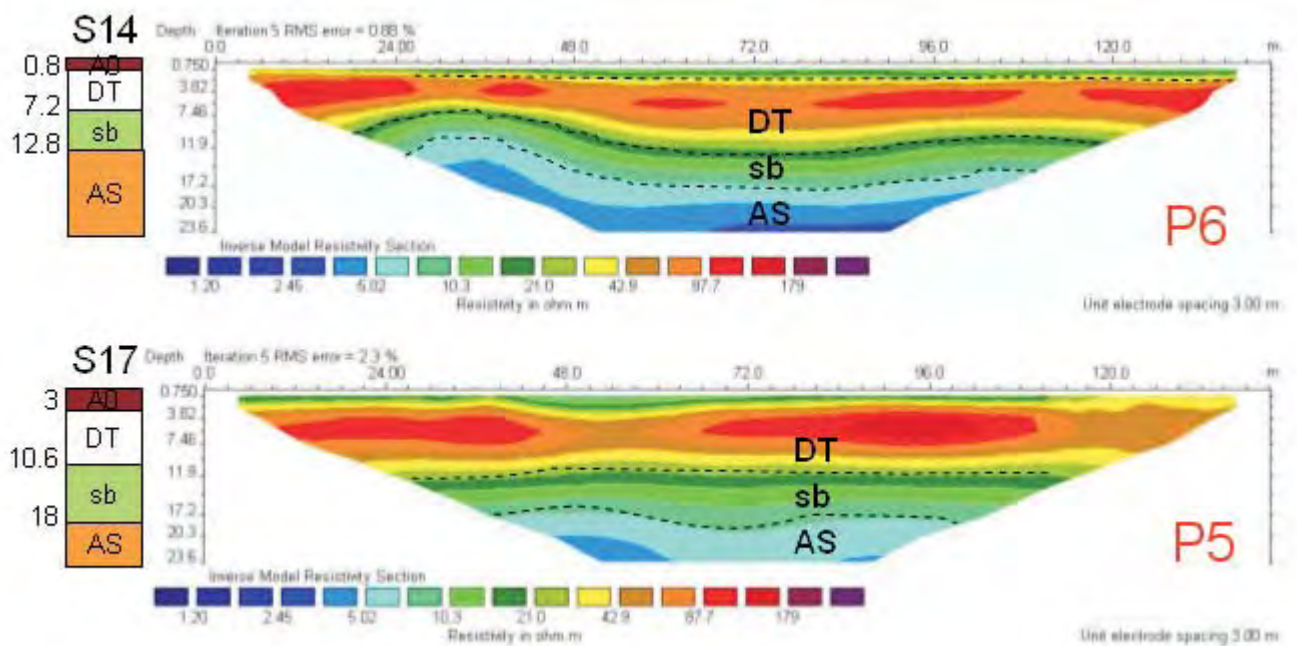


Fig. 11 – ERT Profile interpretation of 2D resistivity models realized in the Brindisi area. AS, subapennine Clays; DT, Terraced Deposits; sb, Brindisi sands. Location in the frame to the right and in figure 2.

– Modelli di resistività 2D ottenuti dall'interpretazione di profili ERT, nel Brindisino. AS, Argille subapennine; DT, Depositi di Terrazzo; sb, sabbie di Brindisi. L'ubicazione è riportata nel riquadro a destra ed in figura 2.

tain two overlapping and hydraulically independent aquifers.

A deep aquifer lies in the Mesozoic limestones (Altamura limestone hydrogeologic unit), made up of fractured and karstic carbonatic rocks, and in the porous (from 43% to 49%, ANDRIANI & WALSH, 2002) overlying Pleistocene deposits (Gravina Calcarene hydrogeologic unit). Fresh-water deep aquifer overlies more dense sea water and the thickness of this fresh water above the interface with saline water can be estimated based on the relationship of Ghyben-Herzberg. Unlike the

shallow ground water, found only in places, the deep ground water extends across the whole of the Apulia region. The deep aquifer, lying below the subapennine Clays, contains water under pressure and is therefore of the Artesian type (fig. 14 and fig. 15). The deep ground water is replenished by rainfall where the Cretaceous formation outcrops, by underground outflows from the adjoining “Murge” hills, and by seepage from the shallow aquifer corresponding to the numerous wells used for drinking water, irrigation and industrial uses that are present in the studied area. The hydraulic

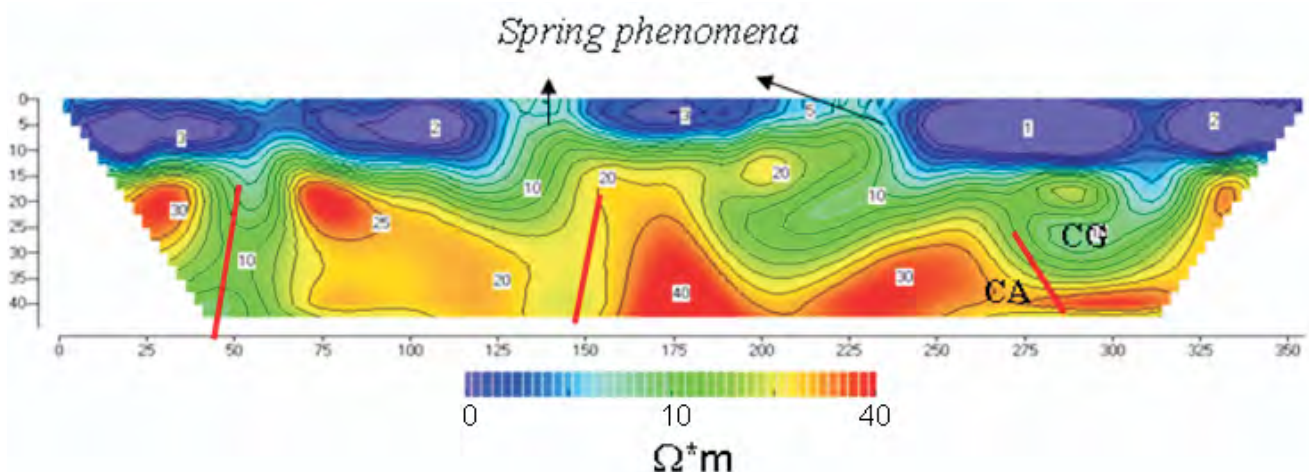


Fig. 12 – ERT Profile interpretation of 2D resistivity models realized in the Taranto area. Probable faults are signed with a red line. CA, Altamura Limestone; CG, Gravina Calcarene.

– Modelli di resistività 2D dall'interpretazione di profili ERT, nel Tarantino. Le faglie probabili sono segnate in rosso. CA, Calcare di Altamura; CG, Calcarene di Gravina.



Fig. 13 – Minor spring phenomena near Mar Piccolo.  
– Fenomeni sorgentizi minori presso il Mar Piccolo a Taranto.

gradients, oriented toward the coast, are very modest (0,5 ‰), even at some distance from the coast.

A distinctive characteristic of the Ionian coast is the presence of spring phenomena (the most important are “Borraco”, “Galese” and “Chidro”, fig. 2). According to ZORZI & REINA (1957), COTECCHIA *et alii*, (1975) and DAURÙ *et alii* (1990), geophysical researches have shown that these points of preferential ground water flow correspond to the zones where the sediments have a greater degree of permeability, due to fracturing and/or karst and principally corresponding to faults in the calcareous and calcareous–dolomitic mass of the Cretaceous. In these high permeability zones the groundwater under pressure rises, perforating and eroding the clay mantle (fig. 14). Other minor superficial springs are the result of the perforation of impermeable continental layers that occlude shallow aquifer.

A shallow porous aquifer, formed by the Middle–Upper Pleistocene marine calcarenitic and sandy deposits overlying the lower Pleistocene

clays, holds a phreatic ground water body. This aquifer is of the phreatic type, with semiconfined conditions where its upper part is overlain with sediments of low permeability (recent continental deposits).

Based on lithostratigraphy, this aquifer can be subdivided into several hydrogeologic units that differ from previous literature (RADINA, 1968; COTECCHIA, 1977; CHERUBINI *et alii*, 1987; RICCHETTI & POLEMIO, 1996). The subapennine Clays (Early Pleistocene) constitute the impermeable base of the aquifer ( $3 \cdot 10^{-7}$  m/sec, RICCHETTI & POLEMIO, 1996) in both areas. At least in the Brindisi area, the Pleistocene aquifer system involves two hydrogeologic units and not only one as in the mentioned bibliography. The greatest permeability ( $5 \cdot 10^{-4}$  m/sec, CONSORZIO BASI, 2002) is found in the calcarenite deposits (Terraced Deposit hydrogeologic unit, Middle–Late Pleistocene). As the fraction of silt increases, the permeability of the deposit decreases. The lower section of the aquifer, characterized by the presence of silty-sandy sedi-



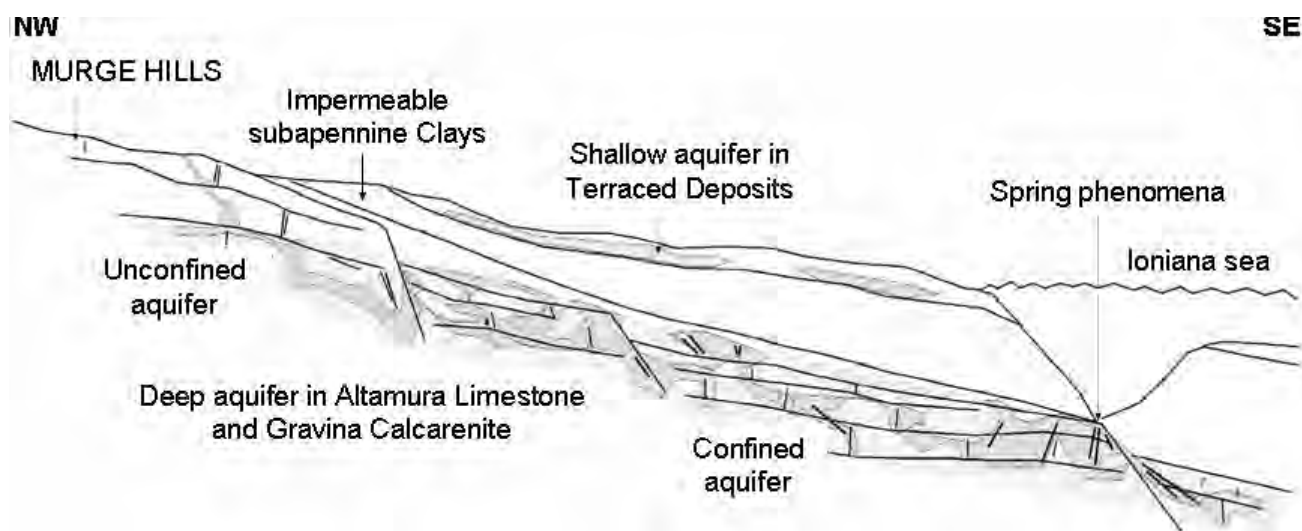


Fig. 14 – Hydrogeologic scheme of the Taranto study area.  
– *Schema idrogeologico del Tarantino.*

ments (Brindisi sands hydrogeologic unit, Early-Middle Pleistocene), has low permeability (on average  $4 \cdot 10^{-5}$  m/sec, CONSORZIO BASI, 2002). The saturated part of the shallow aquifer has a thickness varying from a few decimetres to over 30 m and flows towards the sea. The lack of homogeneously distributed and temporarily comparable data does not permit the elaboration of a piezometric map.

## 6. - CONCLUSIONS

The stratigraphic succession of the Brindisi - Taranto plain was reconstructed for hydrogeologic purposes integrating geological and geophysical surveys, which highlighted the heterogeneity of the subsoil. The results of this research, especially about the shallow aquifer, modify the previous geological and hydrogeological models (fig. 14 and fig. 15). The Brindisi sands are here formalized: the type-section near Cerano cliff, where the contact with the overlying and underlying units is exposed, has been described. To this unit are ascribed the sequences studied by DI GERONIMO (1969), GENTILE *et alii* (1996) and COPPA *et alii* (2002). This study points out the necessity to clarify the stratigraphy of Pleistocene sediments of the Taranto area, particularly for the possible identification of the Brindisi sands, probably included also in the western area in subapennine Clays and particularly in its upper sandy interval. In the Taranto area, BELLUOMINI *et alii* (2002) describe a transgressive clayey-sandy unit (about 4 m thick) that is of Middle Pleistocene age overlying the subapennine Clay Formation but a lack of borehole log data does not permit the determination of the

extension in the subsoil of this unit and its real thickness. The Taranto unit could correlate with the Brindisi sands but more studies are necessary. The two formations can be differentiated not only in terms of composition, but also in terms of permeability, that is higher in the Brindisi sands compared to subapennine Clays. These two formations are easily distinguished for their distinct electrical properties. The Brindisi sands have resistivity values that range from 8 to 20 ohm\*m while subapennine Clays are characterized by values below 5 ohm\*m. Based on this lithostratigraphy the shallow aquifer can be subdivided into several hydrogeologic units that differ from previous literature.

Brindisi sand hydrogeologic unit (permeability of  $4 \cdot 10^{-5}$  m/sec) constitute the lower section of the aquifer, Terraced Deposit hydrogeologic unit (permeability of  $5 \cdot 10^{-4}$  m/sec) the upper part and subapennine Clays the impermeable base (permeability of  $3 \cdot 10^{-7}$  m/sec).

ERT surveys have shown themselves to be a useful tool in the individualization of spring phenomena that are situated at the bottom and along the edges of the natural basins and channels flowing especially into Mar Piccolo with a non-homogeneous distribution along the west coast.

From the paleogeographic point of view, the South Salento sediments of Galatone Formation have been recognized for the first time near Talsano (western coast): this lithostratigraphical attribution indicates an Oligocene lacustrine environment also for the Taranto area. Furthermore, the identification of the existing wells has provided an initial overall picture of the distribution and density of the points of extraction from the deep aquifer, highlighting its possible overexploitation.



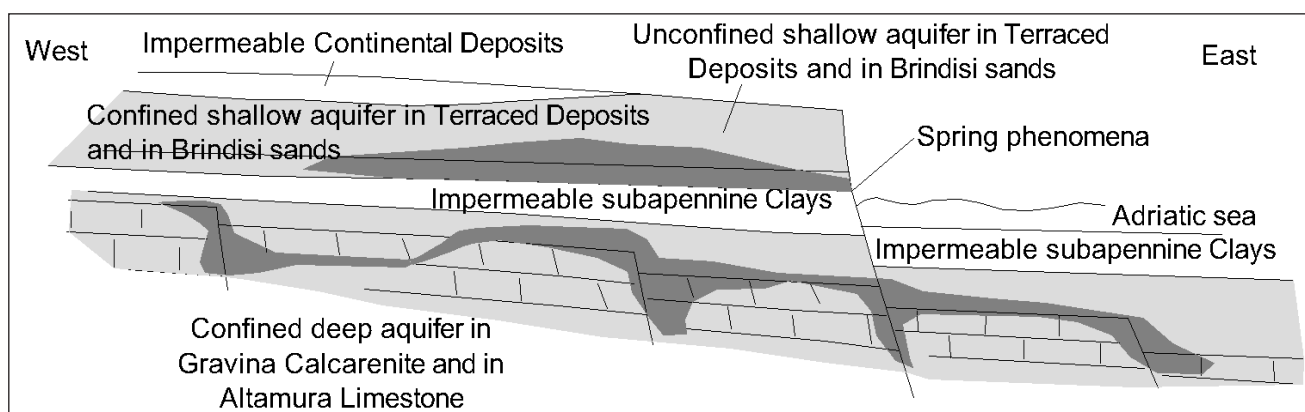


Fig. 15 – Hydrogeologic scheme of the Brindisi study area.  
– Schema idrogeologico del Brindisino.

## Acknowledgements

The authors acknowledge the careful revision by S. RUSI and another anonymous Referee.

## REFERENCES

- ANDRIANI G.F. & WALSH N. (2002) - *Physical properties and textural parameters of calcarenitic rocks: qualitative and quantitative evaluations*. Engineering Geology, **67**: 5-15.
- BELLUOMINI G., CALDARA M., CASINI C., CERASOLI M., MANDRA L., MASTRONUZZI G., PALMENTOLA G., SANSÒ P., TUCCIMEI P. & VESICA P.L. (2002) - *The age of Late Pleistocene shorelines and tectonic activity of Taranto area, southern Italy*. Quaternary Science Reviews, **21**: 525-547.
- BENTIVENGA M., COLTORTI M., PROSSER G. & TAVARNELLI E. (2004) - *A new interpretation of terraces in the Taranto Gulf: the role of extensional faulting*. Geomorphology, **6**: 383-402.
- BOSSIO A., ESU D., FORESI L.M., GIROTTI O., IANNONE A., LUPERTO SINNI E., MARGIOTTA S., MAZZEI R., MONTEFORTI B., RICCHETTI G. & SALVATORINI G. (1999) - *Formazione di Galatone, nuovo nome per un'unità litostratigrafica del Salento (Puglia, Italia meridionale)*. Atti Soc. Toscana Sc. Nat., Mem., Serie A, **105**: 151-156.
- CHERUBINI C., MARGIOTTA B., SGURA A. & WALSH N. (1987) - *Caratteri geologico-tecnici dei terreni della città di Brindisi*. Mem. Soc. Geol. It., **37**: 689-700, 20 ff., 2 tabb.
- CIARANFI N., GHISETTI F., GUIDA M., IACCARINO G., LAMBIASE S., PIERI P., RAPISARDI L., RICCHETTI G., TORRE M., TORTORICI L. & VEZZANI L. (1983) - *Carta Neotettonica dell'Italia meridionale*. Pubbl. no. 515 Prog. Fin. Geod. C.N.R., Bari, 62 pp.
- CIARANFI N., PIERI P. & RICCHETTI G. (1992) - *Note alla carta geologica delle Murge e del Salento (Puglia centromeridionale)*. Mem. Soc. Geol. It., **41**: 449-460.
- CONSORZIO BASI (2002) - *Verifica dello stato qualitativo delle acque sotterranee: 1-40ee all'entrata e all'uscita del polo industriale di Brindisi*. Archives of Brindisi Genio Civile.
- COPPA M.G., DE CASTRO P., MARINO M., ROSSO A. & SANFILIPPO R. (2002) - *The pleistocene with Aequipecten opercularis (Linneo) of "Campo di Mare" (Brindisi, Italy)*. Bollettino della Società Paleontologica Italiana, **40** (3): 405-429.
- COTECCHIA V. (1977) - *Studi e ricerche delle acque sotterranee e sull'intrusione marina in Puglia (Penisola Salentina)*. Quad. Ist. Ricerch. Acqua, **20**: 1-462.
- COTECCHIA V., TADOLINI T., TAZIOLI G.S. & TULIPANO L. (1973) - *Studio idrogeologico della zona della Sorgente Chiaro (Taranto)*. 2° Convegno Internazionale sulle Acque Sotterranee, Aprile – Maggio 1973, Bari: 3-15.
- CARDARELLI E. & FISCHANGER F. (2006) - *2D data modelling by electrical resistivity tomography for complex subsurface geology*. Geophysical Prospecting, **54**: 121-133.
- D'ARGENIO B. (1974) - *Le piattaforme carbonatiche periadriatiche. Una rassegna dei problemi del quadro geodinamico mesozoico dell'area Mediterranea*. Mem. Soc. Geol. It., **13**: 137-159.
- D'ARGENIO B., PESCATORE T. & SCANDONE P. (1973) - *Schema geologico dell'Appennino meridionale (Campania e Lucania)*. Acc. Naz. Lincei, **182**: 49-72.
- DAURÙ M., LOLLINO G. & TADOLINI T. (1990) - *Stima per il monitoraggio automatico di parametri chimico-fisici delle acque all'opera di captazione della sorgente sottomarina Galeso, mar piccolo di Taranto*. Geologia Applicata ed Idrogeologia, **25**: 265-277.
- DI GERONIMO I. (1969) - *I depositi quaternari della costa tra Brindisi e Torre Canne (Puglia)*. Atti Acc. Gioenia Sc. Nat. Catania, S. 6, 20, (Suppl. Sc. Geol.): 195-224.
- DOGLIONI C., MERLINI S. & CANTARELLA G. (1999) - *Fore-deep geometries at the front of the Apennines in the Ionian Sea (Central Mediterranean)*. Earth and Planetary Science Letters, **168**: 243-254.
- FURMAN A., FERRÈ T.P.A. & WARRICK A.W. (2004) - *Optimization of ERT surveys for monitoring transient hydrological events using perturbation sensitivity and genetic algorithms*. Available at [www.vadosezonejournal.org](http://www.vadosezonejournal.org). Vadose Zone J., **3**:1230-1239.
- GENTILE G.M., MONTERISI L. & VENTRELLA N.A. (1996) - *Erosione del litorale adriatico ed arretramento della falesia a sud di Brindisi (Puglia)*. Mem. Soc. Geol., **51**: 781-791.
- LEUCCI G., MARGIOTTA S. & NEGRI S. (2004) - *Geophysical and Geological Investigations in a Karstic Environment (Salice Salentino, Lecce, Italy)*. Journal of Environmental and Engineering Geophysics (JEEG), **9** (1): 25-34.
- LOKE M.H. (2004) - *Res2DInv ver 2.14*. Geotomo Software. [www.geoelectrical.com](http://www.geoelectrical.com).
- MARGIOTTA S. & NEGRI S. (2005) - *Geophysical and stratigraphical research into deep groundwater and intruding seawater in the mediterranean area (the Salento Peninsula, Italy)*. Natural Hazards and Earth System Sciences **5**: 127-136.
- MARGIOTTA S., MAZZONE F., NEGRI S. & CALORA M. (2008) - *The role of integrated high resolution stratigraphic and geophysical surveys for groundwater modelling*. Hydrology and Earth System Sciences Discussion, **5**: 1-40.
- RADINA, B. (1968) - *Risultati geologici di perforazioni eseguite nei dintorni di Brindisi*. Bollettino della Società dei Naturalisti in Napoli, **57**: 207-218.

- RICCHETTI G. (1967) - *Osservazioni preliminari sulla geologia e morfologia dei depositi quaternari nei dintorni del Mar Piccolo (Taranto)*. Atti della Accademia Gioenia di Scienze Naturali in Catania, **18**: 123-130.
- RICCHETTI G. (1980) - *Contributo alla conoscenza strutturale della Fossa bradanica e delle Murge*. Boll. Soc. Geol. Ital., **99**: 421-430.
- RICCHETTI G., CIARANFI N., LUPERTO SINNI E., MONGELLI F. & PIERI, P. (1988) - *Geodinamica ed evoluzione sedimentaria e tettonica dell'Avampese Apulo*. Mem. Soc. Geol. It., **41**: 57-82.
- RICCHETTI E. & POLEMIO M. (1996) - *L'acquifero superficiale del territorio di Brindisi: dati geoidrologici diretti e immagini radar da satellite*. Mem. Soc. Geol. It., **51**: 1059-1074, 11 ff.
- SELLI R. (1962) - *Il Paleogene nel quadro della geologia dell'Italia meridionale*. Mem. Soc. Geol. It., **3**: 737-789.
- TEDESCHI C. (1969) - *Terreni ed opere di fondazione della Centrale Termoelettrica di Brindisi*. Rivista italiana di geotecnica, **3**, Napoli.
- ZORZI L. & REINA C. (1957) - *Valutazione e sfruttamento delle risorse idriche sotterranee della Conca di Brindisi*. Giorn. Genio Civile, **10**: 743-754, Roma.

# A comprehensive hydrogeological view of the Friuli alluvial plain by means of a multi-annual quantitative and qualitative research survey

*Quadro idrogeologico generale della Pianura alluvionale friulana sulla base di indagini quantitative e qualitative pluriannuali*

MARTELLI G. (\*), GRANATI C. (\*)

**ABSTRACT** - In order to define a global hydrogeological model of the Friuli alluvial plain, the present work investigates the relationships between the regional unconfined and multilayered aquifer systems integrating geological, hydrogeological, geochemical and isotope data.

The Neogenic and Quaternary mostly clastic sediments of both continental and marine origin, locally more than 1000 meters thick, gave rise to a sequence of megafan-shaped progradated sedimentary bodies, both lengthwise and cross-wise granulometrically differentiated.

The geometry of the relating saturated zone has been reconstructed by both deterministic and stochastic methods.

By means of the isophreatic map of the High Plain (APF), the active recharge to the confined system of the Low Plain (BPF) has been calculated. The groundwater flow conditioning by means of the regional tecto-dynamics is showed.

The hydrogeological model, integrated with hydrogeochemical and isotope data collected from wells, springs and rivers, allowed some considerations about recharge provenience and hydraulic connection within the confined aquifer system.

**KEY WORDS:** Friuli Plain, hydraulic connection, multilayered aquifer, recharge, water-table aquifer.

**RIASSUNTO** - Lo scopo del presente lavoro è stato quello di definire un modello di circolazione idrica sotterranea della pianura friulana studiando le relazioni fra i due sistemi acquiferi presenti nell'area (falda freatica dell'Alta Pianura e sistema multistrato della Bassa pianura) attraverso l'interpretazione integrata di dati geologici, idrogeologici, idrochimici e isotopici. Le elaborazioni dei dati piezometrici, le carte di distribuzione dei macrocostituenti e l'analisi dei dati isotopici sui campioni esaminati hanno consentito, per il sistema acquifero multistrato della Bassa Pianura, di trarre delle conclusioni sulle caratteristiche della ricarica e sui fenomeni di drenanza.

**PAROLE CHIAVE:** acquifero multistrato, drenanza, falda libera, pianura friulana, ricarica.

## 1. - INTRODUCTION

More and more often, the use of research techniques and elaboration methodologies that are peculiar to geological, geophysical, geochemical and geostatistical fields turns out the necessity and suitability of assuming an integrated multi-disciplinary approach within hydrogeological surveys addressed to detailed tridimensional characterizations of geological structures, to descriptions of recharge mechanisms and groundwater flow paths as well as to spatial distribution settlements of the hydraulic properties of aquifers associated to complex depositional systems (i.e. alluvial plains). As a rule, the cognitive bases of hydrogeological researches are quantitatively and qualitatively heterogeneous and typically scattered both in space and in time dimension.

The aim of the present work is to synthesize, as an integration of the foregoing knowledge, the results attained by the Authors within the over seven-year surveys hinged on geometric, hydrodynamic and hydrochemical features of the indifferiated and multi-layered aquifers of the Friuli Plain eastward of Tagliamento River.

The outstanding issues of hydraulic head and qualitative measurements carried out within a local experimental monitoring network (MARTELLI *et alii*, 2007a), together with the hypotheses concerning the recharge and circulation patterns of the regional groundwaters (supported by geostatistical elaborations of piezometric, pluviometric and cli-

(\*) Dipartimento di Georisorse e Territorio, Università degli Studi di Udine, via Cotonificio 114 - 33100 Udine



mate data, as well as chemical and isotopic analyses), will be exposed and discussed. In every respect, the aquifer reservoirs of the southern sector of the Friuli - Venezia Giulia region represent a strategic resource at a regional scale.

## 2. - THE FRIULI PLAIN AND ITS AQUIFERS

The Friuli Plain (fig. 1) on the left side of the Tagliamento River represents the extreme eastern part of the Po Plain, to whom it preserves some of the most peculiar hydrogeological patterns (ANTONELLI & STEFANINI, 1982; DAL PRÀ *et alii*, 1989; REGIONE EMILIA-ROMAGNA, ENI-AGIP, 1998; REGIONE LOMBARDIA, ENI-AGIP, 2002). The depositional processes that occurred in the

Upper Pleistocene, conditioned by both the geological-structural evolution of the area and the sea level fluctuations following from the climatic events of Quaternary glaciations (FLORINETH & SCHLUCHTER, 2000; OROMBELLI & RAVAZZI, 1996), produced the sedimentation of clastic materials (of fluvio-glacial, marine, lagoon and marshy origin) prograding in size, along a N-S direction, within a coalescent system of alluvial mega-fans (FONTANA, 2006). Such detrital materials lie over, in order, (a) terrigenous-carbonatic marine deposits of the Miocene transgression (outcropping at the southern boundary of the Carnic Pre-Alps and to the S of Udine), (b) the Grivò (Upper Palaeocene – Lower Eocene) and the Cormons (Ypresian) arenaceous-marly Flysch, as an evidence of an active mountain chain foredeep system in motion from

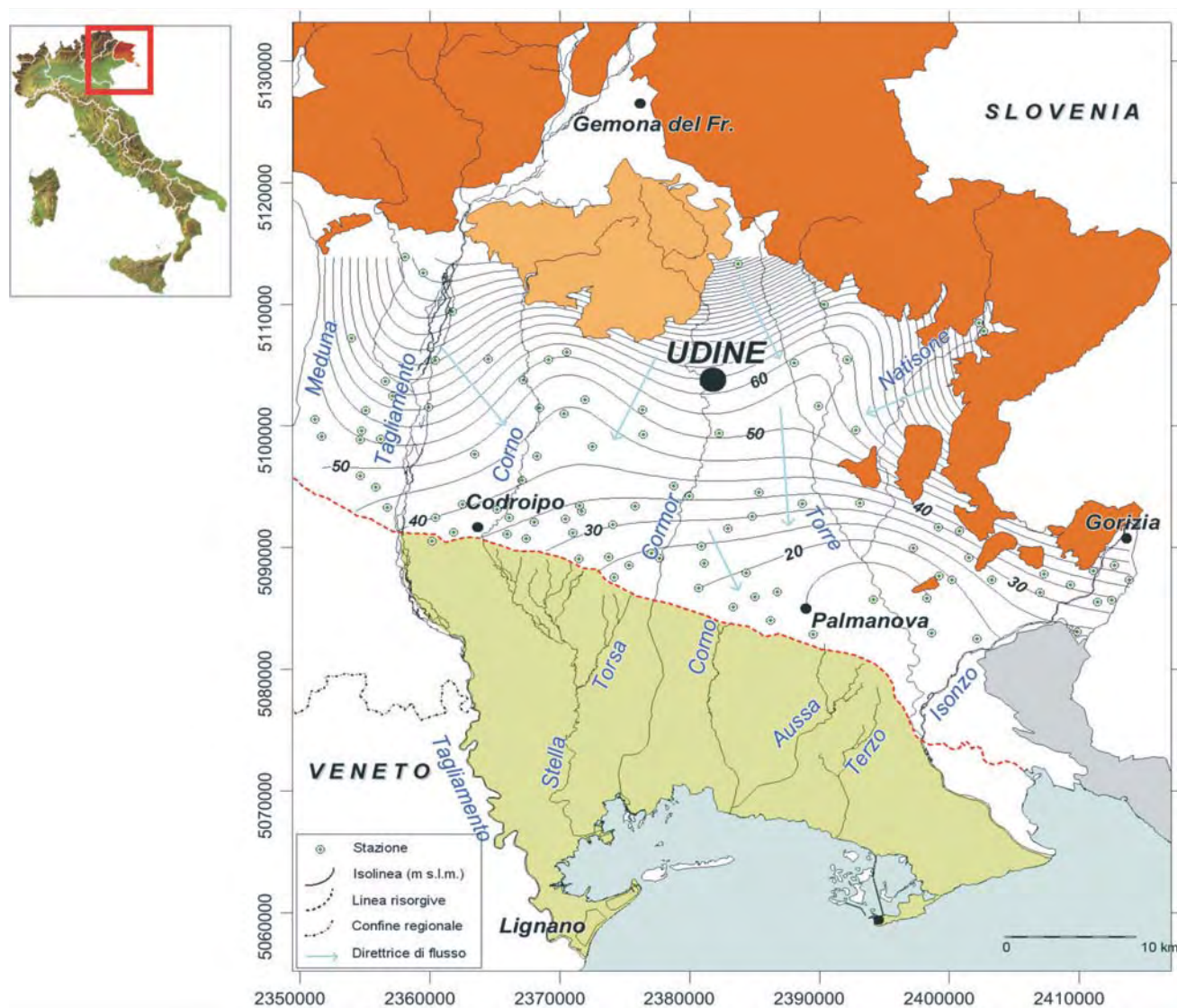


Fig. 1 – Isophreatic map of the High Plain unconfined aquifer system (from MARTELLI & GRANATI, 2007a). Dot symbols indicate the location of the piezometric gauge network, while arrows mark the main groundwater flow directions.

– Carta, in proiezione Gauss-Boaga, dell'andamento freaticometrico (m s.l.m.) della falda dell'Alta Pianura friulana (da MARTELLI & GRANATI, 2007a). I simboli indicano i singoli pozzi della rete di rilevamento regionale, mentre le frecce individuano le principali direzioni di deflusso idrico sotterraneo.

the western sector of the Slovenian basin to the eastern sector of the Veneto basin, and (c) the Mesozoic carbonate platform, over 6.000 meters thick and conditioned by buried and sometimes seismically active overthrust fronts, oriented in a Dinaric direction and overlapping towards SW (BURRATO *et alii*, 2008; CALORE *et alii*, 1995; CASTELLARIN & CANTELLI, 2000; CATI *et alii*, 1989a, 1989b; GALADINI *et alii*, 2005). The thickness of the Neogenic and Quaternary deposits increases from NE (about 50 meters at the foot of the moraine hills) towards SW (over 900 meters at the western border of the plain) (REGIONE AUTONOMA FRIULI-VENEZIA GIULIA, 2004). The pre-Quaternary substratum behaves as a permeability boundary for groundwaters circulating within the alluvial materials.

The geometric pattern of the Quaternary deposits has been conditioned by both the geological-structural evolution of the area and the Pleistocene glacial-eustatic fluctuations, that worked together in order to outline the main hydrogeological subdivision of the Friuli Plain in two distinct sectors.

In the High Plain (area of about 1150 km<sup>2</sup>, stretching between the Tagliamento moraines, the central and eastern Pre-Alps and the spring belt), the thick coarse-grained detrital body of fluvio-glacial origin (gravels irregularly cemented in conglomerate horizons and intercalated with layers of sand and, less frequently, of clay) holds, owing to its marked high permeability characteristics, a wide and continuous water-table aquifer, whose depth-to-water decreases from the moraines foot (about 75 meters to the N of Udine) to the most southern sector near the spring belt (MARTELLI & GRANATI, 2007b). The springs, extending for about 40 kilometers in the E-W direction, discharge about 80 m<sup>3</sup>/s (CONSORZIO DI BONIFICA LEDRA-TAGLIAMENTO, 1982).

Southward from springs, the hydrogeological behaviour of the Low Plain (about 740 km<sup>2</sup>) is a direct consequence of the presence of a complex and articulated sequence of wide and continuous silty-clayey deposits, sandy and subordinately gravelly horizons: within such multi-layered system, at least eight confined and variously branched super-imposed aquifer horizons are recognisable. Owing to the strict hydraulic link existing between High and Low Plain, the confined aquifers are fed by groundwaters coming from the phreatic system (about 820 millions of m<sup>3</sup>/year) (MARTELLI *et alii*, 2003; MARTELLI & GRANATI, 2007b). This connection assures a common feeding area, located to the north of the spring belt (MOSETTI, 1983; STEFANINI, 1978), to both of the aquifer systems: the 25% of the whole recharge contributions is

due to effective meteoric infiltration and the remaining 75% to relevant seepage from losing rivers of the High Plain hydrographic network (MARTELLI & GRANATI, 2007b).

The annual groundwater volume drawn from the Low Plain confined aquifers, representing the main regional reservoir for drinking and domestic uses, has been estimated at 526 millions of m<sup>3</sup>/year (GRANATI *et alii*, 2000; MARTELLI *et alii*, 2004; MARTELLI & GRANATI, 2007b). About 84% of withdrawals concerns the most shallow aquifer horizons (till 112 m bsl): a progressive loss in both pressure and natural productivity is evidenced by a large number of wells in the northern sector of the Low Plain (MARTELLI & GRANATI, 2007b).

### 3. - THE GEOLOGICAL-STRUCTURAL FRAME OF THE STUDIED AREA

The involvement of multi-disciplinary approaches and operative methodologies representatively marks the studies, undertaken in the last decades and refined in the most recent past, whose aim can be singled out in the hydrogeological characterisation of the site of interest; such studies are propaedeutic to quantitative groundwater flow and transport modelling calibrated to a suitable use scale (GRANATI, 2007; DRIUTTI, 2009).

The knowledge of the Friuli Plain deep structure follows from deep boreholes and geophysical surveys (AGIP, 1972; CALORE *et alii*, 1995; CASSANO *et alii*, 1986; CATI *et alii*, 1989a, 1989b; MARTINIS, 1971) that started in the fifties by ENI-AGIP for hydrocarbon research and that have been recently synthesized and improved by Trieste University (REGIONE AUTONOMA FRIULI-VENEZIA GIULIA, 2004) even through a new deep drilling project in the Grado lagoon (DELLA VEDOVA *et alii*, 2009; FANTONI *et alii*, 2003; REGIONE AUTONOMA FRIULI-VENEZIA GIULIA, 2004).

The lithostratigraphical data coming from water-wells closely spread in the area of interest (GRANATI *et alii*, 1999, 2000), from a few to over 500 meters deep, represent the main survey tool for the Neogenic and Quaternary alluvial body and its aquifer systems (GIOVANNELLI *et alii*, 1985; MAROCCO, 1988; MAROCCO *et alii*, 1988; MARTELLI & GRANATI, 2007a, 2007b; MARTELLI & RODA, 1998).

The conceptualisation and characterisation of the aquifers' spatial structure (MARTELLI & GRANATI, 2006) started off from lithostratigraphical evidences associated to over a thousand water-wells gathered among (a) the regional archive of water-wells and drillings realised in the Quaternary alluvial horizon and in the unfastened deposits of the Friuli region (REGIONE AUTONOMA FRIULI-



VENEZIA GIULIA, 1990), (b) technical reports in applications for large (Udine Civil Engineers Office) and small (Provincial Direction of Regional Technical Services) supplies of drinking water, trout breeding, industrial and agricultural groundwater drawings, and (c) technical reports in applications for deep geothermal groundwater drawings (Industrial Regional Direction).

Beginning with class codification processes (on the basis of hydrogeological criteria) of the materials defined by the drilling operators and pursuing with correlations between productive aquifer horizons and lithologically similar layers characterised by the same average depth, it has been possible to reconstruct in detail (MARTELLI & GRANATI, 2006) the geometry of the Low Plain confined aquifer system: the existence of eight artesian layers, identified with a capital letter (from A to H in the increasing depth direction) accordingly with the past scientific literature conventions (MARTELLI *et alii*, 2004; STEFANINI & CUCCHI, 1977), has been confirmed between 19 m bsl and over 500 m bsl.

#### 4. - THE HIGH PLAIN WATER-TABLE AQUIFER BEHAVIOUR

The annual averaged phreatimetric pattern of the High Plain aquifer system came out from geo-statistical elaboration of data collected within the regional water-table monitoring network (MARTELLI & GRANATI, 2007b): 96 hydraulic head measurement stations, supplied with data coming from 20 or more observation years in the period 1967-2004, have been taken into account.

At a regional scale, the main groundwater flow directions (fig.1), as evidenced by the drainage axes in correspondence of the Corno River and the Torre – Natisone – Isonzo hydrographic network, single out a fan-shaped arrangement, with a NW-SE flow direction in the western sector and a NE-SW direction in the eastern one, with a SE deflection near the spring area. The groundwater recharge from the Tagliamento River is particularly evident in the left river side.

The groundwater flow conditioning by the regional tecto-dynamic pattern comes out (fig. 2) from overlaying the above-mentioned isophreatimetric map and the Friuli Plain structural map (POLI *et alii*, 2008). The Palmanova line, active until the Palaeogene and whose trace can be seen in the lower right corner of the map, represents the buried front of the Dinaric belt under the Miocene and Quaternary deposits. The Pozzuolo, Udine and Medea faults show deformation evidences in the Upper Pleistocene (BURRATO *et alii*, 2008; GALADINI *et alii*, 2005): in particular, the

former one causes a Miocene molasse outcrop along the left side of the Cormor river to the SW of Udine and consequently a resulting thickness lowering of the Quaternary alluvial body (less than 75 meters) near the tectonic displacement (REGIONE AUTONOMA FRIULI-VENEZIA GIULIA, 2004). The whole tectonic lines act as a water divide between the western and the eastern sectors, tied to the Tagliamento River and the Torre – Natisone hydrographic network dynamics respectively. The drainage axes, shown by the water table map, also appear strictly connected to the dinaric and south-alpine paleogeography.

The map of the annual averaged water table excursion (fig. 3) shows the link between hydrographic network and groundwaters. It has been drawn through data of 132 water-wells collected in the period 1998-2007. The greatest values are located in correspondence with the Tagliamento (14 meters) and the upper Torre (9 meters) rivers, as well as radial decreasing values can be observed moving both towards the northern moraines and the southern spring belt (about 1 meter).

#### 5. - HYDROCHEMICAL CHARACTERISATION OF THE HIGH PLAIN UNCONFINED AQUIFER

The improvement of the knowledge concerning the High Plain groundwater flow system could not leave the analysis of the main chemical-physical features (main dissolved ions, pH, temperature, conductivity) out of consideration. The elaborations involved time series of data (tab. 1 and fig. 4) as follows:

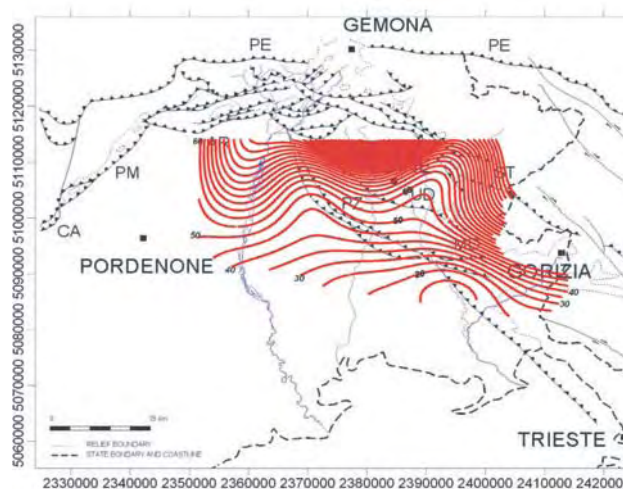


Fig. 2 – Main regional tectonic features (ZANFERRARI *et alii*, 2008), hydrographic network and High Plain phreatimetric field on the left side of the Tagliamento river (MARTELLI & GRANATI, 2007a).

– Principali lineamenti tettonici regionali (ZANFERRARI *et alii*, 2008), rete idrografica principale e andamento freaticometrico dell'Alta Pianura friulana in sinistra Tagliamento (MARTELLI & GRANATI, 2007a).



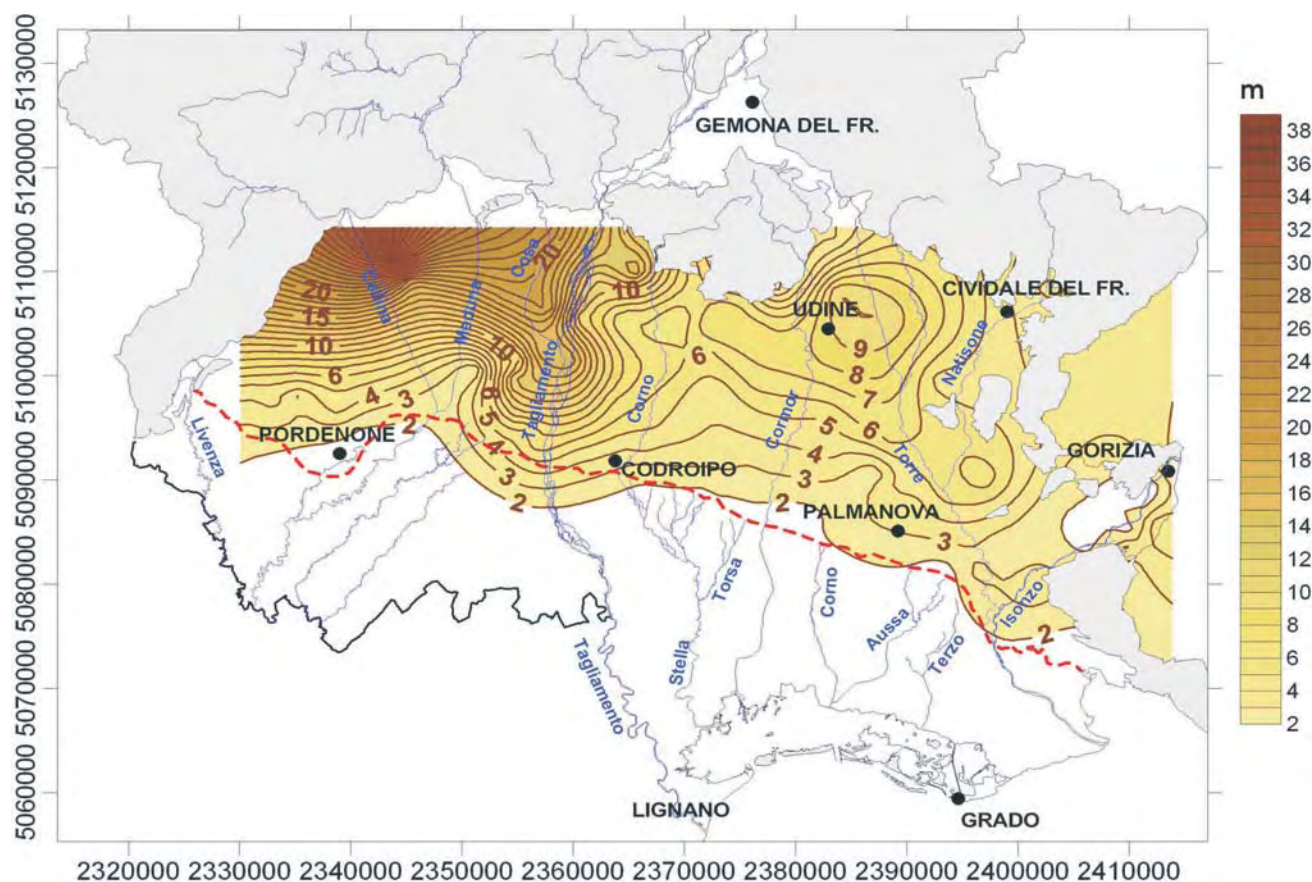


Fig. 3 – Annual averaged (1998-2007) phreatimetric excursion (in metres) of the High Plain unconfined aquifer. The regional border is marked by the black bold line; the red dotted line shows the average position of the spring alignment.

– Mappa dell'escursione freaticca media annua (1998 – 2007), in metri, dell'acquifero indifferenziato dell'Alta Pianura friulana. In grassetto è rappresentato il confine regionale; con tratteggio rosso, è indicata la posizione media dell'allineamento delle risorgive.

- observations collected in 34 sampling points of the regional qualitative monitoring network for the period 1982- 1992;

- measurements carried out (project PRIN 2005) in correspondence of 17 springs, 1 phreatic well and the 4 main rivers of the sector (Tagliamento, Torre, Natisone and Isonzo) for the period 2003-2007 (MARTELLI & GRANATI, 2008a; BORTOLAN PIRONA, 2008).

As evidenced by the Schoeller diagram (fig. 5), both river waters and groundwaters of the northern sector of the Friuli Plain show a  $\text{Ca-HCO}_3$  hydrochemical facies. Limestones, dolomitic limestones and dolomites are widely present in both the mountain basins of the Friuli rivers and the Quaternary alluvial deposits.

According to the hydraulic head outputs, that put in evidence a remarkable groundwater recharge action by the Tagliamento River in the most western sector of the studied plain, both groundwaters and spring waters of such area belong to a  $\text{Ca-SO}_4$  facies: the relevant  $\text{SO}_4^{=}$  amount that characterises the Tagliamento waters is due to the dissolution of Permian gypsum (Bellerophon formation) that

outcrops in the Carnic Alps (STEFANINI, 1978). The same waters are relatively poor in  $\text{HCO}_3^-$  owing to the interfering action of calcium coming from sulphates (STEFANINI, 1972). Starting from the area close to the Tagliamento River, where  $\text{SO}_4^{=}$  ranges from 80 to 130 mg/l (fig. 6), the concentration of such anion in High Plain groundwaters decreases moving eastward accordingly with the increasing distance from the river and it becomes close to zero in the most eastern sector pertaining to the recharge contributions of the Torre – Natisone hydrographic system: the sulphate concentration in the upper Torre waters ranges between 2 and 16 mg/l, while calcium joins values of about 60 mg/l. The seepage waters of the Tagliamento River, although progressively diluted, preserve their distinctive chemical character according to the regional tectonic pattern.

The map of the calcium spatial distribution (fig. 7) shows the lowest concentrations in correspondence of a central sector stretched between the Cormor and the Torre rivers, as a divide, according to the phreatimetric evidences, of the western area from the eastern one (pertaining re-

Tab. 1 – *Main physical-chemical parameters determined for sampled groundwaters of the Friuli High Plain, spring waters and rivers.*

– Valori dei principali parametri chimico-fisici rilevati in campioni idrici prelevati da 35 pozzi della falda freatica dell'Alta Pianura friulana, da 17 affioramenti di risorgiva e da 4 corsi d'acqua.

Codice	Temp. (°C)	pH	Cond. (μS/cm)	Ca <sup>++</sup> (mg/l)	Mg <sup>++</sup> (mg/l)	Na <sup>+</sup> (mg/l)	K <sup>+</sup> (mg/l)	Cl <sup>-</sup> (mg/l)	SO <sup>4=</sup> (mg/l)	Sr <sup>-</sup> (mg/l)	NO <sup>3-</sup> (mg/l)	HCO <sup>3-</sup> (mg/l)
213	12,8	7,4	545	82,1	26,9	3,2	1,0	5,0	81,3	0,4	19,6	304,0
214	12,8	7,4	554	84,8	27,1	3,5	0,7	4,0	83,8	0,4	22,4	
215	10,3	7,4	544	78,9	28,1	4,0	1,3	5,1	59,2	0,3	26,3	
216	13,3	7,4	564	84,3	29,8	3,6	0,8	5,0	49,9	0,3	26,2	351,0
217	13,3	7,4	600	82,2	28,7	16,1	1,3	20,7	52,9	0,3	24,4	
219	13,1	7,3	583	86,3	29,2	4,5	1,4	5,9	52,4	0,3	26,8	360,0
220	13,1	7,4	530	78,3	25,3	3,5	2,0	7,1	43,8	0,3	74,7	
253	13,7	7,6	482	74,8	22,1	3,1	1,2	4,7	21,4	0,2	20,5	
255	14,5	7,4	551	90,9	20,7	3,4	1,2	5,2	15,7	0,2	23,9	386,0
256	14,5	7,4	581	90,8	27,4	3,8	1,9	6,7	28,0	0,2	29,0	
234	13,0	7,5	532	87,6	22,9	3,1	1,5	4,9	18,6	0,2	23,0	351,0
235	13,4	7,8	350	61,3	9,5	4,1	1,9	4,2	9,5	0,1	9,5	222,0
245	12,1	7,6	418	68,7	13,9	3,0	1,5	4,8	10,4	0,2	18,1	
246	14,5	7,6	551	83,0	21,1	6,2	5,6	7,5	19,0	0,1	32,3	310,0
247	12,9	7,8	345	60,0	9,9	2,9	1,1	3,4	7,7	0,2	7,5	
248	14,3	7,2	662	104,1	17,4	23,8	1,9	16,9	26,4	0,3	3,6	
254	14,2	7,6	403	62,6	17,9	3,1	1,2	3,5	10,1	0,1	18,2	
236	12,2	7,7	472	79,8	19,6	3,4	1,0	3,2	122,3	0,9	3,7	199,0
238	13,2	7,7	498	76,7	23,5	4,1	1,3	5,0	74,9	0,4	14,7	
242	12,5	8,0	474	71,4	20,4	6,3	8,2	5,8	76,4	0,5	11,0	
218	12,5	7,4	516	72,5	27,4	5,3	1,0	7,6	42,7	0,2	18,7	309,0
228	12,9	7,7	432	64,0	18,9	2,9	1,2	5,3	24,5	0,2	14,6	
232	12,1	7,6	453	73,9	22,4	4,3	2,1	5,5	34,4	0,3	13,5	
233	13,9	7,8	340	51,4	17,0	2,4	0,8	4,8	10,2	0,1	13,3	234,0
237	12,8	7,9	433	64,9	19,6	4,2	4,3	5,9	71,3	0,5	6,7	258,0
239	13,2	7,6	629	90,6	35,0	12,3	8,3	17,7	28,2	0,1	62,9	
240	13,1	7,7	450	64,6	25,0	3,2	0,8	4,9	27,1	0,1	14,0	286,0
241	12,3	7,5	544	79,3	28,2	4,5	1,3	6,1	52,3	0,2	31,6	
243	13,4	7,7	367	53,8	18,4	3,1	0,8	4,3	18,1	0,1	12,8	
244	12,8	7,6	439	61,1	23,7	4,8	0,9	5,3	21,9	0,1	21,4	
249	12,8	7,7	383	58,6	20,0	3,3	0,8	4,0	16,2	0,1	13,5	
250	13,1	7,6	490	71,6	25,7	5,5	1,0	8,2	32,8	0,2	17,6	310,0
251	13,3	7,8	382	55,8	18,0	3,3	0,7	4,8	15,2	0,1	15,9	
252	15,1	7,9	277	48,7	9,0	2,1	1,1	2,8	7,2	0,2	56,1	177,0
37	12,0	7,8	340	42,1	24,2	3,8	0,8	8,1	32,0		16,2	
TAG	19,9	7,5	435	72,3	18,8	3,2	0,4	5,1	127,3		2,8	151,2
TOR	16,7	7,6	191	34,6	9,3	1,5	0,4	4,0	3,7		2,9	132,2
NAT	22,7	7,7	247	42,6	5,2	1,9	0,4	4,0	4,4		2,6	145,5
ISO	20,8	7,6	216	38,4	6,9	1,3	0,2	3,7	3,3		2,0	140,7
RIS1	10,0	7,8	543	65,4	21,1	3,1	1,0	4,2	48,1	0,2	7,0	240,9
RIS2	12,3	7,8	644	88,9	25,1	6,2	1,5	10,1	67,6	0,8	10,8	341,6
RIS3	12,2	7,7	640	77,9	26,7	7,2	2,0	10,1	63,2	0,9	15,1	317,2
RIS4	10,6	7,9	685	81,2	26,4	2,8	1,0	6,7	67,1	0,8	19,4	311,9
RIS5	12,1	7,8	589	77,4	25,4	2,6	0,6	5,8	69,2	0,9	17,6	292,8
RIS6	12,6	7,9	668	87,6	27,5	3,5	1,5	8,0	44,8	0,7	20,9	366,0
RIS7	11,7	7,6	661	89,6	29,4	3,4	0,9	8,4	64,7	0,7	22,3	353,8
RIS8	10,3	7,6	619	85,1	29,5	2,9	0,7	5,6	87,6	0,7	11,5	324,5
RIS9	11,9	7,3	786	105,6	34,9	3,0	0,7	9,6	130,1	1,2	13,6	361,1
RIS10	14,8	7,6	532	73,2	25,1	2,2	0,5	4,2	81,2	< 0,01	10,9	258,6
RIS11	14,0	7,9	575	74,9	27,8	3,5	0,8	5,8	47,8	0,4	16,2	329,4
RIS12	13,5	7,5	722	97,7	31,3	7,3	1,5	16,7	30,4	< 0,01	37,5	400,2
RIS13	14,4	7,4	624	83,3	29,3	5,6	0,9	8,8	38,4	< 0,01	25,3	363,6
RIS14	14,3	7,2	748	98,9	33,0	6,6	1,0	11,8	45,3	< 0,01	28,7	407,5
RIS15	13,5	7,2	649	98,5	28,7	5,6	1,6	13,4	21,1	< 0,01	26,1	412,4
RIS16	12,0	7,7	448	68,6	20,0	2,9	0,9	3,8	9,4	< 0,01	11,6	288,0
RIS17	12,8	7,2	513	80,5	20,8	3,2	1,5	4,7	14,0	< 0,01	12,6	333,7



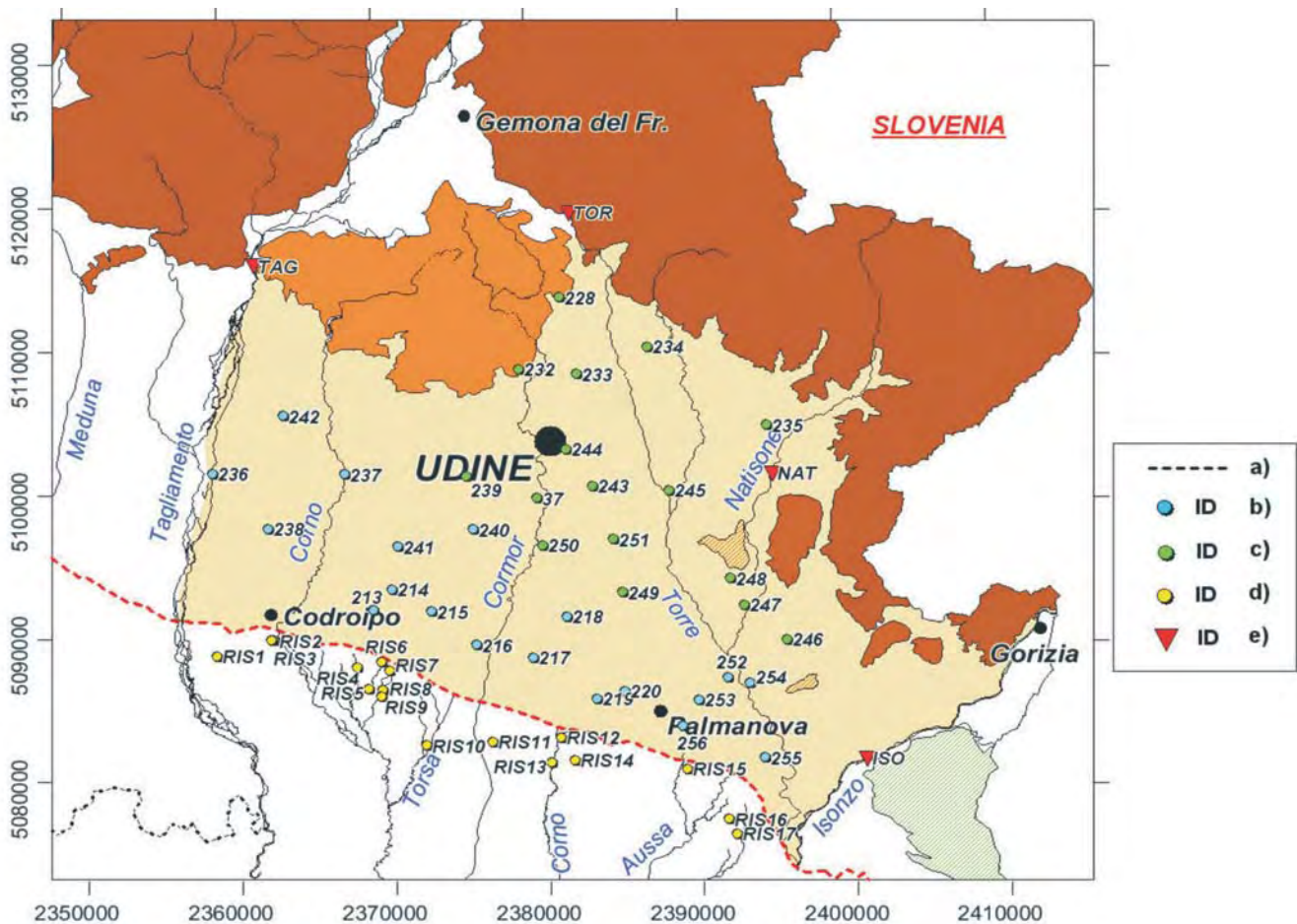


Fig. 4 – Physical-chemical sampling sites in the High Friuli Plain (APF). Legend: a) spring belt; b) sampling wells to the South of main regional tectonic features; c) sampling wells to the North of main regional tectonic features; d) sampled springs; e) sampled rivers.

- Ubicazione dei punti di campionamento chimico-fisico nell'Alta Pianura Friulana (APF). Legenda: a) allineamento medio degli affioramenti di risorgiva; b) pozzi posti a Sud dei principali elementi tettonici regionali; c) pozzi posti a Nord dei principali elementi tettonici regionali; d) risorgive; e) corsi d'acqua superficiali.

spectively to the Tagliamento and the Torre-Natisone system recharge contributions). The higher calcium values in the western sector are due to the sulphate contribution, as well as the ones pertaining to the spring area, accordingly with the main groundwater flow directions.

The thematic maps that describe the spatial variability of chlorine, sodium and nitrate content (figg. 8-10) show maximum concentrations in the same areas. High nitrates are connected to local pollution phenomena of agricultural origin. Peak concentrations of chlorine and sodium close to the Cormor River, also supported by past documentary evidences (STEFANINI, 1972), need further investigations.

Spring waters, whose alignment marks in surface the transition between the two Friuli Plain hydrogeological systems, show chemical patterns that are similar to the ones proper to western phreatic groundwaters: they are characterised by a  $\text{Ca-HCO}_3$  facies, with a sulphate content decreasing from W to E accordingly with an increasing distance from the Tagliamento River (fig. 11).

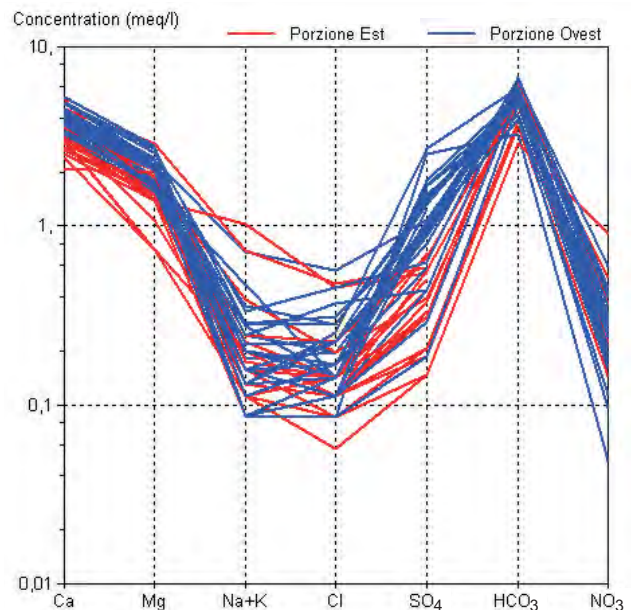


Fig. 5 – Schoeller diagram for Friuli High Plain groundwaters sampled to the South (red lines) and to the North (blue lines) of the main regional tectonic features.

- Diagramma di Schoeller relativo alle acque freatiche dell'Alta Pianura friulana, differenziate in base alla localizzazione rispetto ai principali lineamenti tettonici regionali.



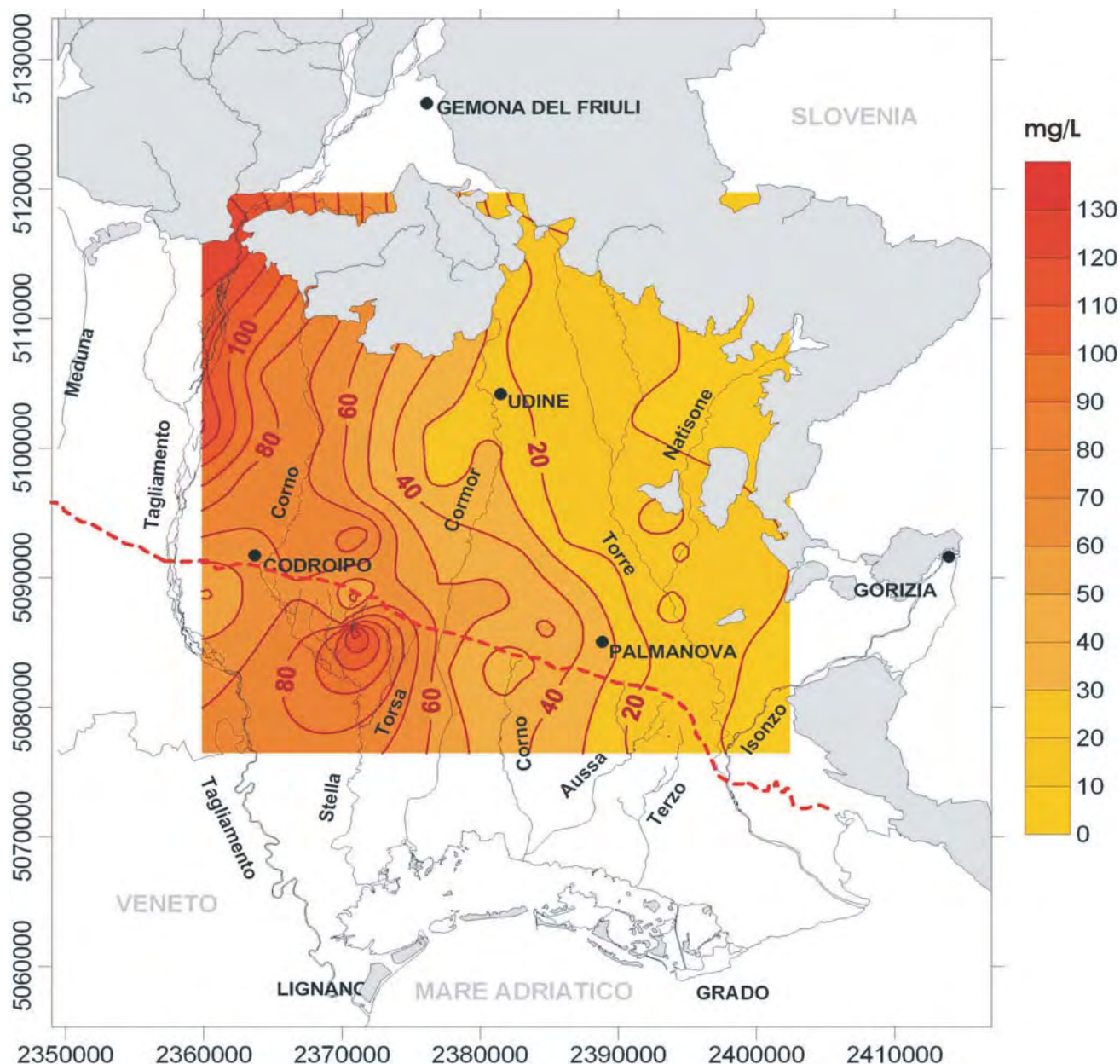


Fig. 6 – Sulphates distribution in High Plain groundwaters, surficial and spring waters.  
 - Carta della distribuzione dei solfati nelle acque sotterranee, superficiali e di risorgiva dell'Alta Pianura friulana.

## 6. - PIEZOMETRIC CHARACTERISTICS OF THE LOW PLAIN AQUIFER SYSTEM

The quantitative piezometric survey related to the sequence of confined aquifer levels that can be found in the Friuli Low Plain between 19 and more than 500 m bsl required the arrangement, together with ex APAT – Italian Geological Service (MARTELLI *et alii*, 2007a), of an experimental monitoring network involving 134 water-wells within the studied area. The hydraulic head data collected in the period 2003-2007 allowed (MARTELLI & GRANATI, 2006, 2007b; MARTELLI

& GRANATI, 2007a), by means of geostatistical methods of variographic analysis, to reconstruct the groundwater flow fields pertaining to the single aquifer levels, mapping out (fig.12) the annual averaged spatial distribution of piezometric head. Except Aquifer E (179/216 m bsl), for which no isomaps have been drawn owing to the small available measurement points, and the deepest Aquifer H (over 276 m bsl), marked by complex and peculiar flow circuits (as confirmed by the after-mentioned geochemical and isotopic results), a main NW-SE flow direction is recognisable for the remaining aquifers (MARTELLI *et alii*,

2007a). The most shallow Aquifer A (19/80 m bsl), whose average hydraulic gradient is about  $1,0 \cdot 10^{-3}$ , shows a rather articulated piezometric topology. The similar piezometric distributions that are appraisable for Aquifer B (80/112 m bsl) and Aquifer C (112/148 m bsl), whose hydraulic gradients are about  $1,8 \cdot 10^{-3}$  e  $1,9 \cdot 10^{-3}$  respectively, let foresee, together with the qualitative evidences, a possible mutual hydraulic connection (MARTELLI & GRANATI, 2006, 2007b). Analogous considerations pertain Aquifer D (148/179 m bsl) and Aquifer F (216/262 m bsl), characterised by an average hydraulic gradient of about  $2,0 \cdot 10^{-3}$  e  $8,2 \cdot 10^{-3}$  respectively. An hydraulic head increase with depth is recognisable as a general trend, in

spite of the wide variability range evinced at the same depth by the inner pressures within Aquifers C, D, E.

As regards the piezometric excursions, the isomaps, however conditioned by the inhomogeneous measurement sites' spatial distribution, show the highest values close to the spring belt till 200 m bsl. The extreme variations concerning Aquifers A (average excursion 1,4 meters) and B (average excursion 2,0 meters) are located near the Aussa-Corno hydrographic system, while the corresponding maxima in Aquifers C (average excursion 2,0 meters), D (average excursion 2,7 meters) and E (average excursion 2,4 meters) are recognisable close to the upper

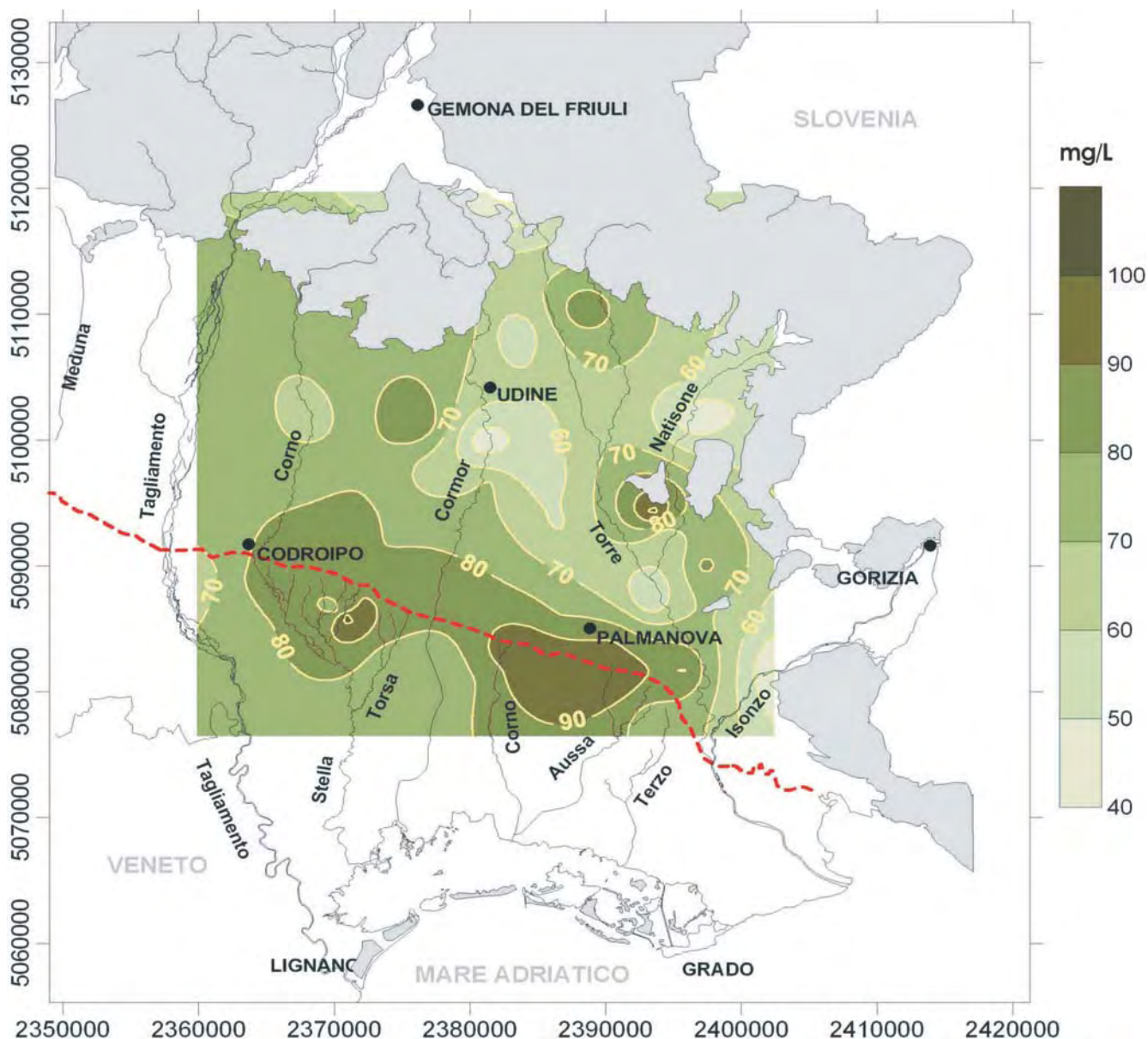


Fig. 7 – Calcium distribution in High Plain groundwaters, surficial and spring waters.  
– Carta della distribuzione del calcio nelle acque sotterranee, superficiali e di risorgiva dell'Alta Pianura friulana.



Torsa-Stella hydrographic system. Within Aquifer F (average excursion 2,6 meters), the excursion decrease develops radially starting from a maximum located in the central sector near the middle Cormor River.

The highest piezometric variability of Aquifer H (average excursion 1,3 meters) characterises the sector close to the lower Tagliamento River. Figure 13 shows the excursion patterns for Aquifers A and D.

## 7. - HYDROCHEMICAL CHARACTERISATION OF THE LOW PLAIN CONFINED AQUIFERS

Geochemical surveys, turned to improve both the main groundwater circuits' definition and the recharge areas of the Low Plain confined aquifers on the left side of the Tagliamento River (PRIN 2005), have been recently carried out on the basis of the data (major ions, pH, temperature, conduc-

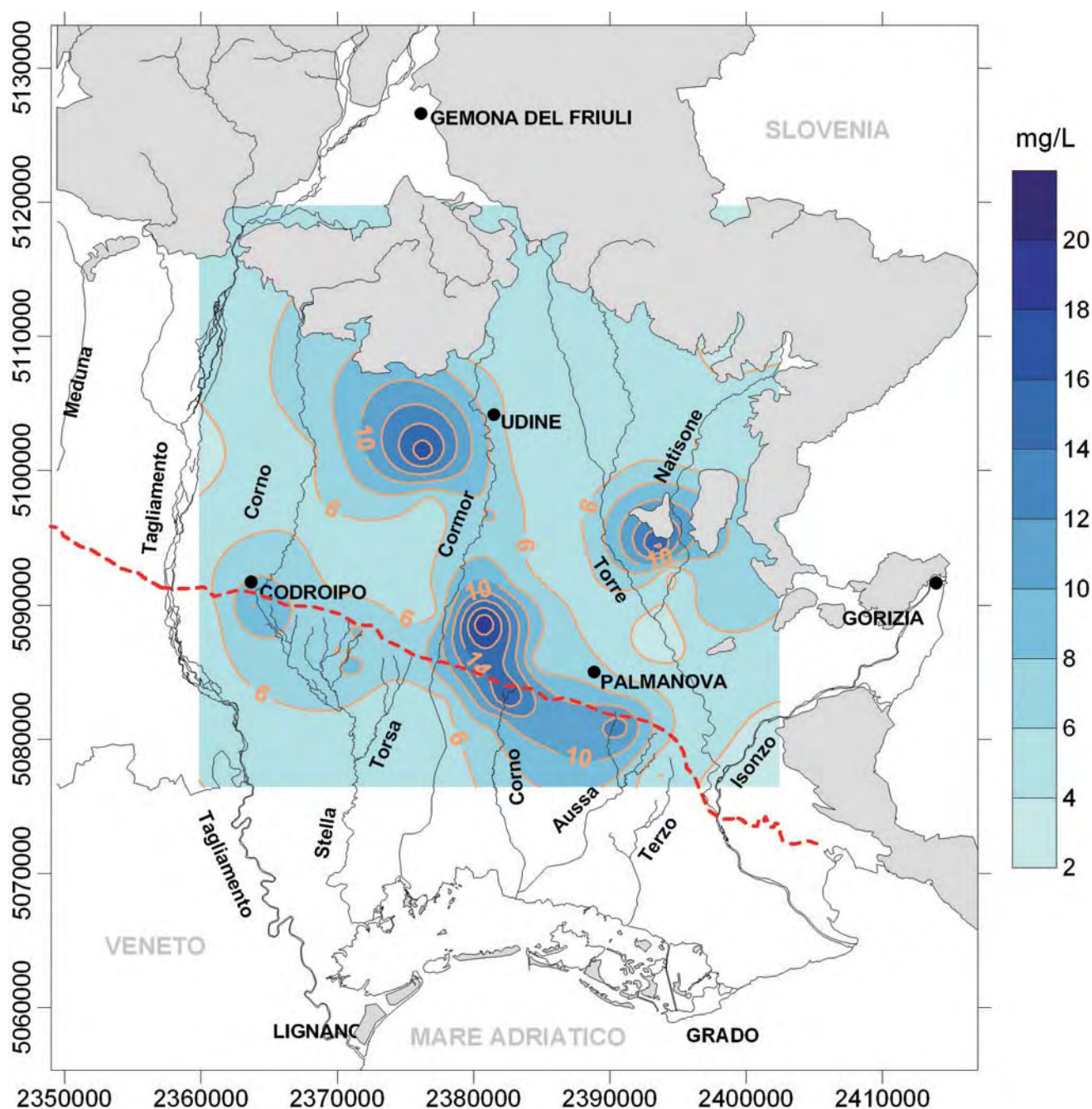


Fig. 8 – Chlorine distribution in High Plain groundwaters, surficial and spring waters.  
- Carta della distribuzione del cloro nelle acque sotterranee, superficiali e di risorgiva dell'Alta Pianura friulana.



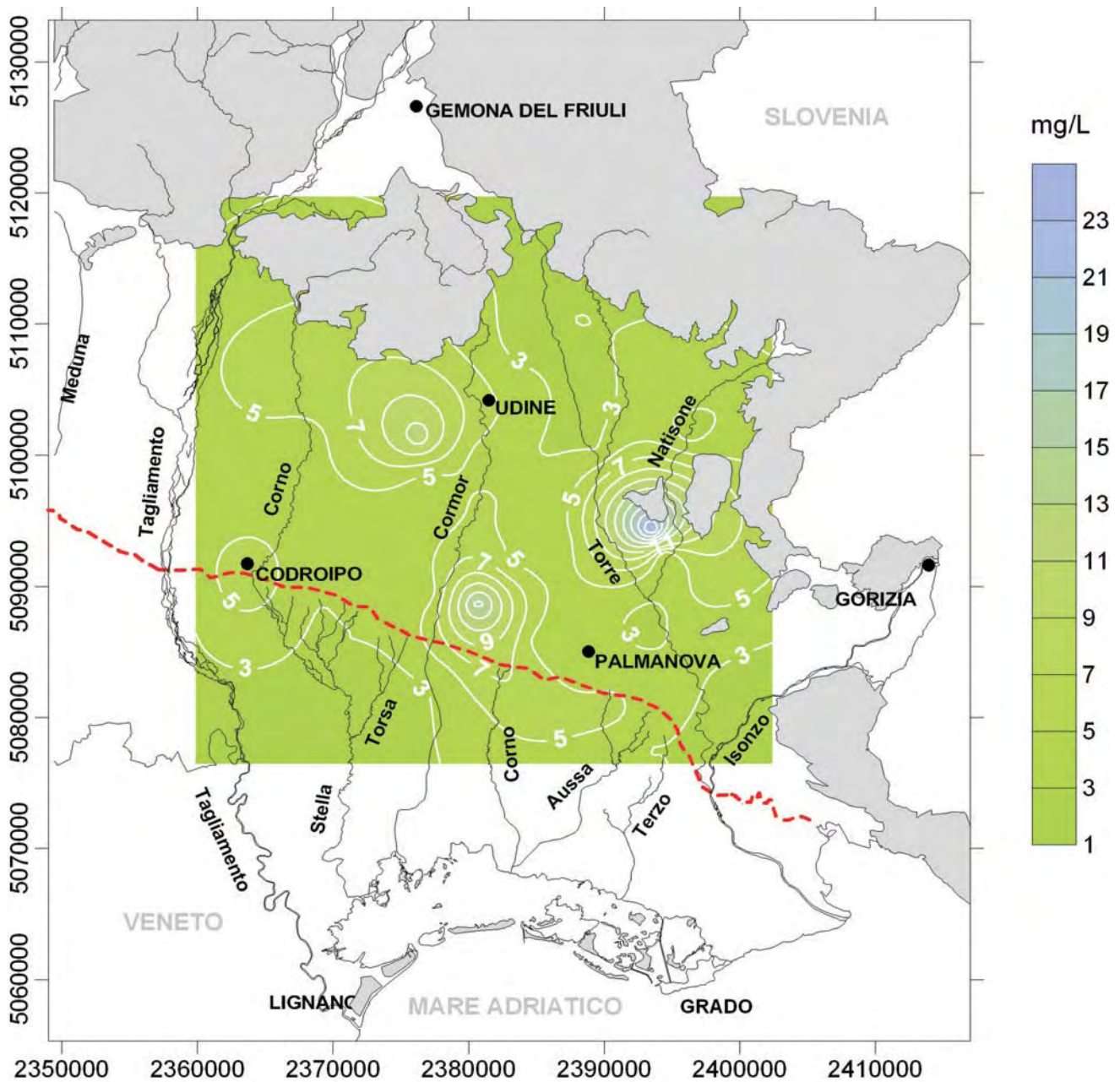


Fig. 9 – Sodium distribution in High Plain groundwaters, surficial and spring waters.  
 – Carta della distribuzione del sodio nelle acque sotterranee, superficiali e di risorgiva dell'Alta Pianura friulana.

tivity) collected in April, July, October 2006 and March 2007 through qualitative measurements on 36 artesian wells reaching aquifer levels more than 180 m bsl deep (1 well for Aquifer D, 6 for Aquifer E, 6 for Aquifer F, 4 for Aquifer G, 19 for Aquifer H). The interest for the deep flow patterns is strictly connected to the effects of the increasing groundwater withdrawals, owing to both the qualitative impoverishment of the most shallow confined levels and the increasing geothermal ex-

ploitation of the deep thermal waters (over 300 m bsl), that can be found along the coastal area in correspondence of the Cesarolo structural high (BARNABA, 1990; CALORE *et alii*, 1995; MARTELLI & GRANATI, 2008a, 2009). The collected data have been compared and completed with the ones coming from:

- 23 wells reaching the confined aquifer levels less than 180 m bsl deep (14 wells in Aquifer A, 5 in Aquifer B, 1 in Aquifer C, 3 in Aquifer D), moni-

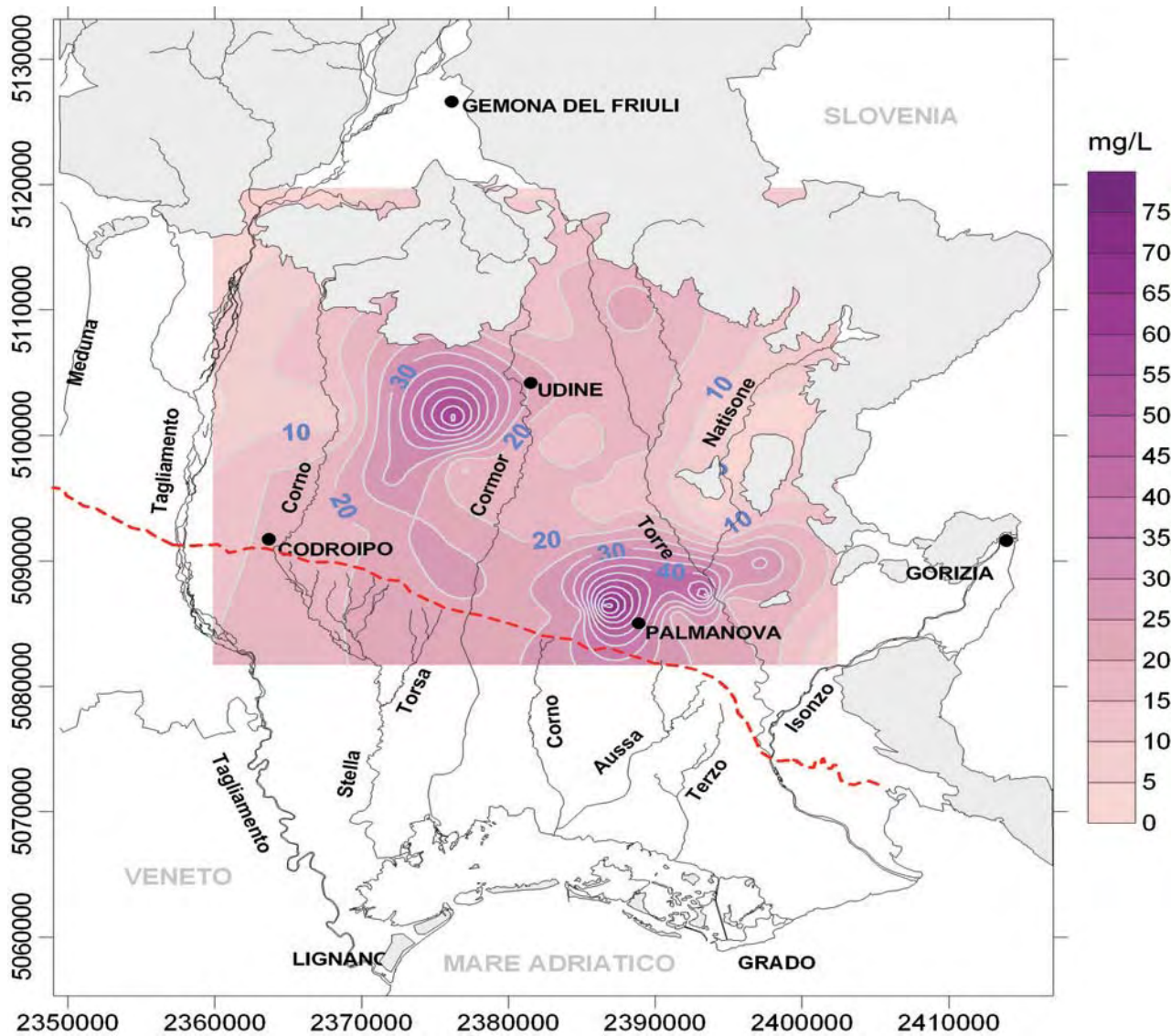


Fig. 10 – Nitrate distribution in High Plain groundwaters, surficial and spring waters.  
– Carta della distribuzione dei nitrati nelle acque sotterranee, superficiali e di risorgiva dell'Alta Pianura friulana.

tored by ARPA in June-July-August and October-November-December 2006 (BORTOLAN PIRONA, 2008; MARTELLI & GRANATI, 2009);

- 255 wells of the regional archive (REGIONE AUTONOMA FRIULI-VENEZIA GIULIA, 1990), reaching the whole recognised aquifer levels (44 wells in Aquifer A, 32 in Aquifer B, 11 in Aquifer C, 40 in Aquifer D, 7 in Aquifer E, 53 in Aquifer F, 10 in Aquifer G, 59 in Aquifer H), analysed by OGS in 1989 within the regional geothermal anomalies surveys (OSSERVATORIO GEOFISICO SPERIMENTALE DI TRIESTE, 1989).

Table 2 displays the values, sometimes averaged on the available measurements for each water-well, of the main determined chemical-physical parameters (fig. 14).

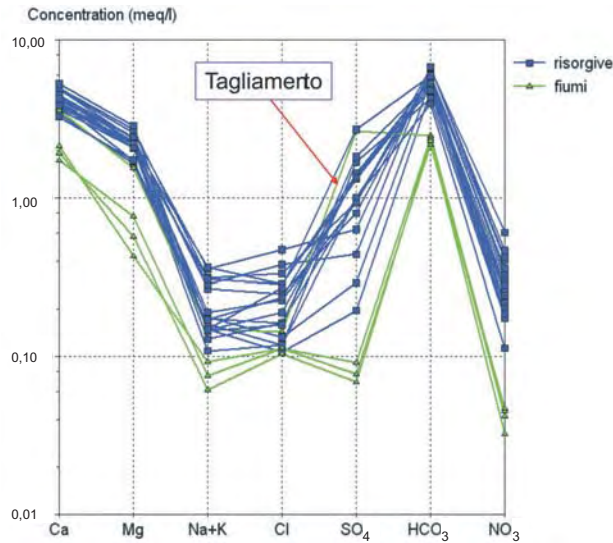


Fig. 11 – Schoeller diagram for Friuli High Plain surficial and spring waters.  
– Diagramma di Schoeller relativo alle acque superficiali e di risorgiva dell'Alta Pianura friulana.



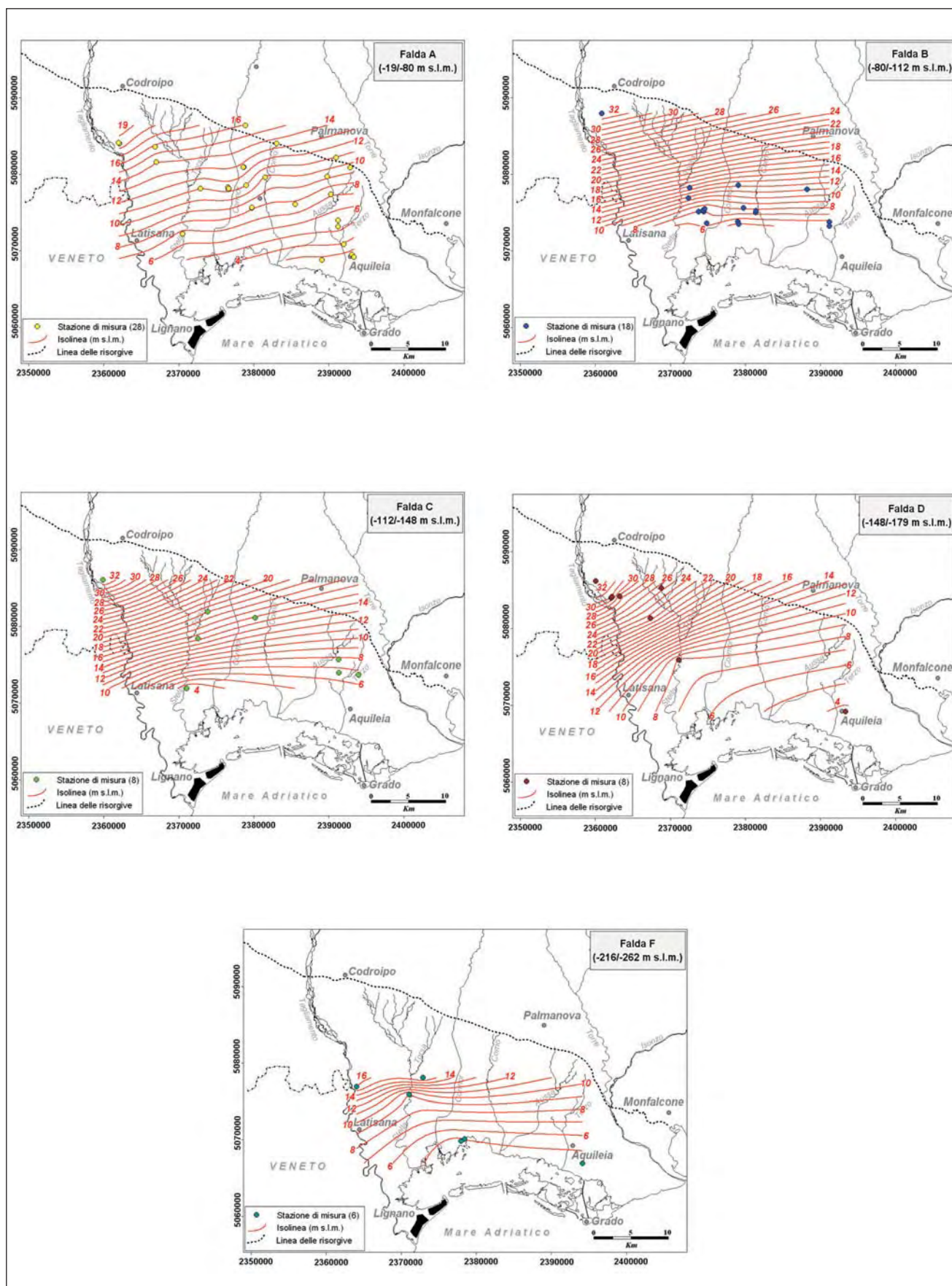


Fig. 12 – Aquifers A, B, C, D, F: hydraulic head contour lines (September-October 2003) (from MARTELLI & GRANATI, 2007a).  
 – Falde A, B, C, D, F: ricostruzioni piezometriche relative a misure effettuate nel periodo settembre-ottobre 2003 (da MARTELLI & GRANATI, 2007a).



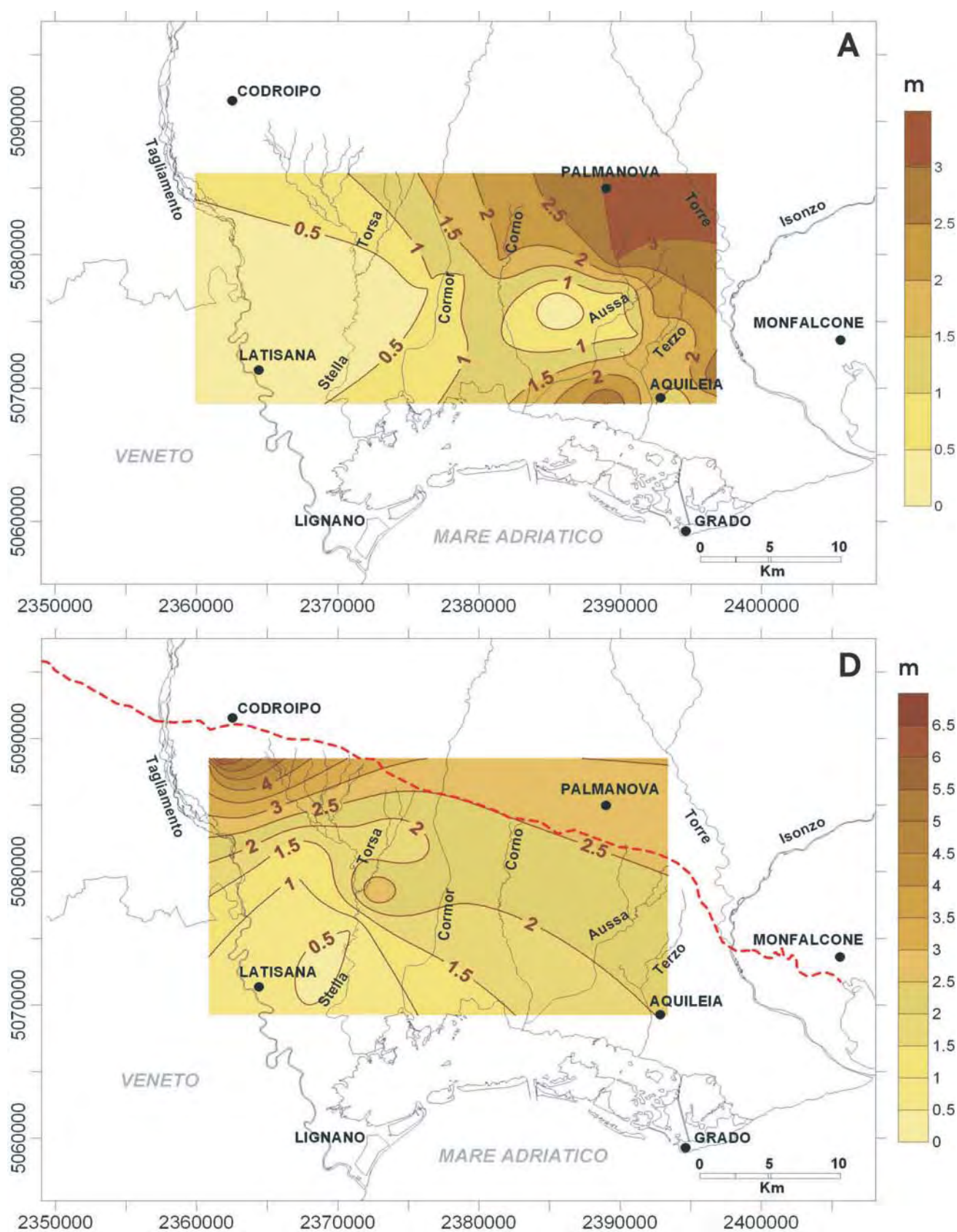


Fig. 13 – Annual averaged phreatimetric excursions (in m) of the Low Plain confined aquifers A,D.  
 – Mappe dell'escursione piezometrica media annua (in m) dei livelli acquiferi A e D della Bassa Pianura friulana.

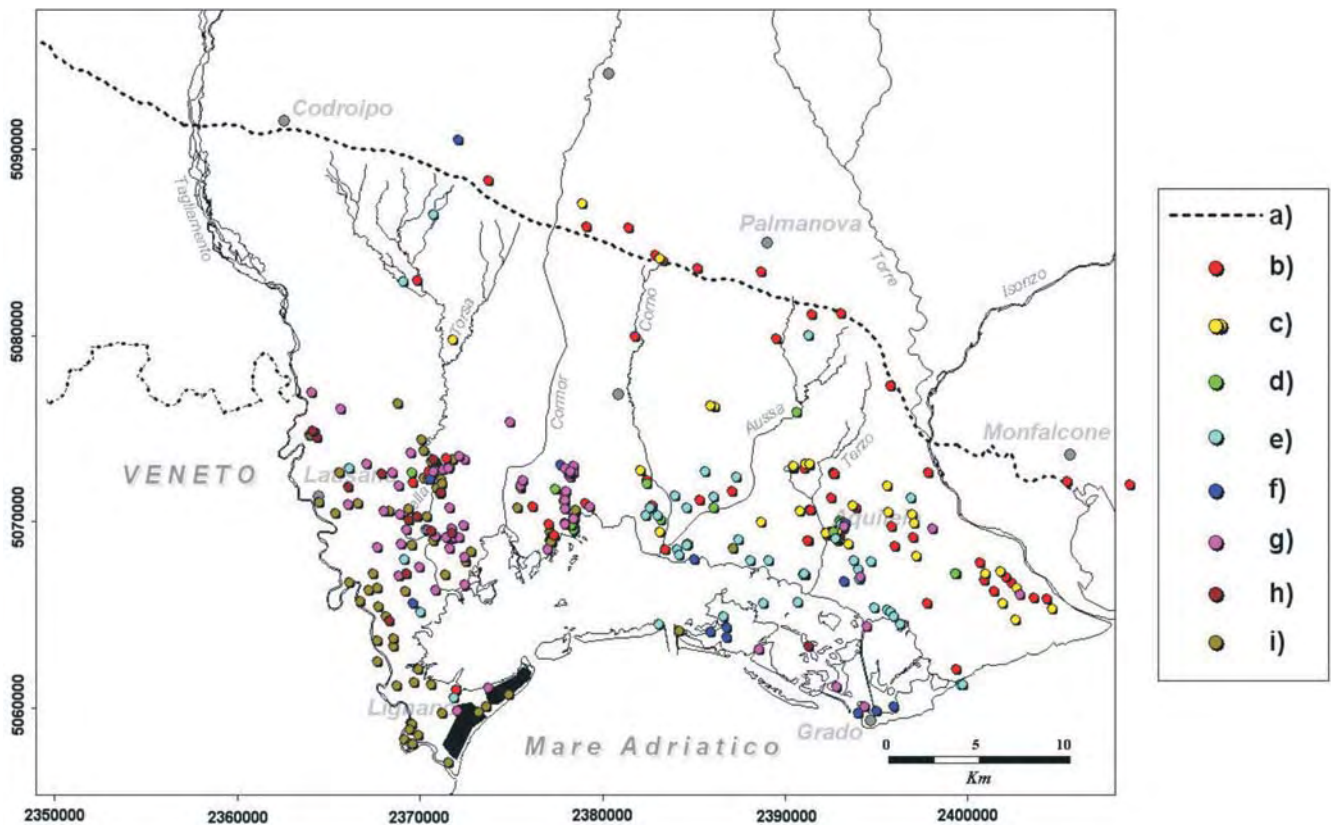


Fig. 14 – Hydrochemical sampling sites in the Low Friuli Plain. Legend: a) spring line; b) Aquifer A; c) Aquifer B; d) Aquifer C; e) Aquifer D; f) Aquifer E; g) Aquifer F; h) Aquifer G; i) Aquifer H.

– Distribuzione dei punti di campionamento idrochimico negli acquiferi confinati della Bassa Pianura Friulana. Legenda: a) linea delle risorgive; b) Falda A; c) Falda B; d) Falda C; e) Falda D; f) Falda E; g) Falda F; h) Falda G; i) Falda H.

The  $\text{Ca-HCO}_3$  facies (figg. 15-16), that can be associated to a flow circulation totally developing within the Quaternary clastic carbonate sediments, marks groundwaters till 150 m bsl (Aquifers A, B, C). Groundwaters of the lower Aquifers D and E show transition characteristics towards the  $\text{Na-HCO}_3$  facies, which becomes predominant in the deeper Aquifers F, G, H. Over 300 m bsl (Aquifer H), the  $\text{Na-Cl}$  facies can also be recognised (MARTELLI & GRANATI, 2009).

Within the most shallow Aquifers A, B, C, D (till 200 m bsl), the spatial distribution of sulphate content displays, although with a rather complex behaviour, a decreasing trend in the NW-SE direction according to the recharge origin (fig. 17); the highest concentrations can be distinguished between the Stella and the Ausa-Corno rivers. Topologically different sulphate distributions characterise groundwaters of the deeper Aquifers F, G, H (over 200 m bsl).

Analyzing the main chemical-physical data vs. depth (MARTELLI & GRANATI, 2009), a water temperature increase (fig. 18), according to a gradient

of about  $4^\circ\text{C}/100$  m higher than the conventional one, can be singled out.

The conductivity (fig. 19) displays an increasing trend under 300 m bsl, consistently with deep groundwater flow patterns characterised by long residence times (MARTELLI & GRANATI, 2008a) leading to high contents of dissolved salts of geochemical origin.

Calcium and magnesium solute concentrations (fig. 20) decrease in a similar way; the values related to water samples coming from aquifer levels between 200 and 400 m bsl are clearly scattered (MARTELLI & GRANATI, 2009).

The alkaline metals (sodium, potassium) dissolved contents also show a similar increase with depth (fig. 21), together with a remarkable scattering of concentration values within the deepest confined levels (MARTELLI & GRANATI, 2009).

Unlike the  $\text{Cl}^-$  ion (fig. 22), that undergoes an increasing concentration under 400 m bsl, and the  $\text{HCO}_3^-$  ion (fig. 23), that shows a clear spread of values, the sulphate amounts (fig. 24) are remarkably scattered till 300 m bsl, accor-

Tab. 2 – *Main physical-chemical parameters determined for sampled groundwaters of the Friuli Low Plain multi-layered aquifer system.*

– Valori dei principali parametri chimico-fisici rilevati in campioni idrici prelevati da pozzi attingenti ai livelli confinati del sistema acquifero multifalda della Bassa Pianura friulana.

ID	Fonte	Quota filtri (-m slm)	Conduc ( $\mu\text{S}/\text{cm}$ )	pH	TDS (mg/l)	Ca <sup>2+</sup> (mg/l)	Mg <sup>2+</sup> (mg/l)	Na+ (mg/l)	K+ (mg/l)	Cl <sup>-</sup> (mg/l)	HCO <sup>3-</sup> (mg/l)	SO <sub>4</sub> <sup>2-</sup> (mg/l)	NO <sup>3-</sup> (mg/l)	Sr <sup>-</sup> (mg/l)	SiO <sup>2</sup> (mg/l)
<i>Falda A</i>															
463	ARPA	50,0	512	7,7		81,5	21,5	5,5	2,0	8,0	311,0	36,6	16,5		
608	ARPA	63,0	638	7,3		94,5	30,5	6,0	2,0	11,0	381,0	32,6	38,4		
609	ARPA	63,0	651	7,5		96,0	31,0	5,5	2,0	10,0	363,0	40,8	49,7		
614	ARPA	61,0	556	7,5		77,0	27,5	5,5	1,0	10,5	308,0	40,1	38,3		
618	ARPA	48,0	591	7,4		85,0	30,0	8,5	2,0	13,0	341,5	39,1	35,9		
619	ARPA	67,0	613	7,6		89,0	31,0	8,0	1,5	12,5	335,5	52,4	42,8		
620	ARPA	62,0	506	7,7		71,0	26,5	2,0	1,0	4,5	220,5	104,9	17,2		
1293	ARPA	70,0	469	7,4		79,5	17,0	3,5	1,5	5,5	296,0	12,4	23,2		
1295	ARPA	54,0	610	7,4		97,5	27,0	4,5	1,0	11,0	363,0	26,9	33,3		
1300	ARPA	40,0	463	7,6		67,0	24,5	2,5	1,0	6,0	271,5	19,9	23,1		
1303	ARPA	40,0	663	7,2		104,5	32,0	6,5	1,5	11,5	354,0	53,8	51,1		
1312	ARPA	37,0	480	7,6		68,5	26,5	3,0	1,0	4,0	293,0	28,6	15,3		
1316	ARPA	40,0	423	7,8		59,5	24,5	3,0	1,0	3,5	174,0	112,0	3,7		
1320	ARPA	40,0	546	7,8		79,0	28,0	10,0	2,0	15,0	317,0	26,0	24,0		
0050010	OGS	29,5	375			57,3	19,4	3,8	0,9	8,4	200,0	13,5		0,4	10,5
0050013	OGS	29,9	370			58,1	19,7	2,9	0,7	3,4	200,0	13,5		0,3	7,5
0050024	OGS	70,8	350			53,3	20,4	7,1	0,9	2,6	200,0	0,5		0,3	12,7
0050025	OGS	70,9	330			51,7	21,9	7,2	1,0	1,7	202,0	29,0		0,3	12,7
0050028	OGS	60,4	395			59,3	21,9	2,6	0,6	2,8	210,0	15,3		0,2	6,6
0050056	OGS	65,2	390			54,5	23,8	5,4	1,4	2,5	220,0	20,7		0,4	11,5
0050069	OGS	28,0	370			52,1	21,9	3,3	1,0	2,7	214,0	19,8		0,3	11,2
0280012	OGS	78,8	440			64,1	20,9	6,8	1,1	2,6	240,0	38,4		0,4	15,9
0280030	OGS	79,5	370			32,0	8,0	43,0	1,4	1,7	228,0	0,5		0,1	17,8
0280036	OGS	77,5	375			53,7	23,3	7,9	1,1	1,3	198,0	48,6		0,4	17,3
0280061	OGS	59,7	375			41,7	17,5	20,0	1,5	0,7	230,0	0,4		0,3	16,6
0650012	OGS	59,0	360			56,9	17,7	1,9	0,7	4,7	206,0	11,9		0,1	5,2
0650014	OGS	27,7	395			62,5	19,9	2,9	0,5	2,3	230,0	24,7		0,2	8,1
0650017	OGS	62,5	360			57,3	15,6	4,8	0,9	1,9	214,0	15,7		0,4	12,1
0650023	OGS	16,9	450			82,6	15,6	2,8	1,2	5,5	248,0	19,3		0,2	3,7
0780007	OGS	72,2	390			43,7	21,1	7,2	4,1	3,4	224,0	0,8		0,2	13,8
0780013	OGS	64,7	370			45,7	22,1	4,6	1,7	3,1	218,0	15,3		0,2	8,3
0780014	OGS	54,3	400			52,1	19,2	10,0	1,9	1,5	250,0	3,1		0,2	13,3
0780015	OGS	50,2	370			48,1	20,9	4,8	1,7	2,7	215,0	16,0		0,2	7,4
0780019	OGS	72,0	360			50,1	18,5	2,9	0,7	5,7	192,0	11,7		0,2	7,7
0780021	OGS	67,0	365			44,1	20,7	8,4	2,1	2,3	217,0	6,3		0,2	11,6
0780026	OGS	72,2	400			49,7	19,7	10,8	2,3	2,1	243,0	0,5		0,2	16,7
0780043	OGS	76,1	415			57,7	19,0	8,4	1,3	2,3	212,0	22,1		0,3	15,0
0780069	OGS	68,5	425			50,1	20,7	7,8	2,1	3,3	216,0	11,9		0,2	7,4
0830045	OGS	26,2	565			25,3	13,4	61,0	5,6	26,8	316,0	0,5		0,3	10,4
0910010	OGS	78,6	500			75,8	23,6	2,5	0,6	5,3	174,0	115,0		0,7	3,3
0910027	OGS	73,5	455			42,9	18,7	35,0	3,6	0,9	250,0	1,0		0,3	15,4
0990041	OGS	24,6	375			52,1	12,1	14,8	0,8	22,1	163,0	14,0		0,2	3,8
0990054	OGS	37,7	430			76,1	13,8	3,3	1,7	5,0	235,0	16,2		0,1	3,0
1140013	OGS	66,2	390			47,7	21,6	8,4	0,9	1,0	190,0	54,7		0,3	13,9
1340010	OGS	42,3	445			50,9	19,7	20,8	1,7	1,8	276,0	1,0		0,3	17,0
1340016	OGS	50,8	380			47,7	16,5	13,6	1,2	0,4	198,0	30,6		0,3	14,6
1610039	OGS	74,5	435			48,5	21,1	7,4	1,7	1,2	202,0	33,8		0,3	14,8
1610050	OGS	76,8	505			60,1	27,2	4,7	0,9	6,2	214,0	59,9		0,4	13,2
1920002	OGS	79,8	405			45,3	18,2	12,0	1,7	0,3	216,0	7,9		0,3	16,8
1920022	OGS	28,0	400			66,1	20,2	2,2	0,7	4,0	222,0	14,8		0,1	4,9
1920023	OGS	30,0	400			65,7	20,7	2,3	0,7	4,3	215,0	14,4		0,1	4,6
1920024	OGS	30,5	395			68,1	18,0	2,2	0,7	4,3	220,0	15,9		0,1	4,5
1920025	OGS	27,5	390			64,1	19,9	2,2	0,7	4,1	216,0	13,0		0,1	4,9
1920043	OGS	63,0	405			65,7	20,4	2,4	0,6	3,2	226,0	13,5		0,2	7,3
1920045	OGS	60,6	360			52,9	21,9	2,9	0,6	2,4	200,0	13,5		0,4	9,4
1920046	OGS	63,6	365			54,9	20,9	2,9	0,6	2,8	200,0	23,0		0,4	9,4
1950032	OGS	49,6	370			52,1	20,9	4,8	0,8	0,6	192,0	44,5		0,4	11,7
1950048	OGS	56,8	380			56,5	20,2	4,6	0,9	2,3	214,0	34,9		0,4	13,8

next page



<i>Falda B</i>														
637	ARPA	85,0	664	7,2		99,0	42,0	6,0	1,0	11,0	439,0	65,2	0,3	
1304	ARPA	90,0	544	7,5		81,0	29,5	6,5	1,0	10,0	311,0	36,2	31,6	
1310	ARPA	90,0	371	7,8		50,5	23,5	5,5	1,0	1,0	204,0	66,0	0,8	
1325	ARPA	86,0	505	7,4		72,0	27,0	7,0	1,0	13,0	299,0	31,3	26,9	
1328	ARPA	93,0	470	7,4		70,5	25,5	3,5	1,0	4,0	242,0	70,3	12,7	
0050030	OGS	99,0	365			53,7	21,4	2,8	0,6	3,0	196,0	19,8		0,2 7,2
0050036	OGS	98,0	380			58,9	21,6	3,5	1,0	6,7	201,0	13,5		0,2 5,7
0050054	OGS	109,0	370			56,1	19,9	2,6	0,6	3,3	204,0	16,2		0,3 7,8
0050058	OGS	100,0	375			55,7	21,6	3,6	0,8	5,2	198,0	13,1		0,4 10,0
0050059	OGS	99,2	385			54,5	22,4	3,6	0,8	5,5	210,0	31,9		0,4 9,9
0050060	OGS	100,0	325			50,9	22,6	4,0	0,8	2,7	215,0	12,0		0,4 11,5
0050061	OGS	99,0	375			60,5	22,8	4,4	1,1	2,0	228,0	29,0		0,3 9,4
0050062	OGS	89,0	355			50,5	21,9	3,8	0,7	3,0	200,0	23,4		0,4 11,0
0280037	OGS	83,2	370			54,5	20,2	8,6	1,2	1,6	200,0	47,0		0,3 17,3
0280060	OGS	89,0	370			34,5	13,1	30,8	1,4	1,6	228,0	0,9		0,2 16,9
0650006	OGS	96,6	385			56,1	21,4	3,2	0,7	2,6	214,0	36,7		0,3 7,3
0650008	OGS	99,7	380			56,1	20,9	2,4	0,6	3,4	218,0	18,9		0,2 7,3
0650020	OGS	97,7	365			50,1	20,4	5,4	0,8	1,9	216,0	21,8		0,4 11,4
0650022	OGS	98,0	370			59,3	17,5	1,7	0,8	3,5	208,0	12,2		0,2 4,4
0650026	OGS	95,9	400			62,9	19,9	2,8	0,8	7,1	209,0	14,4		0,2 5,8
0650030	OGS	100,4	345			46,1	19,2	4,1	0,8	3,7	191,0	8,6		0,2 10,4
0780003	OGS	100,0	365			44,1	19,9	8,0	1,5	2,4	212,0	3,2		0,2 13,7
0780010	OGS	99,9	350			48,5	17,3	5,6	1,1	1,5	208,0	9,9		0,2 10,8
0780012	OGS	100,5	360			48,9	18,7	6,2	1,2	1,3	214,0	7,6		0,2 12,0
0780016	OGS	95,3	370			46,1	21,9	5,0	1,7	2,2	210,0	14,6		0,2 10,4
0780018	OGS	95,6	360			49,7	19,7	2,9	0,7	5,1	193,0	11,7		0,2 7,7
0780027	OGS	90,9	400			50,1	19,7	10,4	2,2	3,7	240,0	0,9		0,2 17,9
1610003	OGS	92,7	535			60,1	30,6	4,2	1,0	7,4	236,0	46,6		0,5 9,1
1610042	OGS	99,2	405			46,9	20,2	6,3	0,9	1,3	164,0	54,9		0,4 12,8
1920014	OGS	89,8	365			36,1	28,7	4,6	0,9	0,8	200,0	35,3		0,3 16,5
1920026	OGS	102,6	350			52,1	20,9	2,5	0,5	2,7	190,0	13,5		0,2 6,7
1920027	OGS	103,6	350			53,7	19,7	2,8	0,6	2,8	200,0	13,5		0,2 7,4
1920029	OGS	83,6	350			52,5	21,6	2,5	0,8	3,0	197,0	13,5		0,2 6,7
1920032	OGS	97,6	400			62,1	22,9	2,4	0,6	4,1	218,0	13,7		0,1 6,8
1920033	OGS	87,8	390			60,5	22,8	2,6	0,5	3,3	222,0	16,7		0,2 7,3
1920042	OGS	95,8	390			54,5	25,0	2,3	0,5	3,7	218,0	13,5		0,1 6,4
1920047	OGS	109,8	350			52,9	21,1	3,0	0,6	2,5	202,0	13,5		0,3 9,2
<i>Falda C</i>														
1299	ARPA	141,0	477	7,5		70,0	24,5	3,0	1,0	6,0	289,5	16,1	21,9	
0050027	OGS	126,5	345			50,9	20,7	6,6	1,2	1,6	207,0	15,0		0,3 13,2
0050044	OGS	126,8	365			52,1	21,9	3,1	0,6	2,5	200,0	16,7		0,2 6,2
0050063	OGS	118,0	395			56,1	24,3	2,7	0,6	3,1	214,0	14,9		0,3 9,1
0280029	OGS	133,8	325			42,5	17,5	15,6	1,4	1,0	217,0	11,0		0,3 17,8
0650018	OGS	148,7	345			46,1	20,2	5,2	0,8	3,0	154,0	7,4		0,2 10,9
0910013	OGS	140,4	375			29,3	12,4	38,0	1,4	0,7	234,0	0,8		0,2 16,7
0910016	OGS	141,5	400			40,1	16,0	28,4	2,4	2,3	244,0	2,2		0,3 13,7
1340014	OGS	147,6	355			38,9	16,5	17,2	1,3	1,0	212,0	9,2		0,2 15,1
1610038	OGS	127,0	555			64,1	30,1	4,6	1,0	10,3	232,0	58,0		0,5 12,0
1610044	OGS	126,6	405			46,5	20,4	6,4	0,9	0,8	164,0	55,6		0,4 12,0
1950046	OGS	122,7	350			47,7	17,5	11,4	1,2	2,6	200,0	21,0		0,4 16,9
<i>Falda D</i>														
1294	ARPA	169,0	433	7,6		60,5	24,5	3,5	1,0	5,5	253,0	26,7	14,2	
1317	ARPA	152,0	410	7,8		55,5	25,0	2,0	1,0	2,0	155,5	114,0	2,1	
1330	ARPA	170,0	390	7,8		54,0	22,5	2,0	0,5	7,0	174,0	93,0	2,1	
29	DGT	179,0	509	8,5	305	15,6	5,9	81,1	5,0	4,8	292,8	0,1	0,0	
0050003	OGS	162,0	335			49,7	22,1	8,8	1,4	2,6	225,0	20,0		0,3 15,8
0050004	OGS	170,7	385			48,9	25,3	4,7	1,2	3,1	206,0	27,0		0,4 12,0
0050005	OGS	163,7	380			53,3	22,4	4,7	1,2	3,7	210,0	28,3		0,4 11,9
0050006	OGS	170,0	385			52,9	23,1	4,7	1,2	3,8	208,0	28,3		0,4 11,9
0050009	OGS	170,0	380			52,9	20,9	10,3	1,3	3,1	222,0	17,1		0,4 13,3
0050016	OGS	169,1	340			47,7	18,0	10,7	1,9	1,8	205,0	11,0		0,3 16,0
0050018	OGS	171,1	365			32,0	11,2	44,4	3,4	2,7	220,0	9,0		0,2 15,0
0050019	OGS	171,1	445			48,1	19,4	13,6	1,8	4,7	212,0	22,7		0,3 15,8
0050020	OGS	171,1	440			44,1	22,9	10,0	1,2	3,3	182,0	48,4		0,3 11,8
0050038	OGS	155,5	340			52,1	21,9	3,0	0,6	3,0	190,0	16,0		0,1 8,9
0050043	OGS	151,5	395			58,1	22,1	3,7	0,8	7,4	212,0	21,6		0,3 7,5
0050046	OGS	176,3	410			55,3	19,4	15,3	2,0	9,9	212,0	33,3		0,4 13,6
0050047	OGS	170,2	340			55,7	15,3	2,2	0,8	3,7	180,0	12,6		0,1 5,7
0050050	OGS	168,0	400			62,1	20,7	2,9	0,8	5,9	207,0	14,6		0,2 5,7
0050052	OGS	149,4	370			56,9	16,5	3,3	0,6	4,7	210,0	8,8		0,4 12,6
0050065	OGS	159,5	380			56,5	21,6	3,2	0,7	2,8	210,0	15,7		0,4 10,0
0650005	OGS	160,5	385			56,9	20,7	3,2	0,6	3,4	212,0	27,0		0,3 7,3

next page

0780039	OGS	169,9	540			27,6	15,1	66,0	8,9	30,0	283,0	3,1		0,2	14,5
0780047	OGS	171,3	450			32,5	13,9	44,0	4,3	12,0	224,0	11,0		0,2	18,3
0780048	OGS	165,6	590			28,8	11,2	80,0	6,4	43,0	245,0	11,7		0,2	14,6
0780071	OGS	167,5	410			45,7	18,5	11,2	1,2	0,9	174,0	46,8		0,3	16,2
0780080	OGS	167,7	525			28,8	14,3	66,0	9,1	29,0	287,0	2,7		0,2	14,6
0800011	OGS	178,2	340			38,5	17,3	15,4	1,2	1,6	194,0	16,0		0,3	14,9
0830017	OGS	179,0	615			18,0	10,2	86,0	4,4	7,4	388,0	0,5		0,2	17,7
0910024	OGS	164,0	420			41,7	20,4	12,8	1,4	1,1	176,0	46,8		0,3	16,8
1140043	OGS	178,4	350			36,1	14,1	22,4	1,4	1,9	214,0	1,8		0,2	16,0
1340041	OGS	159,9	365			37,3	13,9	30,4	2,0	1,3	238,0	1,4		0,2	16,6
1340048	OGS	149,9	430			41,7	18,2	33,2	3,5	2,1	284,0	1,1		0,2	14,3
1610045	OGS	167,3	405			47,7	19,7	6,6	0,9	0,8	158,0	56,2		0,4	12,6
1610046	OGS	164,1	405			46,5	20,4	6,6	0,9	0,8	170,0	54,7		0,3	10,4
1610048	OGS	164,0	505			61,7	26,3	4,8	0,9	6,5	208,0	58,9		0,4	12,6
1920001	OGS	168,2	410			45,3	20,2	6,6	0,9	1,7	160,0	56,0		0,4	13,9
1920015	OGS	169,1	415			47,3	19,9	6,8	0,9	1,3	160,0	59,6		0,3	13,0
1920018	OGS	179,0	415			46,5	19,9	6,4	0,9	1,3	158,0	59,6		0,4	12,9
1920055	OGS	158,8	365			46,5	22,4	4,1	0,8	1,4	204,0	28,1		0,4	13,6
1950028	OGS	155,7	385			56,1	19,9	4,3	0,8	3,7	196,0	47,3		0,4	12,4
1950030	OGS	153,7	350			49,7	19,9	3,5	0,7	2,4	172,0	49,8		0,5	10,4
1950031	OGS	164,1	345			47,3	20,4	3,9	0,7	1,7	168,0	50,6		0,4	11,1
1950045	OGS	161,8	365			50,5	21,9	3,2	0,6	2,4	200,0	26,1		0,4	10,8
1950049	OGS	159,7	355			71,7	19,7	5,4	0,9	2,0	198,0	28,1		0,4	11,3
<b>Falda E</b>															
10	DGT	215,0	384	7,2	293	41,7	20,1	5,7	1,4	4,7	234,2	15,5	0,0		
25	DGT	198,0	392	6,8	270	41,3	20,9	10,7	1,1	1,1	219,4	34,7	0,0		
27	DGT	202,0	318	8,6	258	44,7	21,8	2,8	0,6	1,4	158,5	75,7	1,9		
33	DGT	215,0	428	7,5	289	25,9	11,8	57,2	8,2	15,5	232,4	3,8	50,8		
34	DGT	213,0	434	7,4	297	23,6	11,1	61,2	8,9	26,1	235,5	3,8	0,2		
36	DGT	216,0	243	6,9	204	37,5	13,1	6,6	0,7	11,4	163,9	8,8	6,1		
0050039	OGS	195,0	345			54,1	20,9	3,3	0,6	2,6	198,0	17,0		0,1	8,9
0280028	OGS	185,2	385			56,5	23,3	8,3	1,0	1,4	198,0	63,9		0,3	17,4
0780072	OGS	187,0	425			42,9	18,2	20,4	4,6	2,4	214,0	17,6		0,3	15,6
0780073	OGS	188,3	685			16,8	6,6	129,0	6,5	34,8	264,0	1,4		0,1	13,1
0780074	OGS	188,9	410			44,9	17,3	16,4	1,7	0,7	180,0	43,8		0,3	16,9
1340008	OGS	209,2	360			36,1	13,9	30,0	1,9	0,8	134,0	0,7		0,2	16,5
1920016	OGS	200,9	415			44,5	21,1	8,0	1,1	0,7	170,0	51,1		0,3	13,9
<b>Falda F</b>															
2	DGT	218,0	371	8,2	269	32,2	16,6	18,8	2,5	3,4	213,7	16,1	0,6		
9	DGT	220,0	379	7,4	284	46,1	21,3	5,8	0,7	1,1	204,4	50,3	0,0		
14	DGT	238,0	370	8,6	258	25,7	12,9	37,8	1,2	1,2	248,3	0,1	0,1		
26	DGT	233,0	368	8,0	265	36,8	21,2	11,5	0,9	1,3	200,4	42,7	0,9		
31	DGT	220,0	449	9,4	300	22,9	11,1	63,6	5,9	7,5	288,5	0,2	0,0		
35	DGT	218,0	422	7,5	289	26,5	12,5	51,1	7,5	13,7	248,9	3,3	2,8		
0050017	OGS	218,0	360			51,7	22,4	7,6	1,7	2,5	212,0	24,0		0,3	16,8
0050040	OGS	236,0	340			20,8	8,0	70,0	3,8	4,5	215,0	0,9		0,1	14,7
0280010	OGS	257,2	325			32,8	13,4	26,0	1,3	0,8	210,0	0,9		0,2	18,5
0280013	OGS	230,0	370			36,9	11,7	28,8	1,3	1,3	220,0	0,5		0,2	17,4
0280018	OGS	227,2	300			32,5	14,1	31,0	1,3	1,5	200,0	2,2		0,2	17,9
0280019	OGS	233,0	325			33,7	14,8	29,4	1,3	1,1	210,0	0,5		0,2	20,6
0280021	OGS	237,4	399			57,7	24,8	6,8	1,0	1,6	205,0	49,5		0,4	17,9
0280022	OGS	237,4	315			31,7	15,1	30,0	1,2	0,9	210,0	0,7		0,2	20,1
0280023	OGS	238,1	320			32,1	14,8	31,0	1,3	1,0	210,0	1,8		0,2	19,8
0280024	OGS	258,3	310			32,9	14,1	30,0	1,3	1,0	208,0	5,0		0,2	19,9
0280025	OGS	232,0	315			34,5	14,6	30,0	1,2	0,8	210,0	3,1		0,2	19,9
0280031	OGS	258,7	370			38,5	10,7	32,5	1,5	0,7	222,0	0,5		0,2	17,0
0280032	OGS	218,1	370			32,1	13,9	33,0	1,4	2,1	226,0	0,5		0,2	16,1
0280034	OGS	237,6	325			31,2	14,6	32,0	1,3	0,7	212,0	0,9		0,2	20,1
0280038	OGS	238,8	325			31,3	15,1	34,5	1,3	1,4	223,0	0,7		0,2	20,3
0280039	OGS	239,4	370			34,5	11,4	35,5	1,3	0,8	228,0	0,5		0,2	16,9
0280040	OGS	238,5	370			32,1	11,7	35,0	1,3	1,3	232,0	0,5		0,2	16,9
0780009	OGS	219,0	370			48,9	19,0	6,2	1,2	2,0	216,0	7,6		0,2	12,4
0780044	OGS	234,3	462			19,6	8,5	80,0	3,7	1,1	266,0	2,0		0,1	17,9
0800046	OGS	246,0	350			30,9	12,6	34,0	1,1	1,9	222,0	0,7		0,2	16,3
0800048	OGS	259,3	370			26,9	10,5	33,6	1,4	0,6	236,0	0,7		0,2	17,3
0830020	OGS	219,3	540			26,9	10,7	66,0	4,7	3,0	342,0	0,5		0,3	15,3

0830030	OGS	249,1	470			75,4	22,4	2,0	0,6	3,7	166,0	115,0		0,8	3,9
0910011	OGS	239,4	375			29,3	12,2	40,0	1,4	1,8	234,0	0,7		0,2	15,6
1140002	OGS	247,0	360			32,5	15,3	27,2	1,4	0,6	220,0	0,8		0,2	16,7
1140004	OGS	246,2	360			35,3	14,1	26,8	1,4	1,1	218,0	0,5		0,2	16,3
1140034	OGS	259,4	345			24,2	11,2	55,0	1,6	1,1	237,0	1,0		0,1	18,0
1140037	OGS	249,5	375			26,5	9,5	47,0	1,4	0,7	234,0	0,5		0,1	17,3
1140038	OGS	240,3	365			28,5	12,4	37,6	1,3	0,4	238,0	0,8		0,2	15,8
1140039	OGS	240,8	360			28,1	12,9	36,0	1,4	0,8	234,0	0,9		0,2	15,8
1140040	OGS	247,5	435			43,3	19,2	26,5	2,7	0,9	272,0	0,7		0,3	15,4
1140046	OGS	244,6	370			28,3	10,9	38,5	1,3	0,9	230,0	1,1		0,1	17,2
1140047	OGS	243,0	350			35,7	14,8	21,2	1,4	0,3	212,0	1,1		0,2	15,6
1140048	OGS	240,1	430			43,7	18,5	26,5	2,4	0,4	270,0	0,9		0,3	15,7
1140050	OGS	242,7	355			29,3	13,4	31,2	1,3	1,0	224,0	0,5		0,2	14,3
1140052	OGS	240,0	355			29,3	13,6	31,0	1,2	1,0	220,0	0,9		0,2	16,6
1140053	OGS	238,8	355			31,7	14,3	28,5	1,1	1,1	222,0	0,6		0,2	16,9
1140058	OGS	260,0	325			28,8	13,6	38,0	1,3	1,0	218,0	1,0		0,2	18,1
1140060	OGS	247,6	380			32,9	12,2	35,0	1,4	1,5	240,0	0,9		0,2	17,3
1340001	OGS	258,3	360			21,8	11,2	66,0	1,8	0,9	240,0	1,0		0,1	15,2
1340003	OGS	258,0	365			26,9	10,7	48,0	1,4	0,6	232,0	1,6		0,1	17,3
1340005	OGS	258,2	345			28,5	12,9	40,4	1,5	0,7	230,0	1,6		0,2	17,4
1340011	OGS	237,3	370			29,7	11,7	39,0	1,3	0,9	228,0	1,0		0,2	16,8
1340013	OGS	257,3	350			37,7	15,3	20,0	1,1	1,0	202,0	8,1		0,2	16,5
1340022	OGS	260,0	370			32,1	14,1	32,5	1,3	0,9	230,0	0,8		0,2	16,7
1340026	OGS	255,8	305			31,4	14,0	29,0	1,2	0,9	208,0	1,0		0,2	17,7
1340027	OGS	260,5	330			40,1	15,8	17,4	1,1	1,4	196,0	17,7		0,2	15,6
1340032	OGS	252,0	360			26,5	10,2	48,0	1,5	2,0	240,0	1,5		0,1	16,6
1340039	OGS	258,4	345			44,1	14,3	17,8	1,2	2,0	198,0	29,5		0,2	18,9
1340045	OGS	239,2	370			25,7	10,0	48,4	1,5	0,4	244,0	1,4		0,1	16,5
1340049	OGS	255,0	370			26,1	10,9	50,5	1,6	1,0	246,0	1,4		0,1	16,7
1510019	OGS	251,2	300			37,7	16,5	19,0	1,0	0,9	192,0	11,0		0,2	18,8
1560011	OGS	219,2	355			52,9	19,9	3,0	0,6	2,5	206,0	21,1		0,2	6,8
<i>Falda G</i>															
4	DGT	267,0	460	8,1	283	23,7	12,6	38,0	1,7	3,7	245,2	0,3	0,0		
6	DGT	263,0	467	7,2	342	63,3	20,5	3,5	0,6	4,9	168,9	111,5	7,7		
23	DGT	269,0	413	7,0	288	24,3	11,7	59,7	1,9	1,4	310,1	0,7	0,1		
30	DGT	269,0	517	6,9	369	25,4	12,3	79,2	5,5	30,7	297,7	4,1	1,6		
0800038	OGS	266,3	325			39,3	15,3	16,0	1,1	1,2	200,0	15,3		0,2	16,8
1140045	OGS	266,7	340			24,7	11,2	51,0	1,4	1,3	225,0	1,0		0,1	18,6
1140049	OGS	269,8	355			30,5	13,4	30,5	1,2	1,8	212,0	0,9		0,2	16,4
1140055	OGS	267,8	300			30,9	13,8	30,0	1,3	1,0	207,0	1,0		0,1	17,5
1340012	OGS	262,7	350			36,9	16,0	18,0	1,1	0,7	204,0	12,1		0,2	16,4
1340024	OGS	267,4	380			31,7	13,6	36,0	1,3	1,3	234,0	0,8		0,2	17,2
1340025	OGS	268,5	430			54,9	18,7	14,8	1,4	0,9	262,0	0,8		0,3	17,4
1340033	OGS	267,3	320			35,7	15,1	21,2	1,3	1,3	208,0	10,3		0,2	15,3
1340034	OGS	262,8	325			36,1	14,6	21,2	1,3	1,4	206,0	10,1		0,2	14,9
1340050	OGS	269,4	365			24,2	10,4	62,0	1,8	0,9	250,0	1,0		0,1	16,3
<i>Falda H</i>															
1	DGT	325,0	370	8,4	256	22,0	10,3	36,1	1,5	1,6	218,9	5,6	0,5		
3	DGT	500,0	556	8,4	339	23,9	13,2	39,1	1,7	3,4	254,3	0,1	0,0		
5	DGT	492,0	510	8,8	334	24,2	13,3	38,3	1,7	3,8	247,3	0,1	0,0		
7	DGT	281,0	370	7,1	243	38,8	18,5	9,8	0,8	1,6	211,5	24,7	0,0		
8	DGT	494,0	557	8,6	351	25,3	13,0	38,5	1,7	3,6	255,6	0,1	0,8		
11	DGT	362,0	493	7,9	359	42,3	21,0	5,6	0,7	1,0	188,8	53,9	0,0		
12	DGT	346,0	436	8,3	286	25,6	15,8	15,3	1,0	1,6	207,6	0,2	0,8		
13	DGT	298,0	353	8,2	247	26,7	13,5	29,4	1,4	3,5	234,1	0,1	0,0		
15	DGT	359,0	401	8,2	266	22,3	10,1	45,6	1,3	1,6	252,6	0,0	0,7		
16	DGT	358,0	366	8,4	254	23,0	10,4	45,7	1,4	1,2	250,8	0,3	0,1		
17	DGT	359,0	353	7,3	240	25,0	12,7	33,1	1,7	2,4	237,5	0,0	0,0		
18	DGT	359,0	419	7,9	270	24,1	12,4	49,7	2,4	9,3	263,4	0,3	0,0		
19	DGT	359,0	404	6,7	271	25,9	12,8	33,3	1,6	2,5	240,4	0,2	1,2		
20	DGT	507,0	2538	8,7	1292	6,3	4,3	380,7	17,5	346,4	490,1	0,7	6,6		

next page



21	DGT	495,0	1289	9,0	740	6,7	2,7	200,8	20,8	145,5	358,5	0,0	1,0		
22	DGT	575,0	2094	8,3	1138	10,7	5,5	304,2	13,4	265,3	473,4	0,2	2,8		
24	DGT	524,0	663	8,6	404	15,3	8,1	111,8	4,9	11,5	325,8	0,1	0,9		
28	DGT	414,0	389	8,1	250	24,7	11,9	40,7	1,8	2,2	236,1	0,4	0,0		
32	DGT	598,0	9420	7,4	4819	82,1	48,5	1326,8	63,4	2233,4	272,3	92,0	20,9		
0280011	OGS	436,0	280			28,9	13,4	21,0	1,4	1,2	182,0	0,9		0,1	21,3
0280042	OGS	351,6	340			31,7	11,9	27,5	1,7	1,6	210,0	0,7		0,1	16,0
0280059	OGS	308,5	365			36,9	13,9	28,0	1,4	0,8	228,0	0,7		0,2	17,2
0780070	OGS	281,3	425			27,6	11,7	5,1	2,5	1,8	224,0	12,6		0,2	15,1
0800004	OGS	604,6	4475			40,9	22,6	813,0	51,0	1451,0	480,0	6,4		0,4	26,4
0800009	OGS	429,6	770			19,2	9,2	138,0	6,8	44,2	426,0	0,5		0,1	16,1
0800012	OGS	457,0	600			14,4	7,3	108,0	5,0	18,0	370,0	0,5		0,1	16,1
0800021	OGS	523,1	555			19,2	7,5	86,0	4,4	14,6	336,0	0,5		0,1	14,6
0800024	OGS	488,3	695			15,6	7,5	135,0	6,3	24,8	402,0	0,5		0,1	16,5
0800025	OGS	279,6	415			24,8	10,9	59,5	2,1	1,3	270,0	1,1		0,1	17,5
0800026	OGS	574,7	1540			7,6	4,3	360,0	20,0	326,0	478,0	4,5		0,0	23,1
0800028	OGS	451,8	430			22,0	7,3	64,0	3,6	12,4	260,0	0,5		0,1	15,4
0800031	OGS	467,1	400			28,1	10,2	50,0	2,7	4,3	266,0	0,7		0,1	18,0
0800039	OGS	445,9	640			20,4	8,5	114,0	5,3	24,2	374,0	1,8		0,1	17,5
0800040	OGS	473,2	760			12,0	5,3	143,0	8,7	29,3	450,0	0,5		0,0	18,1
0800043	OGS	450,0	690			14,0	5,1	143,0	7,5	29,9	394,0	1,1		0,0	17,1
0800050	OGS	495,5	1040			6,4	2,4	144,0	16,9	143,0	428,0	0,9		0,1	21,5
0800052	OGS	366,3	390			27,7	9,7	48,0	1,7	1,6	252,0	0,7		0,1	16,9
0800059	OGS	495,5	985			6,8	2,7	130,0	15,4	152,0	360,0	1,4		0,1	19,1
0800063	OGS	299,4	710			20,0	6,8	130,0	5,0	8,9	456,0	1,3		0,1	19,6
0800064	OGS	499,0	780			12,4	2,7	155,0	8,5	19,2	476,0	0,9		0,0	18,3
0800065	OGS	565,0	990			5,9	3,0	260,0	13,4	97,0	538,0	1,0		0,0	21,0
0830001	OGS	416,4	735			4,0	1,0	122,0	14,0	26,8	424,0	0,9		0,0	20,2
0830003	OGS	414,6	695			4,4	1,5	98,0	16,3	36,5	382,0	0,9		0,0	19,1
0830007	OGS	568,0	44200			230,0	1430,0	6400,0	424,0	19785,0	154,0	2745,0		7,4	0,1
0830008	OGS	499,2	3900			60,1	12,6	413,0	55,5	1239,0	240,0	5,4		0,8	19,6
0830009	OGS	486,4	970			7,2	2,7	138,0	12,4	143,0	372,0	0,5		0,1	16,0
0830016	OGS	498,0	860			5,6	2,9	118,0	14,6	68,5	412,0	0,7		0,0	13,8
0830019	OGS	395,5	845			5,2	2,2	126,0	14,4	71,1	408,0	0,9		0,0	14,0
0830023	OGS	558,4	435			32,1	12,2	32,8	4,0	1,6	274,0	0,9		0,3	15,5
0830037	OGS	532,4	900			6,4	2,7	114,0	21,5	123,5	340,0	0,4		0,1	19,3
0830038	OGS	498,9	700			4,0	1,9	100,0	17,0	35,3	384,0	2,9		0,0	19,8
0830047	OGS	459,0	645			4,8	1,9	94,0	14,0	8,8	404,0	0,6		0,0	14,0
0830048	OGS	475,3	945			3,6	1,5	140,0	16,5	97,1	426,0	0,6		0,0	20,4
0910005	OGS	357,8	365			28,5	13,4	34,5	1,9	3,7	216,0	0,4		0,1	17,9
0910006	OGS	357,9	365			30,1	12,6	33,0	1,9	3,7	216,0	0,4		0,1	17,8
0910007	OGS	357,7	360			31,3	11,7	32,5	1,9	2,5	216,0	0,4		0,1	17,8
0910008	OGS	359,0	365			31,7	11,7	33,0	1,9	3,3	214,0	0,7		0,1	17,9
0910014	OGS	299,2	400			40,9	16,0	26,4	2,3	1,3	244,0	0,9		0,3	15,8
1140031	OGS	282,9	395			25,7	9,0	51,5	1,5	0,7	252,0	1,1		0,1	17,2
1140033	OGS	296,4	405			39,3	14,8	30,5	2,1	0,9	252,0	0,7		0,3	17,3
1140035	OGS	329,9	400			25,7	10,2	50,0	1,6	0,6	246,0	0,7		0,1	17,3
1140036	OGS	330,2	380			33,7	13,1	33,5	1,6	0,6	230,0	0,7		0,2	16,9
1140042	OGS	299,3	375			27,3	11,4	40,0	1,4	1,2	234,0	1,1		0,2	16,3
1140054	OGS	497,1	275			28,9	14,8	10,0	0,7	1,3	166,0	0,9		0,1	11,9
1140056	OGS	296,0	370			31,3	12,6	35,5	1,3	1,0	230,0	0,8		0,2	17,4
1140059	OGS	277,8	310			30,3	14,4	29,0	1,2	0,7	207,0	1,0		0,1	18,0
1140071	OGS	408,1	305			30,5	17,3	12,8	1,5	2,7	194,0	0,7		0,1	13,6
1140076	OGS	511,3	400			26,5	17,6	59,0	2,3	9,3	258,0	1,0		0,1	20,1
1170014	OGS	289,2	270			26,5	15,3	11,6	1,0	1,9	184,0	0,5		0,1	12,8
1340002	OGS	279,2	330			34,5	13,1	24,4	1,5	1,6	206,0	7,5		0,2	15,9
1340020	OGS	515,7	370			28,1	11,4	39,0	2,9	2,4	220,0	1,4		0,1	17,9
1340021	OGS	298,0	380			42,5	20,4	12,8	1,2	1,0	200,0	32,3		0,3	14,8
1340023	OGS	277,0	380			32,1	12,6	35,0	1,3	0,3	230,0	0,8		0,2	17,2
1340029	OGS	477,0	530			15,6	8,5	85,0	4,7	3,2	344,0	0,9		0,0	16,2
1340035	OGS	417,8	315			22,0	11,7	36,0	2,3	3,5	214,0	0,5		0,1	14,5
1340037	OGS	404,5	505			22,0	8,0	84,0	3,3	5,8	320,0	0,5		0,1	17,7
1340038	OGS	298,9	345			44,1	14,1	17,8	1,1	0,4	192,0	28,1		0,2	18,9
1340051	OGS	279,9	330			33,9	14,4	29,0	1,7	0,9	215,0	1,0		0,2	18,1

ding to the recharge coming from the High Plain unconfined aquifer. At greater depths (MARTELLI & GRANATI, 2008a, 2008b), the sulphate contents are low and almost uncorrelated with depth.

## 8. - ISOTOPE REMARKS

In order to improve the knowledge about the flow and recharge patterns of the Friuli Plain aquifers, isotope analyses ( $^{18}\text{O}$ ,  $^2\text{H}$ ,  $^{14}\text{C}$ ) have been

carried out (MARTELLI *et alii*, 2007b) on the basis of water samples collected, during the period April 2003 – March 2007, from:

56 wells reaching each confined aquifer level of the Low Plain multi-layered system and 1 well pertaining to the High Plain unconfined aquifer system;

- 17 surfacing spring waters between the Tagliamento and Torre rivers;
- 4 main local rivers (Tagliamento, Torre, Natisone, Isonzo).

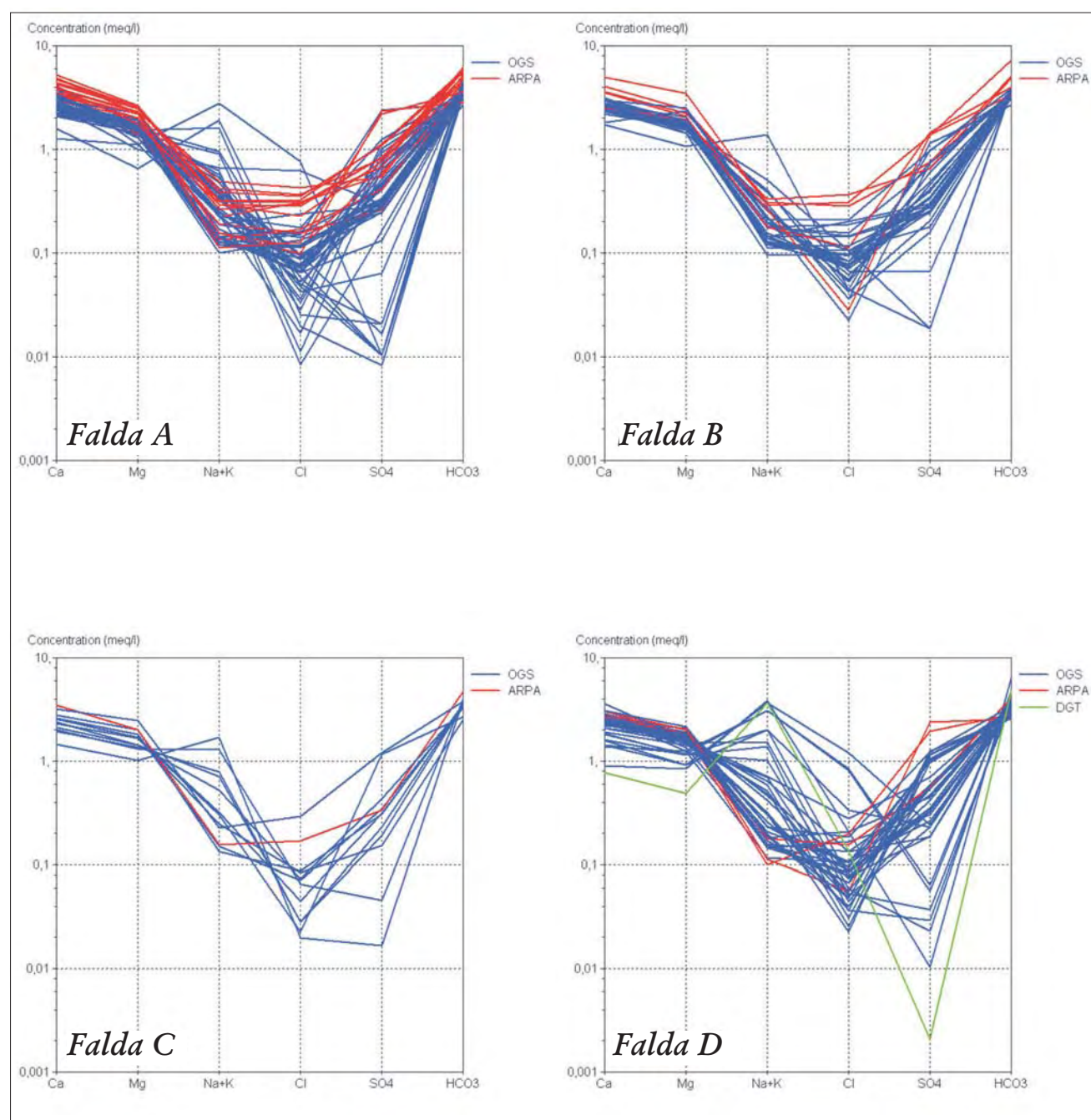


Fig. 15 – Schoeller diagrams concerning groundwaters of Low Plain Aquifers A, B, C, D.  
– Diagrammi di Schoeller relativi alle acque delle Falde A, B, C, D della Bassa Pianura friulana.

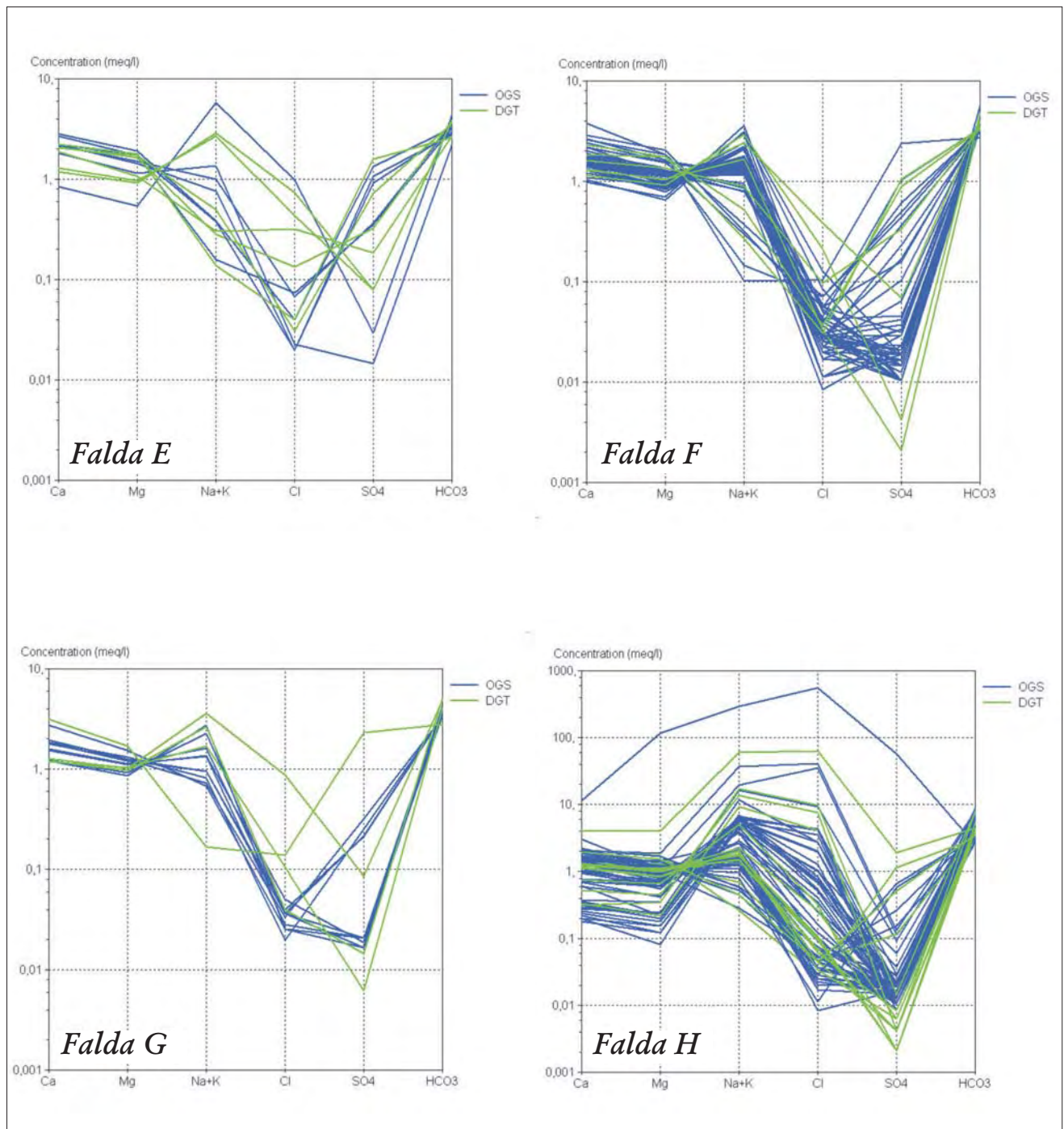


Fig. 16 – Schoeller diagrams concerning groundwaters of Low Plain Aquifers E, F, G, H.  
 – Diagrammi di Schoeller relativi alle acque delle Falde E, F, G, H della Bassa Pianura friulana.

Data related to the hydrogen and oxygen isotope composition have been evaluated (MARTELLI & GRANATI, 2008b), together with the age calculated from the  $^{14}\text{C}$  contents, for water samples coming (March – November 2007) from 19 artesian wells of the Low Plain (3 new-acquired and 16 already involved in heavier isotopes determinations) and from the above-mentioned phreatic well of the High Plain (tab. 3). The  $\delta^2\text{D}$  and  $\delta^{18}\text{O}$

analyses were performed on a FINNIGAN GLF 1086 automatic equilibration device and a DELTA PLUS FINNIGAN mass-spectrometer (Department of Earth Sciences, University of Parma); the  $^{14}\text{C}$  content was analysed at the Hydroisotop GmbH Laboratory in Schweitenkirchen (D).

Preliminary analyses (MARTELLI *et alii*, 2007b) outlined as most of deep groundwaters does not



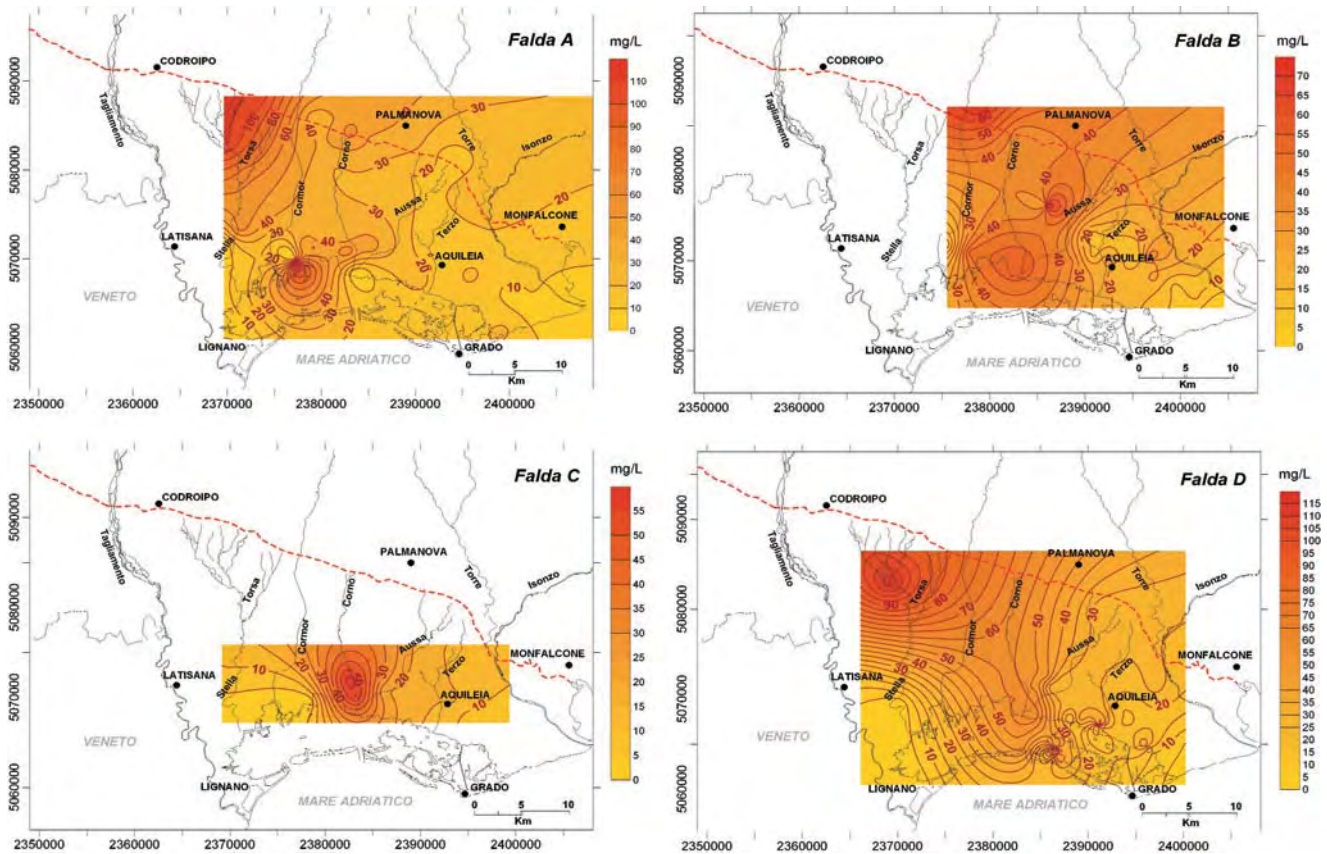


Fig. 17 – Sulphate distribution in groundwaters of Low Plain Aquifers A,B,C,D.  
 – Carte della distribuzione dei solfati nelle acque delle Falde A, B, C, D della Bassa Pianura friulana.

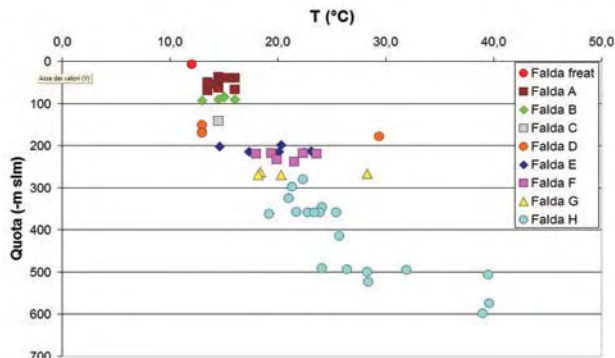


Fig. 18 – Temperature (°C) versus withdrawal depth in the Low Plain confined aquifers.

– Variazione della temperatura (°C) con la quota di attingimento idrico sotterraneo dei pozzi campionati nella Bassa Pianura friulana.

reveal remarkable seasonal fluctuations in the  $\delta^{18}\text{O}$  and  $\delta\text{D}$  contents, pointing out permeability and flow conditions in the relative aquifer horizons such as to allow a recharge contribution mixing. With regard to the  $\delta^{18}\text{O}$  spatial variability, the water samples of the most shallow confined aquifer levels (A, B, C, D) become increasingly more negative towards NW, while spring waters show progressively less negative values moving eastward; the deepest groundwaters (F, G, H) are isotopically lighter towards the

coastal sector, according to greater flow depths, higher recharge areas and/or old recharge contributions. Tagliamento and Isonzo rivers are characterised by negative  $\delta^{18}\text{O}$  values owing to their high mountain basins.

The diagram in figure 25 displays the relationship between  $\delta^{18}\text{O}$  and  $\delta\text{D}$  contents in river, spring and groundwater samples. Groundwater radiocarbon datings are also reported. The similar out-

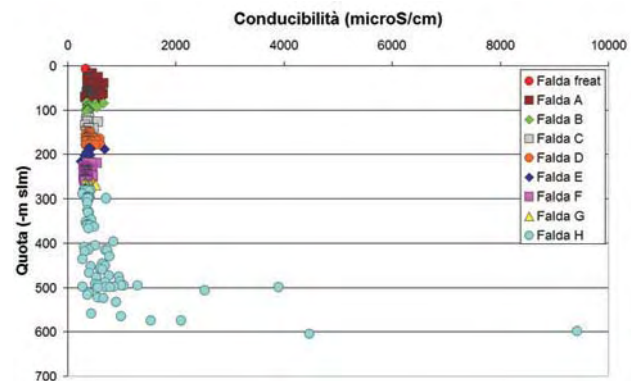


Fig. 19 – Conductivity (µS/cm) versus withdrawal depth in the Low Plain confined aquifers.

– Variazione della conducibilità (µS/cm) con la quota di attingimento idrico sotterraneo dei pozzi campionati nella Bassa Pianura friulana.

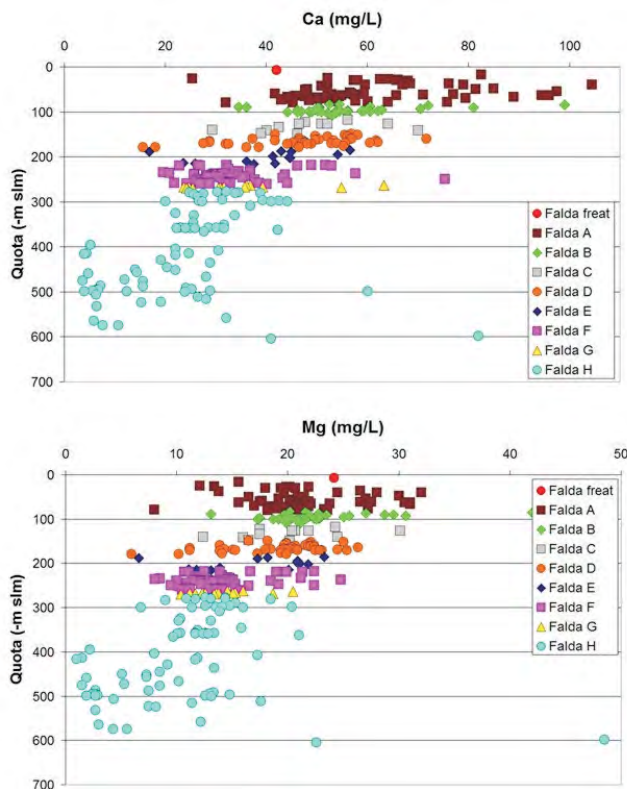


Fig. 20 –  $\text{Ca}^{++}$  (mg/l) and  $\text{Mg}^{++}$  (mg/l) contents versus withdrawal depth in the Low Plain confined aquifers.

– *Variazione dei parametri  $\text{Ca}^{++}$  (mg/l) e  $\text{Mg}^{++}$  (mg/l) con la quota di attingimento idrico sotterraneo dei pozzi campionati nella Bassa Pianura friulana.*

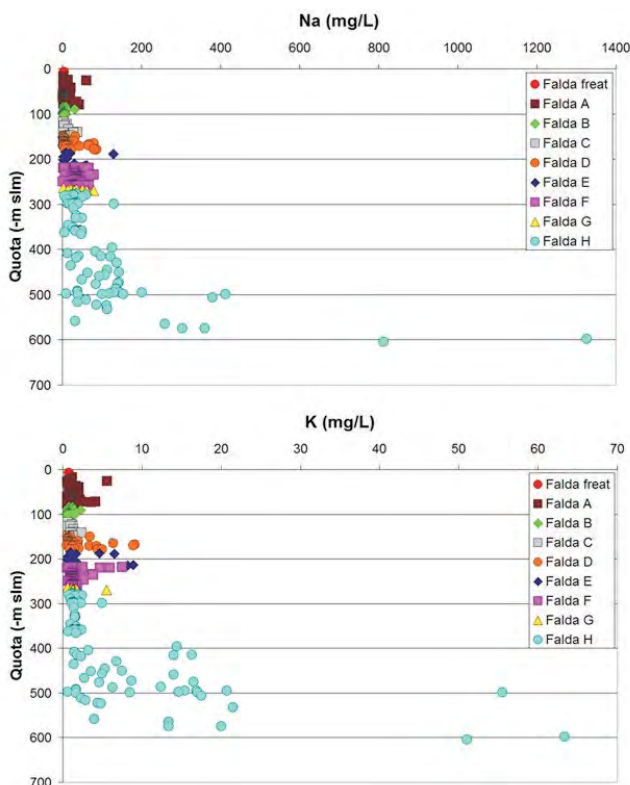


Fig. 21 –  $\text{Na}^{+}$  (mg/l) and  $\text{K}^{+}$  (mg/l) contents versus withdrawal depth in the Low Plain confined aquifers.

– *Variazione dei parametri  $\text{Na}^{+}$  (mg/l) e  $\text{K}^{+}$  (mg/l) con la quota di attingimento idrico sotterraneo dei pozzi campionati nella Bassa Pianura friulana.*

coming isotope ratios that characterise surface, phreatic, spring and meteoric waters regarding MWL<sub>S</sub> (Northern Italy Meteoric Water Line:  $\delta D = 7,7094 \delta^{18}\text{O} + 9,4034$ ) and GMWL (Global Meteoric Water Line:  $\delta D = 8,20 \delta^{18}\text{O} + 11,27$ ) (LONGINELLI & SELMO, 2003; LONGINELLI *et alii*, 2006) support both the meteoric origin of recent aged waters (MARTELLI *et alii*, 2007b) and their hydraulic connection.

Groundwaters coming from Aquifers A, B, C (till 150 m bsl) show an isotope signal consistent with the one determined for phreatic and spring waters, that means present or recent recharge.

The most isotopically negative groundwaters ( $\delta^{18}\text{O} = 9,5 - 10,5\text{‰}$ ) are almost exclusively associated to aquifer levels more than 270 m bsl deep and are undoubtedly old (up to 36000 years).

Mixing processes characterise groundwaters with an isotope signal between -8 and -9‰, coming from aquifer levels more than 180 m bsl deep and pointing out really different ages.

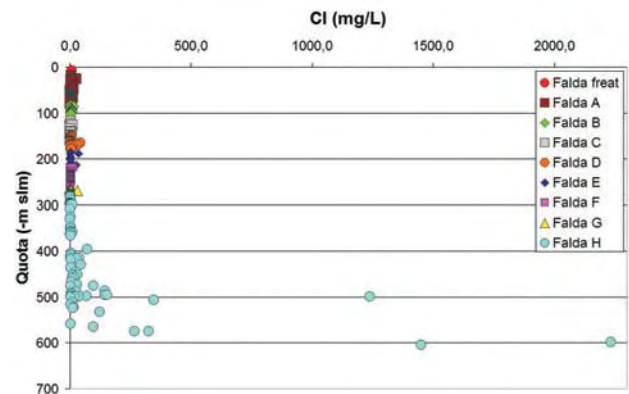


Fig. 22 –  $\text{Cl}^{-}$  (mg/l) content versus withdrawal depth in the Low Plain's confined aquifers.

– *Variazione del parametro  $\text{Cl}^{-}$  (mg/l) con la quota di attingimento idrico sotterraneo dei pozzi campionati nella Bassa Pianura friulana.*

The diagram  $\delta^{18}\text{O}$  vs. Cl (fig. 26) shows some of the most remarkable mixing phenomena, especially as far as the deepest confined levels are concerned:

- the red arrow marks deep fresh-waters moving towards shallow levels, with a mixing between old and recent fresh-waters;
- the blue arrow displays a mixing between old recharged fresh-waters and saline paleo-waters;
- the green arrow is indicative of a mixing between fresh and saline old waters.



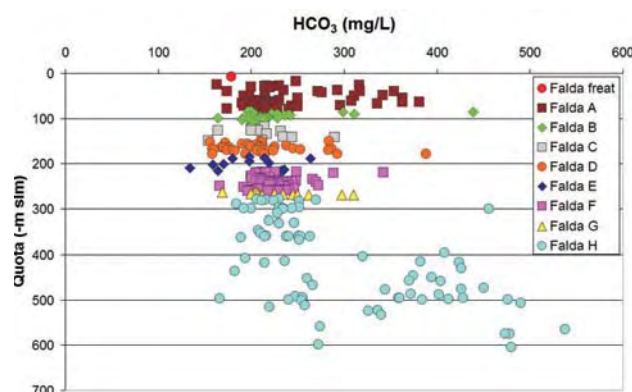


Fig. 23 –  $\text{HCO}_3^-$  (mg/l) content versus withdrawal depth in the Low Plain confined aquifers.

– *Variazione del parametro  $\text{HCO}_3^-$  (mg/l) con la quota di attingimento idrico sotterraneo dei pozzi campionati nella Bassa Pianura friulana.*

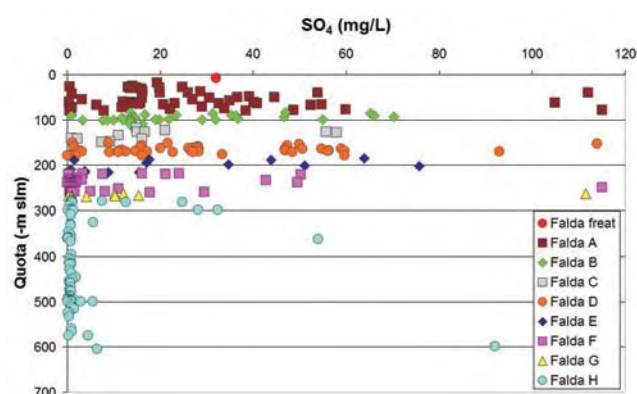


Fig. 24 –  $\text{SO}_4^-$  (mg/l) content versus withdrawal depth in the Low Plain confined aquifers.

– *Variazione del parametro  $\text{SO}_4^-$  (mg/l) con la quota di attingimento idrico sotterraneo dei pozzi campionati nella Bassa Pianura friulana.*

## 9. - CONCLUSIONS

Owing to the above-mentioned surveys and elaborations, the following considerations can be pointed out:

- the local geological and structural patterns played a determinant role in conditioning the High Plain groundwater flow circulation; the divide between western and eastern groundwaters is evidenced in terms of both hydraulic head and chemistry; the same data also confirm the strict connection between the main regional hydrographic systems and the High Plain unconfined aquifer;
- the Low Plain confined aquifer levels till 300 m bsl are fed by groundwaters coming from the High Plain water-table aquifer;
- the Low Plain confined aquifer system exhibits mutual connections between its levels, in terms both of pressure (as supposed on the basis of the similar hydraulic head distributions in the Aquifers B-C and Aquifers D-F) and of mass

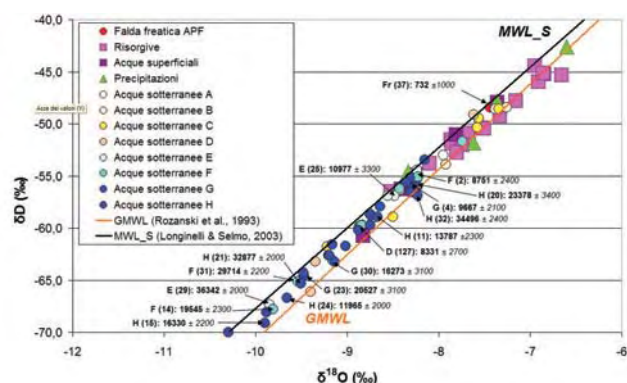


Fig. 25 – Relationship between  $\delta^{18}\text{O}$  and  $\delta\text{D}$  of groundwaters, surface waters, spring waters and meteoric waters, together with  $^{14}\text{C}$  dating results (mean of corrected ages by INGERSON & PEARSON, 1964, and MOOK, 1980).

– *Relazione tra  $\delta^{18}\text{O}$  e  $\delta\text{D}$  per acque sotterranee, superficiali, di risorgiva e di precipitazione, con indicazione dei risultati di datazioni con radiocarbonio. Le età indicate derivano dalla media delle età corrette secondo INGERSON & PEARSON (1964) e MOOK (1980).*

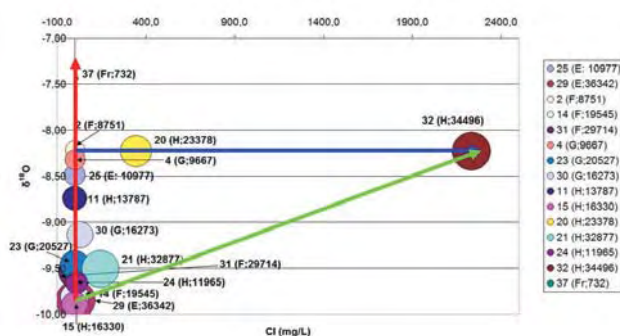


Fig. 26 -  $\delta^{18}\text{O}$  (‰) versus  $\text{Cl}^-$  (mg/l) in Friuli Plain groundwaters;  $^{14}\text{C}$  dating results are also indicated.

– *Relazione tra  $\delta^{18}\text{O}$  (‰),  $\text{Cl}^-$  (mg/l) ed età determinate mediante analisi al radiocarbonio delle acque sotterranee della Pianura Friulana.*

transport (as evidenced by geochemical and isotopical outputs about deep and shallow groundwater mixings).

On account of such statements, a sustainable exploitation of the Low Plain aquifer system needs the assumption of two distinct withdrawal approaches, connected to the recharge origin and speed features. In fact, the confined levels till 300 m bsl are fed by the High Plain groundwaters, while the deepest productive horizons, whose present exploitation is valued at about 5 millions of  $\text{m}^3/\text{year}$  (MARTELLI & GRANATI, 2006, 2007a, 2007b), are involved in complex and low flow circuits, related to prealpine/alpine recharge areas.

## Acknowledgements

*The Authors are grateful to the Referees for their thoughtful suggestions and constructive reviews.*



Tab. 3 – *Isotopic data and  $^{14}\text{C}$  dating results (mean of corrected ages by INGERSON & PEARSON, 1964, and MOOK, 1980) concerning Friuli Plain's groundwaters, spring waters and surficial waters.*

– Sintesi dei campionamenti isotopici effettuati su acque di falda, superficiali e di risorgiva della Pianura friulana, con indicazione dei risultati delle datazioni con radiocarbonio; l'età riportata deriva dalla media delle età corrette secondo INGERSON & PEARSON (1964) e MOOK (1980).

ID	$\delta^{18}\text{O}$ -VSMOW (‰)	dD	Età ( $^{14}\text{C}$ )	ID	$\delta^{18}\text{O}$ -VSMOW (‰)	dD	Età ( $^{14}\text{C}$ )
<b>Falda freatica</b>				23	-9,47	-64,61	20527
37	-7,44	-48,41	732	30	-9,14	-63,27	16273
<b>Falda A</b>				<b>Falda H</b>			
128			11739	1	-9,48	-64,34	
152	-8,30	-56,12		3	-8,35	-55,55	
84	-7,95	-52,99		5	-8,31	-55,19	
85	-7,38	-48,56		7	-8,15	-53,47	
<b>Falda B</b>				8	-8,29	-56,13	
130	-7,26	-48,41		11	-8,74	-58,78	13787
150	-8,42	-56,35		12	-8,31	-56,57	
64			6953	13	-8,74	-59,72	
74	-7,92	-53,87		15	-9,90	-69,13	16330
<b>Falda C</b>				16	-9,88	-68,08	
131	-7,58	-50,33		17	-8,88	-60,21	
146	-9,22	-61,76		18	-9,16	-61,55	
151	-8,50	-58,91		19	-9,01	-61,73	
72	-7,56	-49,48		20	-8,23	-56,03	23378
96	-7,34	-48,55		21	-9,51	-65,30	32877
<b>Falda D</b>				22	-8,67	-58,90	
29	-9,85	-67,35	36342	24	-9,66	-66,69	11965
127	-8,87	-59,83		28	-9,20	-62,63	
162	-9,40	-66,10		32	-8,23	-56,86	34496
127			8331	125	-9,49	-64,01	
138	-9,20	-62,60		<b>Risorgive</b>			
159	-9,35	-63,21		RIS1	-8,52	-56,52	
58	-7,62	-49,12		RIS2	-8,10	-53,78	
<b>Falda E</b>				RIS3	-7,86	-51,55	
25	-8,49	-56,90	10977	RIS4	-7,67	-50,90	
33	-8,83	-59,71		RIS5	-7,85	-51,85	
34	-8,56	-56,92		RIS6	-7,33	-49,25	
36	-8,23	-54,43		RIS7	-7,74	-52,00	
124	-10,30	-69,98		RIS8	-7,53	-50,42	
<b>Falda F</b>				RIS9	-7,51	-50,47	
2	-8,22	-55,05	8751	RIS10	-8,26	-54,87	
9	-8,43	-56,19		RIS11	-7,80	-52,76	
10	-7,74	-51,68		RIS12	-6,85	-45,21	
14	-9,81	-67,78	19545	RIS13	-7,16	-47,76	
26	-8,75	-58,60		RIS14	-6,91	-45,98	
27	-8,86	-59,78		RIS15	-6,66	-45,34	
31	-9,54	-65,14	29714	RIS16	-6,95	-44,45	
35	-8,72	-59,03		RIS17	-6,86	-45,13	
111	-8,84	-59,74		<b>Corsi d'acqua</b>			
126	-9,16	-63,08		TAG	-8,83	-60,72	
<b>Falda G</b>				TOR	-7,81	-51,05	
4	-8,32	-55,64	9667	ISO	-8,41	-56,25	
6	-8,64	-57,92		NAT	-7,36	-47,94	

## REFERENCES

- AGIP (1972) - *Acque dolci sotterranee. Inventario dei dati raccolti dall'AGIP durante la ricerca e la produzione di idrocarburi in Italia*. Grafica Palombi, Roma, 914 pp.
- ANTONELLI R. & STEFANINI S. (1982) - *Nuovi contributi idrogeologici ed idrochimici sugli acquiferi dell'alta pianura veronese*. Mem. Sc. Geol., **35**, 35-67, Padova.
- BARNABA P.F. (1990) - *Considerazioni geologiche sul sottosuolo e sulle risorse idrotermali della zona di Latisana-Foce del Tagliamento (Province di Udine e Venezia)*. Mem. Sc. Geol., **42**, 343-359, Padova.
- BORTOLAN PIRONA A. (2008) - *Le risorgive del Friuli orientale: idrogeologia e idrochimica*. Tesi di Laurea specialistica in Scienze Ambientali, Università Ca' Foscari, Venezia, a.a.2007-08, 359 pp.
- BURRATO P., POLI M.E., VANNOLI P., ZANFERRARI A., BASILI R. & GALADINI F. (2008) - *Sources of Mw5+ earthquakes in northeastern Italy and western Slovenia: an updated view based on geological and seismological evidence*. Tectonophysics, **453**, 157-176.
- CALORE C., DELLA VEDOVA B., GRASSI S., MARSON I., NICOLICH R. & SQUARCI P. (1995) - *A hydrothermal system along the coastal area of Friuli-Venezia Giulia region (NE Italy)*. Transactions of "Geothermal Resources Council - World Geothermal Congress". May 1995, Firenze, **2**, 1269-1274, Firenze.
- CASSANO E., ANELLI L., FICHERA R. & CAPPELLI V. (1986) - *Pianura Padana. Interpretazione integrata di dati geofisici e geologici*. In: AGIP, 73° Congresso Soc. Geol. It., 29 Settembre-4 Ottobre 1986, 27 pp., Roma.
- CASTELLARIN A. & CANTELLI L. (2000) - *Neo-Alpine evolution of the Southern Eastern Alps*. Journal of Geodynamics, **30**, 251-274, Oxford.
- CATI A., SARTORIO D. & VENTURINI S. (1989a) - *Carbonate platforms in the subsurface of the Northern Adriatic area*. In: G.B. CARULLI *et alii* (Eds.): Proceedings of the International Symposium on "Evolution of the karstic carbonate platform: relation with other periadriatic carbonate platforms", 1-6 June 1987, Trieste. Mem. Soc. Geol. It., **40**, 295-308, Padova.
- CATI A., FICHERA R. & CAPPELLI V. (1989b) - *Northeastern Italy. Integrated processing of geophysical and geological data*. In: G.B. CARULLI *et alii* (Eds.): Proceedings of the International Symposium on "Evolution of the karstic carbonate platform: relation with other periadriatic carbonate platforms", 1-6 June 1987, Trieste. Mem. Soc. Geol. It., **40**, 273-288, Padova.
- CONSORZIO DI BONIFICA LEDRA-TAGLIAMENTO (1982) - *Studio per la determinazione del bilancio idrologico dell'alta pianura friulana compresa tra i fiumi Isonzo e Tagliamento*. Relazione - Reg. Aut. F.V.G., Dir. Reg. LLPP, Consorzio Ledra-Tagliamento - Rapporto interno, 140 pp., Udine.
- DAL PRÀ A., FABBRI P. & BELLENGHI G. (1989) - *Esempi di sfruttamento delle falde artesiane nella media pianura veneta in aree non servite da acquedotti pubblici. Modalità di utilizzazione, quantità dei prelievi, vantaggi ed effetti negativi*. Mem. Sc. Geol., **41**, 115-130, 18 figg., Padova.
- DELLA VEDOVA B., NICOLICH R., CASTELLI E., CIMOLINO A. & BARISON E. (2009) - *The geothermal potential of the carbonatic platform buried beneath the Veneto and the Friuli coastal areas: results from the Grado-1 borehole (NE Italy)*. In: Epitome di "GeolItalia 2009 - VII Forum Italiano di Scienze della Terra", Rimini 9-11 settembre 2009: 141.
- DRUOTTI S. (2009) - *Studio di un acquifero di pianura mediante codice MODFLOW con applicazione ad un modello di dispersione di inquinante*. Tesi di Dottorato in Ingegneria Civile e Ambientale, 258 pp.
- FANTONI R., DELLA VEDOVA B., GIUSTINIANI M., NICOLICH R., BARBIERI C., DEL BEN A., FINETTI I. & CASTELLARIN A. (2003) - *Deep seismic profiles through the Venetian and Adriatic foreland (N-Italy)*. Mem. Sci. Geol., **54**, 131-134.
- FLORINETH D. & SCHLUCHTER C. (2000) - *Alpine Evidence for Atmospheric Circulation Patterns in Europe during the Last Glacial Maximum*. Quaternary Research, **54**, 295-308, Washington.
- GALADINI F., POLI M.E. & ZANFERRARI A. (2005) - *Seismogenic sources potentially responsible for earthquakes with M > 6 in the eastern Southern Alps (Thiene-Udine sector, NE Italy)*. Geophys. J. Int., **161**, 739-762.
- GIOVANNELLI M.M., RIZZI LONGO L., STOLFA D. & ZUCCHI STOLFA M.L. (1985) - *Considerazioni paleoecologiche sui sondaggi S19-Lignano e S20-Bevazzana (delta del Fiume Tagliamento)*. Gortania, Atti Museo Friul. Storia Nat., **7**, 87-112, 6 figg., 5 tabb., Udine.
- GRANATI C. (2007) - *Ricostruzione degli acquiferi della Bassa Pianura friulana e simulazione di flusso con approccio stocastico*. Tesi di Dottorato in Ingegneria Civile e Ambientale, 308 pp.
- GRANATI C., RODA C. & MARTELLI G. (1999) - *Utilizzazione della cartografia numerica regionale per lo studio dei pozzi della Bassa Pianura Friulana*. In: Università degli Studi di Udine, Centro Interdipartimentale Cartesio, Prima Conferenza sulle Informazioni Territoriali nel Friuli-Venezia Giulia, 10 Settembre 1999, Udine, 19 pp.
- GRANATI C., MARTELLI G. & RODA C. (2000) - *Valutazione preliminare del volume di acqua estratta annualmente in Provincia di Udine dal sottosuolo della Bassa Pianura Friulana*. IGEA, **15**, 13-26, Torino.
- GRASSI S. (1994) - *Alcune osservazioni sulle caratteristiche geochimiche delle acque sotterranee della Bassa Pianura Friulana*. Atti Soc.Tosc.Sci.Nat., Memorie, Serie A, **101**, 1-15.
- GRASSI S. (1999) - *Natura e provenienza delle acque idrotermali della Bassa Pianura Friulana*. In: Regione Aut. FVG, Atti dell'incontro di lavoro "Potenzialità geotermiche della Bassa Pianura Friulana: stato dell'arte e proposte operative", Trieste, 18 febbraio 1999, 15-17.
- LONGINELLI A. & SELMO E. (2003) - *Isotopic composition of precipitation in Italy: a first overall map*. Journal of Hydrogeology, **270**, 75-88.
- LONGINELLI A., ANGLESIO B., FLORA O., IACUMIN P. & SELMO E. (2006) - *Isotopic composition of precipitation in Northern Italy: reverse effect of anomalous climatic events*. Journal of Hydrology, **329**, 471-476.
- MAROCO R. (1988) - *Considerazioni sedimentologiche sui sondaggi S19 e S20 (delta del F.Tagliamento)*. Gortania, Atti Museo Friul. Storia Nat., **10**, 101-120, 4 figg., Udine.
- MAROCO R., STOLFA D., ZUCCHI STOLFA M.L. & LENARDON G. (1988) - *Considerazioni sedimentologiche, paleoecologiche e geochimiche sul sondaggio S15 (Canale di Morgo-Laguna di Grado)*. Gortania, Atti Museo Friul. Storia Nat., **10**, 81-100, Udine.
- MARTELLI G. & RODA C. (1998) - *L'acquifero della Bassa Pianura Friulana in Comune di S. Giorgio di Nogaro*. Quaderni di Geologia Applicata, **5** (1), 15-38, Bologna.
- MARTELLI G., GRANATI C. & RODA C. (2003) - *Distribution of coarse-grained sediments in the Friuli alluvial plain (Northern Italy) from the surface till the depth of 50 metres*. Quaderni di Geologia Applicata - Serie Aiga, **2** (1), 131-146, Bologna.
- MARTELLI G. & GRANATI C. (2006) - *The confined aquifer system of the Friuli Plain (North Eastern Italy): analysis of sustainable groundwater use*. Giornale di Geologia Applicata, **3**, 59-67.
- MARTELLI G. & GRANATI C. (2007a) - *Lithostratigraphical and hydrogeological characteristics of the aquifers of the Low Friuli Plain and sustainability of groundwater extractions*. Mem. Descr. Carta Geol. d'It., **76**, 241-266.
- MARTELLI G. & GRANATI C. (2007b) - *Valutazione della ri-*

- carica del sistema acquifero della bassa pianura friulana. *Giornale di Geologia Applicata*, **5**, 89-114.
- MARTELLI G. & GRANATI C. (2008a) - *Le caratteristiche idrochimiche dei corpi idrici profondi della Pianura Friulana*. *Rend. Soc. Geol. It.*, **3**, 536-537.
- MARTELLI G. & GRANATI C. (2008b) - *Preliminary remarks on the age of groundwater of the Friuli plain multilayer aquifer*. *Giornale di Geologia Applicata*, **10**, 77-82.
- MARTELLI G. & GRANATI C. (2009) - *Caratteristiche idrochimiche generali delle falde profonde della Pianura friulana*. *Italian Journal of Engineering Geology and Environment* (in printing).
- MARTELLI G., GRANATI C. & ROSSI S. (2004) - *The multistrata aquifer system in the Low Friuli Plain (NE Italy)*. In: *Proceedings of ISES 2004*, 8-10 September, Istanbul, Turkey, 267-274.
- MARTELLI G., GRANATI C. & RODA C. (2007a) - *Criteri per la realizzazione di una rete di monitoraggio quantitativa e sperimentazione*. In: APAT, Mem. Descr. Carta Geol. d'It., "Progetto per il monitoraggio degli acquiferi della bassa pianura friulana in provincia di Udine", Firenze, 27-84.
- MARTELLI G., GRANATI C., TOSCANI L., IACUMIN P. & SELMO E. (2007b) - *Risultati preliminari delle indagini isotopiche svolte sulle acque delle falde profonde della Bassa Pianura Friulana*. *Giornale di Geologia Applicata*, **6**, 93-101.
- MARTINIS B. (1971) - *Geologia generale e geomorfologia del Friuli-Venezia Giulia*. In: *Enciclopedia monografica del Friuli-Venezia Giulia*, **1** (1), 85-172, 84 figg., Udine.
- MOSETTI F. (1983) - *Sintesi sull'idrologia del Friuli-Venezia Giulia*. *Quaderni ETP*, **6**, 159 pp., Udine.
- OROMBELLI G. & RAVAZZI C. (1996) - *The late glacial and early Holocene: chronology and paleoclimate*. *Il Quaternario*, **9** (2), 439-444, Roma.
- OSSERVATORIO GEOFISICO SPERIMENTALE DI TRIESTE (1989) - *Studio delle anomalie geotermiche della Bassa Pianura Friulana. Rilievo di superficie e censimento dei pozzi d'acqua calda*. REL 89-77/MNS-1/22-12/89. Conv. n.4455 con Reg. Aut. Friuli-Venezia Giulia, Trieste.
- POLI M.E., ROGLEDI S. & ZANFERRARI A. (2008) - *Tettonica*. In: APAT - Servizio Geologico d'Italia - Regione Autonoma Friuli Venezia Giulia, "Note illustrative della carta geologica d'Italia alla scala 1:50.000: Foglio 066 "Udine"": 121-132.
- REGIONE AUTONOMA FRIULI-VENEZIA GIULIA (1990) - *Catasto regionale dei pozzi per acqua e delle perforazioni eseguite nelle alluvioni quaternarie e nei depositi sciolti del Friuli-Venezia Giulia. Stratigrafie. Cartografia. Dir. Reg. Ambiente*, **1-5**, Trieste.
- REGIONE AUTONOMA FRIULI-VENEZIA GIULIA (2004) - *Carta del sottosuolo della Pianura Friulana. Note illustrative, Tav. 1 (Carta delle isopache del Quaternario), Tav. 2 (Carta del tetto dei carbonati)*. A cura di: R. NICOLICH, B. DELLA VEDOVA & M. GIUSTINIANI, Litografia Artistica Cartografica, Firenze.
- REGIONE EMILIA-ROMAGNA, ENI-AGIP (1998) - *Riserve idriche sotterranee della Regione Emilia-Romagna*. G. DI DIO (Ed.), S.EL.CA, 120 pp., Firenze.
- REGIONE LOMBARDIA, ENI DIVISIONE AGIP (2002) - *Geologia degli acquiferi padani della Regione Lombardia. Geology of the Po plain aquifers in the Lombardy region*. In: C. CARCANO & A. PICCIN, S.E.L.C.A., Firenze.
- STEFANINI S. (1972) - *Le acque freatiche tra il F.Livenza ed il T. Torre (Friuli-Venezia Giulia)*. *Mem. Soc. Geol. It.*, **11**, 342-365, Roma.
- STEFANINI S. (1978) - *La falda freatica nell'Alta Pianura friulana*. *Quaderni IRSA*, **34** (14), 343-360, Roma.
- STEFANINI S. & CUCCHI F. (1977) - *Gli acquiferi nel sottosuolo della Provincia di Udine (Friuli-Venezia Giulia)*. *QUADERNI IRSA*, **34** (6), 131-147.



## The architecture of alluvial aquifers: an integrated geological-geophysical methodology for multiscale characterization

*Una metodologia integrata, geologico-geofisica,  
per la caratterizzazione multiscala dell'architettura  
degli acquiferi alluvionali*

MELE M. (\*), BERSEZIO R. (\*), GIUDICI M. (\*),  
RUSNIGHI Y. (\*), LUPIS D. (\*)

**ABSTRACT** - The aim of this work is the improvement of a methodology for the integration of near-surface geoelectrical data (Vertical Electrical Soundings, VES, and Electrical Resistivity Ground Imaging, ERGI) with geological-geomorphological data, in order to characterize the hydrostratigraphy of alluvial plains at different scales. Data integration is based on the mapping of sedimentary bodies that are defined by their geological boundaries, geometry and facies, and traced laterally from subsurface control points (borehole and well logs) with the aid of the vertical electrostratigraphic sequence.

The methodology was applied to the Quaternary alluvial valley of the Sillaro extinct meandering river (Lodi plain south of Milan between the Adda and Lambro terraced valleys). The local stratigraphy consists of LGM sand-gravel meandering river deposits (palaeo-Sillaro) overlying i) a clay to fine sand aquitard (flood plain, Upper Pleistocene), ii) alternating gravel-sand aquifer bodies formed by braiding to meandering depositional systems (Middle-Upper Pleistocene) and iii) a basal aquiclude of silty-clays (flood-plain, Middle Pleistocene). The methodology yields: i) the geological/geomorphological model, ii) the hydrostratigraphic model describing the low rank hierarchical units (hydrofacies) and their evolutive trends up to the assemblage of high rank hydrostratigraphic systems, iii) the characterization of site-specific parameters which affect electrical resistivity (groundwater conductivity, textures, saturation, cementation), iv) planning of the geoelectrical surveys and data acquisition (VES), v) electrical resistivity calibration, correlation of subsurface electrical resistivity models and multiscale interpretation, vi) improvement of details of the subsurface structure (ERGI) and vii) integration between hydrostratigraphy and electrostratigraphy.

89 VES and 3000 m of ERGI sections were acquired

over an area of 30 km<sup>2</sup>. For shallow investigations at the detailed scale (0-5 m, unsaturated zone) the integration of data yielded the assemblage of stratigraphic units and their apparent electrical resistivity maps, both representative of coarse-grained point-bar deposits and fine-grained oxbow-lake/overbank deposits. For deeper investigations at the regional scale (>5 m, saturated zone) VES models were correlated by vertical polarity of electrical contrasts and lateral persistence of electrical resistivity. Hence, we identified the "electrostratigraphic units" (EsU) that represent 3-D geophysical bodies defined by their electrical contrast with the adjacent units, internal electrical properties, apparent geometry and lateral extent, forming an electrostratigraphic sequence. The EsUs are directly related to heterogeneous and stratified sedimentary volumes. 2-D ERGI sections permitted to improve the characterization of the near-surface transitions between electrostratigraphic units at metric scale. Integration between geological and geoelectrical data permitted to: i) define scale, hierarchy and vertical-lateral continuity of subsurface electrostratigraphic units in relation to the local hydrostratigraphic units, ii) develop and validate the subsurface hydrostratigraphic models of the valley of palaeo-Sillaro river to a maximum depth of 80 m and iii) propose a multidisciplinary methodology to characterize the hydrostratigraphic settings of alluvial plains at different scales.

**KEY WORDS:** aquifer, electrical tomography, hydrostratigraphy, Po plain, vertical electrical soundings.

**RIASSUNTO** - Scopo di questo lavoro è lo sviluppo di una metodologia per l'integrazione dei dati derivanti dall'esplorazione geoelettrica da superficie (*Vertical Electrical Soundings*, VES, ed *Electrical Resistivity Ground Imaging*, ERGI) con le basi

(\*) Università degli Studi di Milano, Dipartimento Scienze della Terra "A. Desio", via Mangiagalli 34, 20133 Milano, Italy

di dati stratigrafico-sedimentologici e geomorfologici, per la ricostruzione e caratterizzazione di sistemi e complessi idrostratigrafici di origine alluvionale a scale differenti. L'integrazione dei dati è basata sulla mappatura di corpi sedimentari distinguibili in base ai loro limiti geologici, geometria esterna, organizzazione interna delle facies e tracciabili dai punti di controllo in superficie sulla base delle sequenze elettrostratigrafiche verticali.

La metodologia è stata applicata alla valle alluvionale quaternaria del Sillaro, un paleo-fiume a meandri che scorreva tra le valli terrazzate dei fiumi Adda e Lambro, nell'attuale pianura lodigiana a sud di Milano. La stratigrafia locale è costituita da depositi fluviali sabbioso-ghiaiosi di età LGM relativi alla piana a meandri del paleo-Sillaro che ricoprono i) un acquitardo argilloso-sabbioso fine (piana di esondazione; Pleistocene superiore), ii) alternanze di corpi acquiferi ghiaioso-sabbiosi rappresentati da sistemi deposizionali con carattere da *braided* a meandriforme (Pleistocene medio-superiore) e iii) un acquitardo limoso-argilloso basale (piana di esondazione; Pleistocene medio).

La metodologia prevede: i) la definizione del modello geologico/geomorfologico, ii) la definizione del modello idrostratigrafico a partire dalle unità di rango minimo (idrofacies) e loro associazioni verticali fino all'assemblaggio delle unità di rango superiore (sistemi idrostratigrafici), iii) la caratterizzazione dei parametri sito-specifici che influenzano la resistività elettrica dei terreni (conducibilità delle acque sotterranee, tessitura, saturazione, cementazione), iv) la pianificazione delle indagini geoelettriche e l'acquisizione dei dati (VES), v) la calibrazione della resistività elettrica, la correlazione dei modelli di resistività di sottosuolo e l'interpretazione multiscale, vi) il miglioramento del dettaglio delle strutture sepolte e delle loro eterogeneità orizzontali (ERGI) e vii) l'integrazione tra idrostratigrafia ed elettrostratigrafia.

89 VES e 3000 m lineari di sezioni ERGI sono stati acquisiti in un'area di 30 km<sup>2</sup>. A bassa profondità e a scala di dettaglio (0-5 m, zona insatura) l'integrazione dei dati ha consentito di caratterizzare le unità stratigrafiche ed il loro assemblaggio in superficie attraverso mappe di resistività apparente rappresentative della distribuzione dei depositi grossolani di *point-bar* e dei depositi a grana fine di esondazione e riempimento passivo di canale. A profondità più elevate e a scala di indagine regionale (>5 m, zona satura) i modelli VES 1-D sono stati correlati sulla base della polarità verticale del contrasto elettrico e sulla persistenza laterale dei valori di resistività elettrica. In questo modo, sono stati identificati come "unità elettrostratigrafiche" (EsU) dei corpi geofisici 3-D definiti in base al contrasto elettrico con le unità adiacenti, dalle proprietà elettriche interne, alla geometria apparente e all'estensione laterale. Le EsU sono direttamente legate ai corpi sedimentari eterogenei e stratificati e la loro successione verticale determina una sequenza elettrostratigrafica VES riconoscibile. Le sezioni 2-D ERGI hanno consentito di migliorare la caratterizzazione delle transizioni latero-verticali tra unità elettrostratigrafiche fino ad una scala di dettaglio metrica.

L'integrazione tra dati geologici e geoelettrici ha consentito di: i) definire scala, gerarchia e continuità latero-verticale delle unità elettrostratigrafiche di sottosuolo in relazione alle locali unità idrostratigrafiche, ii) sviluppare e validare i modelli idrostratigrafici della valle del paleo-Sillaro fino ad una profondità massima di 80 m p.c. e iii) proporre una metodologia multidisciplinare per la caratterizzazione dell'architettura idrostratigrafica delle piane alluvionali a scale differenti.

PAROLE CHIAVE: acquiferi, idrostratigrafia, Pianura Padana, sondaggi elettrici verticali, tomografia elettrica.

## 1. - INTRODUCTION

### 1.1. - GEOLOGICAL AND GEOPHYSICAL APPROACHES TO AQUIFER CHARACTERIZATION

The characterization of sedimentary architecture and the achievement of a valid representation of aquifers heterogeneity at different scales (hydrofacies, hydrostratigraphic system/complex; ANDERSON, 1997; MAXEY, 1964) is a key topic to forecast flow and transport processes in the subsurface of alluvial plains. The recognition of aquifer geometries and internal facies organization is still mainly based on direct methods such as continuous recovery boreholes (geognostic logs, water wells), especially in alluvial plains characterised by extensive human activities. The results that can be obtained from these punctual and expensive investigations are often limited to i) the characterisation of textural properties of the sediments, ii) the definition of sedimentary associations and vertical evolutive trends and iii) lithostratigraphic correlations.

Open problems related to the use of such data are represented by: i) the lateral correlation of stratigraphic surfaces, which bound aquifer bodies at the sampling points; ii) the spatial distribution and density of the hard-data, which could affect the subsurface reconstruction; iii) the definition of the hydraulic properties and iv) the lateral and vertical extent and the relative interconnection of the sedimentary bodies.

DC resistivity methods such as Vertical Electrical Soundings (VES; DAHLIN, 2001) and Electrical Resistivity Ground Imaging (ERGI; BAINES *et alii*, 2002) yield respectively the 1-D and 2-D electrical resistivity distribution in the ground. In the case of porous aquifers, the bulk electrical resistivity is controlled by the prevailing process of current conduction ("shale" vs. electrolytic conduction) determined by the occurrence of fine-grained sediments and saline groundwaters which enables the current conduction through the porous media as a function of porosity, clay content, sediments textures and pore-fluid salinity. VES technique is a cost-and-time effective exploration tool. It can be employed in many different geological settings and enables to collect a large amount of 1-D electrostratigraphic data on wide areas providing multi-scale imaging of stratified aquifers. VES vertical resolution relies on the well-known equivalence and suppression principles and only major resistivity variations can be identified at increasing depth, as a complex combination of thickness and resistivity contrasts (KELLER & FRISCHKNECHT, 1966; REYNOLDS, 1997; TELFORD *et alii*, 1990).

To improve the spatial resolution of vertical/horizontal transition between silt-clay aquitard/aquiclude and sand-gravel aquifers, ERGI technique



yields a large number of resistivity measurements along oriented sections, hundred of meters long (BAINES *et alii*, 2002; BERSEZIO *et alii*, 2007; BOWLING *et alii*, 2007).

When textural/porosity/silt-clay fraction contrasts among beds are present and when the data interpretation is independently constrained with the pore-fluid properties, these features make the DC methods a powerful exploration tool to differentiate litho-textural associations (silt-clay aquitard/aquiclude; sand and gravel aquifers; BAINES *et alii*, 2002; BERSEZIO *et alii*, 2007; BRATUS & SANTARATO, 2009; GOURRY *et alii*, 2003; HICKIN *et alii*, 2009; ZAHLEA *et alii*, 2005).

## 1.2. - AIM OF THE WORK

This work aims to improve an integrated methodology to merge near-surface geoelectrical data with geological and hydrostratigraphic data, used as constraints for the definition of *geophysical bodies* with specific relationships with the *sedimentary bodies* at different scales. At this purpose, after a correlation between the bulk electrical resistivity of the porous media and the pore-fluid saturation and

chemistry, the electrical resistivity is considered as a “proxy” of the sedimentary facies characterized by a litho-textural content and a prevailing process of current conduction (“shale” vs. electrolytic conduction). Assuming that the sedimentary heterogeneity can be described with hierarchical elements at different scales (hydrofacies, hydrostratigraphic system/complex/group; HUGGENBERGER & AIGNER, 1999; MAXEY, 1964; MIALI, 1996) and recalling that the resolution of DC surveys decreases with depth, this integrated approach allows to interpret the resistivity distribution as a function of the hierarchical properties of aquifers, i.e., the vertical trends and proportions of facies with prevailing “shale” or electrolytic conduction.

## 1.3. - THE CASE STUDY

The integrated methodology was applied to the Lodi Quaternary alluvial plain south of Milan, Italy (fig. 1) which belongs to the Neogene Po plain foredeep basin, bounded to the North, by the frontal thrusts of the Southern Alps and to the South by the external arcs of the Northern Apennines (ENI-REGIONE LOMBARDIA, 2002; PIERI

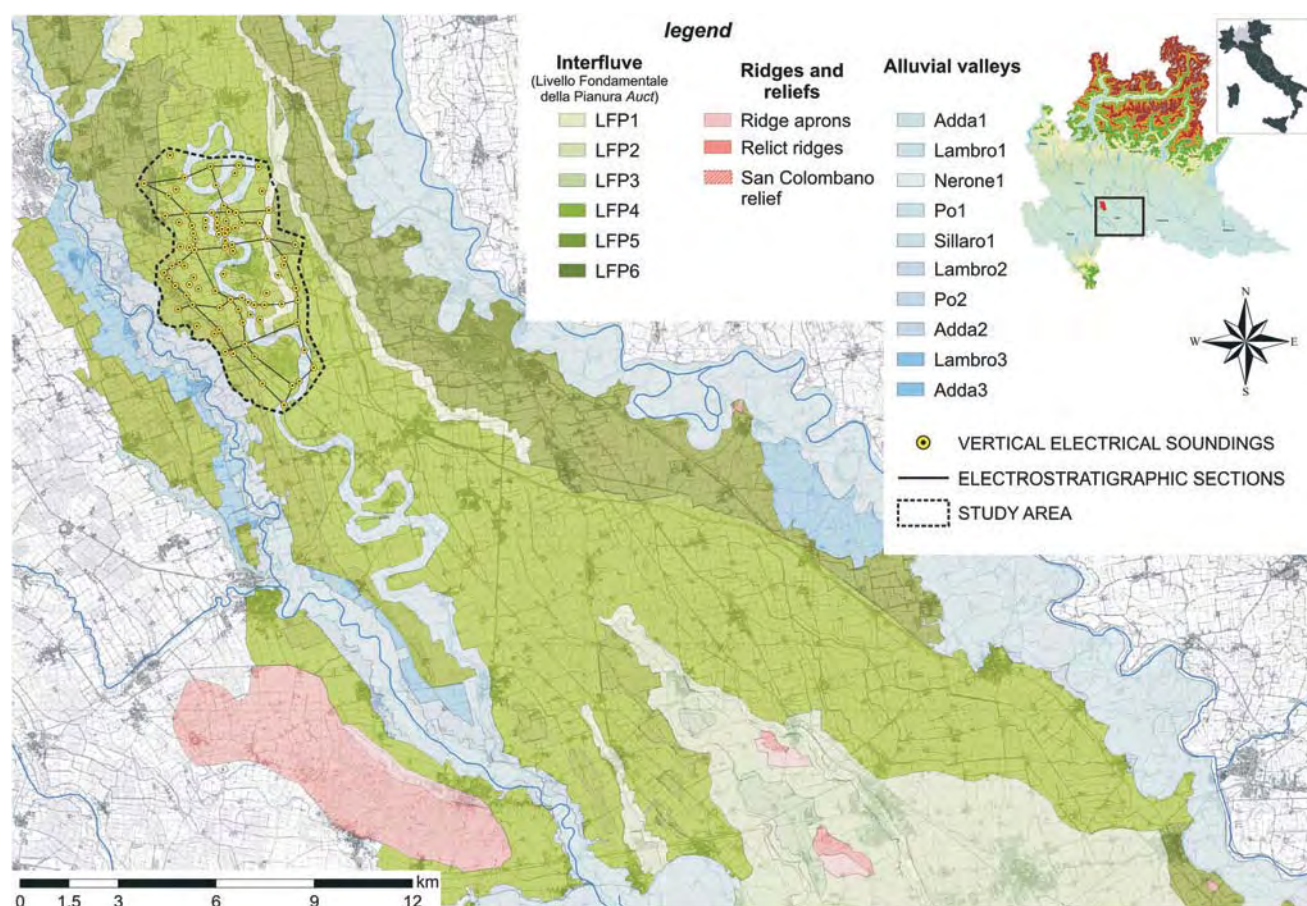


Fig. 1 - Lodi alluvial plain: location of the study area (dashed box; geological map from BAIO *et alii*, 2009).  
- La pianura Lodigiana: ubicazione dell'area in studio (a tratteggio; carta geologica da BAIO *et alii*, 2009).



& GROPPi, 1981). The basin was filled during Pliocene by deep marine sediments and, from Early to Middle Pleistocene, by at least three transgressive-regressive cycles (ENI-REGIONE LOMBARDIA, 2002); the youngest marine-to-transitional deposits are referred to the lower portion of Middle Pleistocene (MUTTONI *et alii*, 2003). From Middle Pleistocene an alluvial succession of Alpine provenance spread over the study area with the deposition of fluvial and glacio-fluvial sand-gravel sediments, whose maximum total thickness reaches some hundreds meters and becomes thin (a few meters) above the tectonic relief of San Colombano Hill (ALFANO & MANCUSO, 1996; BERSEZIO *et alii*, 2004) and Casalbusterlengo, Zorlesco and Chiesiolo buried structures (BERSEZIO *et alii*, this volume) to the South. The study area (fig. 1) is 30 km<sup>2</sup> wide and is located across the relict meandering river belt of the Sillaro palaeo-river of LGM-post and glacial age, entrenched in the local "Livello Fondamentale della Pianura" (i.e., basic plain level, LFP from now on; CASTIGLIONI & PELLEGRINI, 2001) between Adda (to the East) and Lambro (to the West) major river valleys.

#### 1.4. - METHODOLOGY

The adopted methodology aims to efficiently map sedimentary bodies, that are defined by their boundaries, geometry and facies organization. The workflow can be summarized as follows:

- i) definition of the geological/geomorphological model on the basis of the surface-subsurface data;
- ii) elaboration of the hydrostratigraphic model describing the low rank hierarchical units (hydrofacies) and their evolutive trends (fining/coarsening upwards sequences), up to the assemblage of high rank hydrostratigraphic systems;
- iii) characterization of site-specific parameters which affect the electrical resistivity (groundwater conductivity, soil saturation, porous matrix cementation);
- iv) planning of the 1-D geoelectrical surveys (VES) and data acquisition;
- v) calibration of the electrical resistivity with the hydraulic and litho-textural properties through the definition of the local petrophysical relationship between physical sediments' properties;
- vi) correlation of subsurface electrical resistivity models and identification of the electrostratigraphic framework;
- vii) improvement of details of the subsurface electrostratigraphic framework with 2-D resistivity imaging (ERGI);
- viii) integration between hydrostratigraphy and electrostratigraphy and elaboration of the final model.

## 2. - CONCEPTUAL MODEL OF THE PALAEO-SILLARO VALLEY

Geological mapping, interpretation and correlation of subsurface data yielded a preliminary conceptual model including several components: geometry (area, shape and thickness of the sedimentary bodies), sedimentology (textures and sediment composition, facies associations, lateral and vertical evolutive trends), stratigraphy (hierarchy, stacking patterns and age of the stratigraphic units) and hydrostratigraphy (estimates of porosity and permeability, relationship with pore-fluids).

### 2.1. - STRATIGRAPHIC FRAMEWORK

According to BERSEZIO *et alii* (2004) five depositional units of Middle Pleistocene-Holocene age form the subsurface of the Lodi plain, down to 100 m below the ground surface (fig. 2, box C).

Their deposition was controlled by the Middle to Upper Pleistocene climatic-tectonic cycles during the glaciations and the last tectonic pulses at the front of the Apennine thrusts (San Colombano, Casalbusterlengo, Zorlesco and Chiesiolo buried structures; BERSEZIO *et alii*, this volume; BINI, 1997b; ENI-REGIONE LOMBARDIA, 2002).

The lowermost subsurface unit (Unit 1; Middle-Upper Pleistocene) has no relationship with the ground surface in the study area. The topmost portion of the overlaying Unit 2 (Upper Pleistocene) and Unit 3 (LGM – Post-glacial) form the present-day topographic surface, the geomorphological LFP *Auct.* in the Lodi plain. It shows an average SSE dip of about 0.15% and is cut by the terrace scarps of the Lambro and Adda valley systems (fig. 2, box A). In the study area Unit 3 corresponds to the depositional system of the palaeo-Sillaro meandering river belt that is confined within a terraced valley with an average width of 3 km. The meandering trace of the abandoned river is well preserved, showing a mean radius of curvature of about 1 km (BERSEZIO, 1986; VEGGIANI, 1982). To the North the terrace scarps expose the top of Unit 2, attributed to the Upper Pleistocene glacio-fluvial Besnate Allogroup (BERSEZIO *et alii*, 2004; BINI, 1997a, 1997b; DA ROLD, 1990). The Lambro valley Post-glacial depositional systems are Units 4 and 5 (fig. 2, box A and C) that will not be dealt with.

### 2.2. - STRATIGRAPHIC MODEL

The stratigraphic model was elaborated by traditional correlation of the available data through litho-textural classification of sediments after MIALL's (1996) classification, modified to specify

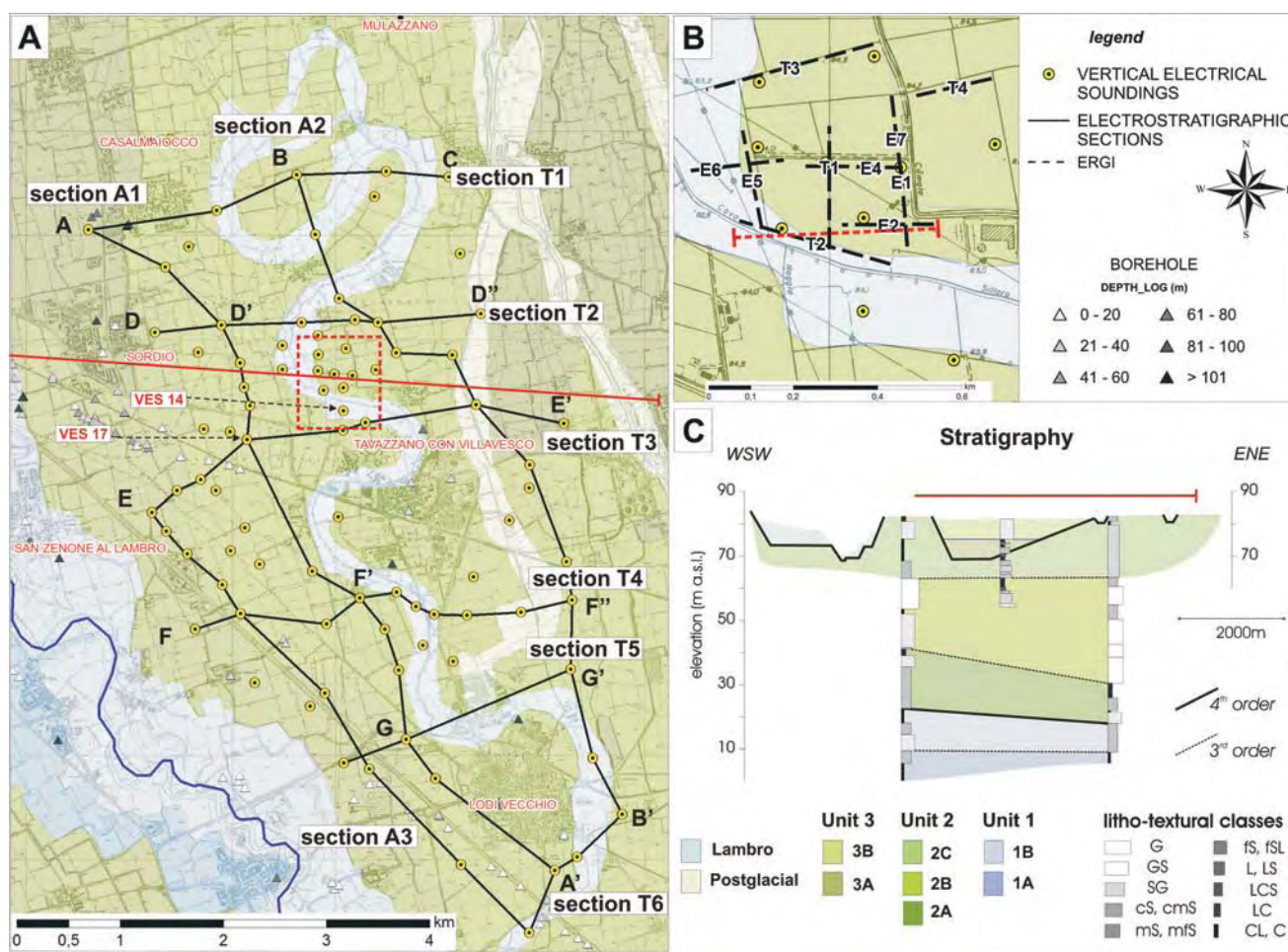


Fig. 2 - Geological map (box A; from BAIO *et alii*, 2009) of the Lodi plain showing the location of the subsurface data points, of the VES, of the area covered with a detailed ERGI survey (dashed box; the location of the ERGI profiles is shown in box B) and of the traces of the hydrostratigraphic (fig. 3) and electrostratigraphic (fig. 5, 7 and 9) sections. Simplified geological section across the palaeo-Sillaro valley (red continuous line in box A) is shown in box C.

- Carta geologica (A; da BAIO *et alii*, 2009) della pianura lodigiana, che illustra la posizione dei dati di sottosuolo, dei VES, dell'area coperta con il rilievo ERGI di dettaglio (rappresentata con il quadrilatero a tratteggio rosso in A; l'ubicazione dei profili ERGI è riportata nell'inserito B) e le tracce delle sezioni idrostratigrafiche (fig. 3) ed elettrostratigrafiche (fig. 5, 7 and 9). Una sezione geologica semplificata attraverso la valle del paleo-Sillaro (linea rossa continua nell'inserito A) è mostrata nell'inserito C.

the grain size association of the sedimentary facies.

The hierarchy of the sedimentary discontinuities was determined after the identification of the sharp boundaries between gravel-sand beds above fine grained sediments.

Four informal hierarchical orders were defined, starting from the minimum rank sequences, or genetic units (minimum fining-upwards, stationary or coarsening upwards vertical trends). The stack of these lowest rank units originates the stratigraphic hierarchy of depositional elements, stratigraphic sub-units and stratigraphic units shown in table 1.

The hierarchical classification enabled to identify three highest-rank stratigraphic units, bounded by 4<sup>th</sup> order stratigraphic surfaces that are formed by stacked sub-units bounded by 3<sup>rd</sup> order stratigraphic surfaces (fig. 2, box C). The 4<sup>th</sup> order units correspond, from the bottom to the top, to the Unit 1, 2 and 3 described by BERSEZIO *et alii*, (2004). Unit 1 (Middle Pleistocene, maximum de-

tectable thickness 25 m) consists of sand, silt and clay facies, arranged in fining upwards sequences, tens of meters thick. It is bounded at the top by a planar erosional surface, at an elevation between 30 m and 40 m above sea level. Two sub-units (1A, 1B) are bounded by 3<sup>rd</sup> order surfaces. Sub-unit 1A is characterized by organic-rich silt-clay, fining upwards sequences; sub-unit 1B consists of sand-silt fining upwards sequences, up to 15 m thick. Unit 2 (Middle-Late Pleistocene, maximum detectable thickness 45 m) is formed by stacked gravel and sand depositional elements, with rare fine grained layers. It is bounded at the top by the present-day topography in the northern area and by the concave erosional surface at the base of the uppermost Unit 3, to the south. From its base and upwards, Unit 2 is formed by three sub-units (2A, 2B, 2C) bounded by 3<sup>rd</sup> order surfaces. Sub-unit 2A consists mainly of sands and gravelly-sands, up to 10 m thick, and subordinated fine grained layers. Sub-

unit 2B is the coarsest sedimentary body, characterized by gravel and sandy-gravel fining-upwards sequences, up to 25 m thick. Sub-unit 2C is a sand and silty-clay facies association, forming two fining-upwards sequences; its total thickness ranges from 5 m, due to the top truncation, and 25 m.

Unit 3 (Latest Pleistocene, LGM – Post-glacial, maximum thickness 15 m) is characterized by sand-gravel and silt-clay facies. It was formed by the palaeo-Sillaro meandering depositional system. Unit 3 is bounded at the top by the present-day topography. The 4<sup>th</sup> order basal erosional unconformity truncates Unit 2 down to the base of sub-unit 2C, laying between 70 m and 75 m above sea level. This buried erosional surface is connected with the emerging terrace scarps which bound the palaeo-Sillaro valley. Unit 3 includes two sub-units (from the base to the top: 3A and 3B), which define two sand-gravel fining upwards sequences.

### 2.3. - HYDROSTRATIGRAPHY

The stratigraphic model provides the base for hydrostratigraphy from the low rank units (hydrofacies) up to their assemblage into aquifer/aquitard systems and complexes. The hierarchy of stratigraphic and hydrostratigraphic units is presented

in tab. 1, the elements for hydrofacies characterization are presented in tab. 2. The facies association was at first described by litho-textural classes; then porosity and hydraulic conductivity were estimated and compared with bibliographic data (BERSEZIO *et alii*, 1999; JUSSEL *et alii*, 1994; KLINGBEIL *et alii*, 1999) and with the results of laboratory tests upon analogue sedimentary facies exposed in the study area (DELL'ARCIPIRETE *et alii*, 2008). The resulting hydrofacies scheme (in the sense of ANDERSON, 1997) was simplified in a threefold classification of broad and semi-quantitative permeability classes (tab. 2) to facilitate comparisons with the electrical properties resulting from VES and ERGI surveys.

Hydrofacies were assembled into hydrostratigraphic systems (sensu MAXEY, 1964; DOMENICO & SCHWARTZ, 1990): sand/gravel aquifer systems (high to intermediate permeability hydrofacies) and aquitard/aquiclude systems (low permeability hydrofacies), associated with rare intermediate permeability hydrofacies on the base of the spatial distribution and relative interconnection of, respectively, sand-gravel and silt-clay bodies as portrayed by the hydrostratigraphic sections across the palaeo-Sillaro valley (fig. 3).

Two aquifer systems (S2-S4) were identified,

Tab. 1 - *Stratigraphy and hydrostratigraphy in the palaeo-Sillaro valley.*  
- Stratigrafia e idrostratigrafia della valle del paleo-Sillaro.

Stratigraphic units (age)	Stratigraphic sub-units	Depositional elements	Minimum genetic units	Thickness (m)	Hydrostratigraphic units	
Unit 3 (Latest Pleistocene, LGM + Postglacial)	3B	sand, gravelly sand fining upward sequence	· silt to clay fining upwards sequences	3 - 8	aquifer system S4	complex C2
			· clayey silt lenses			
	3A	sand, gravelly sand fining upward sequence	· gravelly sand to silt and clay fining upwards sequences	5 - 10		
			· clayey silt lenses			
Unit 2 (Middle-Late Pleistocene)	2C	sand to silt-clay fining upward sequence	· sand to silt fining upwards sequences	5 - 20	aquitard system S3	
			· organic-rich clayey silt lenses			
	2B	gravel, sandy gravel bodies	· non-cyclical gravel bodies	15 - 25	aquifer system S2	
			· gravel to sand fining upwards sequences			
			· clayey silt lenses			
	2A	gravel bodies, sand, gravelly sand fining upward sequence	· gravel to sand fining upwards sequences	5 - 15		
			· clayey silt lenses			
Unit 1 (Middle Pleistocene)	1B	sand to silt-clay fining upward sequence	· sand to silt and clay fining upwards sequences	10 - 15		
			· clayey silt lenses			
	1A	silt-clay fining upward sequence	· clayey silt lenses	10 - 15	aquitard system S1	



Tab. 2 - *Hydrofacies characterization (textural classes, permeability classes and thickness range of minimum rank hydrofacies units, corresponding to stratigraphic depositional elements and genetic units; see table 1).*

- Caratterizzazione delle idrofacies (classi tessiturali e di permeabilità e spessori caratteristici delle idrofacies di rango minimo corrispondenti ad elementi stratigrafici deposizionali e unità genetiche; si confronti con tabella 1).

Textural Classes	Hydrofacies					Thickness range (m)
	Porosity		Hydraulic conductivity estimates K (m/s)			
	BERSEZIO <i>et alii</i> , 1999 JUSSEL <i>et alii</i> , 1994 KLINGBEIL <i>et alii</i> , 1999	DELL'ARCIPRETE <i>et alii</i> , 2008	BERSEZIO <i>et alii</i> , 1999 JUSSEL <i>et alii</i> , 1994 KLINGBEIL <i>et alii</i> , 1999	DELL'ARCIPRETE <i>et alii</i> , 2008	Permeability classes	
G	0.4	0.43	2.5 x 10 <sup>-1</sup> - 1.0 x 10 <sup>-2</sup>	3.2 x 10 <sup>-2</sup>	high	0-15
GS	-	0.4	-	4.6 x 10 <sup>-3</sup>		0-15
SG	0.2-0.3	0.42	1.0 x 10 <sup>-2</sup> - 1.0 x 10 <sup>-4</sup>	1.3 x 10 <sup>-3</sup>		0-10
cS/cmS	0.4	0.43	5 x 10 <sup>-3</sup> - 1.7 x 10 <sup>-5</sup>	5.2 x 10 <sup>-4</sup>	intermediate	0-8
mS/mfS		0.44		4.2 x 10 <sup>-4</sup>		0-8
fS/fSL	-	0.45	5 x 10 <sup>-3</sup> - 1.7 x 10 <sup>-5</sup>	1.6 x 10 <sup>-4</sup>	low	0-15
L/LS	-	-	-	-		0-10
LAS	-	0.5	-	-		0-10
LC	-	-	-	6.0 x 10 <sup>-6</sup>		0-10
CL/C	-	-	-	-		0-15

separated by an aquitard system (S3) and bounded at the base by a widespread basal aquitard (S1).

These units form two aquifer complexes (C1-C2) that presumably correlate in some way with the Aquifer Groups A and B and with the topmost portion of Group C of ENI-REGIONE LOMBARDIA (2002). The phreatic aquifer system S4 hosts the local water table. The aquitard S3 corresponds to the fine sand to silt-clay succession of the Upper Pleistocene flood plain (sub-unit 2C). In the northern sector of the study area, the separation between aquifer S2 and S4 is limited due to the

presence of the palaeo-Sillaro depositional system which truncates the aquitard system S3. Aquifer S2 overlies a basal aquiclude of silty-clays formed by the Middle Pleistocene transitional-to-marine succession (sub-unit 1A) which hosts the salt-fresh water interface (ENI- REGIONE LOMBARDIA, 2002).

### 3. - ELECTROSTRATIGRAPHY

The assemblage of stratigraphic units and their physical properties (thickness, lateral extent, geome-

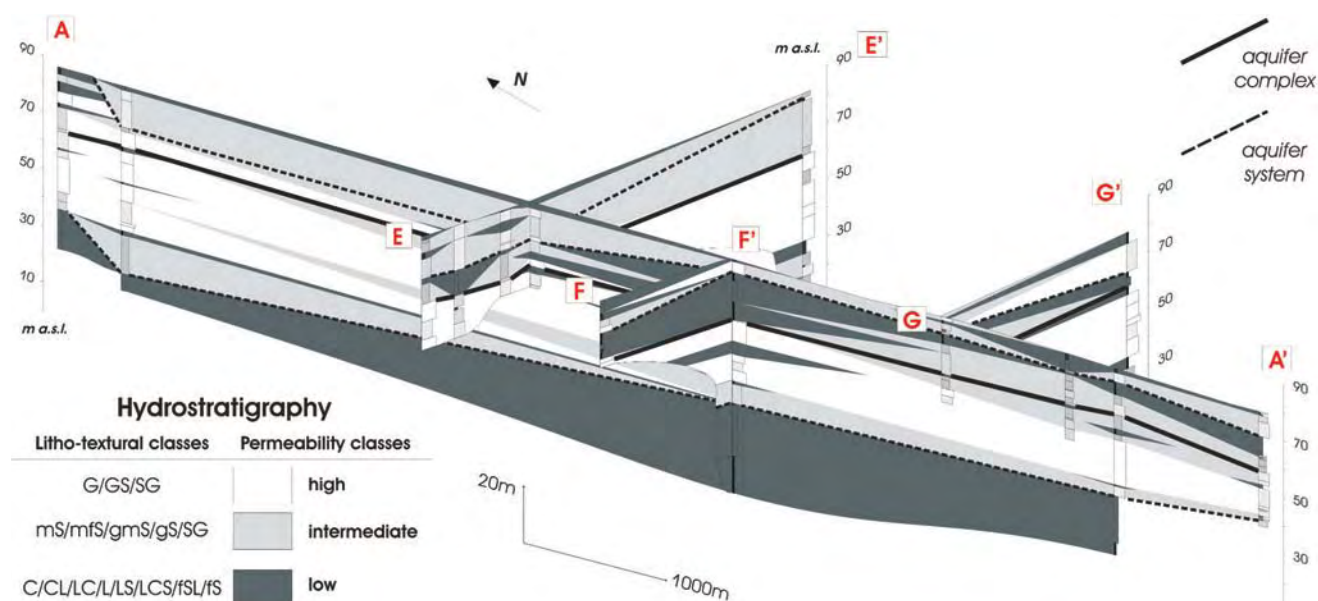


Fig. 3 - 3-D fence diagram of NNW-SSE and WSW-ENE hydrostratigraphic sections across the palaeo-Sillaro valley (see figure 2 for location and lithotextural codes).  
- Correlazione a siepe delle sezioni idrostratigrafiche attraverso la valle del paleo-Sillaro (l'ubicazione e i codici litologici e tessiturali sono riportati in figura 2).

Tab. 3 - *Characteristics of survey areas and of geophysical prospecting.*  
 - Caratteristiche delle aree di studio e delle prospezioni geoelettriche effettuate.

Width	Area (km <sup>2</sup> )	DC survey type	Horizontal resolution	Vertical resolution		Exploration depth
				Near surface	Depth	
Regional study area	30	89 VES	hundred of meters	dm to m	m to tens of M	50-70 meters below ground level
		(half spacingmax=300 m)				
Detailed study area	<1	10 ERGI	meters	meters	m to tens of M	40 meters below ground level
		(48 electrodes; 5 m spacing)				

try, litho-textural associations, hydrofacies) were used as the conceptual framework for the definition of two survey areas of different horizontal width (regional study area and detailed study area; fig. 2; tab. 3).

In order to interpret the electrical resistivity distribution in terms of litho-textural properties, the site-specific physical parameters which affect the electrical resistivity as qualitatively expressed by the Archie's law (groundwater conductivity, saturation and cementation; ARCHIE, 1942; KELLER & FRISCHKNECHT, 1966; REYNOLDS, 1997; TELFORD *et alii*, 1990) were monitored during the field acquisition of geoelectrical data. The characterization of these parameters can be summarized as follows:

- the average pore-fluid conductivity in the study area is 550  $\mu\text{S}/\text{cm}$ , corresponding to an average electrical resistivity of 18  $\Omega\text{m}$ . This value was estimated by i) direct sampling of the surface groundwater at deep excavation points and analysis with a portable conductivity meter and ii) bibliographic data (SISTEMA INFORMATIVO FALDA SIF, PROVINCIA DI MILANO) relative to chemical analyses of groundwater extracted from water wells;
- the pore fluid saturation was determined in relation to the depth of the water table, which is shallow (from 0.9 m to 2.5 m below ground level) in correspondence to the present-day, topographically depressed, Sillaro underfit stream and deeper (between 4.1 m and 6.3 m b.g.l.) in correspondence to the top of older terraces within the palaeo-Sillaro valley;
- on the base of the available subsurface data (geognostic boreholes, water-well stratigraphy) no evidence of cementation was detected in the investigated stratigraphic succession.

### 3.1. - REGIONAL STUDY AREA

The regional survey consisted of 89 VES collected with Schlumberger array. The average exploration depth is about 70 m b. g. l., over a 30 km<sup>2</sup> wide area (tab. 3) where Unit 3 is outcropping, but for a limited extent in the northern sector, where

Unit 2 is found (fig. 2, box A and C). Each VES sounding was carried out with half-spacing of the current dipole varying between 1 m and 300 m (the half-spacing of the potentiometric dipole varied from 0.5 m to 50 m) and a maximum of 17 apparent electrical resistivity measurements for each sounding. Some VES were acquired as close as possible to the position of subsurface data (namely, water wells) in order to calibrate the results. The distance between soundings ranges from 200 m to 1000 m, for an areal density from 2 VES/km<sup>2</sup> up to 12 VES/km<sup>2</sup>; this choice was aimed at obtaining 1-D resistivity models at an horizontal scale comparable with the size of the depositional elements (tab. 1).

#### 3.1.1. - Data processing

The elaboration of 1-D models was performed by: 1) fixing the number of resistive and conductive layers that comprise the electrostratigraphic sequence on the basis of the minimum, maximum and inflexion points of the apparent resistivity curves (KELLER & FRISCHKNECHT, 1966); 2) cali-

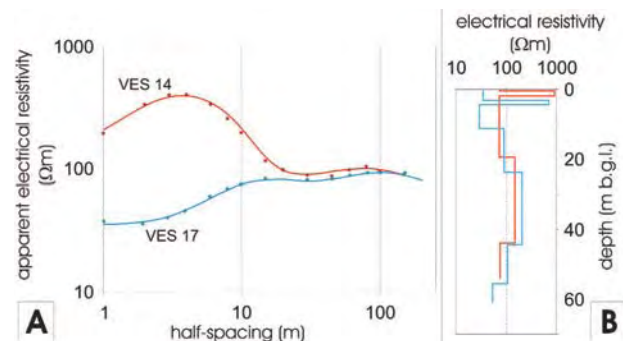


Fig. 4 - Example of the best-fitted apparent electrical resistivity curves (box A; dots represent field data) and the corresponding 1-D inverse models (box B) obtained for two VES collected respectively within (VES 14, red curve: RMS 4.8%) and outside (VES 17, blue curve: RMS 2.4%) the present-day Sillaro underfit stream (VES ubication is shown in fig. 2, box A).

- Esempio di curve di resistività elettrica apparente simulate ( riquadro A: i punti rappresentano le misure acquisite) con i corrispondenti modelli inversi 1-D ( riquadro B) per due VES posizionati rispettivamente all'interno (VES 14, curva rossa: RMS 4.8%) e all'esterno (VES 17, curva blu: RMS 2.4%) del paleo-alveo del Sillaro.

brating 1-D models of electrical resistivity with the RES1D software (LOKE, 2001). The inverse procedure required a maximum of 5 iterations and the models with a high RMS error were re-processed with an increasing number of layers in order to decrease the RMS error. Finally the number of electrolayers ranges from 3 to 7, for a maximum investigation depth of 70 m b. g. l. (fig. 4). Most of the models are well fitted; 11 models only show relative RMS error greater than 3%.

### 3.1.2. - *Electrostratigraphic interpretation*

Correlation of VES 1-D models was based on two criteria: 1) the discontinuities between electrolayers were characterized on the base of the vertical polarity of the resistivity contrast (vertical stacking of resistive above conductive layer or vice versa) determining the local vertical electrostratigraphic sequence; 2) the polarity of resistivity contrasts between electrolayers was correlated among the 1-D models in order to delimitate the subsurface sediment volumes with the lowest internal variation of electrical resistivity.

These two criteria allowed to recognize the *geo-electrical bodies* in the subsurface that could be traced through the investigated volume by the horizontal variation of the vertical electrostratigraphic sequence identified in VES models and are characterized by an increasing thickness at increasing depth, according to the equivalence and suppression principles (KELLER & FRISCHKNECHT, 1966).

They represent 3-D bodies showing i) a clear resistivity contrast with the adjacent bodies, ii) peculiar internal electrical properties and iii) a typical apparent geometry and vertical/horizontal extent. Considering the analogy with the definition of “lithostratigraphic units” (NASC, 1983; NASC, 2005), each geoelectrical body was informally defined “electrostratigraphic unit” (EsU). Differently from a lithostratigraphic unit, an EsU can be defined only by the resistivity contrasts, that can be traced over significant distances preserving the same vertical polarity.

Nine electrostratigraphic correlation sections were elaborated (fig. 2, box A), with a kilometeric horizontal extent and longitudinal and transverse orientation with respect to the main drainage axis (NNW-SSE) of the palaeo-Sillaro valley. These sections were mounted on a 3-D panel (fig. 5, box A) to check their coherence at the intersection points and to build up the electrostratigraphic framework of the investigated volume.

On the base of their lateral persistence, the EsUs were subdivided in (tab. 4):

- widespread units, that could be identified in several 1-D models and characterized by good lateral

continuity in the study area;

- lens-shaped units, identified in a single or a few 1-D models.

The widespread EsUs were used to define the electrostratigraphic model of the study area at a regional scale and they were coded, from top to bottom, respectively with the letters from A to G (tab. 4).

The uppermost EsUs A and B (fig. 5, 7 and 9) mainly identify the vertical variation of electrical resistivity due to the near-surface facies/hydrofacies transition within the unsaturated zone. These EsUs are defined respectively as a conductive body ( $<70 \Omega\text{m}$ ) and an underlying high-resistive body (170-1500  $\Omega\text{m}$ ), with metric/sub-metric thickness.

The deeper EsUs (unit C, D, E, F; fig. 5, 7 and 9) characterize the saturated zone below the water table (generally coincident with the base of EsU B; fig. 7, box B). They represent both conductive and resistive bodies characterized by a thickness that increases with depth up to tens of meters. EsUs C to F represent an alternation of conductive and resistive bodies. EsU G ( $<70 \Omega\text{m}$ ) is the deepest conductive unit and is identified in few 1-D models corresponding to the VES that reached the maximum exploration depth (fig. 5; fig. 9); for this reason, its identification is quite uncertain. The lense-shaped EsUs (unit L; fig. 5 and 7) do not conform with the electrostratigraphic framework defined at a regional scale and represent local features with small lateral extent. Therefore their geometry remains more uncertain and in some cases different equivalent correlations could be proposed.

### 3.2. - DETAILED SURVEY AREA

In order to improve the details of the horizontal transitions between the electrostratigraphic

Tab. 4 - *VES electrostratigraphic model for the palaeo-Sillaro valley (regional study area) based on the widespread EsUs.*

- Modello elettrostratigrafico VES della valle del palaeo-Sillaro (area di studio a scala regionale).

EsU	Electrical resistivity $\rho$ range ( $\Omega\text{m}$ )	Thickness range (m)	Depth range
			(m b.g.l.)
A	$< 70$	0.5 - 9	0 - 10
B	170 - 1500	0.5 - 5	0.5 - 6
C	20 - 70	5 - 10	5 - 15
D	70 - 100	10 - 15	15 - 25
E	110 - 200	10 - 25	25 - 45
F	70 - 90	10 - 30	25 - 60
G	$< 70$	-	$> 60$ -70



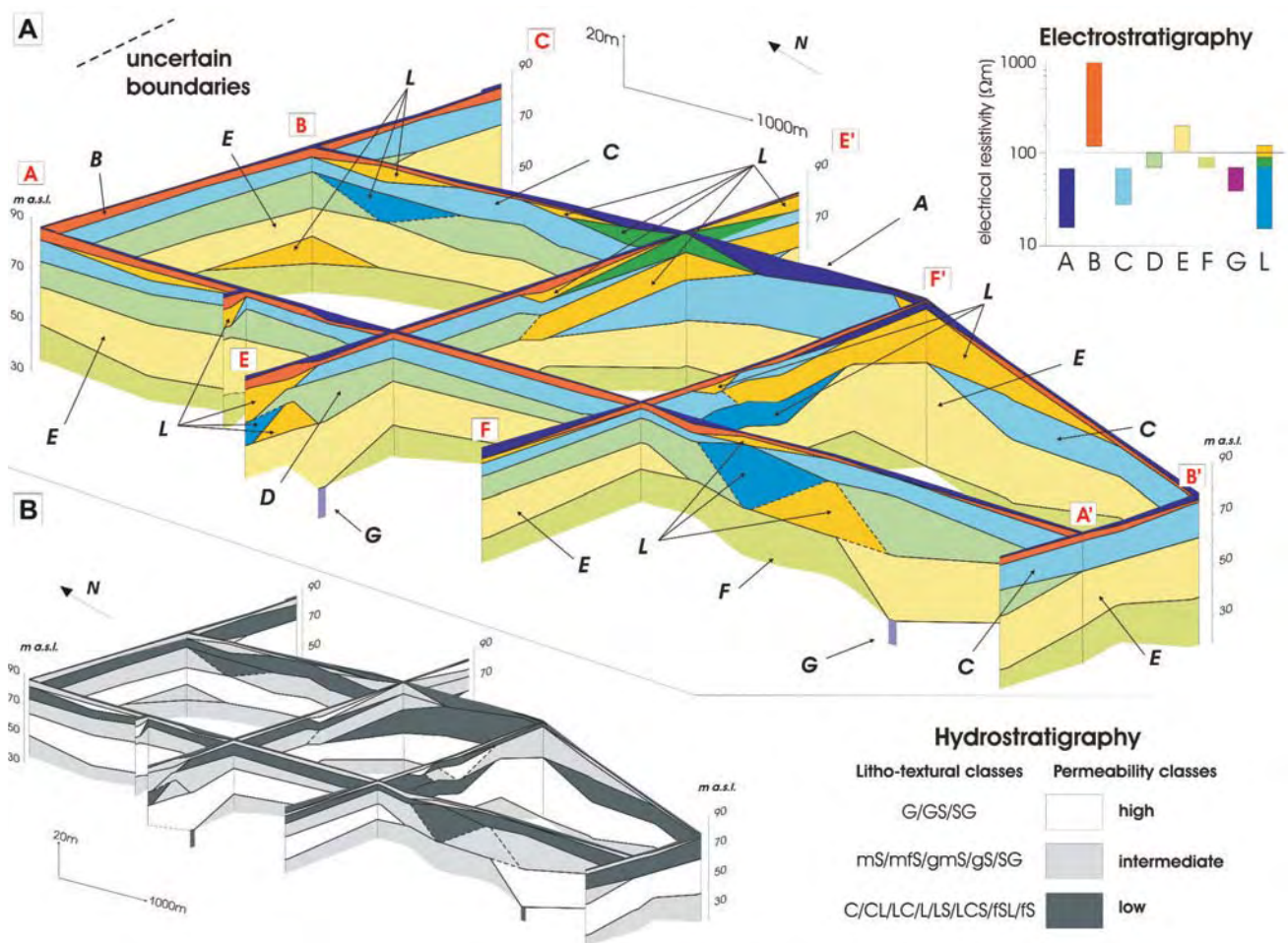


Fig. 5 - Fence diagrams of NNW-SSE (A1, A2) and WSW-ENE (T1, T2, T3, T4 and T6) VES electrostratigraphic sections (box A; see figure 2, box A for location) and plot of EsUs' electrical resistivity (upper right corner; units from A to F refers to EsUs described in table 4, units L refers to the lense-shaped EsUs). In the lower plot (box B): 3-D panel of electrostratigraphic sections (same as box A) interpreted in terms of the dominant hydraulic properties at the regional scale across the palaeo-Sillaro valley.

- Correlazione a siepe delle sezioni elettrostratigrafiche ( riquadro A: ubicazione in figura 2, riquadro A) ottenute dai VES e resistività elettrica delle EsUs ( riquadro in alto a sinistra destra; le unità da A a G si riferiscono alle EsUs descritte in tabella 4; le unità L rappresentano EsUs lenticolari). Riquadro in basso (B): pannello di correlazione 3-D tra le sezioni elettrostratigrafiche nella valle del paleo-Sillaro, interpretate in funzione delle proprietà idrodinamiche alla scala regionale.

units at the metre-scale, a 2-D ERGI survey was planned within a selected area (fig. 2, box A). In particular, ERGI profiles were located to investigate a point-bar complex of the palaeo-Sillaro river (Unit 3), with a grid normal and parallel to the point-bar elongation (fig. 2, box B). Ten sections were acquired with 48 electrodes using a Wenner-Schlumberger array, electrode spacings from 3 m to 5 m and a roll-along acquisition scheme for a maximum length of the array of 410 m. The maximum number of apparent electrical resistivity measurements for a single section was 1220.

### 3.2.1. - Data processing

For each ERGI section a preliminary datum removal of bad measurements (less than 10% of the total), mainly due to poor coupling between electrode and ground, was performed. Inversion of

field apparent resistivity data was performed with the RES2DINV software (LOKE & BARKER, 1995).

The final 2-D resistivity models were obtained after a maximum of 8 iterations, using the L1-norm optimization method, which is quite robust and reduces the effect of outliers in the field data sets (FARQUHARSON & OLDENBURG, 1998). Relative RMS error ranges from a minimum of 1.2% to a maximum of 13.4%, with an estimated maximum depth of investigation of 40 m below the acquisition surface.

### 3.2.2. - Electrostratigraphic interpretation

The robust inversion yielded 2-D models characterized by areas of approximately uniform electrical properties which are separated from each other by sharp boundaries (LOKE *et alii*, 2003) and directly related to the regional electrostratigraphic

framework defined through the VES survey. These areas represent the analogue of the EsUs defined through the correlation of the VES electrostratigraphic sections. The ERGI sections were fixed on a 3-D panel (fig. 6, box A) to verify the internal coherence of the subsurface electrical resistivity at the intersections. However, the geoelectrical boundaries between EsUs have no straightforward correspondence in the ERGI sections, because the 2-D resistivity distribution obtained from ERGI is determined for a great number of blocks whose spatial extent depends on the electrode spacing. The correspondence between these regions and EsUs was explored by comparing 2-D sections with the nearest VES electrostratigraphic section.

In figure 6 (box B) the correspondences between the uppermost conductive regions (0-15 m b.g.l.; 30-40  $\Omega\text{m}$ ) with the EsUs C and D and between the lowermost resistive regions (> 15 m b.g.l.; 130-160  $\Omega\text{m}$ ) with the resistive EsU E are shown at a metric horizontal scale. Due to the large electrode spacing, ERGI survey cannot yield accurate reconstructions for the near-surface unsaturated zone.

#### 4. - INTEGRATION OF HYDROSTRATIGRAPHIC AND ELECTROSTRATIGRAPHIC MODELS

In order to integrate the hydrostratigraphy with the electrostratigraphic model of the palaeo-Sillaro valley, a calibration between the electrical resistivity measurements and the hydraulic and litho-textural estimates was attempted, considering separately the unsaturated and the saturated zone and fixing the average electrical conductivity of local groundwater in the Lodi plain (18  $\Omega\text{m}$ ). In the unsaturated zone (<5 m b.g.l.), a direct calibration between electrical resistivity and hydrofacies was obtained at VES stations thanks to hand-auger drilling down to 5 m b.g.l.: the depth of the boundaries between near-surface EsUs was compared with the depth of hydrofacies transitions and with the local groundwater level (fig. 7, box B). In the saturated zone (>5 m b.g.l.), an indirect calibration was attempted, comparing the electrostratigraphic framework at increasing depths with the vertical litho-textural associations (i.e. hydrofacies) interpreted from the available stratigraphic logs (fig. 7, box C). In order to

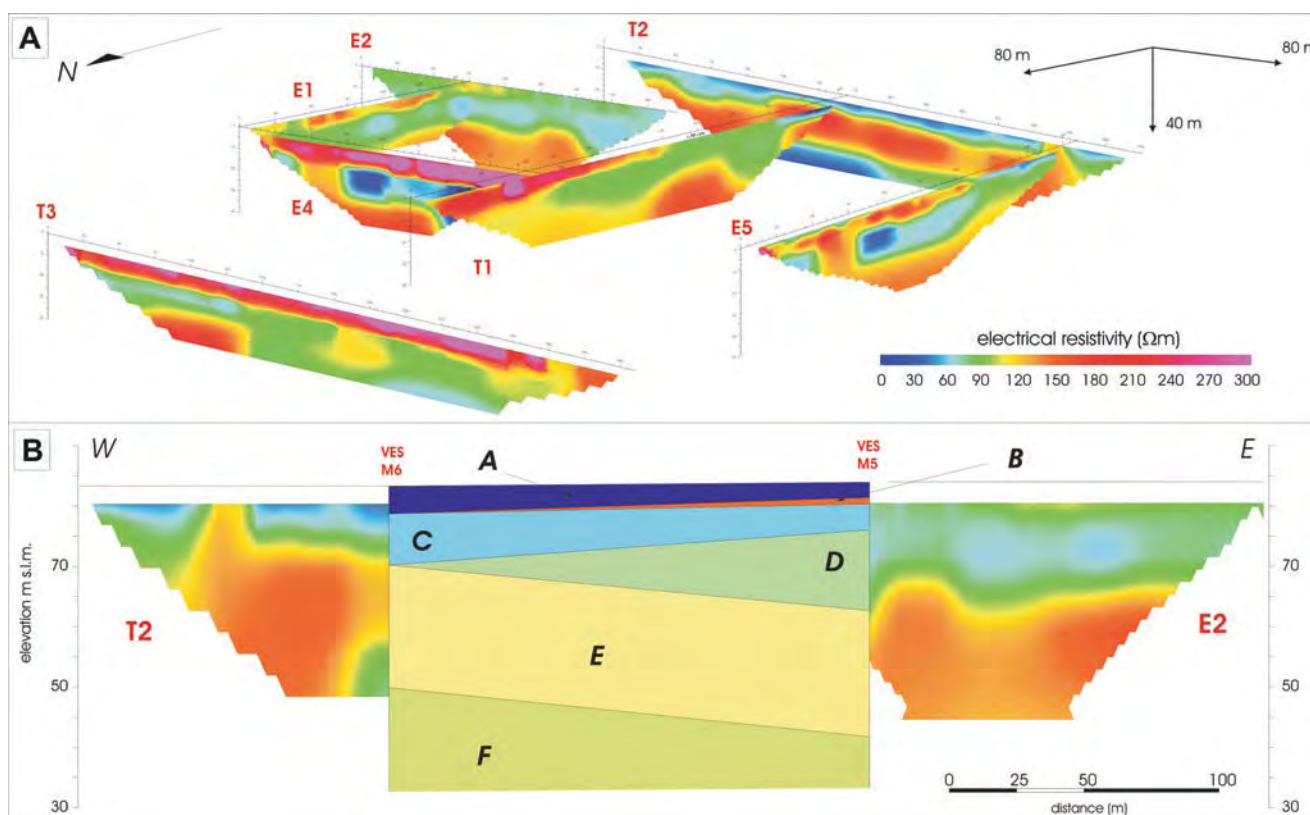


Fig. 6 - 3-D panel of 2-D ERGI models collected in the detailed survey area corresponding to the abandoned Sillaro point bar complex (box A; for location see figure 2, box A and B). The section in the lower plot (box B) corresponds to red dashed line in figure 2 (box B) and compares the electrical resistivity distribution determined from 2-D ERGI high resolution survey (T2, E2) and 1-D VES electrostratigraphic correlation at regional scale.

- Pannello di correlazione tra i modelli ERGI rilevati nell'area di dettaglio in corrispondenza del complesso di barra di meandro del paleo-Sillaro (l'ubicazione è riportata in figura 2, riquadro A e B). La sezione in basso (riquadro B), corrispondente alla linea rossa tratteggiata in figura 2, riquadro B, presenta il confronto tra il rilievo ERGI T2, E) e la corrispondente sezione di correlazione elettrostratigrafica basata sui modelli 1-D VES.



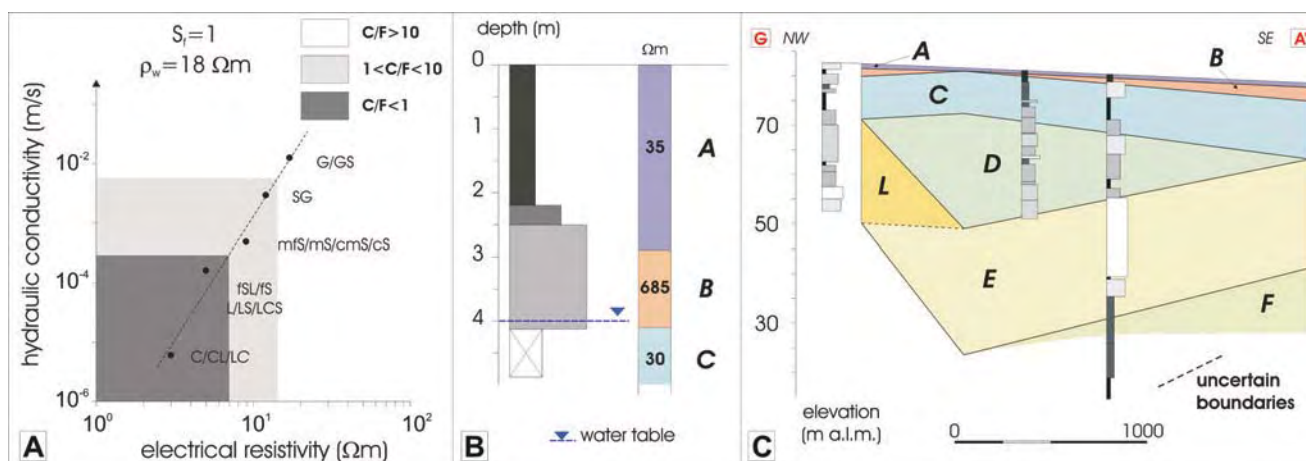


Fig. 7 - Local petrophysical relationship between hydraulic conductivity estimates, electrical resistivity, fluid saturation ( $S_f$ ) and mean groundwater electrical resistivity ( $\Omega m$ ) (box A); the black dots represent the values of electrical resistivity calibrated for different hydrofacies. Direct calibration (box B) between 1-D electrical resistivity and hydrofacies at VES stations in the unsaturated zone (dashed line represents water table; see fig. 2, box C for lithotextural codes). Indirect calibration between electrostratigraphic framework and hydrofacies associations (box C) based on stratigraphic boreholes along electrostratigraphic section A1 (ubication is shown in figure 2, box A).

- Correlazione petrofisica locale ( riquadro A) tra stime di conducibilità idraulica, resistività elettrica, saturazione ( $S_f$ ) e resistività media della acque sotterranee ( $\Omega m$ ); i punti neri indicano i valori di resistività elettrica calibrati per le diverse idrofaccies. Calibrazione diretta tra VES e idrofaccies ( riquadro B) ai punti di rilievo geoelettrico nella zona insatura (la linea a tratteggio rappresenta la tavola d'acqua; i codici tessiturali sono riportati in figura 2, riquadro C). Calibrazione indiretta tra elettrostratigrafia ed associazione di idrofaccies (C) lungo la sezione elettrostratigrafica A1 (ubicazione in fig. 2, riquadro A).

interpret the electrical resistivity as a “proxy” of the hydrostratigraphic properties, the coarse-to-fine litho-textural ratio ( $C/F$ , adimensional; cut-off  $\varnothing=0.3$  mm) was calculated for high-permeability gravel-sandy gravel hydrofacies ( $C/F>10$ ), gravelly sand hydrofacies ( $1<C/F<10$ ) and low-permeability silt-clay hydrofacies ( $C/F<1$ ). The threefold classification based on the  $C/F$  ratio mimics the broad classification of hydrofacies permeability adopted in tab. 2. The variability range of the  $C/F$  ratio was compared to the hydraulic conductivity  $K$  (m/s) and the electrical resistivity  $\rho$  ( $\Omega m$ ) of hydrofacies, both in the unsaturated and in the saturated zone. A local petrophysical relationship between hydraulic and electrical conductivity was established (fig. 7, box A) to reclassify the electrical resistivity at near-surface and at increasing depth in term of the prevailing hydraulic properties (low-intermediate-high permeability) of the equivalent volume (fig. 5, box B).

#### 4.1. - NEAR-SURFACE RECONSTRUCTION

In order to characterize at the detailed scale (shallow depth, 0-5 m, unsaturated zone) the stratigraphic Units 3 and 2, a map of apparent electrical resistivity has been obtained by interpolating data for half spacing of 4 m with an inverse distance method (fig. 8). According to the local near-surface geological and geomorphological model (sand-gravel to silt-clay fining-upwards point-bar sequence, terrace scarps, slopes) and the electrostratigraphic model (tab. 4), regions of low and high apparent resistivity can be interpreted as characterized by respectively high and low thick-

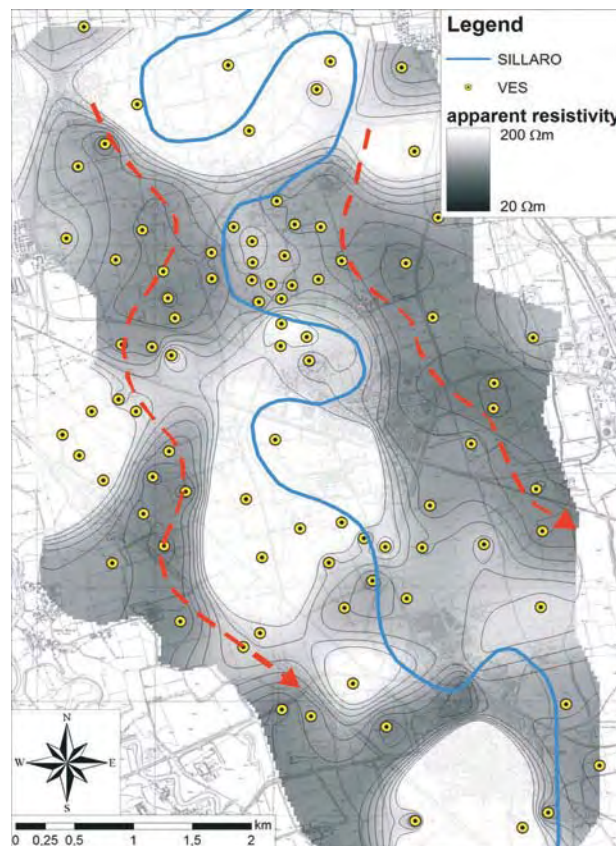


Fig. 8 - Apparent resistivity map (half-spacing 4 m; contours  $20 \Omega m$ ) of the palaeo-Sillaro valley. The dashed lines along the west and east borders of the paleo-Sillaro meandering abandoned trace (continuous line) represent two inferred extinct fluvial traces of the palaeo-Sillaro river that could be observed by the integration of apparent electrical resistivity of near-surface sediments and geomorphological survey.

- Mappa di resistività apparente (semi-spaziatura elettrodica pari a 4 m; equidistanza  $20 \Omega m$ ). Le linee tratteggiate lungo i bordi orientale ed occidentale della traccia meandri-forme del paleo-Sillaro (linea continua) rappresentano due possibili decorsi fluviali abbandonati, rilevabili attraverso l'integrazione della resistività elettrica apparente dei sedimenti superficiali e del rilievo geomorfologico.



nesses of the conductive part of the fining upwards sequences (EsU A, fine litho-textural association, low permeability hydrofacies; tab. 2).

Therefore, the apparent resistivity map yields some useful information about the near-surface horizontal transition between the unsaturated coarse-grained point-bar deposits (EsU B, coarse litho-textural association, high permeability hydrofacies; tab. 2) and the fine-grained oxbow-lake/overbank deposits at regional scale in the unsaturated zone. Within the palaeo-Sillaro valley, two low resistivity areas ( $<70 \Omega\text{m}$ ) were identified to the East and to the West of the meandering trace of the present-day Sillaro underfit stream (fig. 8). These areas could be interpreted as two possible extinct fluvial traces of the palaeo-Sillaro river, in which the topographical depression associated to the avulsed fluvial channel were filled by a pluri-metric thickness of fine-grained sediments. Notice that this interpretation could not be obtained by the simple geomorphological analysis of terrace scarps and slopes, but results from combination of geological and geophysical data. Hence, the map adds substantial information to the near-surface reconstruction.

#### 4.2. - SUBSURFACE RECONSTRUCTION

The integration between the electrostratigraphic and the hydrostratigraphic models by the means of the local petrophysical relationship (fig. 7, box A) permits to validate and revise the hydrostratigraphic framework in the alluvial valley of palaeo-Sillaro river, in terms of vertical hydrostratigraphic successions, average hydrodynamic properties and

distribution of lateral heterogeneities. According to the equivalence and suppression principles which limit the interpretation of DC measurements, shallow EsUs (in the unsaturated zone) coincide with hydrofacies whereas deep EsUs (in the saturated zone) can be interpreted as the geoelectrical images of the connectivity of the sedimentary bodies that are characterized by peculiar facies (i.e. litho-textural), hydraulic and electrical properties at a physical scale comparable with the hierarchical scale of the hydrostratigraphic systems.

From North to South in a depth range of 25-60 m b.g.l., the electrostratigraphic sections shown in figure 9 confirm the presence of coarse-grained resistive sheet-bodies (sand-to-gravel, gravel) with electrical resistivity ranging in the uppermost part from 110 to 200  $\Omega\text{m}$  and estimated hydraulic conductivity ranging from  $1.9 \cdot 10^{-3}$  to  $2.3 \cdot 10^{-2}$  m/s (Unit E) and, in the lowermost part, from 70 to 90  $\Omega\text{m}$  (Unit F; K from  $3.0 \cdot 10^{-4}$  m/s to  $8.4 \cdot 10^{-4}$  m/s). These bodies describe a coarsening upwards sequence that can be interpreted as a stage of progradation of the southernmost termination of a glacio-fluvial braiding fan of alpine origin (sub-units 1B, 2A e 2B) of Middle-Upper Pleistocene age (BERSEZIO *et alii*, 2004). They form the aquifer system S2 at the top of an older sandy-clay meandering river belt of Middle Pleistocene age (sub-unit 1A) characterized by electrical resistivity less than 70  $\Omega\text{m}$  and estimated K less than  $3.0 \cdot 10^{-4}$  m/s (Unit G in fig. 9), corresponding to the aquitard system S1 at the base of the lowermost hydrostratigraphic complex C1. The subsequent backstepping to north of the depositional system during the Upper Plei-

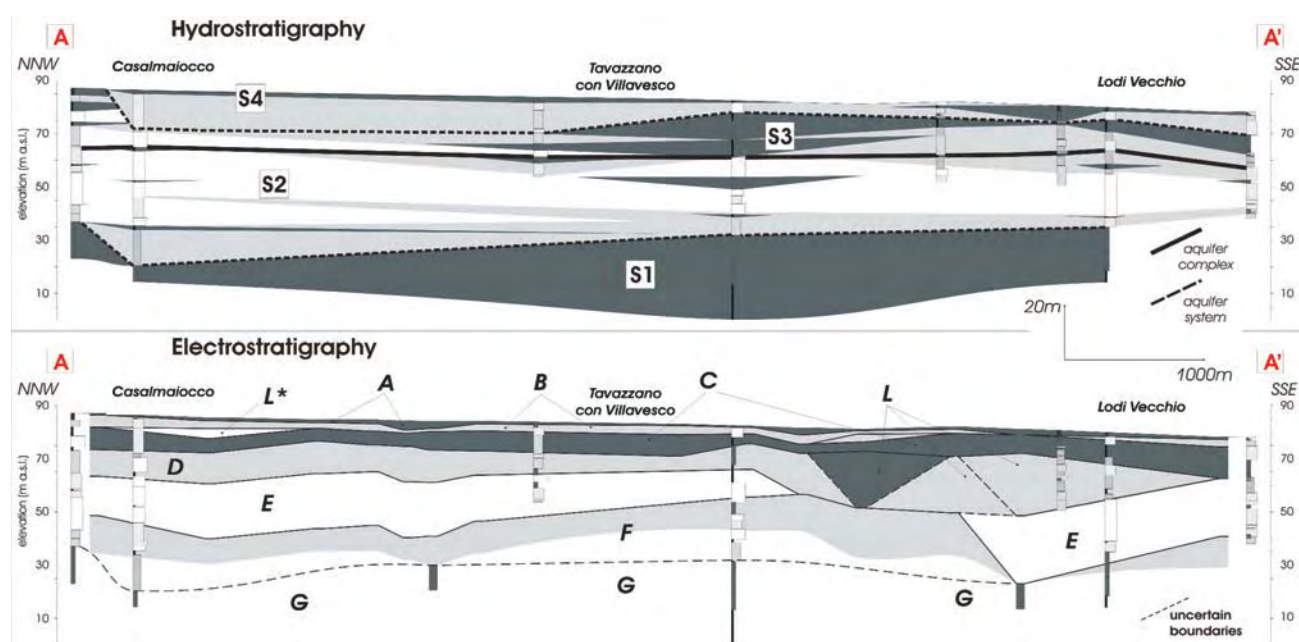


Fig. 9 - Integration of hydrostratigraphy and electrostratigraphy along section A1 (see fig. 2, box A for location and fig. 3 and fig. 5 for permeability classes).  
- Integrazione delle ricostruzioni idrostratigrafica ed elettrostratigrafica lungo la sezione A1 (fig. 2, riquadro A, per l'ubicazione e fig. 3 e fig. 5 per le classi di permeabilità).

stocene, and the development of a sandy meandering system with a clay-rich flood plain over the entire study area is represented by sub-unit 2C plausibly corresponding to EsUs C ( $20 \Omega\text{m} < \rho < 70 \Omega\text{m}$ ;  $1.6 \cdot 10^{-6} \text{ m/s} < K < 3.0 \cdot 10^{-4} \text{ m/s}$ ) and D ( $70 \Omega\text{m} < \rho < 100 \Omega\text{m}$ ;  $3.0 \cdot 10^{-4} \text{ m/s} < K < 1.3 \cdot 10^{-3} \text{ m/s}$ ), that represent the aquitard system S3 at the base the uppermost hydrostratigraphic complex C2. The sharp boundaries between gravel-sand resistive beds of Unit 3, corresponding to aquifer system S4, do not show clear evidences because the high resistivity contrast between near-surface coarse-grained unsaturated sediments (up to  $1500 \Omega\text{m}$ ) and the underlying saturated sediments locally masks the presence of a resistive unit interposed between Units B and D (Unit L\* in fig. 9). In the area of Tavazzano con Villavesco and Lodi Vecchio, the integration of hydrostratigraphy with electrostratigraphic ameliorated the interpretation of the lateral terminations of the coarse grained part of the aquifer system S2 (fig. 9).

## 5. - CONCLUSION

The integration between hydrostratigraphy and electrostratigraphy allowed to develop and cross-validate the subsurface hydrostratigraphic models of the Sillaro palaeo-valley to a maximum depth of 80 m. The evaluation of the hydrostratigraphic significance of electrostratigraphic units was put in relation to the well-known equivalence and suppression principles (KELLER & FRISCHKNECHT, 1966) which limits the interpretation at increasing depth of electrical resistivity estimated from the ground surface with the VES soundings. In the near-surface, EsUs represent vertical resistivity variations related to the litho-textural contrasts at the scale of the hydrofacies (ANDERSON, 1997), as a function of the proportion between fine and coarse textures within the each sedimentary facies (C/F ratio). Through the geostatistical interpolation of the near-surface apparent electrical resistivity, representative maps of the near-surface horizontal transitions between the coarse-grained point-bar deposits (Coarse litho-textural association) and the fine-grained oxbow-lake/overbank deposits (Fine litho-textural association) can be obtained. At increasing depth, EsUs represent vertical resistivity variations related to the litho-textural contrasts within an heterogeneous and hierarchically stratified medium at the hydrostratigraphic systems scale (MAXEY, 1964).

A reliable representation of sedimentary heterogeneities can be obtained by the identification of the regional electrostratigraphic sequence through correlation of 1-D VES models with two

criteria (polarity of contrasts and uniformity of values of electrical resistivity). These criteria provide a tool to put in evidence local heterogeneities, i.e., EsUs that do not conform with the regional electrostratigraphic sequence. An improved mapping of the horizontal transitions (up to a metric scale) between EsUs can be obtained with the 2-D ERGI models. This integrated multidisciplinary approach gives the chance to reduce the disparity between the lateral and the vertical resolution of the hydrostratigraphic reconstruction, traditionally based on point data and allows to obtain a better conceptualization for the mathematical modelling of flow and transport processes in the hierarchically stratified porous media.

## Acknowledgements

*The Authors acknowledge the careful revision of this manuscript by V. Lapenna and A. Łożej. This work was financially supported by the MIUR and the University of Milano through the research projects of national interest "Integrating geophysical and geological data for modelling flow in some aquifer systems of alpine and appenninic origin between Milano and Bologna" (PRIN 2005) and "Integrated geophysical, geological, petrographical and modelling study of alluvial aquifer complexes characteristic of the Po plain subsurface: relationships between scale of hydrostratigraphic reconstruction and flow models" (PRIN 2007). Geophysical field survey was conducted with the partnership of Prof. Annalisa Zaja (Università degli Studi di Padova) and Prof. Roberto Francesc (OGS Trieste). The authors thank Marta Martinelli, Andrea Suardi, Simone Angeloni, Luca Colombera, Fabio Oriani, Davide Gorna and Gabriele Broetto for their helpful support during field acquisition and data interpretation.*

## REFERENCES

- ALFANO L. & MANCUSO M. (1996) - *Sull'applicabilità del metodo dipolare-dipolare continuo nelle ricerche idriche a media profondità in aree di pianura*. Acque Sotterranee, **13** (2/50): 61-71.
- ANDERSON M.P. (1997) - *Characterization of geological heterogeneity*. In: G. DAGAN & S.P. NEUMAN (Eds.): "Subsurface flow and transport: a stochastic approach", Cambridge University Press: pp. 23-43, Cambridge.
- ARCHIE G.E. (1942) - *The Electrical Resistivity Log as an Aid in Determining Some Reservoir Characteristics*. Trans., AIME, **146**: 54-62.
- BAINES D., SMITH D.G., FROESE D.G., BAUMAN P. & NIMECK G. (2002) - *Electrical resistivity ground imaging (ERGI): a new tool for mapping the lithology and geometry of channel-belts and valleyfills*. Sedimentology, **49**: 441-449.
- BAIO M., BERSEZIO R., BINI A., CAVALLI E., CANTONE M., MELE M., PAVIA F., LOSI E., RIGATO V., RODONDI C., SOMMARIGA M. & ZEMBO I. (2009) - *Geological and geomorphological map of the Lodi alluvial Plain: the contribution of surface geology to hydrostratigraphic reconstruction*. Epitome, **3**: 5. ISSN 1972-1552.
- BERSEZIO R. (1986) - *Studio foto geologico e geofisico per la ricostruzione dell'andamento degli antichi alvei: prima ricostruzione dei paleo-alvei della pianura fra Adda e Ticino*. Studi idrogeologici sulla pianura padana, **2**, CLUP, Milano.
- BERSEZIO R., BINI A. & GIUDICI M., (1999) - *Effects of sedimentary heterogeneity on groundwater flow in a quaternary pro-*

- glacial delta environment: joining facies analysis and numerical modeling. *Sedimentary Geology*, **129**: 327-344.
- BERSEZIO R., PAVIA F., BAIO M., BINI A., FELLETTI F. & RODONDI C. (2004) - *Aquifer architecture of the Quaternary alluvial succession of the southern Lambro basin (Lombardy, Italy)*. *Il Quaternario*, **17** (2/1): 361-378.
- BERSEZIO R., GIUDICI M. & MELE M. (2007) - *Combining sedimentological and geophysical data for high-resolution 3-D mapping of fluvial architectural elements in the Quaternary Po plain (Italy)*. *Sedimentary Geology*, **202**: 230-248.
- BINI A. (1997a) - *Problems and methodologies in the study of Quaternary deposits of the southern side of the Alps*. Geological Institute, **2** (2): 11-20.
- BINI A. (1997b) - *Stratigraphy, chronology and palaeogeography of Quaternary deposits of the area between the Ticino and Olona Rivers (Italy-Switzerland)*. Geological Institute, **2** (2): 21-46.
- BOWLING J.C., HARRY D.L., RODRIGUEZ A.B. & ZHENG C. (2007) - *Integrated geophysical and geological investigation of a heterogeneous fluvial aquifer in Columbus Mississippi*. *Journal of Applied Geophysics*, **62** (1): 58-73.
- BRATUS A. & SANTARATO G. (2009) - *The characterization of aquifers by means of resistivity investigations*. *Bollettino di Geofisica Teorica ed Applicata*, **50**: 15-28.
- CASTIGLIONI G.B. & PELLEGRINI G.B. (2001) - *Note illustrative della Carta geomorfologica della Pianura Padana*. *Suppl. Geogr. Fis. Dinam. Quat.*, **4**, 207 pp.
- DA ROLD O. (1990) - *L'apparato glaciale del Lago maggiore, settore orientale*. Ph.D. Thesis, University of Milan, 200 pp.
- DAHLIN T. (2001) - *The development of DC resistivity images techniques*. *Computer and Geosciences*, **27**: 1019-1029.
- DELL'ARCIPIRETE D., FELLETTI F. & BERSEZIO R. (2008) - *Simulation of fine-scale heterogeneity of meandering river aquifer analogues: comparing different approaches*. *geoENVVII*. Geostatistics for Environmental Applications, Springer, *in press*.
- DOMENICO P.A. & SCHWARTZ F.W. (1990) - *Physical and chemical hydrogeology*, pp. 824, John Wiley & Sons, New York.
- ENI-DIVISIONE AGIP & Regione Lombardia (2002) - *Geologia degli Acquiferi Padani della Regione Lombardia*. A cura di: C. CARCANO & A. PICCIN, pp. 130, S.E.L.C.A., Firenze.
- FARQUHARSON C.G. & OLDENBURG D.W. (1998) - *Non-linear inversion using general measures of data misfit and model structure*. *Geophysical Journal International*, **134**: 213-227.
- GOURRY J.C., VERMEERSCH F., GARCIN M. & GIOT D. (2003) - *Contribution of geophysics to the study of the alluvial deposits: a case study in the Val d'Avaray area of the River Loire, France*. *Journal of Applied Geophysics*, **54**: 35-49.
- HICKIN A.S., KERR B., BARCHYN T.E. & PAULEN R.C. (2009) - *Using Ground-Penetrating Radar and Capacitively Coupled Resistivity to Investigate 3-D Fluvial Architecture and Grain-Size Distribution of a Gravel Floodplain in Northeast British Columbia, Canada*. *Journal of Sedimentary Research*, **79** (6): 457-477, doi: 10.2110/jsr.2009.044.
- HUGGENBERGER P. & AIGNER T. (1999) - *Introduction to the special issue on aquifer-sedimentology: problems, perspectives and modern approaches*. *Sedimentary Geology*, **129**: 179-186.
- JUSSEL P., STAUFFER F. & DRACOS T. (1994) - *Transport modeling in heterogeneous aquifers, 1. Statistical description and numerical generation of gravel deposits*. *Water Resources Research*, **30**: 1803-1817.
- KELLER G.V. & FRISCHKNECHT F.C. (1966) - *Electrical methods in geophysical prospecting*, pp. 517, Pergamon Press.
- KLINGBEIL R., KLEINEIDAM S., ASPRION U., AIGNER T. & TEUTSCH G. (1999) - *Relating lithofacies to hydrofacies: outcrop-based hydrogeological characterisation of Quaternary gravel deposits*. *Sedimentary Geology*, **129** (3/4): 299-310.
- LOKE M.H. (2001) - *RES1D ver. 1.00a Beta. 1-D Resistivity, IP and SIP Modeling*. <http://www.geoelectrical.com>.
- LOKE M.H. & BARKER R.D. (1995) - *Least-squares deconvolution of apparent resistivity pseudosections*. *Geophysics*, **60** (6): 1682-1690, doi:10.1190/1.1443900.
- LOKE M.H., ACWORTH I. & DAHLIN T. (2003) - *A comparison of smooth and blocky inversion methods in 2D electrical imaging surveys*. *Exploration Geophysics*, **34**: 182-187.
- MAXEY G.B. (1964) - *Hydrostratigraphic Units*. *Journal of Hydrology*, **2**: 124-129.
- MIALI A.D. (1996) - *The Geology of Fluvial Deposits: Sedimentary Facies, Basin Analysis and Petroleum Geology*, pp. 582, Springer, Berlin.
- MUTTONI G., CARCANO C., GARZANTI E., GHIEMI M., PICCIN A., PINI R., ROGLEDI S. & SCIUNNACH D. (2003) - *Onset of Major Pleistocene glaciations in the Alps*. *Geology*, **31**: 989-992.
- NORTH AMERICAN COMMISSION ON STRATIGRAPHIC NOMENCLATURE (1983) - *North American Stratigraphic Code* Am. Assoc. Petrol. Geol. Bull. (AAPG), **67**: 841-875.
- NORTH AMERICAN COMMISSION ON STRATIGRAPHIC NOMENCLATURE (2005) - *North American Stratigraphic Code* Am. Assoc. Petrol. Geol. Bull. (AAPG), **89** (11): 1547-1591, DOI:10.1306/07050504129.
- PIERI M. & GROPPI G. (1981) - *Subsurface geological structure of the Po Plain, Italy*. Publ. 414, P.F. Geodinamica, CNR, pp. 23, Roma.
- REYNOLDS J.M. (1997) - *An Introduction to Applied and Environmental Geophysics*, pp. 796, Wiley, New York.
- SISTEMA INFORMATIVO FALDA - SIF (DIREZIONE CENTRALE RISORSE AMBIENTALI DELLA PROVINCIA DI MILANO) - [http://www.provincia.milano.it/ambiente/acqua/sotterranea\\_sif.shtml](http://www.provincia.milano.it/ambiente/acqua/sotterranea_sif.shtml).
- TELFORD W.M., GELDART L.P. & SHERIFF R.E. (1990) - *Applied Geophysics (second edition)*, pp. 770, Cambridge University Press, Cambridge.
- VEGGIANI A. (1982) - *Variazioni climatiche e dissesti idrogeologici dell'Alto Medioevo in Lombardia e la rifondazione di Lodi - Sibrum*, **16**, 199-208, Lodi.
- ZALEHA M.J., RITTER J.B. & RUMSCHLAG H.J. (2005) - *Resolving fluvial, glaciofluvial and glacial deposits using electrical resistivity ground imaging (ERGI)*. 8th International Conference on Fluvial Sedimentology, Delft, Book of Abstracts, **324**. TU Delft.



## Groundwater flow modeling supporting a remediation project within a chemical facility

*Modello di flusso della falda utilizzato nell'ambito di un progetto di bonifica di un sito industriale*

PISANI V. (\*), D'ONOFRIO S. (\*), CARLSON F. (\*\*)

**ABSTRACT** - Environmental characterization activities and hydraulic testing were conducted at a chemical plant located in Lombardy, in the upper portion of the Po Plain, in close proximity to a river. The subsoil consists of fluvial and glaciofluvial deposits (sand and gravel mixtures) about 30 m thick and hosting the unconfined aquifer, followed by mixed continental-marine deposits (sandy gravels, interbedded with silty layers) about 50 m thick, hosting a confined aquifer, which is separated from the hydrogeologic unit above by a silty and clayey level and is delimited at its bottom by marine clays representing a regional aquiclude. No further details can be provided on the geographical and geological description of the site, because of their confidential nature.

The purpose of the characterization activities, requested to comply with Italian environmental regulation, was to identify the presence and extent of suspected contamination. One of the investigated areas was a man-made basin (or basin), excavated in the central portion of the facility and used in the past to collect post-process cooling water. Chemical analyses confirmed the presence of constituents within both the sediments at the bottom and the first 0.5 m of native subsoil beneath the basin. The area, notified as contaminated to the Italian Authorities had to be remediated.

Hydrogeological tests were thus conducted to evaluate the local hydrogeological properties of the aquifer beneath the plant and set up a groundwater model to be used as a supporting tool for the remediation of the area. In fact, the bottom of the basin, which was not sealed with any impermeable layer, was located at about 2.5 m of depth and resulted below the local groundwater level, generally found at about 2.2-2.3 m below ground surface. Pumping wells were necessary to decrease the local groundwater level in order to excavate sediments and soil and restore the site by means of clean material and the construction of a concrete basin, in dry and safe conditions.

The local hydraulic properties (Transmissivity, Hydraulic Conductivity and Storativity) obtained from the interpretation of the pumping activities and the general response of the aquifer system to the hydraulic tests were used to calibrate a groundwater flow model, which was built using the

mathematical code MicroFEM®, version 3.60.66, a hybrid finite element-finite difference method for the calculation of heads.

The purpose of the model was to determine the minimum number and the location of pumping wells required to meet the project objectives (namely, impose a groundwater level necessary to conduct field works required for the site remediation at an optimized pumping rate). Based on the model's prediction, two pumping wells were actually installed and operated at the pumping rates defined after several runs of the model. The groundwater levels in the working area could be lowered to the desired level and excavation works were safely completed. The model was therefore a useful tool to support the site-specific remediation plan.

**KEY WORDS:** aquifer testing, finite element method, pumping configuration optimization, remediation, transmissivity, unconfined aquifer.

**RIASSUNTO** - Attività di caratterizzazione ambientale e test idraulici sono stati condotti presso uno stabilimento chimico situato in Lombardia, nella porzione superiore della Pianura Padana, collocato in prossimità di un fiume. Il sottosuolo dell'area è costituito da depositi fluviali e fluvioglaciali (miscele di ghiaia e sabbia) spesso circa 30 m, al cui interno si trova l'aquifero freatico. Ad essi fanno seguito depositi misti continentali e marini (ghiaie sabbiose intercalate da strati limosi) spessi circa 50 m, al cui interno si trova un acquifero confinato, separato dall'unità idrogeologica soprastante da un livello di argilla limosa e delimitato alla base da argille marine che rappresentano l'aquiclude a scala regionale. Per ragioni di riservatezza non vengono forniti ulteriori dettagli in merito all'ubicazione geografica e alla descrizione geologica del sito.

Le attività di caratterizzazione sono state condotte per identificare la presenza e l'estensione di una possibile contaminazione all'interno del sito. Tra le aree indagate era compreso un bacino artificiale, realizzato nella porzione centrale dello stabilimento e che, in passato, veniva utilizzato per raccogliere la acque di raffreddamento utilizzate nei processi industriali svolti in sito. Le analisi chimiche hanno confermato

(\*) CH2M HILL, via XXV Aprile 2 – 20097 San Donato Milanese  
(\*\*) CH2M HILL, 2525 Airpark Drive – 96001 Redding (California)

la presenza di composti chimici sia nei sedimenti al fondo che nei primi 0,5 m di terreno naturale al di sotto del bacino artificiale. L'area, notificata alle autorità italiane come contaminata, necessitava di interventi di bonifica.

Sono state successivamente svolte delle prove idrauliche allo scopo di valutare le proprietà idrogeologiche dell'acquifero nell'area dello stabilimento, e sviluppare un modello idrogeologico della falda da utilizzare come strumento decisionale nell'ambito delle operazioni di bonifica pianificate per il sito. Infatti, il fondo del bacino artificiale, non impermeabilizzato, era posto a circa 2,5 m di profondità e risultava più basso di circa 0,2-0,3 rispetto al livello medio di falda. Era dunque necessario utilizzare dei pozzi di pompaggio per deprimere localmente il livello della falda in modo da poter eseguire, in condizioni di sicurezza e all'asciutto, attività di scavo per rimuovere i sedimenti e il terreno naturale e ripristinare il sito mediante la stesura di terreno pulito e la costruzione di una vasca di cemento.

Le proprietà idrauliche locali (trasmissività, conducibilità idraulica e coefficiente di immagazzinamento) ottenute dall'interpretazione delle prove idrauliche e la risposta in generale dell'acquifero ai test condotti sono state utilizzate per la calibrazione del modello idrogeologico della falda, realizzato utilizzando il codice matematico MicroFEM© 3.60.66, che utilizza un metodo ibrido (elementi finiti-differenze finite) per il calcolo del livello potenziometrico.

Lo scopo del modello era determinare il numero minimo di pozzi di pompaggio, la loro ubicazione ideale e la portata ottimale di emungimento, necessari a raggiungere gli obiettivi del progetto, cioè ad abbassare il livello della falda in modo da poter svolgere le attività richieste per la bonifica del sito.

In base alle risposte fornite dal modello sono stati perciò installati due pozzi di pompaggio, emunti alle portate indicate a seguito di diverse iterazioni del modello. È stato così possibile abbassare la falda al di sotto del bacino artificiale fino a raggiungere il livello desiderato per poter eseguire le operazioni di scavo e rimozione in condizioni di sicurezza e all'asciutto. Il modello si è perciò rivelato uno strumento molto efficace a supporto delle attività di bonifica pianificate per il sito.

**PAROLE CHIAVE:** acquifero non confinato, bonifica, metodo di calcolo agli elementi finiti, ottimizzazione dello schema di pompaggio, test di pompaggio, trasmissività.

## 1. - INTRODUCTION AND STUDY - LIMITATIONS

The present paper describes a case-study of groundwater modeling applied to the remediation of a contaminated site identified inside a chemical facility, operating in Lombardy since the late sixties.

After the direct investigation results confirmed the presence of chemical compounds above regulatory standards in both in the subsoil and within groundwater, the site was notified to the Italian Authorities as requested by the environmental regulation.

During a formal meeting (*Conferenza di Servizi*) the characterization activities conducted at the site were discussed and a series of prescriptions were made by the Authorities, including the execution of additional investigations and the remediation of the contaminated areas.

As part of the remediation, excavation activities were required in an area (a man-made basin) where contamination was found in the saturated portion of subsoil; groundwater level had to be locally decreased to allow remediation of the subsoil. Consequently, a groundwater model was developed in order to design a suitable pumping scheme. In addition to the definition of number of pumping wells and optimization of pumping rate, however, the groundwater flow model was also used as a tool to minimize both the interferences with production activities conducted at the facility and costs related to the site remediation activities.

Given the short timing previewed by the law for the preparation of a Preliminary Remedial Design, a detailed study of the hydrogeological conditions of the unconfined aquifer could not be conducted. Time and cost constraints, unfortunately, represented one of the drivers in the groundwater flow model development; the accuracy and precision of the model's prediction, however, were considered satisfactory under the remediation perspective and allowed for the achievement of the overall project goals, as the excavation activities conducted as part of the remediation, could be conducted under safe and dry conditions.

## 2. - SITE SETTING AND STUDY AREA DESCRIPTION

The investigation site is a chemical facility, extending over an area of about 160,000 m<sup>2</sup> and located in Lombardy, within the northern portion of the Po Plain and in proximity of a river (that will be indicated here as River Alpha).

In order to accomplish with Italian environmental regulations requirements and as a response to local Authorities requests, an environmental characterization study was conducted across the entire facility by means of direct investigations, in order to evaluate the presence, magnitude and extent of contamination related to current and past activities conducted by the plant.

Given the production history, the type and mobility of the chemical compounds of concern and the local geological features, the investigations mainly focused on the shallow portion of subsoil and included the execution of soil borings (mainly drilled to 3-3.5 m of depth, to characterize the unsaturated soil) and the installation of 2" and 3" monitoring wells, generally advanced to a depth of 10-15 m and screened in the upper portion of the unconfined aquifer.

Field investigations described above, combined with the findings of a literature search conducted at a wider scale (logs of deep public and private wells

retrieved at the local Municipality) helped identifying the local geologic features of the subsoil between ground surface and about 45 m below ground surface, which consists of coarse-grained sediments, mainly gravels and sandy gravels, locally interbedded with thin layers of silt. The geological sequence reconstructed based on the logs of the deep wells presented several features similar to those described

for the Po river plain by regional studies (AIROLDI & CASATI, 1989; AIROLDI *et alii*, 1997; BARNABA, 1998) and summarized by GIUDICI *et alii*, 2000.

In detail, at a regional scale the following stratigraphic sequence, here presented from the surface down (fig. 1), can be described:

- Upper unit composed of sandy gravels corresponding to recent alluvial and fluvio-glacial sedi-

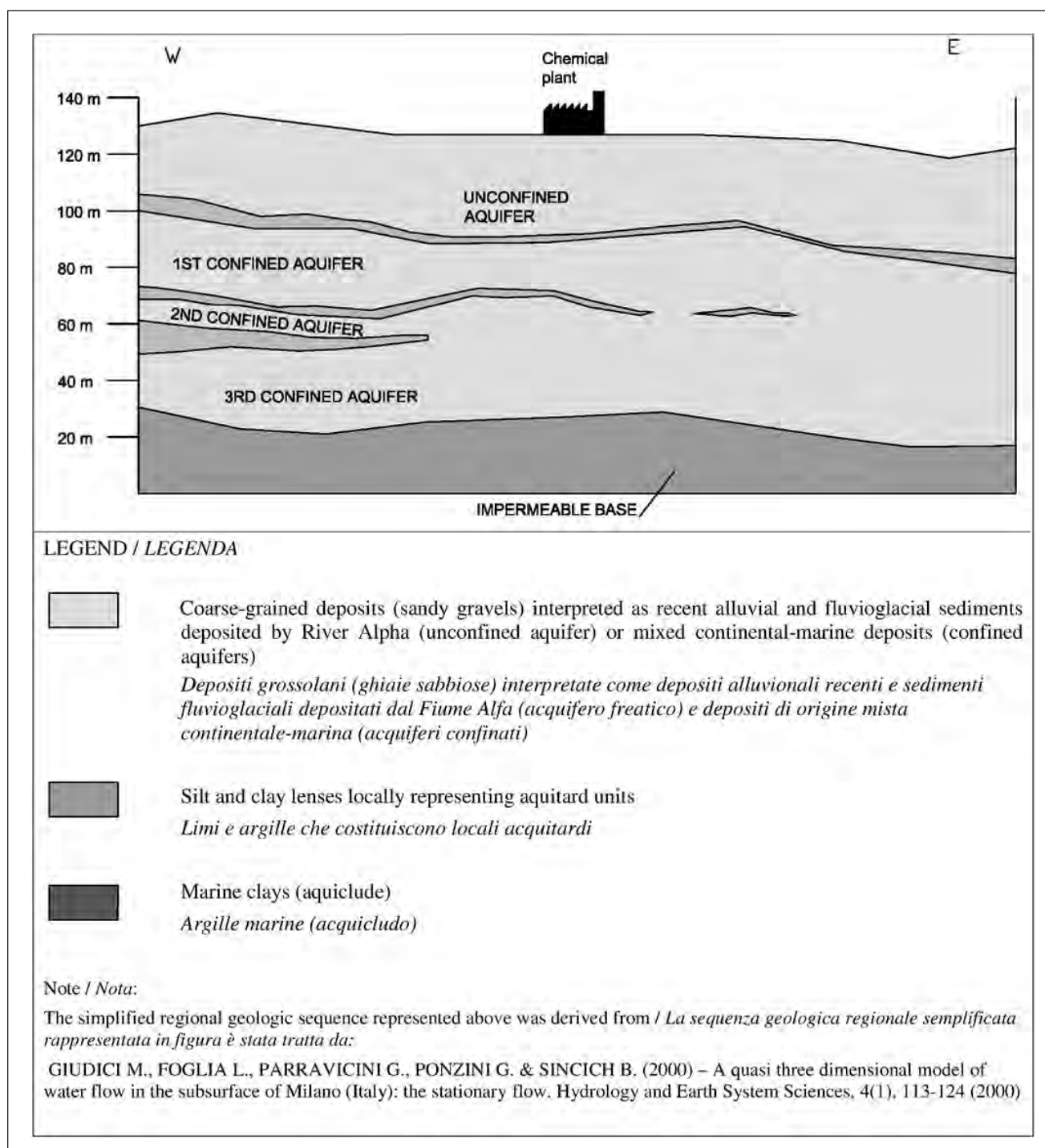


Fig. 1 - Regional stratigraphic sequence.  
- *Successione stratigrafica regionale.*



ments deposited by River Alpha (upper Pleistocene-Holocene). These deposits host an unconfined aquifer. The lower limit of this unit is an erosive surface, located at a depth ranging between 30 and 40 meters;

- Second unit, composed of mixed continental-marine deposits, consisting of sandy gravel layers separated by silt and clay lenses, which subdivide the unit into minor sub-units from an hydrogeological point of view. Two superimposed confined aquifers are identified. The overall thickness of this unit varies between 50 and 90 meters; and

- Basal unit composed of silty-clayey sediments deposited in a marine environment during the lower Pleistocene and Pliocene; these sediments represent the regional aquiclude.

At a regional scale, as confirmed by a piezometric surface map obtained at the local Municipality, groundwater in the unconfined aquifer flows from north to south; groundwater level measurements conducted at the facility indicated that at the local scale the unconfined aquifer flows from northwest to the southeast, with an average hydraulic gradient of 0.0035 beneath the facility, and is locally drained by the River Alpha.

The depth to groundwater at the site ranges from 1.5 to 4.8 m below ground surface (bgs). Within the basin's area the average depth to groundwater is in the order of 2.2 m bgs; the water table is, thus, above the actual bottom of the basin.

The facility currently includes a network of sampling locations used to monitor the local groundwater quality (fig. 2) and consisting of:

- 4 piezometers and 23 monitoring wells screened in the upper portion of the unconfined aquifer (between 3 and 10 m bgs);

- one monitoring well screened in a wider portion of the unconfined aquifer (between 2.5 and 15.5 m bgs); and

- one monitoring well screened in the upper portion of the first confined aquifer (between 47.5 and 52.5 m bgs).

In addition, four pumping wells, P1, P3, P4 and P5 (fig. 2), mainly screened in the confined aquifer, are used by the site for industrial water supply.

The analytical results of collected samples identified the following environmental conditions:

- Groundwater contamination identified in the unconfined aquifer only (sample taken from production wells presented concentrations below the method detection limits), mainly affecting the downgradient areas of the facility;

- A "hot spot"-type subsoil contamination, identified in the shallow layers (within 2 m of depth) of unsaturated soil, at selected locations only, whose position was related to the presence of productive areas or warehouses.

Based on a detailed review of the operational processes formerly conducted in the facility, the presence of contamination within a man-made basin excavated in the central portion of the facility was suspected and direct characterization activities, conducted after the preliminary investigation on soil and groundwater, confirmed that concentrations of chemical compounds detected in the basin's sediments and in the first meter of native soil were above regulatory standards.

The man-made basin, 35 m wide by 35 m long and 2.5 m deep, covering a surface of about 1200 m<sup>2</sup> is located in the central portion of the facility. Even though the basin currently represents a reservoir of clean water kept for fire-fighting purposes, in the past it received cooling water used for the industrial processes, which was discharged into the basin before being channeled outside the facility by means of a pipeline connected to an external canal.

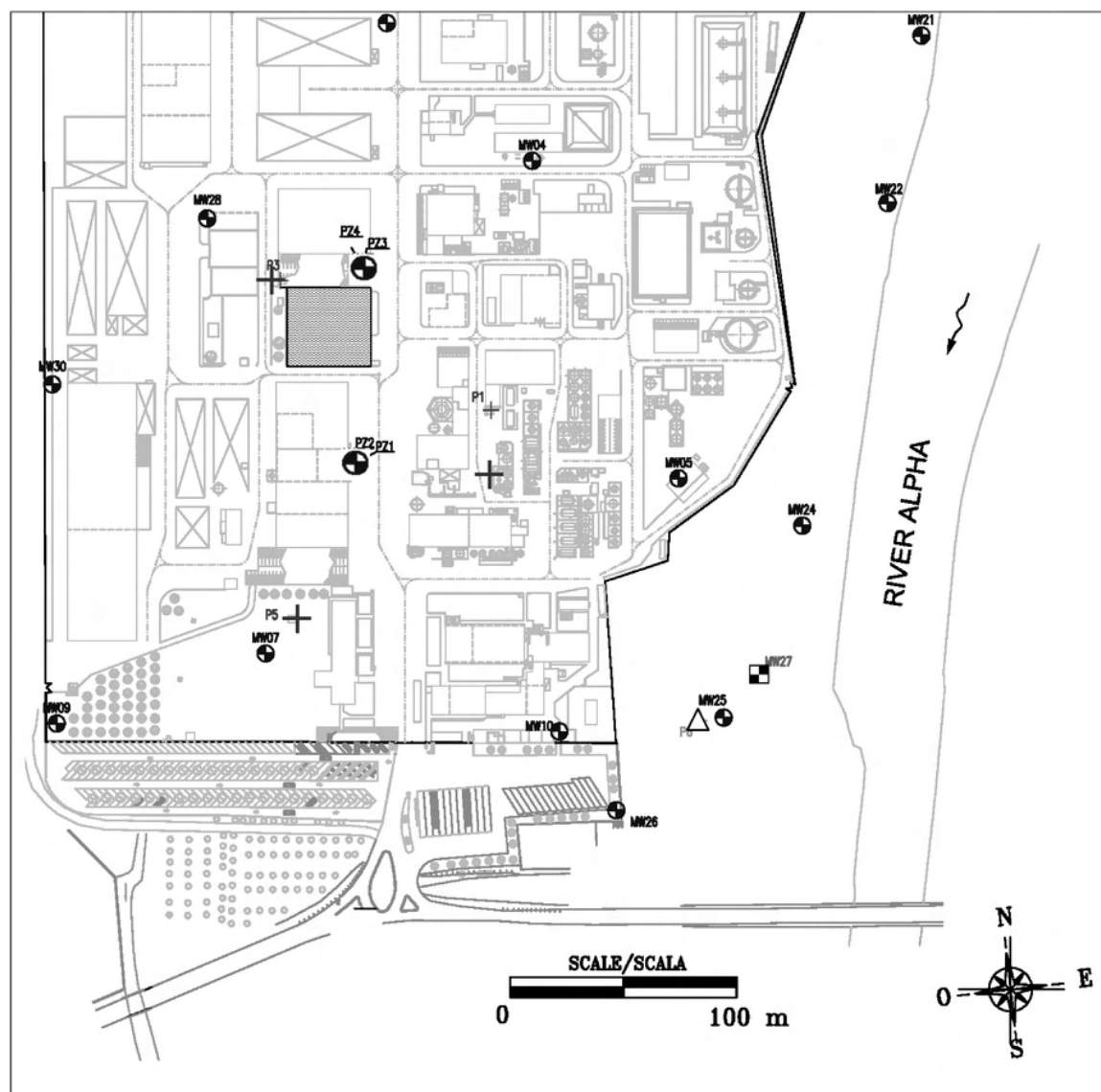
The bottom and walls of the basin were represented by the boundaries of the excavation made to create the basin's depression. Native soil was not protected by any kind of impermeable layer. Therefore, any constituent present in the post-process cooling water was free to accumulate first in the sediments at the bottom of the basin, infiltrate into the natural soil and finally leach into the groundwater. Also, due to the relative depths of the bottom of the basin and the groundwater table (2.5 and 2.2 m below ground surface, respectively), the unconfined aquifer resulted always in contact with the basin's sediments and water. Under normal site use conditions, the basin was about 75% full of water (thus the basin surface resulted about 0.6-0.7 m bgs but nearly 1.7 m above the groundwater level. The basin acted as a recharge source.

### 3. - THE PROBLEM

Soil sampling within the basin indicated the presence of chemical compounds in both the sediments at the bottom and in the upper 0.3-0.4 meters of native soil beneath the basin. A remedial action, as requested by the Italian Authorities during a *Conferenza di Servizi* meeting, was therefore considered necessary and the planned intervention included the removal of the contaminated portion of subsoil.

Because of the relative depths of the bottom of the basin (2.5 m bgs) and the groundwater table in the study area (2.2 m bgs), it was deemed necessary to temporarily lower the groundwater level, in order to allow excavating and removing the soils in safe and dry conditions.

For the purpose of designing the dewatering system, a groundwater flow model of the site was



## LEGEND / LEGENDA






-  Piezometers (PZ1 – PZ4, 1”) and monitoring wells (MW4 – MW32, 3”) screened in the upper portion of the unconfined aquifer (between 3 and 10 m bgs) / *Piezometri (PZ1 – PZ4, 1”) e pozzi di monitoraggio (MW4 – MW32, 3”) fessurati nella porzione superiore dell’acquifero freatico (tra 3 e 10 m dal p.c.)*
-  Monitoring well (P6, 12”) screened in a wider portion of the unconfined aquifer (between 2.5 and 15.5 m bgs) / *Pozzo di monitoraggio (P6, 12”) fessurato in una porzione più estesa dell’acquifero freatico (tra 2,5 e 15,5 m dal p.c.)*
-  Monitoring well (MW27, 4”) screened in the upper portion of the first confined aquifer (between 47.5 and 52.5 m bgs) / *Pozzo di monitoraggio (MW27, 4”) fessurato nella porzione superficiale del primo acquifero confinato (tra 47,5 e 52,5 m dal p.c.)*
-  Production wells (P1 – P5) / *Pozzi produttivi (P1 – P5)*
-  The basin area / *L’area del bacino*

Fig. 2 - Groundwater monitoring network within the chemical plant.  
- Rete di monitoraggio della falda all'interno dello stabilimento chimico.

used as a supporting tool for the design of pumping wells required to meet the project objectives, which included:

- For the basin's area: quantification of the amount of water that had to be extracted to decrease the groundwater surface to the desired level (about 0.6-0.7 m below the undisturbed head conditions), definition of the minimum number and location of pumping wells necessary to obtain the desired groundwater level and optimization of the pumping rates;

- For the area downgradient of the basin and the production areas: evaluate the effectiveness of existing pumping wells on the hydraulic containment of the upper portion of the unconfined aquifer, especially in the southeastern corner of the facility and identify a pumping wells configuration (position and pumping rate) possibly required for the hydraulic containment.

In addition, the following site constraints had to be taken into consideration:

- The number and position of pumping wells required for the basin's remediation had to be selected so that interferences with the plant's operations could be minimized, avoiding interruptions of production activities or damages to underground utilities, and the overall remediation costs could be affordable;

- Groundwater extracted in view of the remediation, possibly contaminated by the chemical compounds leaching from the sediments in the basin, had to be discharged into the on-site wastewater treatment plant prior to being discharged off site. The total amount of groundwater that the wastewater treatment plant was able to process on a daily basis could not be exceeded; a small reduction in the facility's inflow into the plant was agreed to allow for the treatment of the extracted groundwater (which, however, could not exceed 250 m<sup>3</sup>/h);

- The design of the pumping system was required in a very short time, in order to respond to the local Authorities prescriptions within the times established by the law.

#### 4. - THE GROUNDWATER FLOW MODEL

A groundwater flow model of the aquifer was constructed, using the finite element-finite difference code MicroFEM© 3.60.66 (HEMKER C.J. & DE BOER R.G., 1997), which is a hybrid finite element-finite difference method for the calculation of heads. Given the time and budget constraints, a thorough hydrogeological study could not be completed in view of the implementation of the groundwater model.

The modeled area resulted about 7 km wide and 8 km long; the purpose of having such a large area was to minimize the mathematical effects of model boundaries in the area of interest (the facility) and also to include all available hydrogeological features (basically, the Alpha River and regional potentiometric surface contour lines, retrieved from a local Municipality groundwater surface map) to be used as fixed head boundary conditions, in order to minimize assumptions on groundwater flow at the site. Finally, the groundwater flow model was intended as a decisional tool to be possibly used in the future by the facility; therefore, the entire facility boundary was to be covered by the model to allow for any future simulations and hydraulic testing planning and development.

The modeled area was defined by an irregular grid of nodes, with different spacing distances (ranging from 300 meters to 5 meters inside the facility), which were selected in order to have a sufficient detail within the facility, where site-specific data (though pellicular) on geological features and hydrogeological conditions could be obtained by direct observation, and minimize errors at the boundaries, where regional-scale data, retrieved from literature, had to be used.

Given the limited dimensions of the study area (1200 m<sup>2</sup>) and the local geological conditions in relation to a quite uniform regional setting and considering the construction schemes of the existing monitoring wells (which were defined for other purposes than investigating the aquifer for hydrogeological studies), the groundwater flow model had to replicate a case that can be simplified as a horizontal formation of constant thickness, infinite extent, discharged by partially penetrating wells, with finite radius and constant discharge rate.

The numerical code MicroFEM© 3.60.66 was applied to simulate the effects of partial penetration on groundwater flow. As described in the paper presented by Hemker (HEMKER C.J., 1999) this was one of the possible applications of the numerical code that is a hybrid finite element-finite difference method for the calculation of heads (HEMKER C.J., 1997).

The theory and solution to account for the effect of partial penetration on flow in a homogeneous unconfined aquifer flow problem, as originally developed by NEUMANN (1974), and extended by MOENCH (1993, 1996), is applied in the paper presented by HEMKER (1999), who suggests an integrated analytical and numerical solution of the Laplace transform.

Since on-site production wells, screened in the confined aquifer, were used to conduct part of the hydraulic testing, the presence of confined layers was deemed necessary to replicate the main hydro-



geological conditions.

The following configuration, which in the end was confirmed to adequately replicate field observation with the model, was used to model the area in the subsurface (fig. 3):

- a first layer, 20 m thick, representing the saturated portion of the unconfined aquifer, where the

majority of the monitoring wells installed at the site is screened;

- a second layer, 50 m thick, represents a lower portion of aquifer, locally confined by discontinuous clayey layers, where the site pumping wells have their screened section;

- the third layer (40 m thick) representing the

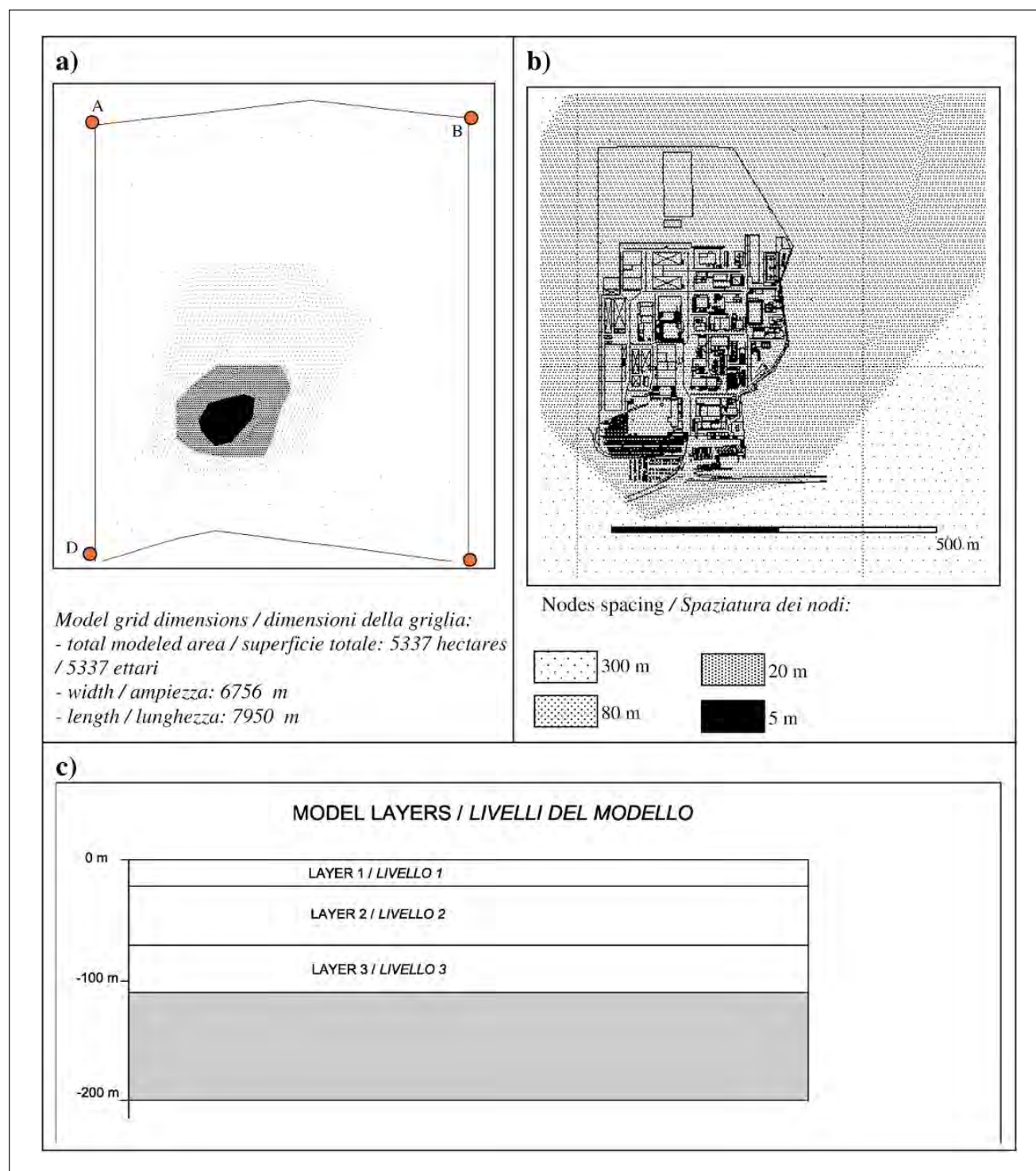


Fig. 3 - Groundwater flow model configuration. a) Model grid dimensions, b) Model grid: detail of the chemical facility area, c) Model layers.  
- Configurazione del modello di flusso della falda. a) Dimensioni della griglia del modello, b) Griglia del modello: dettaglio dell'area dello stabilimento chimico, c) Livelli del modello.

confined aquifer. It is estimated from regional geology that the base of model layer 3 corresponds to the top of the regional aquiclude (marine clay layer).

Hydraulic properties, especially for the portion of the model more distant to the facility, with larger nodes spacing, were first assigned to the different layers based on literature values of hydraulic conductivity (GIUDICI *et alii*, 2000) and corresponded to the following:

- First layer:  $T = 0.04 \text{ m}^2/\text{s}$  ( $3456 \text{ m}^2/\text{day}$ );
- Second layer:  $T = 0.065 \text{ m}^2/\text{s}$  ( $5616 \text{ m}^2/\text{day}$ );
- Third layer:  $T = 0.0104 \text{ m}^2/\text{s}$  ( $898.56 \text{ m}^2/\text{day}$ ).

Fixed head conditions (Dirichelet type) were assigned taking into consideration the regional groundwater surface map retrieved at the local Municipality, where groundwater levels for the Alpha River were also indicated. In order to calibrate model and refine simulations within the facility area, hydraulic testing were conducted at the site.

## 5. - AQUIFER TESTING

The aquifer tests conducted at the site aimed at determining the local hydrogeological features and the response of the hydrogeological system to pumping activities; these data were necessary to define the specific conditions for the hydraulic containment, to evaluate whether these conditions are achieved with current pumping rates and to optimize the number of pumping wells necessary to reduce the groundwater surface elevation at the basin's area in view of its remediation.

Different types of testing were conducted, in the following order: at two selected locations a step drawdown test was conducted to identify the optimal pumping rate for each well. A constant discharge test followed at both locations, operating the wells at the pumping rates suggested by the previous test. Finally, a pulse test (or interference test) was conducted, using the on-site pumping wells normally used by the facility for industrial purposes. Each test will be described below.

### 5.1. - STEP DRAWDOWN TESTS AND COSTANT DISCHARGE PUMPING TEST

In order to obtain hydraulic parameters of the aquifer, step drawdown tests (SDTs) and pump and recovery tests (PRTs) were conducted in two wells: P1 and P6. The first well is located in proximity of the basin's area, while the second well was installed in a position suggested by the model as a good location for a future hydraulic containment system.

The SDT for P1 (tab. 1) had three 120 minute steps, while in test conducted on P6, six steps were

Tab. 1 - *Step drawdown test conducted on P1 and P6.*  
- Prova a gradini condotta nei pozzi P1 e P6.

Step drawdown Test at P1			
Step	Pumping rate	Time length of the step	Notes
1	69.3 m <sup>3</sup> /hour	2 hours	drawdown was measured by means of a manual water level indicator and was recorded at intervals of 5, 10, 15, 20, 30 40, 60, 90 and 120 minutes
2	108.9 m <sup>3</sup> /hour	2 hours	
3	144.7 m <sup>3</sup> /hour	2 hours	
Step drawdown Test at P6			
1	56.2 m <sup>3</sup> /hour	1 hour	drawdown was measured by means of a manual water level indicator and was recorded at intervals of 5, 10, 15, 20, 30 40, and 60 minutes
2	108 m <sup>3</sup> /hour	1 hour	
3	136.2 m <sup>3</sup> /hour	1 hour	
4	180 m <sup>3</sup> /hour	1 hour	
5	221.7 m <sup>3</sup> /hour	1 hour	
6	252 m <sup>3</sup> /hour	1 hour	

applied, each with a duration of one hour.

The constant discharge pumping tests (PRTs) were then conducted for both P1 and P6, at the optimal pumping rates, graphically determined for both wells (fig. 4 for P1 and fig. 5 for P6).

A pumping phase was first conducted with duration of 2 days for P1 and 2.8 days for P6, and the corresponding drawdown was measured at significant locations; a recovery phase (one day for P1, 3.1 days for P6), during which the rise of groundwater level was observed at the end of pumping activity, was then completed.

### 5.2. - PULSE TEST

An interference test (or pulse test) was also conducted and consisted of the observation of groundwater level fluctuations at selected monitoring locations to evaluate the response to different pumping schemes (tab. 2), obtained by turning on and off the existing site production wells. The objective of the test was to verify the effectiveness of pumping system present on-site on hydraulic containment and assess the existence of any hydraulic connections between the unconfined aquifer and the confined layers below (since most of the pumping wells resulted to be screened in both types of unit).

This type of pulse testing (using the normal fluctuations in pumping from supply wells) represents a very low cost method of determining aquifer properties because dedicated wells are not needed and water supply needs of the facility can be ade-

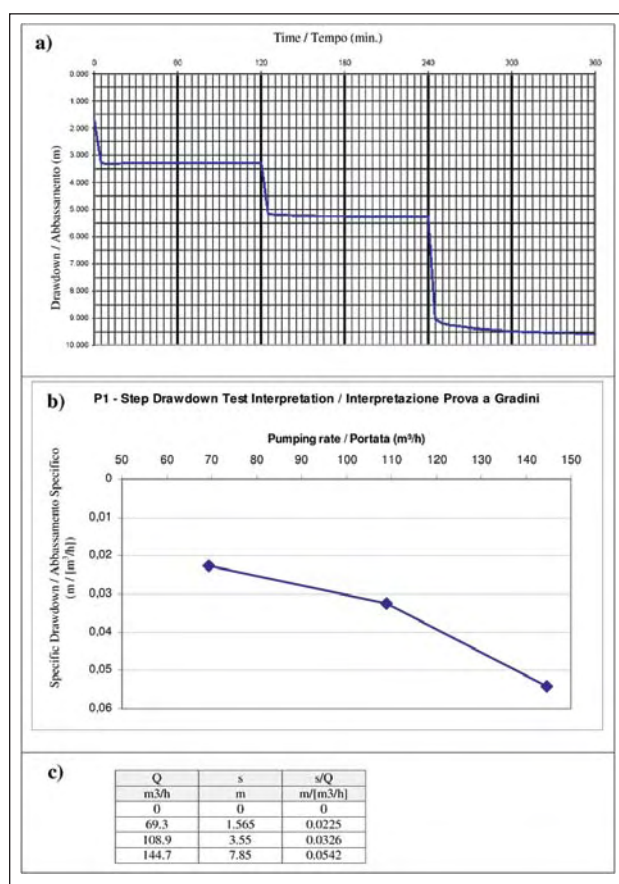


Fig. 4 - Step Drawdown Test (SDT) in pumping well P1. a) Field data: drawdowns vs. time, b) Interpretation of SDT, c) Flow rates, drawdown and specific drawdown measured during the test.

- Prova di portata a gradini nel pozzo produttivo P1: a) Dati di campo: abbassamenti rispetto al tempo, b) Interpretazione della prova a gradini, c) Portate, abbassamenti e abbassamenti specifici misurati durante la prova.

quately satisfied, avoiding an interruption of pumping, possibly required by other types of testing.

The observation points were selected to monitor the central portion of the site, around the three production wells P1, P3 and P5, where the water level response to changes in pumping rates was expected to be detectable and where most of the hydrogeological data gaps were identified. In addition, observation wells were selected in the southeastern portion of the site including monitoring locations, in order to evaluate the influence of the site pumping activities and the extent of the capture zone created by the existing production wells with the current pumping rates.

Groundwater level fluctuations were recorded by means of pressure transducers, with readings taken at 1-minute intervals, and by manual measurements, taken at a 15-minute or 30-minute frequency depending on the location.

The pulse-test was implemented not only to estimate the Zone of Capture (ZOC) of existing production wells and evaluate the preliminary data to quantify the response of the unconfined aquifer to

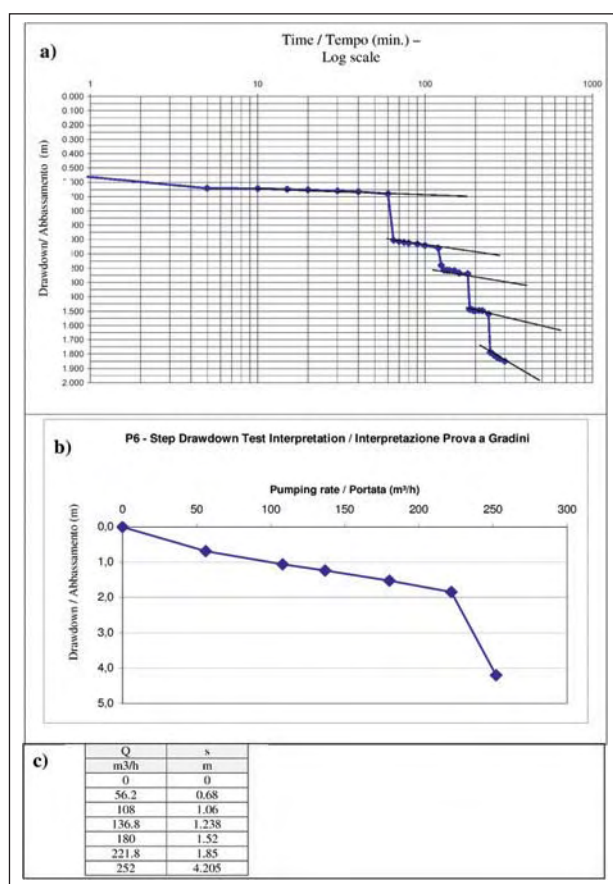


Fig. 5 - Step Drawdown Test in well P6. a) Field data: drawdowns vs. time, b) Interpretation of SDT, c) Flow rates and drawdowns measured during the test.

- Prova di portata a gradini nel pozzo P6. a) Dati di campo: abbassamenti rispetto al tempo, b) Interpretazione della prova a gradini, c) Portate e abbassamenti misurati durante la prova.

different pumping schemes, but also to evaluate the relationships between the unconfined aquifer and the confined aquifer and verify whether the hydraulic control of the unconfined aquifer was effective to guarantee containment also in the southeastern portion of the site.

### 5.3. - HYDRAULIC TESTS INTERPRETATION

The outcomes of the STD and PRT tests were analyzed using the software Aqtesolv to evaluate the local aquifer properties. The average transmissivity (T), vertical resistance (c) and storativity (S) values estimated by the interpretation of the test, applying the Neumann delayed-yield solution (Neumann, 1972, 1975), were initially obtained from the interpretation of the pumping, and recovery tests conducted in P1 and P6 were processed using a software application specifically dedicated to the interpretation of aquifer tests in multi-layer systems, MLU (Multi-Layer Unsteady state).



Tab. 2 – *Pulse Test operation scheme.*  
- Schema operativo del Test a Impulsi.

Step	Time	P1		P3		P4		P5	
		ON/ OFF Pumping rate (m <sup>3</sup> /h)		ON/ OFF Pumping rate (m <sup>3</sup> /h)		ON/ OFF Pumping rate (m <sup>3</sup> /h)		ON/ OFF Pumping rate (m <sup>3</sup> /h)	
		Day 1	Day 2	Day 1	Day 2	Day 1	Day 2	Day 1	Day 2
1	12:00 ÷ 13:00	114	116	0	0	168	134	0	0
2	13:00 ÷ 14:00	112	115	115	180	161	137	180	190
3	14:00 ÷ 15:00	111	114	109	182	163	134	181	188
4	15:00 ÷ 16:00	0	0	165	180	160	135	180	185
5	16:00 ÷ 17:00	0	0	173	183	160	135	0	0
6	17:00 ÷ 18:00	114	113	174	183	162	133	0	0
7	18:00 ÷ 19:00	112	111	145	149	0	0	0	187
8	19:00 ÷ 20:00	0	0	137	149	0	0	185	186

Subsequent optimization phases were conducted until a good match between simulated and observed drawdown could be found (fig. 6, fig. 7).

The values obtained for the three layers considered in MLU resulted:

- Layer 1:  $T = 2453 \text{ m}^2/\text{day}$ ,  $S = 0.3$ ;
- Layer 2:  $T = 1200 \text{ m}^2/\text{day}$ ,  $c = 14 \text{ days}$ ,  $S = 6 \times 10^{-5}$ ;
- Layer 3:  $T = 960 \text{ m}^2/\text{day}$ ,  $c = 23 \text{ days}$ ,  $S = 6 \times 10^{-5}$ .

The storativity coefficients defined for layers 2 and 3 resulted in the range of values typical of confined aquifers. Since the second layer represents a deep portion of the aquifer that can be locally confined by discontinuous clayey layers, and the third layer represents the confined aquifer delimited at its bottom by marine clays, the result was considered satisfactory.

The layers considered in MLU replicated those adopted for the large-scale groundwater flow model; therefore, the values reported above were finally used in the large-scale groundwater flow model. The optimized values were assigned only to

the nodes of the unconfined aquifer, corresponding to the area of influence of the wells (considering the position of the observation wells where pumping caused drawdown effects, though limited). For remaining nodes of the unconfined aquifer and for remaining layers, the initial  $T$  values were not modified. The groundwater model developed using the MicroFEM©, version 3.60.66 mathematical code was then calibrated trying to simulate the potentiometric surface contour under undisturbed conditions and to replicate both the results of the pulse test and the PRT. Several runs were conducted until a good match between field observations, tests results, and the software simulations was obtained (fig. 8).

Once calibrated, the model was used to both evaluate the hydraulic containment under current conditions, and to define the best pumping scheme (number of wells and pumping rates) required for the dewatering of the basin's area.

## 6. - GROUNDWATER FLOW MODEL APPLICATIONS

### 6.1. - HYDRAULIC CONTAINMENT EVALUATION

A groundwater elevation map of the unconfined aquifer under undisturbed conditions was first obtained considering measured data from monitoring wells only (pumping wells data were excluded because no sufficient data were available to delineate, by interpolation, the drawdown cone in the pumped aquifer).

The following observations were made:

- two production wells were pumping at the time of measurement (P3 and P4), as indicated by the water levels in the wells;

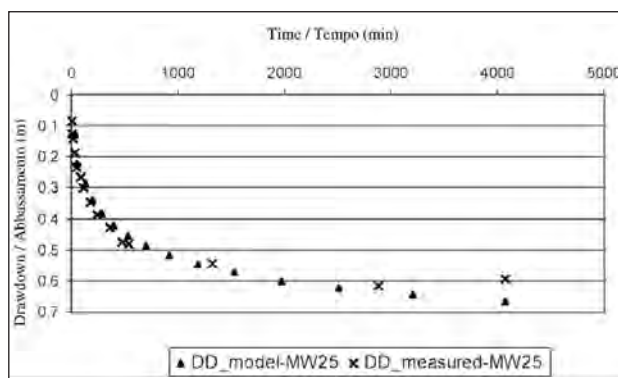


Fig. 6 - Comparison between simulated and measured drawdown during constant discharge (Pump and Recovery Test – PRT) at P6.  
- Confronto tra gli abbassamenti simulati e quelli osservati durante le prove di lunga durata al pozzo P6.

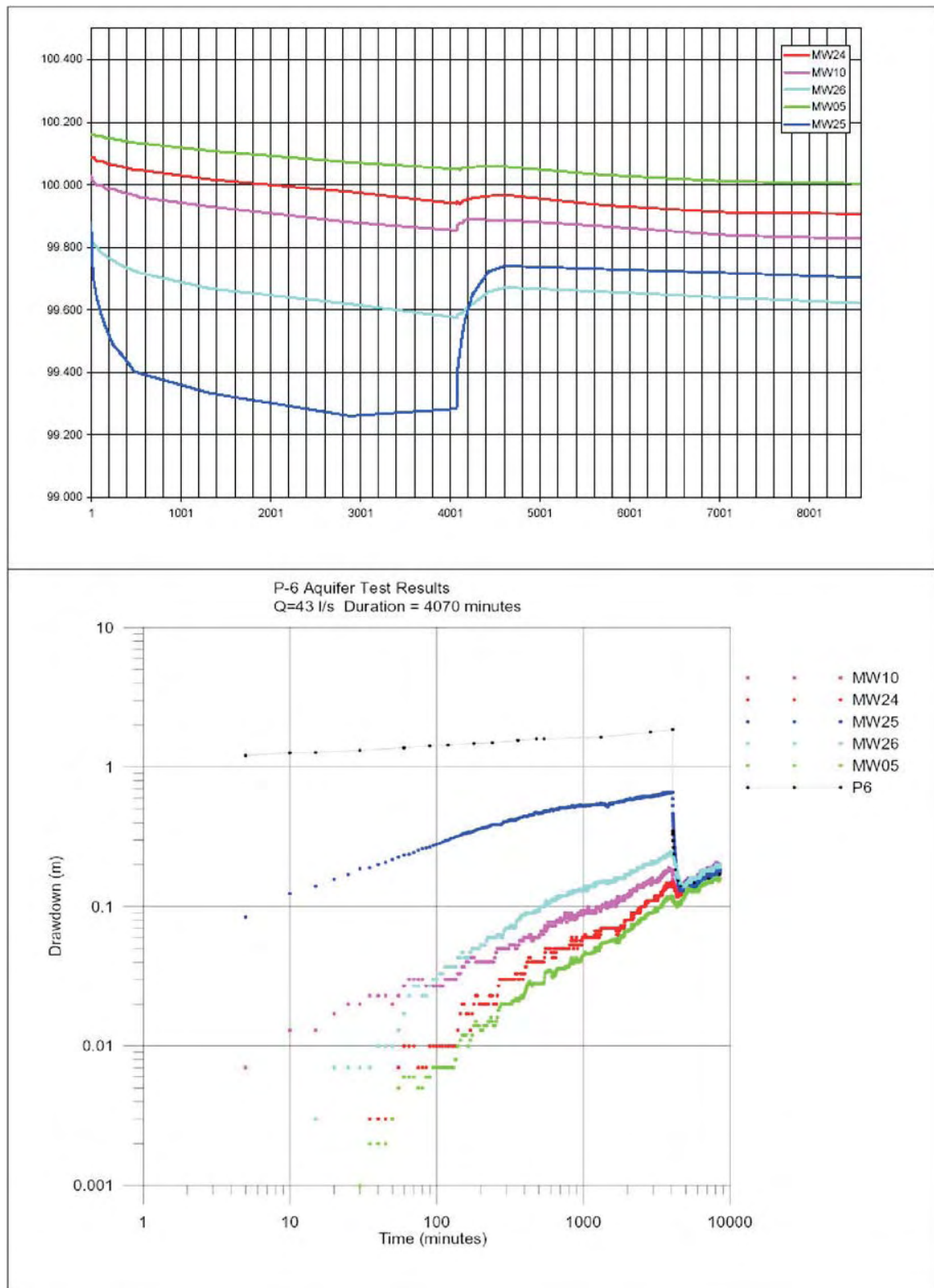


Fig. 7 - Comparison between measured drawdown (above) and simulated drawdown (below) – PRT interpretation using the MLU software.  
 - Confronto tra gli abbassamenti osservati (in alto) e quelli simulati (in basso) – Interpretazione della prova di lunga durata mediante il software MLU.

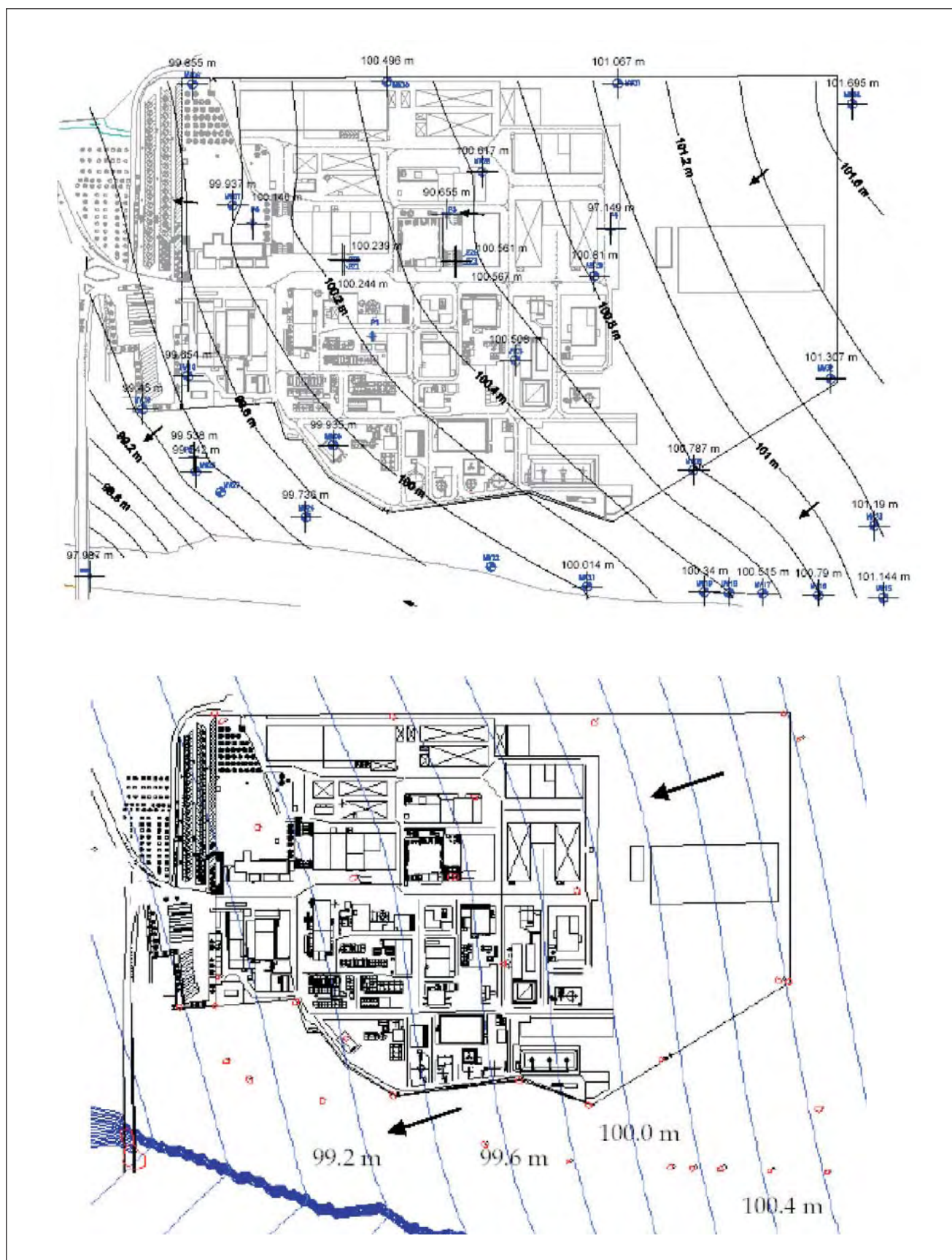


Fig. 8 - Comparison between measured data (above) and simulated data (below) – Groundwater surface map for the unconfined aquifer.  
 - Confronto tra dati misurati (in alto) e simulati (in basso) – Carta potenzimetrica dell'acquifero freatico.



- based on the interpolation, the pumping activity seemed to have a minimum effect on the upper unconfined aquifer in the central portion of the facility (as indicated by the inflections in the potentiometric surface contour lines); and

- the southeastern corner of the facility was not affected by the pumping wells.

Subsequently the outcomes of the pulse-test, which was conducted to verify whether different pumping schemes could modify the response in the unconfined aquifer, were considered. The results are discussed below:

- Monitoring well MW7 was the only location where groundwater level fluctuations presented a clear correlation with pumping activity of well P5 (about 20.5 m distant). The maximum drawdown, associated with an average pumping rate of 180 m<sup>3</sup>/hour, was 0.115 m. The effects of pumping at other production wells on MW7 seemed to be negligible (0.005 m);

- Groundwater level fluctuations measured in the central portion of the site, especially in the piezometer pairs PZ1-PZ2 and PZ3-PZ4 located in proximity of the basin's area, seemed to be the result of pumping activity of P3 and P5; the combined effects of the two pumping wells created a maximum drawdown in the order of 0.02-0.03 m, with a maximum response of about 0.06 m. The influence of P1 on observed drawdowns was quite limited and was not consistent and clearly defined: for instance, a rise in the level, apparently associated with the interruption of pumping activities in P1, can be observed in the intermediate portion of the test in the piezometer pairs. However, different response to pumping interruption were observed at the end of the pulse test in the two days of measurements;

- The southeastern portion of the site seemed to be scarcely or not influenced by the pumping activities at the site; the groundwater level fluctuations measured at the different monitoring wells (on average 150 to 250 m distant from the pumping wells) presented time-trends independent at each location, and not corresponding to on/off cycles of the site pumping wells;

- In summary, the pulse testing showed that the effects of normal pumping operation have only a small and local effect on groundwater levels in the shallow aquifer.

As a subsequent step, the site groundwater flow model was used to evaluate the extent of the capture zone created by the site production wells. In order to achieve this goal, the software was used to draw the flowlines (the ideal paths of groundwater particles in the subsoil) corresponding to the following pumping configuration (using pumping

rates that provided the highest response during the pulse test):

- P3: 160 m<sup>3</sup>/hour (3840 m<sup>3</sup>/day);
- P4: 160 m<sup>3</sup>/hour (3840 m<sup>3</sup>/day);
- P5: 180 m<sup>3</sup>/hour (4320 m<sup>3</sup>/day).

All of the above indicated wells are screened in the lower portion of the unconfined aquifer as well as in the confined aquifer. The flowlines drawn by the software indicated that the pumping is not containing the upper portion of the unconfined aquifer (fig. 9).

As a further step, the model was run including in the pumping scheme the newly installed well P6, which is screened in the upper portion of the unconfined aquifer, considering a flow rate similar to the one applied during the PRT (140 m<sup>3</sup>/hour).

As a final result, it was concluded that:

- the hydraulic containment of the southeastern corner of the site can be achieved using well P6, if it is operated at a pumping rate similar to the one adopted for hydraulic testing (140-150 m<sup>3</sup>/hour, corresponding to about 43 l/s). At lower pumping rates (2500 m<sup>3</sup>/day – 30 l/s), the hydraulic containment of the southeastern corner (possibly receiving chemicals released in groundwater at the basin's area) would not be complete;

- the theoretical pumping rate necessary to contain, using P6, the upper portion of the unconfined aquifer over the entire site (10000 m<sup>3</sup>/day – above 115 l/s) would not be sustainable both considering the characteristics of the well, of the pump that can be installed in it and the volumes of pumped water that the site can treat and discharge daily;

- the theoretical pumping rates necessary to achieve the hydraulic containment of the unconfined aquifer using the production wells (320 m<sup>3</sup>/hour for P3; 320 m<sup>3</sup>/hour for P4 and 350 m<sup>3</sup>/hour for P5) would be again not sustainable, nor feasible. In fact the total extracted volume could not be treated by the wastewater treatment plant, and the technical characteristics of the pumps installed in the wells would not allow reaching the required pumping rates.

Considering the conclusions presented above, a hydraulic containment system for the southeastern corner of the site was developed based on P6 well pumping at 140-150 m<sup>3</sup>/hour (fig. 10).

## 6.2. - DEWATERING OF THE BASIN AREA AND PUMPING SCHEME CONFIGURATION

The groundwater flow model was subsequently run in transient mode, in order to forecast groundwater level changes over time, and simulations were conducted based on the following assumptions:

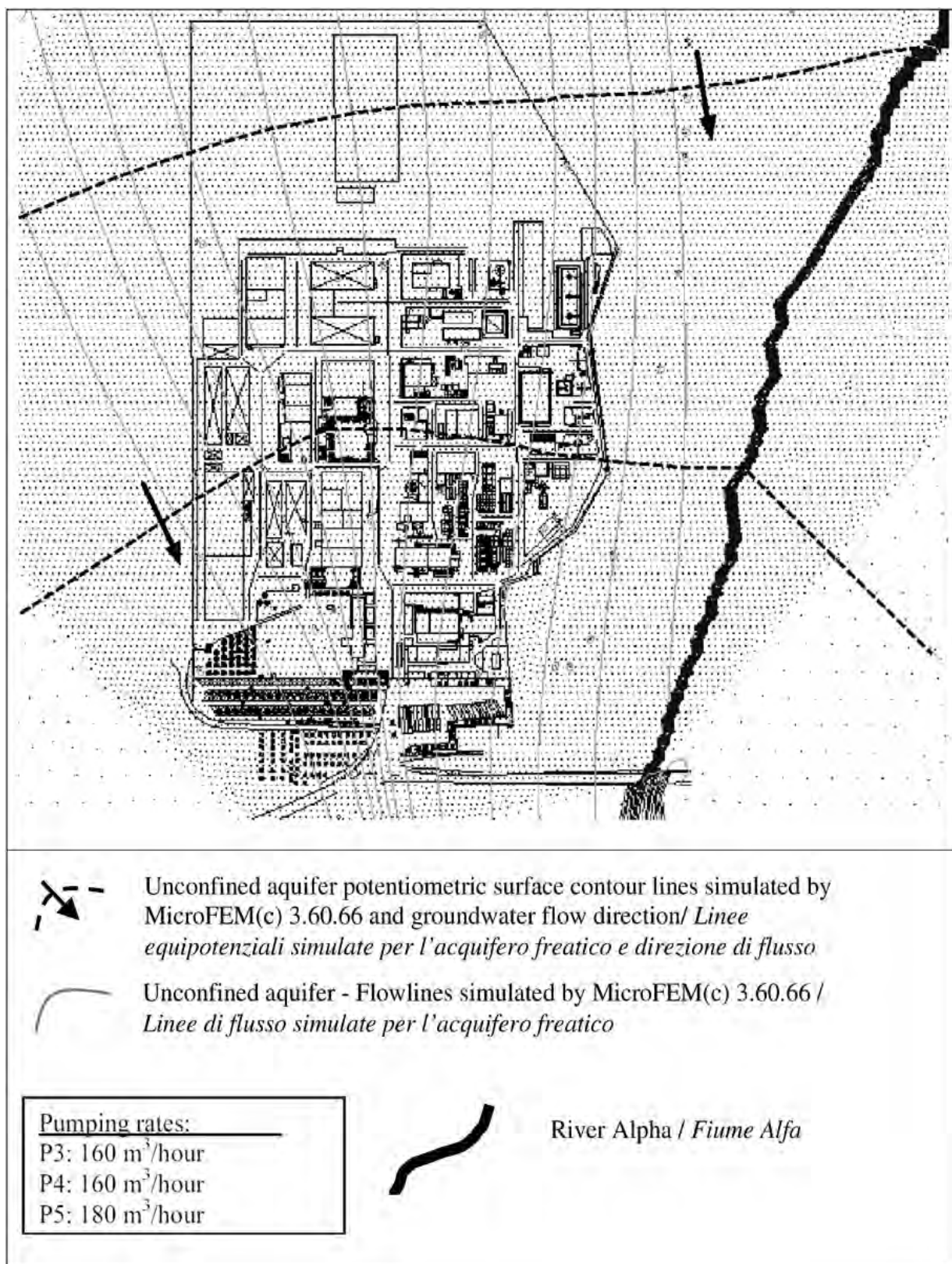


Fig. 9 - Simulated flowlines in the upper unconfined aquifer with pumping wells P3, P4 and P5 operating.  
- *Linee di flusso simulate per la porzione superficiale dell'acquifero freatico, con i pozzi produttivi P3, P4 e P5 in pompaggio.*



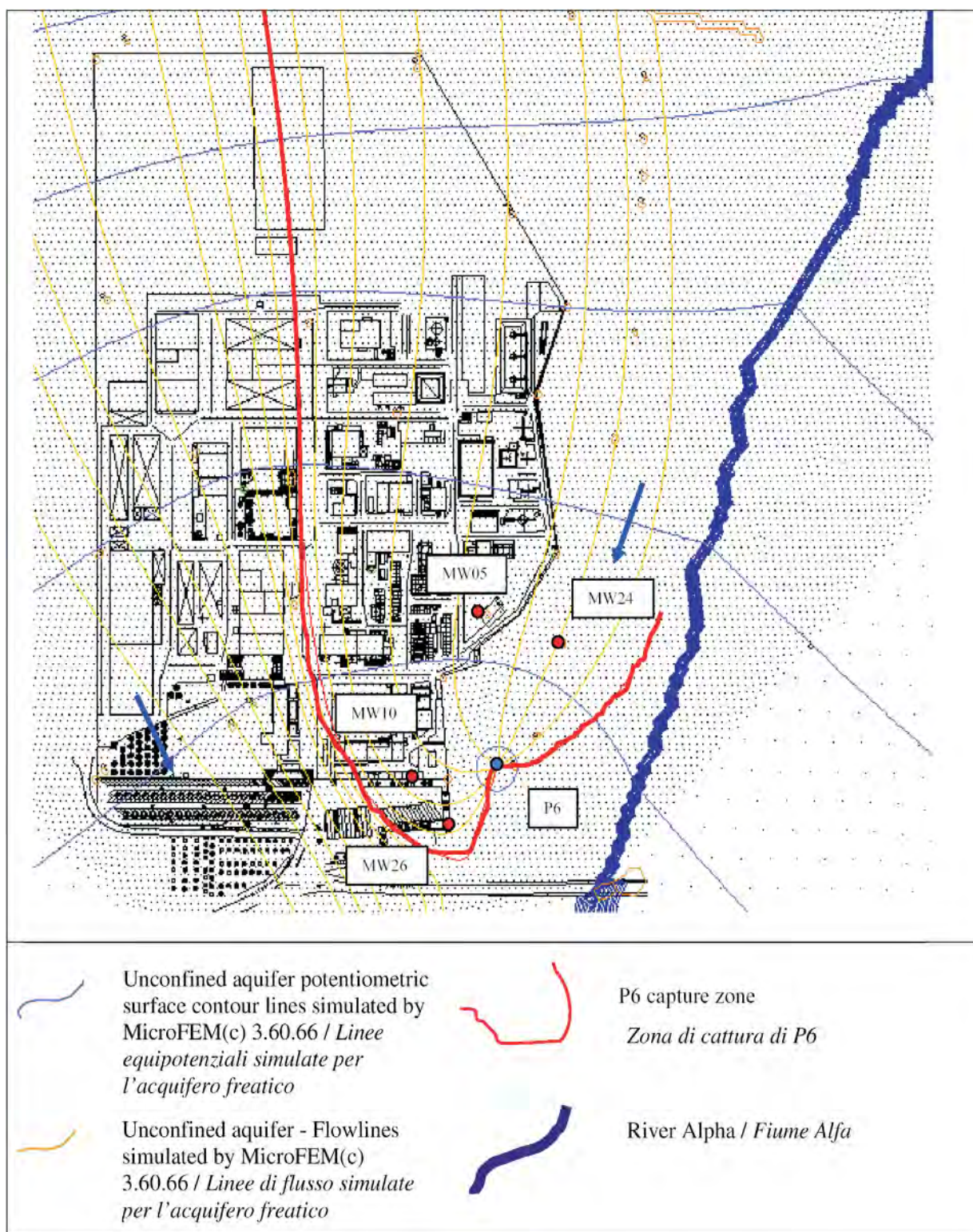


Fig. 10 - Simulated flowlines in the upper unconfined aquifer with well P6 pumping at 140 m<sup>3</sup>/hour.  
 - *Linee di flusso simulate per la porzione superficiale dell'acquifero freatico, con il pozzo P6 in pompaggio a 140 m<sup>3</sup>/ora.*



- Initial conditions represented by the use of the study area prior to remediation. The water level of the basin was artificially maintained about 1.5 m above the natural potentiometric level of the unconfined aquifer, due to the discharge of water extracted from P3. Based on the simulation results, the water level inside the basin could locally affect groundwater level measurements conducted in piezometers located close to the basin itself (PZ3-PZ4).

- The map obtained considering an artificial recharge of the basin shows bending of the potentiometric surface contour lines which is in agreement with groundwater surface maps obtained from the interpolation of field measurements.

A first run of simulations was conducted to evaluate the time necessary for the basin to naturally discharge water and restore equilibrium with the unconfined potentiometric surface, in the hypothesis that the discharge of water extracted from P3 should be interrupted (see upper diagram in fig. 11).

The presence of the basin was simulated assigning to the basin's area an initial head value 1.5 m higher than the one indicated by the model under steady-state conditions, without the artificial recharge of the basin. The model was then run in transient mode; according to the simulation results, the natural discharge would have taken about 8-10

days to reach the equilibrium (which is assumed to be at about the same depth as the bottom of the basin). Therefore, this drawdown would not have been sufficient to ensure to have the first 0.5 m of native soil below the bottom of the basin above the groundwater level.

Subsequently, a simulation was conducted considering the same initial conditions (water level in the basin higher than the natural groundwater level), to evaluate the time-frame required for the dewatering of the basin conducted using one pumping well installed west of the basin and pumping at a flow rate of 35 l/s.

Figure 12 shows the location suggested for the pumping well, while the lower diagram in figure 11 shows the simulated drawdown measured at the center of the basin and along each of the four sides. The location of the well was selected along the western side, cross-gradient of the basin, considering both the site characteristics (logistic) and the hydrogeological features of the area, in order to avoid pumping groundwater from other portions beneath the facility.

- Based on the simulation outcomes, it was initially assumed that a single pumping well could be used to increase the dewatering of the basin to the equilibrium with the natural potentiometric surface level (estimated time required for this phase: about 1 day).

- In case pumping should be continued for further 2-3 days, the groundwater level would be further decreased and the target drawdown would be almost reached.

There was however one data gap that needed to be addressed before the execution of soil removal operation: the actual groundwater level beneath the basin needed to be estimated more accurately, by means of simple groundwater level measurements to be conducted at selected monitoring wells (PZ1, PZ2, PZ3 and PZ4, MW28, MW30, MW7 and MW9), together with the discharge rate of P3 water into the basin and depth to water inside the basin, with respect to the ground surface.

Once gathered, the above mentioned data were used to refine and calibrate the existing groundwater flow model in correspondence of the basin; one pumping well was actually installed west of the basin and operated at a flow rate of 35 l/s in order to evaluate observed results against predictions.

As a subsequent step, a preliminary pumping test was run in correspondence of the location suggested by the model, to evaluate the actual response of the aquifer/basin system to the pumping. The calibrated groundwater model was used in transient mode to replicate the dewatering test conducted on site; the dewatering test was simulated with the following steps:

STEP 1 (duration: 9 hours):

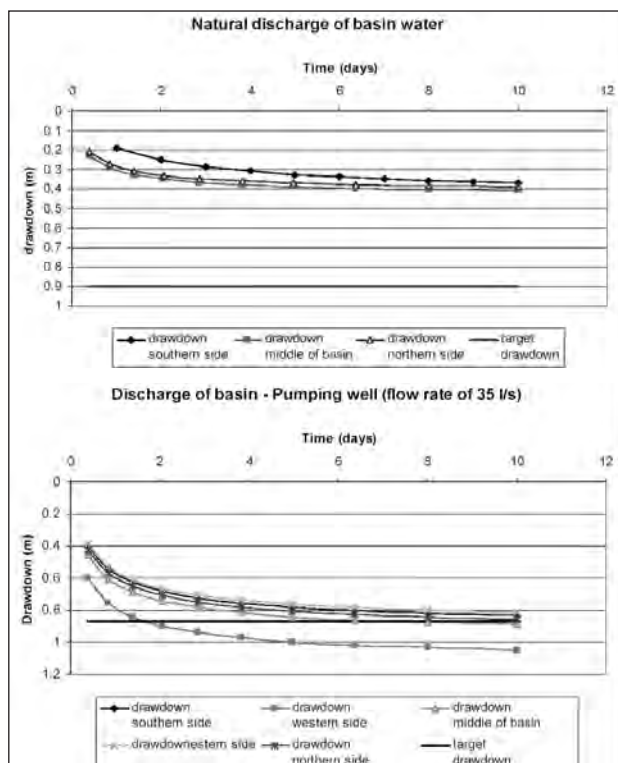


Fig. 11- Simulated discharge of the basin under natural conditions (diagram above) and with a pumping well (diagram below).

- Simulazioni di svuotamento del bacino in condizioni indisturbate (grafico superiore) e con un pozzo in pompaggio (grafico inferiore).

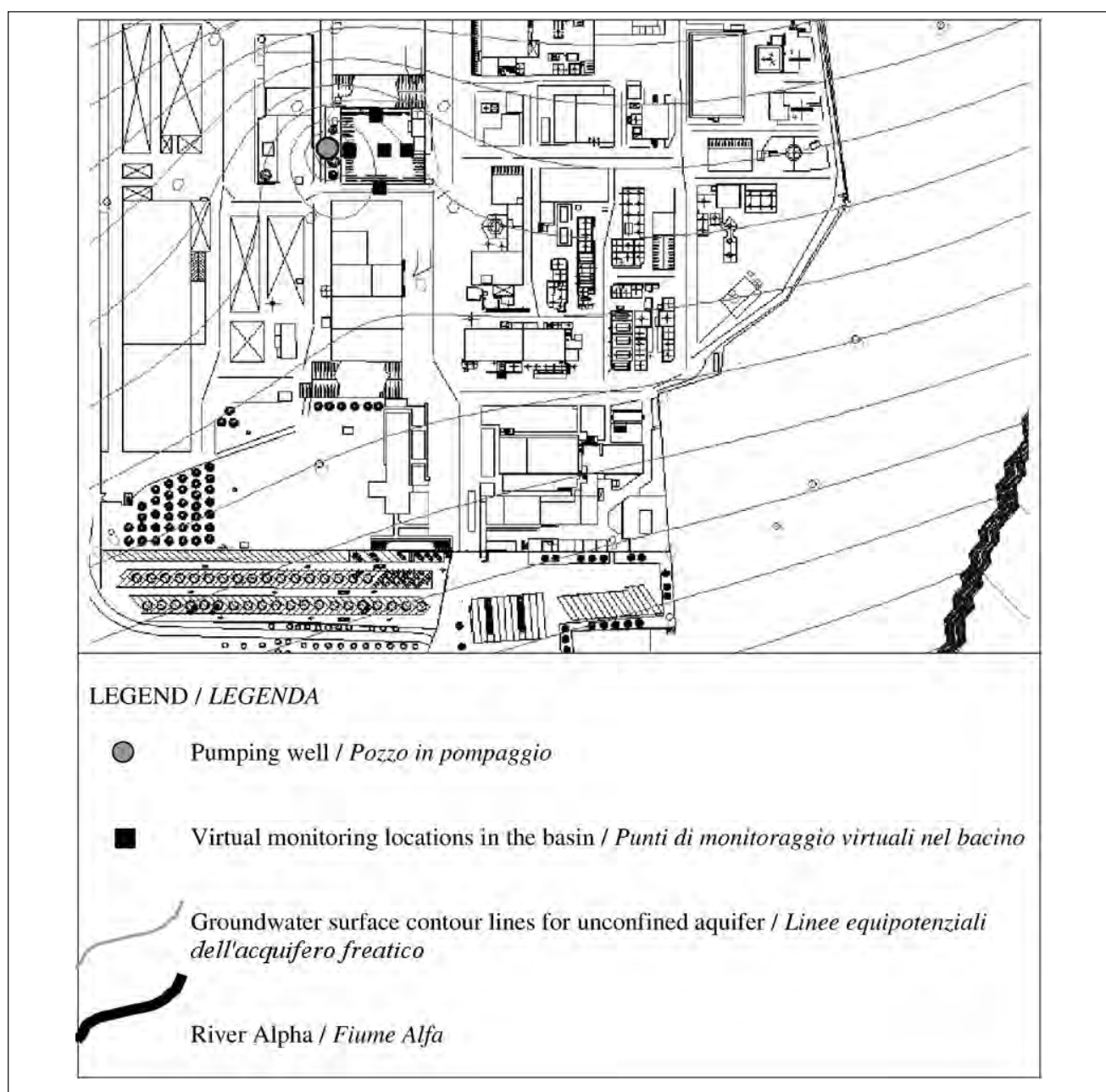


Fig. 12 - Location of pumping well and virtual monitoring locations selected to simulate drawdown inside the basin.  
 - Ubicazione del pozzo di pompaggio e dei punti di monitoraggio virtuali selezionati per simulare l'abbassamento indotto all'interno del bacino.

The basin is full of water and, at the beginning of the test, discharges to groundwater as no impermeable layer is present at the bottom. Two pumping wells are turned on with the following pumping rates:

- P7 = 108 m<sup>3</sup>/hour (30 l/s);
- P8 = 144 m<sup>3</sup>/ hour (40 l/s)

Drawdown recorded at observation wells PZ2 and PZ3 is compared to simulated values.

STEP 2 (duration 17 hours):

The basin is nearly empty and does not discharge to groundwater. The external pumping is interrupted, while the two wells keep pumping at

the same rate. Drawdown is simulated at observation wells PZ2 and PZ3 (no measurement was taken)

STEP 3 (duration 3 hours):

Pumping is interrupted and the groundwater level is observed for three hours. Drawdown recorded at observation wells PZ2 and PZ3 is compared to simulated values (tab. 3).

At the end of the pumping period (26 hours), the model overestimates the drawdown at PZ3, upgradient of the pumping wells, but replicates a similar response to the interruption of pumping activities (in 3 hours, the system recovers about 20 cm in the

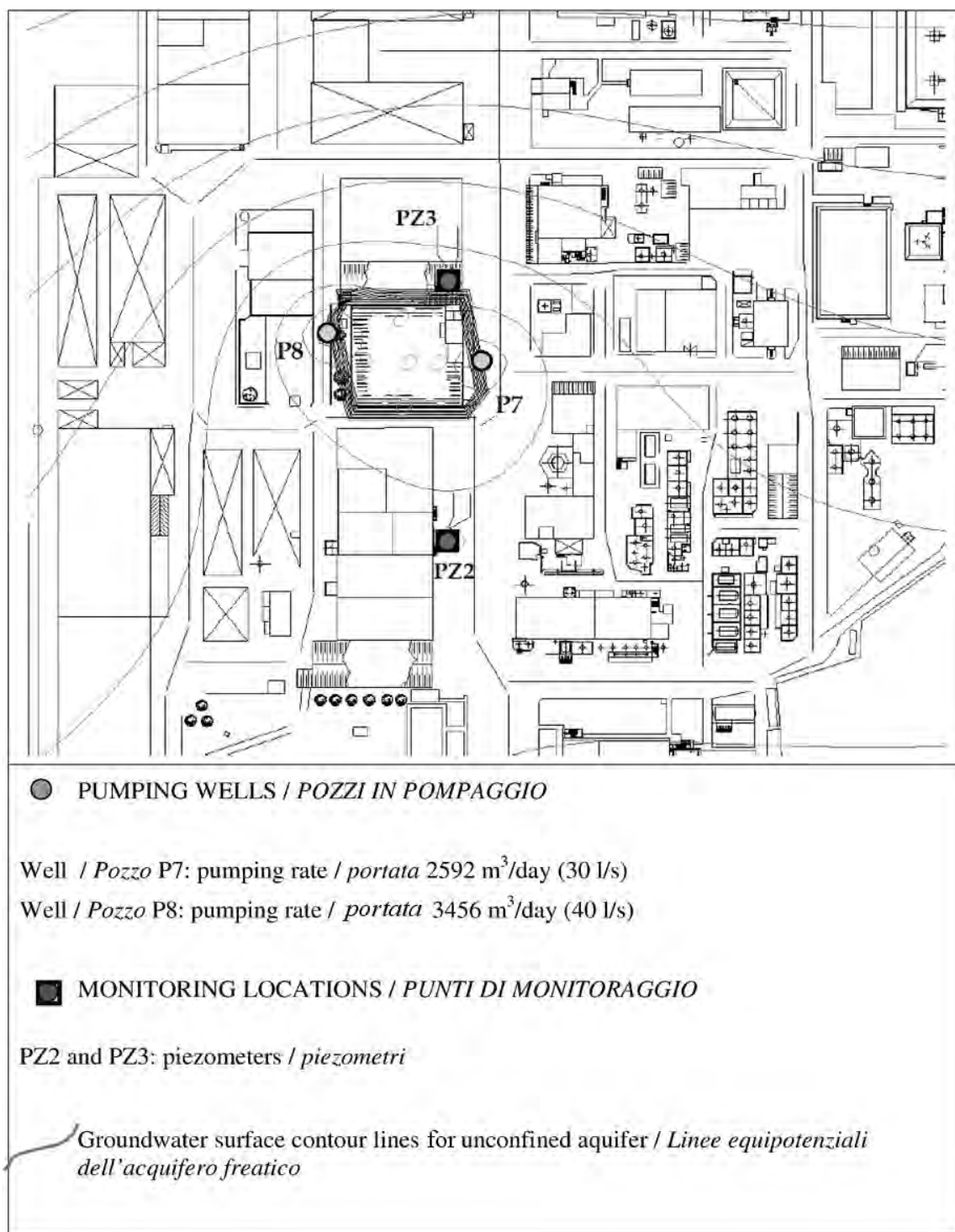


Fig. 13 - Groundwater surface map simulated for the unconfined aquifer at the end of the 26 hours-pumping test.  
 - Carta potenziometrica dell'acquifero freatico simulata al termine della prova di pompaggio di 26 ore.

simulation and 16 cm in the observed test).

On the opposite, the simulation better represent the drawdown at PZ2, downgradient of the basin (maximum observed drawdown: 31 cm; max-

imum simulated drawdown: 32 cm) but the response to the interruption of pumping is different (in 3 hours the system recovers 4 cm in the simulation and 16 cm in the observed test).



Tab. 3 – *Pilot pumping test - Simulated versus observed drawdowns.*  
 – Test pilota di pompaggio - Confronto tra abbassamenti simulati e osservati.

Step	Time (from the beginning of pumping)	Drawdown at PZ2		Drawdown at PZ3	
		measured	simulated	measured	simulated
		(m)	(m)	(m)	(m)
1	2 hours (0.083 days)	0.19	0.03	0.10	0.14
	5 hours (0.21 days)	0.22	0.10	0.17	0.27
	8 hours (0.34 days)	0.27	0.16	0.20	0.37
3	26 hours (1.08 days)	0.31	0.32	0.24	0.55

Though not extremely accurate, the model predictions (fig. 13) were, however, considered adequate for the actual implementation of the pumping system and the execution of remediation works.

The optimized pumping configuration finally defined based on the pumping test outcomes (tab. 4) consisted in two pumping wells (P7 and P8), installed along the east and west sides of the basin. The average pumping rate adopted in the field was 125 m<sup>3</sup>/hour for both wells.

## 7. - CONCLUSIONS

Field works started at the beginning of July 2007 and were completed in about 3 months; due to site constraints, both wells could not always be operated at the optimized pumping rate for the whole period, but groundwater was pumped out at flow rates ranging between 95 and 145 m<sup>3</sup>/h.

The dynamic groundwater levels inside the wells were stable at 7.2 to 8.7 m bgs, while the dynamical level measured at close monitoring points was 2.6 m bgs (at piezometers PZ3 and PZ4, upgradient of the site) and 2.96 (at piezometers PZ1 and PZ2, downgradient of the site). The dynamic level inside the basin was stable at 2.85 at 2.95 m bgs.

The dynamic groundwater level obtained as a consequence of pumping activities (fig. 14) was sufficient to allow excavating machines to enter the working area and remove sediments and native soil to the desired depth and to build an impermeable concrete basin.

The original basin area was first reshaped and

the western and southern banks pulled back. In-place soil reshaping was also necessary to ensure safe working conditions, particularly acceptable banks slopes (35° to 40° maximum). The concrete basin basement was comprised of a 30-cm-thick gravel layer laid from 2.95 to 2.65 m bgs and properly compacted, followed by a 20-cm-high concrete underpinning casting (lean concrete) equipped with a 5-mm-diameter arc-welded net (20x20 cm mesh) and a 40-cm-high concrete bed, installed from 2.45 to 2.05 m bgs. Upon the basin concrete basement installation, 25-cm-thick concrete waterproof walls were finally installed at the all basin sides.

The groundwater flow model specifically developed for the site was thus successfully used to support the remediation throughout the entire duration of the works (fig 14).

Tab. 4 – *Optimized pumping configuration.*  
 – Schema di pompaggio ottimale.

Well ID	Well Diameter (mm)	Well Depth (m bgs)	Screen Interval (m bgs)	Pump depth (m bgs)	Average pumping rate (m <sup>3</sup> /h)
P7	323	12	2 - 12	11	125
P8	323	12	2 - 12	11	125

## Acknowledgements

*The authors are indebted to G. Beretta and an anonymous reviewer for their comments and remarks.*

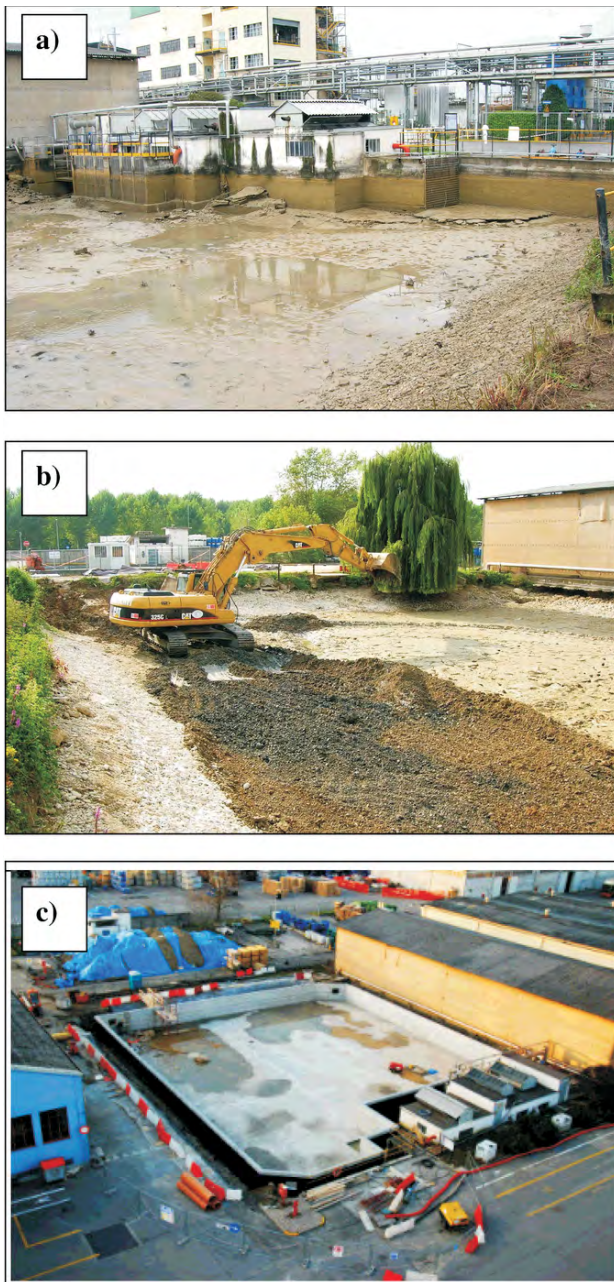


Fig. 14 - Pictures from the remediation works: a) Dewatering of the basin before the beginning of the pumping activity, b) Excavation activities and c) Concrete basing installation.

- Fotografie di varie fasi della bonifica: a) Svuotamento artificiale del bacino precedente la fase di pompaggio, b) Attività di scavo, c) Installazione della vasca di calcestruzzo.

## REFERENCES

- AIROLDI R. & CASATI P. (1989) – *Le falde idriche del sottosuolo di Milano*. Comune di Milano, Italy.
- AIROLDI R., PETERLONGO G., CASATI P. & DE AMICIS M. (1997) – *Oscillazioni del livello della falda idrica sotterranea milanese nel periodo 1990-1995*. *Acque sotterranee*, **53**.
- BARNABA P.F. (1998) – *Considerazioni sui lineamenti idrogeologici del sud-est Milanese: risorse idriche e falda superficiale*. *Acque Sotterranee*, **58**, 9-18.
- GIUDICI M., FOGLIA L., PARRAVICINI G., PONZINI G. & SINCICH B. (2000) – *A quasi three dimensional model of water flow in the subsurface of Milano (Italy): the stationary flow*. *Hydrol. Earth Syst. Sc.*, **4** (1), 113-124.
- HEMKER C.J. & NIJSTEN G.J. (1997) – *Groundwater flow modeling using Micro-Fem: Version 3*, Hemker, Amsterdam.
- HEMKER C.J. (1999) – *Transient well flow in vertically heterogeneous aquifers*. *J. Hydrol.*
- HEMKER C.J. & DE BOER R.G. (1997) – *MicroFEM Version 3.60.66*. Hemker Geohydrolog, Amsterdam.
- HEMKER C.J. & DE BOER R.G. (2000) – *MLU version 3.60* (Nov. 2002) – *Microcomputer Aquifer Test Analysis for Unsteady-State Flow in Multiple-Aquifer Systems*. Elandsgracht 83, 1016 TR Amsterdam, The Netherlands.
- HYDROSOLVE Inc. (1989) – *Aqtesolv for Windows. Advanced Software for Pumping Tests and Slug Tests*.
- MOENCH A.F. (1993) – *Computation of type curves for flow to partially penetrating wells in water-table aquifers*. *Ground Water*, **31**: 966-971.
- MOENCH A.F. (1996) – *Flow to a well in a water-table aquifer: an improved Laplace transform solution*. *Ground Water*, **34**: 593-596.
- NEUMANN S.P. (1972) – *Theory of flow in unconfined aquifers considering delayed response of the water table*. *Water Resour. Res.*, **8**: 1031-1045.
- NEUMANN S.P. (1974) – *Effect of partial penetration on flow in unconfined aquifers considering delayed gravity response*. *Water Resour. Res.*, **10**: 303-312.
- NEUMANN S.P. (1975) – *Analysis of pumping test data for anisotropic unconfined aquifers considering delayed gravity response*. *Water Resour. Res.*, **11**(2): 329-342.

## Conceptualization, modelling and management of alluvial aquifers: case studies of Sangro and Vomano plains (central Italy)

*Concettualizzazione, modellazione e gestione di acquiferi alluvionali: i casi di studio delle piane del Sangro e del Vomano (Italia centrale)*

RUSI S. (\*), TATANGELO F. (\*\*)

**ABSTRACT** - The analysis of complex hydrogeological problems related to alluvial aquifers through conceptualization and numerical modelling is of great relevance particularly for defence and management of groundwater and surface water systems. Assessment of conceptual models and uncertainties related to system geometries, parameter distributions, boundary and internal conditions are essential in application of density-dependent flow and transport numerical modelling.

Investigations and numerical analysis have been carried out on Sangro and Vomano rivers alluvial plains (Central Italy), supported by specific hydrogeological and hydrochemical geodatabases within ESRI ArcGIS platform and developed using finite-difference MODFLOW and density-dependent finite-element FEFLOW numerical codes.

These studies highlight the role of aquifer geometry, recharge conditions and hydrodynamic processes related to main hydrological features and applied stresses. The management of well fields exploitation for drinking and irrigation purposes has also been assessed, considering hydraulic connections with surface water bodies and groundwater hydrochemistry. The alluvial plains waters are characterized by facies of both Apennine origin and up flow from deep underlying mineralized systems; there is also evidence of marine intrusion phenomena along coastal areas. The found chemical-physical layering of groundwater proves to be important to environmental characterization and monitoring.

By focusing on the key-role of rivers as recharge and drainage bodies and hydrogeological properties of major palaeo-rivers, numerical modelling supported an overall analysis of the underground hydrology, including analysis of fundamental components of local hydrogeological balance, flow pathlines and velocity fields, as well as possible problems related to contaminants migration. After calibration processes, models have been used to investigate some major issues, concerning optimisation of well fields pumping regimes as well as establishment of wellhead protection areas.

The salt water intrusion dynamics, which often play a major role along the eastern Italian coastline, are amplified

by localized groundwater exploitations as proved by physical-chemical evidence. Simulated scenarios confirm risks of marine intrusion due to groundwater over-exploitations related to civil uses and irrigation; mobilisation of salt waters normally requires some years to take place but is a persistent phenomenon once established.

Long-term environmental monitoring, system conceptual refinement, numerical models uptuning are of fundamental importance for confidence building on simulation results for comprehension of relevant hydrological processes and adequate decision-making in socio-economic changing times.

**KEY WORDS:** alluvial aquifers, Central Italy, conceptualization, density-dependent conditions, groundwater modelling.

**RIASSUNTO** - L'analisi di problematiche idrogeologiche complesse di acquiferi alluvionali tramite un approccio integrato basato su concettualizzazione e modellistica numerica è fondamentale per la difesa e la gestione dei sistemi idrici superficiali e sotterranei. La definizione dei modelli concettuali, in relazione alla variabilità delle geometrie dei sistemi, dell'entità e distribuzione dei parametri, delle condizioni interne ed al contorno, è presupposto essenziale per l'analisi modellistica di flusso e trasporto in condizioni densità-dipendenti.

Indagini ed analisi modellistiche hanno riguardato gli acquiferi delle piane alluvionali dei fiumi Sangro e Vomano (Italia centrale), sviluppate con il supporto di specifici geodatabase idrogeologici ed idrochimici, implementati in ambiente ESRI ArcGIS, e tramite i codici numerici alle differenze finite, MODFLOW, ed agli elementi finiti, FEFLOW. Gli studi condotti evidenziano il ruolo della geometria degli acquiferi, delle condizioni di ricarica e dei processi idrodinamici in relazione ai principali elementi di rilevanza idrogeologica e degli emungimenti operati. La gestione degli emungimenti, in particolare da campi pozzi per uso idropotabile ed irriguo, è stata valutata in relazione alle condizioni di ricarica, riconducibili prevalentemente ai corpi idrici superficiali, ed alle caratteristiche idrochimiche delle

(\*)Dipartimento di Geotecnologie per l'Ambiente e il Territorio, Università "G. d'Annunzio" Chieti

(\*\*) Ctd Capragrassa 12/1 66041 Atesa (CH)



falde idriche di subalveo. Le acque sotterranee presentano facies di origine appenninica e di risalita da sistemi mineralizzati profondi attraverso fasce tettonizzate; nelle zone costiere sono evidenti salinizzazioni delle acque sotterranee riconducibili sia a fenomeni localizzati di *upconing* che di ingressione del cuneo salino. La zonalità chimico-fisica verticale rilevata risulta di fondamentale importanza per la caratterizzazione ed il monitoraggio ambientale. Le analisi modellistiche, condotte in condizioni 3-D densità-dipendenti, evidenziando il ruolo dei corpi idrici superficiali come principali elementi di ricarica e drenaggio e delle proprietà idrogeologiche dei principali paleoalvei, hanno permesso di ricostruire la circolazione idrica sotterranea, incluso le componenti fondamentali del bilancio idrogeologico locale, tracciare le linee di flusso e definire i campi di velocità, oltre che di valutare problemi relativi alla migrazione di contaminanti. I modelli numerici implementati, a seguito di calibrazione ed analisi di sensitività parametrica, sono stati impiegati per l'analisi di problematiche relative all'ottimizzazione dei regimi di emungimento dei campi pozzi esistenti ed alla definizione delle aree di salvaguardia delle captazioni.

Le dinamiche di intrusione salina, rilevanti nelle zone costiere adriatiche, sono accentuate da emungimenti idrici concentrati, come evidenziato dalle evidenze chimico-fisiche. Gli scenari simulati confermano il rischio di fenomeni di intrusione salina riconducibili a sovraemungimenti; i tempi di mobilitazione delle acque salate sono generalmente lunghi, nell'ordine di anni, ma tali fenomeni sono estremamente persistenti qualora si manifestino.

Il monitoraggio ambientale di lungo periodo e l'affinamento continuo dei modelli concettuali e numerici dei sistemi idrogeologici sono di fondamentale importanza nel processo di sviluppo confidenziale nei risultati degli scenari simulati sia per la comprensione dei processi idrogeologici ed idrochimici rilevanti che per gli aspetti decisionali in un contesto socio-economico ed ambientale recentemente in rapida e talora drammatica evoluzione.

**PAROLE CHIAVE:** acquiferi alluvionali, concettualizzazione, condizioni densità-dipendenti, Italia centrale, modellistica numerica.

## 1. - INTRODUCTION

The conceptual models, based on hydrogeological setting and principal hydrodynamic and hydrochemical aquifer characteristics are fundamental for numerical modelling applications finalized to water resources analysis and management; investigations and numerical analysis have been developed for Sangro and Vomano river plains (Central Italy) and presented (fig. 1), in current paper, as representative case studies for characterization, modelling and management of alluvial aquifers.

Depositional environments and aquifer geometry have been defined with the aid of geological, geomorphological, photogeological, geognostic and geophysical investigations (over 170 boreholes in Sangro plain and over 120 VES and 20 boreholes in Vomano plain).

The hydrological balance was evaluated using data from pluviometric and thermometric sta-

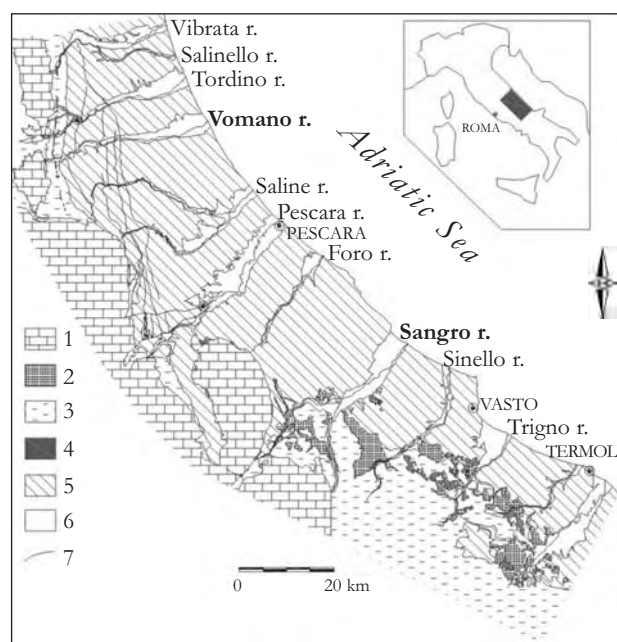


Fig. 1 – Location of the case studies and geolithological scheme. 1) Carbonate sequence (Upper Triassic-Miocene). 2) Varicoloured Clays (Upper Cretaceous-Oligocene). 3) Turbiditic deposits (Laga formation and Molise nappes, Miocene). 4) Evaporitic deposits (Upper Miocene). 5) Pelitic deposits of Abruzzo and Molise foredeep (Plio-Pleistocene). 6) Alluvial deposits (Holocene). 7) Main faults and thrusts in the Mesozoic-Cenozoic and Miocene deposits.

- Ubicazione dei casi di studio e schema geolitologico. 1) Successione carbonatica (Triassico superiore-Miocene). 2) Argille Varicolori (Cretaceo superiore-Oligocene). 3) Depositi turbiditici (Formazione della Laga e coltre molisana, Miocene). 4) Depositi evaporitici (Miocene superiore). 5) Depositi pelitici dell'avanzfossa abruzzese - molisana (Plio-Pleistocene). 6) Depositi alluvionali (Olocene). 7) Principali faglie e sovraccorrimenti nei depositi meso-cenozoici e miocenici.

tions within hydrologic basins; the aquifer hydrodynamics was investigated considering seasonal piezometric measurements in monitoring wells and water springs, and pumping tests, with contemporary acquisition of physical-chemical groundwater parameters; chemical analysis of groundwater samples were used to define hydrochemical facies. Specific salinization processes, such as sea-water intrusion in coastal area and upward migration of deep waters along alluvial plain borders, were analysed by multiparametric profiles and chemical analysis.

Data and information management, analysis and visualisation were undertaken through development of hydrogeological geodatabases in ArcGIS environment (ESRI, 2009), inspired by ArcHydro (MAIDMENT, 2002) and Groundwater Data Model (STRASSBERG & MAIDMENT, 2004) and useful for data exchange with the finite-difference MODFLOW (MCDONALD & HARBAUGH, 1984; MCDONALD *et alii*, 2000) and finite-element FEFLOW (DHI-WASY, 2009) numerical codes; geostatistical and statistical analysis was undertaken within external software environments like GeoDa (ANSELIN, 2004).

A regional numerical model, relative to lower

Sangro alluvial valley (DESIDERIO *et alii*, 2007) was developed to estimate groundwater resources and river-aquifer exchanges, while a local scale numerical model was also developed for saline intrusion phenomena analysis in coastal area, both applied for interpretation purposes (ANDERSON & WOESSNER, 1992) and simulation of different exploitation scenarios.

The Vomano valley aquifer, playing a key-role on water supply at both local and regional scale, has been previously analysed for definition of hydrogeological settings and groundwater dynamics (recharge, geometry, parameter distribution, surface water body interactions and fresh-salt water interface) by DESIDERIO *et alii* (2003), DESIDERIO & RUSI (2003), RUSI *et alii* (2004).

The optimisation of well fields pumping regimes and protection of water resource quality represent some major hot issues for a sustainable development; the application of groundwater modelling techniques has improved the knowledge of hydrogeological framework, useful for problems analysis related to concentrated groundwater exploitations, as sea water intrusion, and impacts of anthropic activities.

## 2. – THE SANGRO ALLUVIAL VALLEY

### 2.1. – GEOLOGICAL SETTING

The lower Sangro valley (fig. 2) is located between the terrigenous alloctonous units of the molisan facies (SELLI, 1962; CATENACCI, 1974; PATACCA *et alii*, 1992) and plio-pleistocene marine deposits of the Abruzzo-Molise foredeep (MOSTARDINI & MERLINI, 1986; GHISETTI & VEZZANI, 1996-97); these units, mainly clayey deposits, constitute the basement of the alluvial deposits (fig. 3) superimposed on top of the Aventino-Sangro gravity flow deposits (ENI-AGIP, 1972), upstream of the confluence with Aventino river, while overlay marine plio-pleistocene deposits downstream (CRESCENTI, 1971; CRESCENTI *et alii*, 1980). The plio-pleistocene basement is mainly constituted by clays, sandy clays and marly clays, while arenaceous conglomerates are predominant near the coastal areas; sometimes the arenaceous conglomerates vary to sandy silts and clayey silts that have typical facies of marine-coastal to fluvio-deltaic environments.

The I, II and III order alluvial terraces are con-

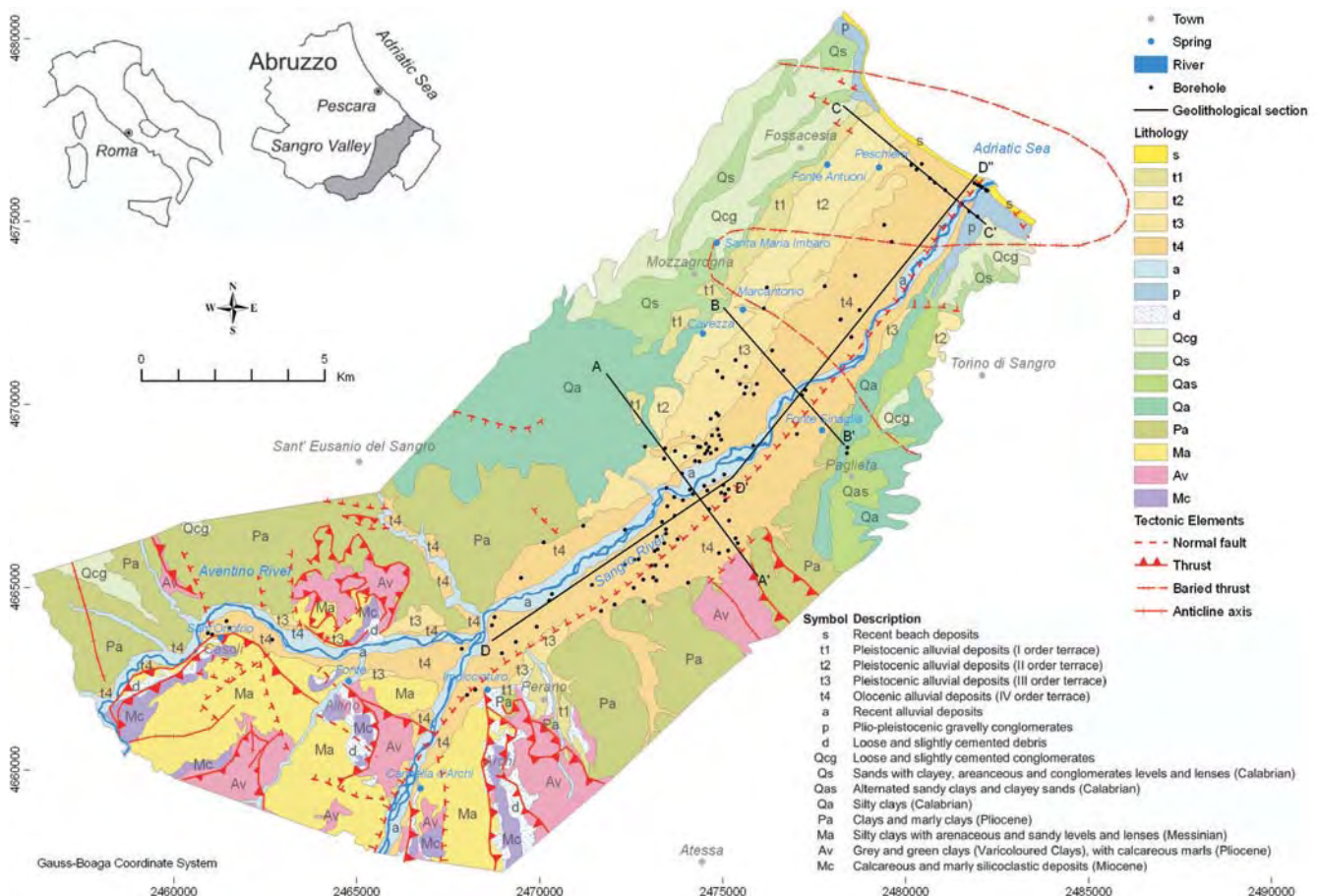


Fig. 2 – Geologic map of the Sangro alluvial plain with boreholes locations; modified after DESIDERIO *et alii*, 2007.

- Carta geologica della pianura alluvionale del Fiume Sangro e ubicazione dei sondaggi geognostici.



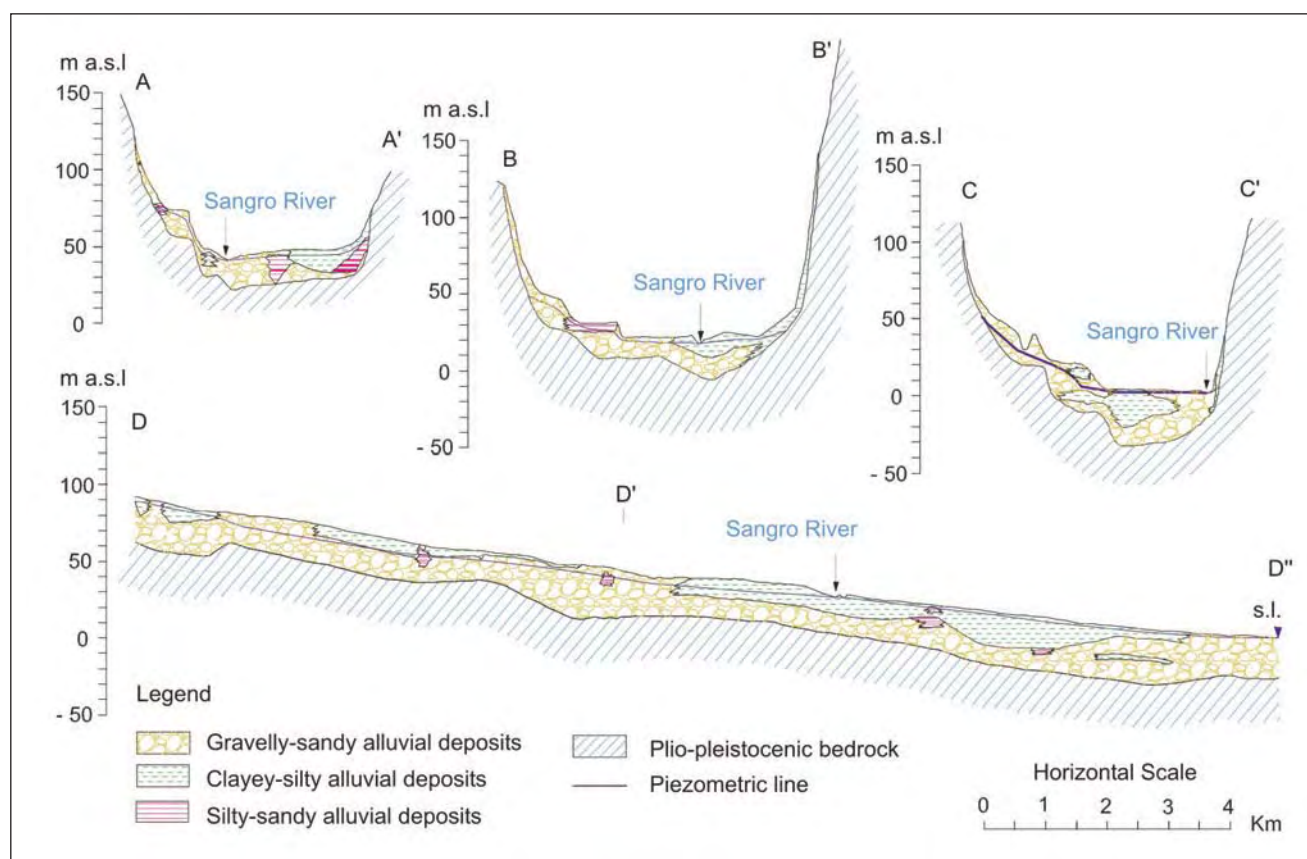


Fig. 3 - Schematic geolithological sections of the Sangro alluvial plain; modified after DESIDERIO *et alii*, 2007.  
- Sezioni geolitologiche schematiche della piana alluvionale del Sangro.

stituted by gravelly sand deposits, sometimes slightly cemented, with silty-sandy-clayey lens and occasional brown-blackish paleosoils. The sandy matrix shows ferritization signs more evident in relation to the deposits age. Sandy and gravelly deposits with silty-sands and clayey lens constitute the IV order alluvial terrace, which has been cut by Sangro river. Thalweg alluvial deposits are mainly formed of gravels and sands.

The alluvial deposits are located in correspondence of a complicated mainly strike-slip faults system related to Volturno-Sangro tectonic lineament (DEMANGEOT, 1965; CASNEDI *et alii*, 1981; GHISETTI & VEZZANI, 1983).

The coastal areas are dominated by gravelly and sandy beach deposits and sandy fluvial deposits related to the latest flandrian marine ingression; huge debris deposits, related to weathering of plio-pleistocenic hills, lay on Sangro river right side.

## 2.2. - HYDROLOGY AND ANTHROPIC SETTING

The hydrological balance was evaluated considering data from 34 pluviometric and thermometric stations (SERVIZIO IDROGRAFICO E MA-

REOGRAFICO, 1955-1995) of the whole Sangro-Aventino hydrologic basin, considering a 40 years observation period; the network has been integrated also by 8 fictitious pluviometric stations.

Applying TURC (1961) and THORNTHWAITE & MATHER (1957) methodologies, the mean precipitation is about 1060÷1080 mm/year while the global surface runoff of about 560÷670 mm/year, with high spatial variations due to orography, distance from sea and provenience of humid currents. The pluviometric regime underlines an Apennine sublittoral climate, with marine influences in coastal area; the minimum precipitation values occur in summer time and along coastal area, while the maximum ones occur in winter and spring months, especially in mountainous zones, when the temperature is also lower.

The Sangro alluvial plains is characterized by an enormous social and economic development that require a huge hydroelectric, irrigation, industrial and civil exploitation of superficial and groundwater resources; the Sangro river flow regime is influenced by dams of Bomba, Casoli, Serranella and Sant'Angelo of Altino hydroelectric stations, with an average discharge to sea of about 30 m<sup>3</sup>/s.



### 2.3. - HYDROGEOLOGY

Sangro aquifer geometry has been defined by surface geological and geomorphological surveys, photogeological multitemporal and multiscale analysis and bibliographical geognostic and geophysical investigations (fig. 2). The aquifer is constituted by recent and ancient alluvial deposits characterized by high variable grain-size.

The thickness of the I, II and III order terraces are between 2÷3 m up to 30 m, while the recent alluvial deposits thickness ranges from a few meters in the upstream and lateral plain areas up to 35÷40 m near the coastline (fig. 3). The upstream area is dominated by sandy-gravelly deposits, with only local thin silty-sandy and silty-clayey deposits, while the central and downstream areas of the valley are dominated by gravelly-sandy deposits with clayey-silty lens on Sangro river left side, and silty-sandy and silty-clayey deposits, on the right side. The silty-clayey deposits on the alluvial succession top are relatively thick in the central valley, about 15 m, and near coastline, up to 20 m; topsoil, mainly consti-

tuted by organic silty clays, is about 1÷2 m thick. The aquifer is unconfined even if the silty-clayey lens often tend to configure as aquitards near coastline and on Sangro river right side (DE RISO *et alii*, 1994), a typical condition of many Abruzzo and Marche alluvial plains (NANNI, 1985; DESIDERIO *et alii*, 1999), and only locally is multilayer.

### 2.4. - HYDRODYNAMICS

The Sangro valley piezometry and its temporal oscillations have been evaluated by seasonal surveys on over 160 wells.

Groundwater flow is mainly influenced by paleo-rivers (fig. 4), from alluvial plain borders towards the main water body. Piezometry is dependent on basement morphology, amounts of seasonal recharge and withdrawals, thus the hydraulic aquifer-river exchanges tend to vary. The main drainage axis lays on Sangro river right side in central-upper alluvial plain, then moves to left side due to the presence of a groundwater divide, and converges again towards the river in coastal area. Large depression cones are related to heavy with-

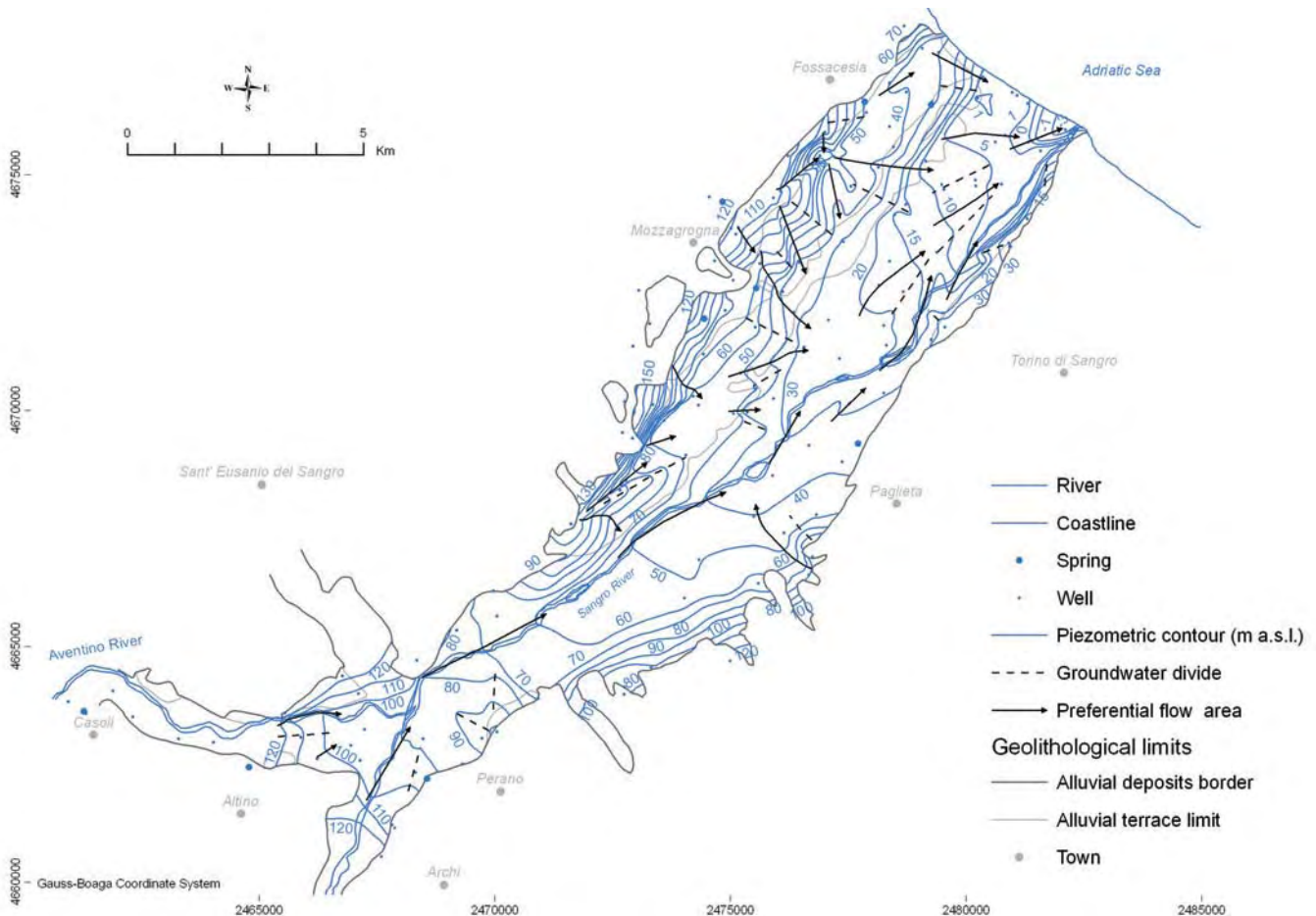


Fig. 4 – Piezometric heads with preferential flow areas and groundwater divides (April 2000), on the basis of more than 160 wells and 10 springs; modified after DESIDERIO *et alii*, 2007.

- *Piezometria con le principali aree di deflusso preferenziali e spartiacque sotterranee (Aprile 2000), ricostruita sulla base di oltre 160 pozzi e 10 sorgenti.*

drawals for irrigation purposes. Upper alluvial terraces contribute to recharge of the preferential drainage axis in relation to surface and basement morphology, hydraulic conductivities, geometry and Plio-Pleistocene system contributions.

Hydraulic gradient is about 4÷5‰ near the recent and IV order terrace deposits and 20÷50‰ in other areas; it is locally higher due to aquifer thinning, hydraulic conductivity variations and local recharge conditions. Groundwater exchange occurs from alluvial terraces towards recent deposits due to sandy-silty overlying layers assuring hydraulic communication; hydraulic gradient increase in coastal area is related to silty-clayey deposits.

Piezometric oscillations are related to amount and distribution of effective recharge related to precipitations, hydrodynamic characteristics of alluvial and overlying deposits, infiltration from surface streams, irrigation and withdrawals. Annual water table oscillations vary from 0.3 up to 1.3 m, with maximum levels recorded in March-April and minimum ones in July-August; variations, after rainfall events, occur within 1÷2 months, due to medium and high hydraulic conductivities. The discharge period varies from 4 up to 5÷6 months, while recharge period varies from 4 up to 8 months.

Aquifer hydrodynamic properties (SCANDELLARI, 1970; CELICO, 1983; DE RISO *et alii*, 1994; DESIDERIO *et alii*, 2007) depend on silt, silty-sandy and silty-clayey deposits distribution with an average hydraulic conductivity value less than  $4 \times 10^{-4}$  m/s. The gravelly-sandy deposits have hydraulic conductivity values varying from  $1.8 \times 10^{-4}$  m/s up to  $4.4 \times 10^{-4}$  m/s. Paleo-river conductivities are about  $2 \times 10^{-3}$  m/s. The Sangro river has strong water exchange, variable through time, with its underlying aquifer. Locally relevant water quantities flow also from secondary valleys. Sangro aquifer water flux towards Adriatic sea is estimated of about  $0.2 \div 0.3$  m<sup>3</sup>/s (DESIDERIO *et alii*, 2007).

Some springs, monitored between October 2000 and November 2001, are located at the contact between terraced alluvial deposits and low conductivity gravity flow and Plio-Pleistocene deposits. Spring discharges, generally modest and concentrated during winter, are normally less than 1 l/s with short time responses of 1÷2 months or even lower, days, to rainfall events; discharge regimes are extremely variable,  $R_v > 100\%$  (MEINZER, 1923), related to limited recharge zones and high hydraulic conductivities.

The wells are used mostly for irrigation, sometimes for civil uses; pumping rates, varying from 1÷5 l/s up to 10÷15 l/s, are discontinuous in time and applied principally during dry seasons.

## 2.5. – HYDROCHEMISTRY

Specific electrical conductivities highlight spatial and temporal changes in Sangro plain varying from about 400 to more than 2000  $\mu\text{S}/\text{cm}$ . The lower values are found in the medium to higher valley in correspondence of preferential flow axis and I, II and III alluvial terraces. Dilution effects cause lowering of specific conductivity values in periods of higher aquifer recharge; in the lower valley there are locally opposite trends due to dissolution of substances in unsaturated zone.

Values higher than 2000  $\mu\text{S}/\text{cm}$ , also more than 7000  $\mu\text{S}/\text{cm}$ , are detected in coastal area due to sea water intrusion related to localized withdrawals; values between 3000 and 11400  $\mu\text{S}/\text{cm}$  were detected in the medium-lower valley, all the way to the river outlet; these anomalies are related to upward migration of deep mineralized waters (DESIDERIO & RUSI, 2004). Groundwater temperatures are influenced by atmospheric variations in lower valley due to a shallow water table. Temperature ranges from 12 up to 18 °C in winter and 15 up to 28 °C in summer. Groundwater temperatures along preferential drainage axis are lower than those of the next recharge areas due to different circulation times.

Spring waters monitoring has shown average specific conductivity values from 695 up to 1624  $\mu\text{S}/\text{cm}$ . Average temperatures, from 13.9 up to 16.6 °C, are essentially related to atmospheric temperature variations.

The dominant hydrochemical facies within Sangro aquifer is bicarbonate-calcium facies (fig. 5). Some waters have bicarbonate-alkaline and sulphate-chloride-earthly alkaline facies; the later is related to mixing with deep and marine mineral-

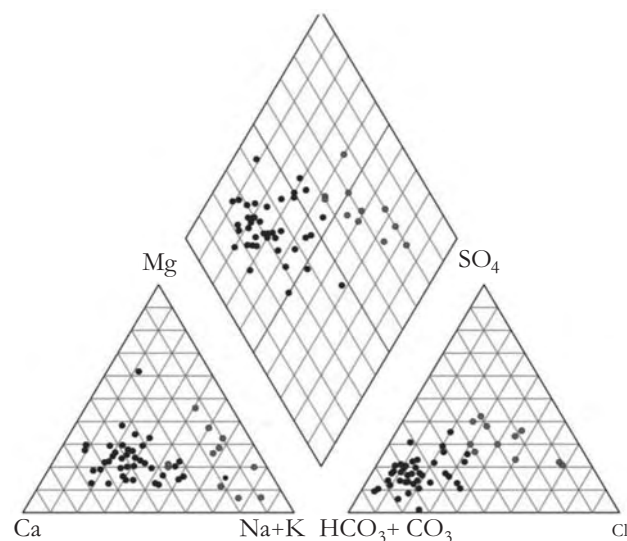


Fig. 5 – Piper's diagram of the Sangro plain groundwaters.  
– Diagramma di Piper relativo alle acque della piana del Sangro.

ized waters. Bicarbonate-calcium waters are mainly distributed in the higher valley and along river thalweg, where appennine origin waters prevail.

#### 2.5.1. - Deep flow mineralization

Mineralised waters, typical of areas with high specific electrical conductivity, normally have sulphate-chlorine-alkaline-earthly alkaline facies, as chloride-sodium and sulphate-sodium. These anomalies are related to saline intrusions (DESIDERIO & RUSI, 2003), due to upward migration of deep mineralized waters from Abruzzo-Molise foredeep, and dissolution of evaporitic deposits within the depositional sequence (DESIDERIO & RUSI, 2004).

Mineralization phenomena are proved on the basis of the  $^{18}\text{O}$  -  $^2\text{H}$  isotopic ratio and  $r\text{SO}_4^{2-}/r\text{Cl}^-$  and  $r\text{Mg}^{2+}/r\text{Ca}^{2+}$  characteristic ion ratios; other typical ion ratios like  $r\text{K}^+/r\text{Na}^+$ ,  $r\text{Sr}^{2+}/r\text{Br}^-$ ,  $r\text{Br}^-/r\text{Cl}^-$  and  $r\text{Li}^+/r\text{Sr}^{2+}$  are also evidence of these phenomena. Mineralized waters along tectonic lineaments on Sangro right side have higher  $r\text{SO}_4^{2-}/r\text{Cl}^-$  and  $r\text{Mg}^{2+}/r\text{Ca}^{2+}$  ion ratios, while water, affected by saline intrusions have lower values than average aquifer deposits.

The unconfined aquifer is recharged mainly by fluvial waters from calcium-bicarbonate facies of Apennine origin, as confirmed by electrical conductivity and groundwater temperature values. River recharge is further testified by groundwater chemistry; close to riverbed the waters present calcium-bicarbonate facies with low saline content. Waters of this type are also found along paleo-river draining Vomano river and its primary tributaries. The high terraces, on the other hand, are recharged mostly by rainwater. Deep flow mineralization is due to Pliocene or Messinian origin waters (NANNI & VIVALDA, 1998, 1999 and 1999a; DESIDERIO & RUSI, 2004, DESIDERIO *et alii*, 2007b), rising along fault-associated fracture zones in plio-pleistocenic basement deposits up to overlying unconfined aquifer. The mixing of sodium-chloride and calcium-sulfate facies Pliocene and Messinian mineralised waters with the calcium-bicarbonate waters of the aquifer lead to different hydrochemical facies in emerging zones. Recharge by the Messinian and Pliocene waters is very slight and mainly influences the groundwater chemistry, causing enrichment in  $\text{Cl}^-$ ,  $\text{Na}^+$ ,  $\text{Mg}^{++}$  and  $\text{SO}_4^{--}$  of calcium-bicarbonate waters originating from fluvial recharge (fig. 5).

#### 2.5.2. - Sea-water intrusion

Piezometric levels show minimum values, sometimes negative, on Sangro river left side near

coastline, related to withdrawals for irrigation purposes during summer ( $10\div 15$  l/s). Local drainage from river occurs where gravelly and sandy alluvial deposits related to paleo-rivers are present. There is a vast recharge area to the western side, which partially compensates summer withdrawals.

The multiparametric profiles conducted on monitoring wells located in the lower valley (fig. 6) show a three dimensional variability of groundwater chemical-physical (T,  $\chi$ , Eh) parameters (fig. 7).

Temperature measurements ranged from 14.4 up to 26.8 °C in July 2005. Vertical temperature changes are generally modest; negative trends were recorded within upper aquifer related to influence of surface temperatures and subsurface hydrodynamics.

Electrical conductivity values change more than 8000  $\mu\text{S}/\text{cm}$  along the vertical. This parameter often increases at just 1÷2 m below the surface in coastal areas. In other wells, even though water exploitations occur (discontinuous and variable, between 1 and 5 l/s), chemical-physical parameters tend to be constant along the vertical, due to greater hydraulic conductivities. Specific electrical conductivity values exceed 2000  $\mu\text{S}/\text{cm}$  near the left side river outlet, where a negative piezometry of more than -1 m a.s.l. exists. These irrigation wells tend to mobilise higher salinity waters. Values larger than 5000  $\mu\text{S}/\text{cm}$  in vertical direction were recorded in wells located at about 1 km from the coastline where no exploitations occur, due to upward migration of deep water from the plio-pleistocenic deposits (DESIDERIO & RUSI, 2004).

The Eh parameter tends to decrease with depth, from 2÷3 m from the water table, then stabilizes on negative values. The reducing conditions are related to circulation within deposits with a silt-clay fraction, sometimes peaty, characterized by low hydraulic conductivities. A possible influence is related with mobilization of deep waters with negative Eh values.

#### 2.6. - MODEL DESIGN, CALIBRATION AND SENSITIVITY ANALYSIS

Scope of Sangro valley groundwater numerical modelling, carried out by the finite-element FEFLOW code (DHI-WASY, 2009), was the quantitative assessment of underground water fluxes and saline intrusion phenomena. The conceptual model is supported by soft ideas (NYKRAVESH *et alii*, 2003; AMINZADEH, 2004). This method enhances peculiar aquifer characteristics. Integrated use of both hard data and soft ideas are fundamental for defining aquifer geometries,



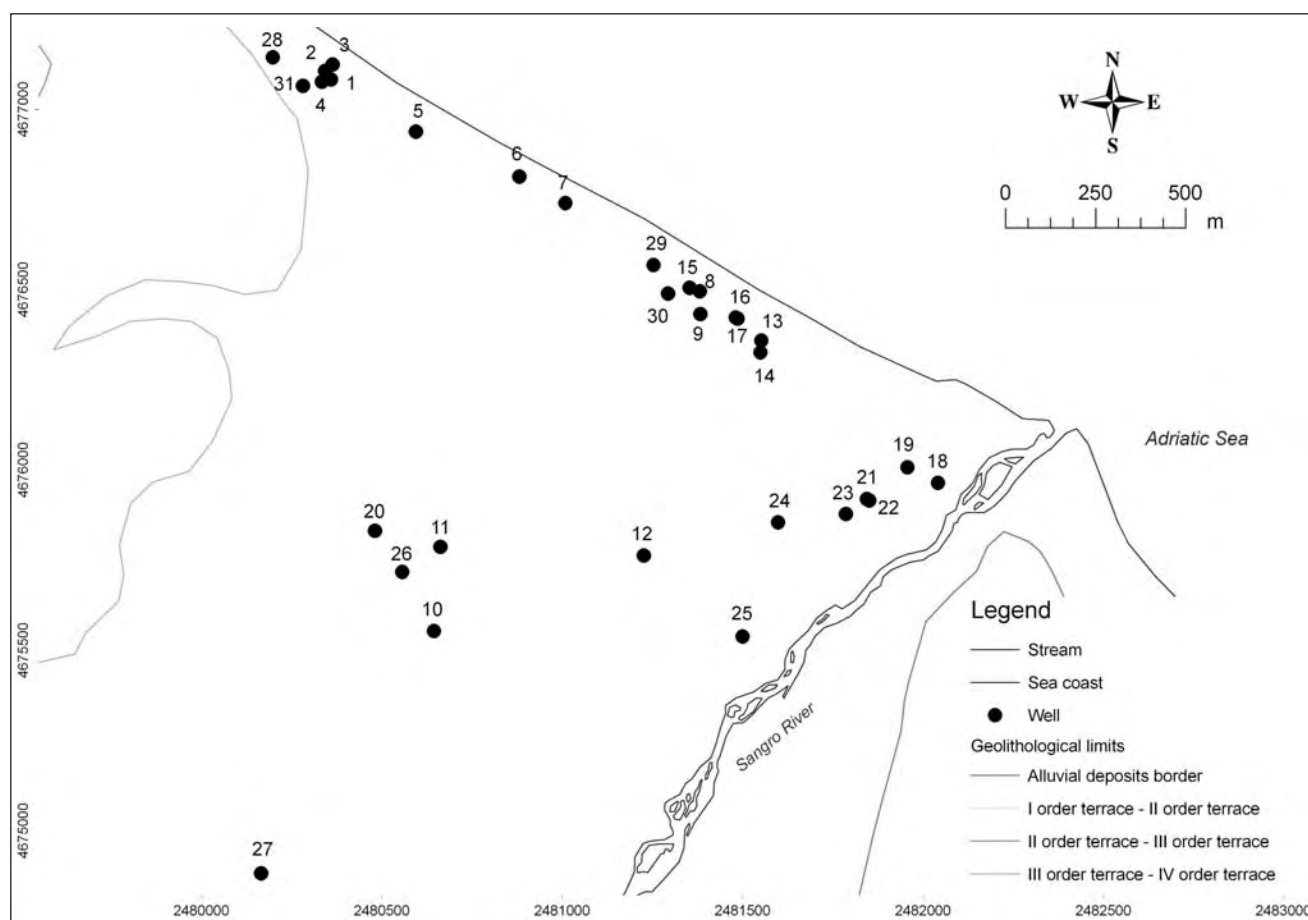


Fig. 6 - Wells used for multiparametric logs.  
 - Pozzi nei quali sono stati eseguiti i profili multiparametrici.

hydrodynamic parameters, effective recharge and issues related with salt water intrusion phenomena. Variability of hydrogeological and hydrogeochemical parameters and boundary conditions was analysed respect to simulation of conservative scenarios.

A regional numerical model was built to assess groundwater resources, river-aquifer water exchange, the influence of palaeo-rivers and fluxes from alluvial terraces; a local model was so used to estimate groundwater fluxes to sea and saline intrusion phenomena, with higher resolution details in coastal area.

The regional 3D mesh (fig. 8), developed over an area of about  $82.67 \times 10^6 \text{ m}^2$ , has 118380 elements and 76360 nodes over 5 vertical layers. The dimensions of the triangular-based prismatic elements gradually vary from  $120 \div 130$  to  $25 \div 30$  m near wells. Steady-state conditions were used during simulations with free and movable conditions (DIERSCH & MICHELS, 1996; DIERSCH, 1998). Geometry settings was defined on the basis of 55 geolithological sections, while hydrogeological parameters were assigned on the basis of available hydrodynamic data.

The hydraulic conductivities and the recharges were distributed on a zone basis (ANDERSON & WOESSNER, 1992; PINDER, 2002; RUSHTON, 2005). Hydraulic conductivities of  $8 \times 10^{-4} \text{ m/s}$  were considered reasonable for the IV order terraces and recent deposits. Hydraulic gradients and borehole logs justify hydraulic conductivity values of about  $2.5 \times 10^{-3} \text{ m/s}$  in areas of preferential flow, with analogies to other Abruzzo coastal alluvial valleys (CELICO 1983; DESIDERIO *et alii*, 2007a). Silty-sandy drift deposits have an hydraulic conductivity of  $4 \times 10^{-4} \text{ m/s}$  (SCANDELLARI, 1970). The regional model is not very reliable in relation to the I, II and III order terraces due to scarce availability of data. Hydraulic conductivities however vary from  $7 \times 10^{-4}$  up to  $2 \times 10^{-3} \text{ m/s}$ . The hydrodynamic parameters, evaluated through numerical modelling, produce plausible piezometric configurations.

Effective recharge was differentiated respect to estimated rainfall recharge and surface lithologies; locally recharge components are also related to irrigation, especially during dry seasons. Sensitivity analysis proves that modest parameter

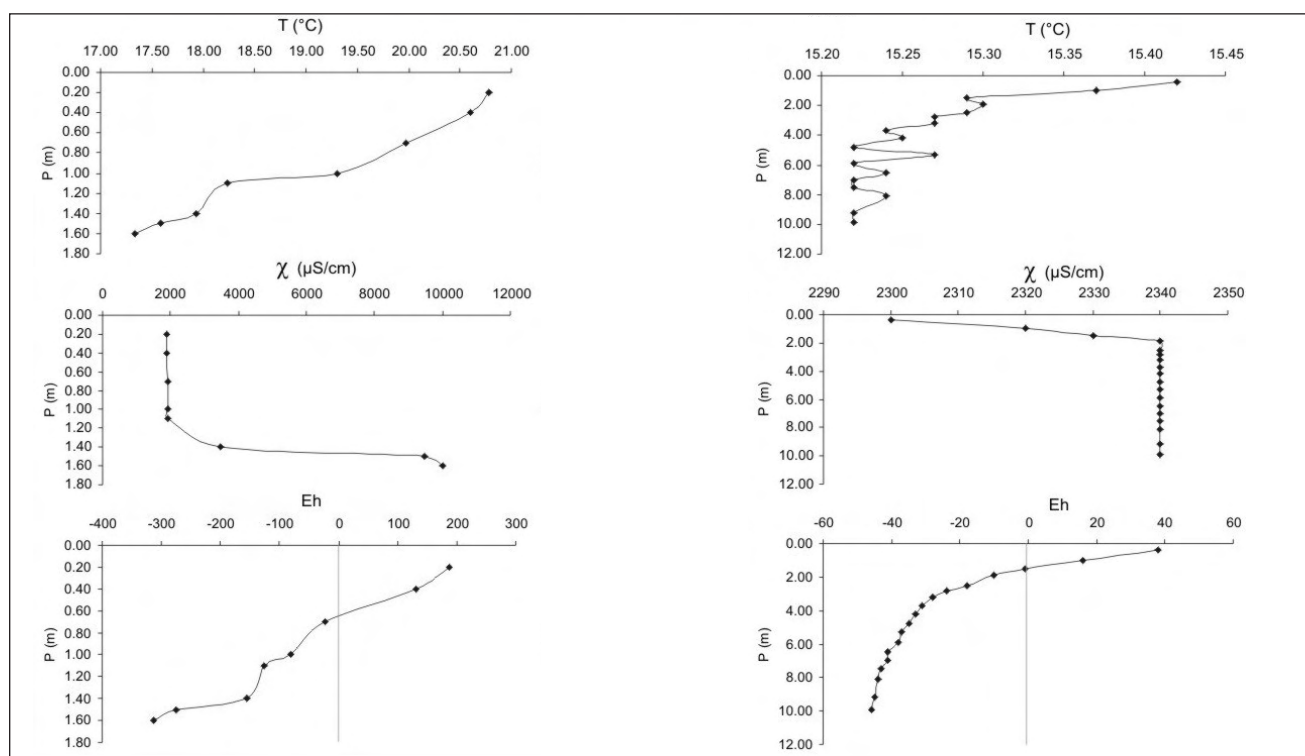


Fig. 7 – Multiparametric logs of a coastal well (at left, n. 7 in figure 6) and a well with mineralized waters (at right, n. 12 in figure 6).  
 – Profili multiparametrici di un pozzo costiero (a sinistra, n. 7 in figura 6) e di un pozzo con acque mineralizzate (a destra, n. 12 in figura 6).

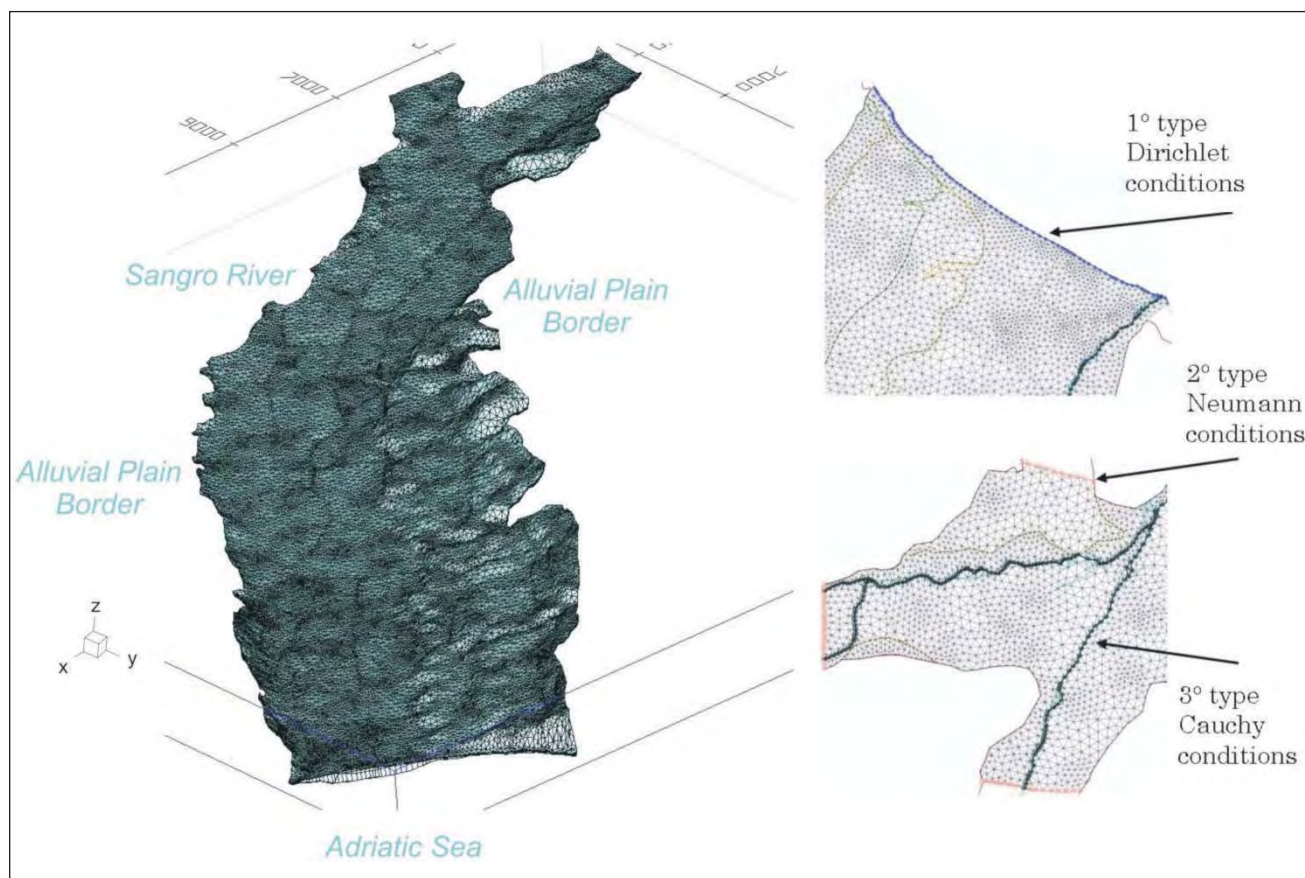


Fig. 8 - 3D mesh and boundary conditions of the Sangro plain regional numerical model (exaggeration factor 10:1); mod. from DESIDERIO *et alii*, 2007.  
 - Mesh 3D e condizioni al contorno del modello numerico, a scala regionale, della piana del Sangro (esagerazione verticale 10:1).

changes have a great influence in hydraulic heads distribution.

Boundary conditions were assigned considering hydrogeological characteristics and model domain extends up to Plio-Pleistocene hills, while the basement is considered impermeable. In the higher alluvial plain border and in correspondence of secondary valleys, fixed flux conditions were applied on the basis of estimated groundwater discharge. Transfer type conditions (DIERSCH, 2002) were applied along Sangro river and constant hydraulic heads, 0 m a.s.l., were applied along coastline.

Averages of piezometric heads, from monitoring program, were used for different observation points during calibration phase; the dominance of positive residual values is justified by the simulation of conditions without exploitations (fig. 9).

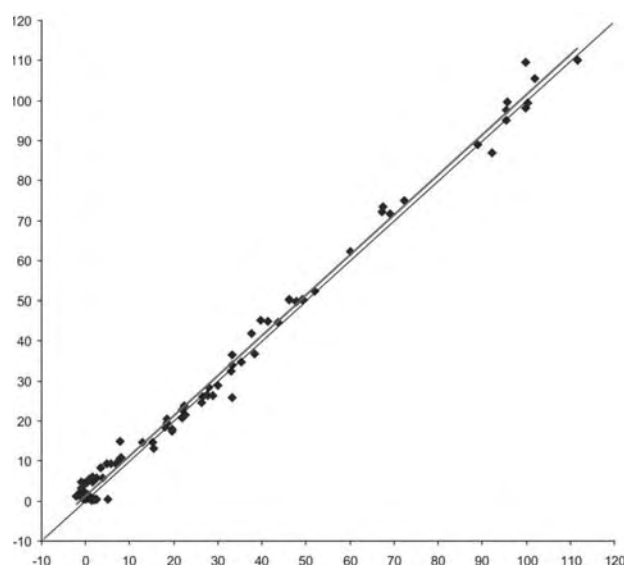


Fig. 9 - Measured vs. simulated value of hydraulic head in the calibration graph of the regional numerical model of Sangro alluvial plain.  
- Confronto tra valori misurati e valori simulati di carico idraulico nel grafico di calibrazione relativo al modello numerico regionale della piana del Sangro.

#### 2.6.1. - Simulation of sea-water intrusion

Conceptual and numerical analysis of Sangro valley aquifers highlights typical problems in groundwater withdrawals and management in coastal areas due to sea-water intrusion and salinization process.

The local numerical models simulates density-dependent flow and transport conditions in the aquifer thus taking into account differences of saline concentrations. The mesh of Sangro local model, which extends over an area of about  $5.93 \times 10^6 \text{ m}^2$ , is constituted by 211680 cells and 116130 nodes over 14 layers. Triangular-based

prismatic elements have orthogonal projections that vary in dimensions from 70 m in the western coastal area to 30 m in areas near the coast and finally 10÷15 m in the proximity of the exploitation wells.

The topmost 7 layers identify the silty-sandy superficial deposits in the western area, and the sandy gravels and silty-clayey lenses in the coastal areas. All remaining layers represent the sandy-gravelly deposits. The distribution of the hydrogeological properties and the effective recharge is derived from the regional model. Constant fluxes in the western area and equivalent hydraulic heads (DIERSCH & KOLDITZ, 1998; DIERSCH, 2002), assuming a sea water density of 1025 g/l for an average salt concentration of 35 g/l, were assumed as boundary conditions. Constraints were applied on the concentrations of incoming and outgoing water fluxes.

The local model was used to simulate scenarios, starting from undisturbed conditions, using different exploitation schemes. The scenario simulating undisturbed conditions was obtained from transient conditions over a long period of 100000 years. The other simulations with ongoing exploitations were run with variable periods going from 30 up to 100 years. Distribution of hydraulic heads and concentrations were calculated at both the end of the time interval and during transient conditions so as to simulate saline intrusion phenomena.

The first scenario considered typical summer exploitations related to irrigation purposes (fig. 10). Variable exploitation rates vary from 0.1 up to 0.2 m<sup>3</sup>/s through several irrigation wells, up to 15÷20 l/s per well. In some stations the exploitation is lower of about 2÷5 l/s and occurs over a short period of few hours. Saline intrusion phenomena occur in these conditions mainly in the areas on the left side of the river near coast. Strong saline intrusion evidences occur in some wells located at short distances from the coast line. These wells are sometimes located on low hydraulic conductivity alluvial deposits. This scenario maximizes the stress conditions of the system due to the fact that the exploitations are not constant on time and superficial recharge is present due to irrigation.

A second scenario with a limited exploitation of only 1 l/s per well, produces reduced saline intrusion phenomena near those wells that are very close to the coast-line where only local high concentrations are recorded.

Other scenarios have been simulated with exploitation rates varying between 0.12 and 0.3 m<sup>3</sup>/s on wells located 2÷4 km from the coast-line and others with wells that are in proximity of the



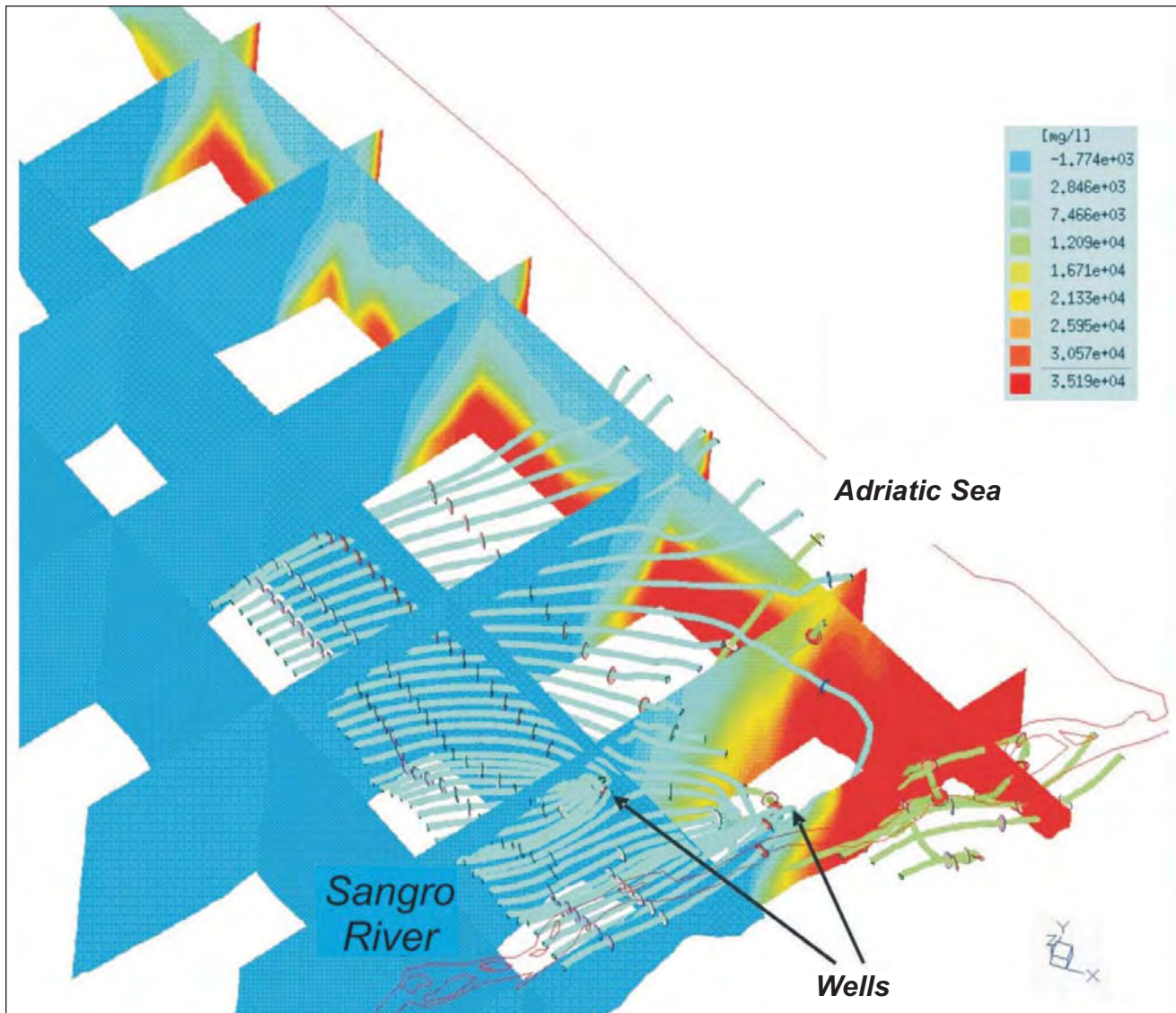


Fig. 10 - Salt water intrusion phenomena near the coastal area and flow lines, typical summer exploitations scenario (total salinity in mg/l; exaggeration factor 10:1); after DESIDERIO *et alii*, 2007.

- Fenomeni di intrusione salina nella zona costiera e linee di flusso, relativamente allo scenario tipico estivo (salinità totale in mg/l; esagerazione verticale 10:1); da DESIDERIO *et alii*, 2007.

river outlet. Intense agricultural schemes are in place in these areas and the absence or reduced presence of superficial irrigation systems increases the need for groundwater exploitations for irrigation. The pumping rates often accelerate the saline intrusion phenomena.

Hydraulic heads tend to reach equilibrium usually within 2÷3 years, while concentrations tend to have significant variability for periods that range from 15 to 25 years.

The different scenarios confirm saline intrusion phenomena due to exploitation in areas near to the river outlet, especially when these are constant through time. Critical conditions of variable concentrations due to strong decrease of piezometric levels are present even after long periods thus proving the persistence of salt water intrusions.

### 3. – THE VOMANO ALLUVIAL VALLEY

#### 3.1. – GEOLOGICAL SETTING

The ancient and recent alluvial deposits of the Vomano river plain (fig. 11) consist of gravel, sandy-gravel and gravelly-sand bodies. Above these, in the middle-low part of the plain, clayey-muddy-sandy and muddy-sandy-clayey deposits are present, varying in thickness from few metres up to 20 m near the coastal belt. Sandy-gravelly deposits crop out in the upper part of the river valley. The substrate beneath the alluvial deposits mainly comprises lithotypes such as the marly clays and clayey marls of the Cellino Formations and Argille Grigio Azzurre (CRESCENTI, 1971; CRESCENTI *et alii*, 1980; CASNEDI *et alii*, 1981;

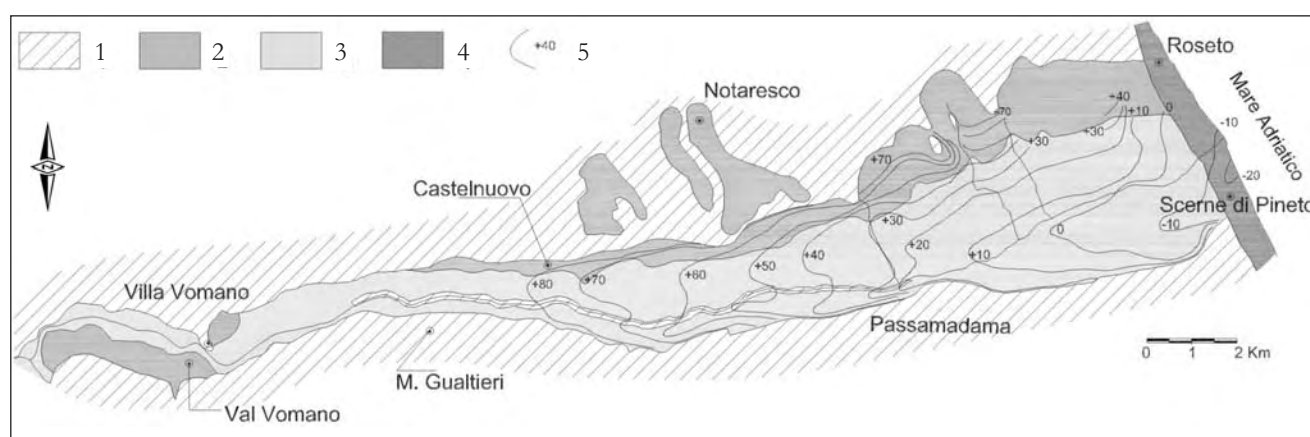


Fig. 11 – Schematic geologic map of the Vomano alluvial plain. 1) Pelitic-arenaceous deposits (Pliocene-Pleistocene). 2) Alluvial terrace (I and II order). 3) Alluvial terrace (III and IV order). 4) Coastal deposits. 5) Substratum morphology (contour lines in m a.s.l.); modified after DESIDERIO *et alii*, 2003.  
 – Schema geologico della piana alluvionale del Vomano. 1) Depositi pelitico-arenacei (Pliocene-Pleistocene). 2) Alluvioni terrazzate (I e II ordine). 3) Alluvioni terrazzate (III e IV ordine). 4) Depositi costieri. 5) Morfologia del substrato (isolinee in m s.l.m.).

VEZZANI & GHISETTI, 1998). In the upper part of the plain, however, the substrate is made up of more permeable lithotypes: these are arenaceous and marly deposits originating from the Laga Formation and the Messinian deposits. The clay basement elevation contours were interpolated after 9 geoelectric prospecting profiles, in the well fields area, including more than 120 Vertical Electrical Soundings (CASSA PER IL MEZZOGIORNO, 1971; CELICO, 1983) and 18 borehole logs (fig. 12).

The top of the substrate of the alluvial deposits is characterised by the presence of a palaeo-thalweg, shifted some hundreds of metres north or south in relation to the present-day riverbed.

### 3.2. - HYDROLOGY AND WELL FIELDS

The hydrological balance was evaluated using data from pluviometric and thermometric stations (SERVIZIO IDROGRAFICO E MAREOGRAFICO, 1955-1995). An average infiltration rate of about 110 mm/yr was estimated by THORNTHWAITE & MATHER (1957) and TURC (1961) methodologies, considering a 30 years observation period (1965-1995). The pluviometric regime underlines an Apennine sublittoral climate, with marine influences; the minimum precipitation values are registered in summer time, while the maximum ones occur in winter and spring months, while the temperature has an opposite trend. The water balance was calculated using more than 30 pluvio-thermometric stations to evaluate the global surface runoff; the superficial hydrographic network is very limited due to high hydraulic conductivity of shallow alluvial deposits and soils so that most of meteoric waters recharges the aquifer, after satisfaction of the soil deficit.

In the eastern part of the Vomano valley, two well fields, Saf 1 and Saf 2 of ACA S.p.A. (a local water agency) are located, not far away from the coastline. The two well fields are located on a highly conductive palaeo-river, as resulted from geophysical prospecting and boreholes. Current overall withdrawal is in the range of 200÷470 l/s, depending upon season, with the average of about 270 l/s. The pumping regimes consist in about 150÷250 l/s for Saf 1 and, when the water request is higher or in emergency conditions as in drought periods, in about 100 l/s for Saf 2, with hydraulic heads up to 3÷4 m below mean sea level in Saf 1 area located near to coastline.

### 3.3. - HYDROGEOLOGY

As emerging from previous hydrogeological studies (CASSA PER IL MEZZOGIORNO, 1971; CELICO, 1983; DESIDERIO *et alii*, 2003), the Vomano valley is characterized by a single phreatic aquifer system, with minor semi-confined layers, overlying an impermeable clay basement (fig. 13). Major hydrogeological features include Vomano river and some, possibly highly conductive, paleo-rivers related to geomorphological and tectonic history of most alluvial valleys of Abruzzo and Marche regions.

The alluvial deposits overlay an impermeable clay basement, with thickness varying from few meters in the proximity of its outcrops, up to about 28 m along the main paleo-river.

The alluvial deposits constitute the III and IV order terraces of Vomano plain; the aquifer system consists mostly of gravel, sandy-gravel and gravelly-sand bodies. In the middle-low plain, clayey-muddy-sandy and muddy-sandy-clayey deposits with much lower hydraulic conductivity

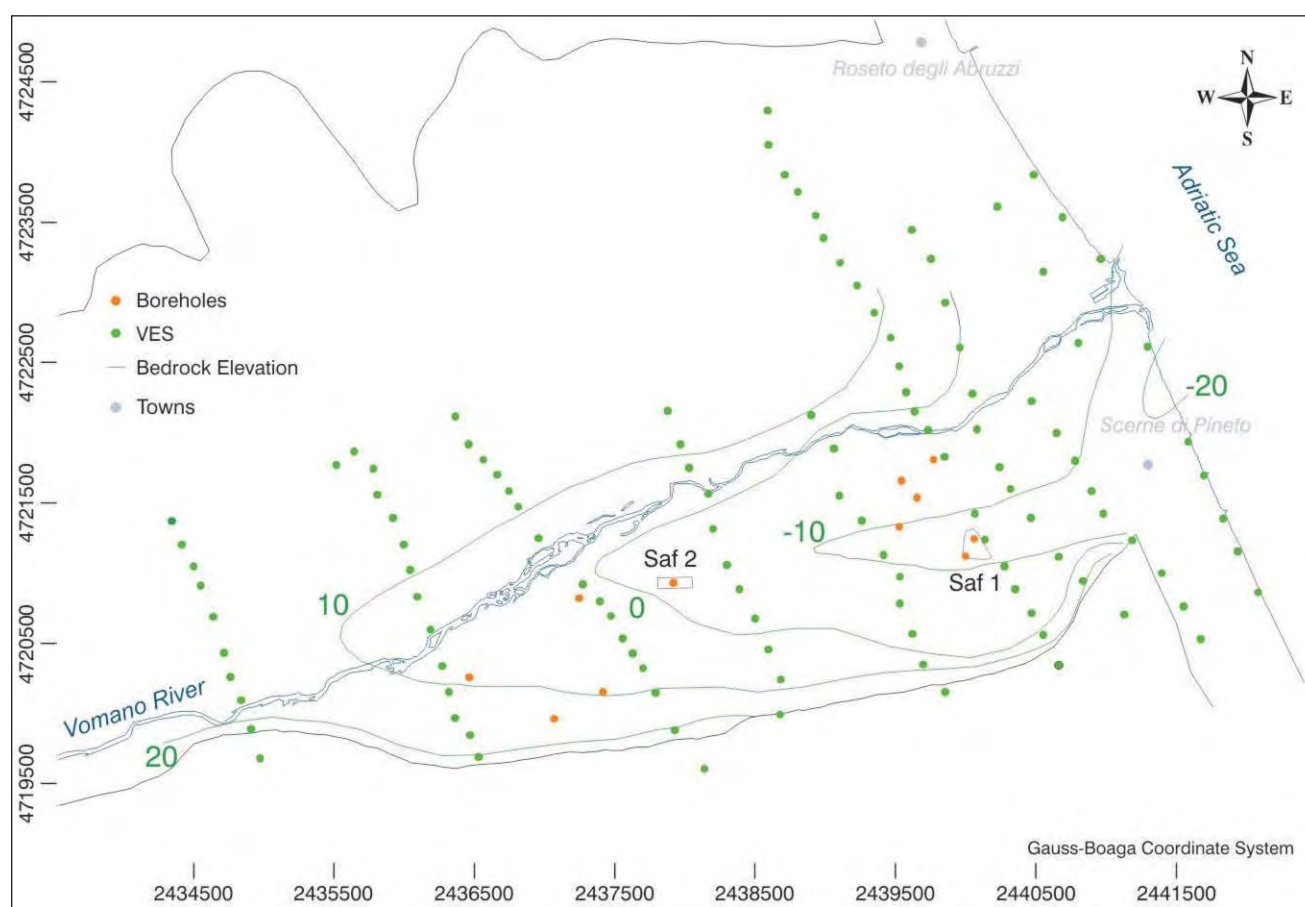


Fig. 12 - Bedrock elevation map with location of VES and boreholes in the lower Vomano alluvial plain.  
 - Carta del substrato con ubicazione dei SEV e dei sondaggi geognostici nella piana alluvionale del Vomano.

values, are responsible for local semi-confined conditions. The silty and clayey soil, is 1÷2 m thick.

The palaeo-river, with a northern deviation close to the coastline, is made by gravelly and sandy deposits, while in the adjacent zones silty matrix gravelly-sands are present; at the valley border sandy silts are prevalent.

The Vomano river thalweg, in the study area, is made by recent alluvial gravelly and locally sandy deposits; hydraulic continuity with aquifers occurs with a prevalent surface water contribution respect to direct precipitation recharge.

### 3.4. – HYDROCHEMISTRY

The unconfined aquifer is recharged mainly by fluvial waters from calcium-bicarbonate facies of Apennine origin, as confirmed by the values of electrical conductivity and groundwater temperature (DESIDERIO *et alii*, 2003). River recharge is further testified by the chemistry of the groundwater: close to the river bed the waters present calcium-bicarbonate facies with low saline content. Waters of this type are also found near the main

drainage axes, which drain the waters of the Vomano river and its primary tributaries through palaeo-thalwegs.

The aquifer is also recharged by deep waters of Pliocene or Messinian origin (DESIDERIO *et alii*, 2003, 2004). These waters, rising along fault-associated fracture zones in the Plio-Pleistocene substrate deposits, are carried to the base of the unconfined aquifer. The mixing of sodium-chloride and calcium-sulfate facies Pliocene and Messinian mineralised waters with the calcium-bicarbonate waters of the aquifer lead to different hydrochemical facies in the aquifer areas close to the zones where the mineralised waters emerge.

Recharge by the Messinian and Pliocene waters is very slight and mainly influences the chemistry of underground waters, causing enrichment in  $\text{Cl}^-$ ,  $\text{Na}^+$ ,  $\text{Mg}^{++}$  and  $\text{SO}_4^{--}$  of the calcium-bicarbonate waters originating from fluvial recharge (fig. 14).

### 3.5. - HYDRODYNAMICS

Vomano valley groundwater circulation is closely dependent on palaeo-rivers.



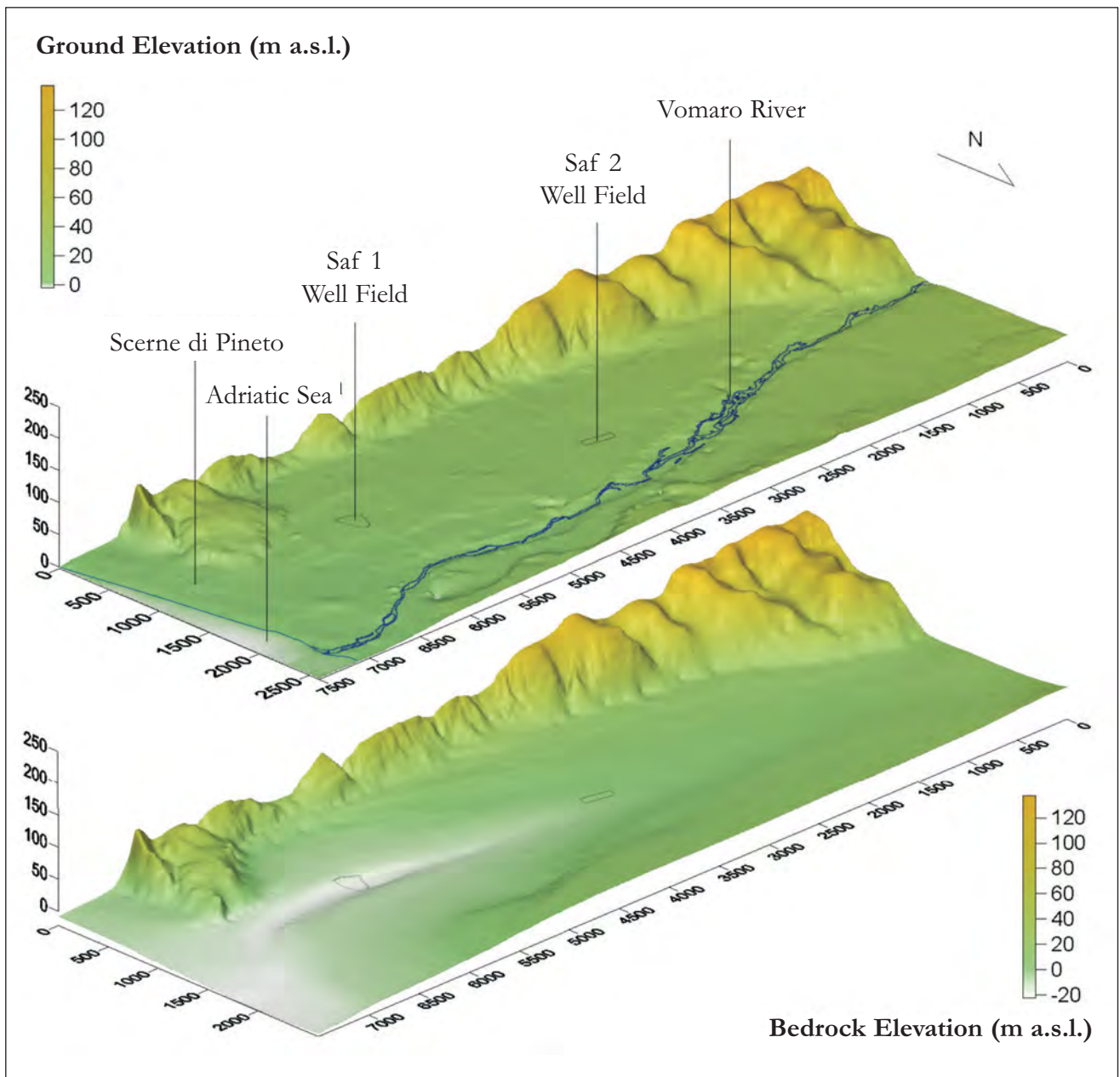


Fig. 13 - A 3D overview of the ground above) and bedrock (below) surfaces (exaggeration factor, 5:1); after RUSI *et alii* 2004.  
 - Vista 3D della superficie topografica (in alto) e del basamento impermeabile (in basso; esagerazione verticale, 5:1).

Piezometry, based on seasonal monitoring of 150 wells during 2000, highlights (fig. 15): - groundwater heads generally intersecting gravels and gravelly sands under overlaying low conductivity silt deposits; - a water circulation depending on basement morphology related to palaeo-rivers; - left side river drainage in medium and lower valley for riverbed gravels and sands; - aquifer drainage into river where flowing directly on basement deposits; - groundwater flow to recent III and IV order terraces from ancient I and II order terraces aquifers, with a prevalent recharge by precipitations.

Aquifer recharge is related to direct precipitation and Apennine contributions in the higher valley; differently in the lower valley it is influenced by river inflows especially along palaeo-rivers, direct precipitations, superficial runoff on hillsides and, during dry seasons, irrigation components.

Several pumping tests of different duration and operative plan were executed in Saf 1 and Saf 2 well fields to evaluate hydrodynamic parameters. The pumping tests were executed with constant flow rates considering the installed pumps typology and aqueduct system (RUSI *et alii*, 2004).

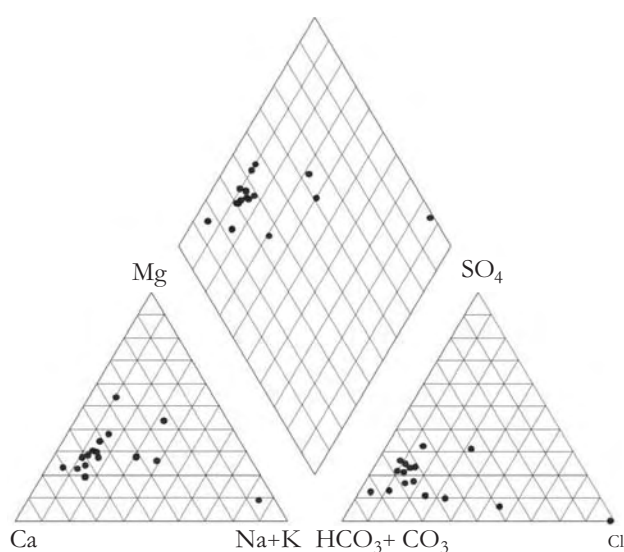


Fig. 14 - Piper's diagram of the Vomano plain groundwaters.  
- Diagramma di Piper relativo alle acque della piana del Vomano.

Some pumping tests were executed on single wells in transient and steady-state conditions for short and long periods (from 3 up to 76 h), monitoring drawdowns in surrounding wells (fig. 16).

Equilibrium was reached in Saf 1 well field about 2 h after the beginning of pumping at the highest possible flow rate allowed by the installed pump (60 l/s). The high aquifer transmissivity involves not only piezometric surface stabilization but even water levels rising in testing and surrounding monitoring wells; these pumping tests were so worked out only considering the steady-state condition (DUPUIT, 1863).

Hydraulic conductivity values range from  $2.0 \times 10^{-3}$  m/s to  $3.1 \times 10^{-3}$  m/s, and average transmissivity is  $4.1 \times 10^{-2}$  m<sup>2</sup>/s, considering an aquifer thickness of 18 m.

It was possible for Saf 2 well field pumping

tests also the transient condition (THEIS, 1935) because the transmissivity is limited due to a smaller aquifer thickness; hydraulic conductivity values range from  $1.5 \times 10^{-3}$  m/s up to  $2.7 \times 10^{-3}$  m/s, with an average transmissivity of about  $2 \times 10^{-2}$  m<sup>2</sup>/s, considering an aquifer thickness of 9.5 m.

Other pumping tests were executed in maximum stress condition allowed by pumping stations (approximately 50 l/s for each well), for about 24 h, to evaluate the hydrodynamic response under overexploitation. The influence of the well fields, in these conditions, was limited in the surrounding areas already at distances of a few hundreds of meters; definitely the influence is limited on short period (one or two days); in any case it is very influential on long periods (some days). Hydraulic conductivity values, based on long time pumping tests and geophysical evidence, are generally in order of  $2 \times 10^{-4}$  m/s up to about  $2.5 \times 10^{-3}$  m/s in correspondence of the palaeo-river.

### 3.6. - MODEL DESIGN AND NUMERICAL ANALYSIS

A finite-difference groundwater flow model was developed for lower Vomano aquifer by using MODFLOW 2000 numerical code, in steady-state and transient conditions for optimization of well fields pumping regime.

The domain was discretised using a regularly spaced grid with 48750 cells, with cell size of 20 m; applying Telescopic Mesh Refinement (TMR) approach (WARD *et alii*, 1987), two site models were implemented around Saf 1 and Saf 2 well fields, with irregularly spaced grids, characterized by a denser refinement near pumping wells (fig. 17).

A constant head boundary of 0 m a.s.l. was used for the coastal zone; no-flow boundaries were specified near southern impermeable hills where the water recharge looks like to be very

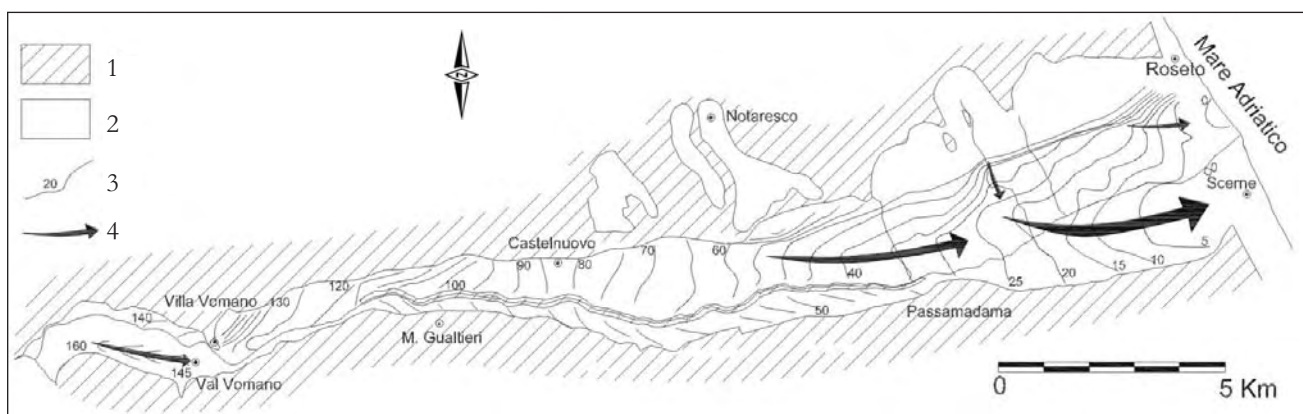


Fig. 15 - Piezometric map of the Vomano alluvial plain. 1) Pelitic-arenaceous bedrock. 2) Alluvial terrace (I - IV order). 3) Piezometric contour (m a.s.l.). 4) Preferential flow area; modified after DESIDERIO *et alii*, 2003.  
- Carta piezometrica della piana alluvionale del Vomano. 1) Substrato pelitico-arenaceo. 2) Alluvioni terrazzate (I - IV ordine). 3) Isopiezometriche (m s.l.m.). 4) Zone e direzioni di drenaggio sotterraneo.



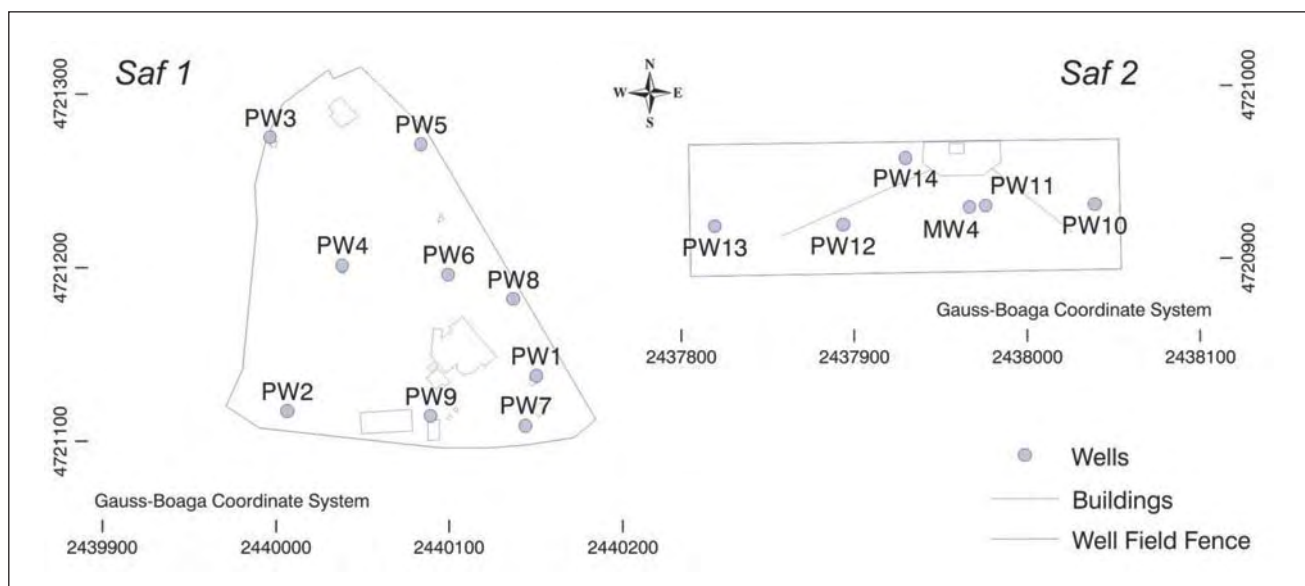


Fig. 16 - Location of Saf 1 and Saf 2 wells used for pumping test.  
 - Ubicazione dei pozzi nei campi Saf 1 e Saf 2 sottoposti a prove di emungimento.

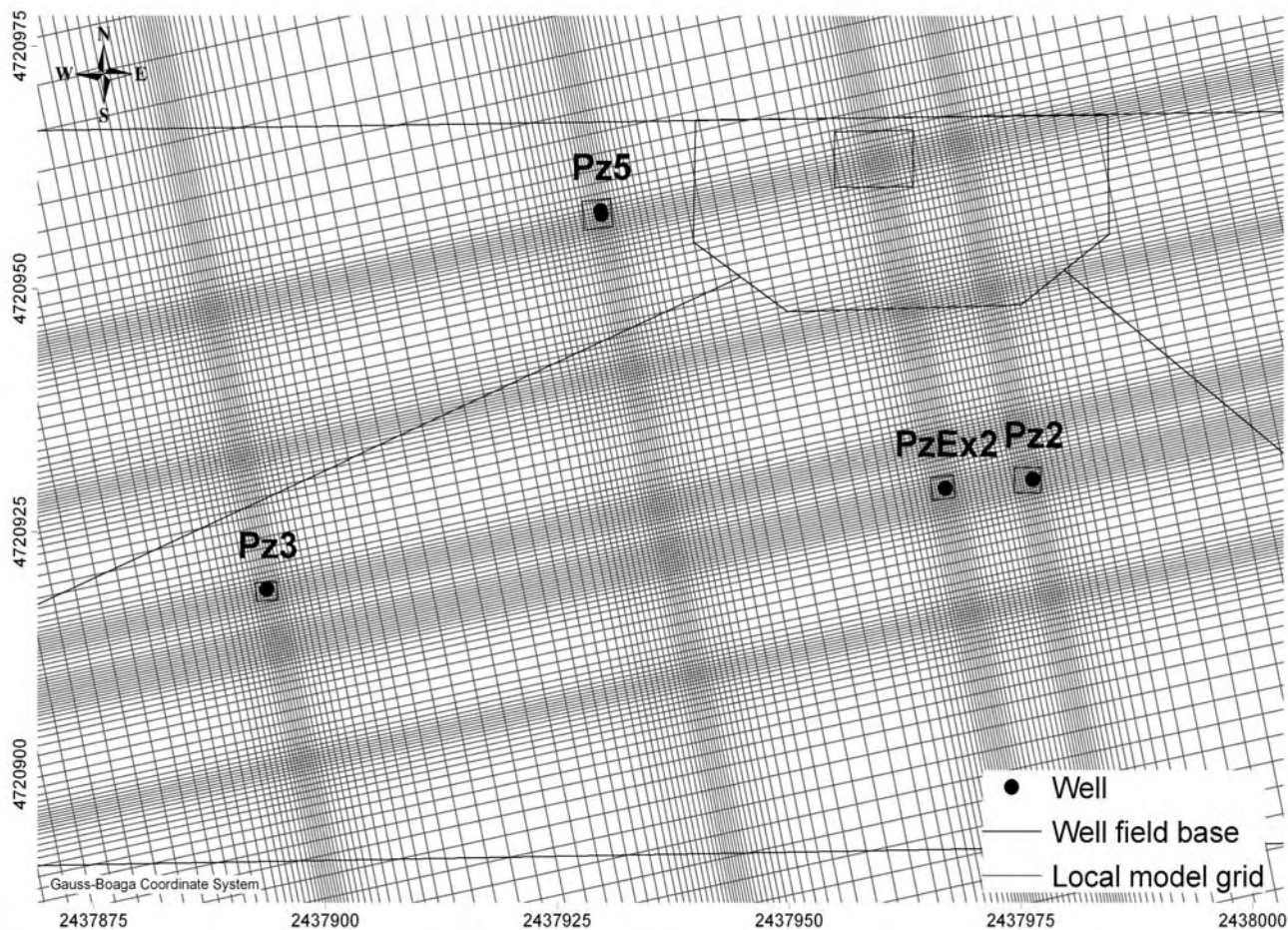


Fig. 17 - Detail of the irregularly spaced grid of the Saf 2 well field local model of the Vomano plain.  
 - Dettaglio della griglia a spaziatura irregolare del modello numerico del Campo Pozzi Saf 2 della piana del Vomano.



small due to the presence of a very thin and low permeable aquifer and lack of a relevant superficial hydrographic network; Vomano river was simulated using variable flow boundaries (Cauchy conditions), and infiltration was assumed constant in time. Different pumping rates were considered, both for steady-state and transient calibrations and simulations.

The model domain was divided in zones with different hydrogeological properties based on the interpretation of well fields pumping tests (fig. 18), geophysical prospecting outcomes and bore-hole logs. The specific focus was to capture the hydrogeological characteristics of the depositional environment. The reference values, obtained by calibration with the best fitting between the calculated and observed drawdown curves, are the most reasonable because they are in accordance with the hydrogeological parameters values evaluated through the pumping tests with DUPUIT (1863) and THEIS (1935) methods and the literature reference values (CASSA PER IL MEZZOGIORNO, 1971; RUSI *et alii*, 2004).

The seasonal measurements of the piezometric heads were executed in 150 wells on the whole Vomano plain to observe the piezometric oscillations. The highest oscillations, some meters, were observed in the study area due to water exploitation for drinking, irrigation and industrial purposes, while in other parts of the

valley the oscillations were smaller, lower than 1 m. Initially the model was calibrated in steady-state conditions using the mean observed water levels and considering the average wells exploitation in the area.

Afterwards the model was calibrated using the drawdown curves both in the case of the single well tests and the overexploitation conditions. The model calculates an adequate piezometric heads distribution for the different stress conditions, even if there are some differences between the computed and observed heads mainly due to uncertainty in parameter values distribution, particularly in the areas located at a certain distance from the well fields, where no pumping tests were available, and in the initial heads distribution. The residuals are minimum at the end of pumping tests for both well fields.

### 3.6.1. - Well fields management

Definitely the calibrated flow model is reasonable to investigate some major issues, concerning the optimisation of the existing well fields pumping regimes as well as the establishment of the wellhead protection zones.

The model supported an overall analysis of the hydrogeological system, highlighting the key-role of the major palaeo-river in controlling aquifer behaviour, as emerging from fundamental

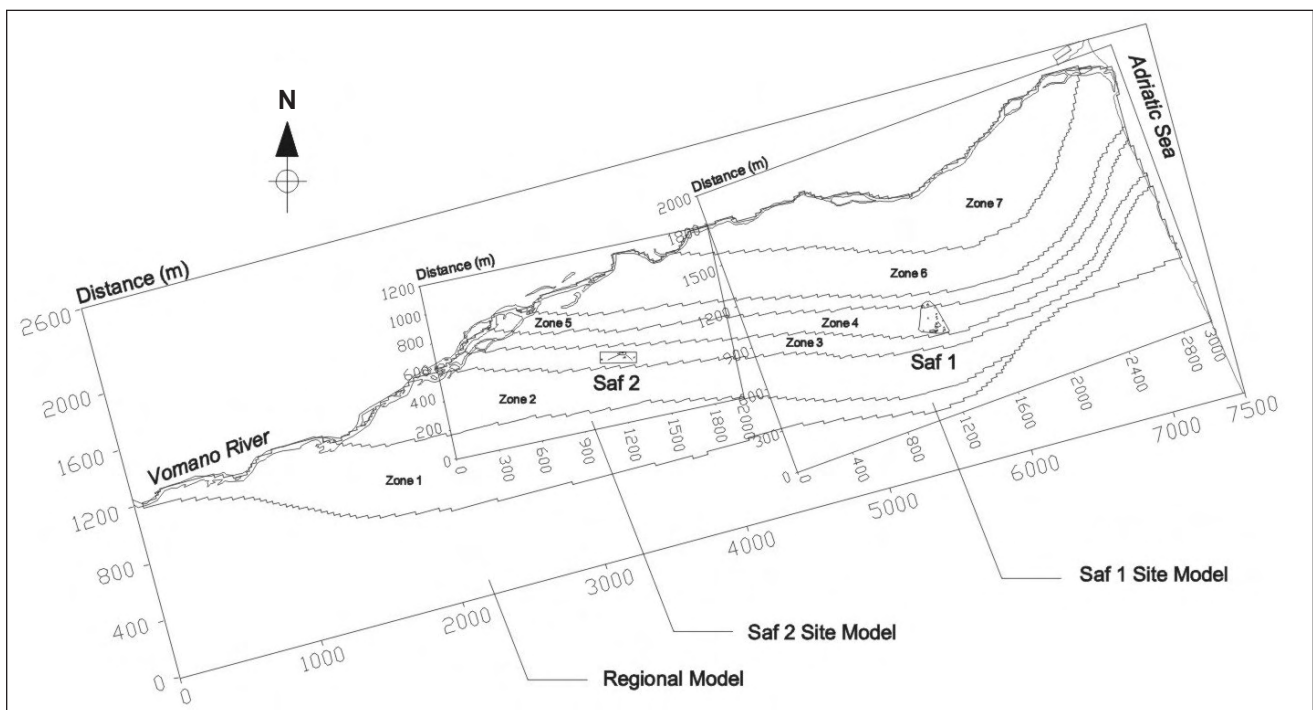


Fig. 18 - The location of the hydrogeological zones with the numerical model domains; from RUSI *et alii*, 2004.  
- Localizzazione delle differenti zone idrogeologiche con individuazione dei domini dei modelli numerici implementati.

components in the local hydrogeological balance, flow paths and velocity fields. The attention was also focused on Vomano river recharging role. At first, the piezometric heads distribution in steady-state conditions and without exploitations was computed (fig. 19), considering the reference parameter values. In this condition the aquifer drains the Vomano river superficial waters in the western area near the Saf 2 well field, while the river drains the aquifer waters along the north area near the Saf 1 well field. The water circulation is mainly influenced by high conductivity palaeo-river, impermeable bedrock geometry and alluvial deposits hydraulic properties as demonstrated by the computed velocity field. The water

budget results were computed using the ZONEBUDGET code (HARBAUGH, 1990), so it was possible to evaluate the river-aquifer water exchanges in different hydrogeological zones, and to estimate the groundwater flow to the Adriatic Sea.

Afterwards the calibrated model was used to simulate different exploitation scenarios, both in steady-state and transient conditions (fig. 19). The sustainable pumping rates were established considering the steady-state conditions, while the periods of overexploitation were determined in transient conditions, assuming respectively the overall withdrawals of 450 l/s and 250 l/s for Saf 1 and Saf 2 well fields, with a pumping rate of 50 l/s for each well.

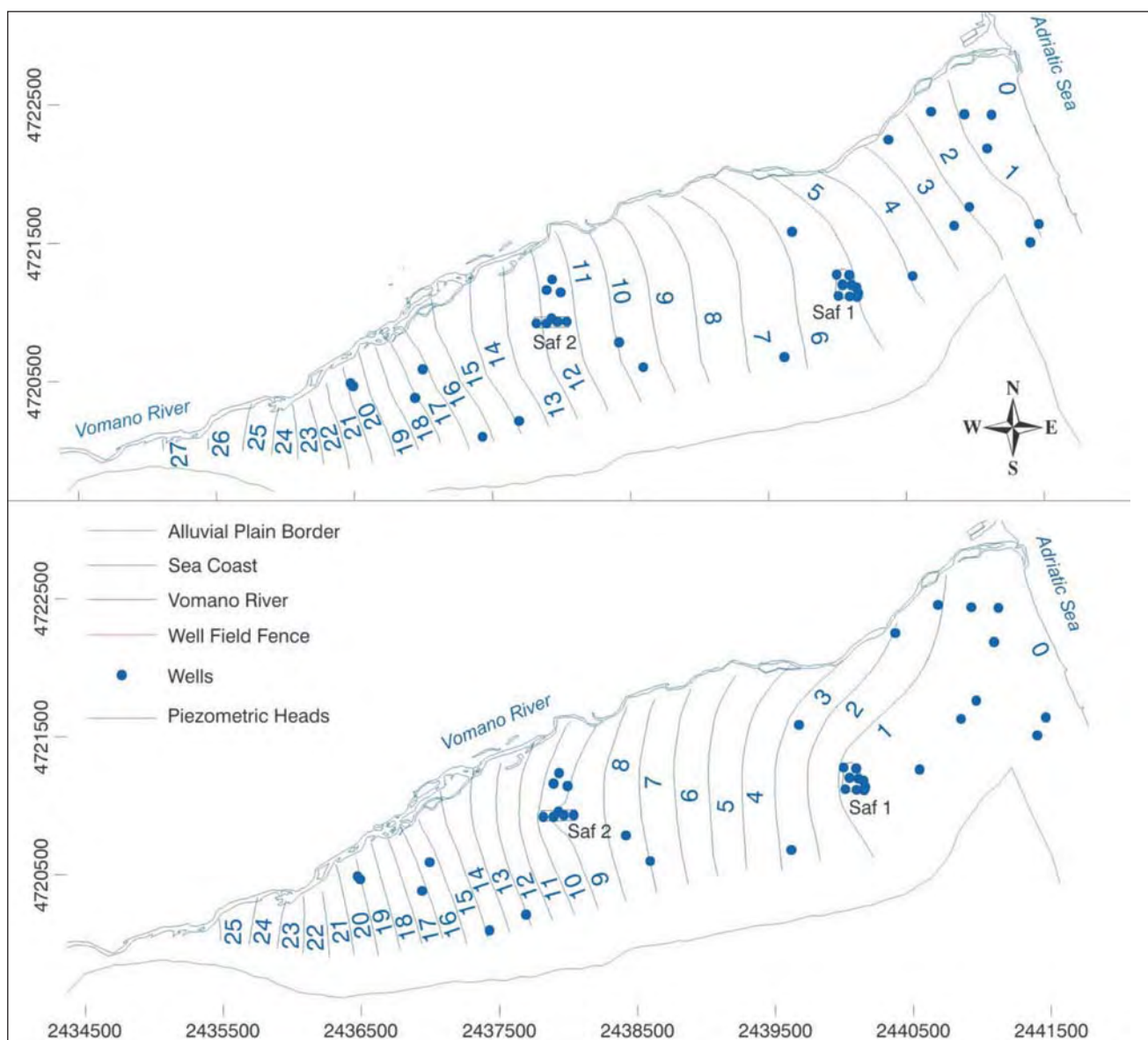


Fig. 19 - Simulated piezometric heads in steady-state condition, without withdrawals (above) and considering the mean withdrawals (below) from the eastern Vomano pumping wells.

- Distribuzione dei carichi piezometrici della zona orientale della Valle del Vomano simulati in condizioni stazionarie, senza emungimenti (in alto) e con emungimenti medi dai pozzi di pompaggio (in basso).

The sustainable pumping regime for the Saf 1 well field is about 150 l/s, due to high aquifer transmissivity (about  $4.1 \times 10^{-2} \text{ m}^2/\text{s}$ ), to be applied alternatively to three wells, maintaining a flow rate of about 50 l/s from each well. The overexploitation of 450 l/s can be supported by the aquifer for a time of about 15 days. In any case it is preferable not to apply overexploitation pumping regime because it can cause salt water intrusion.

The Saf 2 well field can support an overall exploitation of about 100 l/s in steady-state condition, while the overexploitation of 250 l/s can be applied only for short periods (about 5 days), afterwards dry conditions occur in wells with high piezometric drawdown in the aquifer system.

The area is characterized by the presence of industrial plants, agriculture and quarry activities. Preliminary estimate of the wellhead protection areas were made applying the MODPATH particle-tracking code (POLLOCK, 1989). The flow pathlines were computed for scenarios in suggested steady-state conditions for Saf 1 (150 l/s) and Saf 2 (100 l/s) well fields and the wellhead protection areas defined in a conservative way, considering the advective component (fig. 20).

The computed heads and flow pathlines clearly show the water contribution from the river.

### 3.6.2. - Simulation of sea-water intrusion

Salinization problems related to sea-water intrusion in Vomano coastal plain, potentially due to Saf 1 and Saf 2 well fields, have been numerically analyzed with finite-element 3D density-dependent FEFLOW code. Model domain is

extended from Vomano river up to Plio-Pleistocene very low conductivity hills; the mesh is formed by 251770 elements and 141229 nodes over 10 vertical layers and is refined near well fields, for numerical efficiency and stability, with triangular-based prismatic elements gradually varying from about 50 to less than 1 m near wells. Boundary conditions are defined hydraulic heads along Vomano river and coastline, considering here a water density of 1025 g/l. After a calibration tuning, the density-dependent model (CRESTAZ *et alii*, 2007) confirmed the previous numerical results yet highlighting: - high pumping rates for short periods do not induce sea water intrusion related to limited times and high piezometric heads between well fields and coastline due to Vomano river drainage; - overall withdrawals of about 250 l/s from Saf 1 and Saf 2 for a long period induce groundwater salinization along palaeo-river up to lower and principal well fields in about 8÷10 years (fig. 21).

Conceptual and density-dependent numerical analysis highlights the quantitative and qualitative sustainability of withdrawals on short and long periods, that contribute to avoid environmental and socio-economic damage.

## 4. - CONCLUSIONS

Groundwater resources of Sangro and Vomano rivers alluvial plain have been analyzed through flow and transport numerical simulations with MODFLOW and FEFLOW codes, in density-dependent conditions. The conceptual model has been based on geological, geomorphological,

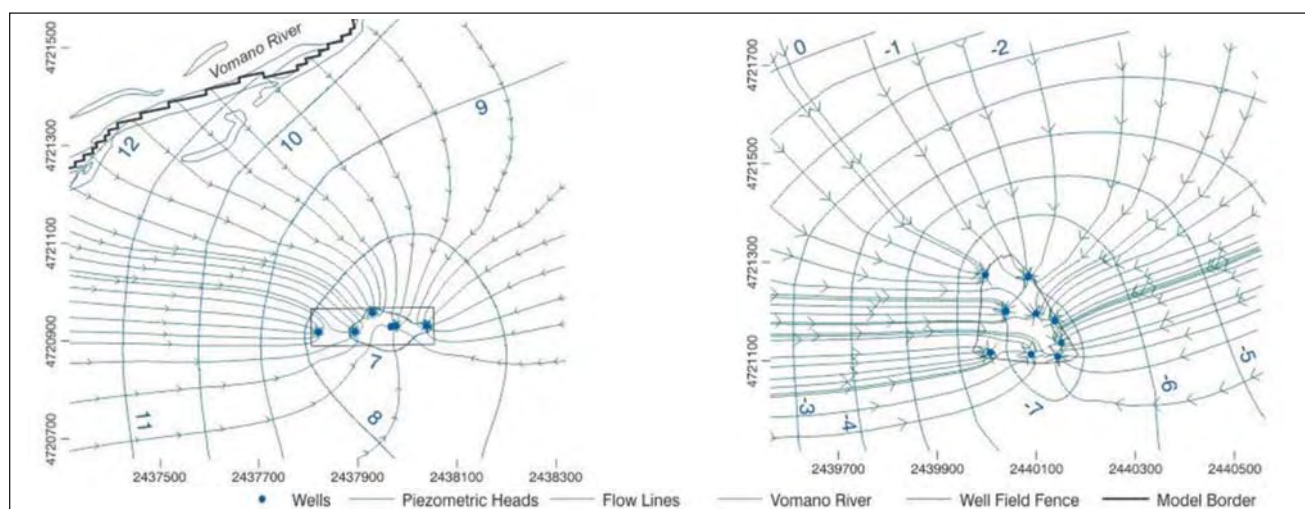


Fig. 20 - Flow pathlines with markers every 30 days. Left: the Saf 2 well field area, considering the simulated steady-state condition with an exploitation of 100 l/s. Right: the Saf 1 well field with an exploitation of 150 l/s.

- Linee di flusso con markers ogni 30 giorni. A sinistra: campo pozzi Saf 2, scenario in stato stazionario, con un'estrazione idrica complessiva di 100 l/s. A destra: campo pozzi Saf 1 con un'estrazione idrica complessiva di 150 l/s.



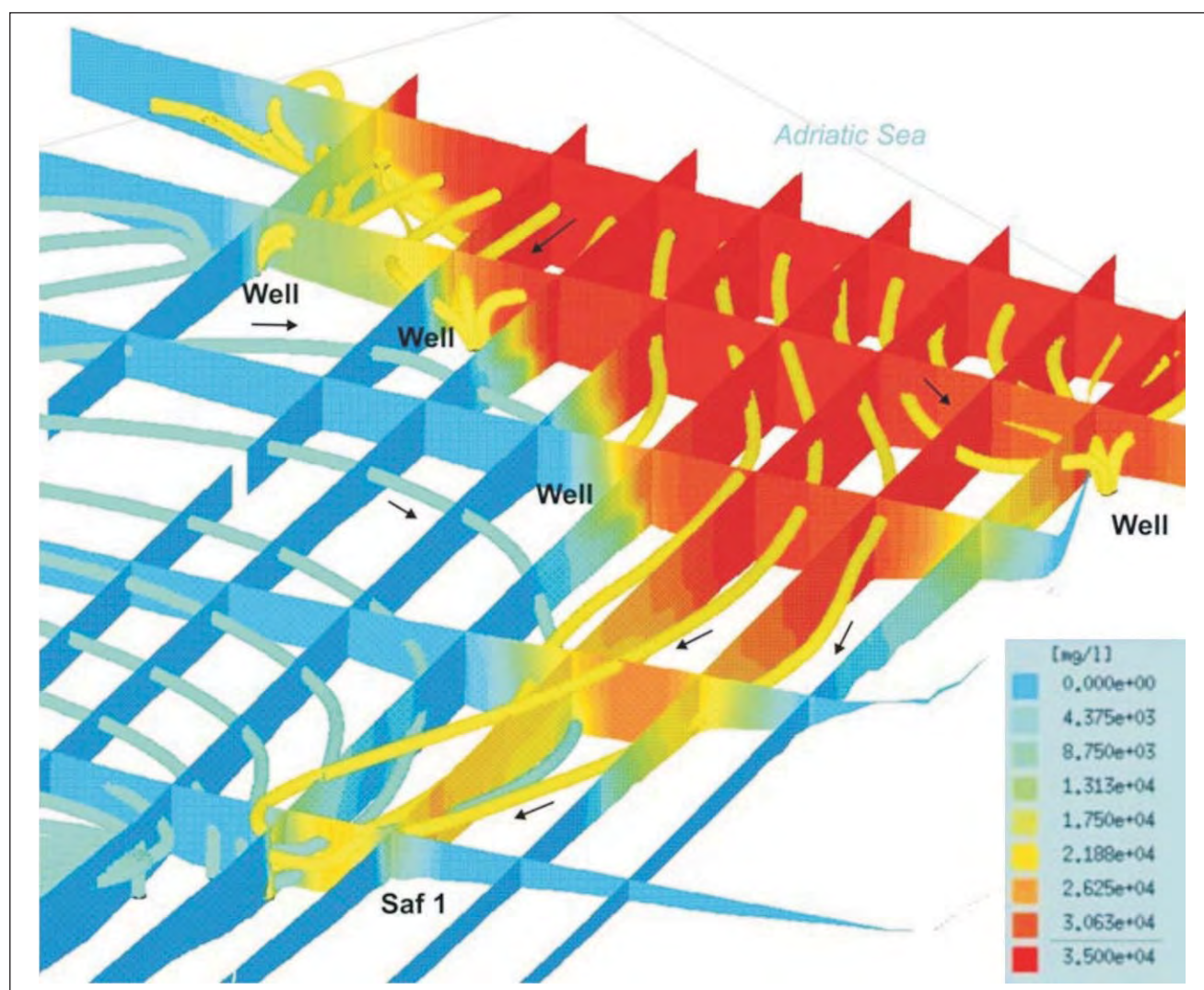


Fig. 21 - Salt water intrusion phenomena near the coastal area and flow lines in the Vomano plain, scenario with withdrawals of about 250 l/s from Saf 1 and Saf 2 well fields for a long period (total salinity in mg/l; exaggeration factor 10:1).

- Fenomeni di intrusione salina nella zona costiera e linee di flusso nella piana del Vomano, relativamente allo scenario con emungimenti di 250 l/s per lungo periodo (salinità totale in mg/l; esagerazione verticale 10:1).

geognostic, geophysical, hydraulic, hydrogeological and chemical data and interpretations.

The alluvial valleys, mainly constituted of both ancient and recent terraced alluvial deposits, are constituted by unconfined aquifers, even if semi-confined conditions are locally reached due to silty-clay lenses. Groundwater flow is strongly influenced by palaeo-rivers, while the influence of higher order terraces is generally modest. The dominant hydrochemical facies is calcium-bicarbonate up to sulphuric-chloride-alkaline to sodium-chloride and sodium-sulphuric facies related to deep up flowing of mineralized waters.

Quantitative assessment of water resources has been possible through numerical modeling in relation to aquifer-river exchanges, influence of palaeo-rivers and water discharges coming from higher order terraces.

Salt-water intrusion phenomena in coastal areas of Sangro aquifer are related to withdrawals for civil and irrigation purposes; vertical chemical trends are evident due to variations in hydrodynamic conditions with depth and mixing with mineralized waters. Simulation results highlight that saline intrusion phenomena can be limited when exploitations are not concentrated during summer and a better spatial configuration of wells is adopted.

The Vomano well field sustainable pumping regimes and wellhead protection areas were defined both in steady-state and transient conditions. The simulated different exploitation scenarios highlight that maximum acceptable exploitation for Saf 1 and Saf 2 well fields is respectively in the order of 150 l/s and 100 l/s, under steady-state conditions, while a pumping regime of 50

l/s for each well can be supported, in transient conditions, by Saf 1 and Saf 2, respectively, for about 15 and 5 days.

The model simulated in an adequate way the aquifer behaviour so it provides a reference hydrogeological framework for evaluation of the aquifer capacities and of the superficial water contributions. It was also useful for water quality protection, through the delineation of flow pathlines in different exploitation conditions.

Numerical analysis highlights the risk of sea-water intrusion if concentrated withdrawals occur near coastline, particularly during higher water request and smaller aquifer recharge periods.

Geolithological and hydrogeological data of the unsaturated zone and river flow measurements could be useful for calibration refining; moreover this research underlines the necessity of a continuous monitoring network of groundwater withdrawals and hydraulic levels for predictive purposes.

#### Acknowledgements

The authors are grateful to the two anonymous reviewers for their appreciated and constructive comments.

#### REFERENCES

- AMINZADEH F. (2004) - *Soft computing for qualitative and quantitative seismic object and reservoir property prediction (Part 1-3)*. EAGE, First Break, **22** (March, April and June 2004).
- ANDERSON M.P. & WOESSNER W.W. (1992) - *Applied Groundwater Modeling: Simulation of Flow and Advective Transport*. Academic Press Inc., San Diego, CA, USA.
- ANSELIN L. (2004) - *GeoDa 0.9.5-I Release Notes*, Spatial Analysis Laboratory and Center for Spatially Integrated Social Science (CSISS), Department of Agricultural and Consumer Economics, University of Illinois, Urbana-Champaign.
- CASNEDI R., CRESCENTI U., D'AMATO C., MOSTARDINI F. & ROSSI U. (1981) - *Il Plio-Pleistocene del sottosuolo molisano*. Geologica Romana, **20**, 1-42.
- CASSA PER IL MEZZOGIORNO (1971) - *Bilancio idrologico della falda alluvionale del fiume Vomano mediante modello analogico*. R.C. Progetto Speciale n.29, Compagnia Mediterranea di Prospezioni, Roma (unpublished work).
- CATENACCI V. (1974) - *Note illustrative della Carta Geologica d'Italia - Foglio 147 Lanciano*. Servizio Geologico d'Italia.
- CELICO P. (1983) - *Idrogeologia dell'Italia centro-meridionale*. Quaderni della Cassa per il Mezzogiorno, **4/2**, 1-230.
- CRESCENTI U. (1971) - *Sul limite Mio-Pliocene in Italia*. Geologica Romana, **10**, 1-22.
- CRESCENTI U., D'AMATO C., BALDUZZI A. & TONNA M. (1980) - *Il Plio-Pleistocene del sottosuolo abruzzese-marchigiano tra Ascoli Piceno e Pescara*. Geologica Romana, **19**, 63-84.
- CRESTAZ E., CASCELLI E., TATANGELO F. & RUSI S. (2007) - *Modellistica densità-dipendente a supporto della definizione delle politiche ottimali di sfruttamento e protezione delle risorse idriche sotterranee in aree costiere*. Acque Sotterranee, **108**, 11-17.
- DE RISO R., DUCCI D., IOVINELLI R. & ROTILIO D. (1994) - *Aspetti idrogeologici ed idrogeochimici della piana alluvionale del Fiume Sangro (Abruzzo)*. Geologica Romana, **30**, 635-644.
- DEMANGEOT J. (1965) *Géomorphologie des Abruzzes adriatiques*. Mem. et Doc., (Ed.) C.N.R.S., Paris.
- DESIDERIO G. & RUSI S. (2003) - *Il fenomeno dell'intrusione marina nei subalvei della costa abruzzese*. Quaderni di Geologia Applicata, **10** (1), 17-31.
- DESIDERIO G. & RUSI S. (2004) - *Idrogeologia e idrogeochimica delle acque mineralizzate dell'Avanfossa Abruzzese Molisana*. Boll. Soc. Geol. It., **123** (3), 373-389.
- DESIDERIO G., NANNI T. & RUSI S. (1999) - *Gli acquiferi delle pianure alluvionali centro adriatiche*. Quaderni di Geologia Applicata, **2** (1) - 1999, 21-30.
- DESIDERIO G., NANNI T. & RUSI S. (2003) - *La pianura del Fiume Vomano (Abruzzo): idrogeologia, antropizzazione e suoi effetti sul depauperamento della falda*. Boll. Soc. Geol. It., **122** (3), 421-434.
- DESIDERIO G., FERRACUTI L. & RUSI S. (2007) - *Structural-Stratigraphic Setting of Middle Adriatic Alluvial Plains and its Control on Quantitative and Qualitative Groundwater Circulation*. Mem. Descr. Carta Geol. d'It., **126**, 147-162.
- DESIDERIO G., RUSI S. & TATANGELO F. (2007a) - *Multidisciplinary approach in the hydrogeologic and hydrogeochemical analysis of the Sangro alluvial valley (Central Italy)*. Geologia Tecnica e Ambientale, **3-4/2007**, 35-57.
- DHI-WASI (2009) - *Institute for Water Resources Planning and Systems Research Ltd*. <http://www.earthsoft.com>.
- DIERSCH H.J.G. & KOLDITZ O. (1998) - *Coupled groundwater flow and transport: 2. Thermobaline and 3D convection systems*. Advances in Water Resources, **21** (5), 401-425.
- DIERSCH H.J.G. & MICHELS I. (1996) - *Moving finite element meshes for simulating 3D transient free surface groundwater flow and transport processes*. XI Int. Conf. on "Computational Methods in Water Resources", **1**, (Ed.) A.A. Aldama et alii, Computational Mechanics Publications, Southampton, 1996, 85-92.
- DIERSCH H.J.G. (1998) - *Treatment of free surfaces in 2D and 3D groundwater modeling*. Mathematische Geologie, **2**, 17-43.
- DIERSCH H.J.G. (2002) - *FEFLOW 5.1. - Reference manual - Physical Basis of Modelling*. Wasy Ltd., Berlin, Germany.
- DUPUIT J. (1863) - *Etudes théoriques et pratiques sur le mouvement des eaux dans les canaux découverts et à travers les terrains perméables*. Dunod, Paris.
- ENI-AGIP (1972) - *Acque Dolci Sotterranee. Inventario dei Dati raccolti dall'AGIP durante la Ricerca di Idrocarburi in Italia*. Grafica Palombi, Roma.
- ESRI (2009) - *Environmental Systems Research Institute*. <http://www.esri.com>.
- GHISETTI F. & VEZZANI L. (1983) - *Deformazioni pellicolari mioceniche e plioceniche nei domini strutturali esterni dell'Appennino centro-meridionale (Maiella e Arco Morrone-Gran Sasso)*. Mem. Soc. Geol. It., **26**, 563-577.
- GHISETTI F. & VEZZANI L. (1996-97) - *Geometrie deformative ed evoluzione cinematica dell'Appennino Centrale*. Studi Geologici Camerti, **14**, 127-154.
- HARBAUGH A.W. (1990) - *A Computer Program for Calculating Subregional Water Budgets Using Results from the U.S. Geological Survey Modular Three-dimensional Finite-difference Ground-water Flow Model*. U.S. Geological Survey, Open File-Report 90-392, 46 p.
- MAIDMENT D. R. (2002) - *Arc Hydro: GIS for water resources*. ESRI Press, Redlands, CA, USA.
- MCDONALD M.G. & HARBAUGH A.W. (1984) - *A modular three-dimensional finite-difference ground-water flow model*. U.S. Geological Survey, Open File-Report 83-875, 528 p.
- MCDONALD M.G., HARBAUGH A.W., BANTA E.R. & HILL M.C. (2000) - *MODFLOW 2000, The U.S. Geological Survey Modular Ground-Water Model - User Guide to Modularization Concepts and the Ground-Water Flow Process*.

- U.S. Geological Survey, Open File-Report 00-92, 121 p.
- MEINZER O.E. (1923) - *Outline of groundwater hydrology, with definitions*. U.S. Geological Survey, Water supply Paper 494, Washington D.C., U.S. Government Printing Office.
- MOSTARDINI F. & MERLINI S. (1986) - *Appennino Centro-Meridionale. Sezioni geologiche e proposta di modello strutturale*. Mem. Soc. Geol. It., **35**, 177-202.
- NANNI T. & VIVALDA P. (1998) - *Salt springs and structural setting of the Marche Adriatic foredeep. Central Italy*. Proceedings of the ninth Water Rock Interaction, Taupo (New Zealand).
- NANNI T. & VIVALDA P. (1999) - *Le acque salate dell'Avanfossa marchigiana: origine, chimismo e caratteri strutturali delle zone di emergenza*. Boll. Soc. Geol. It., **118** (1), 191-215.
- NANNI T. & VIVALDA P. (1999a) - *Le acque solfuree della regione marchigiana*. Boll. Soc. Geol. It., **118** (3), 585-599.
- NANNI T. (1985) - *Le falde di subalveo delle Marche: Inquadramento Idrogeologico, Qualità delle Acque ed Elementi di Neotettonica*. Materiali per la Programmazione, (Ed.) Regione Marche, 1-104, Ancona.
- NYKRAVESH M., AMINZADEH F. & ZADEH L.A. (2003) - *Soft Computing and Intelligent Data Analysis in Oil Exploration*. Elsevier Science, Amsterdam.
- PATACCA E., SCANDONE P., BELLATALLA M., PERILLI N. & SANTINI U. (1992) - *La zona di giunzione tra l'arco appenninico settentrionale e l'arco appenninico meridionale nell'Abruzzo e nel Molise*. Studi Geologici Camerti, Volume Speciale **1991** (2), CROP 11, 417-441.
- PINDER G.F. (2002) - *Groundwater Modeling using Geographical Information Systems*. John Wiley & Sons, Inc., New York.
- POLLOCK D.W. (1989) - *Documentation of Computer Programs to Compute and Display Pathlines Using Results from the U.S. Geological Survey Modular Three-Dimensional Finite-Difference Ground-Water Flow Model*. U.S. Geological Survey, Open File-Report 89-381, 188 p.
- RUSHTON K.R. (2005) - *Groundwater Hydrology*. John Wiley & Sons Ltd., England.
- RUSI S., TATANGELO F. & CRESTAZ E. (2004) - *The hydrogeological conceptualisation and well fields management of the Vomano Valley (Abruzzo, Central Italy) using groundwater numerical modelling*. Geologia Tecnica ed Ambientale, **4/2004**, 5-22.
- SCANDELLARI F. (1970) - *Situazione idrogeologica del basso corso del Fiume Sangro*. Atti 1° Congresso Internazionale sulle Acque Sotterranee, Palermo, 415-426.
- SELLI R. (1962) - *Il Paleogene nel quadro della geologia dell'Italia meridionale*. Mem. Soc. Geol. It., **3**, 737-789.
- SERVIZIO IDROGRAFICO E MAREOGRAFICO (1955-1995) - *Annali Idrologici: Vol. 1 e Vol. 2*. Sezione di Pescara, I.P.Z.S., Roma.
- STRASSBERG G. & MAIDMENT D.R. (2004) - *Arc Hydro Groundwater Data Model*. Geographic Information Systems in Water Resources III, AWRA Spring Specialty Conference, Nashville, May 17-19.
- THEIS C.F. (1935) - *The relation between the lowering of the piezometric surface and the rate and duration of discharge of a well using ground-water storage*. Trans. Amer. Geophys. Union.
- THORNTHWAITE C.W. & MATHER J.R. (1957) - *Instructions and tables for computing potential evapotranspiration and the water balance*. Publication in Climatology, Drexel Institute of Technology, **10/3**.
- TURC L. (1961) - *Evaluation des besoins en eau d'irrigation, évapotranspiration potentielle*. Ann. Agron., **12**.
- VEZZANI L. & GHISETTI F. (1998) - *Carta Geologica dell'Abruzzo 1:100.000*. Regione Abruzzo, Servizio Urbanistica, S.E.L.C.A., Firenze.
- WARD D.S., BUSS D.R., MERCER J.W. & HUGHES S.S. (1987) - *Evaluation of a groundwater corrective action at the Chem-Dyne hazardous waste site using a telescopic mesh refinement modeling approach*. Water Resources Research **23/4**, 603-617.
- WARD D.F., BUSS D.R., MERCER J.W. & HUGHES S.S. (1987) - *Evaluation of a groundwater corrective action at the Chem-Dyne hazardous waste site using a telescopic mesh refinement modeling approach*. Water Resources Research, **23** (4), 603-617.



## Relations between stratigraphy, groundwater flow and hydrogeochemistry in Poirino Plateau and Roero areas of the Tertiary Piedmont Basin, Italy

*Rapporti tra assetto stratigrafico, idrogeologia e idrogeochimica nel settore compreso tra l'Altopiano di Poirino e il Roero (Bacino Terziario Piemontese, Italia)*

VIGNA B. (\*), FIORUCCI A. (\*), GHIELMI M. (\*\*)

**ABSTRACT** - The study concerns the hydrogeologic setting of a vast portion of land, of about 1000 km<sup>2</sup>, between the Poirino Plateau, the thalweg of the Tanaro River and the hills between the towns of Bra and Asti.

The stratigraphic framework of the Messinian-to-Pleistocene succession of this area has recently been redefined on the basis of a multidisciplinary study carried out on the entire western Tertiary Piedmont Basin (TPB). This study, performed by a group of researchers from ENI, the Politecnico di Torino and the University of Turin, was based on the analysis and interpretation of biostratigraphic, sedimentologic, structural data from both outcrops and subsurface (ENI deep wells and seismic sections). The main result of the stratigraphic analysis of the Messinian to Pleistocene succession of the western TPB was the recognition of three main tectono-stratigraphic units or allogroups, bounded at base and top by major tectonically-induced unconformities. These allogroups have been named: Late Messinian Allogroup (LM), Early Pliocene Allogroup (EP) and Late Pliocene Allogroup (LP). Each of these allogroups is made up of informal lithostratigraphic units characterised by relative lithologic homogeneity and referable to one or to a set of marine or continental genetically related depositional environments (e.g. fluvial, deltaic, shelfal, slope, basal depositional systems).

In this work, the correlation between the outcrop and subsurface data has made it possible to define a detailed hydrostratigraphic scheme of the entire area under examination. In fact, the informal lithostratigraphic units recognised

in the multidisciplinary study have been correlated to their respective hydrogeologic units (aquifer analogues), referred to with their same nomenclature. The hydrogeologic units consist of different sedimentary facies. Hydraulic conductivity values have been assigned to the recognized sedimentary facies on the basis of direct measurements or of bibliographic data. Then different aquifer systems have been identified on the basis of the geometry of the aquifer, semi-permeable (aquitards) and impermeable (aquicludes) layers, of the type and geometry of their contacts, and of the hydrodynamical and hydrogeochemical data.

The main aquifer system is located in the basal part of the Villafranchiano B Hydrogeologic Unit and in the permeable sand layers of the Sabbie d'Asti B Hydrogeologic Unit. In the southwestern sector the piezometry of this aquifer system is strongly influenced by the geometry of the unconformity that separates the EP Allogroup from the underlying LM Allogroup and, in the remaining sector, by the geometry of the synclinal structure that involves the Sabbie d'Asti B and the Argille Azzurre B. This piezometry indicates groundwater flows from the Poirino Plateau and Bra Hills towards the Versa Valley (close to Asti) where, in the past, there was an important spring which was tapped for drinking water purposes. At present several wells are in operation and are over-exploiting the aquifer under examination causing a large depression cone. The aquifer system is confined and, below the Eastern Escarpment, is generally artesian. The chemistry of these waters is substantially homogeneous with bicarbonate-

(\*) Dipartimento di Ingegneria del Territorio, dell'Ambiente e delle Geotecnologie, Politecnico di Torino, Corso Duca degli Abruzzi 24, 10129 Torino, Italy. E-mail: bartolomeo.vigna@polito.it; adriano.fiorucci@polito.it

(\*\*) ENI S.p.A., Exploration & Production Division, ESEI, Via Emilia 1, 20097 San Donato Milanese (MI), Italy. E-mail: manlio.ghielmi@eni.it

calcic and bicarbonate-calcic-magnesium facies with decidedly low nitrate contents and iron and manganese levels which are often above the maximum admissible concentrations established by the Italian Law.

A second aquifer system, which at present is not very important but in the past was the only water resource available for the local population, is found in the hilly sector north of the Tanaro River between the villages of *Santa Vittoria d'Alba* and *San Damiano d'Asti*. This aquifer system, located in the sand bodies of the *Argille Azzurre* A Hydrogeologic Unit, is artesian along the main valley bottom and is under pressure in the other zones. The groundwater flow is completely different from the main aquifer system with prevalent directions towards the west and a rather complex recharge mechanism due to recurrent leakage from the aquifers above. This aquifer system is intercepted by deep wells that reach the waterlogged sand bodies below a thick succession of silty clays.

The chemical facies of the waters from this aquifer system are very different one from the other. The presence of chloride-sodic facies shows the existence of marine water that was trapped in the sediment at the moment of the deposition and which still has not been completely displaced by continental water. These latter have been identified in several wells and have bicarbonate-calcic and bicarbonate-magnesium-calcic facies. Bicarbonate-alkaline facies have also been found that can be explained by cationic exchange with the clayey confining layers favoured by long permanence times in the aquifer. The quality of the water is generally poor because of the ammonium, iron and manganese ion contents.

Other less important aquifer systems are present in the *Poirino* Plateau sector in the Villafranchiano C Hydrogeologic Unit and in the Terraced Quaternary Alluvium Hydrogeologic Unit. The piezometry of the latter indicates flow directions opposite to the main aquifer system below and poor quality waters because of high nitrate contents.

**KEY WORDS:** aquifers, hydrogeochemistry, hydrogeology, stratigraphy, Tertiary Piedmont Basin.

**RIASSUNTO** - Lo studio interessa l'assetto idrogeologico di una vasta area (circa 1000 km<sup>2</sup>) compresa tra l'Altopiano di Poirino, il fondovalle del Fiume Tanaro e la zona collinare tra le città di Bra e Asti.

L'assetto stratigrafico di quest'area, relativo alla successione plio-pleistocenica, è stato ridefinito da uno studio multidisciplinare che ha interessato l'intero settore occidentale del Bacino Terziario Piemontese. Per lo studio, condotto da un gruppo di ricercatori di Eni, Politecnico di Torino e Università di Torino, sono stati utilizzati dati di superficie e di sottosuolo che hanno permesso di definire uno schema stratigrafico di dettaglio della successione studiata. Al di sopra dei depositi messiniani della Formazione della Vena del Gesso, sono state riconosciute tre unità stratigrafico-sequenziali principali separate da importanti discontinuità di natura tettonica così denominate: Allogruppo Late Messinian (LM), Allogruppo Early Pliocene (EP) e Allogruppo Late Pliocene (LP). Tali allogruppi sono costituiti da differenti unità stratigrafico-deposizionali riconducibili a uno o più ambienti di deposizione marini o continentali (sistemi deposizionali fluviali, deltizi, di piattaforma, ecc.). Tali unità si caratterizzano per una relativa omogeneità litologica e sono state elevate al rango di unità litostratigrafiche informali.

La correlazione tra la geologia di superficie e i dati di sottosuolo ha permesso di definire un modello idrostratigrafico dell'intera area in esame, in cui le unità litostratigrafiche informali riconosciute nello studio multidisciplinare sono state correlate alle corrispondenti unità idrogeologiche, indicate

ove possibile con la stessa nomenclatura utilizzata per le unità litostratigrafiche informali. Alle diverse associazioni di facies costituenti le varie unità idrogeologiche sono stati assegnati valori di conducibilità idraulica desunti da prove in situ o da letteratura. Sulla base della geometria dei livelli acquiferi, semipermeabili ed impermeabili, della natura e geometria dei loro contatti, dei dati idrodinamici e idrogeochimici sono quindi stati identificati una serie di sistemi acquiferi.

Il sistema acquifero principale è impostato negli orizzonti basali dell'Unità Idrogeologica del Villafranchiano B e dei livelli permeabili dell'Unità Idrogeologica delle Sabbie d'Asti B. La piezometria di tale sistema acquifero è fortemente condizionata, nel settore sud-occidentale dell'area studiata, dalla giacitura dell'unconformity che separa l'Allogruppo EP dal sottostante Allogruppo LM e, nel restante settore, dalla geometria sinclinale che caratterizza il contatto stratigrafico tra le Sabbie d'Asti B e le Argille Azzurre B. L'assetto piezometrico presenta linee di flusso idrico sotterraneo dirette dal settore dell'Altopiano di Poirino – Colline di Bra verso la Valle Versa (in prossimità di Asti) dove in passato era presente un'importante sorgente captata ad uso idropotabile e attualmente sono in funzione numerosi pozzi che sovrasfruttano l'acquifero in esame provocando un vistoso cono di depressione. Il sistema acquifero è in pressione e a valle della "Scarpata Orientale" dell'altopiano di Poirino è generalmente artesiano. La chimica di queste acque è sostanzialmente uniforme con facies bicarbonato-calcica, bicarbonato-calcico-magnesiaca, contenuti di nitrati decisamente bassi e tenori di ferro e manganese sovente più alti della concentrazione massima ammissibile per la normativa italiana vigente.

Un secondo sistema acquifero, ora di modesta importanza ma che in passato ha rappresentato l'unica risorsa idrica disponibile per la popolazione locale, è presente nel settore collinare in sinistra Tanaro tra i centri abitati di Santa Vittoria d'Alba e San Damiano d'Asti. Tale sistema acquifero, impostato nei livelli sabbiosi di mare profondo dell'Unità Idrogeologica delle Argille Azzurre A, è artesiano in corrispondenza dei principali fondovalle e in pressione nelle restanti zone. Il flusso sotterraneo presenta un andamento del tutto differente rispetto al sistema acquifero principale con direzioni prevalenti verso ovest e una ricarica piuttosto complessa legata ad una serie di travasi provenienti dai sistemi acquiferi sovrastanti. Questo acquifero è intercettato da pozzi profondi che attraversano potenti intervalli di argille silteose per raggiungere i corpi sabbiosi acquiferi con acque aventi facies chimiche molto diverse tra loro. La presenza di facies cloruro-sodiche evidenzia l'esistenza di acque marine intrappolate nel sedimento all'atto della deposizione e non ancora completamente sostituite da quelle della circolazione attiva. Queste ultime sono state individuate in numerosi pozzi e presentano facies bicarbonato-calcica e bicarbonato-magnesiaco-calcica. Si rinvenivano, inoltre, facies bicarbonato-alcaline imputabili a fenomeni di scambio cationico con i sedimenti argillosi e quindi caratterizzate da tempi di permanenza in acquifero decisamente lunghi. La qualità delle acque è generalmente scadente a causa degli alti contenuti di ione ammonio, ferro e manganese.

Nel settore dell'Altopiano di Poirino sono presenti altri sistemi acquiferi di secondaria importanza impostati nell'Unità Idrogeologica del Villafranchiano C e nell'Unità Idrogeologica Alluvionale dei Terrazzi Alti. La piezometria di quest'ultima presenta linee di flusso diametralmente opposte (verso ovest) rispetto a quelle dell'acquifero profondo principale e acque di scarsa qualità a causa degli alti contenuti di nitrati.

**PAROLE CHIAVE:** acquiferi, Bacino Terziario Piemontese, idrogeochimica, idrogeologia, stratigrafia.

## 1. - INTRODUCTION

The examined area covers a vast portion of the Piedmont territory (about 1000 km<sup>2</sup>) and falls roughly between the Turin Hill reliefs to the north, the western sector of the Turin-Cuneo plain to the west, the *Tanaro* River to the south-east and the *Asti* reliefs to the north-east (fig. 1).

Faced with the necessity of examining the hydrogeology of an area characterised by a rather complex geological and structural framework as the Piedmont Tertiary Basin (PTB), the work has been performed in different stages in order to correlate the tectono-stratigraphic model with the hydrogeologic context, applying the principle of “*aquifer analogues*” proposed by BERSEZIO (2007).

First, all the data obtained from a multidisciplinary study related to the Pliocene-Pleistocene succession of the western sector of the Piedmont Tertiary Basin (PTB), in which some sequence-stratigraphic (i.e. allogroups and sequences) and lithostratigraphic units were identified (GHIELMI *et alii*, 2002; GHIELMI *et alii*, in preparation), have been analysed. The informal lithostratigraphic units of the geological model has been ascribed to the respective hydrogeologic unit. Finally the identification of the main aquifer systems in the studied succession has been carried out on the basis of the geometry of the different aquiferous horizons, their connection, their lower and upper boundaries (identified by the presence of aquicludes or aquitards), the piezometric levels that has been measured in the wells and the chemistry of the waters.

## 2. - GEOGRAPHIC SETTING

From the morphological point of view (fig. 2), this area includes the entire *Poirino* Plateau, which constitutes a sub-level portion of the same area. It slopes slightly towards the west and is bordered on the north by the Turin Hill reliefs and on the south by the *Bra* Hills with topographical altitudes that vary between 265 (near *Dusino*) and 230 (near *Santena*) m a.s.l. This area has a surface drainage network that collects the water from the Turin Hills, the *Braidese* reliefs and from the plateau itself through two main collectors (the *Banna* Stream and the *Melletta* Stream) and sends it towards the Turin-Cuneo Plain. The eastern margin of the plateau is represented by a clear morphological escarpment (referred to as the Eastern Escarpment) that separates it from the *Asti* reliefs. These reliefs are characterized by a lower topographical altitude (between 260 and 150 m a.s.l.)

than that of the plateau. They are connected to the diversion of the *Tanaro* River and therefore are interested by the consequent deepening and rejuvenation of its catchment as far as the Eastern Escarpment. The remaining part of the territory is made up of a wide hilly area, deeply incised by several streamlets that flow into the *Tanaro* River that comprises the *Asti*, *Roero* and *Bra* hills. Geographically speaking, the *Roero* Hills correspond to a vast portion of land between *Bra*, *Montà* and the *Tanaro* River.

## 3. - METHODOLOGY

In the areas characterised by a remarkable stratigraphic and tectonic complexity, hydrogeologic studies should involve a specific sequence of operative phases. First, it is of fundamental importance to reconstruct in detail the stratigraphic setting of the area through classical geological studies based on biostratigraphic, sedimentologic, structural and sequence stratigraphic analysis of the sedimentary succession, in order to recognize the main stratigraphic units, their sedimentary environments and associated facies, their lateral and vertical stratigraphic and tectonic relationships. Each stratigraphic unit is converted in an hydrogeologic unit (aquifer analogues). The proper hydraulic conductivity value is attributed to each constituent facies of an hydrogeologic unit through the use of literature data or direct in situ measurements (permeability tests, grain-size analysis, slug-tests, aquifer tests). Therefore, different permeability values can be assigned to each hydrogeologic unit and these values can identify aquifers, aquitards, aquicludes and aquifuges.

An aquifer system is characterised by a hydrogeologic structure of known geometry, including the unsaturated zone, the saturated zone and its recharge area (CIVITA, 2005) and it is made up of a set of different hydrogeologic units hydraulically connected to each other. Each aquifer system is therefore recognised on the basis of its hydrodynamic situation and of its hydrogeochemical characterisation and is bounded by aquicludes or aquifuges. Aquifer systems can also be made up of one or several hydrogeologic units characterised by the presence of aquitards and numerous aquifers of small volume so that they can hardly be mapped.

The studied area has proved to be particularly suitable for the application of this approach that also benefitted of the detailed multidisciplinary studies carried out in the western TPB by GHIELMI *et alii*, 2002 and in preparation.



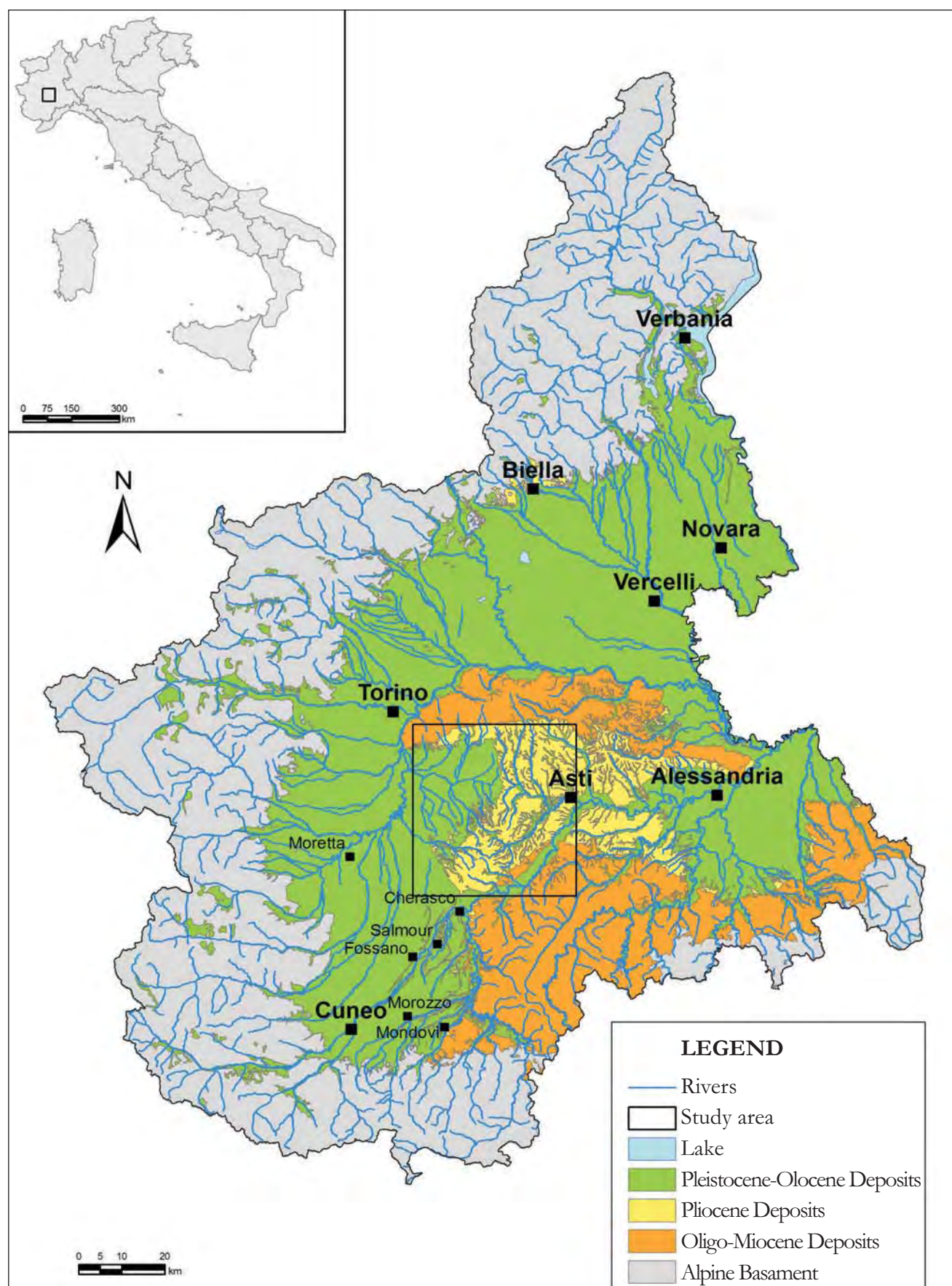


Fig. 1 – Location of the study area on the Lithologic Unit map of Regione Piemonte (Italy) (modified after Regione Piemonte C.S.I., 1990).  
 – Ubicazione dell'area in studio sulla Carta delle Unità Litologiche della Regione Piemonte (Regione Piemonte C.S.I., 1990 - modificata).

#### 4. - TECTONO-STRATIGRAPHIC MODEL OF THE PLIO-PLEISTOCENE SUCCESSION OF THE WESTERN TERTIARY PIEDMONT BASIN

The Pliocene-Pleistocene succession of the Tertiary Piedmont Basin (TPB) has been the subject of numerous geological studies, starting from the works of SACCO (1890, 1912, 1924, 1933), until the recent monographic revision of the Villafranchiano in the type-area by CARRARO (1996). The TPB is considered as an epi-sutural basin, according to the definition given by BALLY & SNELSON (1980), formed in a collisional regime behind the front of the *Monferrato* Front overthrusting the Insubric foreland (GELATI & GNACCOLINI, 1988; BOCCALETTI & MARTELLI, 2004). The oligo-miocenic sedimentary succession of the TPB rests unconformably upon the Alps and the Northern Apennines structural units, hiding their complex geometrical relationships.

The Plio-Pleistocene strata of TPB are bordered towards south and west by the Alpine Units and towards east and northeast by the Oligo-Miocene successions of the TPB (the Turin, *Monferrato* and *Langhe* Hills). The Pliocene and Pleistocene sediments outcrop principally in the area between the towns of *Asti*, *Villafranca* and *Bra*.

They are also exposed on the southern limb of the Turin Hills, on the edges of the *Langhe* hills, along the valley bottoms of the *Tanaro* River and of its main tributary streams as far as the town of *Mondovì*. In the *Cuneo* plain and in the plain to the south of Turin, the Pliocene deposits are overlain by a thin succession of Pleistocene deposits.

Starting from the Upper Miocene and going on until the Pliocene and part of the Pleistocene, various severe phases of structural deformation, connected in the western sector of TPB to some compressive fronts with northwest vergence, led to the creation of a wide sedimentary basin filled with a succession of both marine and continental deposits. The thickness of these deposits reaches 1200-2200 m in the main depocenters of the basin (in the *Moretta* and *Savigliano* sectors) (GHIELMI *et alii*, 2002). As a result of the phases of growth of the compressive fronts, the western TPB is subdivided in a few sub-basins referred to as the *Savigliano* Sub-basin, comprising the central-southern part of the western TPB, the *Moretta* Sub-basin, in the north-western part, and the *Asti* Sub-basin in the north-eastern part (GHIELMI *et alii*, 2002). The northernmost Turin Hills fronts separate these sub-basins from the coeval Western *Po* Plain Fore-deep located in the central Piedmont (MINERVINI *et alii*, 2008). The Pliocene-Pleistocene succession is

represented by an overall transgressive-regressive cycle made up of (from base to top) relatively deep marine clays (*Argille Azzurre* or *Lugagnano* Formations), shelfal to nearshore sands (*Sabbie d'Asti* Formation), deltaic and continental sands, gravels and clays (Villafranchiano). A major unconformity, the *Cascina Viarengo* Surface, subdivides the Villafranchiano succession into two sedimentary units, which are referred to as the Lower Complex and Upper Complex (CARRARO, 1996). The Lower Complex includes two units (from base to top): the Ferrere Unit made up of delta-front sands with tidal influence which, according to BONI *et alii* (1970), belongs to the *Sabbie d'Asti* Formation, and the *San Martino* Unit referred to a delta plain environment (CARRARO, 1996). Also the Upper Complex includes two units: the *Cascina Gherba* Unit, represented by fluvial deposits and the *Maretto* Unit, made up of continental flood-plain deposits (CARRARO, 1996).

In the past the stratigraphic relationships between the different Pliocene-Pleistocene lithostratigraphic units of the western TPB were always considered the record of the aggradational infilling of the basin expressed by a layer-cake stratigraphy. The study presented by GHIELMI *et alii* (2002), based on both outcrop and subsurface data, highlighted, for the first time, the existence of lateral stratigraphic relationships between the *Argille Azzurre* Fm., the *Sabbie d'Asti* Fm. and the Villafranchiano deposits. Moreover these lithostratigraphic units, that seem to show significantly different ages in the different parts of the basin, are framed into different sequence-stratigraphic units (allogroups). As documented in the 2002 study and particularly in a new publication which is presently in preparation by the same authors, during the Messinian and Pliocene the western TPB underwent a few severe phases of compressive and transpressive Apennine structural deformation as suggested by the presence of major unconformities of tectonic origin. Therefore, in these studies, the sequence-stratigraphic analysis was based on the recognition of stratigraphic units bounded at base and top by tectonically-induced major unconformities: the allogroups. Two major unconformities subdivide the Pliocene-Pleistocene succession of the western TPB into three different allogroups: the Late Messinian Allogroup (LM), the Early Pliocene Allogroup (EP) and the Late Pliocene Allogroup (LP). The succession of each allogroup, deposited in relative continuity of sedimentation and attributed to a well defined stratigraphic interval on the basis of the biostratigraphic data, is made up of sediments referred to genetically related depositional environments.



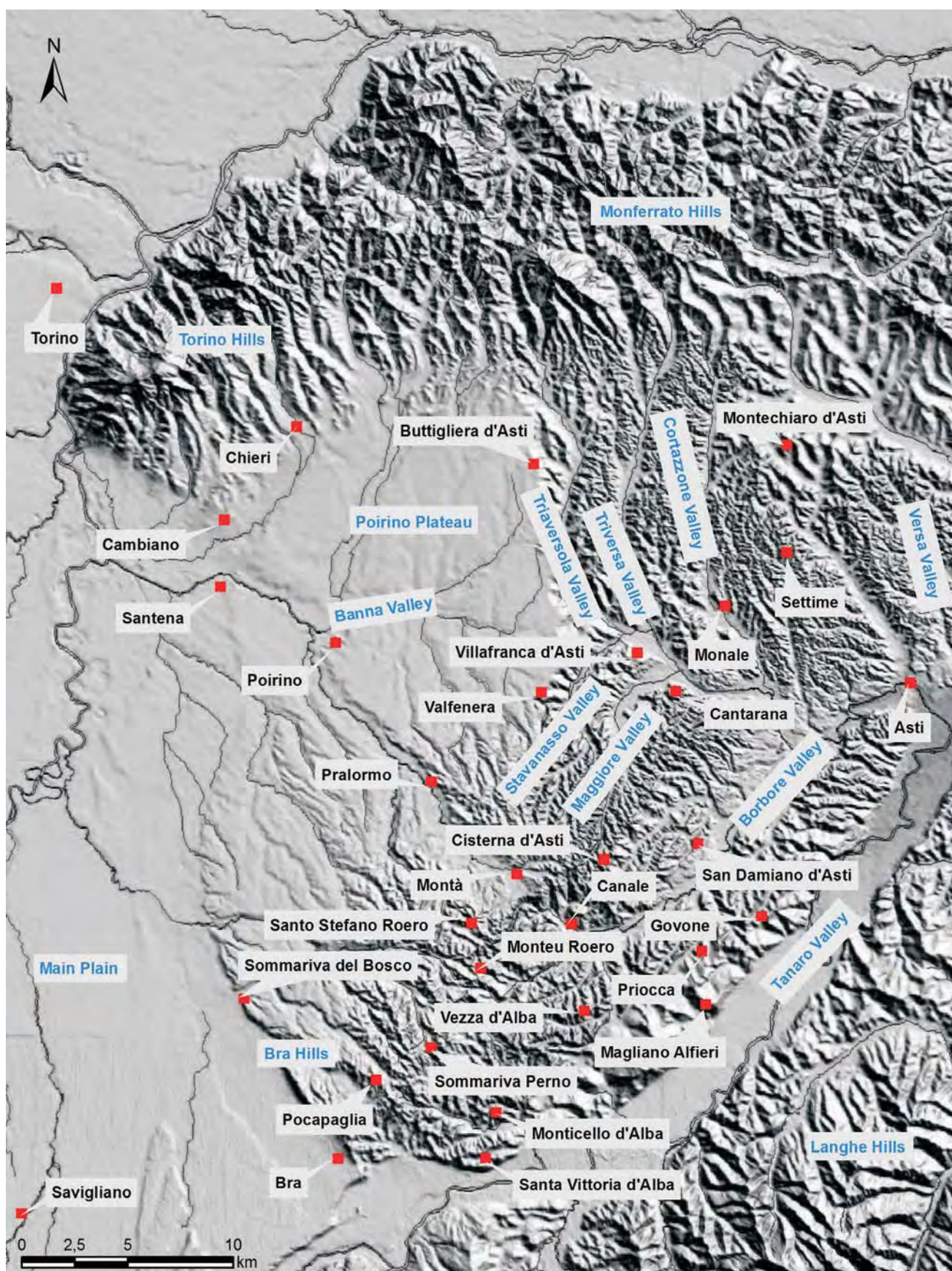


Fig. 2 - Morphologic setting of the study area (processing by Digital Terrain Model of Regione Piemonte 1985 - 1994).  
 - *Assetto morfologico dell'area di studio (elaborazione da modello altimetrico digitale della Regione Piemonte 1985 - 1994).*



#### 4.1. - LATE MESSINIAN ALLOGROUP (LM)

The LM Allogroup includes the post-evaporitic Messinian and Lower Pliocene sediments. The allogroup boundary is represented by a major tectonic unconformity referred to as the “Intra-Messinian Unconformity”. The sediments of the allogroup unconformably overlie the pre- and syn-evaporitic Messinian succession or older Miocene deposits. The Intra-Messinian severe phase of structural deformation caused, in some marginal sectors of the basin, the re-sedimentation of part or, sometimes, of the entire evaporitic succession (with blocks and olistoliths of gypsum and carbonates incorporated in a fine matrix) into the lower part of post-evaporitic succession. These mass-deposits, already described in the outcrops of the southern limb of the Turin Hills front and of south-western *Langhe* Hills as the Chaotic Complex of the Versa Valley (DELA PIERRE *et alii*, 2002, 2003), have also been recognized in the subsurface of other sector of the western TPB (GHIELMI *et alii*, in preparation). The post-evaporitic Messinian succession is made up of gravel, sand and silt of the *Cassano Spinola* Formation (BONI & CASNEDI, 1970). These sediments, characterized by very variable thicknesses, have been interpreted as delta-fan deposits associated to lacustrine and palustrine facies (GHIBAUDO *et alii*, 1985). The “*lago-mare* facies”, deposited in a brackish environment and predominantly made up of greenish clay, belong to the same formation.

The regressive post-evaporitic Messinian succession is overlain, through an sharp lithologic, by transgressive Lower Pliocene deposits mostly represented by relatively deep marine clays with an abundant marine microfauna. These sediments show an abrupt return, in most of the basin, to a rather deep marine sedimentation in consequence of the Pliocene transgression.

Once the basal Pliocene transgressive phase had run out, an important regressive phase started (referred to as “Pliocene progradation” by GHIELMI *et alii*, 2002). This phase gradually led to a partial filling of the western TPB during the first part of Lower Pliocene. Towards the end of the LM Allogroup the basin was characterised by a somewhat complex environmental framework. In the southernmost portion of the western PTB, close to the Alpine basement (between the towns of Cuneo and Mondovì), a deposition of alluvial fan, fluvial and flood-plain sediments took place. These continental sediments have been attributed, by GHIELMI *et alii*, (2002 and in preparation), to the informal Villafranchiano A Unit. Towards the north, in the area roughly between *Fossano* and

*Salmon*, the continental deposits of the allogroup first grade laterally into deltaic and shelfal facies mostly made up of sands, that have been included in the informal *Sabbie d'Asti A* Unit, then into outer shelf, slope and basinal deposits of the informal *Argille Azzurre A* Unit (GHIELMI *et alii*, 2002). The slope deposits consist of clays, locally chaotic, with intercalations of sands and gravels (outcropping above all in the area between the towns of *Morozzo* and *Cherasco*). The basinal sediments (exposed in particular in the study area between *Bra* and *Canale*), are represented by 5-30 m thick sandy bodies alternating with 10-80 m thick clay and silty clay layers. The sand bodies are mostly represented by packages of amalgamated medium to thick sandy beds deposited in a relatively deep water environment by sediment of gravity flows. Moving towards the town of *Asti*, these sediments grade into distal fine-grained basin plain deposits made up of clay with intercalations of thin-bedded silt.

#### 4.2. - EARLY PLIOCENE ALLOGROUP (EP)

This allogroup consist of Lower and Middle Pliocene sediments. The lower boundary of the allogroup corresponds to an important tectonic modification phase of the basin and to a growth phase of the main structural fronts. Throughout the studied area, the boundary is characterized by a pronounced angular unconformity (*Pocapaglia* unconformity) and by a sharp change in the sedimentary facies indicating an abrupt reduction of water depth in consequence of the uplift of the eastern margin of the basin. In the area between the towns of *Bra* and *Monteu Roero*, the continental and deltaic gravels and sands, belonging to the Villafranchiano B informal unit, unconformably overlie the shelfal sands and silts attributed to the *Sabbie d'Asti A* informal Unit (Allogroup LM). To the southwest of the town of *Asti* yellow-brown laminated silty clays of the *Argille Azzurre B* informal unit overlie the deeper typically grey-blue clay of the *Argille Azzurre A*, interpreted as basinal deposits. The EP Allogroup is also made up of deposits that ranges from continental to coastal and marine facies. Moving from the southwest towards the northeast in a basinward direction, continental, fluvio-deltaic and tide-dominated deltaic deposits of the informal Villafranchiano B Unit (corresponding to the “*Complesso Inferiore*” of the Villafranchiano type-area; CARRARO, 1996), predominantly sandy shelfal deposits of the informal *Sabbie d'Asti B* Unit, outer shelf, slope and basinal silty shales of the informal *Argille Azzurre B* Unit outcrop between *Bra* and *Asti*.

#### 4.3. - LATE PLIOCENE ALLOGROUP (LP)

The LP Allogroup is made up of Upper Pliocene and Pleistocene continental sediments. The allogroup boundary corresponds to a severe phase of compressive deformation of the western TPB. A dramatic uplift (referable to the Late Pliocene) interested many sectors of the basin, including also the study area, which were consequently interested by a long period of no deposition and of sub-aerial erosion of the underlying older successions. In the Villafranchiano type-area, the allogroup boundary should correspond to the “*Cascina Viarengo* surface”, angular unconformity identified in the area by CARRARO (1996). This unconformity often represents an important hiatus that can locally encompass the entire Upper Pliocene and part of the middle Pliocene and Pleistocene (CARRARO, 1996; GHIELMI *et alii*, 2002 and in preparation). The sedimentation of upper Pliocene-lower Pleistocene fluvial and flood-plain deposits of the informal Villafranchiano C Unit took place only in the westernmost *Moretta* sub-basin, and in a little sector of the Asti sub-basin (GHIELMI *et alii*, 2002 and in preparation). In the type-area of the Villafranchiano, these strata were included by CARRARO (1996) into the “*Complesso Superiore*” (*Cascina Gherba* and *Maretto* Units).

The LP Allogroup also includes the middle-upper Pleistocene coarse-grained fluvio-glacial deposits of the “Quaternary Alluvium” (alternatively referred to as the “Terraced Fluvial Deposits” following the terminology proposed by CARRARO (1996). The “Quaternary Alluvium” sedimentation, predominantly made up of gravels, mostly developed in the *Cuneo* and *Turin* plain. Fluvio-glacial deposits are also present, to a certain extent, in the *Poirino* Plateau area and in the valley floors of the watercourses. In these areas it is possible to recognize at least three main morphological units: 1) the high terraces, 2) the principal plain (*Cuneo* and *Turin* plain), 3) the present valley floor deposits and the suspended terraces (CAVALLI & VIGNA, 1992). The three units, bounded at the base by erosional surfaces, are interpreted as the result of as many major phases of erosion and subsequent fluvio-glacial deposition controlled by Middle Pleistocene climatic cyclicity.

#### 5. - HYDROGEOLOGIC FRAMEWORK

The first hydrogeologic entry to describe the area was the study by BORTALAMI *et alii*, (1989). The authors showed how the *Cassano-Spinola* conglomerates constitute the deepest aquifer complex, with modest aquifers and rather poor-quality water qual-

ity, while the clays of the *Lugagnano* Formation represent a thick impermeable succession with the presence, on the top of the formation of some sandy intercalations that house limited confined aquifers of limited production. The *Sabbie d'Asti* result to be an aquifer with a remarkable production and which, in the *Versa* Valley zone, house important aquifers under pressure. The Lower Villafranchiano deposits also house aquifers of some importance, while the Upper Villafranchiano ones have a very low production. The deep wells in the *Poirino* Plateau zone exploit the Lower Villafranchiano and the *Sabbie d'Asti* layers and have fair flows. The ancient alluvial sediments (Upper Villafranchiano) constitute an impermeable complex with totally negligible water reserves. In the aforementioned work, there is no mention of the piezometry of the different aquifers, but the quality of the water of the different aquifers was analysed and the results have shown the presence of several very different hydrogeochemical facies.

A subsequent contribution, by CANAVESE *et alii* (1999), analysed the stratigraphy and the aquifer distribution in the subsurface of the central sector of the *Poirino* Plateau. The authors identified the presence of two main aquifers. The first is a shallow aquifer located in the terraced fluvial deposits (Term 4) and, in the southern sector, in the Upper Villafranchiano deposits (*Maretto* Unit) with a flow, strongly conditioned to a great extent by the morphology of the area, from south-east towards north-west and from east towards west in the direction of the *Turin* plain. A second deeper aquifer is located in the Term 1 (*Sabbie d'Asti* and *Ferrere* Unit) and Term 2 (*San Martino* Unit) deposits as well as in the lower part of the Term 3 (*Cascina Gherba* Unit). The deep water flow is in a west to east direction, that is, overall in an opposite direction compared to the shallow aquifer. The two aquifers are probably separated by an impermeable layer belonging to the upper part of Term 3 (*Maretto* Unit). Chemical analyses were also carried out on the groundwater and different chemical characteristics were encountered for the two aquifers.

##### 5.1. - HYDROGEOLOGIC UNITS

In this study several hydrogeologic units have been identified in the test area on the basis of the previously briefly described stratigraphic model of the Pliocene-Pleistocene succession of the western PTB (aquifer analogues). These hydrogeologic units show rather different hydrogeologic characteristics in comparison with those recognised in the previous investigations. An example of the many differences concerns the *Argille Azzurre* Formation



(or *Lugagnano* Formation). In the study area, the clayey succession of the formation is intercalated with numerous sandy aquifer layers previously never recognised. In former studies, this hydrogeologic unit was in fact considered completely impermeable and to play the role of an aquiclude. In the present work, the main sedimentary facies of the different hydrostratigraphic units have been distinguished. Then a value of hydraulic conductivity has been attributed to the sedimentary facies on the basis of direct measurements or of bibliographic data. The hydrogeologic characteristics of the main stratigraphic units identified in the three allogroups are here briefly described (from the bottom to the top):

- *Cassano-Spinola* Hydrogeologic Unit;
- *Argille Azzurre A* Hydrogeologic Unit;
- *Sabbie d'Asti A* Hydrogeologic Unit;
- *Argille Azzurre B* Hydrogeologic Unit;
- *Sabbie d'Asti B* Hydrogeologic Unit;
- *Villafranchiano B* Hydrogeologic Unit;
- *Villafranchiano C* Hydrogeologic Unit;

- Ancient terraced Pleistocene Alluvium Hydrogeologic Unit;
- Fluvial channel Holocene Alluvium Hydrogeologic Unit.

The Hydrogeologic Units map and the Hydrogeologic Units cross-section are shown in figures 3 and 4 respectively.

#### 5.1.1. - *Cassano-Spinola* Hydrogeologic Unit

The unit is made up of alternating sand, gravel and clay of the *Cassano-Spinola* Formation that outcrop in a narrow belt between the villages of *Santa Vittoria d'Alba* and *Magliano Alfieri*, close to the *Tanaro* River valley floor. The thickness of the formation is variable, with an average value in the outcrops of some tens of metres. The sands and gravels, interpreted as fan-delta deposits, are characterized by a rather low permeability due to the presence of a fine matrix, while the fine-grained facies referred to brackish lagoon, lacustrine and swamp environments are completely impermeable.

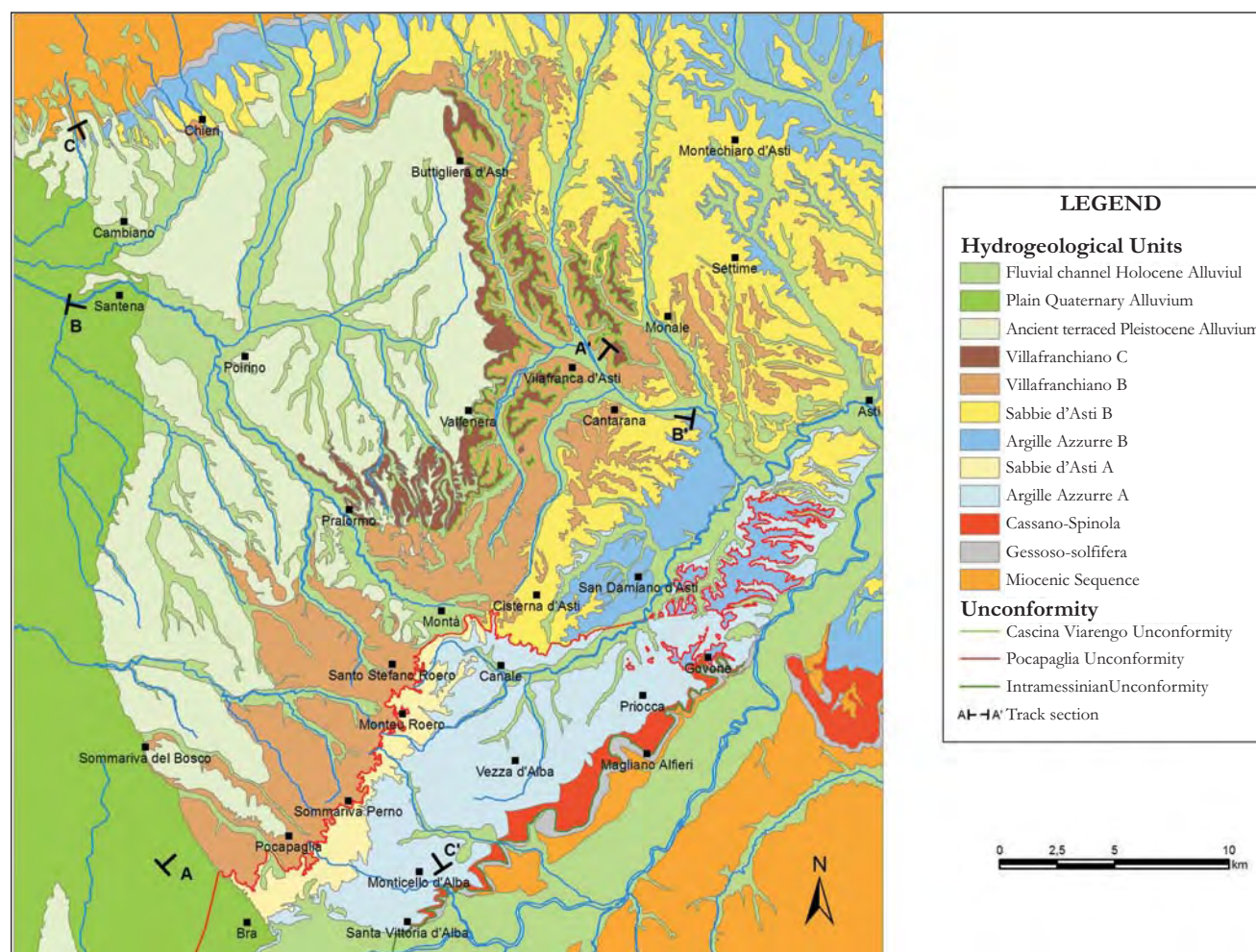


Fig. 3 – Hydrogeologic Units map.  
– Carta delle Unità Idrogeologiche affioranti nell'area in esame.



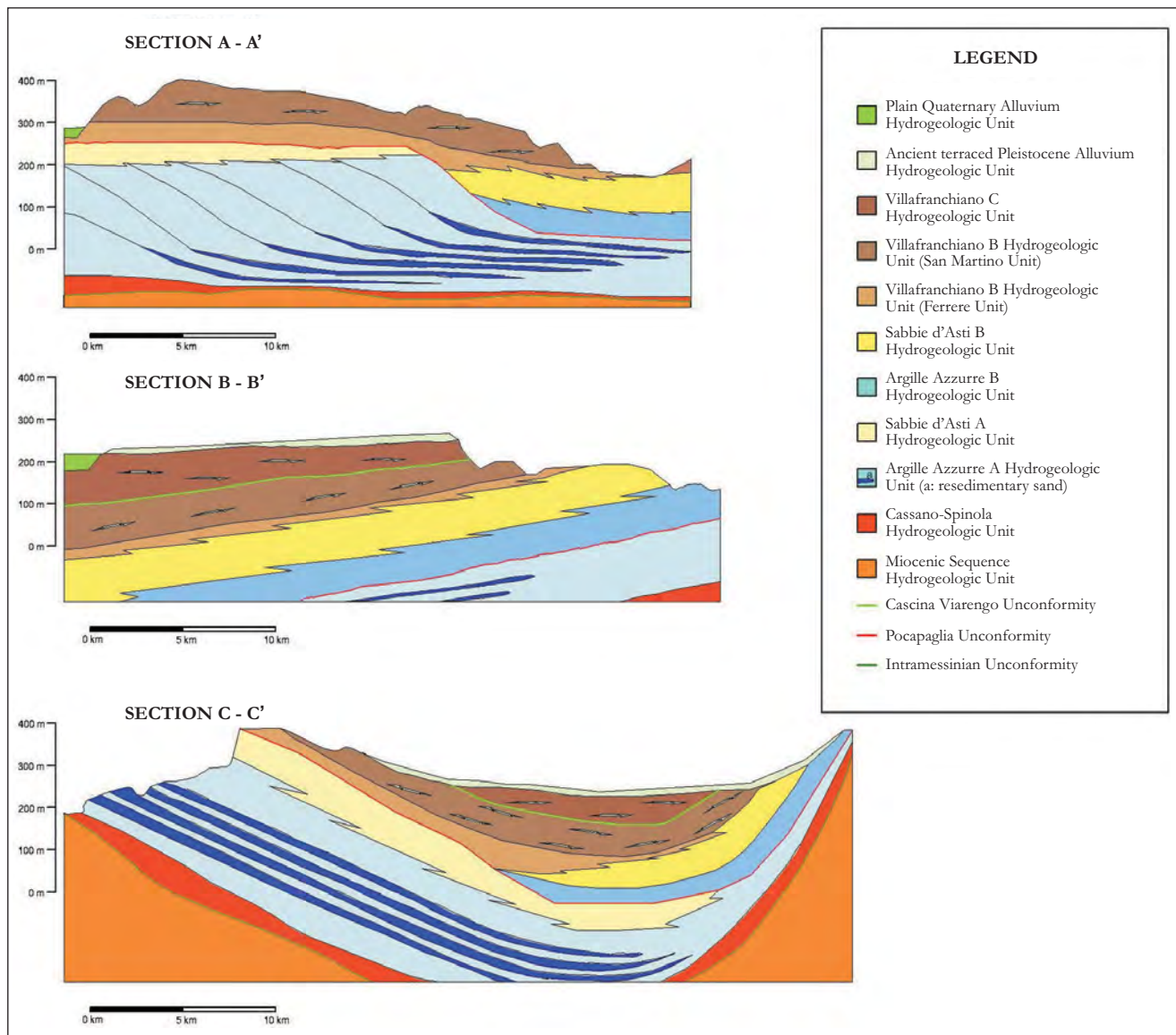


Fig. 4 – Hydrogeologic Units cross-sections. Location in figure 3.  
– Sezioni schematiche delle Unità Idrogeologiche. Ubicazione in figura 3.

#### 5.1.2. - *Argille Azzurre A* Hydrogeologic Unit

The *Argille Azzurre A* Hydrogeologic Unit is represented by a thick succession of alternating clay and fine- to medium-grained sand of the *Argille Azzurre A* informal unit which outcrops between the villages of *Santa Vittoria d'Alba-Pollenzo* and the towns of *Canale* and *Priocca*. The sand bodies, with individual thickness between 5 and 30 m, are mostly represented by packages of amalgamated medium to thick sand beds (fig. 5). From the *Borbore* Stream to the northeast, the examined unit, masked by the overlying *Argille Azzurre B* deposits, is not exposed. The sand bodies, that reach their maximum thickness in the sector between *Monticello d'Alba* and *Vezza d'Alba*, gradually thin and shale out in a northeast direction

towards the city of *Asti*, where the succession is represented by clays with intercalations of thin-bedded very fine-grained sands. The thickness of the entire hydrogeologic unit ranges between 300 m, in correspondence to the eastern margin of the basin, and some tens of metres in the Turin Hill sector.

The permeability of the sands, that depends on the grain-size (ranging predominantly between fine- and medium-grained sand), the compaction (generally elevated) and the presence of silt matrix, usually shows quite low values. A series of hydraulic jump tests carried out in wells of the area has supplied transmissivity values of between  $10^{-5}$  and  $10^{-6}$  m/s, and hydraulic conductivity values, obtained using the QSPEC calculation code (CIVITA, 2005), of between  $10^{-4}$  and  $10^{-5}$  m/s. The



Fig. 5 – Argille Azzurre A Hydrogeologic Unit: grey -blue silty clays alternating with yellowish sand bodies.  
– Unità Idrogeologica delle Argille Azzurre A: alternanze di argille siltose grigio-blu e bancate di sabbie giallastre.

clay intercalations and two thicker clay layers at the top and bottom of the unit are completely impermeable and play an aquiclude role, separating the different sandy aquifer layers.

#### 5.1.3. - Sabbie d'Asti A Hydrogeologic Unit

This hydrogeologic unit outcrops between the towns of *Pocapaglia* and *Montà*, along the Eastern Escarpment of the *Poirino* Plateau, locally known as the “*Rocche di Pocapaglia*”. In the study area, the succession consists of prevailing yellowish bioturbate fine-grained sand and clayey silt (fig. 6), interpreted as outer shelf deposits and characterised by a very low permeability. The thickness of the sequence ranges between 60 and 100 m. In the area of main plain close to the town of *Bra*, the unit, which underlies a thin sequence of quaternary alluvium, seems to be made up of coarser-grained and relatively permeable sand.

This unit therefore takes on the role of aquitard in the *Roero* area and controls the water flow trend of the main aquifer system which is located in the overlying aquifer layers of the *Villafranchiano B* and *Sabbie d'Asti B* Hydrogeologic Units.

#### 5.1.4. - Argille Azzurre B Hydrogeologic Unit

In the study area this hydrogeologic unit is made up of a monotonous succession of clay and silty clay belonging to the informal *Argille Azzurre B* informal unit. These deposits, interpreted as outer shelf, slope and basin deposits, are characterised by a nil permeability, with the exception of thin-bedded, fine-grained sand layers, that can host aquifers. The unit outcrops in the eastern sector between *San Damiano d'Asti* and the town of *Asti*, by the side of the valleys of the main streams of *Asti* area (*Borbore* Valley) and on the southern flank of the *Turin Hill*. The thickness of the sequence is of the order of some hundreds of meter. The hydrogeologic unit, which assumes the role of an aquiclude, influences in the central-eastern sector the circulation of the main aquifer system located in the *Villafranchiano B* – *Sabbie d'Asti B* hydrogeologic units.

#### 5.1.5. - Sabbie d'Asti B Hydrogeological Unit

The *Sabbie d'Asti B* outcrop in the entire sector in the *Asti* hills, between the villages of *Cisterna d'Asti* on the south, the town of *Asti*, the village of *Montebiaro d'Asti* on the north and on the sides





Fig. 6 – Sabbie d'Asti A Hydrogeologic Unit: burrowed fine-grained sands and silts.  
– Unità Idrogeologica delle Sabbie d'Asti A: sabbie fini e silt bioturbati.

of the reliefs of the Turin Hill. The unit is made up of yellowish, medium to coarse-grained sand intercalated with silt. The sand is locally cemented and is characterized by the presence of layers with high concentrations of macrofossils. The *Sabbie d'Asti B* sequence reaches a thickness of less than 100 m (fig. 7). These sediments were deposited by the catastrophic floods of the Villafranchiano fluvio-deltaic system in a shelf environment. The permeability of the different sandy layers results to be somewhat variable and ranges from relatively high values, for the coarser-grained sand (deposited by high-energy and large-volume floods), to lower values for the finer-grained sand (deposited by relatively low-energy and small-volume floods) with hydraulic conductivity between  $10^{-4}$  and  $10^{-6}$  m/s.

#### 5.1.6. - Villafranchiano B Hydrogeologic Unit

The succession of this unit is represented by relatively coarse sediments. It consists, in the lower part, of gravel and medium-grained sand of the *Fer-*

*rere* Unit (CARRARO, 1996) interpreted as mouth-bar deposits (*Pocapaglia – Montà* area) and tide-dominated delta-front deposits (*Cantarana* area), and in the upper part, of delta-plain fine-grained sand and gravel (fig. 8) intercalated with lacustrine clay of the *San Martino* Unit. The thickness of the unit ranges between some tens of metres, in the examined area, and up to more than 300 m in the buried basin depocenter (area between the villages of *Sommariva del Bosco* and *Poirino*). The succession outcrops from the hills close to the town of *Bra* as far as the Villafranchiano type-area (*Villafranca d'Asti, Cantarana*). The permeability of the hydrogeologic unit is variable: it is quite high for the coarser and well-sorted mouth-bar deposits (hydraulic conductivity between  $10^{-3}$  and  $10^{-4}$  m/s), decreases for the delta plain sand and gets nil for the fluvio-lacustrine clay.

#### 5.1.7. - Villafranchiano C Hydrogeologic Unit

The unit is made up of alternating lacustrine clay, prevalently, intercalated with fluvial thick-bedded





Fig. 7 – Sabbie d'Asti B Hydrogeologic Unit: medium- and coarse-grained sands and silts.  
 – Unità Idrogeologica delle Sabbie d'Asti B: alternanze di sabbie medie e grossolane e silt.

sand and gravel belonging to the Upper Villafranchiano sequence (*Cascina Gherba* and *Maretto* Units, CARRARO, 1996). These deposits only outcrop along the syncline axis of the *Asti* sub-basin and presents a reduced thicknesses of the order of some tens of metres. They are still present in the core of the same syncline in the *Poirino* Plateau sector, where they are overlain by a thin sequence of Quaternary alluvial sediments. The coarser layers show a relatively low permeability, because of the abundant fine matrix, while the thick sequence of clay and silt play the role of either aquitard or aquiclude.

#### 5.1.8. - *Ancient terraced Pleistocene Alluvium Hydrogeologic Unit*

This unit, outcropping only in the *Poirino* Plateau, is represented by a thin sequence (about 10 m) of prevailing fine-grained deposits (i.e. fine-grained sand, silt and clay) intercalated with thin layers of gravel. The permeability of the sedimentary succession is somewhat low because of the

presence of an abundant fine matrix. A thick clayey-silt horizon, produced by Pleistocene weathering processes, overlies the whole plateau sector.

#### 5.1.9. - *Fluvial channel Holocene Alluvium Hydrogeologic Unit*

The unit is prevalently made up of fine sediments (fine-grained sand and silt). It outcrops along the incised valleys of the numerous secondary water flows that drain the *Poirino* Plateau (belonging to the hydrographical networks of the *Banna* and *Melletta* streams) and the *Asti* hills (belonging to the hydrographical networks of the *Traversola*, *Triversa*, *Cortazzone*, *Val Andona*, *Stanavasso*, *Maggiore*, *Borbore* and *Versa* streams). The deposits are only some metres thick and their permeability is low.

### 5.2. - AQUIFER SYSTEMS

On the basis of the permeability of the main sedimentary facies forming the hydrogeologic





Fig. 8 – Villafranchiano B Hydrogeologic Unit: sands and gravels interpreted as tide-dominated delta-front deposits (Ferrere Unit).  
 – Unità idrogeologica del Villafranchiano B: sabbie e ghiaie e di fronte deltizio dominato dalle maree (Unità di Ferrere).

units, and of their geometric relationships, it has been possible to recognize the presence of different aquifer systems in the Pliocene-Pleistocene succession of the study area. These aquifer systems, that can involve one or a part of a hydrogeologic unit, or a complex of two or more of them, are characterised by a piezometric network, a recharge area and specific hydrogeochemical characteristics (fig. 9). They are interested by numerous wells used for drinking water, irrigation and industrial uses.

#### 5.2.1. - Villafranchiano B – Sabbie d'Asti B aquifer system

This aquifer system is located in the lower part of the Villafranchiano B Hydrogeologic Unit (Ferrere Unit) and in the coarser layers of *Sabbie d'Asti B* whose facies are heteropic. The deep water circulation of the aquifer is strongly influenced by a syncline, with a east-west axis that gently dips towards the west, involves the whole Pliocene-Pleistocene succession. In the south-eastern sector of

the area, corresponding to the escarpment of the “*Rocche di Pocapaglia*”, the direction of the water flow is controlled by the geometry of the unconformity that separates the EP and LM allogroups (fig. 9) with the basal Villafranchiano aquifer layers in contact with the silty sand of the *Sabbie d'Asti A* Hydrogeologic Unit (aquitard). The deep water circulation in the *Asti* area is controlled by the heteropy contact between the *Sabbie d'Asti B* Hydrogeologic Unit and the time-equivalent *Argille Azzurre B* Hydrogeologic Unit which represents the main aquiclude. The aquifer system is present in almost the whole study area, starting from the *Poirino* Plateau and *Bra* hills, where it is intercepted by deep wells at a depth of more than 250 m. In this sector the aquifer is in pressure and is bordered by thick clayey layers of the middle-upper part of Villafranchiano succession (lacustrine and swamp deposits of the *San Martino*, *Gherba* and *Maretto* Units), with risings of some tens of meter. In the valley bottoms of the *Asti* hills sector, the aquifer system is reached by shallower drillings (between

40 and 80 m) and show artesian conditions in correspondence to the *Stavanasso*, *Traversola* and *Cortazzone* Valleys sectors. In the *Maggiore* Valley area, before the drilling (in 1933) of the numerous wells for human supply of the many municipalities in the area, a spring was present (*Cascina Bonoma* Spring) with a somewhat abundant discharge which was tapped to supply the town of *Asti* (SACCO, 1933).

This spring was located roughly in correspondence to the stratigraphic contact between the aquiferous layers of the basal Villafranchiano B Unit and the *Sabbie d'Asti* B Unit. The wells reach depths of 100 m and intercept several aquiferous layers in the *Sabbie d'Asti* B Unit, which were artesian in the past (up to 18 m above ground level) and now, in consequence of their over-exploitation, level out at about 40 m below the ground level. The aquifer system also extends in the *Asti*

hills sector where is only located in the *Sabbie d'Asti* B Unit in consequence of the complete absence of the Villafranchiano deposits.

The deep water circulation was reconstructed through the measurement of the piezometric levels in more than 190 wells that exclusively involve the tested aquifer system. Other 200 wells can be found in the area which usually interconnect different aquifers of the Upper Villafranchiano succession. These wells were therefore excluded from the calculations relative to the reconstruction of the piezometric network.

The piezometric network of the deep aquifer system (fig. 10) was reconstructed starting from the sector of the *Turin-Cuneo* Plain between the towns of *Bra* and *Cambiano*, where a series of deep wells that reach the aquifer under examination was encountered. In the hilly zone between *Bra*, *Montà*

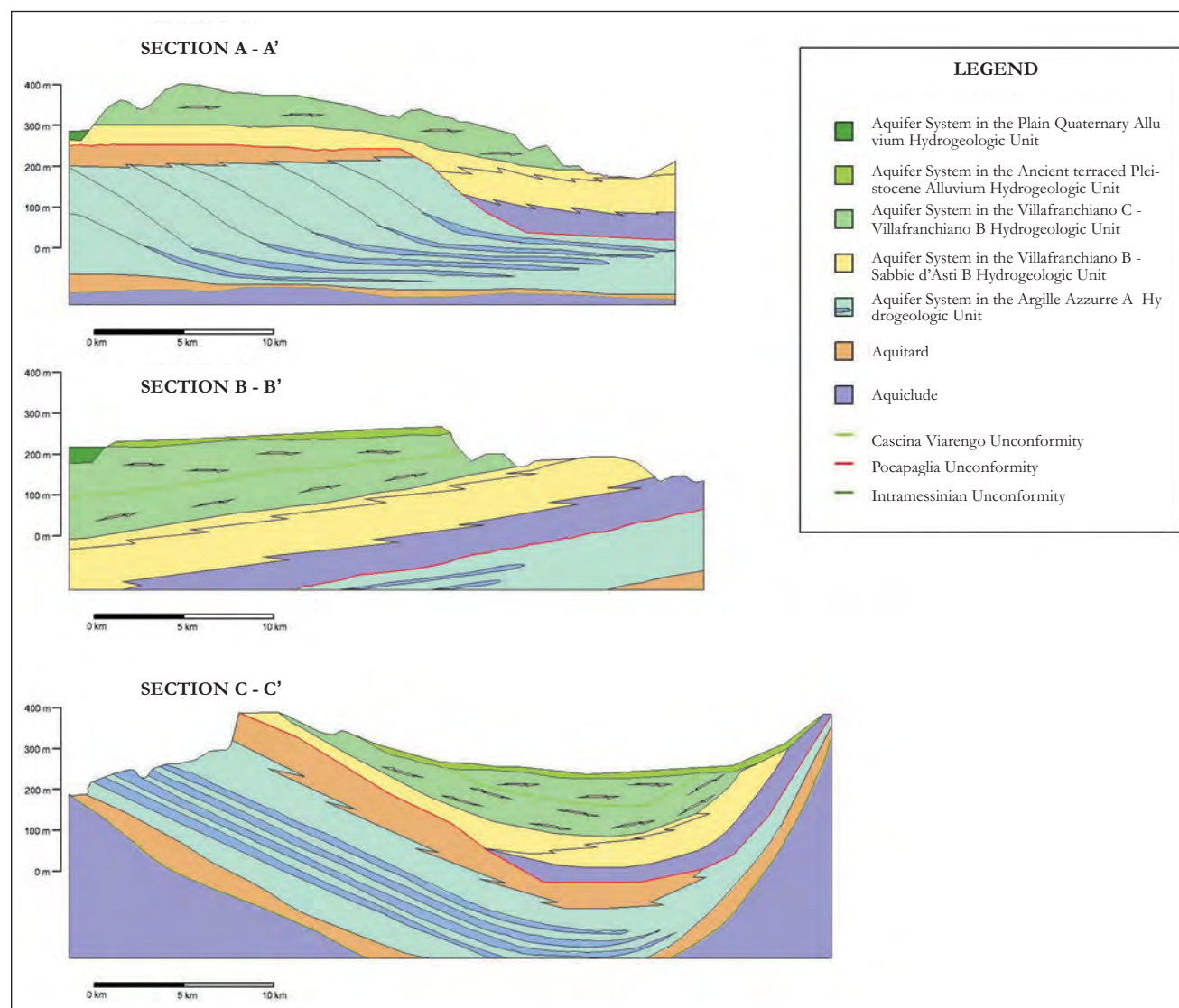


Fig. 9 – Major aquifer systems cross-sections. Location in figure 3.  
– Sezioni schematiche dei sistemi acquiferi maggiori. Ubicazione in figura 3.



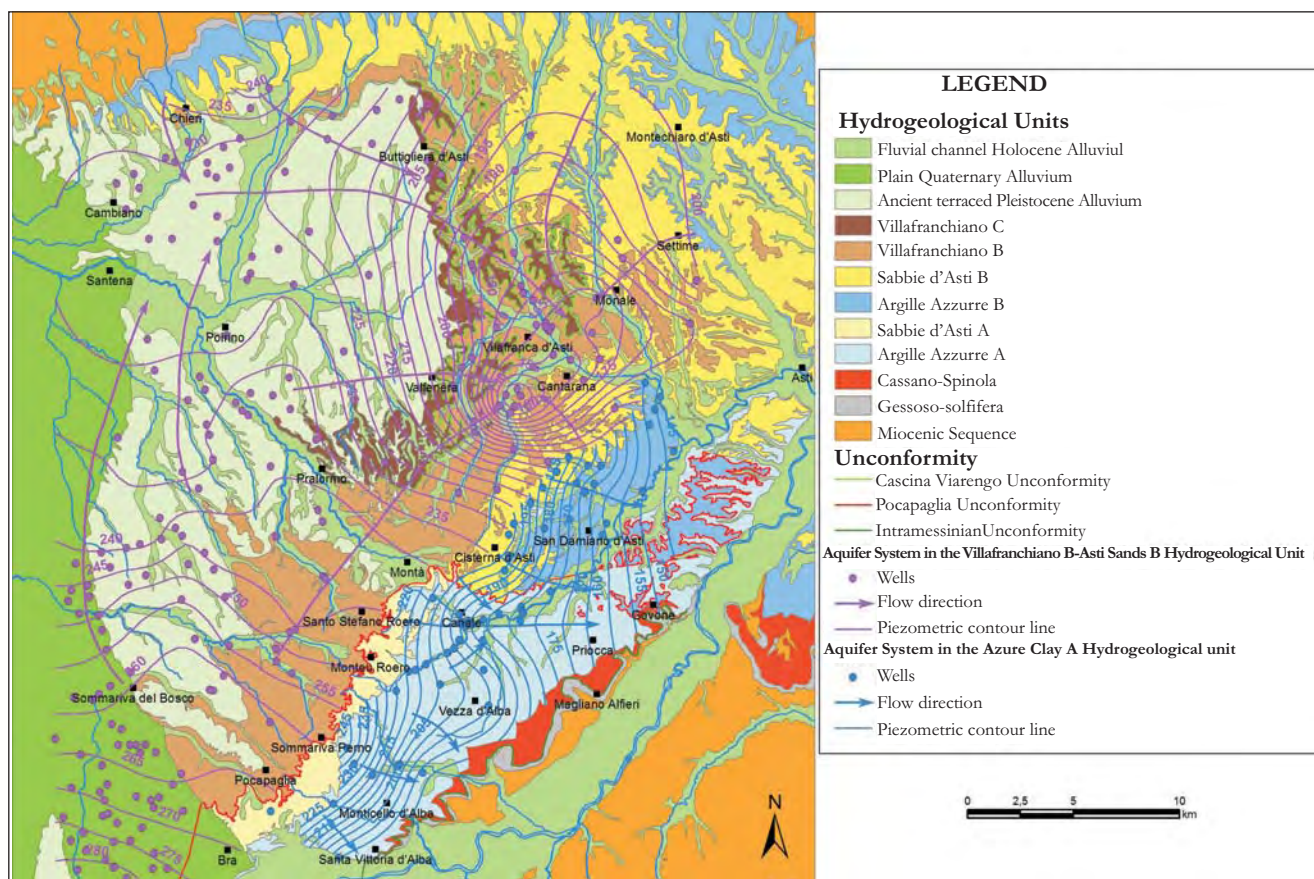


Fig. 10 – Piezometric networks of the main aquifer system in the Villafranchiano B Hydrogeologic Unit – Sabbie d'Asti B Hydrogeologic Unit and of the aquifer system in the Argille Azzurre A Hydrogeologic Unit.

– *Piezometria del sistema acquifero principale delle Unità Idrogeologiche del Villafranchiano B – Sabbie d'Asti B e del sistema acquifero dell'Unità Idrogeologica delle Argille Azzurre A.*

and *Pralormo*, the direction of the underground flow is towards northeast. As far as *Montà* the flow is conditioned by the contact between the Villafranchiano deposits and the underlying *Sabbie d'Asti A* sediments below, which play the role of aquitard. Instead, from *Montà* to the *Maggiore Valley*, the flow is conditioned to a great extent by the drawing action exerted by the *Maggiore Valley* well field, by the geometry of the unconformity between the LM and EP allogroups and by the local hydrostratigraphic layout.

In the area between the village of *Sommariva del Bosco* and the town of *Poirino*, the prevalent direction of the flow is roughly towards the north. In this area, there are two underground water divides that direct the flow towards the zone between the towns of *Santena* and *Cambiano* where there is a sector that is characterised by relatively homogeneous piezometric levels of between 226 and 228 m a.s.l. Towards the east, starting from the *Riva* village zone, an evident underground drainage axis can be identified, which directs the flow towards the *Traversola* and *Triversa* valleys, where there is a series of artesian wells, and then towards *Villafranca d'Asti*, where several wells are tapped for human supply.

On the basis of the available data at present, it results that this aquifer system is supplied in part by the zenithal recharge in the hilly area between *Bra* and *Montà*, where the Lower Villafranchiano deposits outcrop, and in part by the outflows from the extended *Turin-Cuneo* Plain unconfined aquifer, which is located in the Quaternary Alluvium deposits that rest unconformable on the Villafranchiano succession. The contribution from the hilly sector to the northeast between the villages of *Montechiaro d'Asti* and *Settime*, where the *Sabbie d'Asti B* sequence outcrops, is absolutely negligible. The aquifer system in the Villafranchiano B – *Sabbie d'Asti B* Hydrogeologic Units is the main source of underground water tapped for human supply by numerous waterworks organisations. In the *Roero* hills, well fields are located in the villages of *Pocapaglia*, *Sommariva Perno* and *Santo Stefano Roero*. These wells reach depths of more than 150 m with depth-to-water tables between 60 and 95 m. In the *Poirino* Plateau, the aquifer is exploited by the Municipalities of *Chieri*, *Cambiano*, *Buttiglieria d'Asti*, *Santena* and *Poirino* with wells that reach to 300 m of depth with depth-to-water tables between 30 and 70 m. In the *Asti* zone, the aquifer is tapped at dif-

ferent points, in particular by the *Maggiore* Valley well field which supplies the Municipalities of *Asti*, *Ferrere*, *Cantarana*, *Valfenera*, *San Damiano d'Asti* and *Monale*. The examined aquifer system is also exploited by numerous irrigation and industrial use wells. Such an important water resource, intercepted by numerous artesian wells (*Triversa*, *Stavanasso* and *Traversola* Valleys), is often not utilised and left to flow towards the secondary water flows.

### 5.2.2. - *Argille Azzurre A* aquifer system

This aquifer system, which at present is not very important from a production point of view, was in the past the only underground water resource in the *Roero* area used for both human supply and irrigation purposes. The aquifer system, housed in the sandy layers of the *Argille Azzurre A* Hydrogeologic Unit, is confined and is generally artesian in correspondence to the valley bottoms. The discharges from the wells are at present very low also in consequence of the way they were built. These wells, which are known as "*calandre*", were constructed starting from the end of the nineteenth century through striking of small diameter pipes perforated for a length of 1 to 2 m at the point, or through a rotation method without the lining pipe system and filter. A maximum depth of over 200 m could be reached. The *calandre* were located close to the inhabited areas and were used to supply small communities and are still used today to supply the many fountains of those towns. The *Argille Azzurre A* Hydrogeologic Unit, which houses the aquifer system, outcrops in the hills between the villages of *Santa Vittoria d'Alba-Pollenzo* and *Canale-Govone*. The wells in this sector usually have depths of between 100 and 120 m and only exploit a few aquifer layers.

Moving towards north-northeast, the well drillings have to pass a thick clayey succession (*Argille Azzurre B*) before reaching the aquifer layers at a depth of between 160 and 240 m. The sandy layers are almost non existent under the town of *Asti*, due to the diminishing of both the grain-size and the thickness of these levels, where there is an absence of water resources.

The examined aquifer system seems to be located in different sand bodies aquifers separated from each other by thick clayey layers that assume the role of aquiclude.

Through a series of water level measurements carried out in the different wells, it was possible to reconstruct the piezometric network of the aquifer system, which showed a direction of the underground flow roughly from west to east (fig. 10), direction completely different from that encountered in the shallower main aquifer. The trend of the

piezometric lines is rather regular and this shows the existence of a multi-layer that is probably supplied by leakage from the *Sabbie d'Asti A* whose facies are in heteropy with the *Argille Azzurre A* deposits. The *Sabbie d'Asti A* deposits, which outcrop in correspondence to the "*Rocche di Pocapaglia*" sector, consist of silty facies and play the role of aquitard, while at a greater depth, towards the depocenter of the basin, they are represented by coarser facies and are therefore waterlogged. The supply of this aquifer system therefore seems to be provided by a rather complex leakage mechanism: fresh water has been intercepted also in the AGIP petroleum exploration wells *Sommariva del Bosco 1*, in the south-western sector of the study area, in correspondence to aquiferous layers of the *Argille Azzurre A* levels at depths of more than 600 m. The displacement phenomenon of the original salty water with the fresh water coming from the sectors below the *Turin-Cuneo* Plain, connected to the remarkable hydraulic charge in this area (more than 270 m a.s.l.), compared to that found in the *Santa Vittoria d'Alba - Pollenzo* and *Canale - Govone* sector (from 190 to 150 m a.s.l.), and to the lateral and vertical continuity of the various water bodies, has played an important role.

### 5.2.3. - *Villafranchiano C - Villafranchiano B* aquifer system

A multi-level aquifer system under pressure can be found in the *Villafranchiano C* and in part of the *Villafranchiano B* (*San Martino* Unit) Hydrogeologic Units. This multi-level aquifer system is located in relatively permeable sandy-gravely horizons of modest thickness. The permeable layers are intercalated with fine-grained sediments, silty sand, sandy silt and clay, which act as an aquitard. It is intercepted by relatively deep wells, prevalently for irrigation or industrial use, in the *Poirino* Plateau which often interconnect the more permeable horizons encountered at different depths. It has a rather poor productivity and the water quality is heavily conditioned by the elevated concentrations of nitrates. The piezometric level has very similar heights to those encountered in the underlying principal aquifer (The aquifer system in the *Villafranchiano B - Sabbie d'Asti B* Hydrogeologic Units), which is directly in contact with the one under examination because of the lack of a laterally continuous seal.

In the available stratigraphic data, obtained from drillings, the sandy-silty-clayey lithologies are usually indicated as clay thus generating erroneous interpretations of the hydrostratigraphic situation. Only a few continuous coring geognostic surveys, carried out to depths of more than 200 m, pro-



vided useful indications on the true hydrogeologic characteristics of these deposits. The role of aquitard that has been assigned to the fine sandy-silty deposits highlights the complexity of the hydrogeologic framework of the tested aquifer system, which seems to be partially supplied by the vertical recharge from the Quaternary aquifer system above, and partially by the overflows from the unconfined aquifer system of the main Turin-Cuneo Plain. The wells that intercept the studied aquifer (usually for irrigation and industrial use) can reach depths of more than 100 m and often interconnect this system with that one located in the overlying Quaternary alluvial deposits. For this reason, it has not been possible to reconstruct the piezometric network or identify the main recharge areas. The elevated concentrations of nitrates encountered in the wells that intercept the aquifer system and the reduced productivity of the aquifer layers would seem to indicate a supply that prevalently comes from the sector above relative to the Poirino Plateau.

#### 5.2.4. - *Ancient terraced Quaternary Alluvium aquifer system*

An aquifer system exists in the Poirino Plateau sector. This system is located mostly in the Ancient terraced Quaternary Alluvium Hydrogeologic Unit, in part in the upper layers of the Villafranchiano C Hydrogeologic Unit and in part in the Fluvial channel Holocene Alluvium Hydrogeologic Unit. The aquifer system, which is locally confined by a thick layer of clay and silt connected to important weathering processes during the Pleistocene, is intercepted by numerous shallow wells that reach depths of between 2 and 20 m used in the past for domestic and/or zootechnical use. They have a very low productivity, while the piezometric network indicates a flow direction that is strongly influenced by the morphology of the slopes and by the surface drainage network and which shows a predominant direction from east to west (fig. 11). This direction is therefore opposite that of the principal deep aquifer. The recharge of the aquifer system under examination is provided by local infiltration phenomena which heavily conditions the quality of the water with high nitrate concentrations.

#### 5.2.5. - *Other aquifer systems*

Apart from those previously described, in the area under examination there are other aquifer systems of limited importance which are located in the shallower part of the previously described Pliocene Units and in correspondence to the thal-

wegs of the different rivers and streams that can be found in the Asti hills area. These aquifer systems are usually intercepted by very shallow wells for domestic use.

Deeper wells intercept an aquifer system under pressure located in the gravel and sand of the Upper Messinian *Cassano-Spinola* Hydrogeologic Unit and which is characterized by very reduced discharges.

## 6. - GEOCHEMISTRY

The data relative to the water of the deep aquifer systems and in particular those located in the Villafranchiano B – *Sabbie d'Asti B* Hydrogeologic Units and the *Argille Azzurre A* Hydrogeologic Unit are examined in this chapter.

Although a large quantity of chemical analyses was carried out on samples drawn from over 200 wells that intercept the more superficial aquifer systems, these data are here not described or commented on as they are characterised by remarkable human induced impact phenomena, as shown by the high nitrate contents. These wells often have elevated depths, but they also intercept and interconnect different aquifer systems. Thus the drawn samples cannot be considered representative. As the conditioning of most of the wells, in particular the location of the drains and of the plugged levels, was not known, only the chemical analyses enabled us to verify the mixing of the different waters and, when this occurred, to exclude these samples.

### 6.1. - VILLAFRANCHIANO B – SABBIE D'ASTI B HYDROCHEMISTRY

The aquifer system located in the Villafranchiano B Hydrogeologic Unit and *Sabbie d'Asti B* Hydrogeologic Unit is intercepted by several wells and the sampling of the water was carried out in many of these together with the relative chemical analyses. Numerous wells, even though reaching remarkable depths, intercept and interconnect the waters from the overlying aquifer systems (the Villafranchiano C Hydrogeologic Unit aquifer system and the Upper Terrace Quaternary Alluvium Hydrogeologic Unit) which are generally characterised by the presence of elevated nitrate contents. For this reason, 72 different analyses carried out in the same number of wells that only intercept the aquifer system under examination and which had a nitrate content of below 5 mg/l (that is, considered without signs of human induced impact) were considered for the geochemical characterisation.

The waters in the Villafranchiano aquifer system have a specific electric conductivity that varies be-



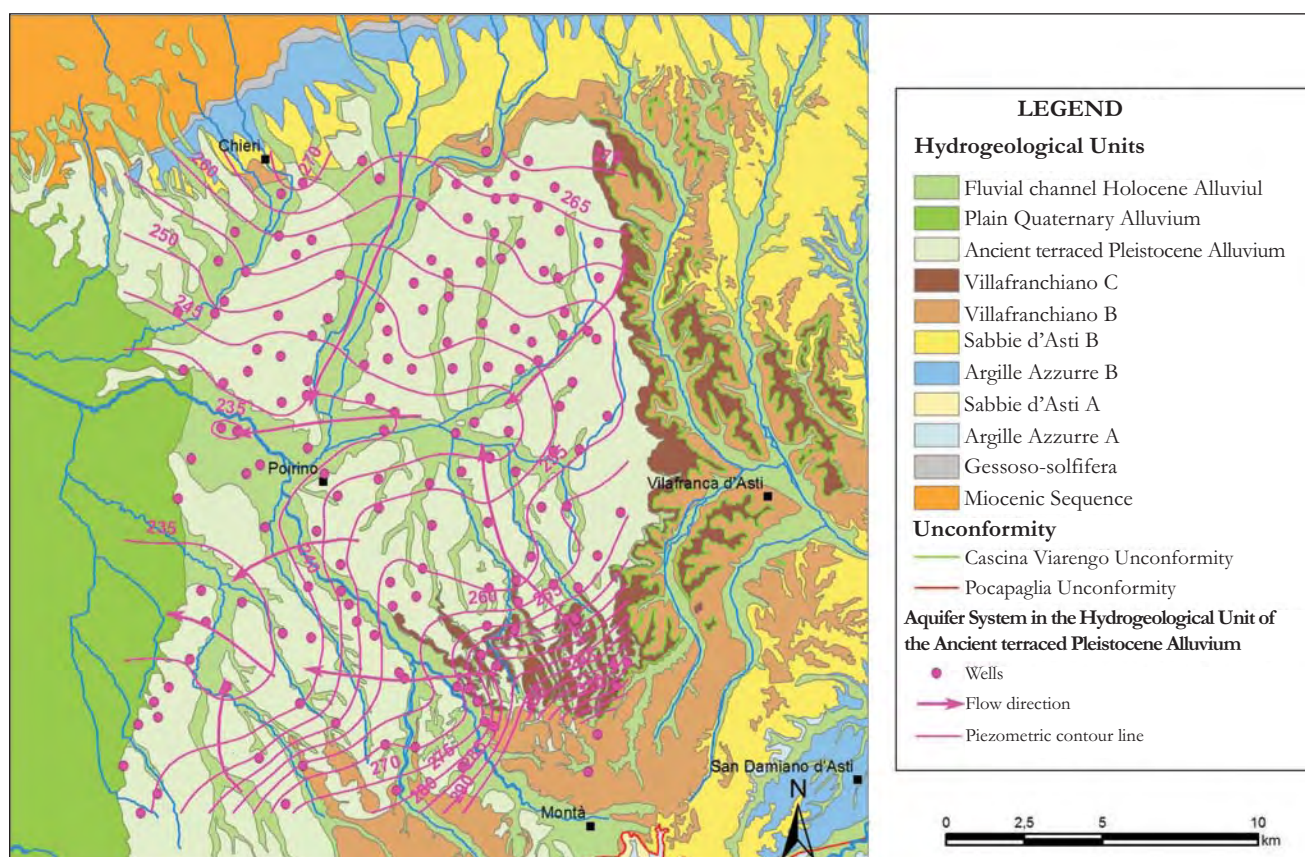


Fig. 11 – Piezometric network of the aquifer system in the Hydrogeologic Unit of the Ancient Terraced Pleistocene Alluvium.  
 – *Piezometria del sistema acquifero dell'Unità Idrogeologica dei Terrazzi Antichi Pleistocenici.*

tween 284 and 854  $\mu\text{S}/\text{cm}$  with a mean value of  $417 \pm 104 \mu\text{S}/\text{cm}$ . These values make it possible to classify these waters as medium-mineral and are therefore, at least for this parameter, suitable for human consumption. The total hardness values, which fall between 13 and 53 French degrees with a mean value of  $22 \pm 6$  French degrees, also underline a potentially utilizable underground water resource for human supply. Instead, either the iron or manganese values, and in some cases both, are higher than the maximum admissible concentrations for water destined for human consumption, according to the Italian laws currently in force.

Taking into consideration the fact that a sufficient number of data were available, a simple statistical analysis was performed for the principal ions (calcium, magnesium, sodium, bicarbonate, sulphate and chloride), in which not only the mean and standard deviation were evaluated, but also the most frequent values. For this purpose, a range obtained dividing each parameter into ten classes of equal extent was considered and then the percentage of cases that fell into each single class was assessed. The thus obtained frequency diagrams are shown in fig 12. The common factor of all the considered parameters is that more than 75% of

the cases fall into three or four contiguous classes that are positioned towards lower values. The only exception is represented by the sodium which presents a typically Gaussian distribution, although with a maximum frequency which is not in the central position but moved slightly towards the lower values. Overall, the values indicate a generally poorly mineralised aquifer with limited cases of higher mineralisation, but always contained within values that can be considered not excessive, as shown by the overall range.

The type of water of all the samples is  $\text{Ca}^{2+} > \text{Mg}^{2+} > (\text{Na}^+ + \text{K}^+) - \text{HCO}_3^- > \text{SO}_4^{2-} > \text{Cl}^-$ . More information can be obtained from some characteristic ratios calculated by expressing the ion concentrations in  $\text{meq}/\text{l}$ .

The  $\text{Mg}^{2+}/\text{Ca}^{2+}$  ratio varies from 0.151 to 0.796, thus showing a greater presence of the calcium ion than the magnesium ion. However, in 86% of the cases, this ratio is below 0.500; therefore the facies is generally of a calcium type and calcic-magnesium only to a lesser extent.

The  $\text{Mg}^{2+}/(\text{Na}^+ + \text{K}^+)$  ratio is always in favour of the magnesium ion as the values are between 1.072 and 7.538. However, the values are not well distributed, considering that 83% of the cases fall

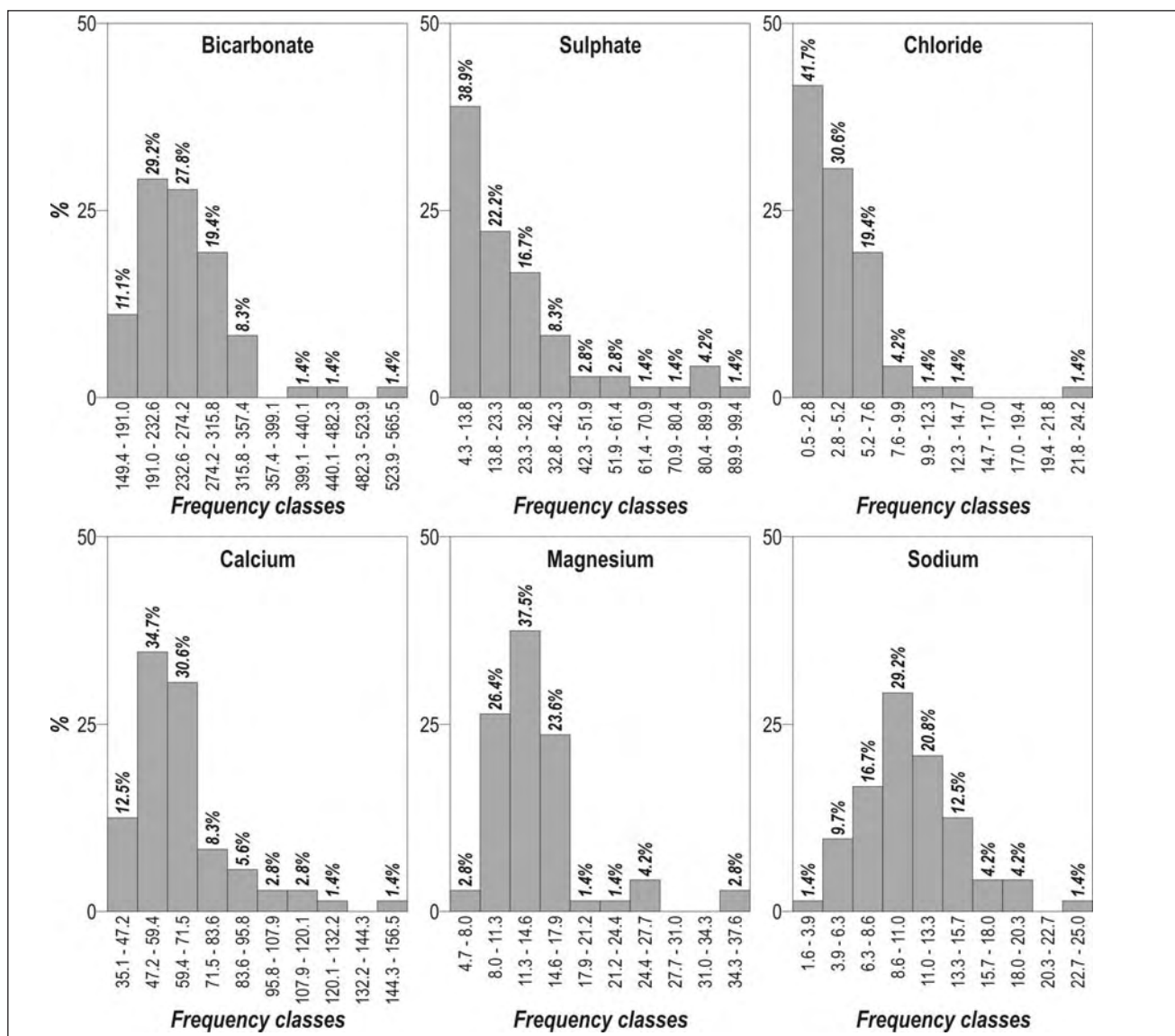


Fig. 12 – Frequency diagrams of the main parameters relative to water chemistry of the aquifer system in the Villafranchiano B Hydrogeologic Unit – Sabbie d'Asti B Hydrogeologic Unit (Values of each class expressed by mg/l).  
 – Diagrammi di frequenza dei principali parametri relativi alle acque del sistema acquifero delle Unità Idrogeologiche del Villafranchiano B – Sabbie d'Asti B (I valori delle singole classi sono espressi in mg/l).

into the first third of the range (1.072 – 3.227). This shows that the alkaline ions, in the cation component, are not generally negligible.

As far as the alkaline ions are concerned, the  $\text{Cl}^-/(\text{Na}^+ + \text{K}^+)$  ratio, which varies between 0.019 and 1.267, is particularly interesting. This ratio is above the unit only in two points (V19 and V41) and below 0.500 in about 88% of the cases. The datum that emerges is that the alkaline ions dissolved in the waters in this aquifer system generally cannot be attributed to the presence of chlorides; therefore the alkaline value should be attributed to other factors such as ionic exchange phenomena or a relevant presence of alkaline feldspatos in the lithic component of the aquifer system.

The  $\text{HCO}_3^-/\text{SO}_4^{2-}$  ratio varies from 1.572 to

37.668 and is widely distributed as it has a mean value of  $13.283 \pm 9.152$ . As far as the characteristic ratio is concerned, the spatial trend described by the isovalue lines is of particular interest (fig. 13). In fact it can be noted that the values are lower in the southern area of the aquifer and increase following the flow lines of the aquifer. The highest values are distributed in correspondence to the principal drainage axis. The obtained data are plotted in a Durov diagram (figs. 14 and 15) where a substantial difference is not clearly shown. The individual points in the cation triangle are concentrated towards the calcium ion vertex, with the exception of four samples (V01, V02 V03 e V04) which are moved slightly towards the centre of the triangle, in consequence of a greater presence of magnesium and alkaline ions. In



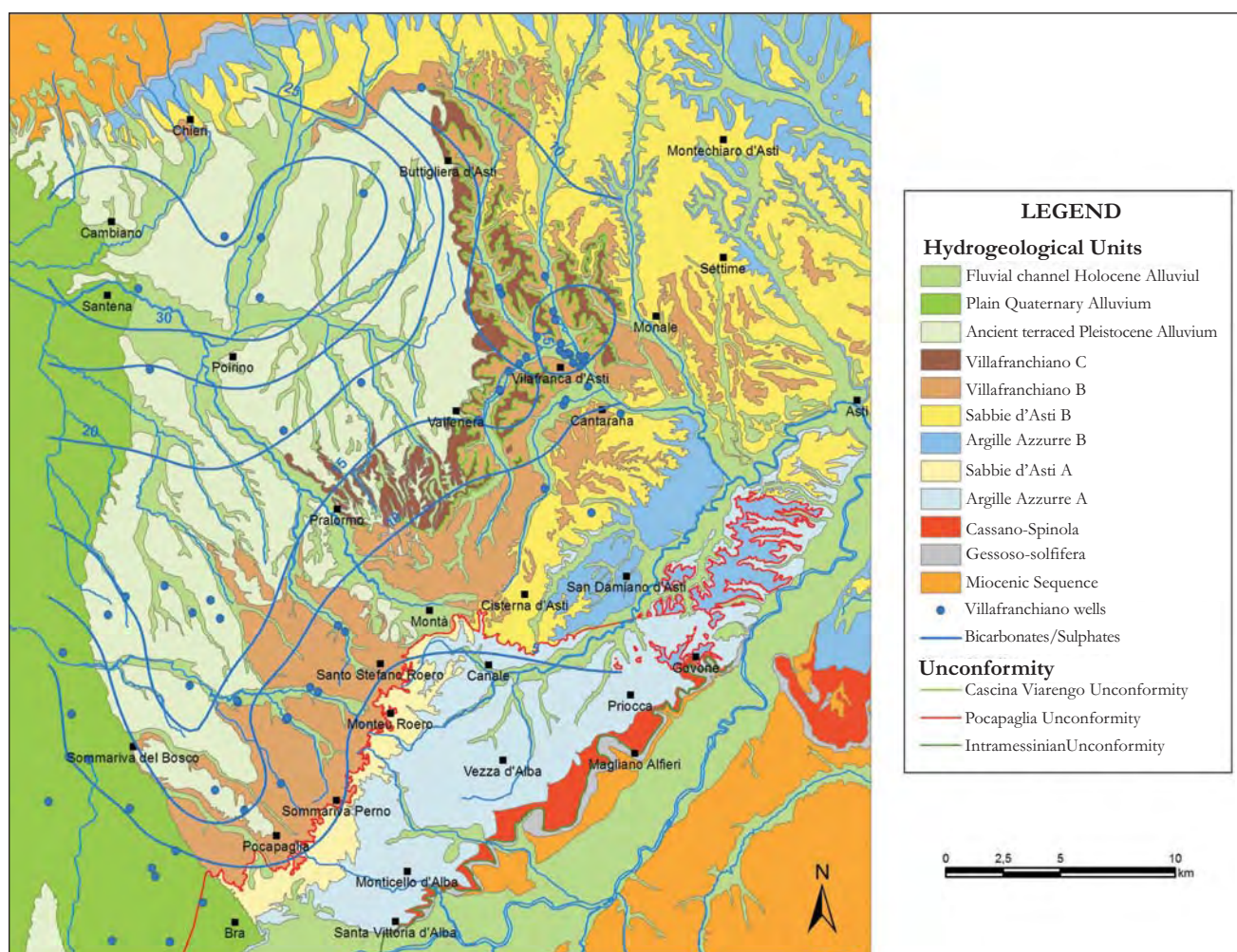


Fig. 13 – Isovalue lines of the  $\text{HCO}_3^-/\text{SO}_4^{2-}$  ratio relative to the aquifer system in the Villafranchiano B Hydrogeologic Unit – Sabbie d'Asti B Hydrogeologic Unit.  
– Carta degli isovalori del rapporto  $\text{HCO}_3^-/\text{SO}_4^{2-}$  relativo al sistema acquifero delle Unità Idrogeologiche del Villafranchiano B – Sabbie d'Asti B.

the anion triangle, the points are distributed along the bicarbonate-sulphate side, because of the low values of the chloride ions found in all the samples. The points are concentrated towards the vertex of the bicarbonate, with the exception of four samples located in the southern part of the aquifer (V49, V62, V63 and V68) which are moved more towards the sulphates.

## 6.2. - ARGILLE AZZURRE A HYDROCHEMISTRY

In order to geochemically characterise the aquifer system located in the *Argille Azzurre A* Hydrogeologic Unit, chemical analyses were carried out on 29 samples drawn from the same number of wells that only intercept the studied aquifer system. In consequence of the limited number of samples, a statistical analysis was not carried out.

The obtained data describe a very complex geochemical situation. Six different types of water were encountered:

Type 1  $\text{Ca}^{2+} > \text{Mg}^{2+} > (\text{Na}^+ + \text{K}^+) - \text{HCO}_3^- > \text{SO}_4^{2-}$

$> \text{Cl}^-$  (14 samples);

Type 2  $\text{Mg}^{2+} > \text{Ca}^{2+} > (\text{Na}^+ + \text{K}^+) - \text{HCO}_3^- > \text{SO}_4^{2-}$   
 $> \text{Cl}^-$  (3 samples);

Type 3  $(\text{Na}^+ + \text{K}^+) > \text{Ca}^{2+} > \text{Mg}^{2+} - \text{HCO}_3^- > \text{SO}_4^{2-}$   
 $> \text{Cl}^-$  (2 samples);

Type 4  $(\text{Na}^+ + \text{K}^+) > \text{Mg}^{2+} > \text{Ca}^{2+} - \text{HCO}_3^- > \text{SO}_4^{2-}$   
 $> \text{Cl}^-$  (5 samples);

Type 5  $(\text{Na}^+ + \text{K}^+) > \text{Ca}^{2+} > \text{Mg}^{2+} - \text{HCO}_3^- > \text{Cl}^-$   
 $> \text{SO}_4^{2-}$  (2 samples);

Type 6  $(\text{Na}^+ + \text{K}^+) > \text{Mg}^{2+} > \text{Ca}^{2+} - \text{Cl}^- > \text{HCO}_3^-$   
 $> \text{SO}_4^{2-}$  (3 samples).

The six types of water that were encountered can be grouped together into three basic hydrogeochemical facies: a bicarbonate calcic facies to which types 1 and 2 belong, a bicarbonate-alkaline facies to which types 3, 4 and 5 belong and a chlorine-alkaline facies to which type 6 belongs.

The obtained data, which are reported in the Durov diagram (fig. 16), clearly shows the presence of the six types of water and the three facies. In the diagram it is also possible to note that intermediate facies exist between the bicarbonate-cal-



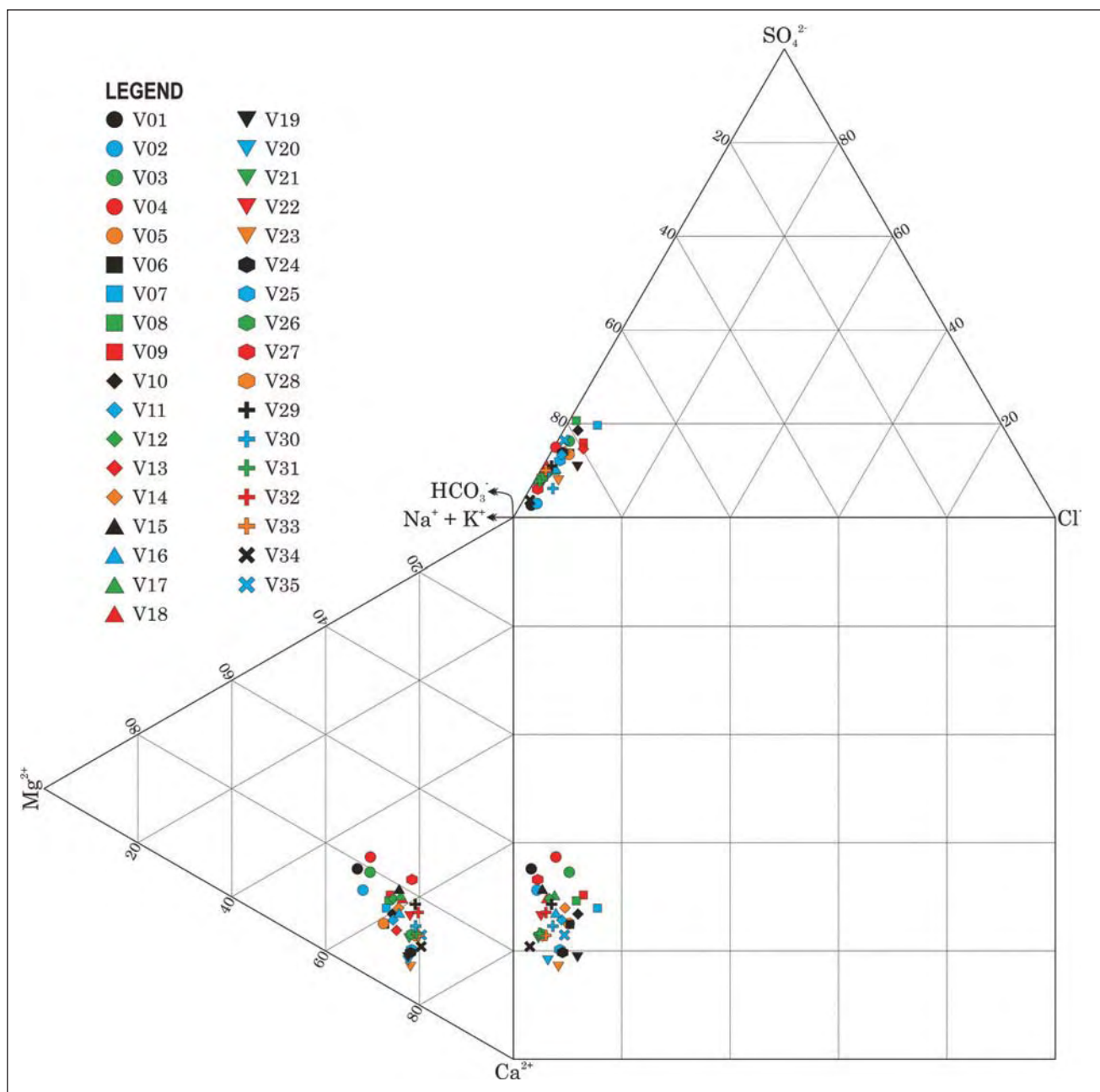


Fig. 14 – Durov diagram of groundwater chemistry in aquifer system of Villafranchiano B Hydrogeologic Unit – Sabbie d'Asti B Hydrogeologic Unit (samples from V01 to V35).

- Diagramma di Durov delle acque del sistema acquifero delle Unità Idrogeologiche del Villafranchiano B – Sabbie d'Asti B (campioni V01 – V35).

cic facies and the bicarbonate-alkaline facies, due to the variation in the main characteristic ratios.

The deep marine sand bodies alternated with thick layers of silty clay that characterise the studied aquifer system must originally have been saturated by marine water (chloride-sodium). After the remarkable deformation of the *Argille Azzurre A* succession during the Pliocene, a water flow was activated that progressively substituted the marine water with fresh water from the aquifer system recharge areas. As many of these sand bodies are laterally and vertically sealed by clay, the marine

water could not have been washed away completely and some remained trapped within them. The marine water began to be progressively substituted by fresh water only when the sand bodies saturated by marine water were intercepted by the drilling and they were triggered into circulation, even though with slow flow. Documents are available which demonstrate that this salt water was used to make bread during de II World War, when it was particularly difficult to find normal salt. The different chemical facies encountered in the various samples might be therefore connected to the mixing phe-

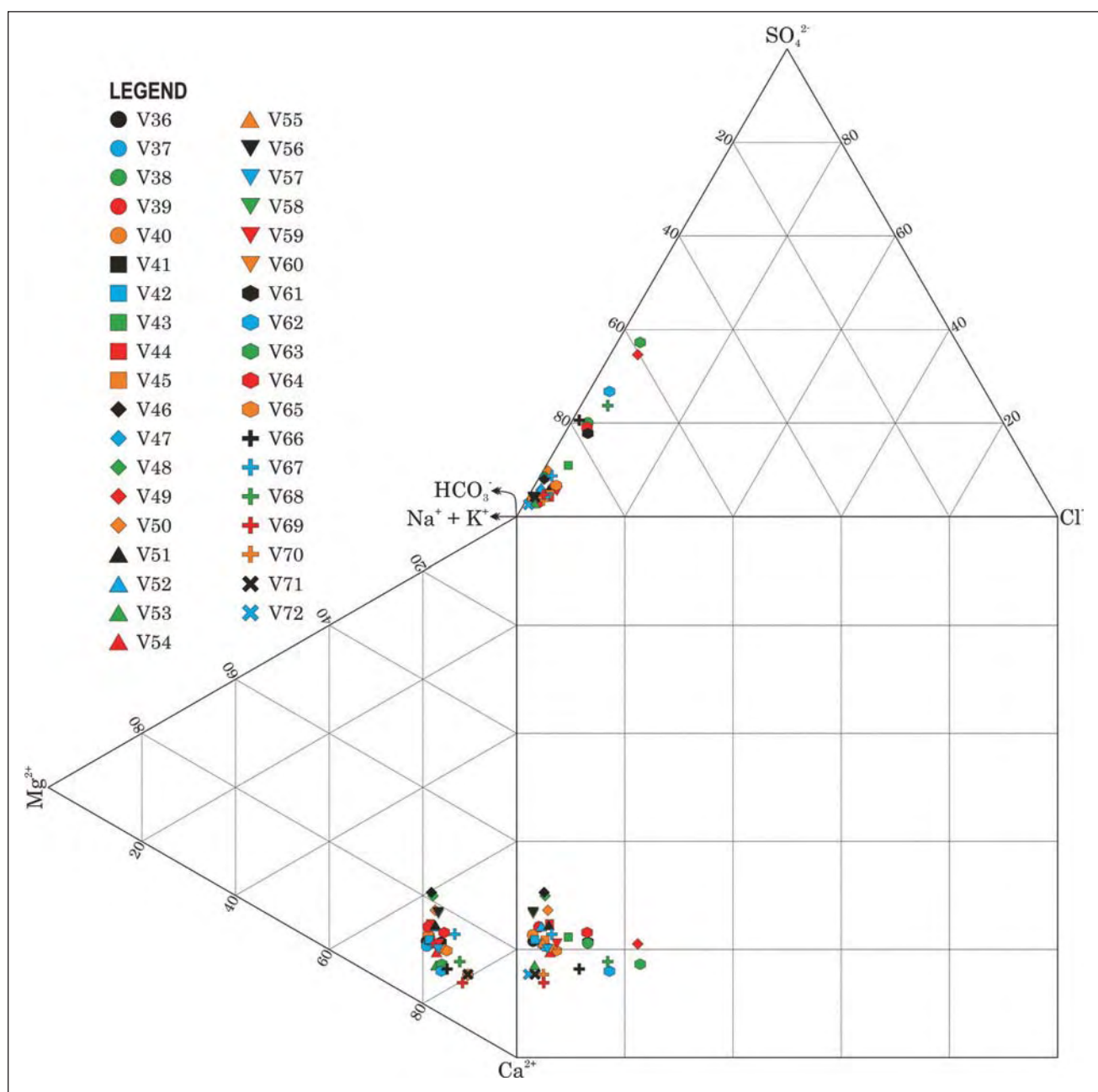


Fig. 15 – Durov diagram of groundwater chemistry in aquifer system of Villafranchiano B Hydrogeologic Unit – Sabbie d'Asti B Hydrogeologic Unit (samples from V36 to V72).

- Diagramma di Durov delle acque del sistema acquifero delle Unità Idrogeologiche del Villafranchiano B – Sabbie d'Asti B (campioni V36 – V72).

nomena generated by the excavation of the wells which interconnect several aquifer levels with different types of water.

The displacement phenomenon is surely fundamental to justify the presence of the bicarbonate-calcic water, but not for the presence of bicarbonate-alkaline water. It is therefore necessary to consider the permanence times of the neo-infiltration water in the aquifer and the cationic exchange phenomena. It is possible that the bicarbonate-calcic water in these sediments progressively become bicarbonate-alkaline because of

the presence of clayey deposits with which the cationic exchange processes occur. The cationic exchanges should have been favoured by the extremely slow velocity of the underground flow and by the consequent long permanence times.

The quality of the water extracted from the aquifer system for drinkable purposes is poor because of the high salt content and, above all, due to the abundant presence of iron, manganese and ammonium ions which are very often above the maximum admissible concentrations established by the Italian laws in force for drinkable water.

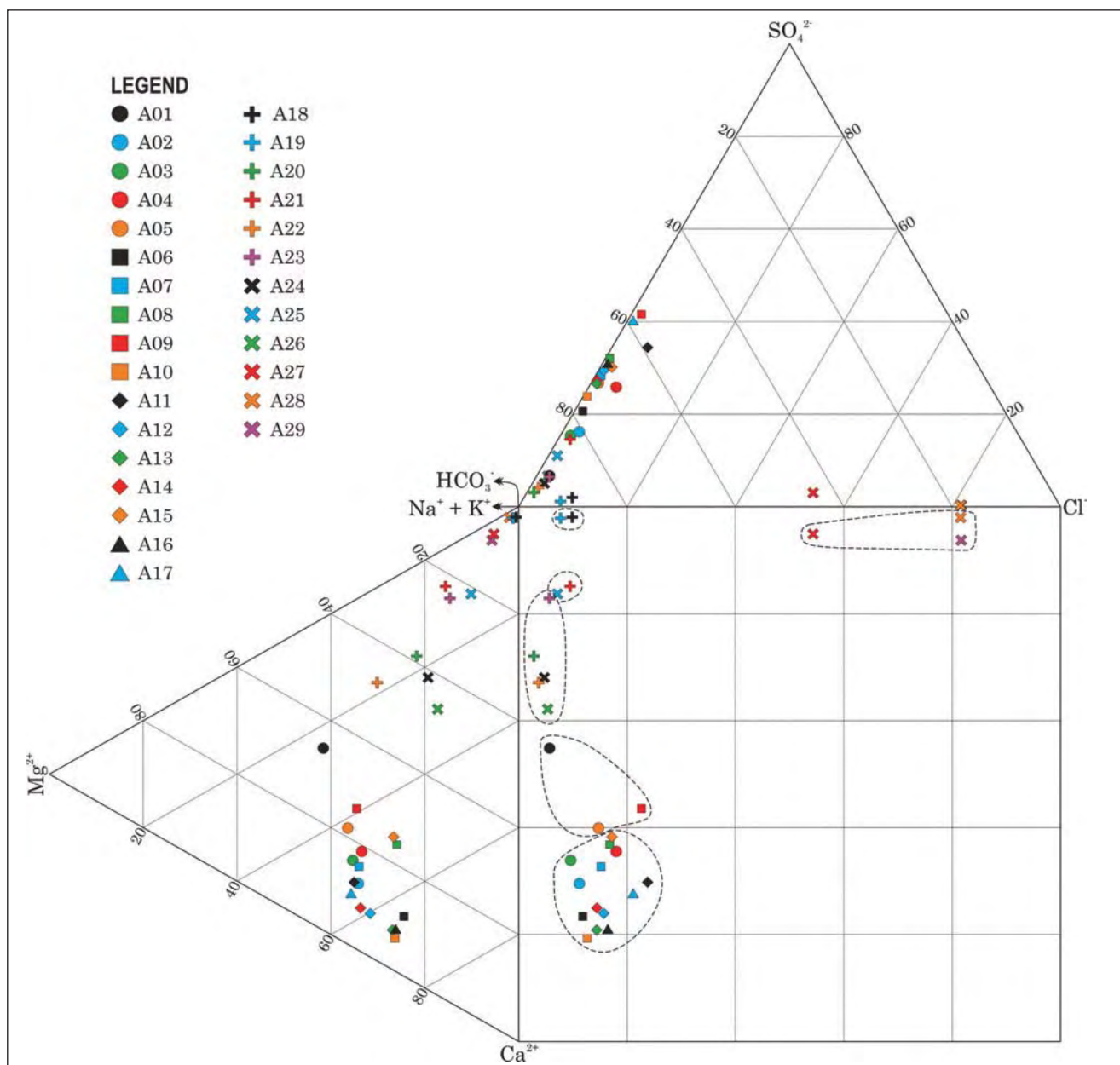


Fig. 16 – Durov diagram of groundwater chemistry in aquifer system of Argille Azzurre A Hydrogeologic Unit.  
- Diagramma di Durov delle acque del sistema acquifero dell'Unità Idrogeologica delle Argille Azzurre A.

## 7. - CONCLUSIONS

The geological model of the upper Messinian to Pleistocene succession is based on a set of informal stratigraphic units corresponding to hydrogeologic units that have been associated to their constituent hydrofacies. The hydrogeologic units that have been recognized in the area are:

- Cassano-Spinola;
- Argille Azzurre A;
- Sabbie d'Asti A;
- Argille Azzurre B;
- Sabbie d'Asti B;
- Villafranchiano B;

- Villafranchiano C;
- Ancient terraced Pleistocene Alluvium;
- Fluvial channel Holocene Alluvium.

The aquifer systems have been identified by the hydrogeologic correlations of many wells, the analysis of deep subsurface data (ENI deep wells and seismic sections), in situ surveys and the analysis of the water levels measured in numerous wells in the area. On the basis of this large data-base, it has been possible to reconstruct the piezometric network of the major aquifer systems and to define their hydrogeochemical characteristics.

The main aquifer system, which is widely exploited by numerous wells for drinkable water and



irrigation use, is located in the Villafranchiano B Hydrogeologic Unit and the *Sabbie d'Asti B* Hydrogeologic Unit, units which are in hydraulic communication. The main aquifer system is bounded on the top by another aquifer system mainly located in the Villafranchiano C Hydrogeologic Unit and made up of a set of aquifers and aquitards. The hydrodynamic data did not allow a clear distinction between the two superimposed aquifer systems. A distinction between the wells that only intercept the first aquifer system from those that interconnect the two systems has been possible thanks to chemical analysis of groundwater (in particular of the nitrate contents). In fact the waters in the main aquifer system show a rather homogeneous hydrochemical facies, regardless of which hydrogeologic unit is locally intercepted.

A second aquifer system, of local importance, is located in a series of aquiferous horizons separated by thick aquicludes but characterised by a single piezometric network, that have been included into the *Argille Azzurre A* Hydrogeologic Unit. The chemical analyses carried out on the waters sampled in the different horizons have shown the presence of different hydrogeochemical facies. The chlorine-alkaline hydrogeochemical facies are connected to the partial and local displacement of ancient saltwater of marine origin by the flow of the present-day water circulation; the bicarbonate-alkaline ones are due to long permanence times of the neo-infiltration water in the aquifer where it has undergone cationic exchange phenomena, while bicarbonate-calcic and calcic-magnesium facies are typical of the main water flow.

From the results here presented, it is possible to deduce that multi-disciplinary studies, such as those described in this paper, are important to clearly understand water circulation modalities in deep aquifers characterised by a remarkable geological-structural complexity.

## Acknowledgements

*The Authors are indebted to the Referees Renzo Valloni and Stefano Margiotta for their careful revision of the manuscript.*

## REFERENCES

- BALLY A.W. & SNELSON S. (1980) – *Realms of subsidence*. In: A.D. Miall, Editor, *Facts and Principles of World Petroleum Occurrence*. Canadian Society of Petroleum Geologists, **6**, 9–94.
- BERSEZIO R. (2007) – *Aquifer Analogues*. Mem. Descr. Carta Geol. D'It., **76**, 39–50.
- BOCCALETTI M. & MARTELLI L. (2004) – *Note illustrative della Carta Sismotettonica della Regione Emilia-Romagna*. S.E.L.C.A., Firenze, pp. 59.
- BONI A. & CASNEDI R. (1970) – *Note illustrative della Carta Geologica d'Italia alla scala 1:100.000*, Fogli 69 e 70, *Asti e Alesandria*. Poligrafica & Cartevalori, Ercolano, 1–96.
- BORTOLAMI G.C., CAVALLERO E., FORNO M.G. & MOSSO E. (1989) – *Studio idrogeologico del bacino di Asti. Caratteristiche e potenzialità degli acquiferi*. Atti Congresso Internazionale Geoingegneria “Sottosuolo”, Torino, 27–30 settembre 1989, **1**, 431–440.
- CANAVESE P.A., BERETTA G.P., DE LUCA D.A., FORNO M.G. & MASCIOTTO L. (1999) – *Stratigrafia e distribuzione degli acquiferi nel sottosuolo del settore centrale dell'Altopiano di Poirino (Torino)*. Il Quaternario (It. Journ. Quatern. Sc.), **12** (2): 195–206.
- CARRARO F. (Eds) (1996) – *Revisione del Villafranchiano nell'area-tipo di Villafranca d'Asti*. Il Quaternario (It. Journ. Quatern. Sc.), **9** (1): 5–119.
- CAVALLI C. & VIGNA B. (1992) – *Il Villafranchiano nel sottosuolo della Pianura Cuneese*. Il Quaternario (It. Journ. Quatern. Sc.), **8** (2), 423–434.
- CIVITA M. (2005) – *Idrogeologia applicata e ambientale*. Casa Editrice Ambrosiana, Milano, pp. 794.
- DELA PIERRE F., CLARI P., CAVAGNA S. & BICCHI E. (2002) – *The Parona chaotic complex: a puzzling record of the Messinian (Late Miocene) events in Monferrato (NW Italy)*. Sedim. Geol., **152**, 289–311.
- DELA PIERRE F., PIANA F., FIORASO G., BOANO P., BICCHI E., FORNO M.G., VIOLANTI D., CLARI P. & PAOLINO R. (2003) – *Note illustrative della Carta Geologica d'Italia alla scala 1:50.000, Foglio 157, Trino*. Litografia Geda, Nichelino (TO), pp. 147.
- GELATI R. & GNACCOLINI M. (1988) – *Sequenze deposizionali in un bacino episeturale, nella zona di raccordo tra Alpi ed Appennino settentrionale*. Atti Tic. Sc. Terra, **31**, 349–397.
- GHIBAUDO G., CLARI P. & PERELLO M. (1985) – *Litostratigrafia, sedimentologia ed evoluzione tettonico-sedimentaria dei depositi miocenici del margine Sud-Orientale del Bacino Terziario Ligure-Piemontese (Valli Borbera, Scrivia e Lemme)*. Boll. Soc. Geol. It., **104**, 349–397.
- GHIELMI M., ROGLEDI S., VIGNA B. & VIOLANTI D. (2002) – *Evoluzione tettono-sedimentaria della successione plio-pleistocenica nel settore del Piemonte centro-meridionale*. Atti 81ª Riunione estiva della Società Geologica Italiana, Torino 10–12 settembre 2002, 181–182.
- GHIELMI M., ROGLEDI S., VIGNA B. & VIOLANTI D. – *Bacino Terziario Piemontese Occidentale: Studio multidisciplinare della successione plio-pleistocenica e messiniana*. (in preparazione).
- MINERVINI M., GHIELMI M., ROGLEDI S. & ROSSI M. (2008) – *Tectono-Stratigraphic Framework of the Messinian-to Pleistocene Succession in the Western Po-Plain Foredeep (Italy)*. Atti 84º Congresso della Società Geologica Italiana, Sassari 15–17 settembre 2008, **3** (2), 562–563.
- REGIONE PIEMONTE (1985 – 1994) – *Digital Terrain Model of Regione Piemonte*. [www.regione.piemonte.it/sit/argomenti/pianifica/cartografia/dwd/DTM\\_notatecnica](http://www.regione.piemonte.it/sit/argomenti/pianifica/cartografia/dwd/DTM_notatecnica)
- REGIONE PIEMONTE C.S.I. (1990) – *Carta delle Unità Litologiche della Regione Piemonte alla scala 1:100.000*. Formato digitale, Arcview shapefiles, Torino
- SACCO F. (1890) – *Il bacino terziario e quaternario del Piemonte*. R. Univ. Torino, Tip. Bernardoni, Milano, pp. 643.
- SACCO F. (1912) – *Geoidrologia dei pozzi profondi della Valle Padana (Parte I)*. Ann. R. Acc. Agric. Torino, **54** (1911): 391–581.
- SACCO F. (1924) – *Geoidrologia dei pozzi profondi della Valle Padana (Parte II)*. Min. LL. PP., Serv. Idr., Uff. Idr. Po, pp. 180.
- SACCO F. (1933) – *Geoidrologia dei pozzi profondi della Valle Padana (Parte III)*. Min. LL. PP., Serv. Idr., Uff. Idr. Po, pp. 532.

## General analytical solutions of the linearized Richards equation for a half-space and a finite-thickness domain

*Soluzioni analitiche generali dell'equazione di Richards linearizzata per un semispazio e un dominio di spessore finito*

VINCENZI S. (\*), MENZIANI M. (\*),  
PUGNAGHI S. (\*)

**ABSTRACT** – This paper aims to describe a compilation of solutions of the linearized one-dimensional Richards equation, solved both in a half-space and in a finite-thickness domain. The solution (the soil water content at any time and depth) can be represented as the sum of two components, one related to the initial condition and to null boundary conditions and the other related to the boundary conditions and to a null initial condition. The sum of the two quoted components is the general solution of the Richards equation in integral form; the analytical expression of the soil water content distribution is therefore obtained if the integrals in the solution can be solved. Besides the integral form solution, another solution holding for any initial and boundary conditions represented with step functions is described in the paper. The initial condition is always the soil water content profile (e.g. the one experimentally measured) while the boundary conditions are different for the two domains. For the half-space domain, the boundary condition can be the soil water content at the surface or the surface flux (e.g. the measured precipitation or evaporation). For this domain, the solution, with the initial-boundary conditions expressed as step functions, is obtained using a procedure, which accounts for the effects of the hydrological conditions of the soil on the flux at the surface. Therefore, this procedure is able to switch between successive atmosphere-controlled and soil-controlled phases of infiltration or evaporation, as required by the given boundary condition. The procedure provides the ponding time, the desiccation time and the surface water flux during the soil-controlled phases. For the finite-thickness domain, the top and bottom boundary conditions are given as time dependent soil water content trends. Also for the finite-thickness domain, a solution, obtained approximating the initial-boundary conditions with step functions, is derived using the basic solution. It provides the soil water content profile evolution, the top and bottom instantaneous and cumulative fluxes and the water gained by the soil layer in a specified time interval. Lastly, a comparison between the procedure results and an exact analytical solution is discussed.

**KEY WORDS:** homogeneous materials, mathematical models, moisture, one-dimensional models, porous materials, surficial aquifers, theoretical models, unsaturated zone.

**RIASSUNTO** – Questo lavoro è un sommario di soluzioni dell'equazione unidimensionale linearizzata di Richards per un semispazio ed un dominio di spessore finito. La soluzione cercata è il contenuto volumetrico d'acqua del suolo. Essa è la somma di due componenti: la soluzione ottenuta con condizione iniziale assegnata e con condizione al contorno nulla e la soluzione ottenuta con condizione iniziale nulla e condizione al bordo assegnata. La forma integrale della soluzione così ottenuta fornisce l'espressione analitica del contenuto volumetrico d'acqua se gli integrali che contiene sono risolvibili. Il lavoro, oltre a presentare la soluzione generale in forma integrale, fornisce le soluzioni per qualsiasi condizione iniziale e al contorno, approssimate con funzioni a gradini. La condizione iniziale è, per entrambi i domini, il profilo verticale di contenuto volumetrico d'acqua del suolo. La condizione al contorno, per il semispazio, può essere sia il flusso sia il contenuto volumetrico d'acqua alla superficie; per lo strato di spessore finito, le condizioni su entrambi i bordi sono sempre il contenuto volumetrico d'acqua. Il profilo verticale del contenuto volumetrico d'acqua, misurato in una stazione idrometeorologica, è già una funzione a gradini perfettamente utilizzabile come condizione iniziale, analogamente il flusso d'acqua misurato all'interfaccia aria-suolo (precipitazione o evaporazione) è, a sua volta, una funzione a gradini immediatamente utilizzabile come condizione al bordo per la soluzione del problema. Per questo dominio (semispazio) è stata messa a punto una procedura che tiene conto degli effetti delle condizioni idrologiche del suolo sul flusso alla superficie. La procedura è in grado di gestire automaticamente il passaggio da una fase di evaporazione o infiltrazione controllata dall'atmosfera ad una controllata dal suolo e viceversa, come richiesto dalla condizione al contorno assegnata. La procedura fornisce anche il tempo al quale il suolo non è più

(\*) Dipartimento di Ingegneria dei Materiali e dell'Ambiente, Università di Modena e Reggio Emilia, via Vignolese 905, 41125 Modena

in grado di assorbire o cedere l'acqua fornita o richiesta dall'atmosfera; inoltre calcola i valori istantanei e cumulativi del flusso alla superficie, del ruscellamento, dell'acqua guadagnata da una colonna di suolo e del flusso uscente dal fondo di tale colonna. Viene inoltre mostrato e discusso un confronto tra i risultati di questa procedura e una soluzione analitica. Infine, anche per lo strato di spessore finito, è presentata una soluzione ottenuta approssimando le condizioni iniziali e ai bordi con funzioni a gradini e vengono calcolati i valori istantanei e cumulativi del flusso al bordo superiore e inferiore e dell'acqua guadagnata dalla colonna di suolo.

**PAROLE CHIAVE:** acquifero superficiale, mezzo omogeneo, mezzo poroso, modello matematico, modello monodimensionale, modello teorico, umidità del suolo, zona non satura.

## 1. – INTRODUCTION

The space and time evolution of the soil water content in an unsaturated medium is described by the Richards equation (RICHARDS, 1931). This equation is highly non linear because of the dependence of both the hydraulic conductivity and the soil water potential on the soil water content. Therefore, several numerical routines have been developed to solve the Richards equation with numerical schemes. However, it is well recognized that analytical solutions of differential equations describing physical problems provide general insights and concisely identify the relationships among the variables of the studied problems, allowing rational approximations and simplifications. Therefore, although numerical methods are powerful in solving complex non-linear problems, analytical solutions maintain their utility and can also provide a useful check to numerical procedures. Some particular cases, exact and approximated analytical solutions of the Richards equation have been derived by, e.g., SANDERS *et alii* (1988), HOGARTH *et alii* (1989), HOGARTH *et alii* (1992), PARLANGE *et alii* (1992), ROSS & PARLANGE (1994), PARLANGE *et alii* (1997), HOGARTH & PARLANGE (2000). Moreover, analytical solutions of the linearized Richards equation have been derived in integral form by WARRICK (1975) and BASHA (1999) resulting in closed form solutions only for constant flux boundary conditions. CHEN *et alii* (2001) derived analytical solutions of the linearized Richards equation for a variety of time dependent fluxes, before surface saturation, while CHEN *et alii* (2003) presented a linearized solution technique for a variety of surface fluxes after ponding. To obtain limiting cases of the real soil solutions, WANG & DOOGE (1994) proposed some analytical solutions of the Richards equation using a uniform initial condition and a quantized flux boundary condition. Two different approaches were used by MENZIANI *et alii* (2005) to obtain exact solutions of the

Richards equation: one is used to solve the non-linear equation without the gravity term, the other allows to derive solutions to the linearized equation. A hybrid procedure, making use of initial-boundary conditions approximated by step functions, has been carried out by MENZIANI *et alii* (2007).

In the present work, a compilation of solutions of the linearized one-dimensional Richards equation is presented. This work is based on two spatial schemes: a half-space and a finite-thickness domain. The computed soil water content at any time and depth is always the sum of two components. One component is related to the initial condition and one or two null boundary conditions; the other is related to the boundary conditions and to a null initial condition. The sum of the two components gives the general solution of the Richards equation in integral form. This integral form is not always solvable; here some exact solutions are given.

Finally, another solution, holding for any initial and boundary conditions represented with step functions, is described in the paper.

## 2. – MATHEMATICAL FORMULATION

In this paragraph, the mathematical formulation to solve the onedimensional linearized flow equation to study infiltration and evaporation processes in a homogeneous medium is presented. A half-space and a finite-thickness domain are the two schemes used to model a nondeformable soil. For both schemes, the linearized Richards equation is changed in a new equation containing only dimensionless variables, suitable for general application. For the finite-thickness domain scheme only this first part will be developed while more detailed results will be given for the half-space domain.

Assuming  $t$  as the time,  $z$  as the soil depth (positive downward)  $D$  as the constant hydraulic diffusivity and  $V = \partial k / \partial \theta$  as the first derivative of the hydraulic conductivity ( $k(\theta)$ ), the following equation

$$\frac{\partial Y}{\partial t} = D \cdot \frac{\partial^2 Y}{\partial z^2} - V \cdot \frac{\partial Y}{\partial z} \quad (1)$$

can be used to describe the space and time evolution of the volumetric soil water content,

$$\theta(z, t) \quad (0 \leq \theta \leq 1)$$

or to describe the evolution of the corresponding flux, defined as:

$$\Phi(z, t) = V \cdot \theta - D \cdot \frac{\partial \theta}{\partial z} \quad (2)$$



In order to use the linear differential equation (1), the relationship between the hydraulic conductivity and the water content is assumed to be linear. The problem to determine  $\mathcal{G}(z, t)$  is an initial condition problem (except for periodic boundary conditions) therefore an initial condition is required:

$$\mathcal{G}(z, 0) = \mathcal{G}_i(z) \quad (t = 0) \quad (3a)$$

or:

$$\Phi(z, 0) = \Phi_i(z) \quad (t = 0) \quad (3b)$$

The space domain is  $z \geq 0$  for a half-space or  $0 \leq z \leq H$  for a finite-thickness domain of depth  $H$ .

For the half-space only one boundary condition is given:

$$\mathcal{G}(0, t) = \mathcal{G}_0(t) \quad (t > 0) \quad (4a)$$

or:

$$\Phi(0, t) = \Phi_0(t) \quad (t > 0) \quad (4b)$$

while for the finite-thickness domain two boundary conditions are required:

$$\begin{aligned} \mathcal{G}(0, t) &= \mathcal{G}_0(t) & (t > 0) \\ \mathcal{G}(H, t) &= \mathcal{G}_H(t) & (t > 0) \end{aligned} \quad (5a)$$

$$\begin{aligned} \text{or: } \Phi(0, t) &= \Phi_0(t) & (t > 0) \\ \Phi(H, t) &= \Phi_H(t) & (t > 0) \end{aligned} \quad (5b)$$

From the hydraulic parameters of the medium, a characteristic length  $\delta = D/V$  can be defined, which allows to introduce the dimensionless variables:

$$\zeta = z/\delta \quad \eta = D \cdot t / \delta^2$$

Using these two dimensionless variables, equation (1) results:

$$\frac{\partial Y}{\partial \eta} = \frac{\partial^2 Y}{\partial \zeta^2} - \frac{\partial Y}{\partial \zeta} \quad (\zeta \geq 0; \eta \geq 0) \quad (6)$$

When treating with the finite-thickness domain,  $H$  (the depth of the layer) represents a reference (or scale) length and, in this case, it is convenient to define the dimensionless space and time variables as follows:

$$\zeta = z/H \quad \eta = D \cdot t / H^2$$

and equation (1) becomes:

$$\frac{\partial Y}{\partial \eta} = \frac{\partial^2 Y}{\partial \zeta^2} - \lambda \cdot \frac{\partial Y}{\partial \zeta} \quad (0 \leq \zeta \leq 1; \eta \geq 0); \quad \lambda = (V \cdot H)/D \quad (7)$$

## 2.1. – HALF-SPACE DOMAIN: PERIODIC BOUNDARY CONDITION

In some hydrological problems, a periodic boundary condition (PBC) is particularly useful to describe the soil volumetric water content or the flux at the surface. The solution, in this case, is easily obtained because this is no more an initial condition problem.

Considering a PBC, with amplitude  $\mathcal{G}^*$  and angular frequency  $\omega$ , for the soil volumetric water content:

$$\mathcal{G}_0(t) = \mathcal{G}^* \cdot e^{i\omega t}$$

and assuming that the method of separation of variables is appropriate, the searched solution can be written as:

$$\mathcal{G}(z, t) = e^{i\omega t} \cdot \mathcal{G}(z)$$

Now, considering the half-space scheme, the solution of equation (6) is:

$$\mathcal{G}(\zeta, \eta) = \mathcal{G}^* \cdot e^{-\left[ -1 + \frac{\sqrt{1+\mu^4}}{\sqrt{2}} \right] \frac{\zeta}{2}} \cdot e^{i \left[ \left( \frac{\delta}{\delta_0} \right)^2 \cdot \eta + \frac{-\mu^2}{\sqrt{2} \cdot \sqrt{1+\mu^4}} \cdot \frac{\zeta}{2} \right]}$$

Where:  $\mu^2 = 8 \cdot \omega \cdot D / V^2$  and  $\delta_0^2 = D / \omega$  which is the characteristic depth of the problem for the considered period;  $\delta, \zeta, \eta$  are defined above.

Of course,  $\omega = 0$  corresponds to the stationary state and  $\mathcal{G}(\zeta, \eta) = \mathcal{G}^*$ .

A solution  $\Phi(\zeta, \eta)$ , similar to  $\mathcal{G}(\zeta, \eta)$ , can be obtained considering a PBC for the flux at the surface. In this case, to get the soil volumetric water content, the integration of the water flux have to be performed (see the following equation (11)).

## 2.2. – HALF-SPACE DOMAIN: GENERAL SOLUTION

Here it will be examined the case of a homogeneous half-space. To solve equation (6) an initial condition and one time dependent boundary condition have to be assigned.

Considering for the soil water content any continuous function of the vertical depth as initial condition and any continuous function of the time as boundary condition, the general solution of equation (6), due to its linearity, can be obtained as the sum of two solutions:

$$\mathcal{G}(\zeta, \eta) = \mathcal{G}_1(\zeta, \eta) + \mathcal{G}_2(\zeta, \eta) \quad (8)$$

Where  $\mathcal{G}_1(\zeta, \eta)$  represents the solution of equation (6) with the initial condition (3a) and a null boundary condition and  $\mathcal{G}_2(\zeta, \eta)$  represents the solution of equation (6) with a null initial condition and the boundary condition (4a). That is:

$$\mathcal{G}_1(\zeta, \eta) = \frac{e^{\frac{\zeta+\eta}{4}}}{\sqrt{\pi}\sqrt{4\cdot\eta}} \cdot \int_0^\infty \mathcal{G}_1(\zeta') \cdot e^{-\frac{\zeta'}{2}} \left[ e^{-\frac{(\zeta-\zeta')^2}{4\eta}} - e^{-\frac{(\zeta+\zeta')^2}{4\eta}} \right] \cdot d\zeta' \quad (9a)$$

and, by means of the Duhamel theorem (CARSLAW & JAEGER, 1986), one obtains:

$$\mathcal{G}_2(\zeta, \eta) = \frac{2}{\sqrt{\pi}} \cdot \int_0^\eta \mathcal{G}_0(\eta') \cdot e^{-\frac{(\eta-\eta')-\zeta}{4(\eta-\eta')}} \cdot \frac{4 \cdot \zeta \cdot d\eta'}{2 \cdot [4 \cdot (\eta-\eta')]^{\frac{3}{2}}} \quad (9b)$$

The sum of equations (9a) and (9b) is the integral form of the solution of equation (6) but the integrals in the aforementioned equations can be difficult or even impossible to be solved analytically.

Similarly, if the flux is the unknown function in equation (6), the general solution can be obtained as the sum of two solutions:

$$\Phi(\zeta, \eta) = \Phi_1(\zeta, \eta) + \Phi_2(\zeta, \eta) \quad (10)$$

Where  $\Phi_1(\zeta, \eta)$  represents the solution of the flux-based form of equation (6) with the initial condition (3b) and a null boundary condition and  $\Phi_2(\zeta, \eta)$  represents the solution of the flux-based form of equation (6) with a null initial condition and the boundary condition (4b). Their expressions are equal to (9a) and (9b) with  $\Phi$  instead of  $\mathcal{G}$ .

Once the solution  $\Phi(\zeta, \eta)$  has been computed, the soil volumetric water content  $\mathcal{G}(\zeta, \eta)$  is obtained from equation (2):

$$\mathcal{G}(\zeta, \eta) = \frac{e^\zeta}{V} \cdot \int_\zeta^\infty e^{-\zeta'} \cdot \Phi(\zeta', \eta) \cdot d\zeta' \quad (11)$$

remembering that:  $\lim_{\zeta \rightarrow \infty} e^{-\zeta} \cdot \mathcal{G}(\zeta, \eta) = 0$ .

### 2.3. – FINITE-THICKNESS DOMAIN: GENERAL SOLUTION

Let us consider now the case of a homogeneous H-thick finite-thickness domain. To solve equation (7) an initial condition and two time dependent boundary conditions have to be assigned. As for the previous domain, the general solution of equation (7) is given by the sum of two solutions as described by equation (8). Again, the solution  $\mathcal{G}_1(\zeta, \eta)$  is derived for null boundary conditions and an arbitrary initial condition (3a) and  $\mathcal{G}_2(\zeta, \eta)$  is derived for a null initial condition and two (usually different) arbitrary boundary conditions (5a). That is:

$$\mathcal{G}_1(\zeta, \eta) = e^{\frac{\lambda \cdot \zeta}{2}} \cdot \sum_{n=1}^{\infty} B_n \cdot e^{-\Lambda_n \cdot \eta} \cdot \sin(n \cdot \pi \cdot \zeta) \quad (12a)$$

$$\text{with } \Lambda_n = \left( n^2 \cdot \pi^2 + \frac{\lambda^2}{4} \right)$$

where:

$$B_n = 2 \cdot \int_0^1 \mathcal{G}_1(\zeta) \cdot e^{-\frac{\lambda \cdot \zeta}{2}} \cdot \sin(n \cdot \pi \cdot \zeta) \cdot d\zeta$$

Also in this case, for a null initial condition and two continuous time functions as boundary conditions, the general analytical solution of equation (7) is obtained using the Duhamel theorem.

$$\mathcal{G}_2(\zeta, \eta) = e^{\frac{\lambda \cdot \zeta}{2}} \sum_{n=1}^{\infty} \left\{ 2n\pi \cdot e^{-\Lambda_n \cdot \eta} \sin(n\pi\zeta) \cdot \left[ \int_0^\eta \mathcal{G}_0(\eta') \cdot e^{\Lambda_n \cdot \eta'} \cdot d\eta' - (-1)^n \cdot e^{-\frac{\lambda \cdot \eta}{2}} \int_0^\eta \mathcal{G}_H(\eta') \cdot e^{\Lambda_n \cdot \eta'} \cdot d\eta' \right] \right\} \quad (12b)$$

The sum of equations (12a) and (12b) is the solution of equation (7) in integral form. The analytical expression of the soil water content distribution  $\mathcal{G}(\zeta, \eta)$  is obtained if the integrals in the above equations can be solved.

### 3. – HALF-SPACE DOMAIN: PROCEDURE

In this section, a procedure to compute the half-space solution, obtained approximating the initial-boundary conditions with step functions, is described. First of all, let us present the solution obtained assuming a null initial condition and a constant boundary condition.

#### 3.1. – HALF-SPACE DOMAIN: NULL IC AND CONSTANT BC

Let us assume the following initial-boundary conditions:

$$\begin{aligned} \mathcal{G}_1(\zeta) &= 0 & (\eta = 0) \\ \mathcal{G}_0(\eta) &= \mathcal{G} & (\zeta = 0) \end{aligned}$$

Due to the choice of the null initial condition the component (9a) of the solution is null, therefore the problem reduces to the determination of (9b)

$$\mathcal{G}(\zeta, \eta) = \frac{\mathcal{G}}{2} \cdot \left[ \operatorname{erfc}\left(\frac{\zeta-\eta}{2\sqrt{\eta}}\right) + e^\zeta \cdot \operatorname{erfc}\left(\frac{\zeta+\eta}{2\sqrt{\eta}}\right) \right] \quad (13)$$

Using the same initial-boundary conditions for the water flux a similar solution is found with  $\Phi$  instead of  $\mathcal{G}$ .

#### 3.2. – PROCEDURE

This procedure computes the solution of the linearized Richards equation, approximating the initial-boundary conditions with step functions.

The initial condition is the soil volumetric water content, while the boundary condition is the surface flux. In fact, the soil volumetric water content profile and the precipitation or evaporation are usually measured at hydro-meteorological stations.

As explained, the solution is the sum of  $\mathcal{G}(\zeta, \eta)$ , that is the component obtained assuming a null boundary condition and an arbitrary initial condi-

tion, and  $\vartheta_2(\zeta, \eta)$ , that is the component obtained assuming a null initial condition and an arbitrary boundary condition. The procedure changes the boundary condition from the water flux to the soil water content and vice versa, according to the atmosphere-controlled or soil-controlled phase respectively.

### 3.2.1. – null BC and arbitrary IC

Let us assume an arbitrary initial condition approximated by:

$$\vartheta_1(\zeta) = \vartheta_0 + \sum_{n=1}^N (\vartheta_n - \vartheta_{n-1}) \cdot H(\zeta - \zeta_n)$$

$N$  is the total number of discontinuities (at:  $\zeta_1, \zeta_2, \dots, \zeta_N$ ) where the initial condition assumes the values:  $\vartheta_1, \vartheta_2, \dots, \vartheta_N$  (besides  $\vartheta_0$ , which is the soil water content value between  $\zeta = 0$  and  $\zeta = \zeta_1$ ).

$H(\zeta - \zeta_n)$  is the Heaviside function (JONES, 1966).

The last soil water content value  $\vartheta_N$  is constant between  $\zeta = \zeta_N$  and infinity. With a null flux as boundary condition and taking into account the principle of superposition, the solution is given by the sum of  $N+1$  terms.

$$\begin{aligned} \vartheta_1(\zeta, \eta) = & \frac{\vartheta_0}{2} \left[ \operatorname{erfc} \left( \frac{\eta - \zeta}{2 \cdot \sqrt{\eta}} \right) + e^{\zeta} \cdot \left[ \operatorname{erfc} \left( \frac{\eta + \zeta}{2 \cdot \sqrt{\eta}} \right) - 2 \cdot \sqrt{\eta} \cdot \operatorname{ierfc} \left( \frac{\eta + \zeta}{2 \cdot \sqrt{\eta}} \right) \right] \right] + \\ & + \sum_{n=1}^N \frac{(\vartheta_n - \vartheta_{n-1})}{2} \cdot \left[ \operatorname{erfc} \left( \frac{\eta + \zeta_n - \zeta}{2 \cdot \sqrt{\eta}} \right) + e^{\zeta} \cdot \left[ \operatorname{erfc} \left( \frac{\eta + \zeta_n + \zeta}{2 \cdot \sqrt{\eta}} \right) - 2 \cdot \sqrt{\eta} \cdot \operatorname{ierfc} \left( \frac{\eta + \zeta_n + \zeta}{2 \cdot \sqrt{\eta}} \right) \right] \right] \end{aligned} \quad (14)$$

### 3.2.2. – null IC and arbitrary BC

#### 3.2.2.1. – atmosphere-controlled phase

During the pre-ponding phase or pre-desiccation-phase the rate of the flux at the surface is atmosphere-controlled. Supposing to be in this phase, let us assume an arbitrary flux boundary condition approximated with a step function:

$$\Phi_0(\eta) = q_0 + \sum_{m=1}^M (q_m - q_{m-1}) \cdot H(\eta - \eta_m)$$

$M$  is the total number of discontinuities (at:  $\eta_1, \eta_2, \dots, \eta_M$ ) where the boundary condition assumes the values:  $q_1, q_2, \dots, q_M$  (besides  $q_0$ , which is the surface flux value between  $\eta = 0$  and  $\eta = \eta_1$ ). Assuming a uniform initial condition  $\vartheta_1(\zeta) = 0$  and taking into account the principle of superposition, the solution of the problem will be a linear combination of  $(J_\eta + 1)$  terms, with  $J_\eta \leq M$ .  $J_\eta$  is the number of the discontinuities before  $\eta$ ; e.g. if  $\eta_2 < \eta < \eta_3$  then  $J_\eta = 2$ .

$$\begin{aligned} \vartheta_2(\zeta, \eta) = & \frac{q_0}{2 \cdot V} \left[ 1 + \operatorname{erf} \left( \frac{\eta - \zeta}{2 \cdot \sqrt{\eta}} \right) + e^{\zeta} \cdot \left[ 2 \cdot \sqrt{\eta} \cdot \operatorname{ierfc} \left( \frac{\eta + \zeta}{2 \cdot \sqrt{\eta}} \right) - \operatorname{erfc} \left( \frac{\eta + \zeta}{2 \cdot \sqrt{\eta}} \right) \right] \right] + \sum_{m=1}^{J_\eta} \frac{(q_m - q_{m-1})}{2 \cdot V} \cdot \\ & \cdot \left[ 1 + \operatorname{erf} \left( \frac{\eta - \eta_{m-1} - \zeta}{2 \cdot \sqrt{\eta - \eta_{m-1}}} \right) + e^{\zeta} \cdot \left[ 2 \cdot \sqrt{\eta - \eta_{m-1}} \cdot \operatorname{ierfc} \left( \frac{\eta - \eta_{m-1} + \zeta}{2 \cdot \sqrt{\eta - \eta_{m-1}}} \right) - \operatorname{erfc} \left( \frac{\eta - \eta_{m-1} + \zeta}{2 \cdot \sqrt{\eta - \eta_{m-1}}} \right) \right] \right] \end{aligned} \quad (15)$$

The solution of the linearized Richards equation is given by the sum of equation (14) and (15) during the atmosphere-controlled phase.

#### 3.2.2.2. – soil-controlled phase

If the precipitation rate exceeds the soil hydraulic conductivity at saturation, the downward infiltration rate into an initially unsaturated soil corresponds to the rainfall rate until the ponding is reached. Thereafter, the rate of infiltration will depend on the soil hydraulic characteristics and the phase is called “soil-controlled phase”. Similarly, during drying periods, the evaporation mechanism switches from atmosphere to soil controlled phase when the soil is no longer able to supply water at the rate required by the atmosphere. At the beginning of the soil-controlled phase a new initial condition is required. It is the discrete soil moisture vertical profile computed during the atmosphere-controlled phase at the ponding time  $\eta_p$  (saturation) or at the desiccation time  $\eta_d$  (air-dry soil, when the rate of the water loss at the surface exceeds the rate of supply from below). The boundary condition is thereafter a soil water content constant value equal to one in case of ponding and equal to zero in case of air-dry soil.

#### 3.2.2.3. – desiccation

If the air-dry soil is reached, a null soil volumetric water content at the surface is the new boundary condition and the new initial condition is the vertical profile of the atmosphere-controlled phase at  $\eta = \eta_d$ .

$$\begin{aligned} \vartheta_d(\zeta, \eta - \eta_d) = & \sum_{n=0}^N \frac{\vartheta_n}{2} \cdot \left[ \operatorname{erfc} \left( \frac{\eta - \eta_d + \zeta_n - \zeta}{2 \cdot \sqrt{\eta - \eta_d}} \right) - \operatorname{erfc} \left( \frac{\eta - \eta_d + \zeta_{n+1} - \zeta}{2 \cdot \sqrt{\eta - \eta_d}} \right) - \right. \\ & \left. e^{\zeta} \cdot \left[ \operatorname{erfc} \left( \frac{\eta - \eta_d + \zeta_n + \zeta}{2 \cdot \sqrt{\eta - \eta_d}} \right) - \operatorname{erfc} \left( \frac{\eta - \eta_d + \zeta_{n+1} + \zeta}{2 \cdot \sqrt{\eta - \eta_d}} \right) \right] \right] \end{aligned} \quad (16)$$

#### 3.2.2.4. – ponding

If the ponding is reached, unitary soil volumetric water content at the surface is the new boundary condition and the new initial condition is the vertical profile of the atmosphere-controlled phase at  $\eta = \eta_p$ .

$$\vartheta_p(\zeta, \eta - \eta_p) = \vartheta_d(\zeta, \eta - \eta_p) + 1 - \frac{1}{2} \cdot \left[ \operatorname{erfc} \left( \frac{\eta - \eta_p - \zeta}{2 \cdot \sqrt{\eta - \eta_p}} \right) - e^{\zeta} \cdot \operatorname{erfc} \left( \frac{\eta - \eta_p + \zeta}{2 \cdot \sqrt{\eta - \eta_p}} \right) \right] \quad (17)$$

As usual the solution (17) is the sum of two parts, the first is the solution (16) obtained with the aforementioned new initial condition and a null soil



water content boundary condition. In this case,  $\eta_p$  instead of  $\eta_d$  has to be used in equation (16). The second part is the solution for a null initial condition and a unitary soil water content boundary condition.

#### 4. – ILLUSTRATIVE EXAMPLES

In the previous section, the general solution of the linearized Richards equation has been obtained in integral form; here particular analytical solutions pertaining to some simple cases of initial-boundary conditions are deduced from the general analytical model.

In this section it is also shown an example of the procedure, which uses the step functions as initial-boundary conditions. It will show the ability of this procedure to take into account the atmosphere-controlled and soil-controlled phases of infiltration or evaporation, as required by the given boundary condition. A comparison between the result of this procedure and an exact analytical solution is then discussed.

A very simple example for the finite-thickness domain is finally presented. The analytical solution used in this example, which assumes constant initial and boundary conditions, represents the basic element to build a procedure similar to the one described for the half-space domain. The solution with the initial-boundary conditions approximated with step functions is a sum of solutions similar to the one here used. Since the boundary conditions for the finite-thickness domain are the soil water content trends, a switch between atmosphere-controlled and soil-controlled phases is not required.

##### 4.1. – HALF-SPACE DOMAIN: NULL IC AND EXPONENTIAL BC

Let us assume the following initial-boundary conditions.

$$\begin{aligned} \vartheta_i(\zeta) &= 0 & (\eta = 0) \\ \vartheta_0(\eta) &= \vartheta_1 \cdot e^{-\gamma \eta} & (\zeta = 0) \end{aligned}$$

The choice of the null initial condition implies that the component (9a) of the solution is null and the problem reduces to the determination of (9b).

According to the boundary condition parameter  $\gamma$ , the solution has three different expressions. This is due to the presence of a square root with a radicand, which is null for  $\gamma = 1/4$ , positive for  $\gamma < 1/4$  and negative for  $\gamma > 1/4$ . Therefore:

- for  $\gamma < 1/4$

$$\vartheta(\zeta, \eta) = \frac{\vartheta_1}{2} e^{\left(\frac{\zeta-2\gamma\eta}{2}\right)} \left[ e^{\zeta \sqrt{\frac{1-4\gamma}{4}}} \operatorname{erfc}\left(\frac{\zeta}{2\sqrt{\eta}} + \sqrt{\eta} \sqrt{\frac{1-\gamma}{4}}\right) + e^{-\zeta \sqrt{\frac{1-4\gamma}{4}}} \operatorname{erfc}\left(\frac{\zeta}{2\sqrt{\eta}} - \sqrt{\eta} \sqrt{\frac{1-\gamma}{4}}\right) \right] \quad (18a)$$

It is easy to verify that, if  $\gamma = 0$ , equation (18a) reduces to equation (13).

- for  $\gamma = 1/4$

$$\vartheta(\zeta, \eta) = \vartheta_1 \cdot e^{\left(\frac{2\zeta-\eta}{4}\right)} \cdot \operatorname{erfc}\left(\frac{\zeta}{2\sqrt{\eta}}\right) \quad (18b)$$

- for  $\gamma > 1/4$

$$\vartheta(\zeta, \eta) = \vartheta_1 \cdot e^{\left(\frac{\zeta-\eta}{2\sqrt{\eta}}\right)^2} \cdot \Re \left\{ W \left( \sqrt{\gamma - \frac{1}{4}} \cdot \sqrt{\eta} + i \frac{\zeta}{2\sqrt{\eta}} \right) \right\} \quad (18c)$$

where  $W(x+iy) \equiv W(z) = e^{-z^2} \cdot \operatorname{erfc}(-i \cdot z)$  is a complex function (of complex variable) whose real and imaginary parts are reported in table 7.9, p. 326 (ABRAMOWITZ & STEGUN, 1965) and in the Appendix II, table II, p. 486 (CARSLAW & JAEGER, 1986). Equation (18c) reduces to equation (18b) if  $\gamma = 1/4$ , the same for equation (18a).

##### 4.2. – HALF-SPACE DOMAIN: UNIFORM IC AND CONSTANT POSITIVE AND NEGATIVE FLUX BC

In order to understand how works the above described procedure, a first application is presented. Uniform soil water content is assumed as initial condition; the flux boundary condition is a step function: starting at  $\eta = 0$  with a positive value; at  $\eta = 10 \cdot \eta_0$  the flux becomes negative with the same absolute value. Here, considering a typical soil,  $\eta_0$  is the dimensionless time corresponding to half an hour. The assumed flux is the boundary condition only during the atmosphere-controlled phases. During the soil-controlled phases, the boundary condition becomes the soil water content at saturation ( $\vartheta = 1$ ) or at desiccation ( $\vartheta = 0$ ). In the presented application, a sequence of two consecutive switches between atmosphere-controlled and soil-controlled phases is solved. The results are for a column of soil of dimensionless thickness  $\zeta = 3$ .

In figure 1a, the thick dashed line corresponds to the uniform soil volumetric water content distribution at the starting time, the initial condition.

The vertical soil moisture distributions at the quoted multiples of  $\eta_0$  are drawn in blue and red during the atmosphere-controlled phases and in cyan and pink during the soil-controlled phases. With the available positive flux applied, the soil surface reaches the saturation at the ponding time  $\eta_p$  and remains saturated until the applied flux becomes negative. At this time a new atmosphere-controlled phase starts and it lasts till the soil is able to convey water to the surface at the poten-

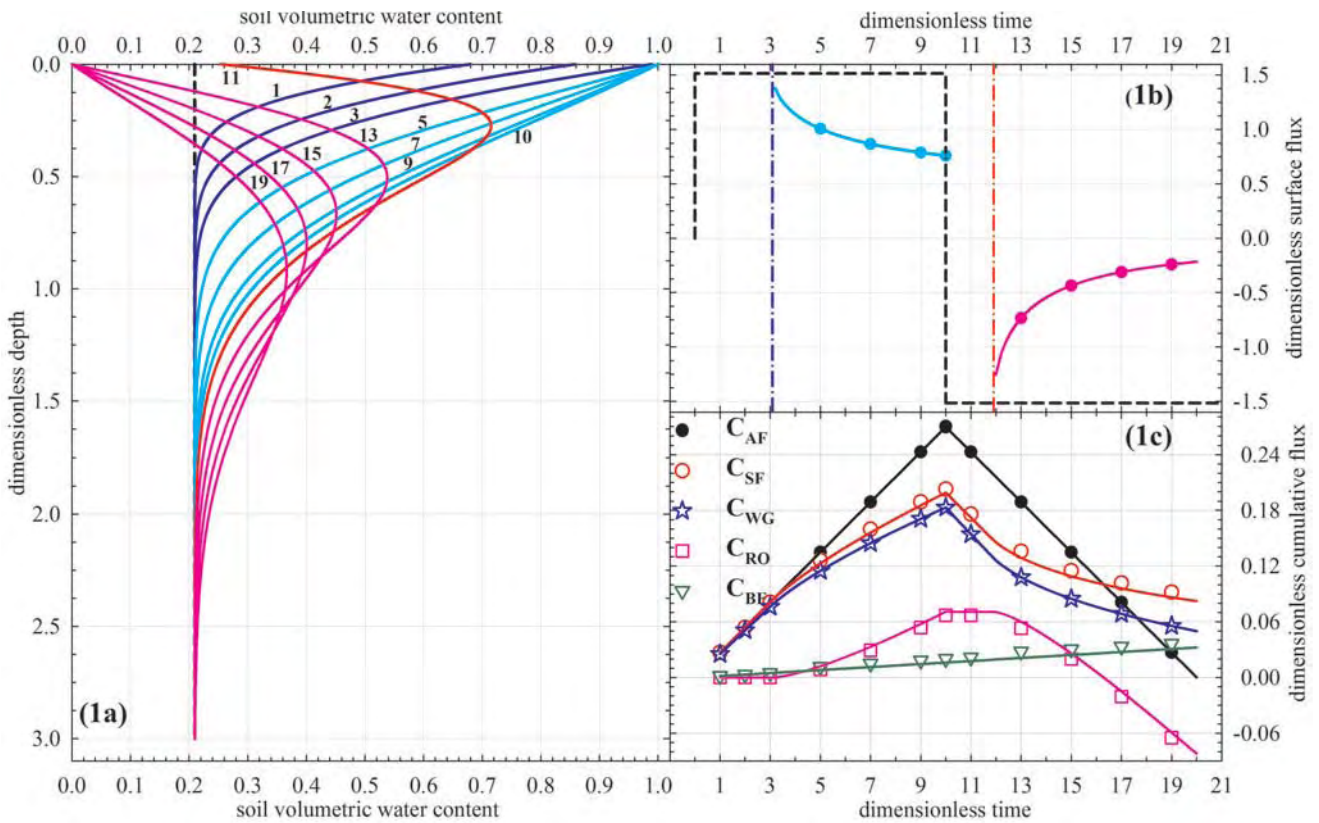


Fig. 1 - (a) soil moisture profiles computed by the procedure at the indicated dimensionless times (multiples of  $\eta_0$ ), the blue and red curves are the solutions during the atmosphere-controlled phases and the cyan and pink ones during the soil-controlled phases; (b) applied surface flux (thick dashed line) and analytical surface flux after ponding time (cyan) or after desiccation time (pink), the two thin dash-dot vertical lines indicate the ponding time (blue) and the desiccation time (red); (c) cumulative flux trends computed by the procedure: applied surface flux ( $C_{AF}$ ), water entered through the surface ( $C_{SF}$ ), water gained by the column of soil of dimensionless height  $\zeta=3$  ( $C_{WG}$ ), runoff (positive) or deficit respect to the evaporation demand (negative) ( $C_{RO}$ ) and water flown through the bottom of the column ( $C_{BF}$ ) during the whole period of time ( $\eta=20\cdot\eta_0$ ).

- (a) profili di contenuto volumetrico d'acqua calcolati dalla procedura ai tempi adimensionali (multipli di  $\eta_0$ ) indicati in figura; le soluzioni durante le fasi controllate dall'atmosfera sono di colore blu e rosso, durante le fasi controllate dal suolo sono di colore ciano e rosa; (b) flusso applicato alla superficie (linea tratteggiata spessa) e flusso analitico alla superficie dopo la saturazione (ciano) o il completo essiccamento (rosa), le due linee verticali (tratto punto) indicano i tempi di raggiunta saturazione (blu) e completo essiccamento alla superficie (rosso); (c) flussi cumulativi calcolati dalla procedura: flusso applicato alla superficie ( $C_{AF}$ ), acqua entrata attraverso la superficie ( $C_{SF}$ ), acqua guadagnata dalla colonna di suolo di altezza adimensionale  $\zeta=3$  ( $C_{WG}$ ), ruscellamento (positivo) o deficit rispetto alla domanda di evaporazione (negativo) ( $C_{RO}$ ) e flusso uscente dal fondo della colonna ( $C_{BF}$ ) durante l'intero intervallo temporale ( $\eta=20\cdot\eta_0$ ).

tial rate, that is, till the air-dry value is reached at the surface. At the desiccation time  $\eta_d$  starts a new soil-controlled phase. After  $\eta=11\cdot\eta_0$  the soil water content profiles show a maximum, moving downward with decreasing amplitude. The thick dashed line in figure 1b corresponds to the boundary condition (flux applied at the surface). The first four cyan circles are the analytically computed surface flux values at the solution times, during the saturation; similarly, the last four circles (pink) are the surface flux values, during the desiccation. They are computed at the dimensionless times reported in figure 1a. The solid lines (cyan and pink) are the analytical surface flux computed each  $\eta_0/5$  dimensionless time interval during the two soil-controlled phases. The two vertical dash-dot lines indicate the times of ponding  $\eta_p$  (blue) and air-dry soil  $\eta_d$  (red). Figure 1c reports the cu-

mulative fluxes obtained by the sum of the instantaneous flux, at the solution time, times the time interval between two consecutive solutions. The symbols indicate the values estimated at the solution times reported in figure 1a while the solid lines are obtained from the solutions computed each  $\eta_0/5$  dimensionless time interval, as for figure 1b. In figure 1c a small difference between symbols and lines can be appreciated; it is due to the time interval between two consecutive solutions. The time interval for the symbols is  $\eta_0$  or  $2\cdot\eta_0$  while, for the solid lines, it is  $\eta_0/5$ .

The computed runoff is the difference between the applied flux (boundary condition) and the analytically computed surface flux; therefore it is a real runoff when it is positive and it is the deficit respect to the evaporation demand when negative.

#### 4.3. – HALF SPACE DOMAIN: NULL IC AND EXPONENTIAL FLUX BC

In this second application, the comparison between the soil water content obtained by the procedure and the results of the analytical solution of the linearized Richards equation subject to a null soil water content initial condition and a decreasing exponential flux boundary condition is presented. Therefore the initial-boundary conditions are:

$$\begin{aligned} \vartheta_1(\zeta) &= 0 & (\eta = 0) \\ \Phi_0(\eta) &= q_1 \cdot e^{-\gamma \cdot \eta} & (\zeta = 0) \end{aligned}$$

In this case the solution of the Richards equation is equal to equation (18a) or (18b) or (18c), according to the value of  $\gamma$ ; in the obtained solution  $\Phi(\zeta, \eta)$ ,  $q_1$  substitutes  $\vartheta_1$ . Then the soil water content  $\vartheta(\zeta, \eta)$  is obtained using equation (11):

$$\begin{aligned} \vartheta(\zeta, \eta) &= \frac{q_1}{V} e^{\left(\frac{\zeta - 2\gamma\eta}{2}\right)} \\ &\left[ \frac{-1}{2\gamma} e^{\left(\frac{\zeta + 2\gamma\eta}{2}\right)} \operatorname{erfc}\left(\frac{\zeta + \eta}{2\sqrt{\eta}}\right) + \frac{e^{\frac{\tau\zeta}{2}}}{1 - \tau} \operatorname{erfc}\left(\frac{\zeta + \tau\eta}{2\sqrt{\eta}}\right) + \frac{e^{\frac{-\tau\zeta}{2}}}{1 + \tau} \operatorname{erfc}\left(\frac{\zeta - \tau\eta}{2\sqrt{\eta}}\right) \right] \end{aligned} \quad (19)$$

where  $\tau = \sqrt{1 - 4\gamma}$ . Equation (19) is valid for  $\gamma \leq 1/4$  and till the saturation is reached.

In this second application of the procedure  $\gamma = 1/4$  has been chosen, so that  $\tau = 0$  and equation (19) is very simple. The soil water content distribution is computed for a column of soil of dimensionless height  $\zeta = 3$ , at multiples of the dimensionless time  $\eta_0$ .

The results are shown in figures 2a, 2b and 2c.

The thick vertical dashed line on the left side of figure 2a is the null initial condition and the decreasing exponential in figure 2b is the boundary condition. The green and cyan solid lines in figure 2a are the solutions of the procedure obtained approximating the exponential boundary condition with a time step of  $\eta_0/6$ . The symbols represent the analytic soil water content profiles obtained using (19) with  $\gamma = 1/4$ . Both procedure and analytic solution are computed at the dimensionless times reported in figure 2a. Up to  $\eta = 6 \cdot \eta_0$ , the applied flux is able to increase the surface moisture without reaching the saturation, as shown by the first four solutions (green curves). As the time goes on, the decreasing exponential flux implies a decrease in the surface moisture, as shown by the last four solutions (cyan curves). In order to qualitatively verify the influence of the “time step” chosen to approximate the boundary condition, the solutions at 1, 2, 4 and 6  $\eta_0$  have been recomputed using a time step of 4  $\eta_0$ ; they are the black lines in figure 2a. In figure 2c only the cumulative applied surface

flux (black), the water gained by the column (blue) and the cumulative bottom flux (green) are reported because the surface flux equals at each time the applied one and, therefore, the runoff is always null.

#### 4.4. – FINITE-THICKNESS DOMAIN: CONSTANT IC AND BCs

A simple example, with constant initial-boundary conditions for the finite-thickness domain, is here presented. In this case the solution of the model is exactly the analytical solution of the problem. In fact, the solution is the sum of equations (12a) and (12b) which are the basic elements to build a procedure similar to the one described for the half-space domain. Uniform soil water content at saturation ( $\vartheta = 1$ ) is assumed as initial condition for the finite-thickness layer of dimensionless depth  $\zeta = 1$ . At the time origin the soil water content at the top of the layer becomes and remains null while the value at the bottom continues to be at saturation. Figure 3a shows the soil water content profiles computed by equations (12a) and (12b) at the dimensionless times: 1, 2, 4, 6, 12, 24, 36, 48, 72, 96, 120, 144, 192, 240  $\eta_0$ . The dashed line is the initial condition and the dotted line is the stationary solution. Figure 3b shows the instantaneous dimensionless flux at the top (pink) and bottom (green) boundaries; the symbols are the values computed at the aforementioned solution times. The fluxes are positive in the increasing depth direction. The square crossed is the value to which both the fluxes tend: that is the stationary flux. Figure 3c shows the cumulative dimensionless flux at the top (red) and bottom (green) boundaries. The total water content trend (blue line and star) is also shown. The full blue star is the total water content at the stationary condition.

## 5. – CONCLUSIONS

In this paper, a compilation of the solutions obtained for the linearized one-dimensional Richards equation, solved both in a half-space and in a finite-thickness domain has been presented. For space reasons, only the most meaningful solutions were described.

The soil water content at any required time and depth results as the sum of two components; one related to the initial condition and to null boundary conditions and the other related to the boundary conditions and to null initial condition. The sum of these two components is the general solution of the Richards equation in integral form and the



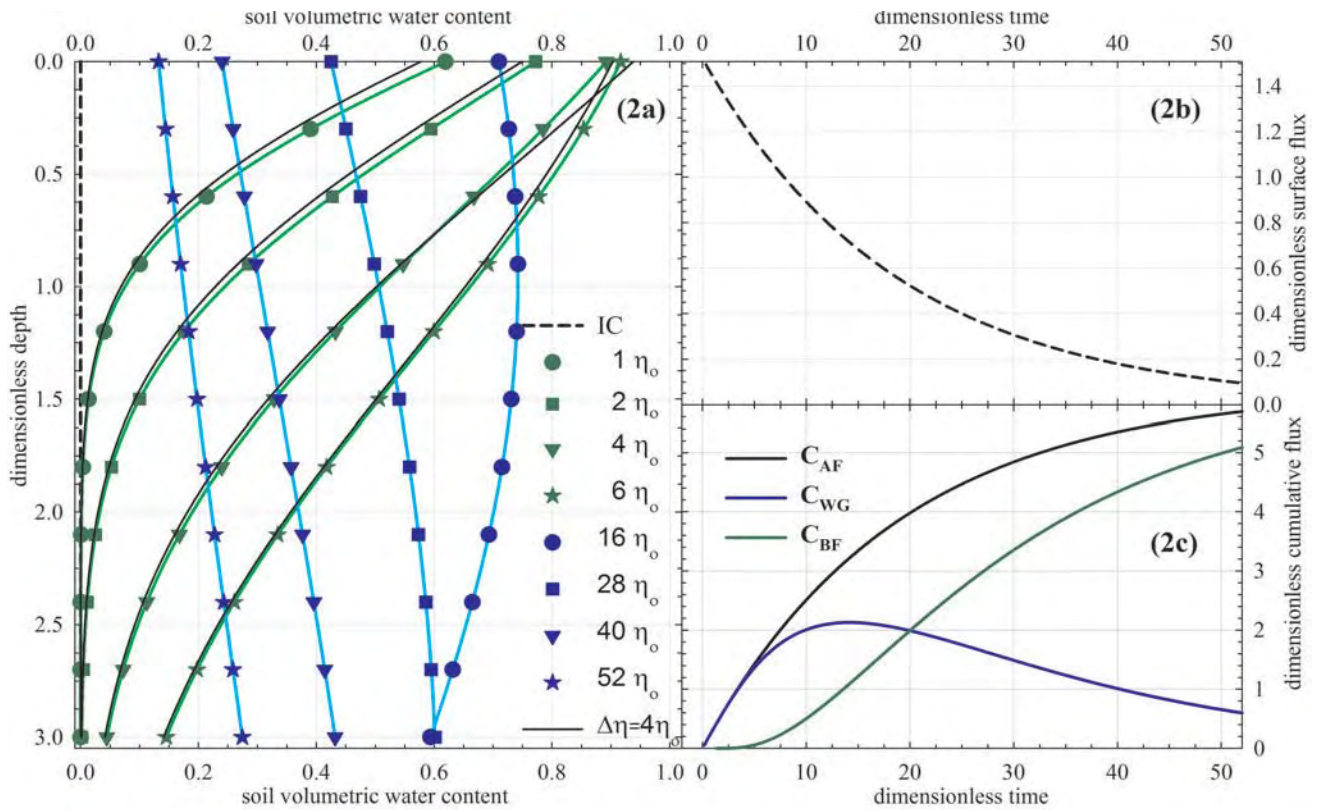


Fig. 2 - (a) soil moisture profiles computed by the procedure (solid lines) and using equation (19) (symbols) at the indicated dimensionless times (multiples of  $\eta_0$ ). The four black lines are the solutions computed by the procedure (at the same times of the green curves) using a worst approximation of the boundary condition; (b) exponential flux applied at the surface; (c) cumulative trends computed by the procedure: applied surface flux ( $C_{AF}$ ), water gained by the column of soil of dimensionless height  $\xi=3$  ( $C_{WG}$ ) and water flown through the bottom of the column ( $C_{BF}$ ) during the whole period of time.

- (a) profili di contenuto volumetrico d'acqua calcolati dalla procedura (linee continue) e con l'equazione (19) (simboli) ai tempi adimensionali (multipli di  $\eta_0$ ) indicati in figura. Le quattro linee nere sono le soluzioni, calcolate agli stessi tempi di quelle verdi, ma con un'approssimazione della condizione al contorno meno accurata; (b) flusso esponenziale applicato alla superficie; (c) andamenti cumulativi calcolati dalla procedura: flusso applicato alla superficie ( $C_{AF}$ ), acqua guadagnata dalla colonna di suolo di altezza adimensionale  $\xi=3$  ( $C_{WG}$ ) e flusso uscente dal fondo della colonna ( $C_{BF}$ ) durante l'intero intervallo temporale.

analytical expression of the soil water content distribution is therefore obtained if the integrals in the solution can be solved. The paper also describes a new method to compute the solutions of the linearized Richards equation, when arbitrary discrete initial and boundary conditions are available (step functions). For the half-space domain the initial condition is the soil volumetric water content and the boundary condition is the flux available at the surface. The experimental readings at a hydro-meteorological station correspond exactly to a step function like the one required by the model. This model also accounts for the switching between successive atmosphere-controlled and soil controlled phases and vice versa. Each phase has its own solution and requires its own initial condition, which is automatically computed by the described procedure. If the linearization of the Richards equation can be considered a valid assumption for a specific soil and its soil water content, the presented procedure is a quite valid tool to estimate the evolution of the soil water content

distribution, the ponding or desiccation time, the water fluxes and the water gained or lost by a column of surface soil. It can also be used, a priori, to define the best spatial domain and the probes depth of a hydrological station to study a specific topic: irrigation, evaporation, ground water recharge and so on. The same can be said about the time step of meteorological readings to be used to estimate the flux applied at the surface.

It must be remarked that the spatial domain of the procedure is a uniform half-space. In many real cases (e.g. in presence of shallow freatic aquifers) the spatial domain is finite and it is better represented by a finite-layer. Here a very simple example for the finite-thickness domain has been presented. The importance of this example is that its analytical solution, which is derived for constant initial and boundary conditions, represents the basic element to build a new procedure similar to the one described for the half-space domain. In fact, the solution with the initial-boundary conditions approximated with step functions is a sum of

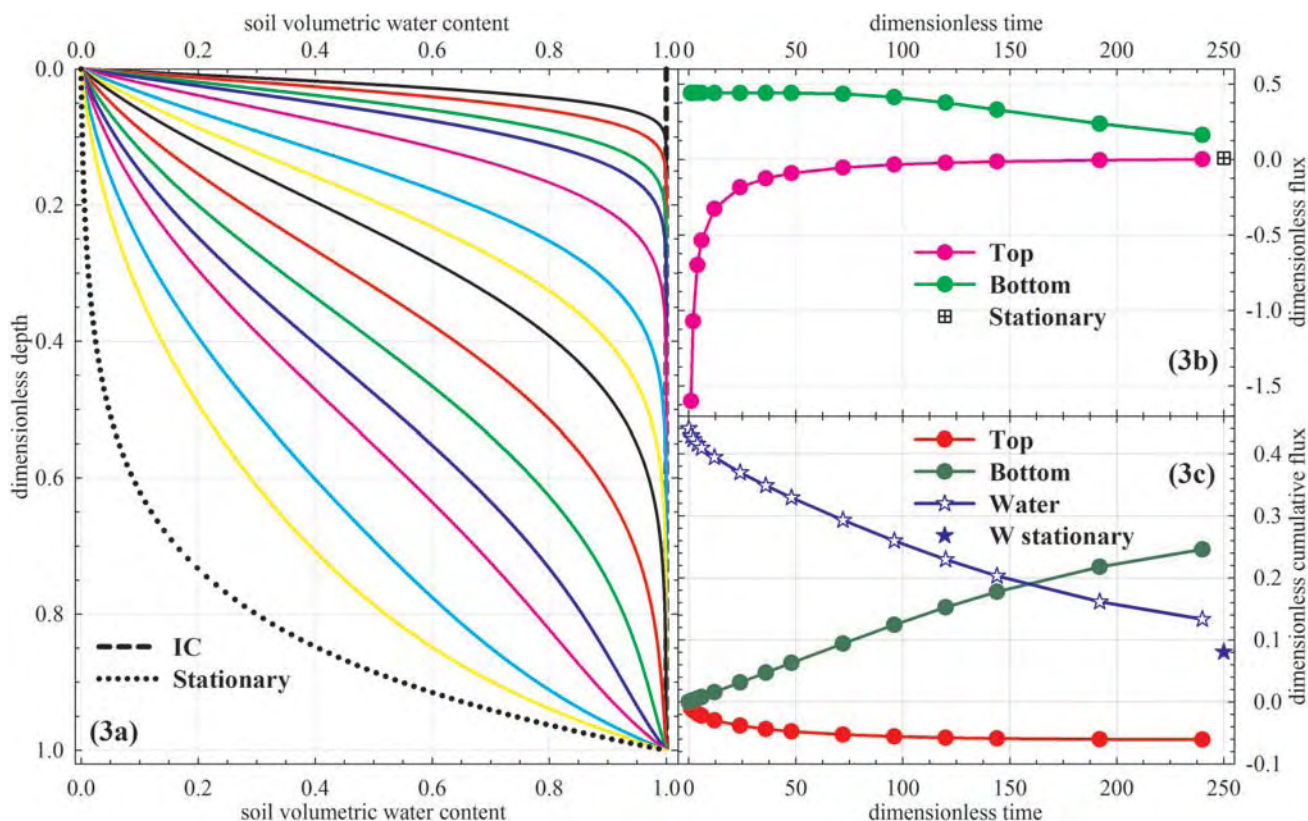


Fig. 3 - (a) soil moisture profiles computed by equations (12a) and (12b) at the dimensionless times: 1, 2, 4, 6, 12, 24, 36, 48, 72, 96, 120, 144, 192, 240  $\eta_0$ . The dashed line is the initial condition ( $\theta=1$ ); the dotted line is the stationary solution; (b) instantaneous dimensionless flux at the top (pink) and bottom (green) boundaries; the symbols are the values computed at the aforementioned solution times. The square crossed is the value of the flux at the stationary condition; (c) cumulative dimensionless flux at the top (red) and bottom (green) boundaries, the symbols are the values computed at the solution times; total water content trend (blue), the symbols (star) are the values computed at the solution times; the full blue star is the total water content at the stationary condition.

- (a) profili di contenuto volumetrico d'acqua calcolati dalle equazioni (12a) e (12b) ai tempi adimensionali: 1, 2, 4, 6, 12, 24, 36, 48, 72, 96, 120, 144, 192, 240  $\eta_0$ . La linea tratteggiata è la condizione iniziale ( $\theta=1$ ); la linea punteggiata è la soluzione stazionaria; (b) flussi istantanei adimensionali ai confini superiore (rosa) e inferiore (verde); i simboli sono i valori calcolati ai tempi delle soluzioni citati sopra. Il quadrato con la croce all'interno è il valore del flusso in condizione stazionaria; (c) flussi cumulativi adimensionali ai confini superiore (rosso) e inferiore (verde), i simboli sono i valori calcolati ai tempi delle soluzioni; andamento del contenuto d'acqua totale (blu), i simboli (stelle) sono i valori calcolati ai tempi delle soluzioni; la stella blu piena indica il contenuto d'acqua alla stazionarietà.

solutions similar to the one here used. In this case (finite-thickness domain), since the boundary conditions are the soil water content trends, the procedure doesn't require a switch between atmosphere-controlled and soil-controlled phases.

#### Acknowledgments

The work here presented is the theoretical part of the models developed by the authors in the framework of National Italian Project: "Esplorazione geofisica e geologica di alcuni complessi acquiferi alluvionali nella pianura Padana tra Milano e Bologna, per la modellazione della circolazione idrica sotterranea" (PRIN 2005043388) and also during the first year of the new one: "Studio integrato geofisico, geologico, petrofisico e modellistico-matematico di complessi acquiferi alluvionali rappresentativi del sottosuolo padano: relazioni tra scala della ricostruzione idrostratigrafica e modelli di flusso" (PRIN 2007F9M9L8). These models will be applied to the experimental data measured at three stations located between the town of Parma and the Taro River. The authors wish to thank "Ciclo Idrico Integrato del-

l'Enia Parma" and "Barilla" for the availability of the places where the instruments are installed.

The Italian Ministero dell'Istruzione, dell'Università e della Ricerca; the Università di Modena e Reggio Emilia; the Fondazione Cassa di Risparmio di Modena in part funded this work.

The authors wish to thank Prof. Mauro GIUDICI and Dr. Emanuele ROMANO for the useful suggestions and revision of the manuscript.

#### REFERENCES

- ABRAMOWITZ M. & STEGUN I.A. (1965) - *Handbook of mathematical functions*. Dover Publication, New York.
- BASHA H.A. (1999) - *Multidimensional linearized nonsteady infiltration with prescribed boundary conditions at the soil surface*. Water Resour. Res., **35**: 75-83.
- CARSLAW H.S. & JAEGER J.C. (1986) - *Conduction of heat in solids*. Clarendon Press, Oxford.
- CHEN JIANN-MOU, TAN YIH-CHI, CHEN CHU-HUI & PARLANGE J.Y. (2001) - *Analytical solutions for linearized Richards equation with arbitrary time-dependent surface fluxes*.

- Water Resour. Res., **37**:1091-1093.
- CHEN JIANN-MOU, TAN YIH\_CHI & CHEN CHU\_HUI (2003) - *Analytical solutions of one-dimensional infiltration before and after ponding*. Hydrol. Process., **17**: 815-822.
- HOGARTH W.L., PARLANGE J.Y. & BRADDOCK R.D. (1989) - *First integrals of the infiltration equation, 2, Nonlinear conductivity*, Soil Sci., **148** (3): 165-171.
- HOGARTH W.L., PARLANGE J.Y. & NORBURY J. (1992) - *Addendum to "First integrals of the infiltration equation"*, Soil Sci., **154**: 341-343.
- HOGARTH W.L. & PARLANGE, J.Y. (2000) - *Application and improvement of a recent approximate analytical solution of Richards' equation*. Water Resour. Res., **36**: 1965-1968.
- JONES D.S. (1966) - *Generalised functions*. McGraw-Hill, New York.
- MENZIANI M., PUGNAGHI S., VINCENZI S. & SANTANGELO R. (2005) - *Water Balance in Surface Soil: Analytical Solutions of Flow Equations and Measurements in the Alpine Toce Valley*. In: "Climate and Hydrology in Mountain Areas", C. DE JONG, D. COLLINS & R. RANZI (Eds.), John Wiley & Sons, 84-100.
- MENZIANI M., PUGNAGHI S. & VINCENZI S. (2007) - *Analytical solutions of the linearized Richards equation for discrete arbitrary initial and boundary conditions*. J. Hydrol., **332**: 214-225.
- PARLANGE M.B., PRASAD S.N., PARLANGE J.Y. & ROMKENS M.J.M. (1992) - *Extension of the Heaslet-Alksne technique to arbitrary soil water diffusivities*. Water Resour. Res., **28**: 2793-2797.
- PARLANGE J.Y., BARRY D.A., PARLANGE M.B., HOGARTH W.L., HAVERKAMP R., ROSS P.J., LING L. & STEENHUIS T.S. (1997) - *New approximate analytical technique to solve Richards equation for arbitrary surface boundary conditions*. Water Resour. Res., **33**: 903-906.
- RICHARDS L.A. (1931) - *Capillary conduction of liquids through porous mediums*. Physics, **1**: 318-333.
- ROSS P.J. & PARLANGE J.Y. (1994) - *Comparing exact and numerical solutions of Richards' equation for one-dimensional infiltration and drainage*. Soil Sci., **157**: 341-344.
- SANDER G.C., PARLANGE J.Y., KUHNEL V., HOGARTH W.L., LOCKINGTON D. & O'KANE J.P.J. (1988) - *Exact nonlinear solution for constant flux infiltration*. J. Hydrol., **97**: 341-346.
- WANG Q.J. & DOOGE J.C.I. (1994) - *Limiting cases of water fluxes at the land surface*. J. Hydrol., **155**: 429-440.
- WARRICK A.W. (1975) - *Analytical solutions to the one-dimensional linearized moisture flow equation for arbitrary input*. Soil Sci., **120**: 79-84.



## INDEX/INDICE

PREFACE/PREFAZIONE.....	Pag. 4
INTRODUCTION/INTRODUZIONE.....	» 5
AMOROSI A. & PAVESI M. – <i>Aquifer stratigraphy from the middle-late Pleistocene succession of the Po Basin</i> Stratigrafia di sistemi acquiferi nella successione medio-e tardo pleistocenica del Bacino Padano.....	» 7
BERSEZIO R., CAVALLI E. & CANTONE M. - <i>Aquifer building and Apennine tectonics in a Quaternary foreland: the southernmost Lodi plain of Lombardy</i> - Origine degli acquiferi e tettonica appenninica in un avampaese quaternario: la pianura lodigiana meridionale in Lombardia.....	» 21
BONOMI T., DEL ROSSO F., FUMAGALLI L. & CANEPA P. - <i>Assessment of groundwater availability in the Milan Province aquifers</i> - Stima della disponibilità idrica negli acquiferi della Provincia di Milano.....	» 31
BONZI L., MARTINELLI G. & SCIUTO P.F. - <i>A Google Map mashup for hydrogeochemical data of Emilia- Romagna Region</i> - Un Google map Mashup per i dati idrogeochimici della Regione Emilia Romagna.....	» 41
BUTTERI M., DOVERI M., GIANNECCHINI R. & GATTAI P. - <i>Hydrogeologic-hydrogeochemical multidisciplinary study of the confined gravelly aquifer in the coastal Pisan Plain between the Arno River and Scolmatore Canal (Tuscany)</i> - Studio multidisciplinare idrogeologico-geochimico dell'acquifero confinato in ghiaie nella fascia costiera pisana tra il Fiume Arno ed il Canale Scolmatore (Toscana).....	» 51
CILUMBRIELLO A., SABATO L., TROPEANO M., GALLICCHIO S., GRIPPA A., MAIORANO P., MATEU- VICENS G., ROSSI C.A., SPILOTRO G., CALCAGNILE L. & QUARTA G. - <i>Sedimentology, stratigraphic architecture and preliminary hydrostratigraphy of the Metaponto coastal-plain subsurface (Southern Italy)</i> - Sedimentologia, architettura stratigrafica e idrostratigrafia preliminare del sottosuolo della piana costiera metapontina (Italia meridionale).....	» 67
DELL'ARCIPRETE D., BERSEZIO R., FELLETTI F., GIUDICI M. & VASSENA C. - <i>Simulation of heterogeneity in a point-bar/channel aquifer analogue</i> - Simulazione dell'eterogeneità in un analogo di acquifero fluviale meandriforme (sistema barra puntiforme/canale).....	» 85
FORNO M.G., DE LUCA D.A., FIORASO G. & GIANOTTI F. - <i>Hydrogeological implication of the Pliocene- Pleistocene torrential and debris flow succession around the Lanzo Ultramafic Massif (Western Alps)</i> - Significato idrogeologico della successione torrentizia e di debris flow al margine del Massiccio Ultrabásico di Lanzo (Alpi Occidentali).....	» 97
GIUDICI M. - <i>Modeling water flow and solute transport in alluvial sediments: scaling and hydrostratigraphy from the hydrological point of view</i> - Modellazione del flusso idrico e del trasporto di soluti in sedimenti alluvionali: i passaggi di scala e l'idrostratigrafia dal punto di vista idrologico.....	» 113
GUADAGNINI A., RIVA M. & GUADAGNINI L. - <i>Modeling dissolution experiments and heavy metals competition in porous media</i> - Modellazione ed interpretazione di processi di dissoluzione e di assorbimento competitivo di metalli pesanti in mezzi porosi.....	» 121
IRACE A., CLEMENTE P., PIANA F., DE LUCA D.A., POLINO R., VIOLANTI D., MOSCA P., TRENKWALDER S., NATALICCHIO M., OSSELLA L., GOVERNA M. & PETRICIG M. - <i>Hydrostratigraphy of the late Messinian- Quaternary basins in southern Piedmont (northwestern Italy)</i> - Idrostratigrafia dei bacini messiniano- quaternari del Piemonte meridionale (Italia nord-occidentale).....	» 133
LONGINELLI A. & SELMO E. - <i>Isotope geochemistry and the water cycle: a short review with special emphasis on Italy</i> - La geochimica isotopica ed il ciclo delle acque: un breve sguardo retrospettivo con particolare riferimento all'Italia.....	» 153

MARGIOTTA S., MAZZONE F. & NEGRI S. - <i>Stratigraphic revision of Brindisi-Taranto Plain: hydrogeological implications</i> - Revisione stratigrafica della piana Brindisi-Taranto e sue implicazioni sull'assetto idrogeologico.....	pag. 165
MARTELLI G. & GRANATI C. - <i>A comprehensive hydrogeological view of the Friuli alluvial plain by means of a multi-annual quantitative and qualitative research survey</i> - Quadro idrogeologico generale della Pianura alluvionale friulana sulla base di indagini quantitative e qualitative pluriannuali..... »	181
MELE M., BERSEZIO R., GIUDICI M., RUSNIGHI Y. & LUPIS D. - <i>The architecture of alluvial aquifers: an integrated geological-geophysical methodology for multiscale characterization</i> - Una metodologia integrata, geologico-geofisica, per la caratterizzazione multiscala dell'architettura degli acquiferi alluvionali..... »	209
PISANI V., D'ONOFRIO S. & CARLSON F. - <i>Groundwater flow modeling supporting a remediation project within a chemical facility</i> - Modello di flusso della falda utilizzato nell'ambito di un progetto di bonifica di un sito industriale..... »	225
RUSI S. & TATANGELO F. - <i>Conceptualization, modelling and management of alluvial aquifers: case studies of Sangro and Vomano plains (central Italy)</i> - Concettualizzazione, modellazione e gestione di acquiferi alluvionali: i casi di studio delle pianure del Sangro e del Vomano (Italia centrale)..... »	245
VIGNA B., FIORUCCI A. & GHIELMI M. - <i>Relations between stratigraphy, groundwater flow and hydrogeochemistry in Poirino Plateau and Roero areas of the Tertiary Piedmont Basin, Italy</i> - Rapporti tra assetto stratigrafico, idrogeologia e idrogeochimica nel settore compreso tra l'Altopiano di Poirino e il Roero (Bacino Terziario Piemontese, Italia)..... »	267
VINCENZI S., MENZIANI M. & PUGNAGHI S. - <i>General analytical solutions of the linearized Richards equation for a half-space and a finite-thickness domain</i> - Soluzioni analitiche generali dell'equazione di Richards linearizzata per un semispazio e un dominio di spessore finito..... »	293

Finito di stampare nel mese di novembre 2010  
dalla Tipolitografia CSR - Via di Pietralata, 157 - 00158 Roma  
Tel. 064182113 (r.a.) - Fax 064506671